Chiral N-heterocyclic carbene (NHC) ligands in Pd-catalyzed cross-coupling reactions

Katayev, Dmitry

UNIVERSITÉ DE GENÈVE
Section de Chimie et Biochmie
Département de chimie organique

FACULTÉ DES SCIENCES

Professeur E. Peter Kündig

Chiral *N*-Heterocyclic Carbene (*NHC*) Ligands in Pd-Catalyzed Cross-Coupling Reactions

THÈSE

présentée à la Faculté des sciences de l'Université de Genève

pour obtenir le grade de Docteur ès sciences, mention chimie

par

Dmitry Katayev

de

Kaluga (Russie)

Thèse N° 4503

GENÈVE

Atelier d'impression ReproMail-UniMail

2012

Ce manuscrit est le résultat des travaux de recherche effectués de septembre 2008 à octobre 2012 au sein du groupe du Professeur Ernst Peter Kündig au Département de Chimie Organique à l'Université de Genève.

Premièrement, je voudrais exprimer ma gratitude au Professeur Kündig pour m'avoir donné la possibilité d'effectuer ma thèse dans son laboratoire. Son leadership professionnel et ses conseils ont eu une forte influence positive sur mon développement professionnel et personnel.

Ce fut un plaisir d'avoir comme jury pour cette thèse le Professeur Frank Glorius (Université de Münster) et le Professeur Clément Mazet (Université de Genève). Je tiens à les remercier d'avoir pris le temps de lire et de juger mon travail de recherche.

Ce travail n'aurait pu être réalisé sans l'aide généreuse des équipes responsables des outils analytiques de l'Université de Genève : analyses RMN par le Dr. Damien Jeannerat et André Pinto, la spectrométrie de masse par Mmes Eliane Sandmeier et Nathalie Oudry ainsi que les analyses par diffraction au rayon-X par le Dr. Gerald Bernardinelli et le Dr. Céline Besnard. Je voudrais également remercier le Dr. Yi-Xia Jia et le Dr. Masafumi Nakanishi pour leur collaboration productive, le Professeur Raghavan B. Sunoj et le Dr. Evgeny Larionov pour les études DFT et le Professeur Thomas Bürgi pour les calculs de dichroisme circulaire vibrationnel (DCV).

Je remercie également tous mes collègues, passés et présents, pour l'atmosphère conviviale et pour leur soutien permanent durant toute la durée de mon séjour à Genève.

J'aimerais remercier spécialement le Professeur Clément Mazet, le Professeur Evgeny Katayev et le Dr. Alastair Lennox pour leur aide exceptionnelle lors de la correction et de la mise en forme de ce manuscrit.

Хочу выразить огромную благодарность и глубокую признательность своим родным и близким за мудрые советы и поддержку в пути к науке.

Index

Résumé en Français 1

I. General Introduction 6

I.1. History of *N*-Heterocyclic Carbenes as Ligands 6
I.2. Structural Diversity of *N*-Heterocyclic Carbene Ligands 7
I.3. Electronic Properies of *N*-Heterocyclic Carbene Ligands 7
I.4. Steric Properties of *N*-Heterocyclic Carbene Ligands 10
I.5. Synthesis of *NHC* Precursors 12

I.5.1. Synthesis of Imidazolium Salts 12
I.5.2. Synthesis of 4,5-Dihydroimidazolium Salts 14

I.6. *NHC* Ligands in Asymmetric Transition-Metal Catalyzed Reactions 15

I.6.1. Chiral Units Located in the Alkyl Side Chains 16
I.6.2. Chiral Backbone in the Heterocycle 19
I.6.3. Axially Chiral NHC Ligands 21
I.6.4. Planar Chiral NHC Ligands 24
I.6.5. Trans-Cyclodiamine Derived Chiral NHC Ligands 25
I.6.6. Oxazoline Based Chiral NHC Ligands 27
I.6.7. Chiral NHC Ligands with Rigid Backbones 28
I.6.8. Summary 28

I.7. Design and Development of a New Family of Chiral *NHC* Ligands in the *Kündig* Group 29
I.8. Project Outline 30

II. Asymmetric Synthesis of Oxindoles *via* Intramolecular Palladium-*NHC*-Catalyzed *α*-Arylation of Amides 32

II.1. Importance of Oxindoles in Medicinal Chemistry 32
II.2. Enantioselective Oxindole Synthesis *via* Metal-Catalyzed Intramolecular Reactions 33
II.3. Results: Chiral *NHC* Ligands in Palladium-Catalyzed *α*-Arylation of Amides 39

II.3.1. Synthesis of Chiral Amines 39

II.3.2. Synthesis of Chiral NHC Ligands (Ligand Precursors) 40
II.3.3. Synthesis of 3-Alkyl-3-Aryloxindoles 42
II.3.3.1. Optimization of Reaction Conditions 42
II.3.3.2. Substrate Scope 44
a) Synthesis of Substrates 44
b) Catalysis 47
*II.3.3.3. Determination of the Absolute Configuration of (S)-**90*** 52
II.3.4. Origin of Asymmetric Induction 52
II.3.5. Mechanistic Studies of Pd(NHC)-Catalyzed α-Arylation Reaction 56
II.3.5.1. Analysis of the Catalytic Cycle 56
*II.3.5.2. Structure of Palladacycles (S,S)-**101a** and (S,S)-**101b*** 62
II.3.6. Synthesis of New Chiral N-Heterocyclic Carbene Ligands 63
II.3.6.1. Synthesis of Chiral Amines 63
II.3.6.2. Synthesis of Imidazolium and Dihydroimidazolium Salts 64
II.3.7. Synthesis of Spirooxindoles 65
II.3.7.1. Optimization of Reaction Conditions 65
II.3.7.2. Synthesis of Substrates 67
II.3.7.3. Catalysis 68
II.3.7.4. Synthesis of New Preformed Catalysts 73
II.3.8. DFT Investigations 75
II.3.9. Catalytic Enantioselective Synthesis of a 3-Aryl-3-benzyl-oxindole Exhibiting anti-Tumour Activity 77
II.3.10. Conclusion 80

III. Asymmetric Synthesis of Indolines *via* Palladium-*NHC*-Catalyzed C(sp^3)-H/C(Ar) Coupling Reactions 82

III.1. Functionalization of non-Activated C(sp^3)-H Bonds 82
III.2. Synthesis of the Indoline Scaffold 87
III.2.1. Importance of Indolines in Medicinal Chemistry 87
III.2.2. Synthesis of Indolines 87

III.3. Concept 88
III.4. Results: Fused Indolines by Pd-Catalyzed Asymmetric C-C Coupling Involving an Unactivated Methylene Group 89
III.4.1. Synthesis of New Catalysts 89
III.4.2. Optimization of Reaction Conditions 89
III.4.3. Synthesis of Carbamates 91
III.4.4. Substrate Scope for the Synthesis of Fused Indolines 95
III.4.5. Determination of Absolute Configuration 98
III.4.6. Proposed Mechanism for Enantioselective Pd(NHC)-Catalyzed Synthesis of Fused Indolines via C(sp^3)-H Activation of the Unactivated Methylene Group. 98
III.4.7. Highly Enantioenriched 2-Substituted and 2,3-Disubstituted Indolines via Regiodivergent Reaction of a Racemic Mixture (RRM). 99
III.4.8. Conclusion 112

IV. Experimental Section 114

IV.1. General Remarks 114
IV.2. Synthesis of Chiral Amines 115
IV.3. Synthesis of Imidazolium and Dihydroimidazolium Salts (Chiral Carbene Precursors) 119
IV.3.1. Synthesis of Imidazolium Salts 119
IV.3.2. Synthesis of Dihydroimidazolium Salts 121
IV.4. General Procedure for the Synthesis of Amides 123
IV.5. Catalytic Asymmetric Intramolecular *α*-Arylation Reactions 141
IV.5.1. General Procedure for Catalytic Asymmetric Intramolecular α-Arylation Reactions 141
*IV.5.2. General Procedure for Kinetic Measurements of the Influence of Additives on the Catalytic Asymmetric Intramolecular α-Arylation of Amide (**61**)* 141
*IV.5.3. General Procedure for Pd-Catalyzed α-Arylation of Amide (**61**) with Various Precatalysts* 141
IV.6. General Procedure for the Synthesis of [Pd(η^3-cinnamyl or allyl)(*NHC*)I] Complexes 157
IV.7. Catalytic Enantioselective Synthesis of a 3-Aryl-3-benzyl-oxindole (**51**) Exhibiting anti-Tumor Activity 165
IV.8. Synthesis of *N*-Cycloalkyl-2-Bromoaniline 171

IV.8.1. Representative Procedure 1 for N-Alkyl-2-Bromoaniline by Reductive Amination 171
IV.8.2. Representative Procedure 2 for Palladium-Catalyzed N-Arylation 171
IV.8.3. Synthesis of Enantioenriched Carbamates 183
*IV.8.4. Preparation of Enantio-pure (R)- and (S)-Methyl-(2-bromophenyl)(1-phenylpropan-2-yl)carbamate (**198**)* 186

IV.9. Palladium-Catalyzed Synthesis of Indolines 187

IV.9.1. Representative Racemic Synthesis of Indolines Using $PCy_3 \cdot HBF_4$ as a Ligand 187
*IV.9.2 Racemic Synthesis of Indoline (**251**) Using $PCy_3 \cdot HBF_4$ as a Ligand* 187
*IV.9.3. Racemic Synthesis of Indoline (**251**) Using IPr·HCl as a Ligand* 188
IV.9.4. Representative Procedure for the Asymmetric Pd(NHC)-Catalyzed C-H Activation 188
IV.9.5. Pd(NHC)-Catalyzed Synthesis of Indolines via Regiodivergent Reaction from Enantiopure Carbamates 203

IV.10. Synthesis of (2*R*,3*S*)-2-Methyl-3-Phenylindoline (**293**) 208
IV.11. IR and Vibrational Circular Dichroism (VCD) Spectra 208

IV.11.1. Computational Methods 209
IV.11.2. Discussion of Results 209

ANNEX 1 (Compounds Index) 217

ANNEX 2 (Crystallographic Data) 228

Abbreviations 243

Literature 245

Ligands Carbènes *N*-Hétérocycliques (*NHC*) Chiraux et Couplages Croisés Catalysés au Palladium

1. Introduction

Isolables et stables, les premiers carbènes *N*-hétérocycliques (*NHC*) ont été signalés par *Arduengo* en 1991. Leurs propriétés uniques telles que leur caractère fortement σ donneur et faiblement π accepteur les ont conduit à devenir une classe de ligand incontournable en catalyse homogène. Cependant, leur succès en catalyse asymétrique est rare et de nouveaux ligands chiraux *NHC* sont nécessaires.

Mis au point par les groupes de *Herrmann* et *Enders*, les carbènes chiraux, dérivés de la phénéthylamine chiral, sont devenus un type très important de ligands chiraux. Des efforts de recherche se sont concentrés à modifier les groupes aromatiques et l'épine dorsale du ligand *N*-hétérocyclique (Fig.1).

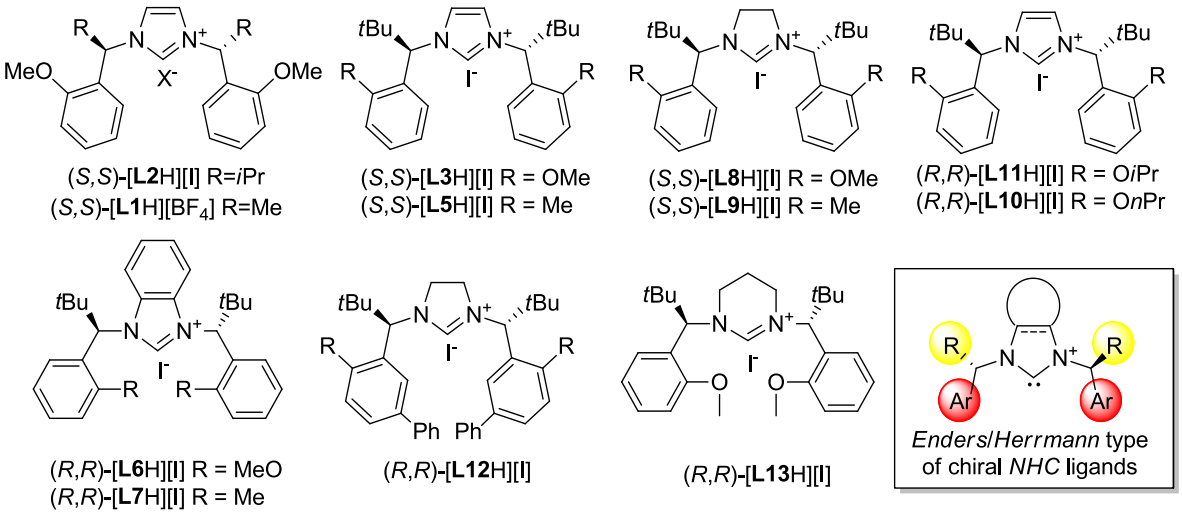

Fig. 1 *NHC* chiraux encombrés développés dans notre laboratoire.

En 2007, le groupe du Prof. *Kündig* a développé de nouveaux *NHC* chiraux encombrés de type *Enders*/*Herrmann* portant des groupes alkyles de tailles différentes sur le centre stéréogénique (Fig. 1). Ces ligands ont trouvé une excellente application en α-arylation asymétrique des amides catalysée au palladium pour accéder à des 3-alkyl-, 3-alcoxy-, 3-amino-3-aryl-oxindoles avec des rendements élevés et des énantiosélectivités excellentes.

2. Résultats

2.1. Synthèse asymétrique des oxindoles via des réactions d'α-arylation intramoléculaire des amides catalysée par des complexes palladium-NHC

Le champ d'application et les limitations de l'*α*-arylation des amides catalysées au palladium ont été étudiés en utilisant les carbènes chiraux développés dans notre groupe. Des oxindoles substitués par différents groupes 3-alkyl-3-aryl et portant des substituant différents sur la partie aniline, ont été préparés avec de très bons rendements et des énantiosélectivités élevées (Schéma 1).

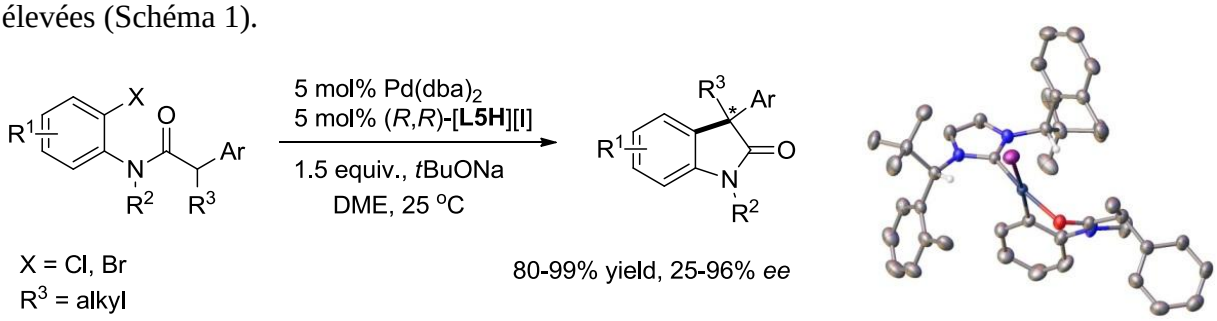

Schéma 1 Synthèse d'oxindole 3,3-disubstitués par arylation des amides catalysée par des complexes Pd-*NHC*.

Les excellentes valeurs d'énantiosélectivité s'expliquent par la présence des groupements *tert*-butyle volumineux sur le centre stéréogénique et des substituants en position ortho des aryles. L'importance des substituants ortho-aryle a été révélée dans les structures cristallines des intermédiaires palladacycle contenant les ligands chiraux *NHC* et le substrat. La position et l'orientation des éléments de «StereoControl» du ligand sont fixées par la minimisation de la contrainte allylique ($A^{1,3}$) produisant un transfert efficace de l'information chirale. Des études mécanistiques de cette transformation ont révélé l'importance des additifs alcènes pour augmenter le TON et le TOF. Des études cinétiques montrent que la réaction est du premier ordre par rapport au substrat. Des études détaillées de DFT ont également été effectuées pour obtenir une meilleure compréhension de cette réaction.

Sur la base de l'analyse aux rayons X des intermédiaires palladacycles portant le ligand **L5** nous avons supposé que la substitution des groupes *ortho*-Me par des cycles aromatiques accolés pourrait amener à des complexes Pd-*NHC*, encore plus performants d'un point de vue de l'induction asymétrique (Fig. 2).

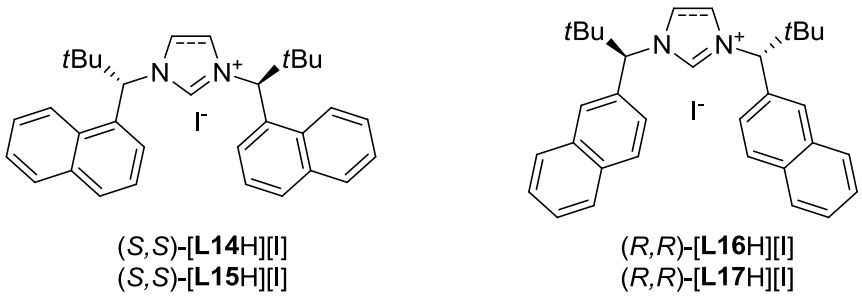

(*S,S*)-[**L14**H][I]
(*S,S*)-[**L15**H][I]

(*R,R*)-[**L16**H][I]
(*R,R*)-[**L17**H][I]

Fig. 2 Nouveaux ligands carbènes *N*-hétérocycliques développés.

Les sels d'imidazolium insaturés ont été synthétisés à partir de l'*α*-alkyl-arylamine ortho-substituée par le procédé décrit par le groupe impliquant dans un premier temps la formation de diimine puis la fermeture de l'hétérocycle, en utilisant du chloromethylpivalate et en présence de AgOTf. Les sels de dihydroimidazolium ont été préparés en suivant la procédure en quatre étapes développée dans l'équipe qui implique la formation de la diimine suivie de sa réduction en diamine correspondante avec du $NaBH_4$. La fermeture du cycle est réalisée dans ce cas en utilisant du triéthylorthoformiate en présence de tétrafluoroborate d'ammonium.

Ces nouveaux ligands carbènes *N*-hétérocycliques ont été utilisés avec succès dans des synthèses d'oxindoles reconnues difficiles comme par exemple la préparation de spiro-aza-et spirooxindoles (Schéma 2).

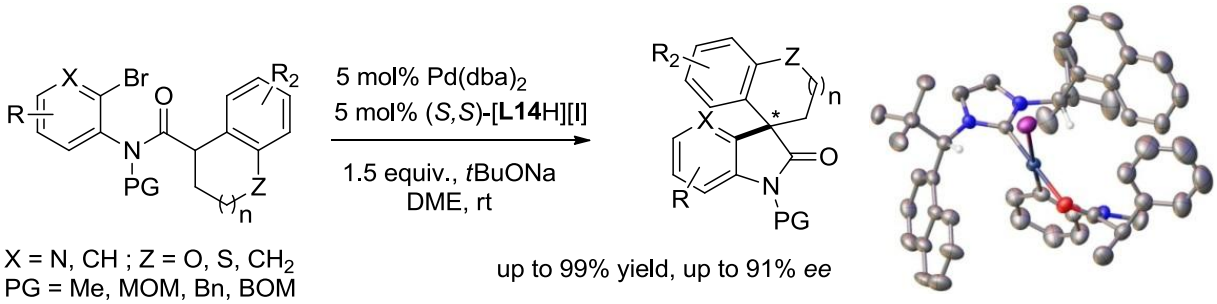

Schéma 2 Synthèse énantiosélective de spiro-aza- et spirooxindoles par Pd-(*NHC*) catalysée par arylation d'amides.

Enfin, nous avons appliqué avec succès cette méthodologie d'*α*-arylation d'amide catalysée à l'aide de complexes Pd-*NHC* à la synthèse totale du composé biologiquement actif hautement énantio-enrichi **51**. La séquence implique 6 étapes avec un rendement global de 45% (Schéma 3). Ces études démontrent que le système [Pd-*NHC*] peut être utilisé dans la

formation de liaison C-C asymétrique à un stade avancé dans la synthèse de structures complexes.

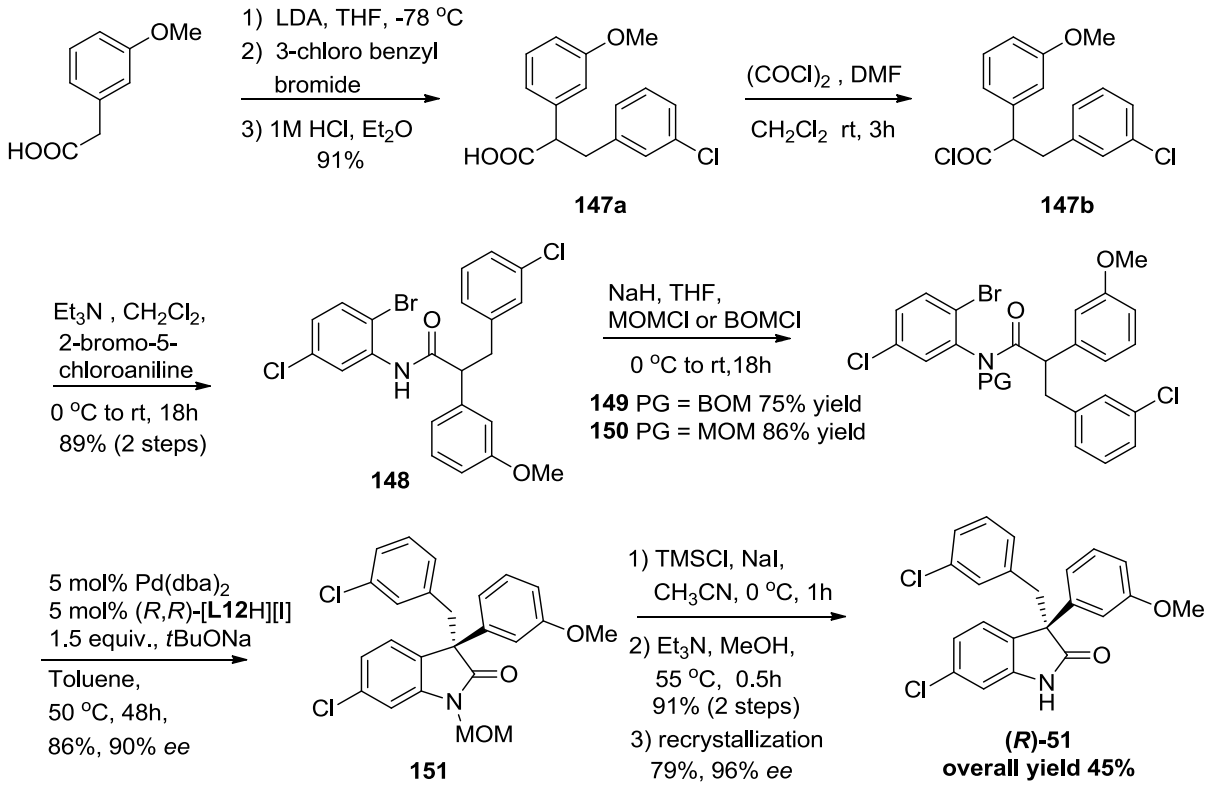

Schéma 3 Synthèse catalytique énantiosélective de la (*R*)-**51**.

2.2. Synthèse asymétrique d'indolines via des réactions de couplage C(sp^3)-H/C(Ar) catalysées par des complexes de palladium-NHC

La formation de liaison C-C catalysée par un métal de transition et suivant une stratégie d'activation C-H a émergé récemment comme une méthode puissante en chimie organique. Dans ce domaine, un défi majeur demeure l'activation sélective de liaisons C (sp^3)-H non activées d'alkyle. En utilisant les ligands *NHC* développés dans le groupe en combinaison avec un précurseur de Pd, nous avons réalisé le couplage énantiosélectif entre un C_{Ar} et un groupe CH_2 pour préparer des indolines de jonction *trans* (Schéma 4). Bien que les températures élevées (140 - 160 °C) soient nécessaires pour cette réaction, une excellente reconnaissance asymétrique d'une liaison C-H énantiotopique d'une unité méthylène non activée est atteinte. Nous avons constaté expérimentalement que la taille du noyau cycloalkyle est d'une importance cruciale dans ce système.

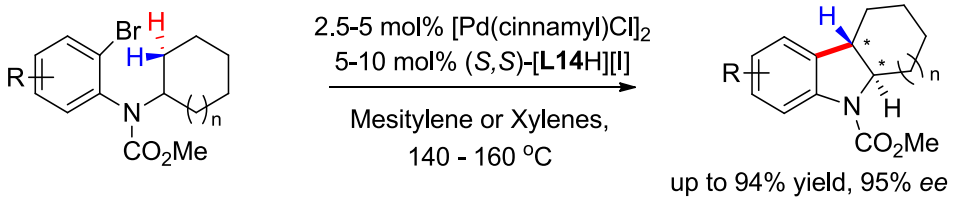

Schéma 4 Enantiosélective Pd-(*NHC*) catalysée par la synthèse des indolines fusionnés.

Ces premiers résultats ont été étendus à la synthèse d'indolines substituées en position 2 et 2,3 (Schéma 5). Dans le cas de substrats comportant des groupes symétriques $NCHR_2$, une très haute induction asymétrique a été obtenue (jusqu'à 97% *ee*). Pour des substrats composés de groupes NCHRR, les catalyseurs Pd-phosphine et Pd-IPr ont montré une nette préférence pour l'activation d'un groupe Me alors que les catalyseurs chiraux Pd-*NHC* conduisent cette transformation vers une réaction régio-divergente du mélange racémique. Dans le cas idéal, lorsqu'il y a la compétition entre l'activation C-H d'un groupe Me et l'activation C-H d'un fragment benzyle, le catalyseur transforme un énantiomère du mélange racémique en une indoline très énantiomériquement enrichie *via* l'activation C_{Me}-H alors que l'autre énantiomère est transformé en une indoline par l'activation $C_{méthylène}$-H hautement asymétrique. A notre connaissance, ce sont les premiers exemples d'une synthèse directe d'indolines *trans* 2,3-disubtituées avec d'excellentes énantiosélectivités et également de réactions regiodivergentes de mélanges racémiques impliquant l'activation CH.

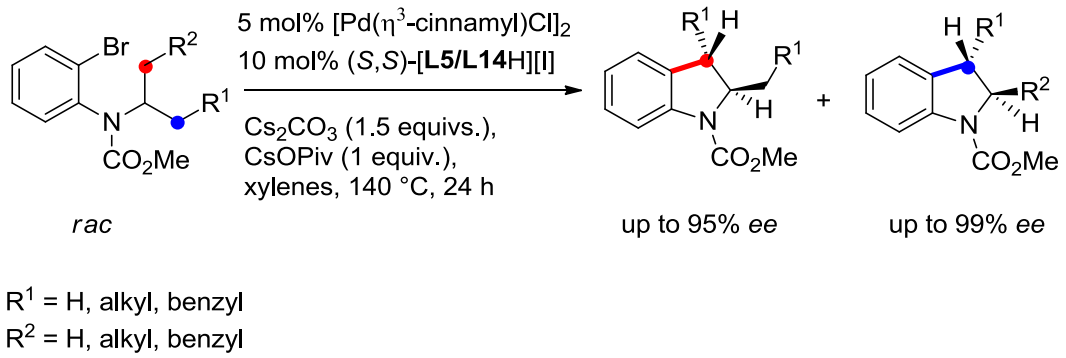

Schéma 5 Indolines hautement énantio-enrichie par réaction régio-divergente d'un mélange racémique.

I. General Introduction

I.1. History of *N*-Heterocyclic Carbenes as Ligands

N-Heterocyclic carbenes (*NHC*s) have become a very important class of molecule, which find use in transition-metal (TM) coordination chemistry and organo-catalysis. The beginning of the story goes back a century when *Chugaev* reacted potassium tetrachloroplatinate with methyl isocyanide, followed by the addition of hydrazine.[1,2] Surprisingly, this reaction did not produce the dimeric species bearing tetracyanide platinum cores linked by hydrazine. The real structure of the formed salt **1** and its biscarbene derivative **2** was solved only 50 years later.[3-6]

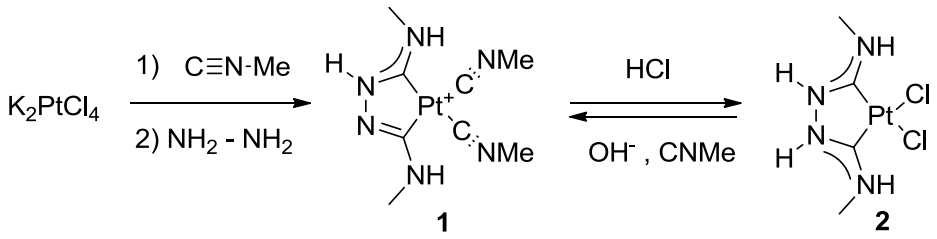

Scheme 1. *Tschugajeff*'s (*Chugaev*) carbene complexes.

The field of coordination chemistry of *NHC*s as ligands for transition metals was pioneered by *Öfele* [7] and *Wanzlick* [8] independently in the early 1960's, through the description of the synthesis and structures of chromium and mercury complexes, respectively, containing *NHC* ligands (Figure 1). A few years later *Lappert* [9,10] extended the coordination chemistry of *NHC*s, of which a good example is the rhodium-carbene complex shown in Figure 1.

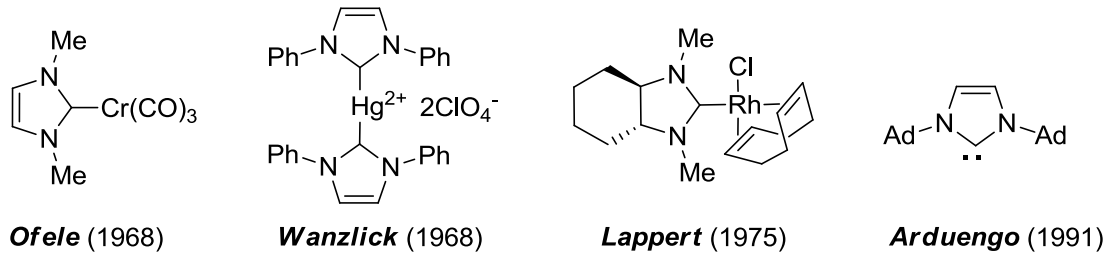

Figure 1. First *NHC*-complexes and the *Arduengo*'s carbene.

Over the next decade little attention was paid to the development of this field until *Arduengo*[11] reported the isolation and characterization of the first free and stable *N*-heterocyclic carbene (Figure 1). The fact that this compound can be isolated led to a rapid broadening of the applications of *NHC*s in synthesis. At the present time, *N*-heterocyclic

carbenes form a class of important compounds and are used as ligands for transition metals and catalysts.

I.2. Structural Diversity of *N*-Heterocyclic Carbene Ligands

A large number of various *NHC*s have been synthesized since *Arduengo*'s discovery.[12-19] Examples of the most common *NHC*s are shown in Figure 2. Over the last decades, *NHC* cores have been modified by changing both substituents at the nitrogen atoms and at the skeleton ring structure.

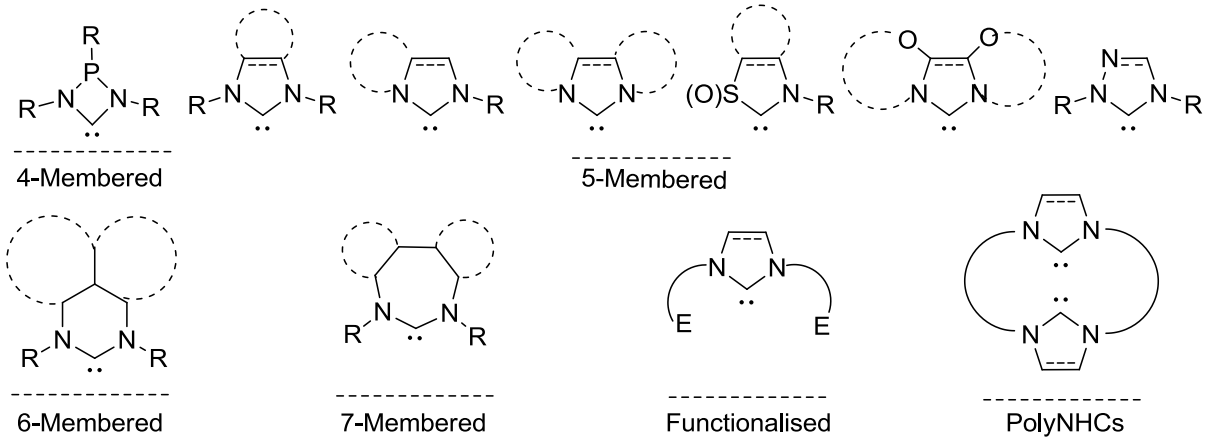

Figure 2. Structural diversity of *NHC* ligands.

However, only *NHC*s derived from imidazolium or 4,5-dihydroimidazolium salts have found wide application in homogeneous catalysis to date. Arguably the most important example is the use of *NHC*s in ruthenium metathesis catalysts developed by *Grubbs* and co-workers. Substitution of one of the two tricyclohexylphosphine ($P(C_6H_{11})_3$) ligands in Grubbs I catalyst with the carbene SIMes led to important improvements, in terms of catalyst activity and stability, which allowed one to extend the substrate scope.[20]

I.3. Electronic Properties of *N*-Heterocyclic Carbene Ligands

Structurally simple *N*-heterocyclic carbene ligands were considered as phosphine mimics but over the last 20 years important differences between phosphine-based and *NHC* ligands were noted. Despite the fact that both ligands are two-electron donors, the sterics and electronic properties of the ligands are quite different.

The electronic properties of the M(Metal)-*NHC* bond can be described as a sum of three components. A simplified diagram, depicted in Figure 3, illustrates the σ—›*d*, *d*—›π^* and π—›*d* bonding modes occurring between *NHCs* and transition metals (TM). So far, the most important bonding contribution to the M-*NHC* bond is the L—›M *σ*-dative bond. *NHC*s

are generally stronger σ-donors than even the most basic phosphines, and they generate very stable complexes.

Another bonding involves the carbene carbon π^*-orbitals, which can accept electron density from filled *d* (HOMO frontier orbital of the metal center) orbitals of the metal *via* the classic *d*—›π^* backbonding pathway (Figure 3). This π backbonding, if existent, is not a strong contributor to the overall bond strength of the M-*NHC* bond.

Finally, for the electron-deficient metals, *NHC*—›M π-donation could arise from the interaction between the filled *NHC* π-orbital of the carbene and empty *d*-orbital of the metal (Figure 3). Recent studies show that *NHC* ligands can accept electron density from metal π^*-orbitals, thus this contribution cannot be completely neglected.[21]

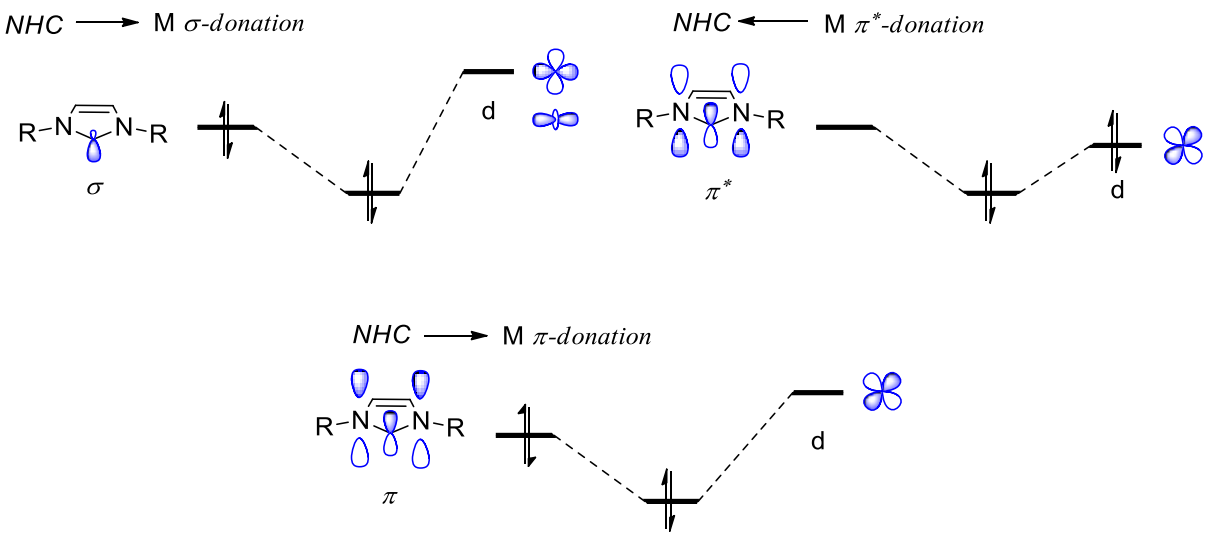

Figure 3. Diagram illustrating the σ—›*d*, *d*—›π^* and π—›*d* bonding modes occurring between *NHCs* and transition metals. The diagram is adapted from reference.[22]

The catalytic ability of transition-metal *NHC* complexes can be dramatically changed upon modification of the steric and electronic properties of the ligand. There are three key parameters in five-membered *NHC*s, which can be modified to tune the properties (Figure 4): (a) *NHC* skeleton (saturated or unsaturated); (b) heterocycle backbone; and (c) *N*-substituents.

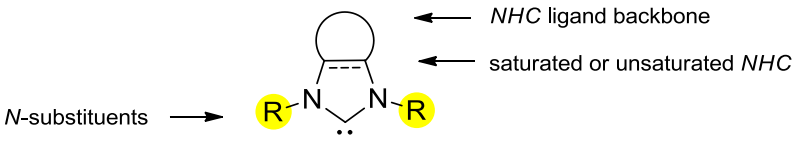

Figure 4. Possible structural modifications, which can change electronic properties of *NHC*s.

Many different methods for the determination of the electronic properties of ligand TM complexes have been used. The *σ*-donor characteristics of the *NHC* ligands can be obtained from their basicity, available from measurements or calculations of the pK_a values of the corresponding azolium salts (pK_a 16-25).[23] Another method relies on calorimetric measurements of the M-*NHC* bond dissociation energies. *Nolan* and co-workers used this methodology for various of Ru-*NHC* complexes.[24] The IR-spectroscopic analysis of the CO-stretching frequencies ν_{av} of $(L)_nM(CO)_n(X)_n$ complexes have emerged as a convenient and simple method to estimate the electronic properties of ligands.[25] With regard to the nature of the *NHC* skeleton (saturated or unsaturated), the *NHC* bond dissociation energy (BDE) in $[Ni(CO)_3(NHC)]$ and $[RuClCp^*(NHC)]$ complexes ($Cp^* = \eta^5$-C_5Me_5) was determined. The measurements showed small variations in values less than 1 kcal/mol.[26,27] Additionally, the spectroscopic analysis of the CO stretching frequency ν_{av} for many $[Ni(CO)_3(NHC)]$ and $[IrCl(CO)_2(NHC)]$ complexes was carried out, which also showed a small variation of ν_{av}, which was often less than 1-3 cm^{-1}.[28,29] These studies led to the conclusion that the nature of the *NHC* skeletons (saturated or unsaturated) does not have a great effect on the electronic properties of the transition-metal complexes. However, experimentally, the saturated and unsaturated *NHC* based transition-metal catalysts show different performances in many transition-metal-*NHC* catalyzed reactions.

The CO-stretching frequency values for $[Ir(CO)_2(Cl)L]$ complexes bearing *NHC* ligands with electronically different substituents in the backbone of heterocycle were determined. These studies showed more significant changes and CO-stretching frequency values varied usually by 6 to 10 cm^{-1} (2020-2035 cm^{-1}). Similar investigations were carried out for the iridium complexes bearing *NHC* ligands with different *N*-substituents. These studies showed that *NHC*s with alkyl *N*-substituents are much better electron donors than those with aryl *N*-substituents. However, differences in the average value of the CO-stretching frequency were still small and less than 6 cm^{-1}.[27]

The comparison between a series *NHC* ligands and some common phosphines are depicted in Figure 5. The ν_{av} of *NHC*s is plotted *vs* the *Tolman* electronic parameter (TEP) together with some tertiary phosphines. The *Tolman* electronic parameter is the carbonyl ν_{CO} IR stretching frequency (the very sharp A_1 high energy mode) in $[Ni(CO)_3L]$ complexes (L = *NHC* or PR_3). The ν_{av} is the average of CO stretching frequencies observed in $[Ir(Cl)(CO)_2L]$ complexes. The diagram demonstrates that lower TEP values correspond to the most typical *NHC* ligands and the latest one is placed in quite a small range of 3-5 cm^{-1}. In contrast,

phosphines are distributed over a larger range of 12 cm^{-1} and generally at higher TEP. We can conclude that *NHC* ligands are very strong σ-donors and the range of electronic properties is very narrow when compared to PR_3 ligands.

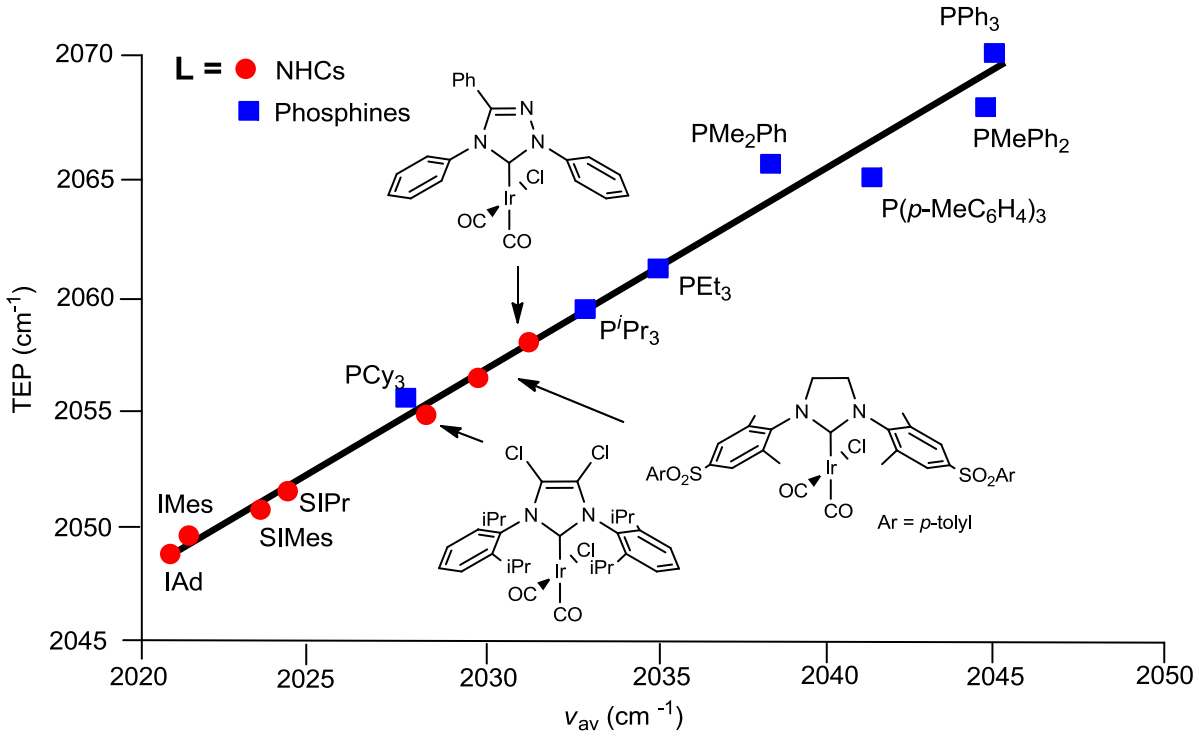

Figure 5. *Tolman* electron parameter (TEP) *vs* average CO stretching frequency (ν_{av}) for *NHC*s and phosphines. The graphic is adopted from reference.[30]

I.4. Steric Properties of *N*-Heterocyclic Carbene Ligands

In transition-metal phosphine complexes, the substituents at the phosphorus atom point away from the metal center, forming a cone-like shape. In contrast, in M-*NHC* complexes, the substituents at the nitrogen atoms of the heterocycle are pointed down, thereby surrounding the metal center (wedge-like shape). Due to the fact, that *NHC* ligands have a C_2 symmetry axis, and phosphines - C_3 symmetry axis, the *Tolman*'s cone[31] angle descriptor for the steric properties of the phosphine ligands cannot be used with *NHCs*.

A number of attempts have been made to measure the steric bulk of *NHC*s, of which *Nolan* and co-workers carried out key investigations in the field. Firstly, they proposed a phosphine-like model for the determination of the steric bulk of *NHC*s based on the crystallographic data of [RuClCp*(*NHC*)] complexes.[24] The two simplified views of an *NHC*-M complex depicted in Figure 6 show the proposed model of *Nolan*, from which two parameters can be calculated: the length parameter A_L and the height parameter A_H. The bond

distance between the metal center and the carbene carbon was considered as the average bond distance and is 2.00 Å. To confirm this model system, two steric parameters were examined *vs* enthalpic relationship, and a good correlation was obtained. However, it was a decisive starting point in attempt to measure the steric parameters of the *NHC* ligands.

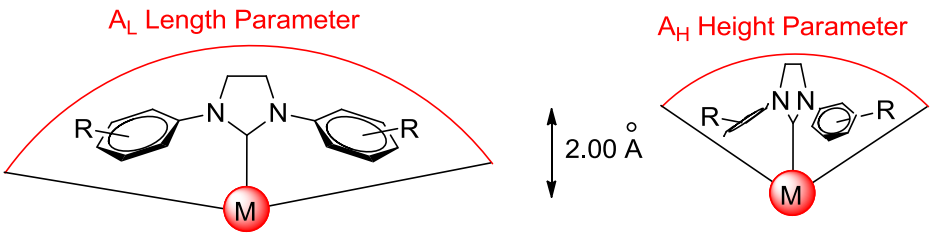

Figure 6. First proposed model by *Nolan* for steric parameter determination of *NHC*s.

In 2003 *Nolan* and *Cavallo* introduced an alternative model system to measure the steric bulk of ligands; ‘‘percent buried volume’’ (%V_{bur}) estimated as a coefficient of the total volume (in percent %) of the coordination sphere occupied by *NHC* ligand around the metal center (Figure 7).[27,32] The free space which is not occupied by the ligand represents a potential coordination space for the substrate in catalytic transformations.

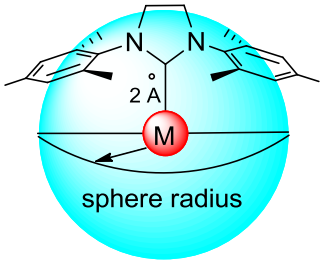

Figure 7. Percent buried volume %V_{bur}.

The percent buried volume can be easily calculated using crystallographic data of *NHC* bearing TM complexes. This model system ‘‘percent buried volume’’ (%V_{bur}) has emerged as a powerful, simple and convenient method to describe the steric properties of *N*-heterocyclic carbene ligands. The percent buried volume (%V_{bur}) has been calculated for many *NHC*-TM complexes including iridium[33], palladium[34], rhodium[35], nickel[28], gold[36] and silver[37] complexes. The data shows, that the percent buried volume (%V_{bur}) for saturated *NHC*s is slightly higher than that for unsaturated analogues. This difference is the consequence of the *NHC* skeleton, where the saturated *NHC* core is slightly distorted compared to the unsaturated analogue, which is planar. To get large value of the percent buried volume one can introduce substituents at C^4 and C^5 atoms of the *NHC* core, which will force the substituents at nitrogen atoms to point closer to the metal center. Such methodology

was applied by *Glorius*[37] in the synthesis of [IBiox(-)-menthyl]·HOTf imidazolium salt, which was used for the formation of silver complex (Figure 8). Presently this ligand is the most sterically demanding C_2-symmetric *NHC*, which has the highest buried volume (%V_{bur}) of ~50%.

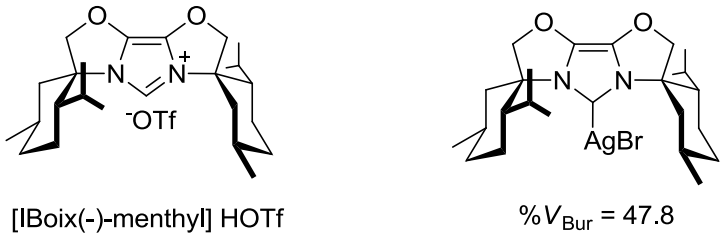

[IBoix(-)-menthyl] HOTf %V_{Bur} = 47.8

Figure 8. The most sterically demanding C_2-symmetric *NHC* ligand developed by *Glorius.*[37]

I.5. Synthesis of *NHC* Precursors

The unsaturated imidazolium salts and saturated 4,5-dihydroimidazolium salts (Figure 9) represent a largest group of stable *N*-heterocyclic carbenes. Due to the fact that our research interest is focused on the C_2-symmetric *NHC* ligands, the following discussion will cover only the synthesis of imidazolium and dihydroimidazolium salts.

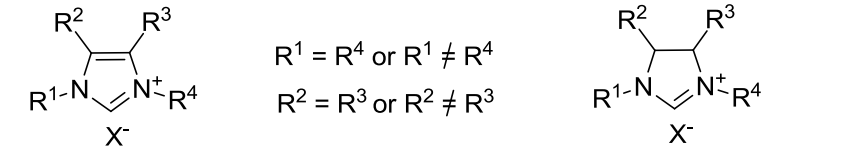

imidazolium salts 4,5-dihydroimidazolium salts

Figure 9. Imidazolium and dihydroimidazolium salts.

I.5.1. Synthesis of Imidazolium Salts

Imidazolium salts can be synthesized by two different methods; 1) substitution reaction at the nitrogen atoms of the imidazole or 2) one-pot or stepwise procedures. The direct substitution at the nitrogen atom can be realized by deprotonation of the nitrogen atom of imidazole, followed by alkylation with an alkyl halide, producing a mono alkylated product. Alternatively, to introduce a first substituent to the imidazole ring, the copper-catalyzed coupling reaction developed by *Buchwald* can be carried out.[38] Using the second equivalent of the alkyl halide, dialkylated product can be generated in moderate to excellent yields (Scheme 2).[39] To introduce different substituents this stepwise alkylation procedure has to be used.[40]

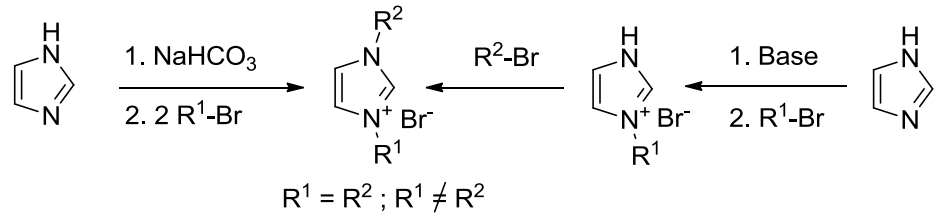

Scheme 2. Synthesis of symmetrical and unsymmetrical *N,N'*-imidazolium salts.

The imidazolium core can be synthesized *via* a multicomponent procedure, where primary amines, glyoxal and formaldehyde react under slightly acidic conditions.[41] This reaction gives access to C_2-symmetric imidazolium salts. Alternatively, symmetrical *N,N'*-substituted imidazolium salts can be synthesized *via* stepwise procedure involving diimine formation, followed by cyclization (Scheme 3).[42,43]

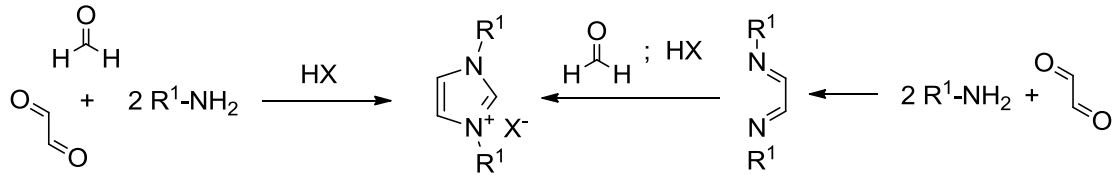

Scheme 3. Synthesis of imidazolium salts by multicomponent or stepwise procedure.

However, the previous methodology failed in the cyclization step during the synthesis of bulky *NHC* ligands, such as bisoxazolines. *Glorius* and co-workers solved this problem by using silver triflate and chloromethyl pivalate and carried out a cyclization of the diimines to the corresponding imidazolium salts in moderate to excellent yields. (Scheme 4).[44]

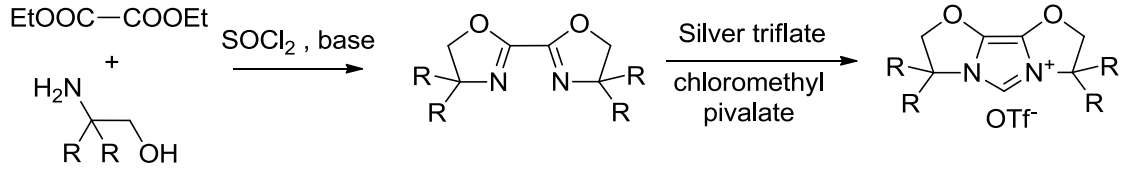

Scheme 4. Synthesis of bisoxazoline derived imidazolium salts.

For the synthesis of the unsymmetrical imidazolium salts, a multicomponent cyclization procedure with a *N*-alkylation step was developed (Scheme 5).[45]

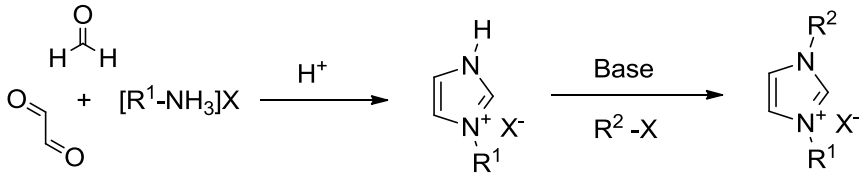

Scheme 5. Synthesis of unsymmetrical imidazolium salts.

In 2008 *Fürstner* and co-workers reported an efficient procedure for the synthesis of unsymmetrical imidazolium salts.[46] The corresponding oxazolium salt, which is easily synthesized from *α*-hydroxyketone or bromoacetaldehyde diethylacetal, was reacted with a primary amine, followed by elimination of water under acidic conditions. This allowed one to obtain the desired salts in moderate to excellent yields (Scheme 6). Moreover, this convenient, scalable and flexible methodology permited the synthesis of the unsymmetrical imidazolium salts bearing substituents at C^4 and C^5 atoms of *NHC* core.

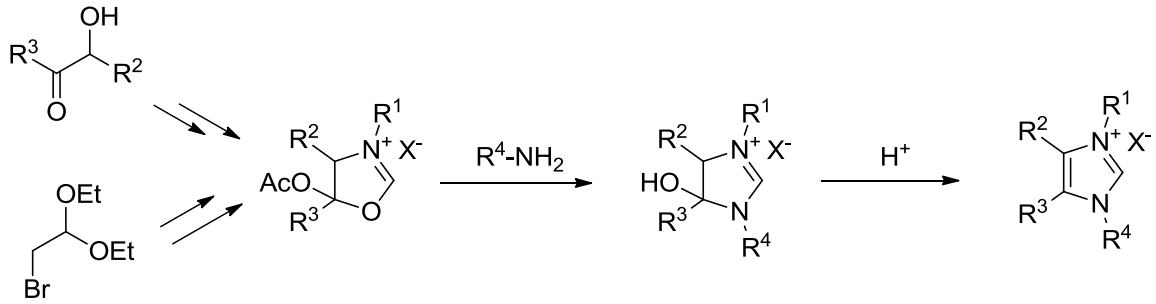

Scheme 6. Unsymmetrical *N,N'*-disubstituted imidazolium salts prepared *via* the method developed by *Fürstner*.

I.5.2. Synthesis of 4,5-Dihydroimidazolium Salts

Diimines can be easily reduced to the corresponding 1,2-diamines, which serve as starting materials for the synthesis of dihydroimidazolium salts. The ring closing of 1,2-diamines in the presence of ammonium tetrafluoroborate and triethylorthoformate lead to products in high chemical yields.[47] This procedure allows one to construct the dihydroimidazolium core bearing alkyl, as well as aryl, substituents at the nitrogen atoms (Scheme 7).

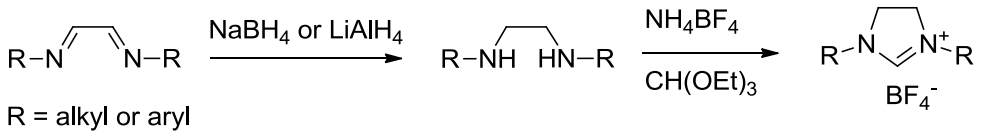

Scheme 7. Synthesis of dihydroimidazolium salts *via* cyclization of 1,2-diamines.

Orru and co-workers developed an interesting procedure for the preparation of the unsymmetrical dihydroimidazolium salts containing substituents at the C^4 and C^5 atoms of the heterocycle.[48-50] The one-pot procedure involves the reaction between an aldehyde or ketone, primary amine and isocyanide. All imidazolidines were easily transformed to the corresponding 4,5-dihydroimidazolium salts *via* established procedures (Scheme 8).

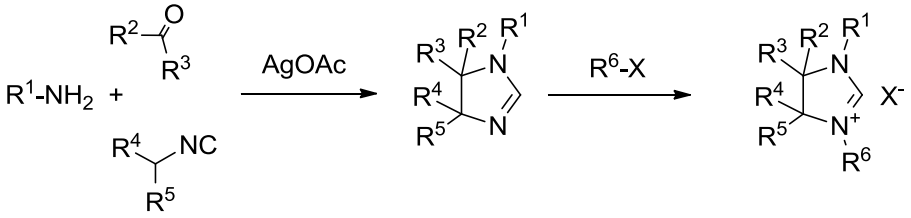

Scheme 8. Synthesis of unsymmetrically substituted imidazolidinium salts.

I.6. *NHC* Ligands in Asymmetric Transition-Metal Catalyzed Reactions

Over the past few decades, a large number of transition metal *NHC* complexes have emerged and successfully been used in many organometallic transformations, including C-C and C-heteroatom bond forming reactions as well as metathesis reactions. The development of chiral *NHC*s is a logical extension in this field.

Chiral *NHC*-ligands and their metal complexes were first reported by *Enders*[51] and *Herrmann*[41] independently in the mid 90s (Figure 10). The complexes were fully characterized and X-ray crystal structures were obtained. Since that time a number of transition-metal complexes bearing chiral *N*-heterocyclic carbene ligands were prepared and utilized in asymmetric catalysis.

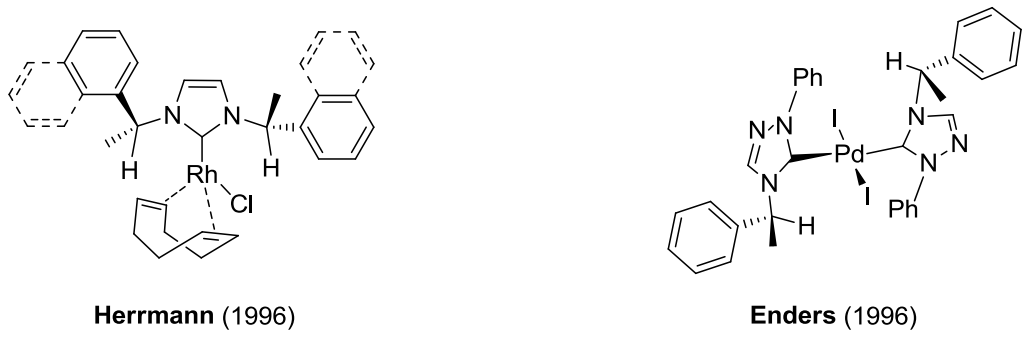

Figure 10. First chiral *NHC*-TM complexes synthesized by *Herrmann* and *Enders*.

Over the last decade considerable progress in the field of asymmetric catalysis based on chiral *NHC*s was observed, but the use of chiral *NHC*s in efficient asymmetric transformations is still limited.[52] Here, we would like to give a short review on the development and the most successful applications of monodentate chiral *NHC* ligands derived from imidazolium or 4,5-dihydroimidazolium salts in the transition-metal-catalyzed transformations dependent on the type of chiral *NHC*. From the methods to introduce the chiral units, chiral *NHC*s can be classified in 7 main groups:

I.6.1. Chiral Units Located in the Alkyl Side Chains

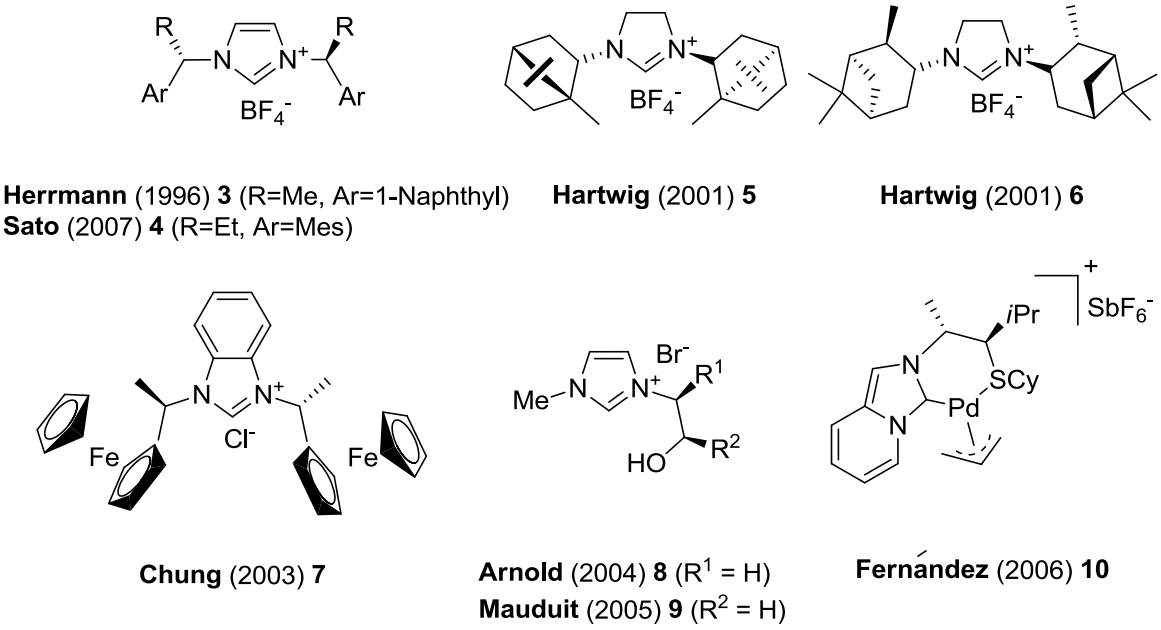

Figure 11. Examples of *NHC* ligands with chiral unites located in the alkyl side chains.

The pioneering work in the development of chiral *N*-heterocyclic carbene ligands was based on the introduction of chiral units in alkyl side chains of the heterocycle. *Herrmann* and *Enders* successfully used this methodology in the synthesis of the first chiral *NHC* ligand **3**[41,51] starting from a chiral arylalkylamine. The complex of the chiral ligand **3** with rhodium was an active catalyst in the asymmetric hydrosilylation of acetophenone, but the enantioselectivity of this transformation was low (Scheme 9).[41]

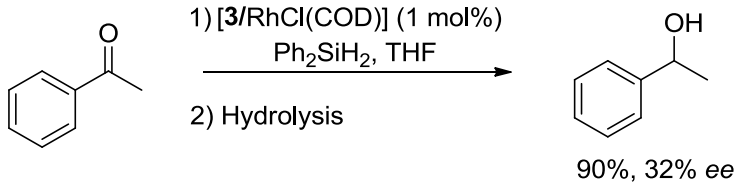

Scheme 9. Asymmetric hydrosilylation using the first chiral *N*-heterocyclic carbene ligands.

The *Alexakis* group expanded the series of chiral arylalkylamine derived *NHC* ligands by using different chiral primary amines. In a systematic optimization of both the ligand substitutions and reaction conditions, ligand **3** showed the best results in terms of the yield (95%) and enantioselectivity (93%) in the Cu(*NHC*)-catalyzed enantioselective 1,4-conjugate addition to cycloheptenone (Scheme 10).[53-55]

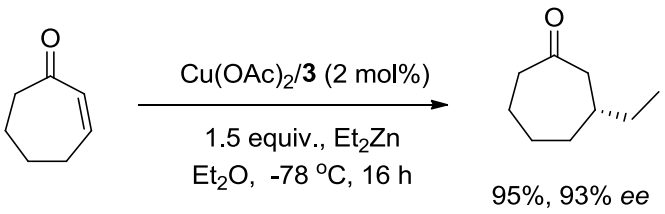

Scheme 10. Enantioselective Cu(*NHC*)-catalyzed conjugate addition of diethylzinc to cyclohept-2-enone.

In 2011, *Glorius* disclosed that the ruthenium complex of the saturated imidazolium salt of **3** is an efficient catalyst for the hydrogenation of quinoxalines[56] (Scheme 11a), benzofurans[57] and benzothiophenes[58] (Scheme 11b), delivering the corresponding products in high regio- and enantioselectivities.

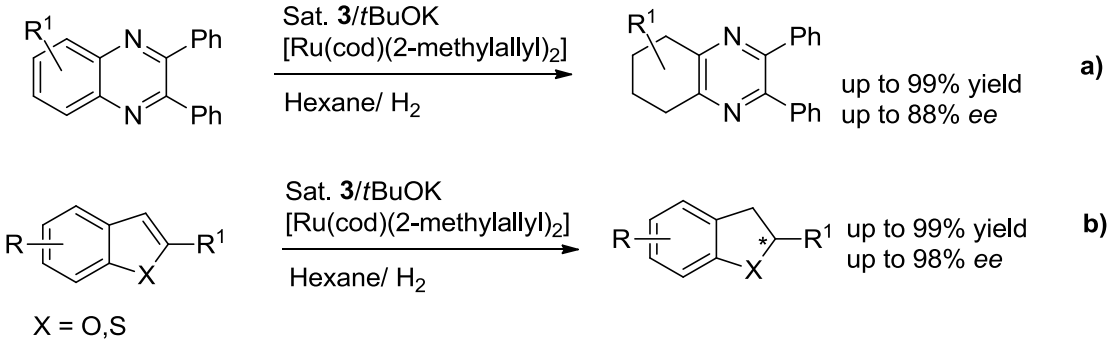

Scheme 11. Asymmetric hydrogenation of quinoxalines **a**) and benzofurans **b**).

Sato developed a Ni(*NHC*)-catalyzed asymmetric three-component coupling of aldehydes with 1,3-diennes and silanes, where the imidazolium salt **4**[59] has 1-(2,4,6-trimethylphenylpropyl) groups on the nitrogen atoms of the heterocycle. This transformation gave product in quantitative yield and excellent (97% *ee*) asymmetric induction (Scheme 12). However, high catalyst loading and reaction times are required for full conversion.

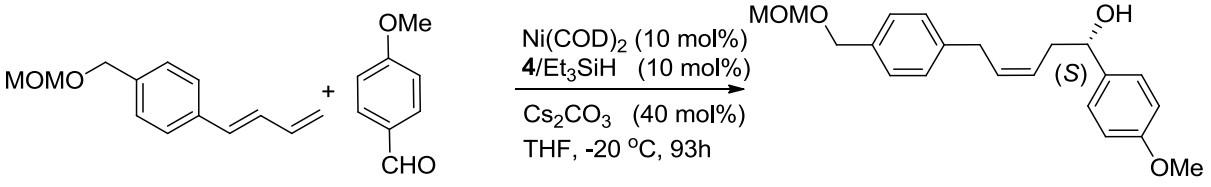

Scheme 12. Asymmetric Ni(*NHC*)-catalyzed three-component coupling reaction.

In 2001, the *Hartwig* group reported the synthesis of chiral ligands **5** and **6**[60] and their application in the asymmetric Pd-catalyzed α-arylation of amides, where moderate enantioselectivities were obtained (Scheme 13).

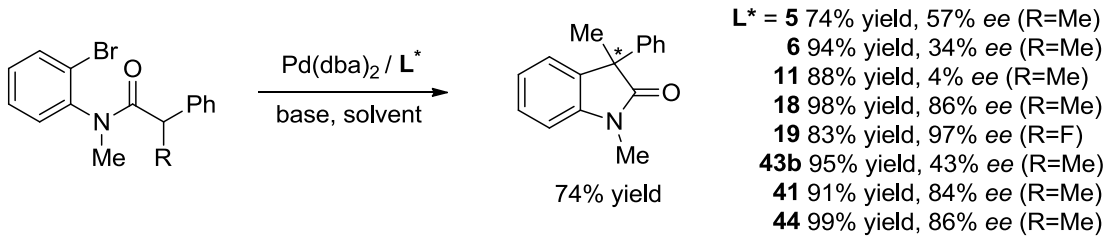

Scheme 13. Asymmetric Pd(*NHC*)-catalyzed α-arylation of amides.

New chiral *NHC* ligand **7**[61], bearing a planar chiral ferrocenyl motif, developed by *Chung* was applied in the Rh(I) and Ir(I)-catalyzed asymmetric transfer hydrogenation reaction. The new complexes displayed excellent activity, but low stereoselectivity for this transformation with a best *ee* of 53% (Scheme 14).

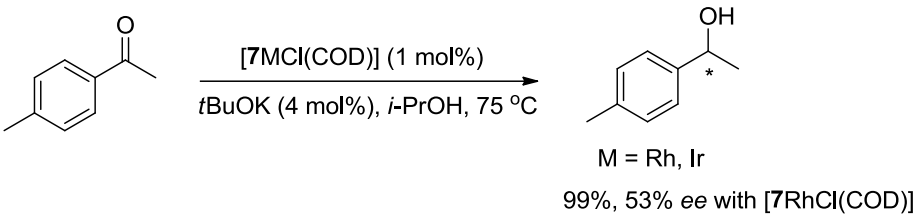

Scheme 14. Rh(I)- and Ir(I)-(*NHC*)-catalyzed asymmetric transfer hydrogenation reaction.

In 2004 *Arnold* and co-workers developed the synthesis of a range of bidentate, alkoxide-*N*-heterocyclic carbene ligands **8**[62]. Their copper complexes were catalytically active, giving in some cases enantioselectivity of 51% for the 1,4-conjugate additions to cyclohexenone. A year later *Mauduit* modified ligands **8** and placed the central chirality at the carbon attached to the nitrogen atom of the heterocycle to form ligand **9**[63], thereby the enantioselectivity of the copper-catalyzed 1,4-conjugate addition to the cyclohexenone improved up to 93% *ee*.

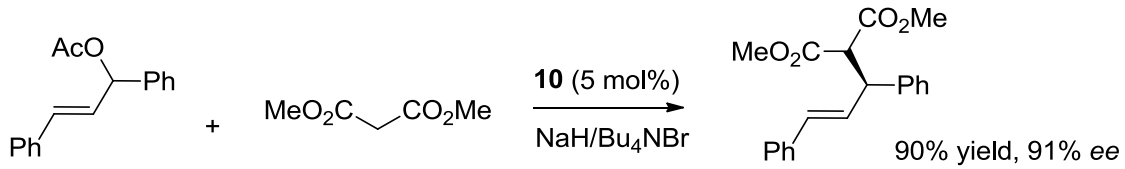

Scheme 15. Pd(*NHC*)-catalyzed asymmetric substitution of 1,3-diphenylpropenyl acetate with dimethyl malonate.

The *Fernández* group reported a new family of sulphur derived *NHC*-Pd cationic complexes and investigated their catalytic activity in the asymmetric allylic substitution of 1,3-diphenylpropenyl acetate with dimethyl malonate. After systematic optimization of the

reaction conditions, complex **10** was found to be the most active in this transformation producing the product in high yield and enantioselectivity (Scheme 15).

I.6.2. Chiral Backbone in the Heterocycle

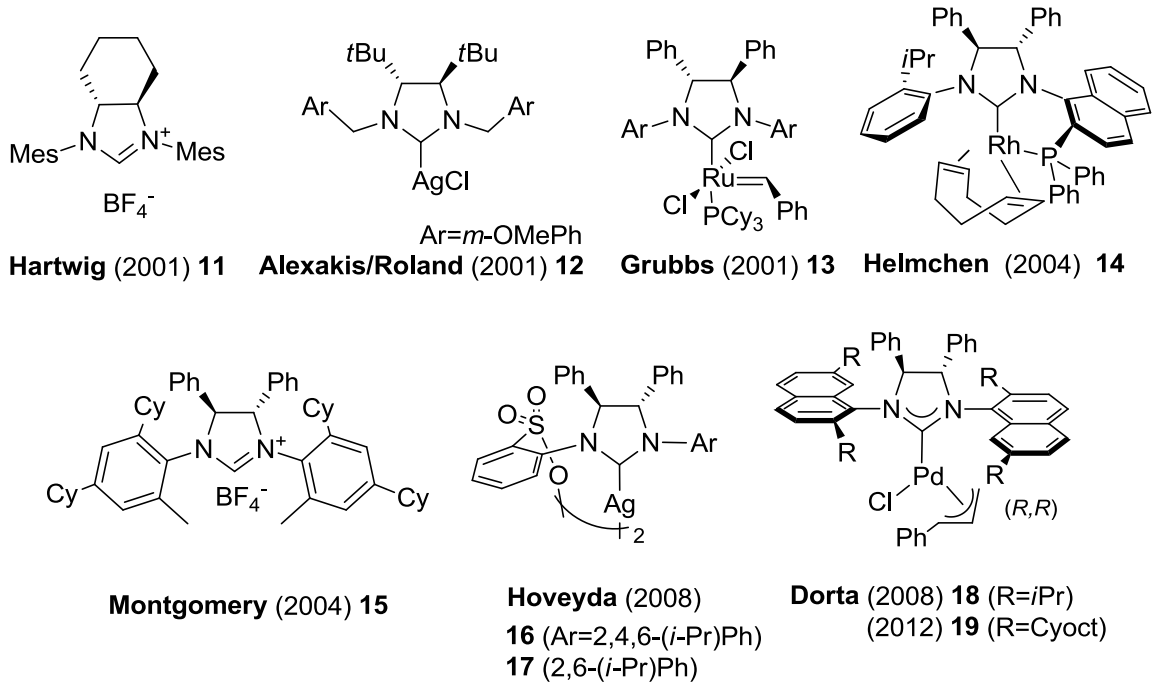

Hartwig (2001) **11** **Alexakis/Roland** (2001) **12** **Grubbs** (2001) **13** **Helmchen** (2004) **14**

Montgomery (2004) **15**

Hoveyda (2008)
16 (Ar=2,4,6-(*i*-Pr)Ph)
17 (2,6-(*i*-Pr)Ph)

Dorta (2008) **18** (R=*i*Pr)
(2012) **19** (R=Cyoct)

Figure 12. Examples of *N*-heterocycle carbene ligands with chiral backbone.

The second strategy to create chiral *NHC* ligands is to introduce chiral elements in the backbone of an imidazoline. Firstly chiral *N*-heterocycle carbene ligand containing *trans*-diaminocyclohexane backbone **11**[60] was prepared by *Hartwig* (Figure 12) and tested in the palladium-catalyzed asymmetric *α*-arylation of amides. Unfortunately, ligand **11** provided poor enantioselectivity in this transformation (Scheme 13).

Alexakis, *Mangeney* [53-55] and *Roland* [64] developed a new family of diaminocarbene ligands with chirality at the backbone of the heterocycle (Figure 12). These new *N*-heterocyclic carbene ligands were very efficient in the asymmetric copper-catalyzed 1,4-conjugate addition of diethylzinc to enones. For the cyclohept-2-enone substrate, the enantiomeric excess can reach up to 88% by using Ag(*NHC*)-complex **12**.

In 2001 *Grubbs* prepared the first enantioselective *NHC*-ruthenium olefin methathesis catalyst **13**[65]. High enantioselectivity (up to 90% *ee*) was obtained in the desymmetrization reaction of achiral trienes. It was found that catalyst **13b** was more efficient than **13a** in terms of the asymmetric induction; moreover, variation of the size of the substituent at the *ortho*-

position of the phenyl group in **13b** led to an improvement of the enantioselectivity of this transformation (Scheme 16).

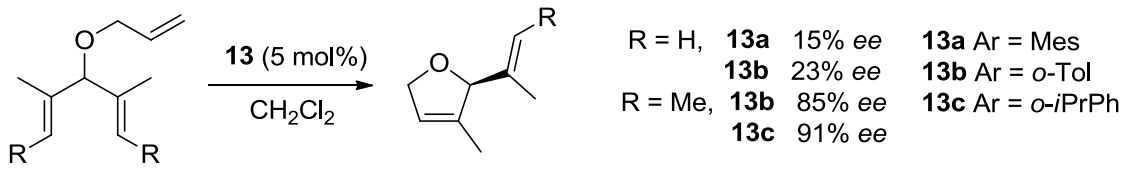

Scheme 16. Enantioselective desymmetrization reaction of trienes using catalyst **13**.

Helmchen and co-workers developed the synthesis of novel chiral diphenylphosphino-functionalized *NHC* ligands, in which its rhodium (I) complex **14**[66] exhibited excellent catalytic activity and asymmetric induction in the hydrogenation of *α,β*-unsaturated esters (Scheme 17).

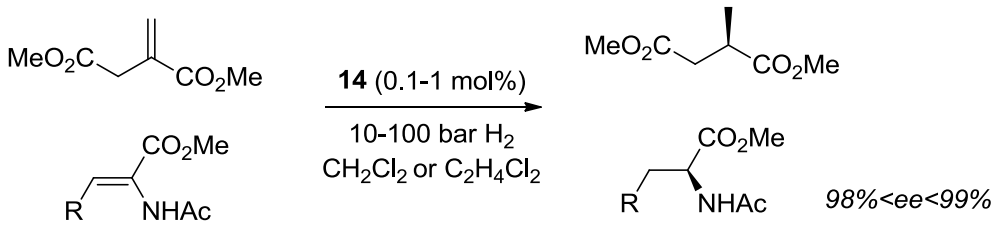

Scheme 17. Asymmetric hydrogenation using chiral Rh(*NHC*)-complex **14**.

In 2007 the research group of *Montgomery* reported the synthesis of ligand **15**, containing chiral units in the backbone of the imidazolinium salt. They also tested this ligand in the asymmetric Ni-catalyzed reductive coupling of alkynes and aldehydes and the corresponding products were generated with *ee* up to 85%. (Scheme 18).[67-69]

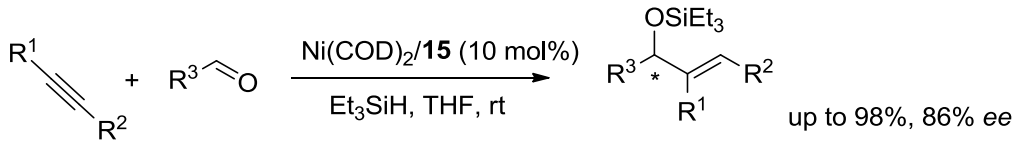

Scheme 18. Ni(*NHC*)-catalyzed aldehyde/alkyne reductive coupling reaction.

Recently, *Hoveyda* published the synthesis and application of the chiral Ag(*NHC*)-complexes **16** and **17**[70,71] in Cu-catalyzed asymmetric allylic alkylations with vinylaluminum reagents. Excellent asymmetric induction up to 98% *ee* was obtained in the presence of $CuCl_2$/**16** or $CuCl_2$/**17** catalysts using trisubstituted vinylaluminum reagents (Scheme 19). Additionally, the *authors* found excellent application of complexes **16** and **17** in highly

enantioselective Ni-catalyzed hydroalumination of aryl- and alkyl-substituted terminal alkynes.[72]

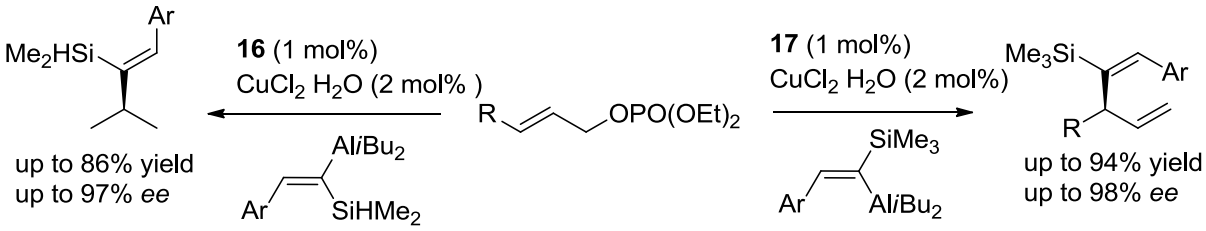

Scheme 19. Cu(*NHC*)-catalyzed asymmetric allylic alkylation (AAA).

Dorta developed a preparation of a novel family of bulky *NHC* ligands containing two *N*-naphthyl groups that can prevent rotation of the *N*-substituents around C-N bonds. The complexes of the ligands with $[Pd(allyl)Cl]_2$ were formed as mixtures, each of them consisingt of three diastereomers. The isomers can be easily separated. The complexes were tested in the Pd-catalyzed α-arylation of amides, where diastereomer **18**[73,74] showed the most successful results (Scheme 13). Modification of the *N*-alkyl side chains to form **19**[75] allowed one to extend the scope of the enantioselective synthesis of 3-fluoro-3-aryl oxindoles (Scheme 13).

I.6.3. Axially Chiral NHC Ligands

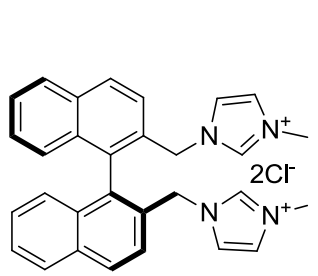

Rajanbabu (2000) **20**

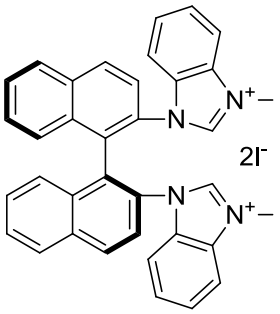

Shi (2003) **21**

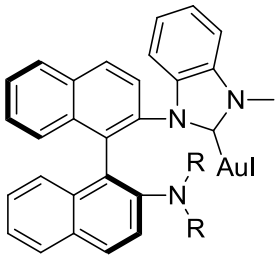

Shi (2011) **22**

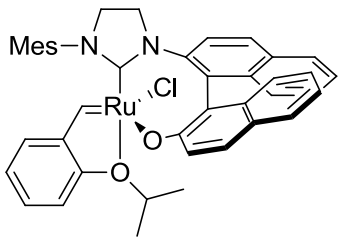

Hoveyda (2000) **23** (R = H)
(2002) **24** (R = Ph)

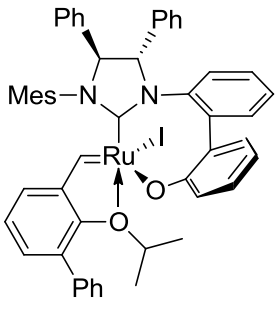

Hoveyda (2005) **25**

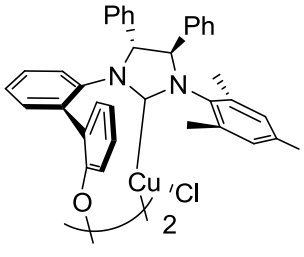

Hoveyda (2005) **26**

Figure 13. *N*-heterocyclic carbene ligands containing elements of axial chirality.

In 2000, *Rajanbabu* reported the first example of axially chiral *NHC* ligand **20**[76] containing the chiral 1,1'-binaphthyl unit, but without any application in catalysis (Figure 13). In this ligand two imidazolium rings are linked to the binapthyl backbone through the methylene bridges. Later, *Shi* developed a new axially chiral *NHC* ligand **21**[77] which was synthesized according to the same strategy as *Rajanbabu*. Ligand **21** is more structurally rigid than **20** due to the fact that imidazolium rings are placed directly at the binapthyl backbone. Novel ligand **21** was applied in the rhodium-catalyzed hydrosilylation of ketones, where excellent *ee* values (92-98%) were obtained. Later, *Shi* and *Zhang* used the palladium complex of ligand **21** as catalyst in the asymmetric conjugate addition of various arylboronic acids to cyclic enones[78] and 2,3-dihydro-4-pyridones[79], delivering products in quantitative yields and excellent enantioselectivities (Scheme 20).

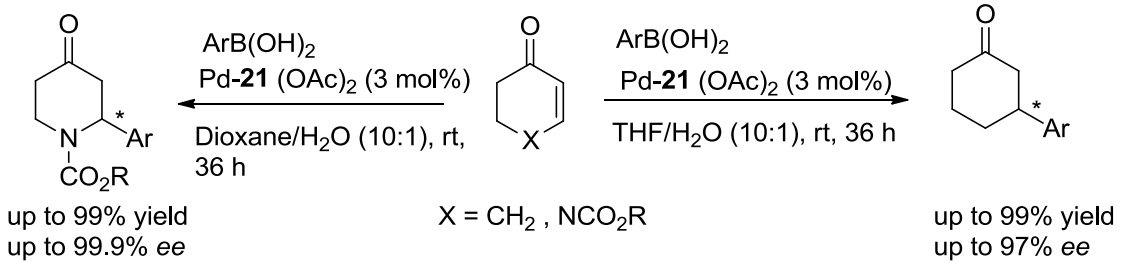

Scheme 20. Pd(*NHC*)-catalyzed asymmetric conjugate addition of arylboronic acids to cyclic enones.

Based on ligand **21** *Shi* and *Zhang* prepared C_2-symmetric cationic *NHC*-Pd(II) diaquo complex, which were applied as catalyst in enantioselective arylation of various *N*-tosylimines with arylboronic acid. Using complex $[(\mathbf{21})_2Pd(H_2O)_2](OTf)_2$ high yields (up to 99%) and enantioselectivities (up to 90%) of the corresponding adducts were obtained (Scheme 21).[80-82]

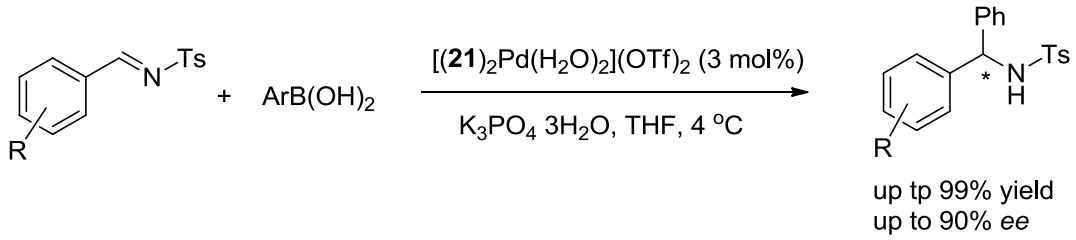

Scheme 21. Pd(*NHC*)-catalyzed asymmetric arylation of *N*-tosylimines with arylboronic acids.

In 2011, *Shi* developed a synthesis of new C_1-symmetric axially chiral *NHC*-Au(I) complexes of the type of **22**[83] bearing binaphtyl or biphenyl framework. The *authors* modified

ligand **21** by replacing one of the two carbene skeleton to amino derivatives, thereby making the ligands less sterically hindered. The Au(I) complexes of **22** were tested in asymmetric cyclizations of 1,6-enynes or allenes. For example, the gold(I)-complex of **22** bearing a pyrrolin-1-yl group delivered product in high 99% chemical yield but only in 58% *ee* (Scheme 22).

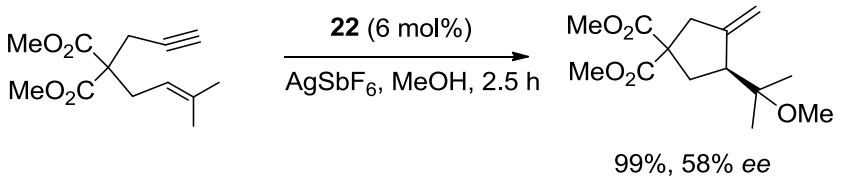

Scheme 22. Asymmetric Au(*NHC*)-catalyzed cyclization of enynes.

In 2002 *Hoveyda* and co-workers developed the synthesis of the ruthenium complex **24**[84,85] bearing a *NHC* ligand with axial chirality. This complex was an efficient catalyst in asymmetric ring-opening/cross metathesis (ROCM) reactions. Moderate to excellent *ee* values were obtained in these transformations (Scheme 23). Later, in 2005, *Hoveyda* developed a new bidentate *NHC* ligand based on optically pure 1,2-dephenylethyendiamine. The ruthenium catalyst of **25**[86] showed similar activity and selectivity to the first-generation Ru(*NHC*) catalysts **23** and **24** in ROCM reactions. The advantage of ruthenium-catalysts **23**-**25** is their ability to promote the AROM/CM reactions under an air. In 2012, *Hoveyda* and co-workers extended the application of *NHC*-based ruthenium complexes in catalysis. The ROCM reaction of oxabicyclic alkenes and enol ethers and a phenyl vinyl sulphide, performed in the presence of only 0.5-5.0 mol% of catalyst **24**, went exclusively with *Z*-selectivities (up to 98% Z) and excellent enantioselectivities (>96% *ee*). Also, in 2012, the *authors* described the application of Cu(*NHC*)-derived complex **26**[87], which worked as an efficient catalyst in allylic alkylation reactions delivering the corresponding addition products in high chemical yields and enantioselectivities (Scheme 24).

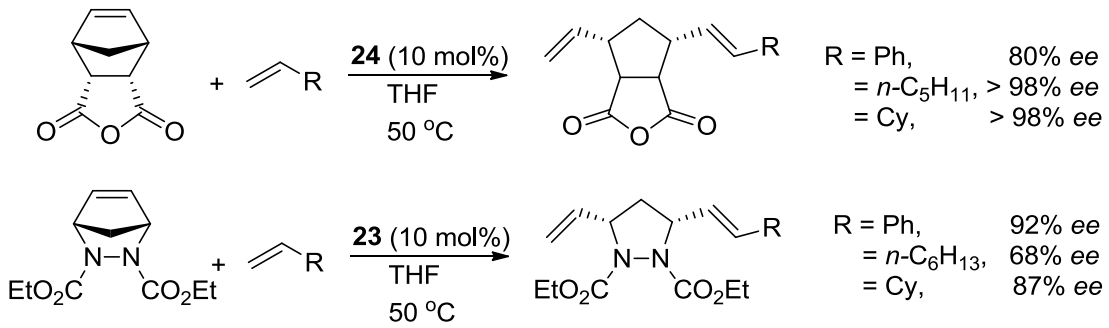

Scheme 23. Application of the chiral Ru(*NHC*) catalysts in catalytic asymmetric ring-opening/cross metathesis.

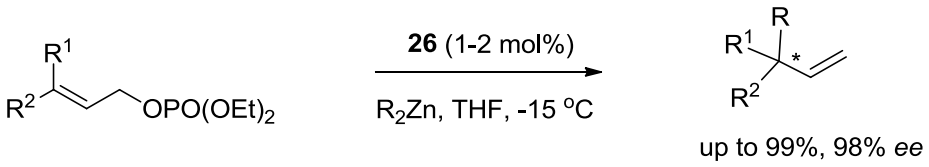

Scheme 24. Enantioselective Cu(*NHC*)-catalyzed allylic alkylation.

I.6.4. Planar Chiral NHC Ligands

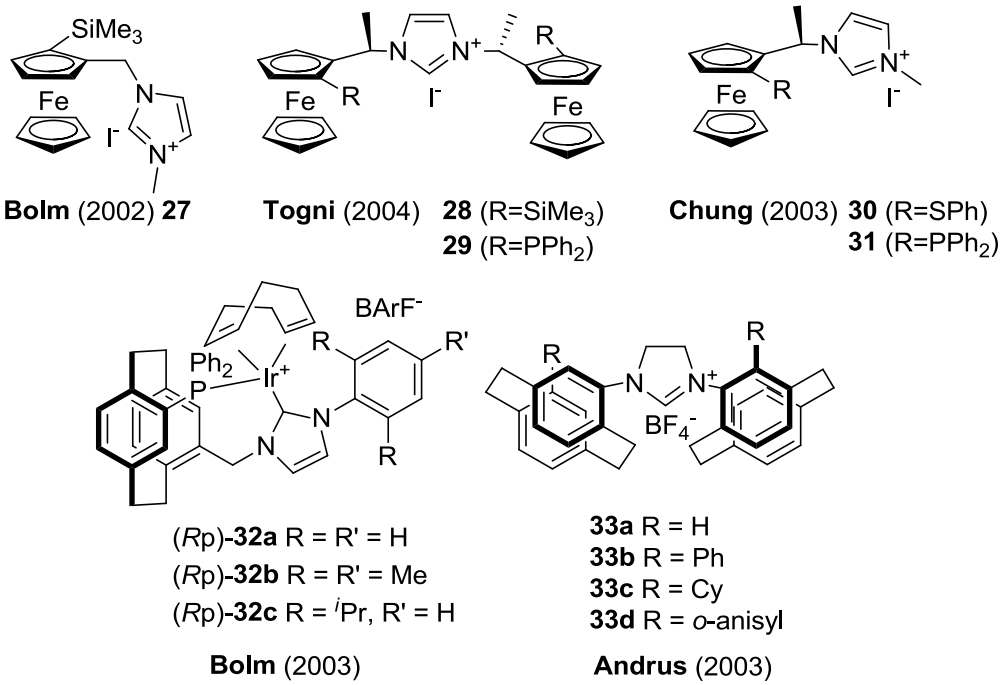

Figure 14. Examples of planar chiral *NHC* ligands.

In 2002, *Bolm* and co-workers reported the synthesis of the first planar chiral *NHC* ligand **27**[88] bearing a ferrocene backbone. Moreover, the chromium and rhodium complexes of **27** were prepared and fully characterized including X-ray analysis. The rhodium complex was tested in the hydrosilylation of ketones, however, only racemic mixtures of the secondary alcohols were obtained. So far, there are no other applications of ligand **27** in asymmetric catalysis.

After the first publication by *Bolm*'s group, *Togni* and *Chung* developed the synthesis of new ferrocene derived *NHC* ligands **28-31**. In the synthesis of C_2-symmetric ligand **28** and **29**[89,90] *Togni* used *Ugi*'s chiral 1-ferrocenylethylamine as a starting material. The same strategy was used by *Chung* in the synthesis of C_1-symmetric chiral ligands **30** and **31**[91], but the second ligated unit was either a diphenylphoshino- **31** or phenylsulfuro- **30** group (Figure 30). Dimeric Rh-**31** and Ir-**30** complexes were found to be inactive in the asymmetric

hydrogenation reaction of dimethylitaconate (Scheme 17). However, the monomeric [Rh(COD)-**30**]BF_4 complex catalyzed this reaction, producing hydrogenated product in moderate yield (44%) and low enantioselectivity (18% *ee*). Tridentate complex Pd-**29**[92], developed by *Togni*, showed high catalytic activity and modest enantioselectivity (up to 75%) in hydroamination reactions (Scheme 25).

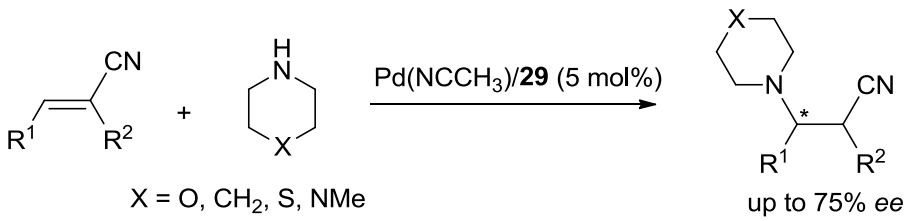

Scheme 25. Pd(*NHC*)-catalyzed asymmetric hydroamination.

In 2003 *Bolm* developed the synthesis of a large family of phosphine iridium-complexes **32**[93,94] containing planar chiral [2,2]paracyclophane skeletons. Their catalytic activity was investigated in the enantioselective hydrogenation of the trisubstituted alkenes, where complex **32a** was found to be the most active catalyst that generates products in high enantioselectivity (up to 82% *ee*).

Major progress was achieved by the group of *Andrus* who developed a new class of *NHC* ligands **33**[95,96], where two planar chiral [2,2]paracyclophane scaffolds are directly linked to the nitrogen atoms of the heterocycle. They were successfully applied to the rhodium complexes in asymmetric conjugate additions of arylboronic acids or potassium aryltrifluoroborates to cyclic or acyclic enones and aldehydes. In the reaction between phenylboronic acid and cyclohexenone both high yield (96% with **33d**) and enantioselectivity (98% *ee* with **33d**) of the product were obtained.

I.6.5. Trans-Cyclodiamine Derived Chiral NHC Ligands

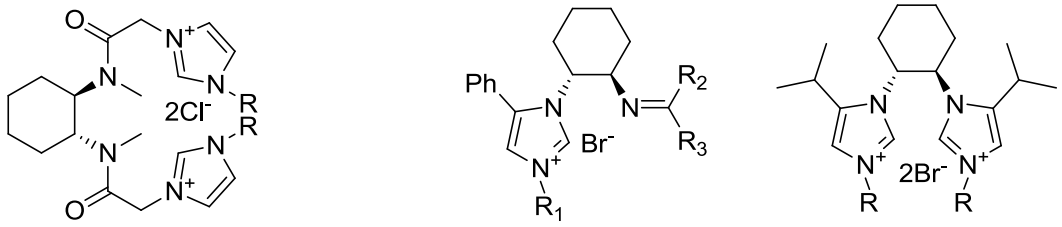

Burgess (2002) **34** **35** **Douthwaite** (2003) **36**

Figure 15. Examples of *trans*-cyclodiamine derived chiral *NHC* ligands.

Enantiomerically pure *trans*-1,2-diaminocyclohexane was extensively used as a building block in the design of many chiral ligands for transition-metal catalyzed reactions.[97,98] The first examples of chiral *NHC* ligands containing *trans*-cyclodiamine cores **34**[99] were introduced by *Burgess* in 2002 (Figure 15). The iridium complex of **34** was found to be a highly active catalyst for the hydrogenation of trisubstituted alkenes (*E*-aryl alkenes) delivering products in excellent enantioselectivities (up to 98% *ee*).

Douthwaite developed carbene-imine ligands **35**[100] which were tested in the palladium-catalyzed asymmetric alkylation reaction, of which the best result are shown in Scheme 26. Later, the *authors* also synthesized bidentate *NHC* ligands **36**;[101] however its palladium complexes showed poor selectivity (11% *ee*) in allylic alkylation reactions.

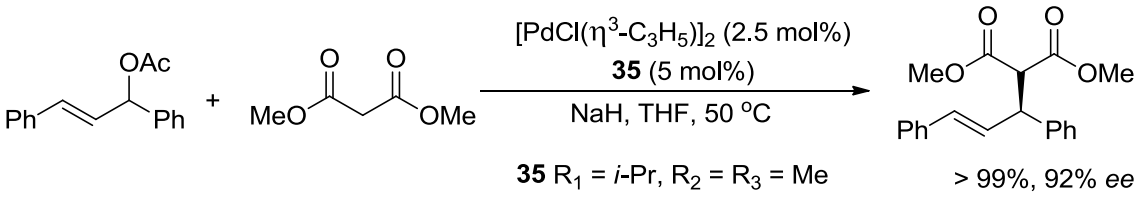

Scheme 26. Pd(*NHC*)-catalyzed enantioselective allylic alkylation.

So far, only a few *NHC* ligands were developed, which work efficiently in asymmetric catalysis. The ligands are based on enantiomerically pure *trans*-1,2-diaminocyclohexane. There is still much room for improvements of these types of *NHC* ligands. Possibly, the introduction of more sterically demanding substituents at C^4 and C^5 position of *NHC* the backbone would exclude free rotation around the carbon-nitrogen bonds. This strategy could help to increase the asymmetric induction of such ligand-metal systems.

I.6.6. Oxazoline Based Chiral NHC Ligands

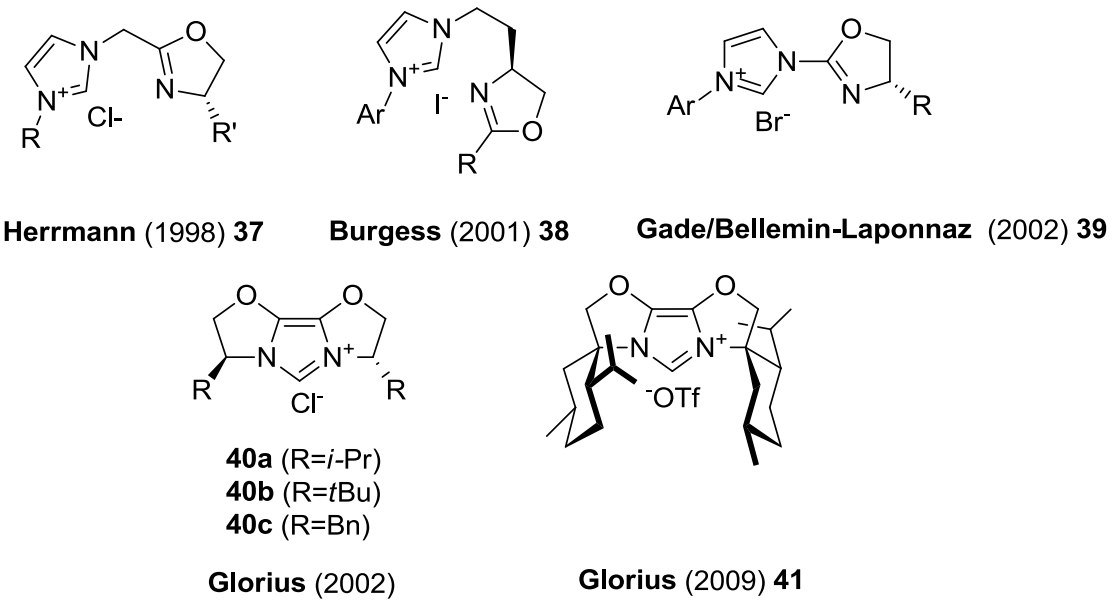

Figure 16. Examples of oxazoline based chiral *NHC* ligands.

In 1998, *Herrmann* reported the first example of a bidentate *NHC*-oxazoline derived ligand **37**[19,102] and its application in the Rh-catalyzed hydrosililation of ketones. In this work moderate enantioselectivities (up to 70% *ee*) were obtained (Figure 16). In 2006, *Pfaltz* and co-workers described a series of iridium complexes with ligand **37** and their application as highly active catalysts in asymmetric hydrogenation of unfunctionalised and functionalised olefins. The reaction afforded products with *ee* up to 90%.[103] The oxazoline derived *NHC* ligand **38**[104,105] developed by *Burgess* showed excellent activity and enantioselectivity in the iridium-catalyzed hydrogenation of alkenes, where only 0.2 to 0.6 mol% of the catalyst was required. The rhodium complexes of bidentate *NHC* ligand **39** developed by *Gade* have found excellent application in the asymmetric hydrosililation reactions[106] (up to 97% *ee*) as well as in asymmetric reduction of various aryl alkyl ketones[107] (up to 91% *ee*).

In 2002 *Glorius* and co-workers designed a new family of conformationally rigid *NHC*s **40**. Ligands **40** were tested in the asymmetric palladium-catalyzed *α*-arylation of amides, however only moderate *ee*'s (up to 43%) were obtained.[44] Later, the *authors* developed new sterically demanding chiral *N*-heterocyclic carbene ligand, IBiox[(-)-menthyl] **41**[37], with a buried volume $\%V_{bur}$ of ~50%. Ligand **41** considerably improved the enantioselectivities in these reactions (Scheme 13).

I.6.7. Chiral NHC Ligands with Rigid Backbones

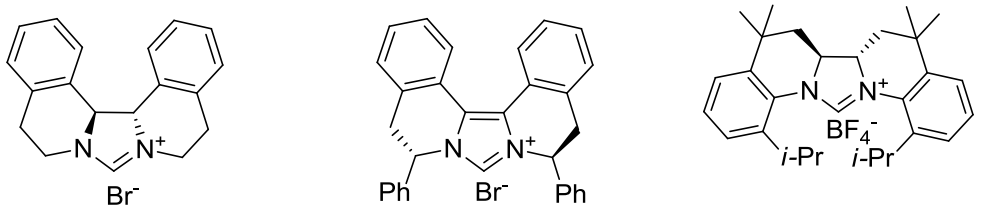

Herrmann (2006) **42** **Herrmann** (2007) **43** **Murakami** (2011) **44**

Figure 17. Examples of chiral tricyclic *NHC* ligands.

In 2006 *Herrmann* reported the first type of chiral *NHC* ligands with rigid backbones **42**[108]. In this ligand, rotations of the *N*-substituents around the C-N bond are limited (Figure 17). The rhodium and iridium complexes of **42** were prepared and fully characterized by X-ray analysis. These complexes were tested in asymmetric hydrosilylation and hydrogen transfer of acetophenone, however very low *ee*'s were observed (up to 28% *ee*).

Later, the group of *Herrmann* developed a more rigid chiral *NHC* ligand **43**[109] which was synthesized from (*S*)-3-phenyl-3,4-dihydroisoquinoline. The iridium complex of **43** was used as a catalyst in the asymmetric hydrogenation of methyl-2-acetamidoacrylate, delivering corresponding products in modest enantioselectivities (up to 67% *ee*).

In 2011, *Murakami* developed chiral *NHC* ligand **44**[110] bearing a 2,2'-bisquinoline-based C_2-symmetric skeleton. The ligand **44** showed excellent results in the palladium-catalyzed α-arylation of amides providing 3-alkyl-3-aryl oxindoles in high enantioselectivities (Scheme 13).

I.6.8. Summary

In summary, chiral monodentate *N*-heterocyclic carbene ligands have broad utility in asymmetric catalysis, but successful applications of such ligands are still rare compared with those involving chiral *N*-, *O*-, and *P*-ligands. In 2009, *Stahl* summarized asymmetric transformations, in which chiral monodentate *N*-heterocyclic carbenes were employed to afford enantioselectivities equal or above 90% *ee*. The transformations include olefin metathesis,[65,111,112] 1,4-addition of boronic acids to enones,[95] hydrosilylation of ketones,[113] intramolecular α-arylation of amides,[114-116] copper-catalyzed conjugate addition to cyclopentanone with diethylzinc,[55] and nickel-catalyzed reductive coupling of 1,3-dienes and aldehydes with triethylsilane.[59] So far, to the best of our knowledge only four more successful

applications of monodentate *NHC* ligands have been reported, including copper-(*NHC*)-catalyzed *β*-borylation of electron-poor alkenes,[117] iridium-(*NHC*)-catalyzed asymmetric hydrosilane reduction of ketones,[118] ruthenium-(*NHC*)-catalyzed asymmetric hydrogenation of benzofurans,[57] and enantioselective synthesis of indolines *via* C(sp^3)-H activation of unactivated simple alkyl groups (a recent development in the group of *Kündig*).[119-121] The latest work will be discussed in detail in chapter III. Thus, new efficient chiral *NHC* ligands for transition-metal asymmetric catalysis are desirable along with the knowledge about the asymmetry transfer.

I.7. Design and Development of a New Family of Chiral *NHC* Ligands in the *Kündig* Group

Pioneered by the groups of *Herrmann*[41] and *Enders*[51] chiral *NHC* ligands derived from chiral phenethylamine and its analogues have become very important chiral ligands (Figure 18). Major attention in their development has focused on the modification of the aromatic group in the *N*-heterocyclic ligand backbone. Little effort has been devoted to the modification of the alkyl R groups at stereogenic benzylic positions (R = Me in almost all cases).

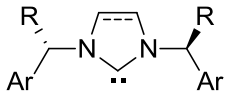

Figure 18. Enders/Herrmann type of chiral *NHC* ligands.

The *Kündig* group proposed that the introduction of sterically more demanding R groups at the ligand stereogenic centers will prevent free rotation along the nitrogen-carbon bond and subsequent steric-hindrance might facilitate a chiral control and will improve the asymmetric induction of the catalyst (Figure 19).

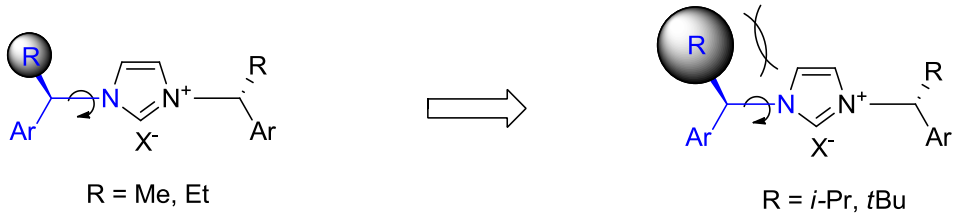

Figure 19. Proposed strategy in the *Kündig*'s group for the development of new chiral *NHC* ligands.

Our group previously reported the synthesis of chiral *ortho*-substituted *α*-alkylbenzylamines and showed their application as chiral auxiliaries[122,123], starting materials

for chiral dibenzoazepines[124], and also as building blocks for chiral bidentate benzoxazine P/N ligands.[122,125] Later, the attention was focused on the synthesis of chiral *NHC* ligands using chiral *orho*-substituted *α*-alkylbenzylamines as starting materials. Thus, a new family of bulky *Enders*/*Herrmann* type chiral *NHC* ligands bearing alkyl groups of different steric demands at the chiral benzylic position was prepared (Figure 20). These ligands have found excellent applications in the asymmetric palladium-catalyzed *α*-arylation of amides delivering 3-alkyl-3-aryl oxindoles[114] and 3-alkoxy- or 3-amino-3-aryl[115] oxindoles in high yields and excellent enantioselectivities.

I.8. Project Outline

The main goals of this work are:

a) Extension of the substrate scope of the palladium-catalyzed *α*-arylation reaction (3-alkyl-3-aryl oxindole synthesis) using bulky chiral *N*-heterocyclic carbene ligands previously developed in the group (Chapter II).

b) Mechanistic studies of the palladium-catalyzed *α*-arylation reaction, including isolation and structural characterization of palladacycle intermediates, kinetic and DFT investigations of the catalytic cycle (Chapter II).

c) Synthesis of new catalysts based on chiral *NHC* ligands, and their application in palladium-catalyzed *α*-arylation of amides (Chapter II).

d) Detailed synthesis of new chiral *N*-heterocyclic carbene ligands (Figure **20**) and their application in the synthesis of 3-alkyl-3-aryl oxindoles, spiro- and *aza*-spirooxindoles (Chapter II).

e) Application of the developed *N*-heterocyclic carbene ligands in the enantioselective synthesis of fused indolines *via* palladium catalyzed C(sp^3)-H activation of an unactivated methylene group (Chapter III).

f) Asymmetric synthesis of 2- and 2,3-disubstituted indolenes *via* regiodivergent reaction of a racemic mixture (RRM) (Chapter III).

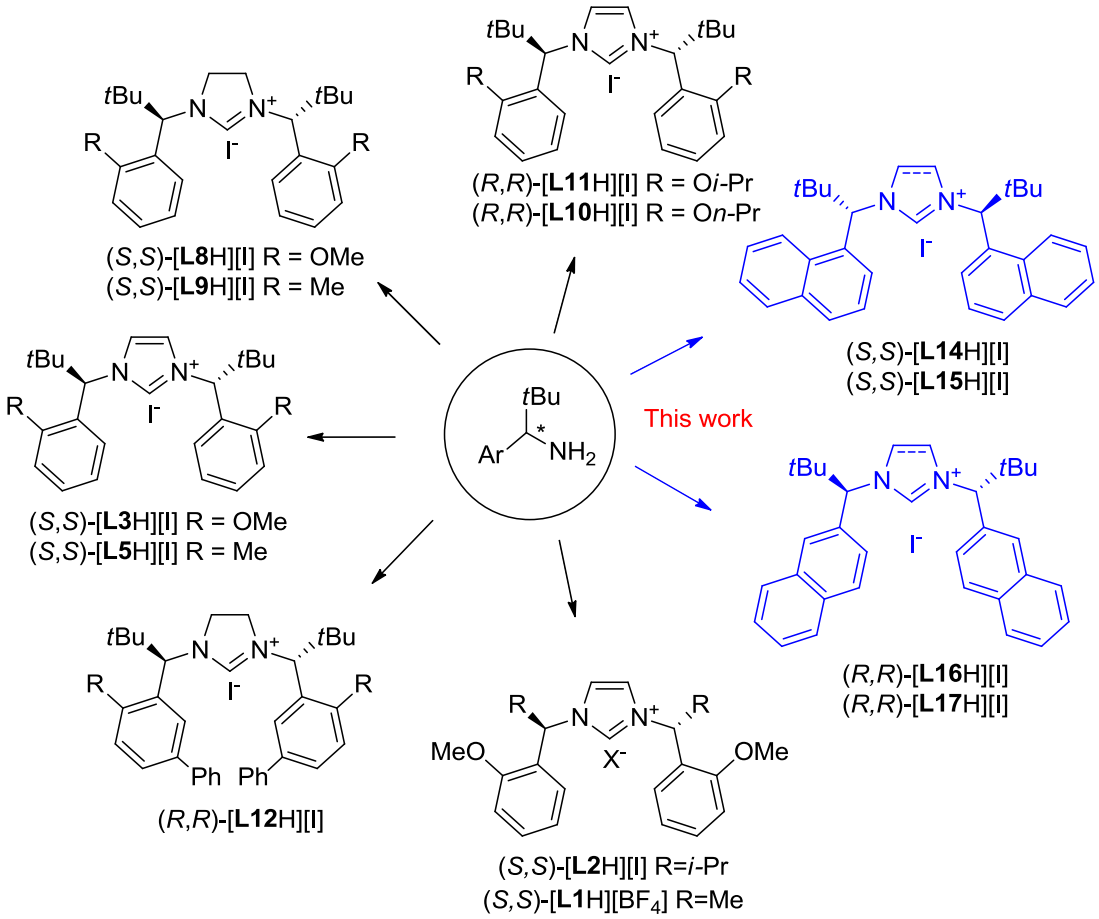

Figure 20. Ligand library of chiral *N*-heterocyclic carbene ligands.

II. Asymmetric Synthesis of Oxindoles *via* Intramolecular Palladium-*NHC*-Catalyzed *α*-Arylation of Amides

II.1. Importance of Oxindoles in Medicinal Chemistry

Oxindoles are constituents of a large family of indole alkaloids,[126] particularly 3,3-disubstituted-oxindoles and oxindoles with spirooxindole skeletons are found in a large number of natural or synthetic products presenting various biologically activities.[127-131] Selected examples are shown in Figure 21.

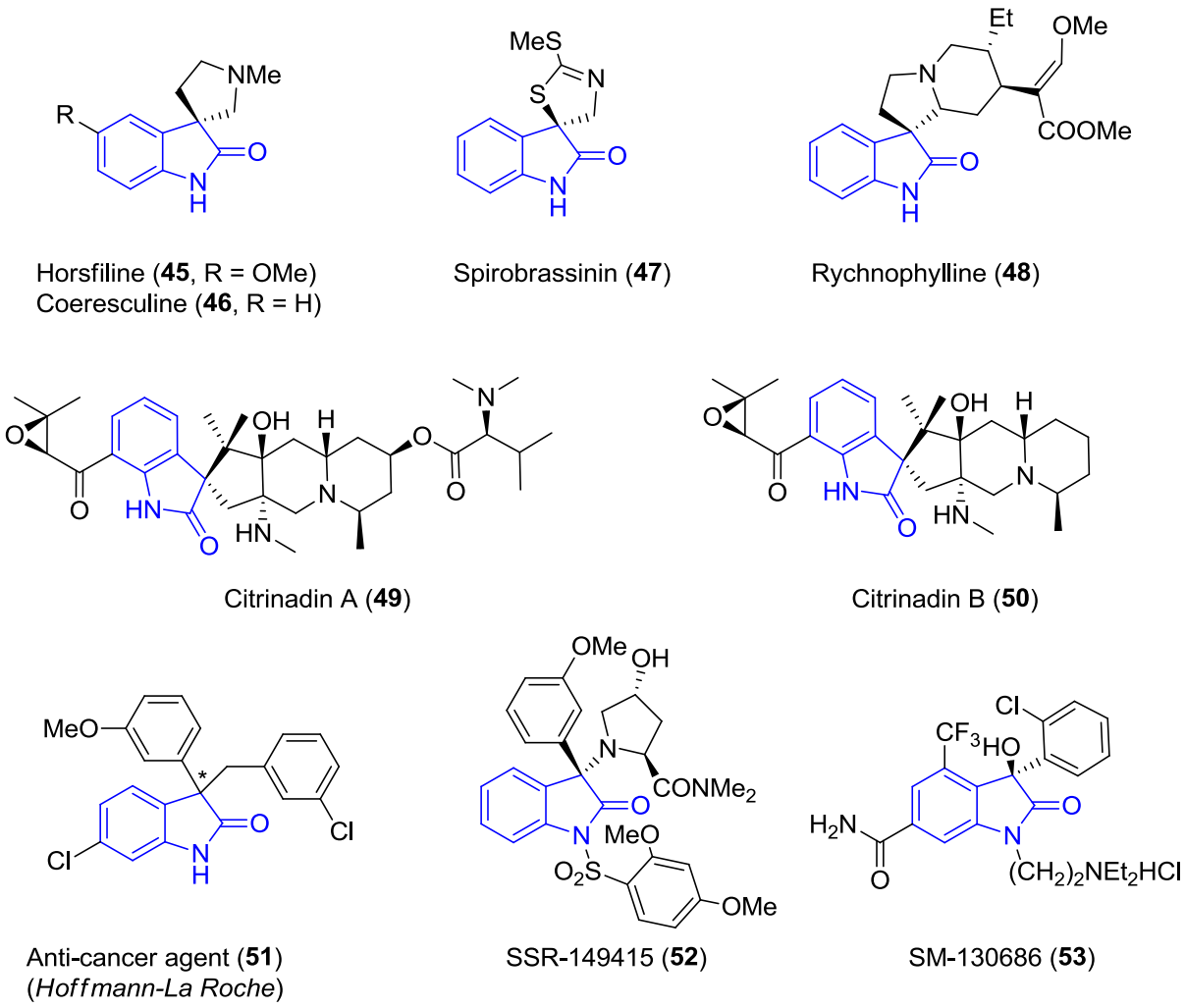

Figure 21. Natural products and biologically active compounds bearing 3,3-disubstituted or spirooxindole scaffolds.

The 3,3-pyrrolidinyl-spirooxindoles constitute a valuable class of biologically active compounds, which can be isolated from natural sources, such as spirooxindole alkaloids **45-48**[132-134](**45** and **46** are used in traditional herbal medicine; **47** is found in the first oxindole phytoalexin; **48** is a non-competitive NMDA antagonist and calcium channel blocker) (Figure

21). Citrinadin A (**49**) and B (**50**) were extracted from marine-derived fungus and fully characterized and are particularly challenging compounds in terms of synthesis. Citinadin B (**50**) shows modest cytotoxicity against murine leukaemia L1210 cells.[135] The non-spirocyclic quaternary stereogenic center at the C-3 position of oxindoles is also present in pharmaceutically active compounds such as **51** are MDM2 antagonist and disrupt nefarious MDM2-p53 interactions[136]. SSR-149415 (**52**)[137,138] is a drug and now is in clinical trials for treatment of anxiety and depression. SM-130686 (**53**)[139-141] containing 3-hydroxy oxindoles framework is a highly potent and orally active nonpeptidic growth hormone secretagogue.

II.2. Enantioselective Oxindole Synthesis *via* Metal-Catalyzed Intramolecular Reactions

Oxindoles are therefore interesting targets for organic chemists. Many elegant methodologies were developed towards the synthesis of the oxindole framework over the past decades.[127-131,142-147] The most common methods are summarized and depicted in Figure 22.

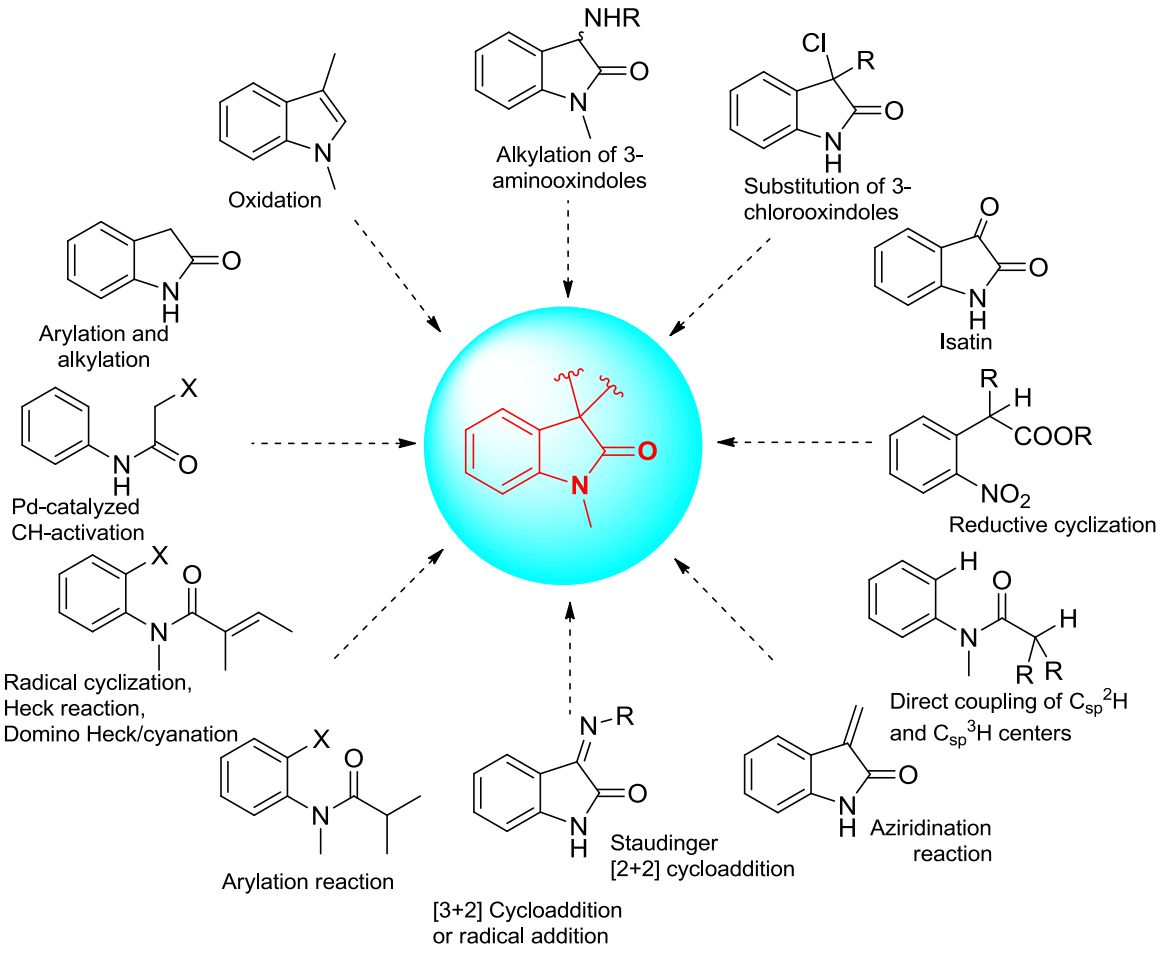

Figure 22. Methods of oxindole synthesis.

Consequently, much activity was also focused on the synthesis of enantiomerically enriched compounds of this family. One of the possible synthetic routes is *via* modification of a pre-existing ring system – typically either a simpler oxindole or an isatin. Recent examples include enantioselective nucleophilic addition to isatins, direct functionalization of 3-substituted oxindoles by alkylation, fluorination of oxindoles at the C-3 position, hydroxylation reaction, aldol reaction, Mannich reaction, Michael addition, amination and cyanoamidation of oxindoles and arylation reactions.[146]

Alternatively, the quaternary stereogenic center at the C-3 position of oxindole can be generated during cyclization reaction of an acyclic precursor. A few intramolecular processes for asymmetric oxindole synthesis were developed so far. A pioneering elegant method here stems from the *Overman* group, who developed an enantioselective *Mizoroki-Heck* reaction for this transformation. Using a Pd/(*S*)-BINAP complex as a catalyst, high chemical yields and enantioselectivities of 3,3-dialkyl-substituted oxindoles were obtained. The spirooxindoles were formed in moderate enantioselectivities under these reaction conditions. Subsequently, this methodology was successfully applied to the total synthesis of the Calabar alkaloid (-)-physostigmine **55** (a parasympathomimetic alkaloid, specifically, a reversible cholinesterase inhibitor). The key step in the construction of an oxindole core starting from butenanilide **54** could reach 95% *ee* for the corresponding product (Scheme 27).[148-152]

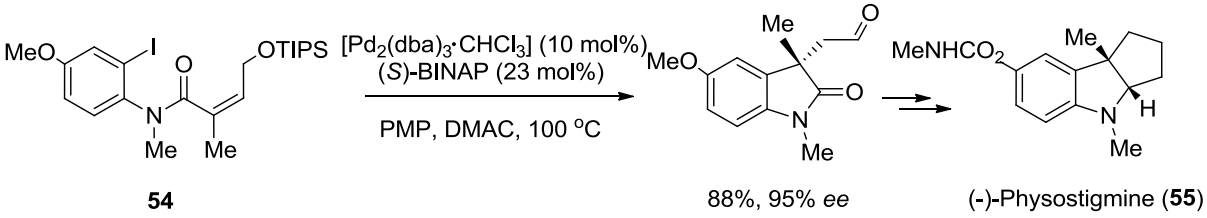

Scheme 27. Asymmetric *Heck* cyclization reaction.

Later the same group applied an intramolecular *Mizoroki-Heck* reaction to the enantioselective synthesis of 3-alkyl-3-aryl oxindoles. The chiral catalyst generated *in situ* from (*R*)-BINAP and $Pd(OAc)_2$ efficiently promoted the cyclization of aryl triflates generating products in enantioselectivities up to 98% *ee* (Scheme 28).[153]

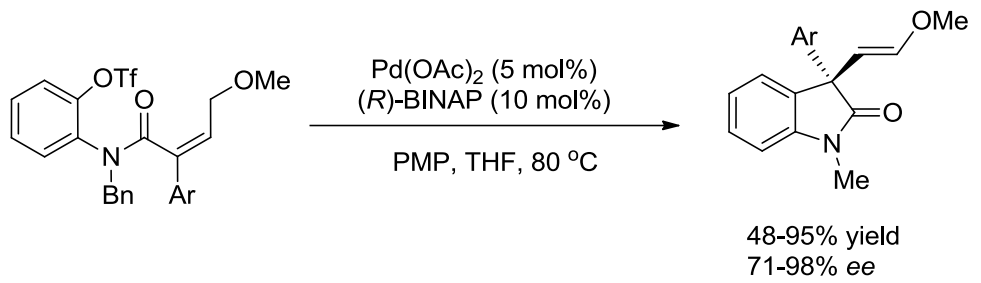

Scheme 28. Asymmetric intramolecular *Mizoroki-Heck* reaction.

In 2003, *Busacca* developed new phosphino-imidazolin ligand **58** and applied it in the enantioselective palladium-catalyzed *Mizoroki-Heck* reaction.[154] In the presence of 11 mol% of **58** and 5 mol% $Pd_2(dba)_3$ the aryl triflate **56** undergoes *Heck* cyclization producing spirooxindole **57** in moderate yield and high 87% enantioselectivity, however only one example was described (Scheme 29).[154]

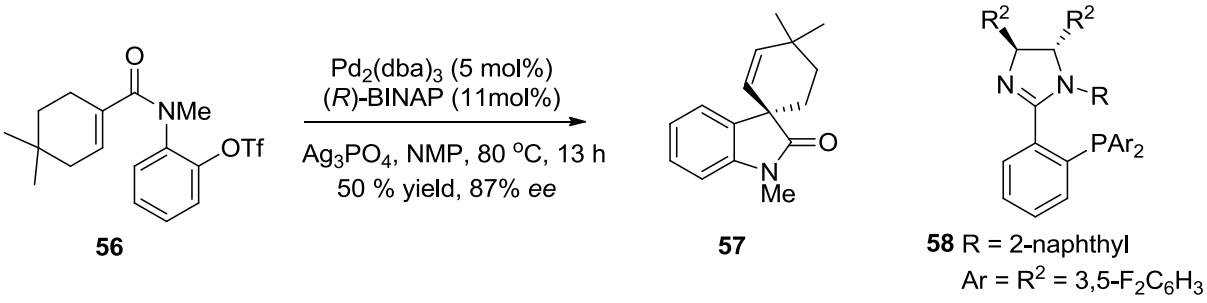

Scheme 29. Spirooxindole framework *via* enantioselective intramolecular *Mizoroki-Heck* reaction.

Zhu[155] extended the studies of *Overman* and developed an enantioselective domino *Heck*-cyanation process, yielding products in moderate to good enantioselectivities (Scheme 30).

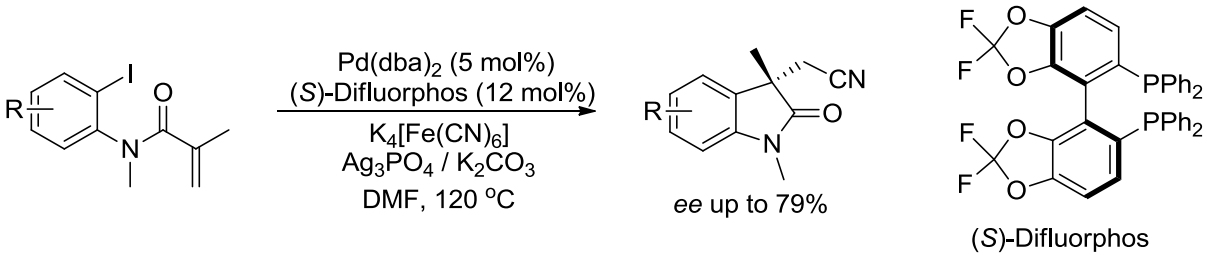

Scheme 30. Palladium-catalyzed enantioselective domino *Heck*-cyanation reaction.

In 2008, the *Takemoto*[156,157] group reported an enantioselective palladium-catalyzed acylcyanation (cyanomidation) of olefins to access a 3-alkyl-3-cyanomethyl-2-oxindole subunit. In the presence of phosporamidite ligand **59** the product forms in up to 86% *ee*

(Scheme 36). A few years later, in 2010, *Douglas* improved the enantioselectivity of the palladium-catalyzed cyanoamidation reaction up to 99% *ee* by using *N*,*N*-(*i*-Pr)$_2$ derivative of octahydro-MonoPhos ligand **60** (Scheme 31). Notably, the substrates with a free N-H bond are tolerated under these reaction conditions, allowing for future protecting-group-free synthesis of alkaloids. The utility of this synthetically useful methodology was demonstrated in the synthesis of several biologically active compounds including (+)-horsfiline (**45**) and (-)-coerulescine (**46**).[158]

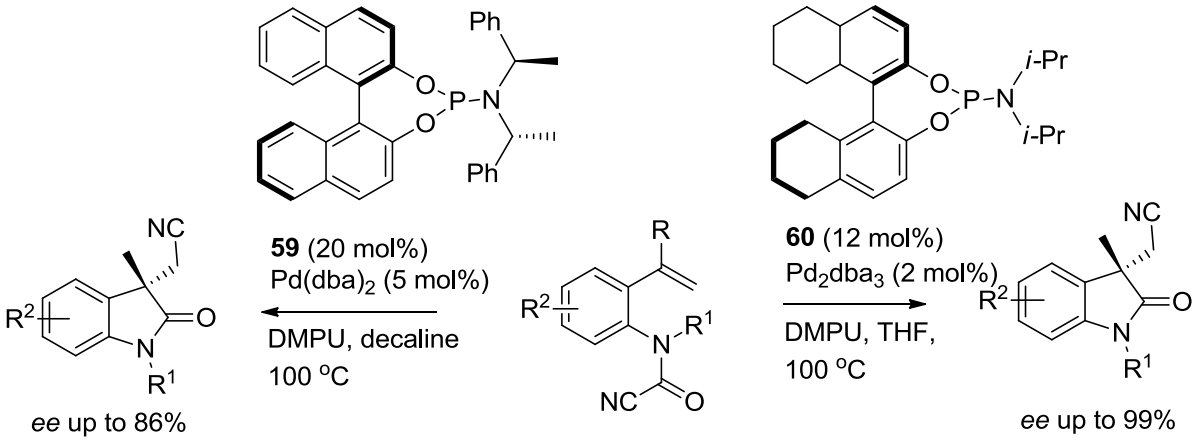

Scheme 31. Intramolecular asymmetric palladium-catalyzed cyanoamidation of olefins.

In the development of the copper-catalyzed enantioselective alkenylation and arylation of isatins using silicon-based nucleophiles, the *Shibasaki* group found that the activity and enantioselectivity dramatically decreased when isatins with substituents at C-4 position were used. To overcome this problem *Shibasaki* developed the enantioselective intramolecular arylation of isatins, where the corresponding 3-aryl-3-hydroxy-2-oxindoles were formed as highly enantioenriched products (Scheme 32).[141] This achievement allowed researchers to utilize a copper-catalyzed intramolecular arylation methodology as a key step in the total synthesis of SM-130686 (highly potent and orally active nonpeptidic growth hormone secretagogue).

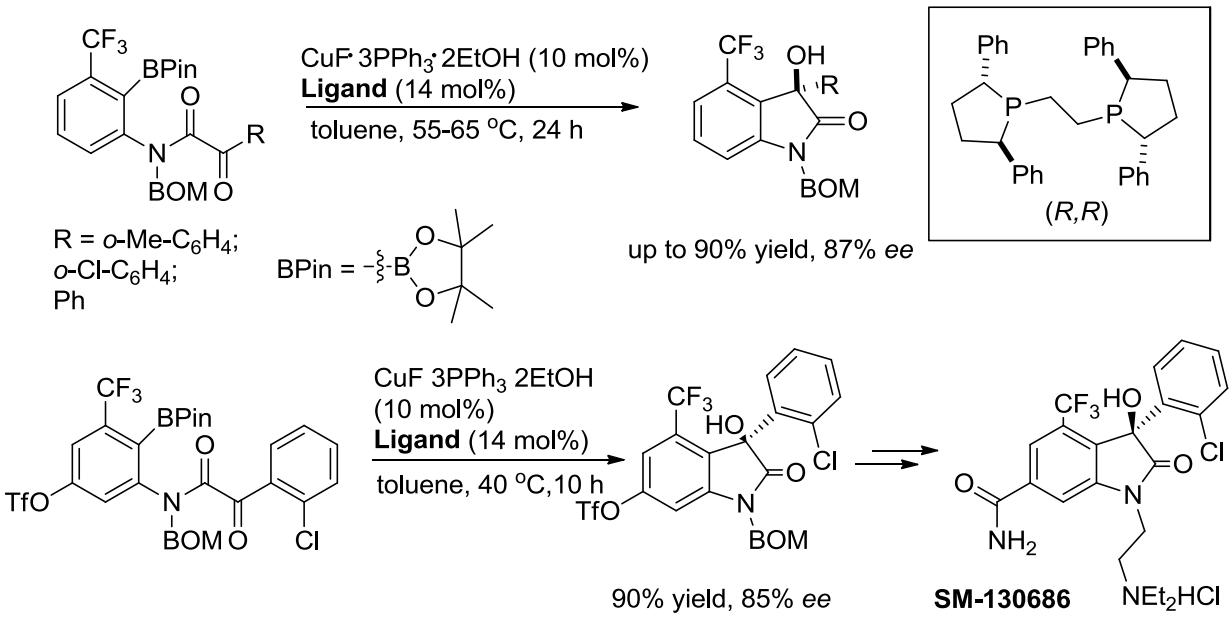

Scheme 32. Cu-catalyzed enantioselective intramolecular arylation of isatins.

Recently, in 2011, *Shibasaki* and co-workers reported the first palladium-catalyzed enantioselective intramolecular aryl-transfer reaction of aryl triflates to ketones. Synthetically useful enantioselectivity of 3-aryl-3-hydroxy-2-oxindoles were promoted by Pd-(*R*)-DifluorPhos catalyst generated *in situ*. A big advantage of this method, that the non-protected amides can be used as substrates (Scheme 33).[159]

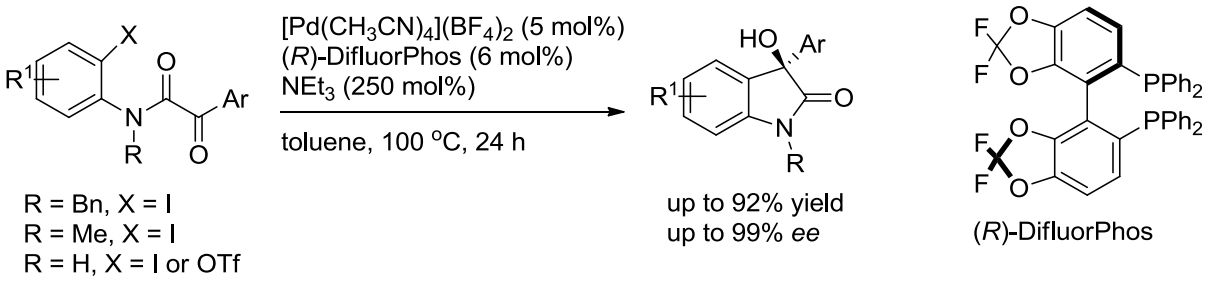

Scheme 33. Palladium-catalyzed enantioselective intramolecular arylation of *α*-ketoamides.

In 2001 *Hartwig*[60] and co-workers reported the results of an extensive study of the palladium-catalyzed intramolecular *α*-arylation reaction of amides to produce 3,3-disubstituted oxindoles. A number of chiral bidentate phosphines, P/N-ligands and monophospines have shown poor to moderate yields and enantioselectivities in this transformation. Promising results were obtained using bulky chiral *N*-heterocyclic carbene ligand **5**, however with enantioselectivities not exceeding 76% (Scheme 34). This study was followed by the groups of *Glorius*[44] and later, *Aoyama*[116], but only moderate (up to 64% *ee*) enantioselectivities were achieved. The breakthrough in this field came in 2007 with the

development of new chiral *NHC* ligand **L5** in our group,[114] where both high yields and asymmetric induction in oxindole synthesis were achieved. Later, *Kündig* found that small modification of aryl groups to form **L12** gave access to highly enantioenriched oxindoles bearing heteroatoms at the oxindole stereogenic center (O and N).[115] Since then, a number of other chiral carbene ligands have been reported to give excellent results (Scheme 34). *Dorta* developed new *NHC* ligands with a chiral *N*-heterocycle and naphthyl side chains and successfully applied palladium complexes incorporating these ligands in 3-alkyl-3-aryl[73], 3-allyl -3-aryl[74] and recently 3-flouro-3-aryl[160] oxindole synthesis. Conformationally restricted chiral ligands developed by *Glorius*[37] and by *Murakami*[110] also showed high asymmetric induction in this reaction. *Trapp*'s group[161] presented the synthesis and application of new six-membered camphor-derived *NHC*-Pd-isonitrile complexes in oxindole synthesis; however the product **62** was formed in 58% *ee* (Scheme 34).

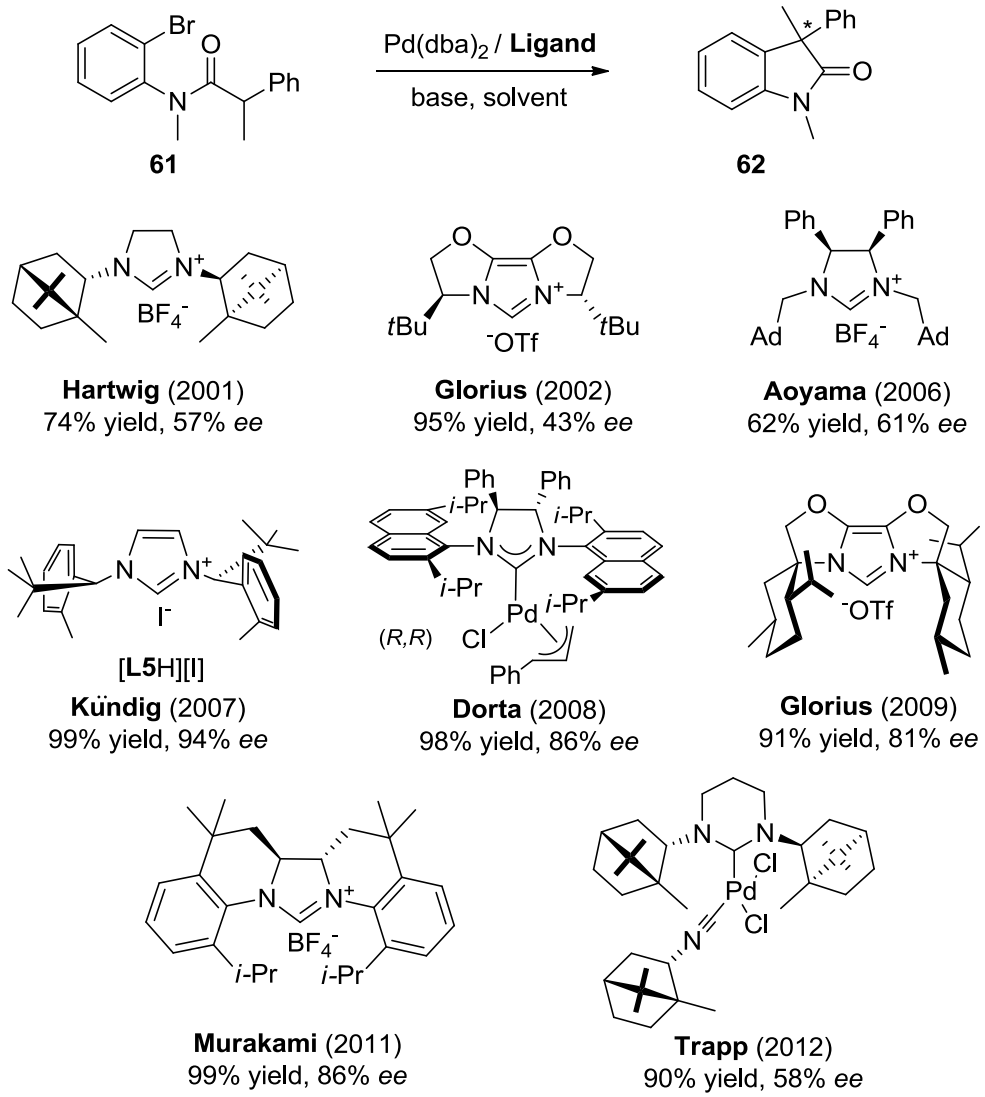

Scheme 34. Progress in the Pd(*NHC*)-catalyzed asymmetric intramolecular *α*-arylation of amides.

II.3. Results: Chiral *N*-Heterocyclic Carbene Ligands in Palladium-Catalyzed *α*-Arylation of Amides

II.3.1. Synthesis of Chiral Amines

Based on the methodologies developed in the *Kündig* group for *N*-heterocyclic carbene ligand synthesis, a series of chiral *NHC* ligands were prepared:

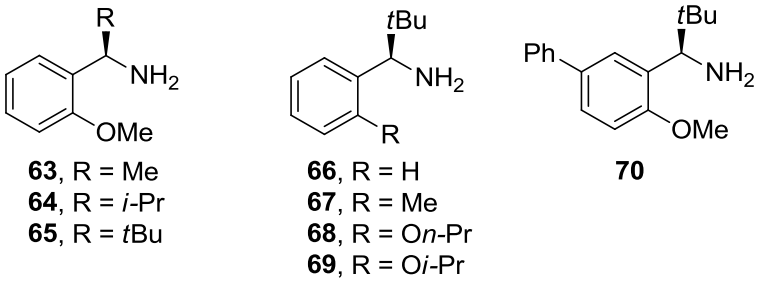

Figure 23. Chiral amines for the synthesis of imidazolium and dihydroimidazolium salts.

Synthesis and resolution of the amines **63-67** and **70** were done according to the procedure developed in the *Kündig* group (Figure 23).[114,115]

Chiral amines **68** and **69** were prepared from amine (*R*)-**65** in high four-step procedure as depicted in Scheme 35. Amino phenol **71a**, synthesized from **65** by reaction with BBr_3, was selectively protected on the more nucleophilic amino group with a *tert*-butyloxycarbonyl group (Boc) to form **71b**. Subsequent treatment of **71b** with alkyl halide in the presence of base (K_2CO_3) allowed the complete conversion to the alkylated phenol. After deprotection of the Boc group amines **68** and **69** were obtained in 99% and 86% yield, respectively.[162]

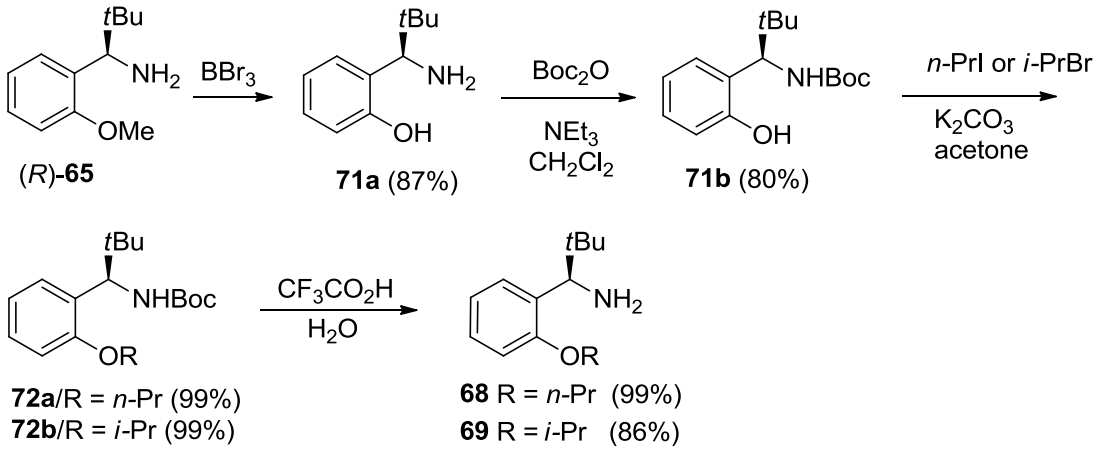

Scheme 35. Synthesis of amines **68** and **69**.

II.3.2. Synthesis of Chiral NHC Ligands (Ligand Precursors)

The first family of ligands synthesized was the unsaturated imidazolium salts starting from the chiral *ortho*-substituted *α*-alkylbenzylamines (Figure 24).[114,115] The imidazolium tetrafluoroborate salt (*R*,*R*)-[**L1**H][BF_4] was synthesized by a standard one-pot procedure in 87% yield (Scheme 36).[163] This method proved inefficient for (*R*,*R*)-[**L2**H][I] and completely failed in the synthesis of (*R*,*R*)-[**L3**H][I] with a bulky *t*Bu group at the benzylic position. (*R*,*R*)-[**L2**H][I] and (*R*,*R*)-[**L3**H][I] were therefore synthesized by the method involving diimine formation, ring closure, and anion exchange (Scheme 36). In the ring-closing step, the method using chloromethylpivalate and AgOTf worked well,[44] giving the imidazolium triflates in moderate yield. The anion exchange of $^-$OTf to I^- allowed us to obtain solid products instead of oily salts. This greatly facilitated purification. Overall, it is a simple process and only the diimine has to be purified.[i] Product yields were moderate (Scheme 36). Similarly, imidazolium iodide (*R*,*R*)-[**L4**H][I] and (*R*,*R*)-[**L5**H][I] were obtained in 14% and 49% yields from (*R*)-**66** and (*R*)-**67** respectively.[114]

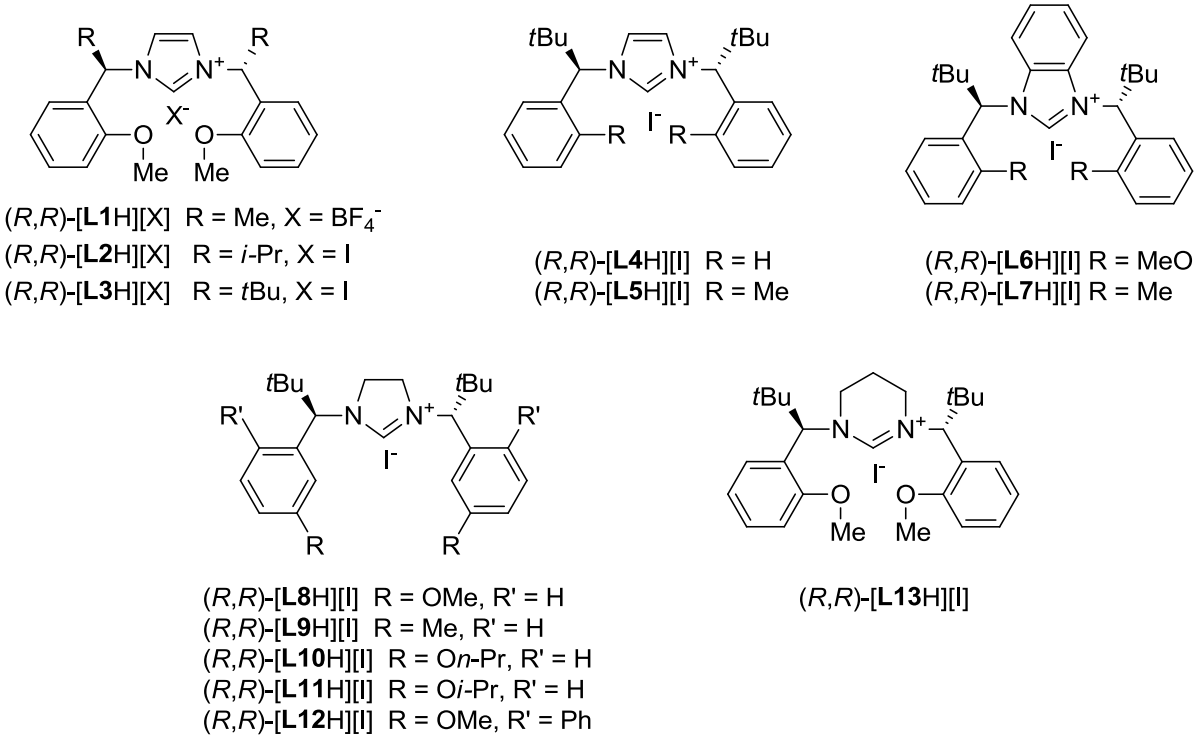

Figure 24. New chiral *NHC* ligands.[ii]

[i] The recrystallization of the diimines from methanol was necessary to achieve better yields of the imidazolium salts in the final ring-closing step.

[ii] A) *NHC* ligands (*R*,*R*)-[**L1**-**4**H][X] and (*R*,*R*)-[**L12**H][X] were resynthesized according procedures developed in the *Kündig* group. B) Ligands (*R*,*R*)-[**L5**-**6**H][I] were prepared in collaboration with Dr. *Y.-X. Jia*.

The dihydroimidazolium salts (*R*,*R*)-[**L8**H][I], (*R*,*R*)-[**L9**H][I], (*R*,*R*)-[**L10**H][I], (*R*,*R*)-[**L11**H][I] and (*R*,*R*)-[**L12**H][I] were synthesized by a four-step procedure that involved diimine formation followed by reduction ($NaBH_4$) to the diamines, ring closure, and anion metathesis (Scheme 36). Ring closure of diamines was carried out with NH_4BF_4 and triethyl orthoformate. Subsequent anion exchange afforded the dihydroimidazolium iodide salts in good to excellent yields (Scheme 36).

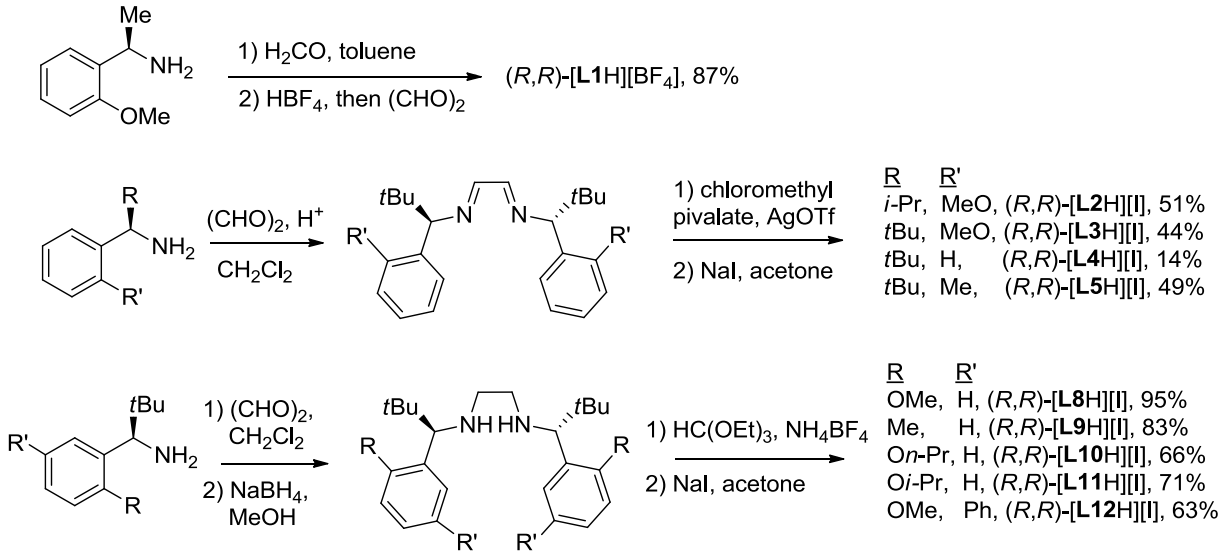

Scheme 36. General procedure for the synthesis of imidazolium and dihydroimidazolium ligand precursors. The *R* amine precursors are depicted.

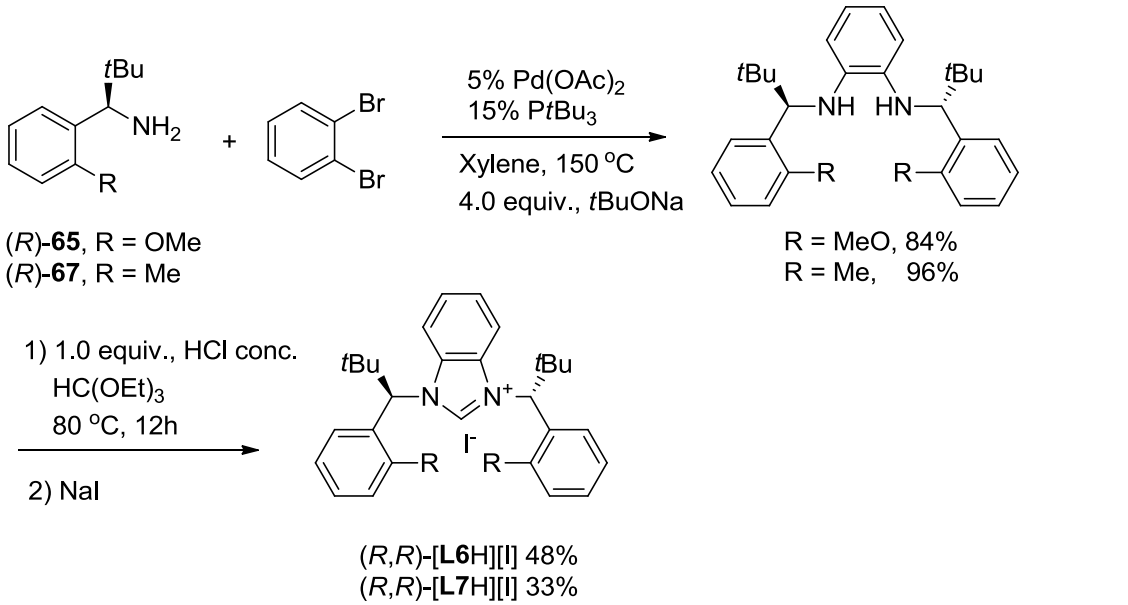

Scheme 37. Synthesis of benzoimidazolium iodide salts (*R*,*R*)-[**L6**H][I] and (*R*,*R*)-[**L7**H][I].

The backbone of ligand heterocyclic ring was further modified to access structurally diverse ligand precursors (*R*,*R*)-[**L6**H][I], (*R*,*R*)-[**L7**H][I] (with a benzoimidazolium ring) and (*R*,*R*)-[**L13**H][I] (with a six-member *N*-heterocycle).

Applying the *Buchwald-Hartwig* amination procedure, the reactions of (*R*)-**65** and (*R*)-**67** with 1,2-dibromo-benzene were carried out with 5 mol% $Pd(OAc)_2$, 15% P*t*Bu_3 and 4 equiv. *t*BuONa in xylene at 150 ^oC for 16 h to give corresponding diimines in high yields. Chiral HPLC showed that no racemization had occurred during this process (Scheme 37). The ring-closing method for the synthesis of dihydroimidazolium salts (*R*,*R*)-[**L8**-**L12**H][I] using NH_4BF_4 and $HC(OEt)_3$ failed when applied to the synthesis of (*R*,*R*)-[**L6**H][I] and (*R*,*R*)-[**L7**H][I]. However, reaction of the chiral diamines with concentrated HCl using triethyl orthoformate as solvent at 80 ^oC gave the requisite benzoimidazolium chloride salt in low yield. By recovering the starting material (diamines) and rerunning the reaction four times followed by anion exchange from Cl^- to I^- with NaI, products (*R*,*R*)-[**L6**H][I] and (*R*,*R*)-[**L7**H][I] were obtained in 48% and 33% yield respectively.

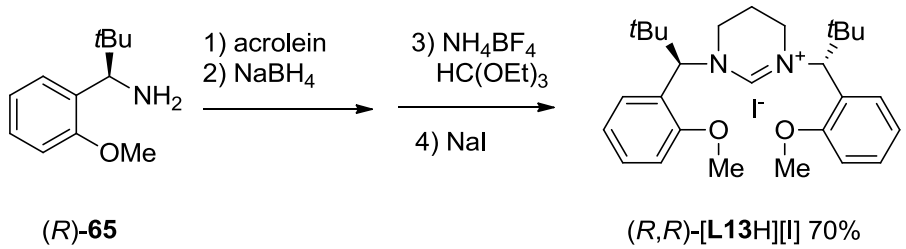

(*R*)-**65** (*R*,*R*)-[**L13**H][I] 70%

Scheme 38. Synthesis of (*R*,*R*)-[**L13**H][I].

N-heterocycle product bearing a six-member ring (*R*,*R*)-[**L13**H][I] was synthesized by a four-step procedure.[164] Reaction of (*R*)-**65** with acrolein followed by *in situ* reduction gave the 1,3-diamine and, cyclization using NH_4BF_4 and $HC(OEt)_3$, followed by anion metathesis with NaI (Scheme 38) afforded the desired product (*R*,*R*)-[**L13**H][I] in 70% overall yield.

II.3.3. Synthesis of 3-Alkyl-3-Aryloxindoles

II.3.3.1. Optimization of Reaction Conditions

Based on the primary studies on the Pd(*NHC*)-catalyzed arylation reaction carried out by Dr. *Y.-X. Jia*[114] (optimization of reaction conditions include the screening of ligands, solvents, bases and a palladium sources) we can conclude that:

- The bulky *t*Bu group at the stereogenic benzylic center is important, but not sufficient to achieve high asymmetric induction.

- The presence of an *orhto*-aryl substituent in addition to the *t*Bu group results in high enantioselectivity.

Table 1. Chiral *NHC* ligands in the palladium-catalyzed α-arylation of **61** to give **62**.[a]

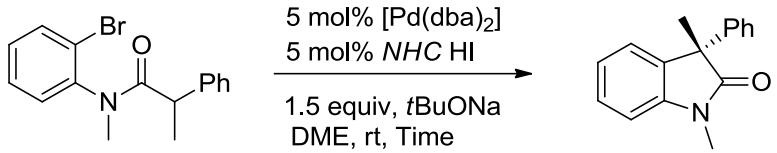

61 **62**

Entry	Ligand precursor	Time (h)	Yield (%)[b]	Ee (%)[c]
1[d]	(*S*,*S*)-[**L3**H][I]	24	96	87 (*S*)
2[d]	(*R*,*R*)-[**L4**H][I]	24	98	57 (*R*)
3[d]	(*S*,*S*)-[**L5**H][I]	24	**99**[e]	**94** (*S*)
4[d,f]	(*S*,*S*)-[**L5**H][I]	24	51	96 (*S*)
5[d]	(*R*,*R*)-[**L6**H][I]	48	67	80 (*R*)
6	(*S*,*S*)-[**L7**H][I]	48	65	91 (*S*)
7	(*R*,*R*)-[**L8**H][I]	14	98	88 (*R*)
8	(*S*,*S*)-[**L9**H][I]	48	55	92 (*S*)
9	(*R*,*R*)-[**L10**H][I]	14	98	75 (*R*)
10	(*R*,*R*)-[**L11**H][I]	14	98	71 (*R*)
11	(*R*,*R*)-[**L12**H][I]	14	98	88 (*R*)
12	(*R*,*R*)-[**L13**H][I]	48	60	68 (*R*)

[a] **61** (0.2 mmol), 0.05 M in DME, $Pd(dba)_2$ (5 mol%), *NHC*·HI (5 mol%), *t*BuONa (1.5 equiv.). [b] Isolated yield. [c] Determined by chiral HPLC. [d] Carried out by Dr. *Y.-X. Jia*. [e] 1 mmol scale. [f] At 10 °C for 24 h.

With a new library of *NHC* ligands in hand, we started to investigate their catalytic activity in the asymmetric palladium-catalyzed α-arylation of **61** to give **62** under previously optimized reaction conditions and the results are listed in Table 1.

Pertinent features are:

- Heterocyclic carbene ligands containing dihydroimidazolium core have almost the same performance as imidazoline carbene ligands. The same trend (*o*-Me > *o*-OMe) in asymmetric induction was found in this series: (*S,S*)-[**L9**H][I] > (*R,R*)-[**L8**H][I] (entries 7 and 8). Large *o*-substituents as in (*R,R*)-[**L10**H][I] (O*n*-Pr) and (*R,R*)-[**L11**H][I] (O*i*-Pr) gave lower product *ee*.

- Modification of the ligand structure as in (*R,R*)-[**L6**H][I], (*S,S*)-[**L7**H][I] and (*R,R*)-[**L13**H][I] led to lower performance (entries 5, 6 and 12).

- The only ligand tested with an aryl group with two substituents was (*R,R*)-[**L12**H][I] (entry 11). The induction was high but it did not reach that of (*S,S*)-[**L9**H][I] or (*S,S*)-[**L5**H][I].

So far, ligand (*S,S*)-[**L5**H][I] was found to be the best ligand precursor with a combination of the bulky *tert*-butyl and the *ortho*-tolyl groups, which are both located at the stereogenic center. However, at this stage, the question of the effect of the *ortho*-tolyl groups on the enantioselectivity of this reaction is still open and need to be answered.

II.3.3.2. Substrate Scope

a) Synthesis of Substrates

The synthesis of the standard substrate **61** was reported in the literature (Scheme 39).[165,166] 2-Bromo-*N*-methylbenzeneamine was prepared by reacting 2 equiv. of the 2-bromoaniline and one equiv. of butyl lithium and methyl iodide in order to prevent double methylation. The oxidation of hydratropaldehyde with sodium chlorite, hydrogen peroxide and monobasic phosponic acid leads to the racemic hydratropic acid**,** which is then transformed to the acid chloride using thionyl chloride. The condensation of the 2-bromo-*N*-methylbenzeneamine with acid chloride formed the desired amide **61**.

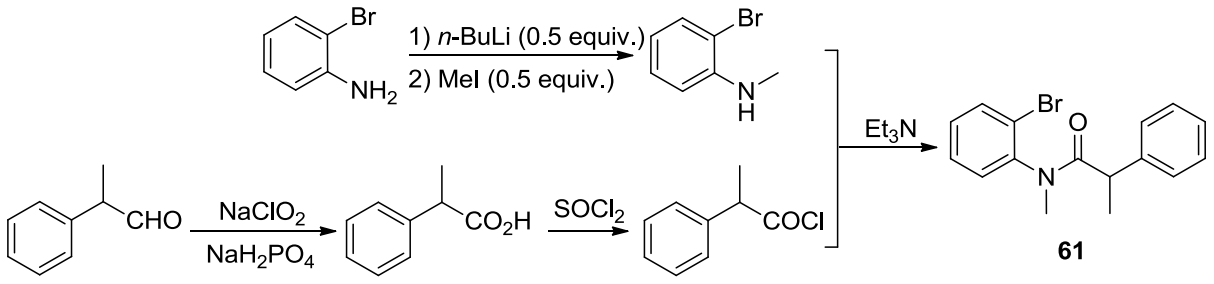

Scheme 39. Literature procedure for the synthesis of **61**.

However, for the study of the substrate scope of the present reaction, we needed a general synthetic route. The substrates bearing different substituents in the aniline part (Table 3), different *N*-protecting groups (Table 2 and 3) and aryl groups at the benzylic position (Table 2) were prepared according the route shown in Scheme 40.

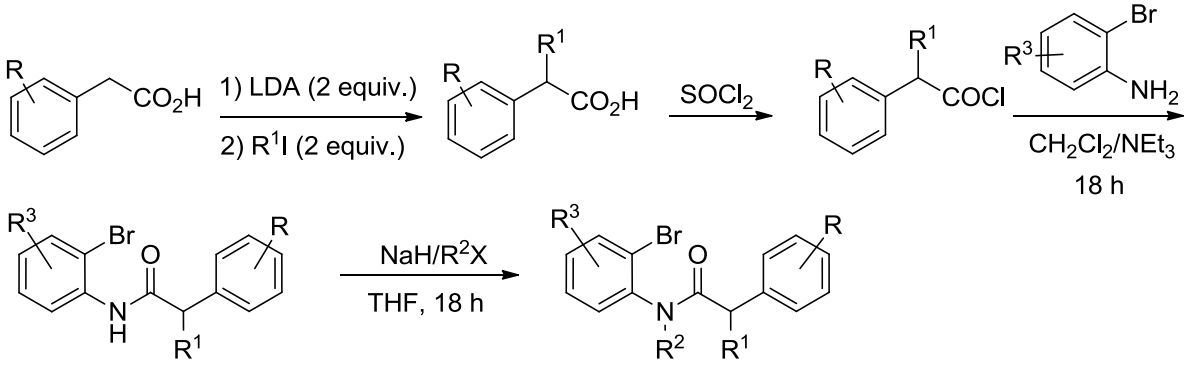

Scheme 40. General methodology to the synthesis of amides.

Table 2. Amides with different aryl and alkyl groups at the benzylic position.

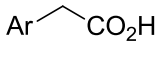	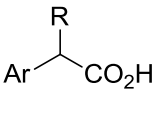	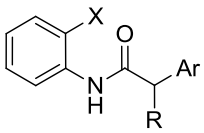	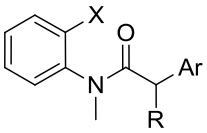
Ar	Yield %[a]	Yield %[b]	**Prod**./Yield %[c]
2-Tol	96 (R = Me)	95 (X = Br)	**73a** / 85
3-Tol	97 (R = Me)	96 (X = Br)	**73b** / 77
4-Tol	91 (R = Me)	94 (X = Br)	**73c** / 87
4-OMe-Ph	96 (R = Me)	54 (X = Br)	**73d** / 92
2-OMe-Ph	93 (R = Me)	95 (X = Br)	**73e** / 74
1-Napht	99 (R = Me)	80 (X = Br)	**73f** / 91
2-Napht	95 (R = Me)	90 (X = Br)	**73g** / 90
Ph	87 (R = Et)	92 (X = Br)	**74a** / 83
Ph	83 (R = *i*-Pr)	90 (X = Br)	**74b** / 79
Ph	84 (R = Bn)	74 (X = Br)	**74c** / 69
4-Tol	96 (R = Me)	59 (X = Cl)	**75a** / 87
2-Napht	95 (R = Me)	93 (X = Cl)	**75b** / 85
Ph	87 (R = Et)	94 (X = Cl)	**75c** / 91
Ph	84 (R = Bn)	75 (X = Cl)	**75d** / 74

[a] *n*BuLi (2.0 equiv.), -30˚C, diisopropilamine, THF, 30 min.; 2.0 (equiv.) MeI, 18 h; 2M HCl [b] Acid chloride (1.1 equiv.), 2-bromoaniline (1.0 equiv.), CH_2Cl_2, NEt_3 (1.5 equiv.), 0 ˚C; rt, 18 h. [c] THF, NaH (1.5 equiv.), 0 ˚C, RI (1.5 equiv.), 18 h.

Starting from the commercially available arylacetic acid, the alkyl group at α-position of the acetic acid was introduced by using 2.0 equiv. LDA and the alkyl iodide. After transforming to acid chloride, the condensation with 2-bromoaniline was performed in the presence of NEt_3 as a base. The alkyl substituents at nitrogen atom were introduced *via N*-alkylation reaction using alkyl halides and NaH as a base.

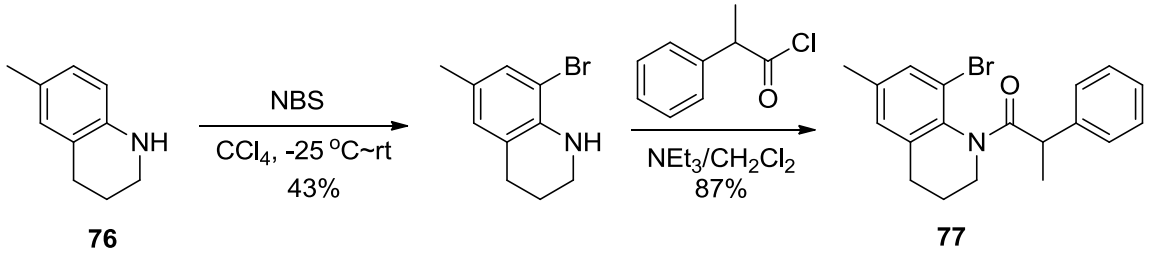

76 **77**

Scheme 41. Synthesis of amide **77**.

Amide **77** was synthesized in two steps involving bromination of amine **76**, followed by alkylation with 2-phenylpropanoyl chloride (Scheme 41).

The synthesis of amide **81** was done according to the general procedure shown in Scheme 40. Carboxylic acid **79** was synthesized *via* alkylation of **78** at α-carbon of acetic acid with LDA. However, the condensation reaction between acid chloride of **79** and 2-bromoaniline in the presence of Et_3N as a base was not efficient. Alternatively, peptide coupling reaction of (*E*)-2-methyl-4-phenylbut-3-enoic acid (**79**) and 2-bromoaniline was achieved using DCC and catalytic amount of DMAP (Scheme 42).

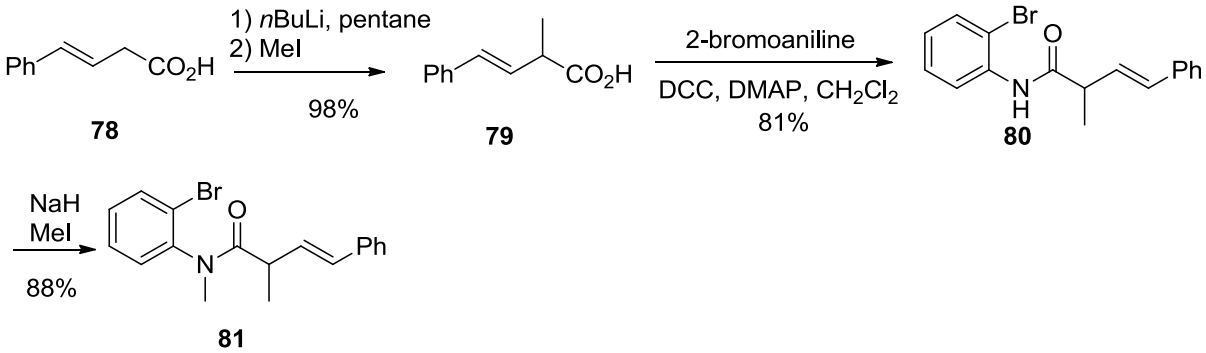

78 **79** **80** **81**

Scheme 42. Synthesis of amide **81**.

Table 3. Amides with different substituents in aniline part.

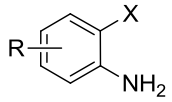	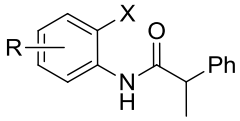	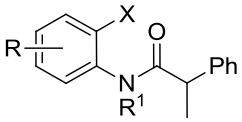
R	Product / Yield %[a,b]	Product / Yield %[a,c]
H (X = Br)	**82** / 89	**61** / 96 (R^1 = Me)
H(X = Br)	89	**83** / 81 (R^1 = Bn)
H (X = Cl)	94	**84** / 85 (R^1 = Me)
C(5)-Me	93	**85a** / 78 (R^1 = Me)
C(5)-*i*-Pr	90	**85b** / 85 (R^1 = Me)
C(5,7)-Me	76	**85c** / 78 (R^1 = Me)
C(6)-CF_3	89	**85d** / 81 (R^1 = Me)
C(6)-F	87	**85e** / 84 (R^1 = Me)
C(6)-OMe	95	**85f** / 89 (R^1 = Me)
C(7)-F	95	**85g** / 44 (R^1 = Me)

[a] Isolated yield. [b] 2-Phenylpropanoyl chloride (1.1 equiv.), 2-bromoaniline (1.0 equiv.), CH_2Cl_2, NEt_3 (1.5 equiv.), 0 ˚C; rt, 18 h. [b] THF, NaH (1.5 equiv.), 0 ˚C, RI (1.5 equiv.), 18 h.

Substrate **89** was prepared in three steps as described in Scheme 43. The ketoacid **86** was reduced to acid **87** according literature procedure using mercury (II) chloride, zinc and hydrochloric acid.[167] Amide **89** was formed in high yield by anilide formation from acid cloride **88** and 2-bromo-*N*-methylaniline.

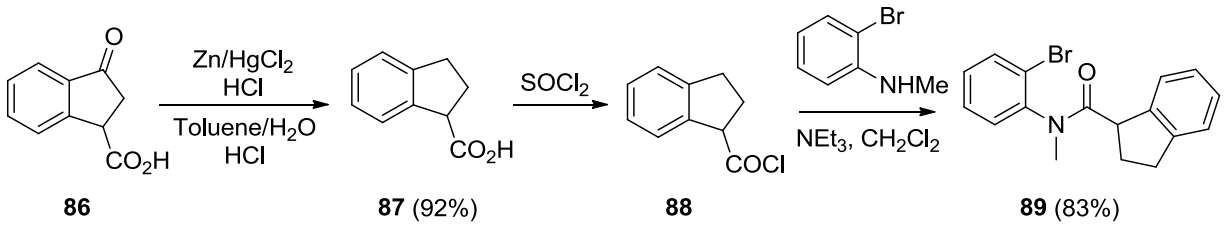

Scheme 43. Synthesis of amide **89**.

b) Catalysis

We next probed the scope and limitation of the reaction by using ligand precursor (*S*,*S*)-[**L5**H][I] under optimized reaction conditions established above (Table 1, entry 3). Initially, substrates bearing different aryl substituents at the benzylic position and also *N*-protecting groups were investigated. Oxindoles **62**, **90**, **91** and **92a-g** were generally obtained in good to excellent enantioselectivities and high yields (Table 4). The enantioselectivity of

the oxindole decreased when the *N*-protecting group was changed from Me to Bn (Table 4, entry 1-2). The attempted conversion of an unprotected amide **82** to the corresponding oxindole failed, showing that a free N-H bond in the substrate is incompatible with this transformation. Hydrogenolysis of (*S*)-**90** using Li/NH_3 afforded (*S*)-**91**. Reactions with substrates incorporating *ortho*-aryl substituents were sluggish and led to products in modest (entry 9) to good (entries 6,7) yields. In these cases the ligand precursor (*S,S*)-[**L3**H][I] performed better than (*S,S*)-[**L5**H][I] (entries 7, 9 and 11).

Table 4. Enantioselective palladium catalyzed α-arylation of substrates **61**, **82, 83 73a-g**.[a]

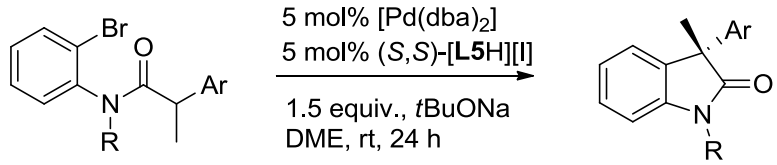

61, 82, 83, 73a-g **62, 90, 91, 92a-g**

Entry	Product	R	Ar	Time (h)	Yield (%)[b]	Ee (%)[c]
1[d]	(*S*)-**62**	Me	Ph	24	99	94
2	(*S*)-**90**	Bn	Ph	24	94	84
3[d]	(*S*)-**91**	H	Ph	24	0[f]	--
4	(*S*)-**92c**	Me	4-Tol	24	99	93
5[d]	(*S*)-**92b**	Me	3-Tol	24	99	93
6	(*S*)-**92a**	Me	2-Tol	24	98	86
7[e]	(*S*)-**92a**	Me	2-Tol	36	98	89
8	(*S*)-**92d**	Me	4-MeO-Ph	14	98	93
9[e]	(*S*)-**92e**	Me	2-MeO-Ph	36	42	84
10	(*S*)-**92f**	Me	1-Napht	36	72	79
11[e]	(*S*)-**92f**	Me	1-Napht	24	98	84
12	(*S*)-**92g**	Me	2-Napht	36	96	95

[a] 0.2 mmol substrate with 0.05 M in DME. [b] Isolated yield. [c] Determined by chiral HPLC [d] 1 mmol scale. [e] With (*S,S*)-[**L3**H][I] as ligand precursor. [f] No reaction.

Next, substrates having different alkyl groups at the benzylic position were investigated in a palladium-catalyzed arylation reaction and the results are summarized in Table 5. Interestingly, increasing the size of the alkyl group at the benzylic position of amide from Me, to Et, *i*-Pr and Bn led to sluggish reactions and lower enantioselectivities. This is particularly striking with R = *i*-Pr (**74b**), and indanyl substrate **89** where product *ee*'s of (*S*)-**93b** and (*S*)-**94** were the modest 50-60% *ee* range (entries 2, 4 and 5). Compared to the reactions in entries 1-3, which required up to 2 days to go to completion, the reaction of substrate **89**, affording the spirocyclic oxindole (*S*)-**94** was complete in <1 h at room temperature, and in 1.5 h at -20 ˚C (entries 4 and 5).

Table 5. Palladium catalyzed *α*-arylation of substrates **74a-c**, **89**.[a]

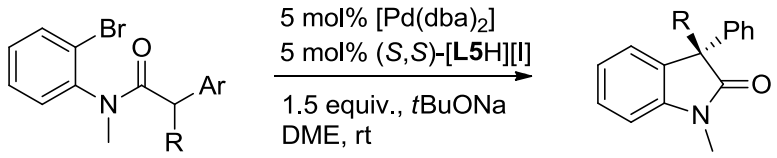

74a-c, 89 **93a-c, 94**

Entry	Product	Time (h)	Yield (%)[b]	Ee (%)[c]
1	(*S*)-**93a**	48	82	90
2	(*S*)-**93b**	48	80	52
3	(*S*)-**93c**	48	86	89
4	(*S*)-**94**	0.9	98	55
5[d]		1.5	98	59

[a] 0.2 mmol substrate with 0.05 M in DME. [b] Isolated yield. [c] Determined by chiral HPLC. [d] -20 ^{o}C.

Table 6 lists the results for the reactions of substrates with different substituents in the aniline part. Yields and enantioselectivities were generally very high for the substrates with

either electron-donating or electron-withdrawing substituents at C(5) or at C(6) positions (Table 6). Erosion of asymmetric induction was observed for the substrates bearing C(7) substituents. Thus, oxindoles (*S*)-**95c** and (*S*)-**95g** were obtained with 25% and 72% *ee*, respectively (Table 6, entries 3 and 7).

Table 6. Palladium catalyzed *α*-arylation of substrates **85a-g**.[a]

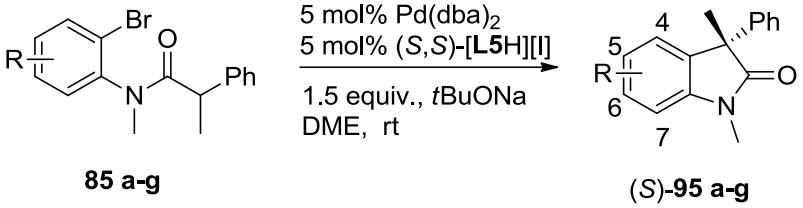

85 a-g (*S*)-**95 a-g**

Entry	Product	R	Time (h)	Yield (%)[b]	Ee (%)[c]
1	(*S*)-**95a**	C(5)-Me	24	98	95
2	(*S*)-**95b**	C(5)-*i*-Pr	24	98	92
3	(*S*)-**95c**	C(5,7)-Me	24	82	26
4	(*S*)-**95d**	C(6)-CF_3	48	98	95
5	(*S*)-**95e**	C(6)-F	48	96	94
6	(*S*)-**95f**	C(6)-OMe	24	98	95
7[d]	(*S*)-**95g**	C(7)-F	24	96	72

[a] 0.2 mmol substrate with 0.05 M in DME. [b] Isolated yield. [c] Determined by chiral HPLC. [d] At 50 ^{o}C.

Incorporation of C(7) substitution into a 6-membered ring structure re-established very high enantioselectivity of the product as shown in Scheme 44 for substrate **77** yielding the tricyclic oxindole (*S*)-**96** in 87% yield with 94% *ee*. All 22 examples above involve oxindoles with an aryl group at the newly formed stereogenic center. An exception is substrate **79** yielding oxindole **97**, albeit with a very modest *ee* of 40% attesting to the fact that the search for catalytic systems for this and a wider range of substrates is by no means over.

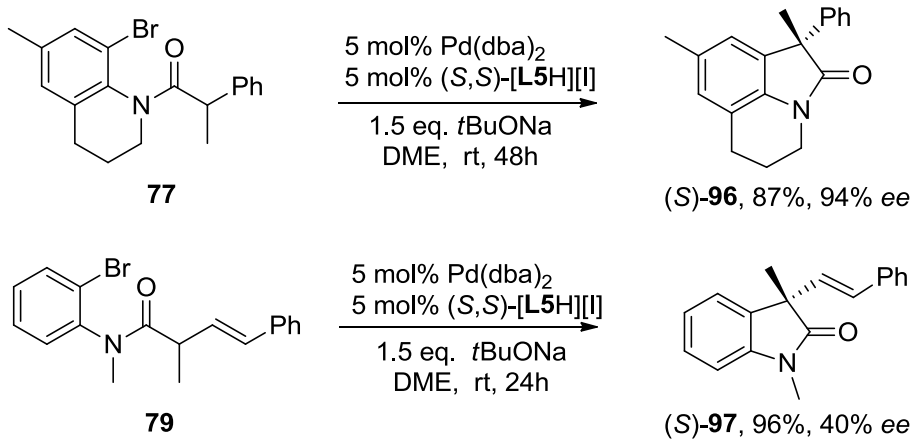

Scheme 44. Palladium catalyzed α-arylation of substrates **77** and **79**.

Finally, our attention was turned to aryl chloride substrates **75** and **84**. Mechanistic studies, performed by *Hartwig*,[60] showed that the reaction involves a rate-limiting oxidative addition of aryl halide. In accordance with the literature precedence for the oxidative addition step,[37,60] slightly higher reaction temperatures are required for aryl chlorides. Gratifyingly, for the aryl-chloride substrates **75** and **84** bearing different alkyl as well as aryl substituents at the benzylic position at 50 ˚C reactions occurred smoothly and because the asymmetric induction is lower than with the bromo-analogs, the values are still in the range between 84 and 91% *ee* (Table 7).

Table 7. Palladium catalyzed α-arylation of chloride-substrates **75** and **84**.[a]

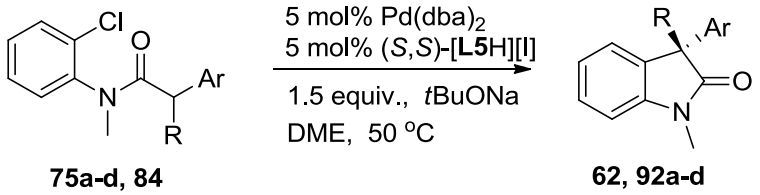

Entry	S.M.	R	Ar	Product	Time (h)	Yield (%)[b]	Ee (%)[c]
1	**84**	Me	Ph	(*S*)-**62**	24	98	90
2[d]	**84**	Me	Ph	(*S*)-**62**	48	21	94
3	**75a**	Me	4-Tol	(*S*)-**92a**	24	98	91
4	**75b**	Me	2-Napht	(*S*)-**92b**	24	98	91
5	**75c**	Et	Ph	(*S*)-**92c**	24	98	84
6	**75d**	Bn	Ph	(*S*)-**92d**	24	97	85

[a] 0.2 mmol substrate with 0.05 M in DME. [b] Isolated yield. [c] Determined by chiral HPLC. [d] At rt.

II.3.3.3. Determination of the Absolute Configuration of (*S*)-**90**.[114]

The absolute configuration of product (*S*)-**90** was determined *via* an X-ray crystal structure analysis of compound (*S*)-**98**. It was obtained by hydrogenolysis and bromination from (*S*)-**90** (Scheme 45). The X-ray structure of **98** showed it to have the *S* configuration (Figure 25). Assignment of other enantiomerically enriched oxindole products was made by analogy (comparison of CD spectra) and is tentative.

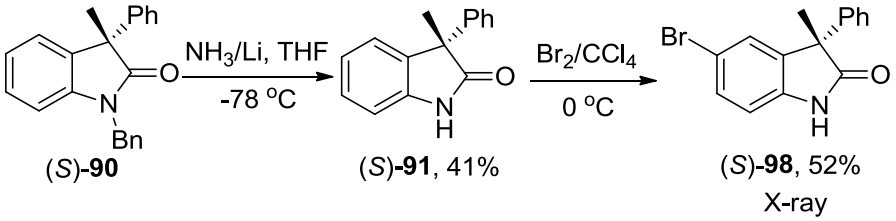

Scheme 45. Synthesis of (*S*)-**98**.

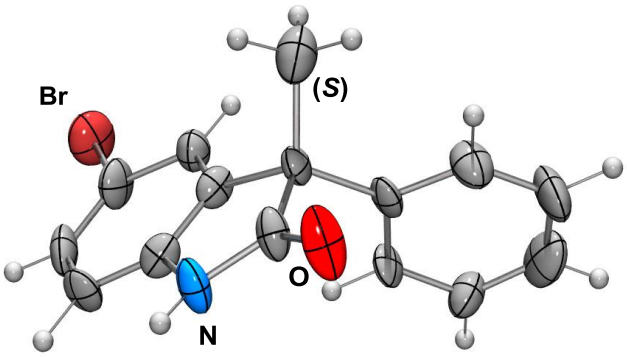

Figure 25. ORTEP-rendered structure of (*S*)-**98**.

II.3.4. Origin of Asymmetric Induction

The ligand screening (Table 1) helped us to ascertain the importance of the bulky *t*Bu groups and the *ortho*-aryl substituents (*o*-tolyl or *o*-anisol) at the stereogenic center. Seeking a rational for this finding, a Pd(*NHC*)-complex was prepared from $[Pd(allyl)Cl]_2$ (**99**), imidazolium salt (*S*,*S*)-[**L5**H][I] and *t*BuONa in DME according to the Scheme 46. After 24 h the complex (*S*,*S*)-**100** was obtained in high yield (83%). The ^{1}H-NMR spectrum of complex (*S*,*S*)-**100** is depicted in Figure 26. We noted the presence of two sets of proton signals. For example, the integration of the CH protons of the allyl group are in a ratio 1(red) : 0.9(blue). This led to the conclusion that we have a mixture of *exo*- and *endo*- isomers of complex (*S*,*S*)-**100** and they do not interconvert on the ^{1}H-NMR timescale.

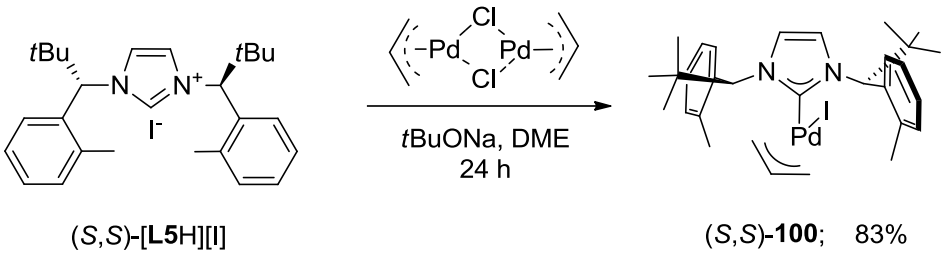

Scheme 46. Synthesis of chiral Pd-*NHC* complex (*S*,*S*)-**100**.

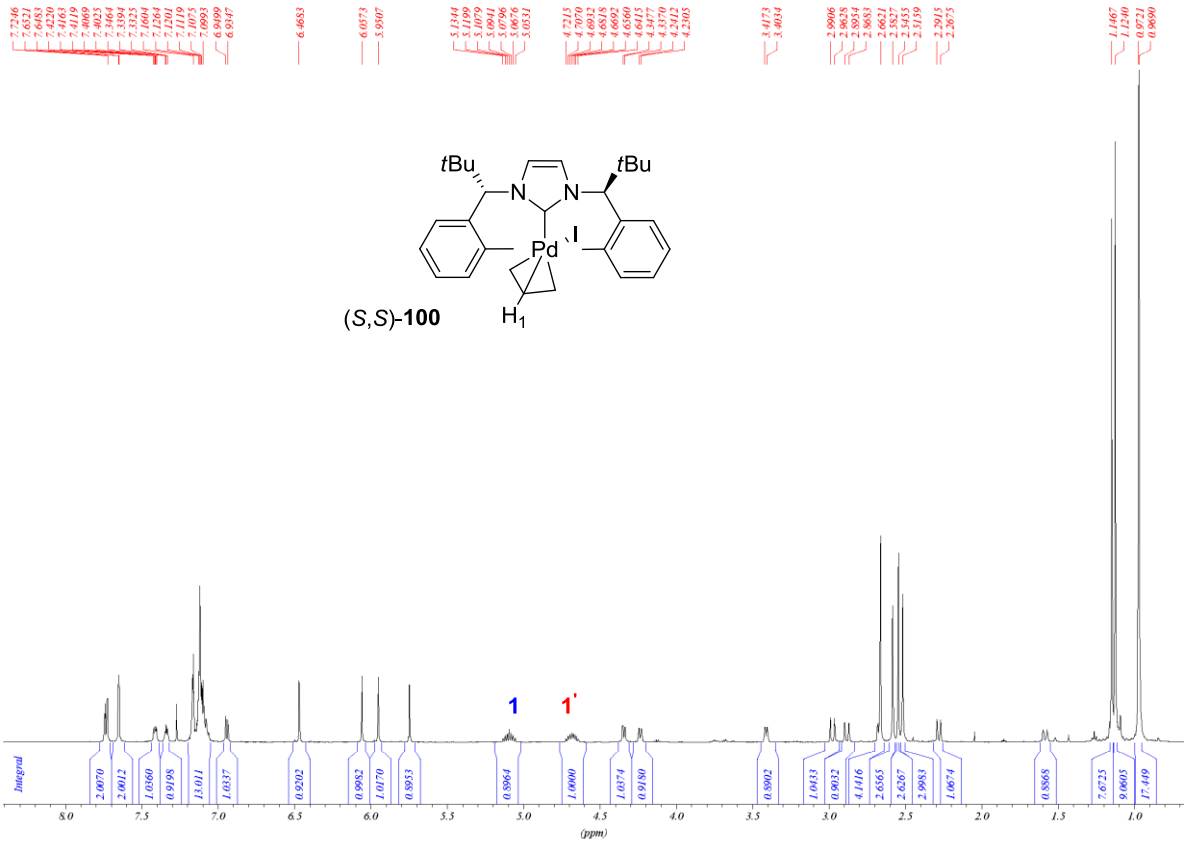

Figure 26. ^{1}H-NMR spectrum of complex (*S*,*S*)-**100**.

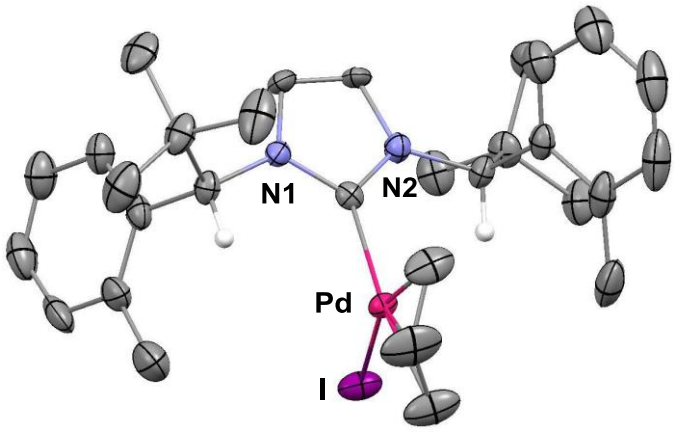

Figure 27. ORTEP structure of [Pd(η^{3}-allyl)(*S*.*S*-**100**)I] (*S*,*S*-**100**).

Recrystallization of complex (*S*,*S*)-**100**[iii] from pentane and acetone afforded crystals suitable for X-ray analysis (Figure 27).[168] In accordance with previous structures of [Pd(allyl(*NHC*)Cl] complexes, the structure of **100** is that of a distorted square planar Pd(II) complex, where one of the carbon atoms of the η^3-allyl group is in *trans* position to the iodide and the other one is in *trans* position to the *NHC* ligand. The Pd-C_{allyl} bond *trans* to the *NHC* ligand is 2.207 Å and that opposite to the iodide is 2.145 Å. The Pd-C_{NHC} bond is 2.044 Å. These values are in the typical range of those previously found in closely analogous complexes.[169]

Our interest then focussed on the chiral ligand and the role of the different ligand elements in generating the chiral site that led to high asymmetric induction. Figure 28 represents the ligand geometry with respect to the Pd-(*S*,*S*)-**L5** bond. For clarity, the allyl and iodide moieties have been left out. The large groups at the stereogenic centers enforce coplanarity of the C(ligand)-Pd bond/C-H bond of the stereogenic center. Rotation around the N-C (stereogenic center) would lead to an increase of allylic strain.[170-172] This fixes the aryl groups in space. Moreover, their orientation is determined by the aryl *o*-substituent (*o*-Me substituents). Again, minimization of $A^{1,3}$-strain is at play and as can be seen in Figure 28, the C(Ar)-CH_3 bond is coplanar with the C-H bond of the stereogenic center. Note that rotating the aryl groups by 180 ^{o} would lead to a situation where the Me groups would enter into conflict with the *t*Bu groups. Thus, the chiral information is transferred from the stereogenic benzylic centers through the *o*-aryl substituents to the palladium center.

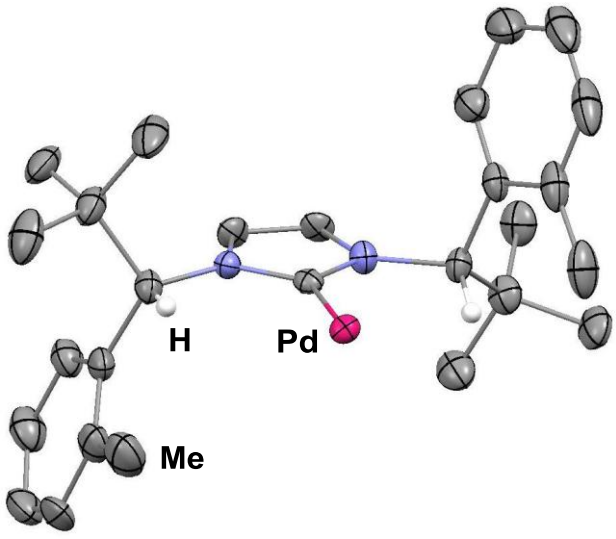

Figure 28. Stereochemical arrangement of key elements in Pd-(*S*,*S*-**L5**) (From the X-ray of complex **100**).

[iii] In 2009 the group of *Stahl* reported the synthesis of the chloro analog of **100**. It was not fully characterized but used directly in a protolytic allyl removal reaction to give the chloro bridged dimer which reacted with silver carboxylates to yield the cyclometallated complex (X-ray).

At this stage, it was particularly interesting to investigate the thermal stability of Pd-(*S*,*S*)-**L5** complex and behavior of stereocontrol elements under different temperature, thus to evaluate the potential utility of complex **100** in catalysis. For that, the ^{1}H-NMR spectrum of complex **100** was measured at different temperatures and the results are depicted in figure 29. d_6-DMSO was used as a solvent. It is clear to see that two CH-allylic proton signals of the isomers of (*S*,*S*)-**100** at 423K are converted to one broad singlet, which could be explained by interconversion of *endo*- and *exo*-isomers of Pd-(*S*,*S*)-**L5** complex. Several mechanisms of apparent allyl rotation have been proposed involving: 1) the π-σ-π isomerization with rotation around the palladium-carbon bond in the η^1-complexe-intermediate[173-175]; 2) the effect of the catalytic amount of anions or polar solvents leading to the formation of 'pentacoordinated' complex, that undergoes geometrical changes *via* switching positions of two ligands (*NHC* and iodine)[174,176,177]; 3) the dissociation of one of the ligands (*NHC* or iodine) to form tricoordinated intermediate[175,178]. Similar picture is observed with the *t*Bu as well as *o*-Me groups of the ligand precursor. Notably, even at 423K complex (*S*,*S*)-**100** showed high stability.[iv]

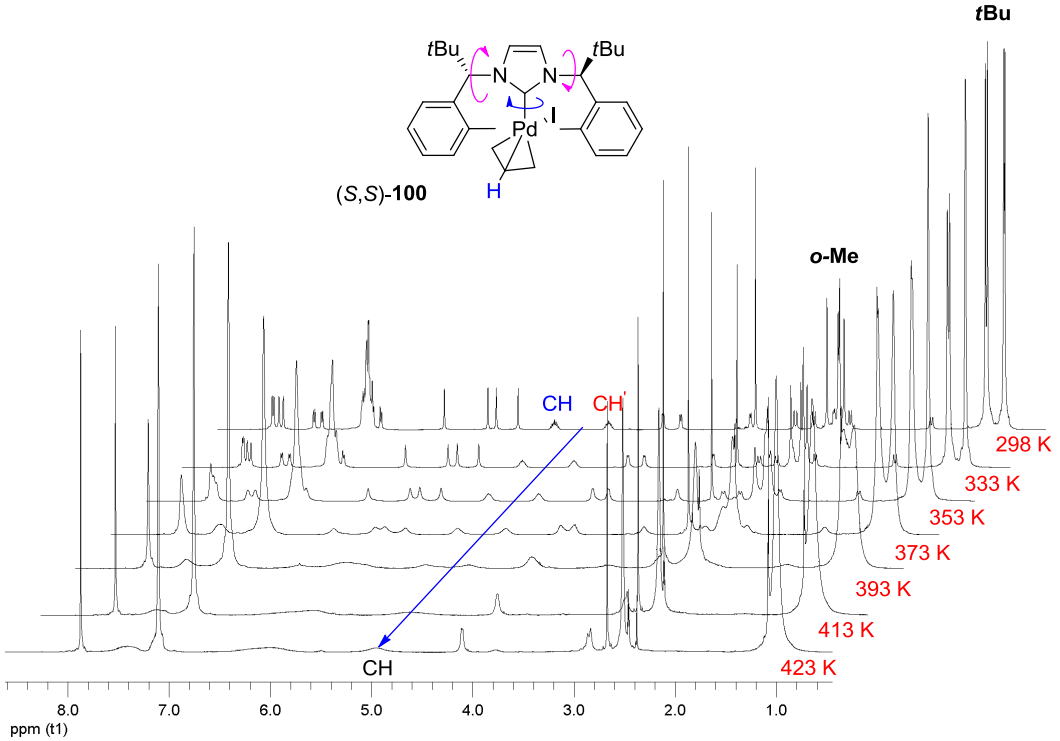

Figure 29. ^{1}H-NMR investigation of complex (*S*,*S*)-**100** at different temperatures.

[iv] The ^{1}H-NMR spectrum showed there was no decomposition of complex (*S*,*S*)-**100** after cooling the solution from 423K to 273K.

Overall, the ligand, when coordinated to palladium (II) adopts a C_2 symmetric chiral structure. The X-ray structure of the imidazolium salt (*R*,*R*)-[**L5**H][I] is different in that both *t*Bu groups in one hemisphere and the aryl groups in the other (Figure 30). The H atoms at the stereogenic centers again are coplanar with the imidazolium ring but in the absence of the large Pd two orientations are possible and one of them is shown in the solid state structure (Figure 30).[114]

The buried volume (%V_{bur}) for ligand **L5** is 37.4 %.[v,179] This, places this ligand in the midst of %V_{bur}'s of common *NHC* ligands (such IMes). It's %V_{bur} far below the value of ~50 % reported for chiral *NHC* ligands by the *Glorius* group and which provided excellent results in the enantioselective arylation of amides.[37] We conclude that exceptional bulk may help but it is not a necessary requirement. Less bulky ligands can give high asymmetric induction provided that their stereodirecting groups are placed judiciously. Our results with ligands (*S*,*S*)-[**L5**H][I] and (*S*,*S*)-[**L9**H][I] attest to this.

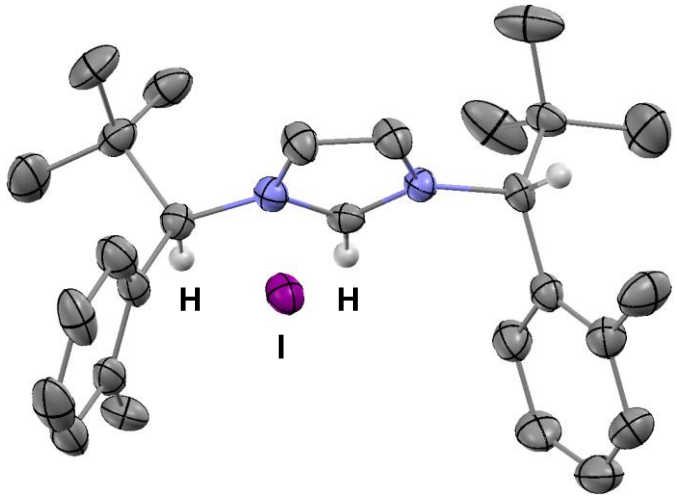

Figure 30. ORTEP structure of (*R*,*R*)-[**L5**H][I].

II.3.5. Mechanistic Studies of Pd(NHC)-Catalyzed α-Arylation Reaction

II.3.5.1. Analysis of the Catalytic Cycle

The mechanism proposed by *Hartwig* for the synthesis of oxindoles by Pd-catalyzed *α*-arylation involves the oxidative addition of the aryl halide, followed by formation of arylpalladium amide enolate in the presence of a base and then the reductive elimination step.[60] Additionally, the *authors* isolated and spectroscopically characterized the intermediate

[v] Calculated using SambVca with the standard parameters: radius of sphere 3.5 Å, distance from sphere 2.1 Å, mesh step 0.05 Å. https://www.molnac.unisa.it/OMtools/sambvca.php

after the oxidative addition, which was proved to be rate-determining step. Based on this fact, the catalytic cycle for *NHC*-Pd-catalyzed cyclization to form oxindoles was proposed and shown in Scheme 47.

In our previous studies on transformation **61** → **62**, we used an *in situ* procedure to generate the chiral Pd(0)*NHC** catalysts. Generation of [Pd(0)**L5**] involved treating a mixture of $Pd(dba)_2$ and the imidazolium iodide [(*S*,*S*)-**L5**H][I] in dimethoxyethane with *t*BuONa. An excess of the base was used, which then generated the amide enolate from the initially formed palladacycle (*S*,*S*)-**101** (Scheme 47).

This catalytic cycle was submitted to DFT analysis (*vide infra*). To verify the kinetic law for the arylation reaction and to compare the reactivity of catalysts with different *NHC* ligands, few experiments were conducted. The use of *in situ* catalyst procedure was compared to that of preformed by Pd-*NHC** catalyst precursors. For this purpose a series of preformed complexes were prepared.

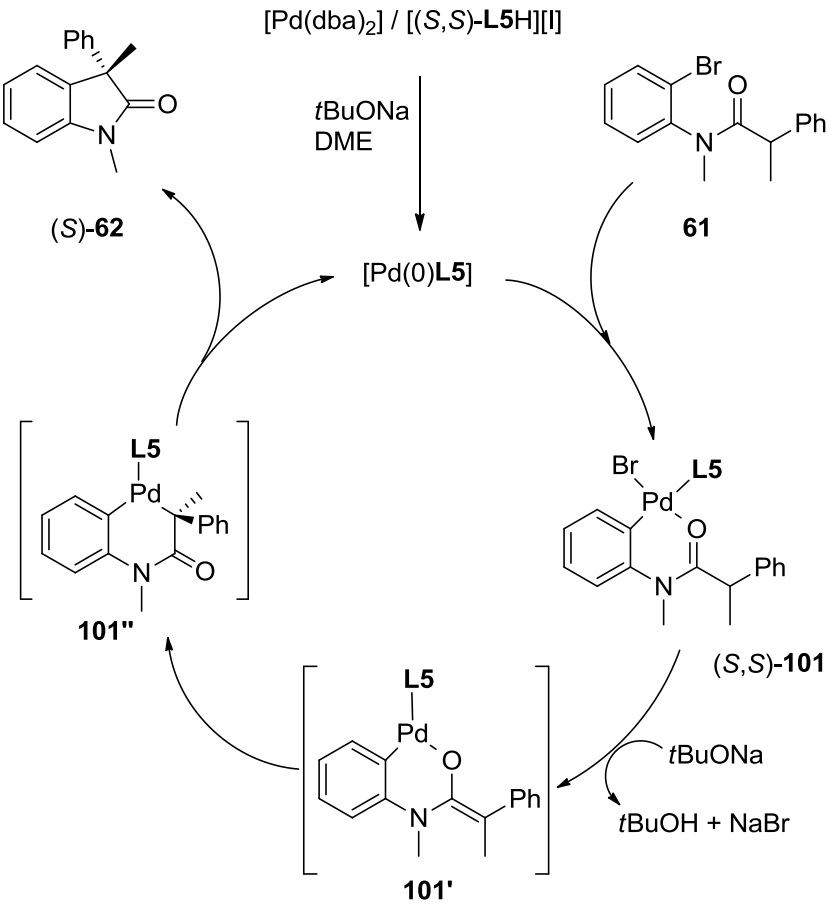

Scheme 47. Catalytic asymmetric intramolecular arylation of anilides.

Nolan showed that a simple modification of the allyl moiety in Pd-allyl complexes dramatically influences the catalytic performance of *Suzuki-Miyaura* cross-coupling

reactions.[180] For example, by increasing steric bulkiness at the terminal allyl group, the active catalytic Pd(0)*NHC* species formed more rapidly.

The synthesis of the precatalyst (*S*,*S*)-**102** were straightforward according to the similar procedure as for the preparation of (*S*,*S*)-**100** reacting $[Pd(cinnamyl)Cl]_2$ dimer with imidazolium salt (*S*,*S*)-[**L5**H][I] in the presence of *t*BuONa as a base for generation free *NHC*. The reaction was carried out in DME at room temperature producing highly air and moisture stable complex (*S*,*S*)-**102** in high yield (89%) (Scheme 48).

In order to isolate palladacycle (*S*,*S*)-**101** and further use it as a precatalyst, the stoichiometric oxidative addition of aryl bromide **61**, chiral imidazolium salt [(*S*,*S*)-**L5**H][I], $Pd(dba)_2$ and *t*BuONa as a base for the *in situ* generation of Pd(II)(*NHC*) was performed. The reaction was carried out in DME at room temperature and complete consumption of **61** was achieved in 18 h giving complex (*S*,*S*)-**101** as a 1:1 mixture of diastereoisomers in total 60% yield (Scheme 48).

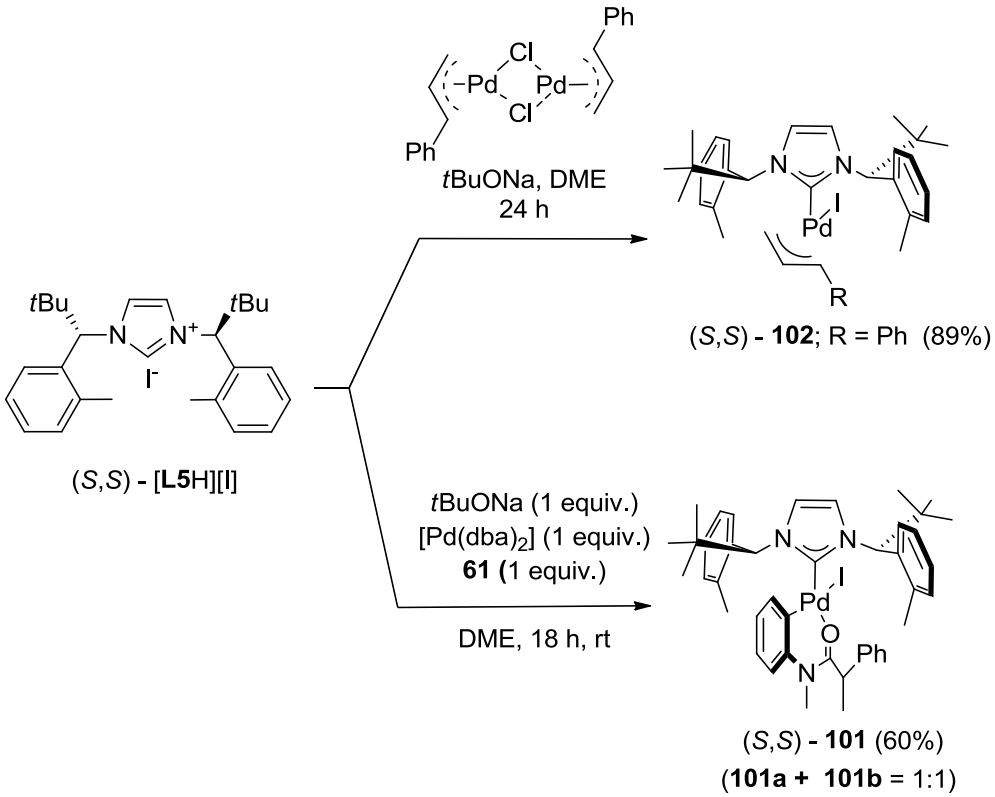

Scheme 48. Synthesis of chiral Pd(*NHC*) complexes.

Table 8 summarizes the results of the reaction depicted in Table 1 (page 43). The catalytic activity of **100**-**102** was compared to the original *in situ* procedure. The reaction using *in situ* generation of the catalyst was monitored by GC. This showed complete conversion of starting material to oxindole **62** in 4 h (Table 8, entry 1). The reactions carried

out with (*S*,*S*)-**100** in the presence of *t*BuONa showed very poor conversion at room temperature (entry 2). In the reaction with (*S*,*S*)-**100**, *t*BuONa first serves as nucleophile to convert the allyl to a more labile alkene ligand. After oxidative addition, *t*BuONa acts as base to generate the enolate. Cinnamyl complex (*S*,*S*)-**102** behaved analogously, even though it was subjected to milder conditions (entry 3). Raising the temperature to 50 ˚C in this case led to the formation of oxindole (*S*)-**62** in a quantitative yield in 48 h with 90% enantioselectivity (entry 4). The use of *t*BuOK proved to be more efficient as shown in entries 5 and 6 but the reaction is still less efficient than the *in situ* procedure. The enolate formation, rearrangement of the *O*-enolate to the *C*-enolate and reductive elimination (Scheme 47) are thus faster than the oxidative addition confirming *Hartwig's* finding that the oxidative addition is the rate-limiting step in the Pd-catalyzed *α*-arylation reaction.[60]

Table 8. Intramolecular arylation of anilide **61** using ether *in situ* generated or preformed Pd(0)-(*S*,*S*)-**L5** catalyst.

Entry[a]	Cat.(5 mol%)	Base (1,5 equiv.)	Time (h)	Yield (%)[b]	Ee (%)[c]
1[d]	*in situ*	*t*BuONa	4	99	94
2	(*S*,*S*)-**100**	*t*BuONa	24	<10	94
3	(*S*,*S*)-**102**	*t*BuONa	24	<10	94
4[e]	(*S*,*S*)-**102**	*t*BuONa	48	99	90
5	(*S*,*S*)-**100**	*t*BuOK	24	98	94
6	(*S*,*S*)-**102**	*t*BuOK	24	98	94
7	(*S*,*S*)-**101**	*t*BuONa	24	65	94
8[f]	(*S*,*S*)-**101**	*t*BuONa	1.5	99	94

[a] 0.2 mmol substrate, 0.05 M in DME, 25°C. [b] Isolated yield. [c] The enantiomeric ratio was determined by chiral HPLC. [d] 5 mol% (*S*,*S*)-[**L5**H][I], 5 mol% $Pd(dba)_2$. [e] At 50˚C. [f] Reaction performed with dba (10 mol%).

Surprisingly, the palladacyle (*S*,*S*)-**101** was a poor performer as a catalyst. After 24 h only 65% conversion of starting material was achieved (entry 7). A clue here was the observation of some catalyst decomposition as indicated by the formation of palladium black. Adding the dba restored catalyst lifetime and under these conditions the original *in situ* procedure could be improved (entry 8). Possibly, that the ligand coordinates to palladium

prior to the reductive elimination and stabilises Pd(0)(*NHC*) active species before the oxidative addition step. This fact led us to the investigation of the additives (Figure 31a).

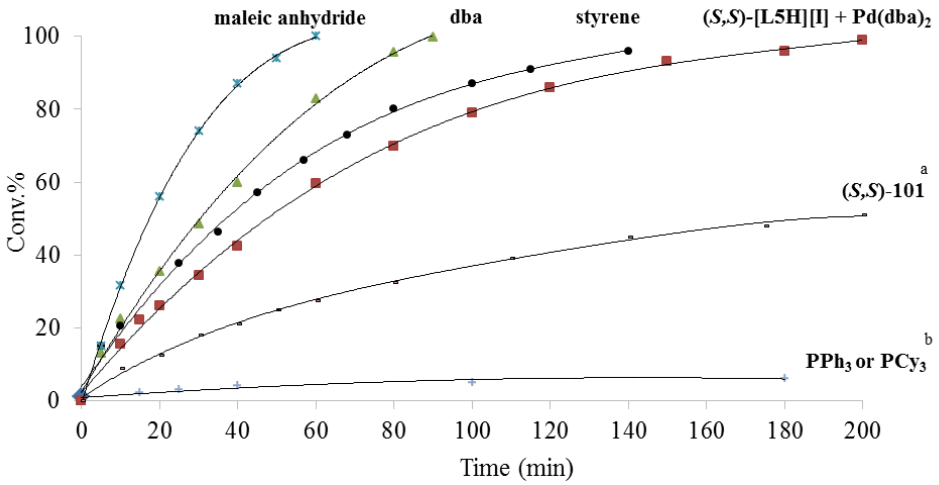

a) Effect of additives on the Pd(0)-(*S*,*S*)-**L5**-catalyzed *α*-arylation of amide **61**.

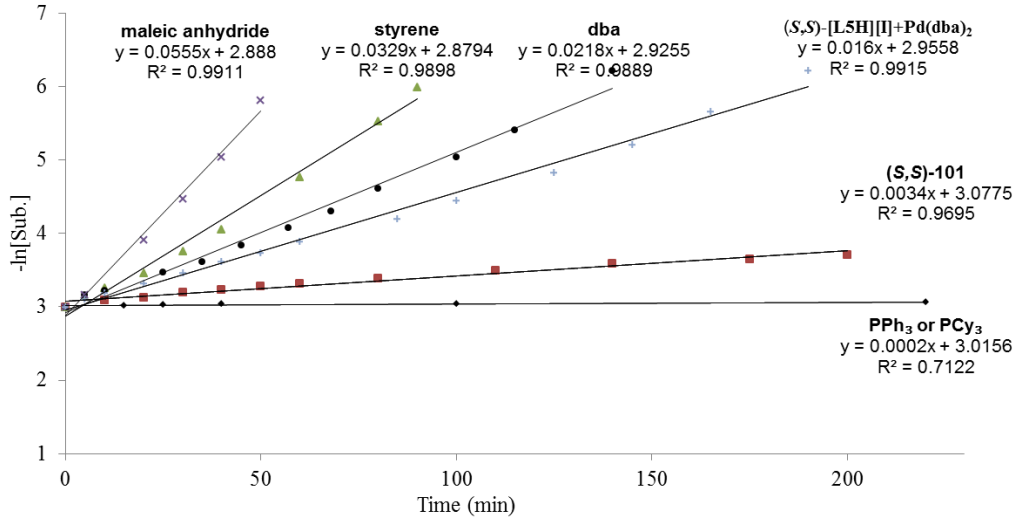

b) Relationship between –ln[sub.**61**] and the reaction time.

Reaction conditions: C[Sub **61**]$_0$ = 0.05M, (*S*,*S*)-**101** 5 mol%, additive (10 mol%), *t*BuONa (1.5 equiv.), DME, rt. Reaction was monitored by GC using decane as internal standard. In all reactions the oxindole (*S*)-**62** formed in 94% *ee*. [a] 65% conversion of **61** after 24 h. [b] 7% conversion of **61** after 24 h.

Figure 31.

Not unexpectedly, P(III)-containing-ligands (PPh_3, PCy_3) interrupted the catalytic cycle whereas alkenes rendered the process more efficient in the following order: styrene < dba < maleic anhydride. In the presence of the alkenes (10 mol%), the half live ($t_{1/2}$) of the first order reaction was 39 min (styrene), 30 min (dba), and 19 min (maleic anhydride). This sequence is in agreement with the DFT studies carried out by *Maseras* and *Espinet* [181,182].

These investigations showed that electron-deficient olefins are able to coordinate to palladium, thus decreasing the activation energy barrier of the reductive elimination step.

As shown in Figure 31b, plots of –ln[sub.**61**] *vs* reaction time are linear and it could be concluded that these reactions are first order with respect to the substrate.

As maleic anhydride was found to be the best additive, the effects of the reaction concentration and the catalyst loading were next investigated and the results are depicted in Figure 32. Initially the catalyst loading was reduced to 2.5 mol% (*S*,*S*)-**101** and the reaction carried out at 0.05 M concentration in the presence of 5 mol% maleic anhydride as an additive. Complete conversion of the amide **61** was found in 340 minutes. When the concentration of the reaction was increased to 0.4 M and after to 0.8 M using 2.5 mol% of (*S*,*S*)-**101** the reaction time was improved to 120 minutes. Thereby, the rate of the reaction strongly depends from the concentration of the substrate in solution.

Finally, the catalyst loading was reduced to 0.5 mol% with [**61**] = 0.8 M, 1 mol% maleic anhydride (reaction time 48 h). This produced 78% conversion of starting material (**61**) and a TON of 156.

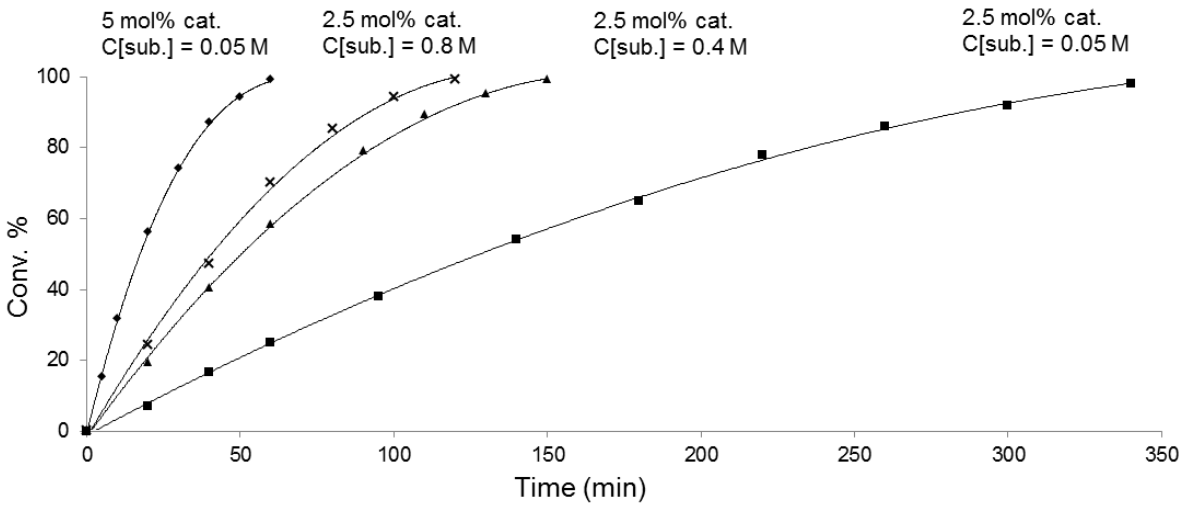

Reaction conditions: C[Sub **61**] = x M, Cat. (*S*,*S*)-**101** y mol%, maleic anhydride (10 mol%), *t*BuONa (1.5 equiv.), DME, rt. Reaction was monitored by GC using decane as internal standard. In all reactions the oxindole (*S*)-**62** formed in 94% *ee*.

Figure 32. Effect of reaction concenration on catalyst loading in Pd-catalyzed *α*-arylation of amide **61**.

II.3.5.2. Structure of Palladacycles (S,S)-101a and (S,S)-101b

The diastereoisomers **101a** and **101b** were carefully separated by column chromatography and were fully characterized. The ^{1}H-NMR spectroscopy investigation revealed that in complex (*S*,*S*)-**101b** one of the *o*-methyl group of *NHC* ligand interacts with the aromatic system of the substrate and is strongly deshielded (for (*S*,*S*)-**101a** is 2.03 ppm, for (*S*,*S*)-**101b**: 2.98 ppm). In the ^{13}C-NMR spectra the carbene carbon atom (N-C-N) appears in the range of 170.0-180.0 ppm. which is in agreement with the previously reported, closely analogous complexes.[59]

Crystals of both diastereoisomers suitable for X-ray analysis were grown by vapor diffusion of pentane into acetone solutions. ORTEP diagrams are shown in Figure 33. (*S*,*S*)-**101a** and (*S*,*S*)-**101b** are slightly distorted square planar Pd(II)(*NHC*) complexes with the iodide *trans* to the substrate aryl and the amide *trans* to the *NHC* ligand. The O-Pd-C_{NHC} angle in (*S*,*S*)-**101a** is 169.05˚, and in (*S*,*S*)-**101b** it is 173.42˚. The Pd-C_{NHC} bond length in palladacycle (*S*,*S*)-**101a** is 1.951 Å and in (*S*,*S*)-**101b** it is 1.967 Å. These distances are in the range of previously reported Pd(II)(*NHC*) complexes.[169] The minimization of allylic strain ($A^{1,3}$), both in the Pd-C-N-C-H and also in H-$C_{benzylic}$-C_{Ar}-C_{ortho}-CH_3 parts of the ligand fix the aryl stereocontrol elements of the *NHC* ligand in the complex (Figure 33).

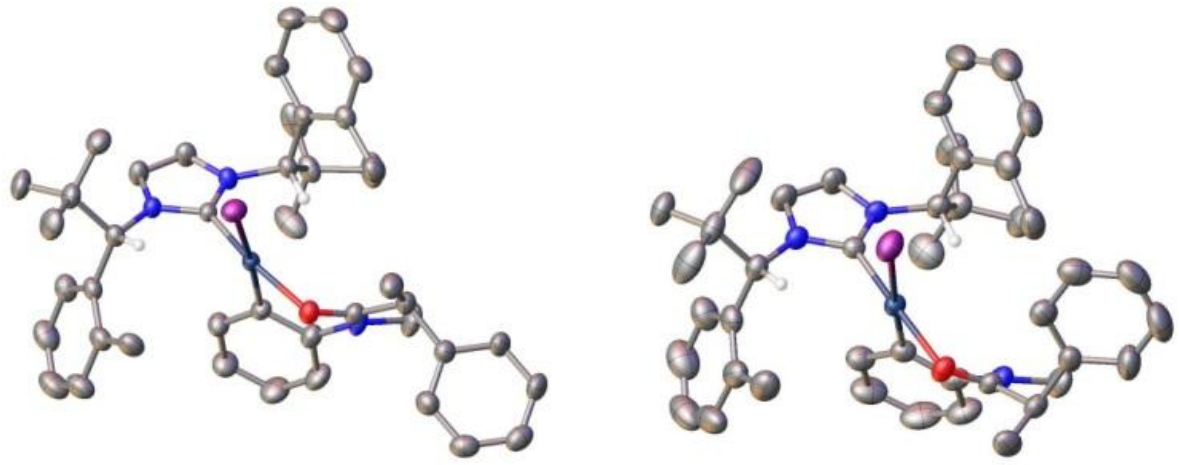

(*S*,*S*)-**101a** (*S*,*S*)-**101b**

Figure 33. ORTEP diagrams of palladacycles (*S*,*S*)-**101a** and (*S*,*S*)-**101b** (50% Probability level for the thermal ellipsoids). All H-atoms except those on the stereogenic centers have been omitted for clarity.

Chiral induction from the palladacycle (*S*,*S*)-**101** may occur during the Pd-*O*-enolate to Pd-*C*-enolate rearrangement (Scheme 47) or during the reductive elimination step. The

process may also be influenced by different rates of deprotonation of the two diastereoisomers (*S*,*S*)-**101a** and (*S*,*S*)-**101b** (Scheme 47).

II.3.6. Synthesis of New Chiral N-Heterocyclic Carbene Ligands

Based on the X-ray analysis of complexes bearing **L5** (discussed above) we hypothesized that the substitution of the *ortho*-Me groups by fused aromatic rings, as depicted in Figure 34 (1-naphthyl derived *NHC* ligand is shown), could make Pd-*NHC* complexes even much better in terms of asymmetric induction.

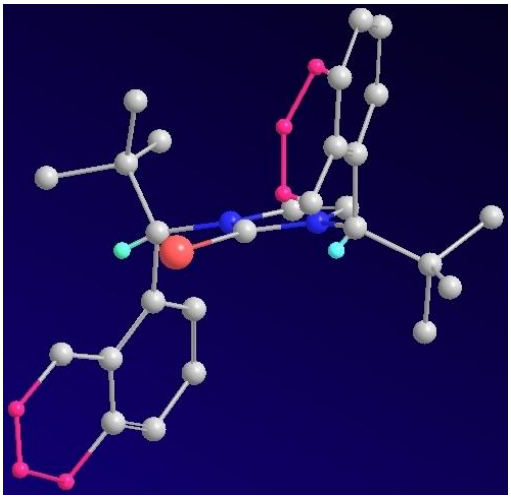

Figure 34. Part of the X-ray of (*S*,*S*)-**L5** showing the Pd-*NHC* ligand arrangement. In pink, the modeled modification of the ligand in which a napthyl fragment is used to extend the aryl plane.

II.3.6.1. Synthesis of Chiral Amines

The synthesis of enantiopure amines **104** and **105** is shown in Scheme 48. Alkylation of corresponding napthonitriles (**103a** or **103b**) with *t*BuMgCl in the presence of a catalytic amount of CuBr followed by *in situ* reduction with $NaBH_4$ afforded (*rac*)-**104** and (*rac*)-**105** in good yields. (*Rac*)-**104** was resolved by forming a diastereoisomeric salt with (*L*)-malic acid in a mixture of isopropanol and ethyl acetate. Other chiral acids (*N*-acetyl leucine, mandelic acid and tartaric acid) showed poor performance as resolving agents.

The (*S*,*S*)-salt of malic acid/**104** crystallized preferentially (6:94 d.r.) and a second recrystallization furnished, after hydrolysis, the amine (*S*)-**104** in 38% overall yield (max.= 50%) and >99% *ee*. For the resolution of amine **105** (*L*)-tartaric acid was found to give the best results. After two recrystallizations of the (*R*,*R*)-salt of tartaric acid/**105** in ethanol and amine recovery, (*R*)-**105** was obtained in 36% overall yield and 99% *ee*.

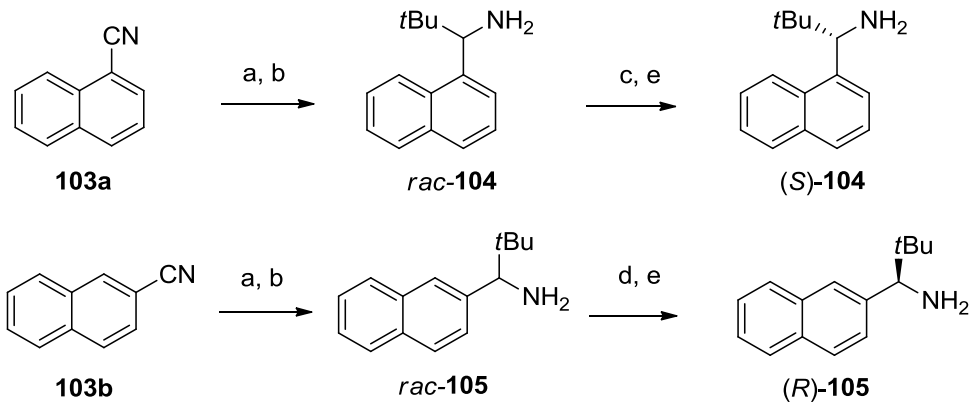

Reagents and conditions: (a) *t*BuMgCl, CuBr (cat.), Et_2O, reflux 24 h; (b) $NaBH_4$, MeOH, -78 to 25 °C, 16 h; *rac*-**104** (65%); *rac*-**105** (76%) (c) (*L*)-maleic acid, *i*-PrOH/EtOAc; (d) *L*(+)-tartaric acid, EtOH; (e) 1M NaOH, Et_2O; (*S*)-**104** (38%), (*R*)-**105** (36%).

Scheme 48. Synthesis of chiral amines (*S*)-**104** and (*R*)-**105**.

II.3.6.2. Synthesis of Imidazolium and Dihydroimidazolium Salts

With the chiral amines in hand, next, the imidazolium salts (*S*,*S*)-[**14**H][I] and (*R*,*R*)-[**L15**H][I] were prepared according to literature methods.[37,44,114] The chiral amines were condensed with glyoxal and the resulting diimines (purified before by crystallization from MeOH) were reacted with chloromethylpivalate in the presence of silver triflate to form the imidazolium triflates. Anion exchange to the corresponding iodides was done with the help of sodium iodide that gave solid products instead of oily triflate salts. Overall, this procedure is quite simple and no further purification of intermediates is needed. The product yields were modest (Scheme 49).

For the synthesis of dihydroimidazolium salts [(*S*,*S*)-**L16**H][I] and [(*R*,*R*)-**L17**H][I] the diimines were reduced with $LiAlH_4$ to the corresponding diamines. Ring-closure was carried out according to the standard procedure with triethyl orthoformate and NH_4BF_4. This afforded the tetrafluoroborate dihydroimidazolium salts. Anion exchange BF_4^-/I^- afforded dihydroimidazolium iodide salts in high yields (Scheme 49).

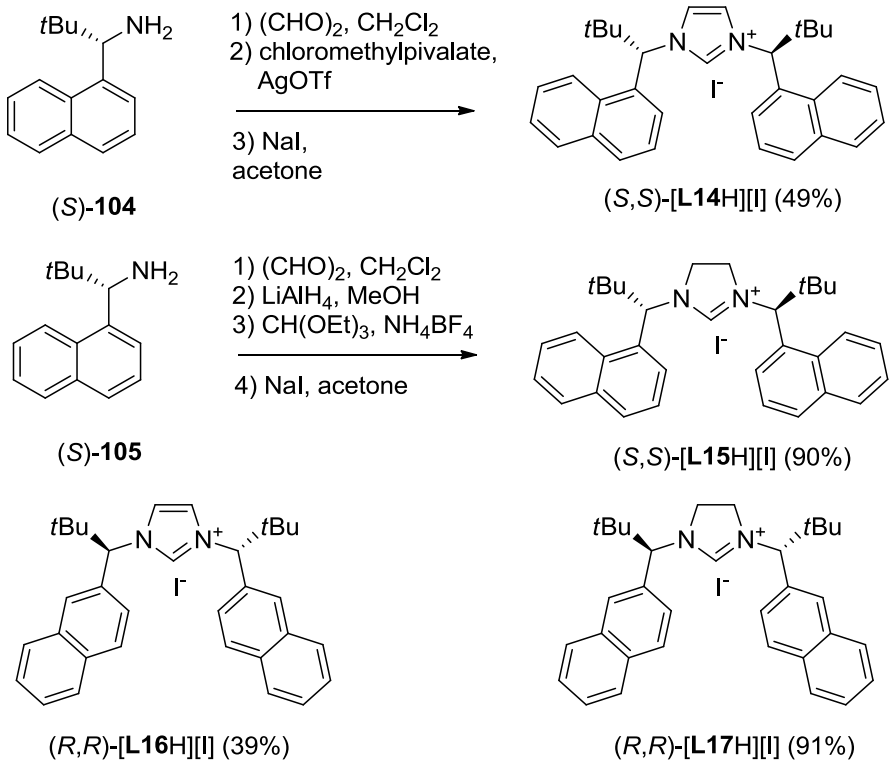

Scheme 49. Synthesis of imidazolium and dihydroimidazolium ligand precursors.

II.3.7. Synthesis of Spirooxindoles

II.3.7.1. Optimization of Reaction Conditions

We began our study by examining new ligand precursor (*S*,*S*)-[**L14**H][I] in the palladium-catalyzed α-arylation reaction under previously established reaction conditions.

Analisis of Table 9 reveals that ligand (*S*,*S*)-[**L14**H][I] gave identical or slightly better yields than reactions with (*S*,*S*)-[**L5**H][I] and it outperformed this ligand in asymmetric induction by 2-3% *ee* a significant improvement in the 90-95% *ee* range. Interestingly, new ligand (*S*,*S*)-[**L14**H][I] produced spirooxindole (*S*)-**94** containing fused five-membered ring at the benzylic position with a improved selectivity (Table 9, entry 5). This result allowed us to have a direct access to enantioenriched spirooxindole.

Table 9. Palladium(*NHC*)-catalyzed *α*-arylation of amides.

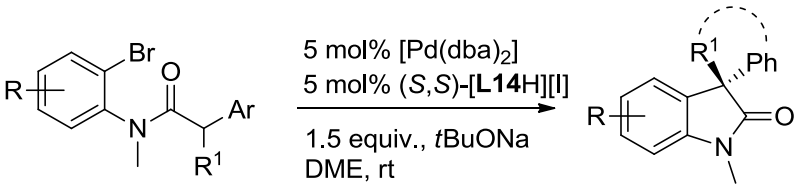

Entry[a]	Product	Ligand	Time (h)	Yield (%)[b]	Ee (%)[c]
1	(*S*)-**62** 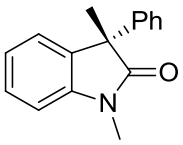	(*S*,*S*)-[**L14**H][I]	24	99	96
2	(*S*)-**95f** 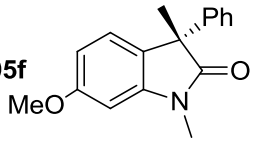	(*S*,*S*)-[**L14**H][I]	24	99	97
3	(*S*)-**95e** 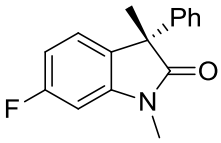	(*S*,*S*)-[**L14**H][I]	24	97	96
4	(*S*)-**93c** 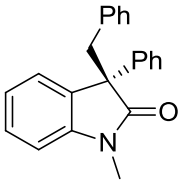	(*S*,*S*)-[**L14**H][I]	24	85	93
5	(*S*)-**94** 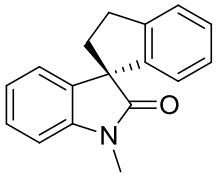	(*S*,*S*)-[**L14**H][I]	20 min	99	81

[a] 0.2 mmol substrate, 0.05 M in DME. [b] Isolated yield. [c] The enantiomeric ratio was determined by chiral HPLC.

In order to improve our results we next investigated *NHC*s bearing *β*-naphthyl substituents at the benzylic positions. However, minor modification of the position of the napthyl group in the imidazolium salt dramatically decreased the enantioselectivity of the spirooxindole (*R*,*R*)-[**L16**H][I] to 29% *ee* (Table 10, entry 6). The dihydroimidazolium salts (*S*,*S*)-[**L15**H][I] and (*R*,*R*)-[**L17**H][I] afforded the product in modest *ee*'s of 64% and 39%, respectively (entries 5 and 7). The ligand (*R*,*R*)-[**L12**H][I] which was found previously more efficient in 3-amino and 3-alkoxyoxindole synthesis,[115] produces **94** in high yield but essentially as racemic product (entry 8).

Table 10. Palladium(*NHC*)-catalyzed *α*-arylation of **89**.

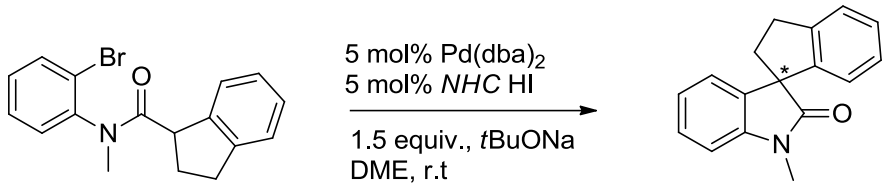

89 **94**

Entry[a]	Ligand	Time (min)	Yield (%)[b]	Ee (%)[c]
1	(*S*,*S*)-[**L5**H][I]	20	98	55
2	(*S*,*S*)-[**L14**H][I]	20	99	81
3[d]	(*S*,*S*)-[**L14**H][I]	24 h	60	70
4[e]	(*S*,*S*)-[**L14**H][I]	24 h	80	80
5	(*S*,*S*)-[**L15**H][I]	20	96	64
6	(*R*,*R*)-[**L16**H][I]	20	97	-29
7	(*R*,*R*)-[**L17**H][I]	20	99	-39
8	(*R*,*R*)-[**L12**H][I]	40	99	-4

[a] 0.2 mmol substrate, 0.05 M in DME. [b] Isolated yield. [c] The enantiomeric ratio was determined by HPLC. [d] Toluene was used as a solvent. [e] $[Pd(allyl)Cl]_2$ was used as a precatalyst.

The imidazolium salt (*S*,*S*)-[**L14**H][I] was found to be the most efficient chiral ligand in this reaction. Changing the solvent to toluene and using (*S*,*S*)-[**L14**H][I] strongly effects on both the yield and enantioselectivity of **94** (entry 3). Switching from $Pd(dba)_2$ to $[Pd(allyl)Cl]_2$ gave an identical enantioselectivity of product **94** but in lower chemical yield (entry 4). Moreover in the last two cases the reaction time had to be increased up to 24 h (entries 3 and 4).

II.3.7.2 Synthesis of Substrates

The synthesis of amides for the enantioselective Pd(*NHC*)-catalyzed *α*-arylation reaction was carried out according to the procedure depicted in Scheme 50. Notably, phenylacetic acids for the synthesis of amides were easily prepared from corresponding commercially available aryl ketones using procedure developed by *Belletire* (Scheme 50).[183] Thereby, using this protocol a range of amides bearing different substituents in aniline part

and different *N*-protecting groups was prepared in good to excellent yields. Additionally, few amides with different size of cycloalkyl groups were synthesized (Scheme 50).

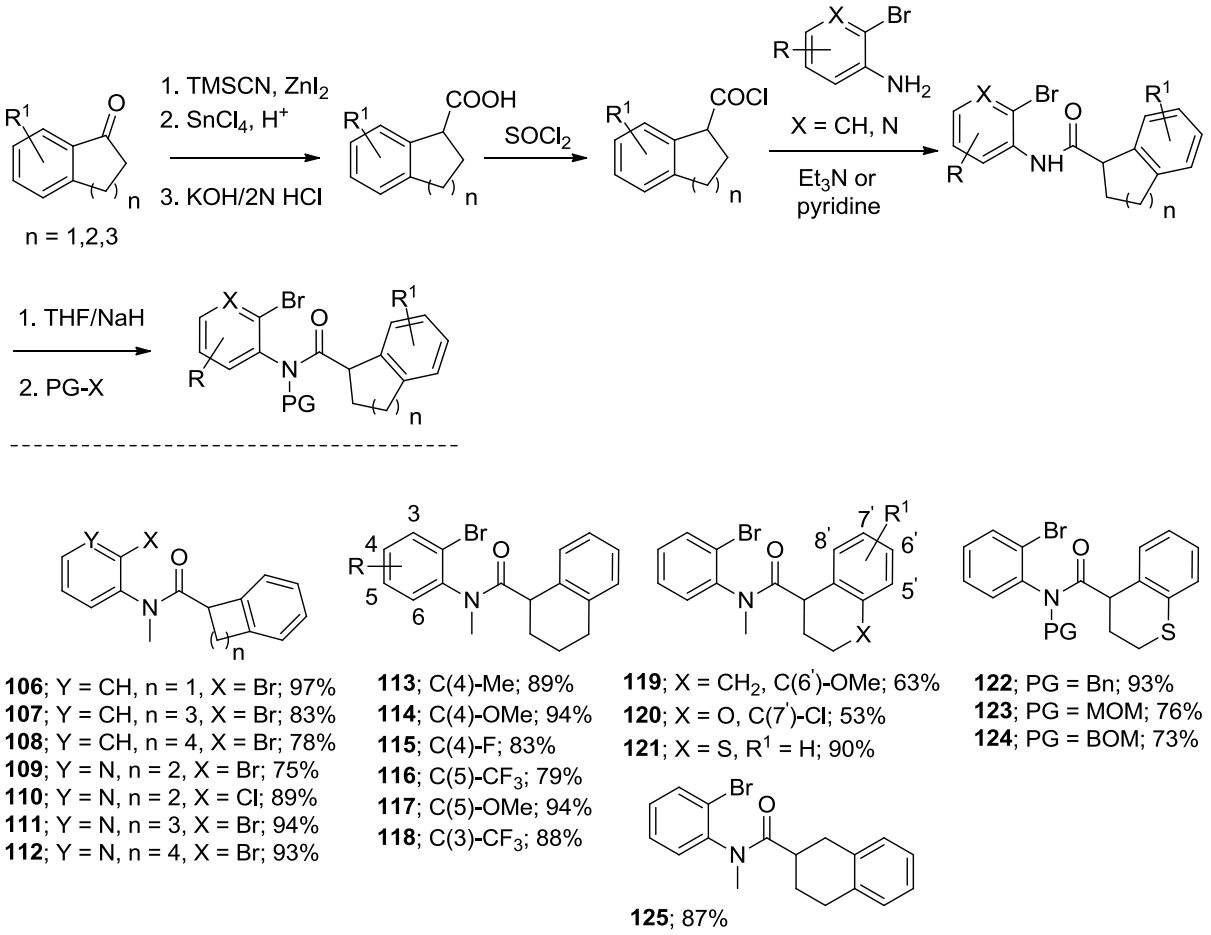

Scheme 50. General procedure for the synthesis of amides. Yields given are over the last 3 steps.

II.3.7.3. Catalysis

The optimized reaction conditions were applied to substrates leading to a range of spirocyclic products (Tables 11-13). Table 11 lists the results of the influence of a size of the fused ring at the benzylic position on the yield and enantioselectivity. We were pleased to find that the reaction is not only limited with amides containing a 5-membered but also produced spirocyclic structures with 6- and 7-membered fused ring system in high yields and enantioselectivities (Table 11, entries 4 and 5). An exception was spirooxindole (*S*)-**126** bearing a 4-membered spirocyclic system, which formed in high yield but poor enantioselectivity (23% *ee*) (entry 1). Notably, using less bulky imidazolium salt (*S,S*)-[**L5**H][I] allowed one to improve the asymmetric induction of spirooxindole (*S*)-**126** to 52% *ee* (Table 11, entry 2).

Table 11. Ring size effect in asymmetric synthesis of spirooxindoles.

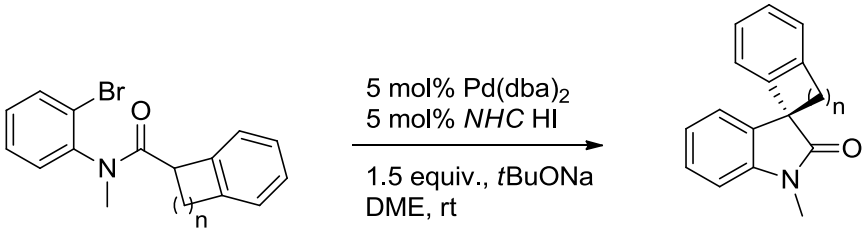

Entry[a]	Product	Ligand precursor	Yield (%)[b]	Ee (%)[c]
1[d]	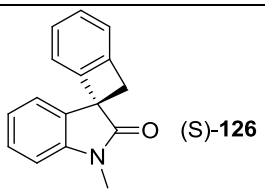 (S)-**126**	(*S*,*S*)-[**L14**H][I]	89	23
2[d]		(*S*,*S*)-[**L5**H][I]	82	52
3[e]	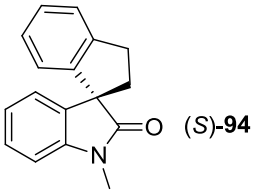 (*S*)-**94**	(*S*,*S*)-[**L14**H][I]	99	81
4[f]	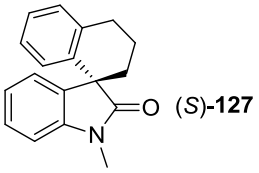 (*S*)-**127**	(*S*,*S*)-[**L14**H][I]	96	86
5[f]	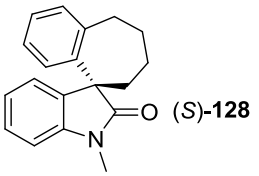 (*S*)-**128**	(*S*,*S*)-[**L14**H][I]	97	83

[a] 0.2 mmol substrate with 0.05 M in DME, absolute configuration of **126**-**128** were assigned by comparison of the circular dichroism (CD) with that of (*S*)-**62**.[114] [b] Isolated yield. [c] The enantiomeric ratio was determined by HPLC. [d] 36 h. [e] 20 minutes. [f] 48 h.

As spirooxindole (*S*)-**127** incorporating a 6-membered fused ring formed in highest enantioselectivity (Table 11, entry 4), we extended these studies to substrates containing an arene functional group. Results are summarized in Table 12. Initially compatibility of functional groups and potential electronic dependence of the reaction were investigated with substrates containing different substituents in the aniline part (Table 12, entries 1-6). Substrates with electron-donating substituents at C(5) gave slightly improved product enentioselectivities (Table 12, entries 1-2). In contrast, spirooxindole with electron-withdrawing group at C(5) formed only in moderate 74% *ee* (entry 3). Both the electron donating and withdrawing groups at C(6) position reduced the product yields and

enantioslectivities (entries 4-5). Strong erosion of asymmetric induction was observed for the oxindole with trifluoromethyl group at C(4) position, which formed in 95% yield within 10 h but as a racemic mixture (entry 6). Perhaps, strong repulsion arise between substituent at C(4) position and naphtyl side chain of carbene ligand in the palladacycle intermediate which could disturb the allylic strain and lead to the formation of the product in poor enantioselectivity. Methoxy substituent in tetrahydronaphthalene part leads to the formation of desired spirooxindole in high yield and 88% enantioselectivity (entry 7). Chroman and thiochroman derivative anilides **120** and **121** underwent spirocyclization smoothly to afford spirooxindoles after 48 h in high 88% and 90% enantioselectivities respectively (entries 8-9).

We next investigated the effects of *N*-protecting groups on the enantioselectivity. Spirooxindole **138** with *N*-benzyl protecting group formed in slightly less enantioselectivity compare with *N*-methyl one (entry 10). Additionally, synthetically important BOM (benzyloxymethyl) and MOM (methyloxymethyl) *N*-protecting groups are found to be suitable in this cyclization reaction giving the corresponding products in high yields and high *ee*'s (86%), even though the reaction had to be heated up to 50 ˚C (entries 11-12). The drop of enantioselectivity was observed when tetrahydronaphthalene-2-carboxamide derivative was tested as a substrate and spirooxindole **141** was formed in 75% yield and modest 56% *ee* (entry 13)

Table 12. Synthesis of spirooxindoles *via* Pd(*NHC*)-catalyzed *α*-arylation of amides.

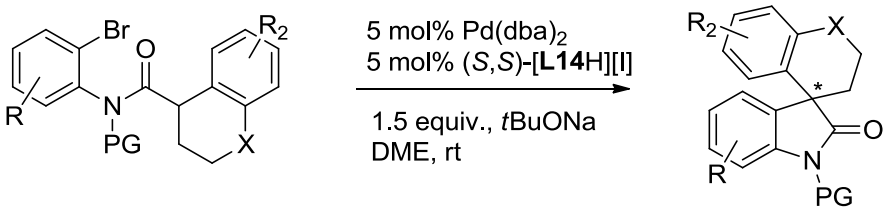

Entry[a]		Product	Time (h)	Yield (%)[b]	Ee (%)[c]
1[d]	(*R*)-**129**	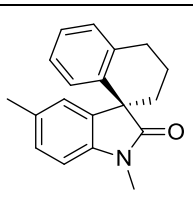	10	98	-87
2[d]	(*R*)-**130**	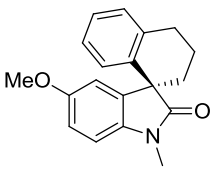	48	95	-89

3[d]	(*R*)-**131**	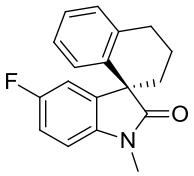	10	89	-74
4[d]	(*R*)-**132**	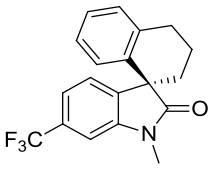	10	77	-51
5[d]	(*R*)-**133**	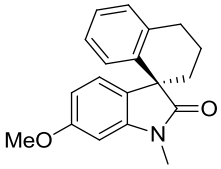	48	91	-77
6	(*S*)-**134**	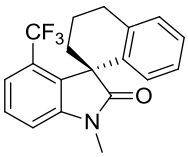	10	95	4
7	(*S*)-**135**	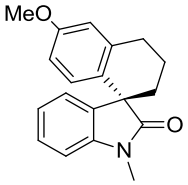	48	92	88
8	(*R*)-**136**	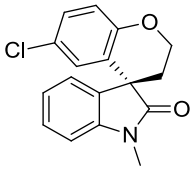	48	98	88
		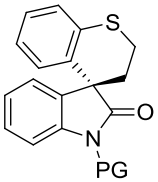			
9	(*R*)-**137**	PG = Me	48	98	90
10	(*R*)-**138**	PG = Bn	48	94	84
11[e]	(*R*)-**139**	PG = MOM	24	97	86
12[e]	(*R*)-**140**	PG = BOM	24	94	86
13	(*S*)-**141**	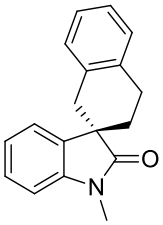	48	75	56

[a] 0.2 mmol substrate with 0.05 M in DME. [b] Isolated yield. [c] The enantiomeric ratio was determined by chiral HPLC. [d] (*R*,*R*)-[**L14**H][I] was used. [e] 50 ˚C.

Another important family of biologically active 3,3-disubstituted oxindoles is *aza*-oxindoles.[184-187] A literature search revealed only a limited number of reports towards the

synthesis of compounds containing the *aza*-oxindole motif.[126,188-200] We were able to extend the use of intramolecular *NHC*-Pd-catalyzed *α*-arylation for the preparation of *aza*-spirooxindoles in an enantioselective fashion. The *ortho*-pyridyl substrates with different size of the cycloalkyl ring were tested and the results are summarized in Table 13. In the case of the oxindole with a spiro-thetrahydronaphthalene motif, the cyclization reaction proceeded fast at room temperature producing the corresponding product in quantitate yield and high enantiomeric excess (Table 13, entry 3). The oxindoles with fused 5- and 7-membered ring formed in slightly lower enantioselectivities 84 and 86% respectively (Table 13, entries 1 and 6). High reaction rates observed for the *otho*-pyridyl based substrates can be attributed to the faster oxidative addition of electron-poor aryl bromides to palladium compared to those with electron-rich substituents.[201] Carrying out the reaction at -10 ˚C allowed to improve the enantioselectivty of *aza*-spirooxindoles **139-141** (entries 2, 4 and 7).

Table 13. Enantioselective synthesis of *aza*-spirooxindoles by Pd(*NHC*)-catalyzed *α*-arylation.

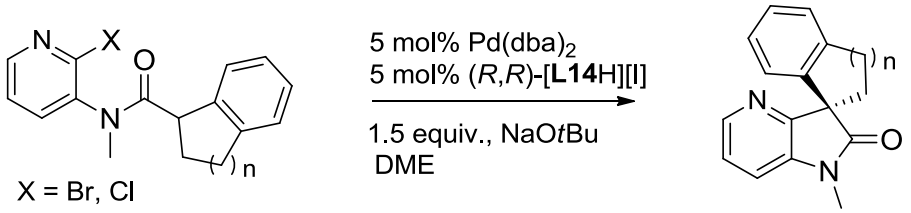

Entry[a]	Product	Time (h)	Yield (%)[b]	Ee (%)[c]
1[d,f]	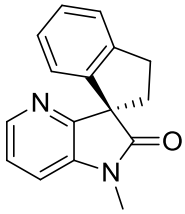 (*R*)-**142**	0.17.	99	84
2[d,g]		24	99	86
3[d,f]	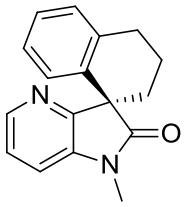 (*R*)-**143**	0.33	99	88
4[d,g]		24	99	91
5[f,e]		24	86	88
6[d,f]	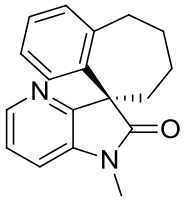 (*R*)-**144**	0.33.	99	86
7[d,g]		24	99	90

[a] 0.2 mmol substrate with 0.05 M in DME. [b] Isolated yield. [c] The enantiomeric ratio was determined by chiral HPLC. [d] X = Br. [e] **110**: X = Cl. [f] 25 ˚C. [g] -10 ˚C.

Finally, we were pleased to see that pyridyl chloride substrate **110** undergo a cyclization reaction even at room temperature producing after 24 h the corresponding product in 86% yield and 88% enantiomeric excess (entry 5).

II.3.7.4. Synthesis of New Preformed Catalysts

Using the same procedure as described earlier for the synthesis of palladacycles (*S*,*S*)-**101**, palladacycle (*S*,*S*)-**146** (Figure 36) was prepared and one of the diastereoisomers was successfully recrystallized from pentane/acetone to give a crystal suitable for X-ray diffraction (Figure 35). A comparison of the structures of the palladacycle (*S*,*S*)-**101** and (*S*,*S*)-**146** showed that all stereoelements of the chiral ligand are located similarly.

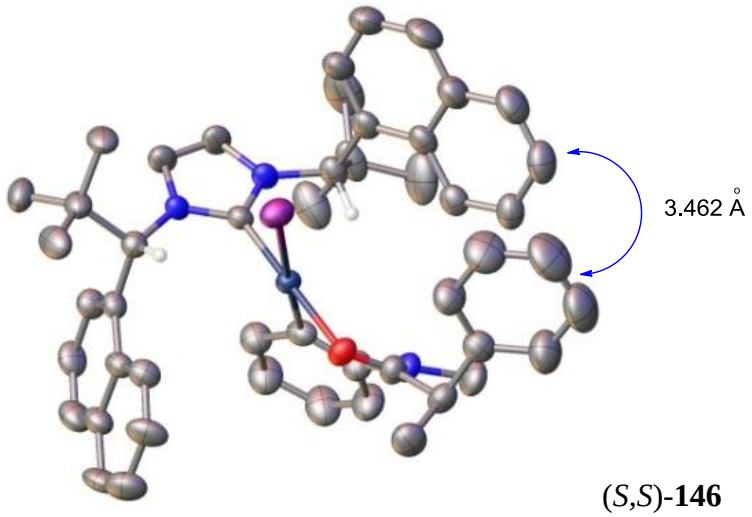

Figure 35. ORTEP-rendered diagram of palladacycle (*S*,*S*)-**146** (50% probability level for the thermal ellipsoids). All hydrogen atoms except for benzylic in imidazolim part have been omitted for clarity.

Palladacycle (*S*,*S*)-**146** includes π–π stacking arrangement between one of the napthyl groups of the *NHC* ligand and the aryl group of the substrate (3.462 Å). This may be of some importance in the transition state leading to the product with high asymmetric induction.

In order to quantify the steric demand of the new *NHC* ligand, the *buried volume* (%V_{bur}) was calculated. For the naphthyl-*NHC* (*S*,*S*)-**L14** ligand the similar value as for (*S*,*S*)-**L5** was found (36.8 %).

We next studied the scope of the precatalysts instead of *in situ* generated systems to identify the most efficient catalyst in terms of reaction times and *ee*'s in the asymmetric palladium-catalyzed α-arylation of amide **61**. Thus, a new palladacycle (*S*,*S*)-**145** was prepared according to a similar procedure as for (*S*,*S*)-**101** and (*S*,*S*)-**146** (Figure 36).

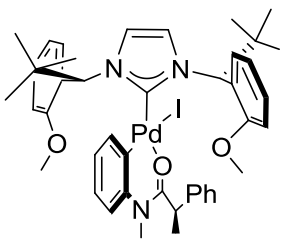

(*S*,*S*) - **145**

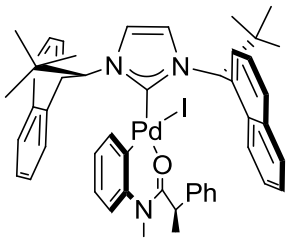

(*S*,*S*) - **146**

Figure 36. New preformed catalysts. Synthesized according to the procedure shown in Scheme 48**.** (*S*,*S*)-**145**-58% yield; (*S*,*S*)-**146**-64% yield.

The catalytic reactions with these complexes were carried out under identical reaction conditions and conversions were monitored by GC (Figure 37). The shortest reaction time in the arylation of amide **61** was achieved using catalyst (*S*,*S*)-**101** with half-time ($\tau_{1/2}$) of 17.5 minutes. More bulky catalyst (*S*,*S*)-**146** showed slightly lower activity (half-time is 23.5 minutes), although oxindole (*S*)-**62** was formed with better enantioselectivity (96%). The complex (*S*,*S*)-**145** containing *ortho*-methoxy aryl substituents in imidazolium part possesses similar activity (half-time is 29.5 minutes) yielding product (*S*)-**62** with 87% enantioselectivity.

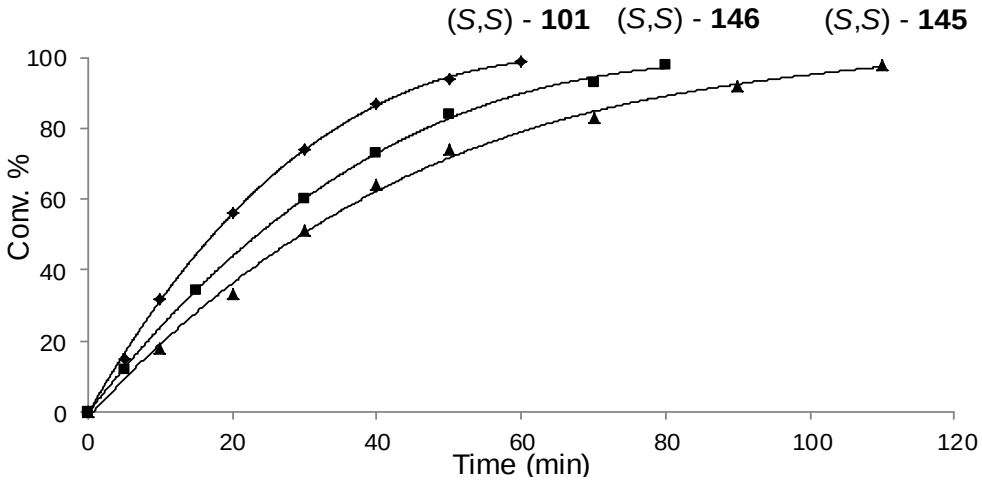

Reaction conditions: [**61**] = 0.05M, catalyst 5 mol%, maleic anhydride (10 mol%), *t*BuONa (1.5 equiv.), DME, rt. Reactions were monitored by GC using decane as an internal standard.

Figure 37. Variation of precatalysts in the palladium-catalyzed *α*-arylation of amide **61**.

The enantioselectivity in this reaction could be controlled by any of the three steps, (a) stereoselective benzylic deprotonation leading to *E* or *Z* enolates, (b) the conversion of *O*-enolate to *C*-enolate, and (c) reductive elimination in the palladacycle leading to cyclization to

product oxindole. We have employed DFT(B3LYP) computations to identify the transition states in an effort to delineate the factors contributing to enantioselectivity as well as to identify the most likely step where the stereoinduction takes place. The computations have separately considered the mechanism emanating for both *R* and *S* enantiomers of the initial racemic substrate used in the reaction.

II.3.8. DFT Investigations[vi]

A number of different mechanistic scenarios were examined for Pd-*NHC**-catalyzed oxindole formation. The major difference between various pathways relates either to geometrical difference in the starting palladacycle or to the mode and timing of the removal of bromide from various intermediates. For the sake of brevity, only the energetically most preferred pathway is discussed here in detail. The effect of solvent continuum is taken into account by computing energies of the cmpounds in the presence of 1,4-dioxane.

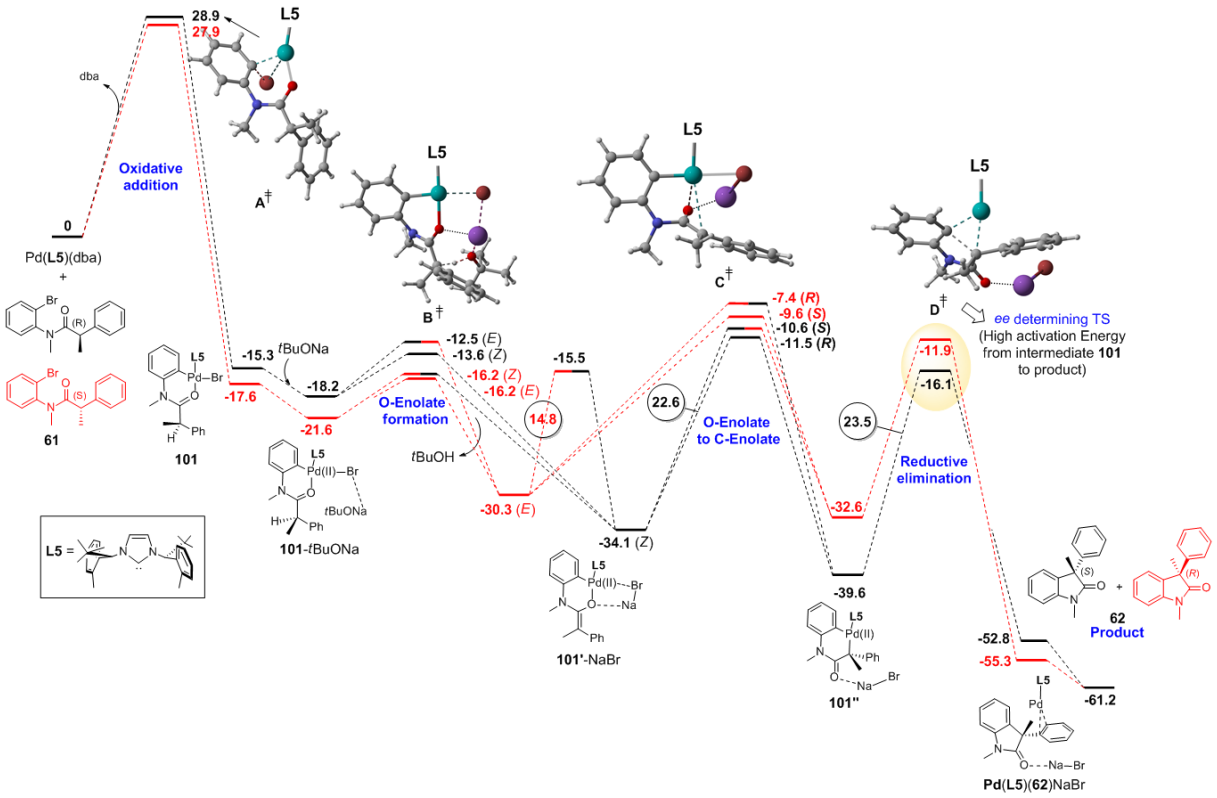

Figure 38. Gibbs free energy diagram (in kcal/mol) of key steps in the asymmetric synthesis of oxindole (*S*)-**62** in solvent (1,4-dioxane). Transition states A‡- D‡ and intermediates shown are those derived from the *R* enantiomer of the starting material.

[vi] DFT investigations were carried out in collaboration with Prof. Dr. *R. B. Sunoj*.

The reaction is envisaged to begin with the formation of [Pd(0)(*NHC**)(dba)] complex from $Pd(0)(dba)_2$. The energy of [Pd(**L5***)(dba)] is taken as the reference for all energetic comparisons. In the first step, an oxidative insertion of Pd-**L5*** to the C_{aryl}–Br bond provides a tetracoordinate Pd(II) intermediate **101**. The oxidative insertion to both enantiomeric forms ((*S*)-**61** and (*R*)-**61**) of the substrate is examined and it was found that the energy difference between oxidative insertion transition states for both (*S*)-**61** and (*R*)-**61** is only one kcal/mol, in favor of the *S* enantiomer.

The next step is the deprotonation of benzylic proton of **101** by *t*BuONa leading to *O*-enolates **101'**. The key featured of the computed energetics can be gathered from the Gibbs free energy profile as given in Figure 38. It can be noticed that the barrier for deprotonation of diastereomer (*S*)-**61** is 5.4 kcal/mol, while that for (*R*)-**61** is 4.6 kcal/mol. The computed energetics further indicates that (*R*)-**61** preferably leads to the *Z*-enolate whereas (*S*)-**61** can result in both *E*-enolate and *Z*-enolate. The step leading to the generation of the enolate intermediate is expected to be not significant in the eventual enantioselectivity of this reaction. Moreover, a key point to note is a likely accumulation of the energetically more favored *Z*-*O*-enolate due to a potential equilibrium between intermediates **101** and **101'** connected *via* TS **B**. Further the barrier for *E* / *Z* conversion (within *O*-enolate) by rotation around the C=C bond is lower than those of the forward reactions.

The next major event in the catalytic cycle is the transition from *O*-enolate **101'** to *C*-enolate **101''**. The barrier for rotation of the *Z*-*O*-enolate to (*R*)-**101''** is found to be lower by 0.9 kcal/mol as compared to that for the *Z*-*O*-enolate to (*S*)-**101''**. This step can influence the stereochemical outcome of the reaction. The *E*-enolate will give rise to palladacycle (*S*)-**101''**, which will eventually lead to (*R*)-**62**. The *Z*-*O*-enolate on the other hand, will convert to (*R*)-**101''** and then to (*S*)-**62**. Hence, different geometric isomers of **101'** will lead to different enantiomers if the interconversion between *E* and *Z*-enolates is prevented.

Finally, a reductive elimination leads to the product oxindole. The configuration at the benzylic carbon moved forward to the product as the reductive elimination is identified to be a concerted process with no additional intermediates. The stereochemistry of the product oxindole therefore depends on the configuration as rendered in the previous step. The intermediate (*R*)-**101''** corresponds to the formation of oxindole (*S*)-**62** whereas (*S*)-**101''** yields (*R*)-**62**. The energy barrier for the reductive elimination in (*R*)-**101''** to (*S*)-**62** is lower in energy by 4.2 kcal/mol than the corresponding conversion of (*S*)-**101''** to (*R*)-**62**. Hence,

the transition state for the formation of (*S*)-**62** is more favorable. This prediction is in concert with the experimental observations.

The analysis of Gibbs free energy profile, as given in Figure 38, reveals that C-Br activation is the rate-limiting step leading to the formation of stable intermediate **101**. The TS for the reductive elimination presents the highest activation barrier (23.5 kcal/mol) step in the formation of a stable oxindole product (**62**). Another important point to note is that intermediates **101'** and **101''**, which lead to *S*-enantiomer are lower in energy. Hence, the stereoselectivity should be controlled by the reductive elimination step. The interconversion between *E* and *Z*-*O*-enolate is expected to play an important role in the catalytic cycle. If *E* and *Z*-enolates were not interconvertible, each would have led to different stereoisomer, resulting in overall reduction in the stereoselectivity.

II.3.9. Catalytic Enantioselective Synthesis of a 3-Aryl-3-benzyl-oxindole Exhibiting anti-Tumour Activity

Enantioenriched oxindoles synthesized above were always model compounds. They have provided the information on the scope and limitations of the reaction but they were neither natural products nor synthetic bioactive agents. In order to apply the asymmetric catalytic method developed in our laboratory towards the synthesis of complex and useful molecules we found that 6-chloro-3-(3-chlorobenzyl)-3-(3-methoxyphenyl)indolin-2-one (**51**) is one of the most active compounds contained in the Roche 2006 patent.[136] The patent reports that 3,3-disubstituted oxindoles are MDM2 antagonists and disrupt nefarious MDM2-p53 interactions. Since p53 is a tumour suppressor protein, MDM2 antagonists can offer a novel approach to cancer therapy. Oxindole **51** is also mentioned in a recent patent dealing with a method for improving the production of influenza viruses and vaccine seeds.[202] The reported synthesis of *rac*-**51** is shown in Scheme 51 involving addition of the *Grignard* reagent to isatin, reduction of 3-hydroxyoxindole derivative followed by an alkylation step. To our knowledge, no report of an enantioenriched oxindole **51** is literature-known.

The target molecule contains a quaternary stereogenic center at the benzylic position and also two aryl chloride groups making the key step of the intramolecular arylation of the precursor amide more challenging due to the potential competition in the transition metal oxidative addition process.

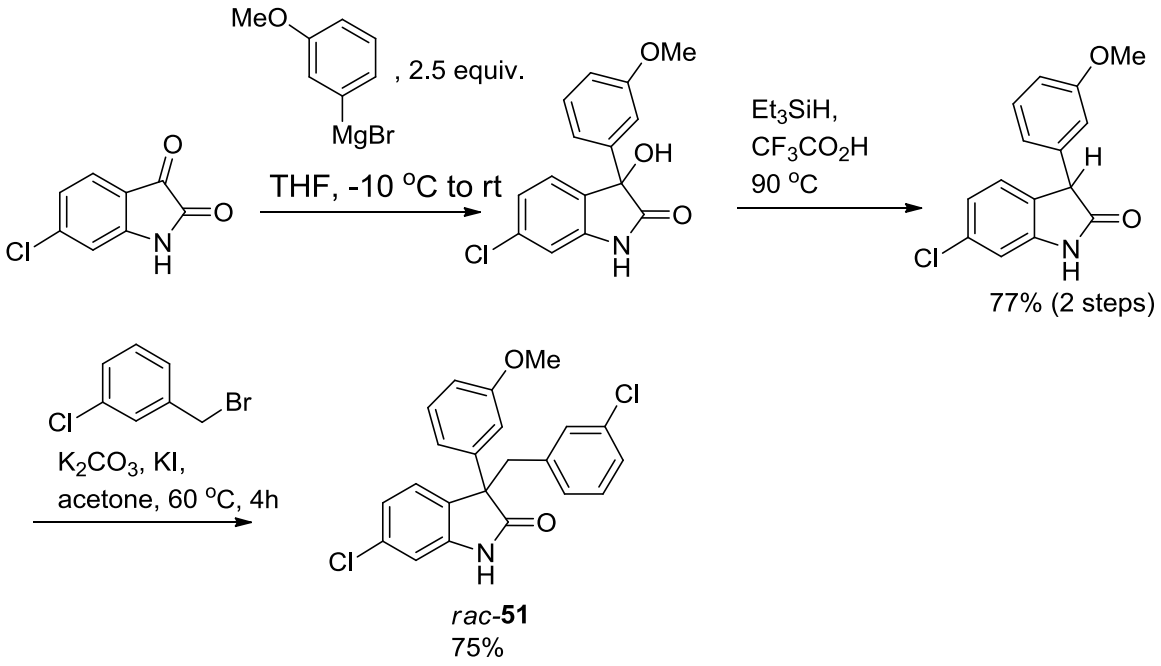

Scheme 51. *F-Hoffmann-La Roche* synthesis of *rac*-**51**.

Our approach to the synthesis of (*R*)-**51** is depicted in Scheme 52. We envisaged that the requisite amide can easily be prepared from the dihaloaniline and the carboxylic acid shown. An asymmetric intramolecular Pd-catalyzed *α*-arylation would then generate the sought for oxindole.

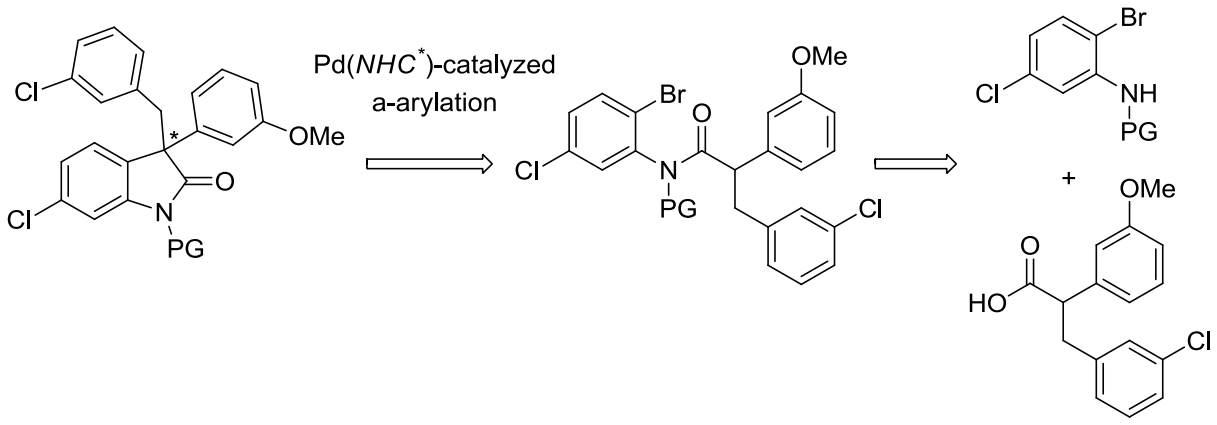

Scheme 52. Our retrosynthetic analysis of **51**.

Commercially available 2-(3-methoxyphenyl)acetic acid was converted to acid **147a** by alkylation with 3-chloro benzyl bromide in the presence of freshly prepared LDA (Scheme 53). 2-Bromo-5-chloroaniline was then coupled with acyl chloride **147b** producing amide **148** in high yield (89% for the two steps). Amides **149** and **150** were synthesized by treating **148** with the corresponding alkoxy chlorides in the presence of NaH in THF.

Earlier data showed that the choice of chiral *NHC* ligand, the solvent, as well as the *N*-protecting group influence both the yield and asymmetric induction. As shown in Table 14, both BOM (benzyloxymethyl) and MOM (methyloxymethyl) groups proved suitable for the transformation in hand with the best yields being obtained when using toluene as solvent at 50 ^{o}C.

Table 14. Pd(*NHC*)-catalyzed α-arylation of substrates **149** and **150**.[a]

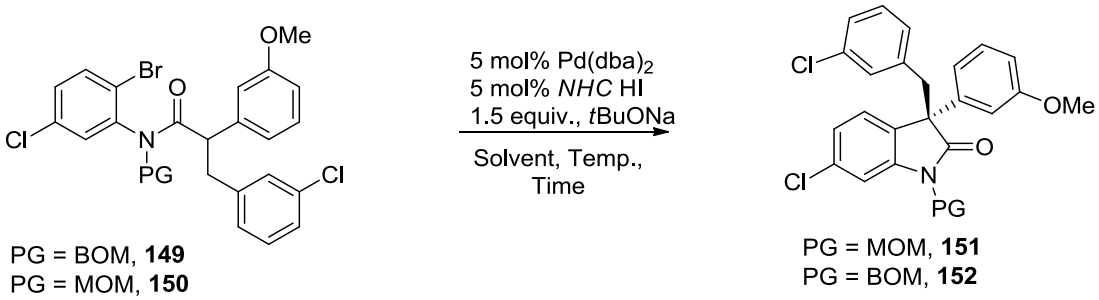

Entry	Substrate	NHC·HI	Solvent	Temp. [˚C]	Time [h]	Yield [%][b]	Ee [%][c]
1	**149**	(*S*,*S*)-[**L5**H][I]	DME	rt	24	28	-84
2	**149**	(*S*,*S*)-[**L14**H][I]	DME	rt	24	31	-86
3	**150**	(*S*,*S*)-[**L14**H][I]	DME	rt	24	30	-89
4	**150**	(*S*,*S*)-[**L14**H][I]	Toluene	rt	48	25	-89
5	**150**	(*S*,*S*)-[**L14**H][I]	Toluene	50	48	85	-87
6	**150**	(*S*,*S*)-[**L5**H][I]	Toluene	50	48	86	-85
7[d]	**150**	(*R*,*R*)-[**L12**H][I]	Toluene	50	48	86	90

[a] 0.2 mmol substrate with 0.05 mmol in DME, absolute configurations are assigned by analogy[114] and are tentative. [d] Isolated yield. [c] The enantiomeric ratio was determined by HPLC on a chiral stationary phase (Chiracel AD-H column). [d] 1 mmol scale.

Conditions used previously with success (5 mol% **L5**·HI or **L14**·HI, 5 mol% $Pd(dba)_2$, 1.5 equiv. *t*BuONa in DME at room temperature afforded the product with good enantioselectivities but in low yields (Table 14, entries 1-3). The reaction was accompanied by decomposition of starting material. Fortunately, changing the solvent to toluene and increasing the temperature to 50 ˚C improved the situation as shown in entries 5-7. While all three chiral ligands (**L5**, **L14** and **L12**) performed very well, ligand (*R*,*R*)-**L12** proved best

giving the oxindole **151** in 86% yield and 90% *ee*. The high yield shows that the Pd-catalyzed cyclization takes place selectively and without interference of the aryl chloride groups present. This procedure was then incorporated into the synthetic protocol for (*R*)-**61**. The methoxymethyl (MOM) protecting group was chosen for its high yield of incorporation into **148** and its ready removal from **151**. The latter reaction was carried out using the *Fukuyama* procedure[203] that consisted of treating **151** with chlorotrimethylsilane (Me_3SiCl) in the presence of sodium iodide (NaI). The *N*-(hydroxymethyl) derivative produced, upon heating with triethylamine (Et_3N) in methanol at 55 °C furnished (*R*)-**51** in 91% yield. Recrystallization from hexane/dichloromethane increased the enantiopurity of (*R*)-**51** to 96% *ee*. The absolute configuration of **51** was assigned as (*R*) by comparison of its circular-dichroism (CD) spectrum with that of similar oxindole structures described in the literature.[114,162]

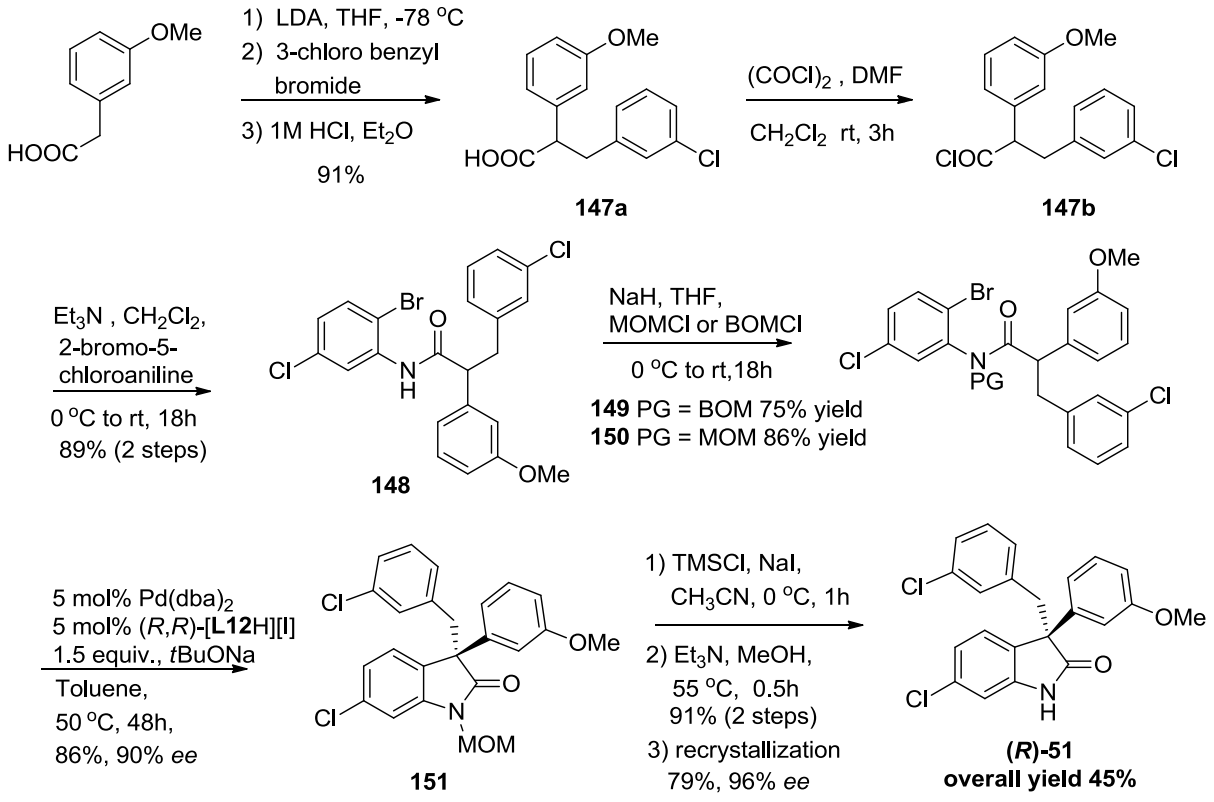

Scheme 53. Catalytic enantioselective synthesis of (*R*)-**51**.

II.3.10. Conclusion

We have synthesized new chiral *N*-heterocyclic carbene ligands and have successfully applied them in the asymmetric palladium-catalyzed α-arylation of amides, such as 3-aryl-3-alkyl-,[114,162] spiro- and *aza*-spirooxindoles in excellent yield and high asymmetric efficiency.

High enantioselectivity of this process resulted from the feature of both, bulky *tert*-butyl groups at the stereogenic centers and *ortho*-aryl substituents. The importance of the *ortho*-aryl substituents was revealed in the crystal structures of palladacycle intermediates containing the chiral *NHC* ligands and the substrate. The place and orientation of the stereocontrol elements of the ligand are fixed by the minimization of allylic ($A^{1,3}$) strain providing efficient transfer of chiral information. Mechanistic studies of this transformation revealed the importance of alkene additives to increase turn-over number (TON) and turn-over frequency (TOF). Kinetic studies show the reaction to be first order in the substrate.

The DFT(B3LYP) computational analysis of the reaction mechanism revealed that the transition states for *O*-enolate to *C*-enolate conversion and the for reductive elimination were found to be the key structure for the formation of desired *S*-enantiomer with a predicted *ee* to be more >98%, which is in agreement with the experimentally observed enantiomer.

In conclusion, we have successfully applied the Pd(*NHC*)-catalyzed asymmetric *α*-arylation of amides to the total synthesis of (*R*)-**51**. The sequence involves 6 steps with overall yield 45%. These studies demonstrate that the Pd(*NHC*)-catalysis can be used in an asymmetric C-C bond formation at a late stage in the synthesis of complex structures.

III. Asymmetric Synthesis of Indolines *via* Palladium-*NHC*-Catalyzed C(sp^3)-H/C(Ar) Coupling Reactions

III.1. Functionalization of non-Activated C(sp^3)-H Bonds

Directed aromatic functionalization methods (electrophilic (S_EAr) and nucleophilic (S_NAr) aromatic substitution, radical nucleophilic substitution (S_{RN}), vicarious nucleophilic substitution (VNS), and directed *ortho* metalation (DoM) reaction) are recognized as extremely powerful methods for the synthesis of various compounds including industrial materials, medicines, and natural products (Figure 39). The discovery of aryl-metal compounds (mainly formed *via* directed *ortho* metalation, metal insertion or metal-halogen or pseudohalogen exchange) led to the fast development of a new family of transition metal catalyzed coupling reactions. In 2010 the Nobel Prize in Chemistry was awarded to the pioneers of palladium-catalyzed cross-coupling reactions, namely to *R. Heck*, *E. Negishi*, and *A. Suzuki*. Thus, the worldwide appreciation showed the tremendous importance of this scientific effort in organic chemistry.

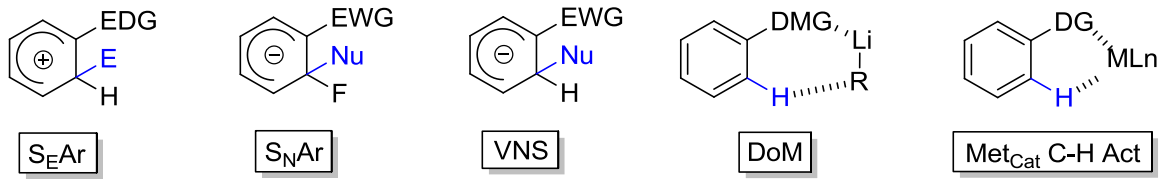

Figure 39. Directed aromatic functionalization methods.

Transition-metal catalyzed C-H functionalization emerged in recent years as a powerful tool for the formation of carbon-carbon or carbon-heteroatom bonds.[204-210] C-H arylation reactions became an attractive alternative to traditional C-C cross coupling reactions because the corresponding substrates do not require further conversion to metalated or halogenated derivatives.[211-218] Extensive mechanistic studies of arylation of alkene-, arene- and heteroarene C(sp^2)-H bonds[219-226] allowed chemists to extend the scope of substrates that can be later functionalized yielding synthetically useful motifs. On the other hand, the activation of non-acidic C(sp^3)-H bonds has been less studied until recently.[227,228] However, over the last decades, an increased interest in the functionalization of non-activated C(sp^3)-H bonds led to significant advances in this field. The recently developed methods towards the functionalization of non-activated C(sp^3)-H bonds can be divided into three main groups: a) Heteroatom-directed C-H arylation; b) Oxidative addition/metalation-induced C-H arylation;

c) Non-directed organometallic C-H arylation reactions (Scheme 54). In terms of our research interest the oxidative addition/metalation-induced C(sp^3)-H arylation reactions (Scheme 54b) will be further discussed in details.

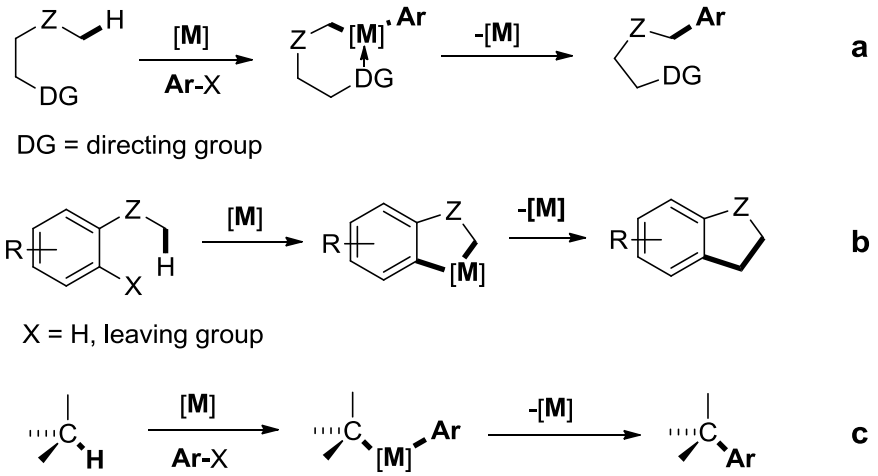

Scheme 54. **a)** Heteroatom-directed C-H arylation; **b)** Oxidative addition/metalation-induced C-H arylation; **c)** Non-directed organometallic C-H arylation.

A series of seminal articles on the synthesis of polycyclic systems from aryl iodides *via* palladium-catalyzed intramolecular C(sp^3)-H activation were reported by *Dyker*[229-231] in the beginning of 1990's. As example, a fused heterocycle was prepared in high yield (90%) *via* trimerization of 2-iodoanisole in the presence of $Pd(OAc)_2$ (10 mol%), potassium carbonate and ammonium salt (Scheme 55).

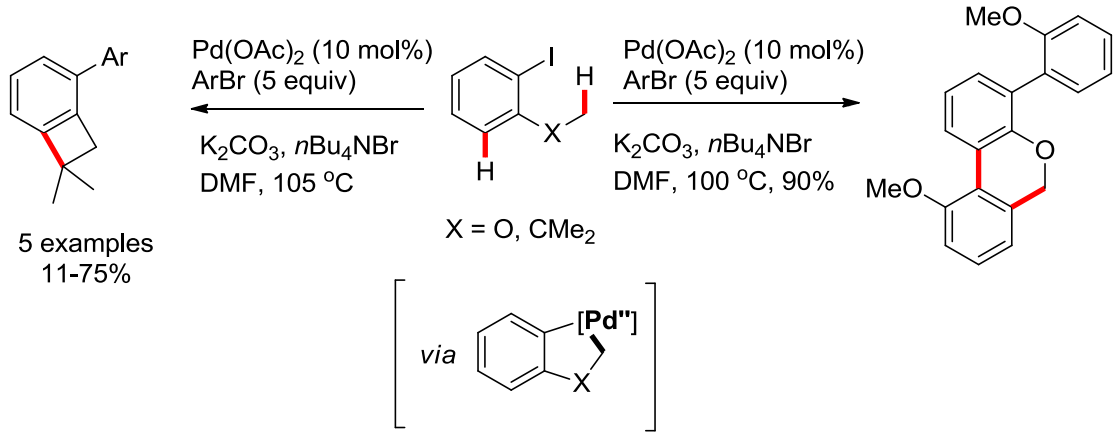

Scheme 55. Palladium(0)-catalyzed synthesis of polycyclic systems.

This transformation involves a sequence of steps. The five-membered palladacycle intermediate forms after the oxidative addition of the Pd(0) catalyst to the aryl iodide, followed by the intramolecular C(sp^3)-H activation. After that, the palladacycle intermediate

undergoes an intermolecular coupling with two other molecules of 2-iodoanisole producing the final product (Scheme 55).

In 2007, *Fagnou* developed the synthesis of 2,2-dialkyldihydrobenzofuranes *via* intramolecular palladium-catalyzed alkylation reactions of aryl bromides and chlorides involving C(sp^3)-H bond cleavage/functionalization. Mechanistic studies including density functional theory (DFT) calculations revealed the importance of the concerted, inner-sphere palladium-deprotonation pathway. The reaction proceeds *via* a three-center agostic interaction in the transition state (Scheme 56).[232] Later on, this methodology was extended to cheaper aryl chlorides.[233]

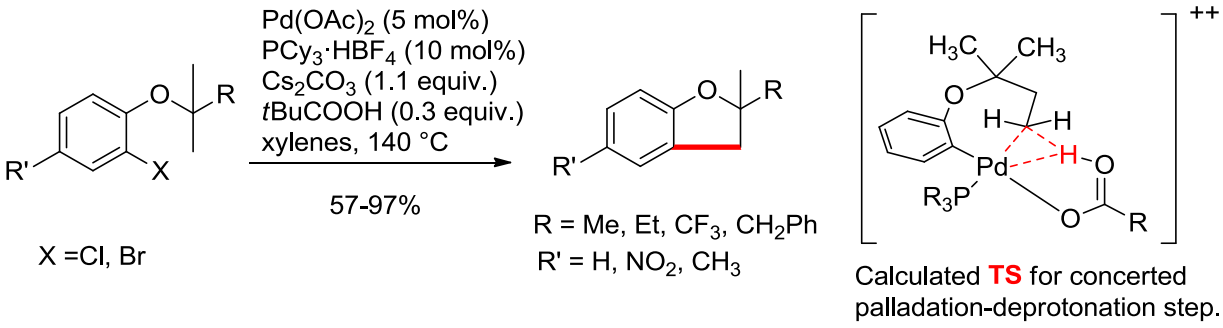

Scheme 56. Palladium-catalyzed alkane arylation.

In 2008, *Fujii* and *Ohno* reported an efficient method for the synthesis of an indoline skeleton *via* a C(sp^3)-H activation process.[234] Under similar reaction conditions, as it was reported by *Fagnou*, the range of 2,2-disubstitued- and fused- indolines was prepared in moderate to quantitative yields (Scheme 57a). For the first time, this study demonstrated that the C(sp^3)-H bond of the alkyl group can be easily activated without the help of heteroatom-directed group or a quaternary carbon moiety.

The substituted (*o*-chloro)-ketophenones were found to be suitable substrates for the intramolecular C(sp^3)-H arylation, leading to indanones in moderate to good yields (Scheme 57b). All these transformations require the addition of a catalytic amount of pivalic acid, which reacts with carbonate base to form a pivalate anion. Pivalate is believed to promote C-H bond cleavage *via* a concerted metalation-deprotonation (CMD) pathway. Even though the optimized reaction conditions performed well for a wide range of substrates shown in Schemes 56, 57a and 57b, other substrates (Schemes 57c and 57d) are unreactive under Cs_2CO_3/PivOH/xylene conditions. Further optimization of the base and solvent combinations

led to K_2CO_3/DMF system, which is better suited for the construction of carbocycles (Schemes 57c and 57d) rather than heterocycles (Schemes 56 and 57a).[233]

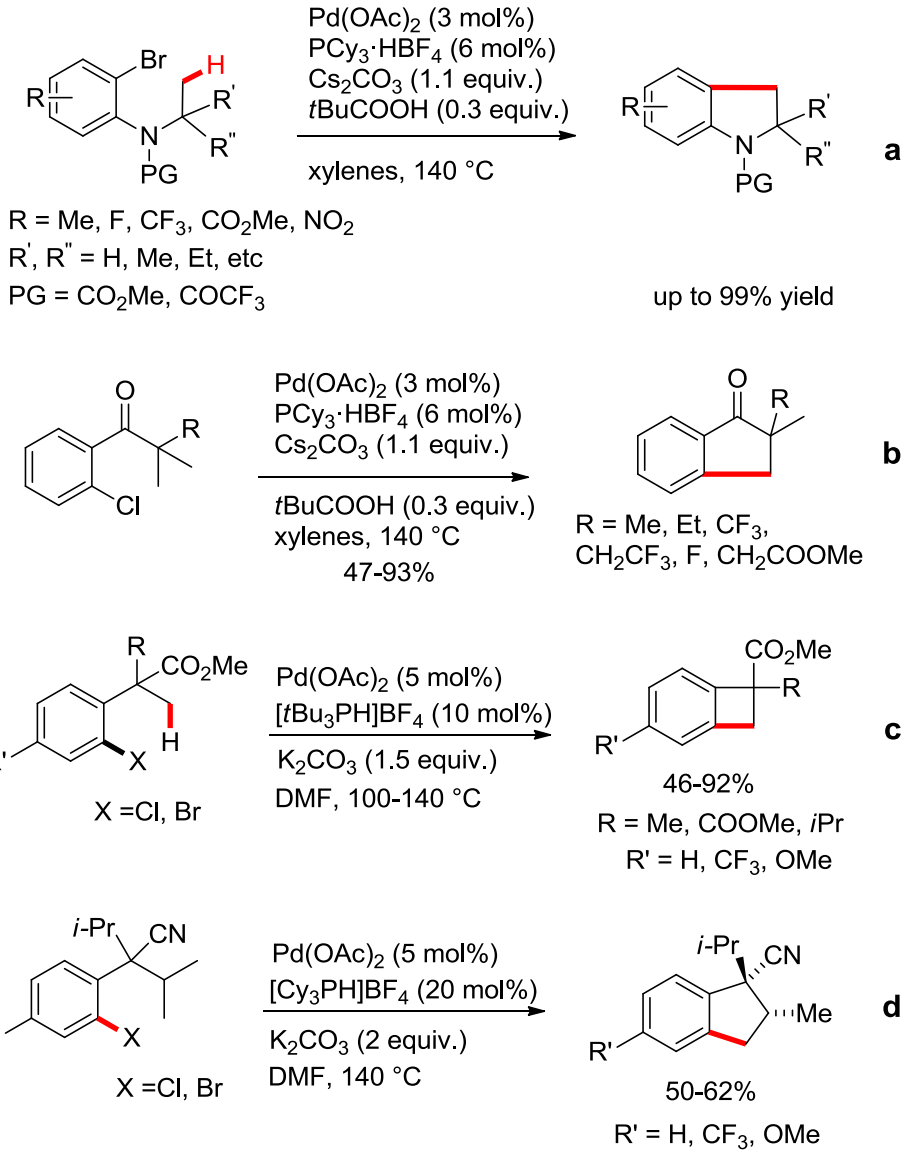

Scheme 57. Synthesis of indolines (**a**), indanones (**b**), cyclobutarenes (**c**) and indanes (**d**) *via* intramolecular C(sp^3)-H arylation reactions.

However, all the transformations mentioned above gave racemic products. Asymmetric transformations, which involve C(sp^3)-H activation are still very rare. Remarkable progress in this field was achieved by *Yu* and co-workers, who developed a palladium-catalyzed enantioselective activation of C(sp^2)-H and C(sp^3)-H bonds (Scheme 58).[235] The *authors* found, that monoprotected *α*-amino acids are efficient chiral ligands for Pd(II)-catalyzed asymmetric C-H activation/C-C coupling reactions. Later, these reaction conditions were applied to the C-H activation of cyclopropanes.[236]

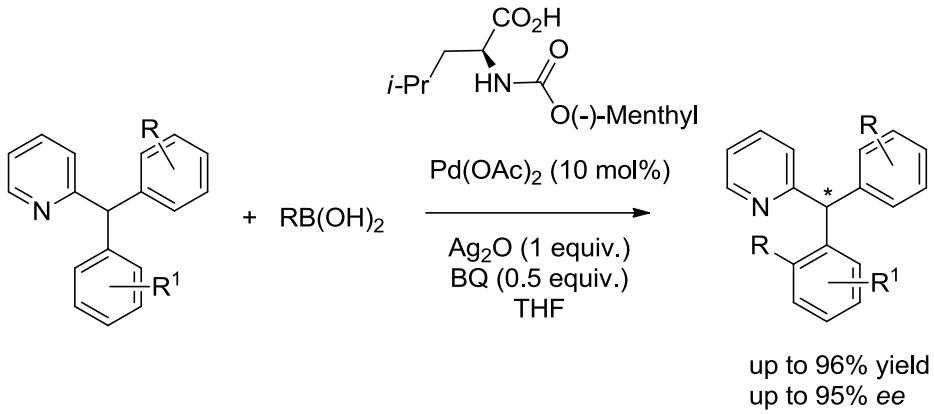

Scheme 58. Enantioselective C-H activation/C-C coupling.

In 2010, *Baudoin* and *Clot* developed an asymmetric intermolecular arylation of unactivated C(sp^3)-H bonds, which are in *β* position to an ester group (Scheme 58). The reaction proceeded in the presence of chiral phosphine ligand giving a range of synthetically interesting functionalized carboxylic esters; however, the enantiomeric ratio of the products formed was limited (e.r. up to 77:23) (Scheme 59a).[237] Recently, in 2012, the same *authors* reported for the first time a diastereo- and enantioselective synthesis of fused cyclopentanes *via* an intramolecular C(sp^3)-H arylation. After optimization of reaction conditions it was found, that in the presence of a chiral Pd/binepine catalyst the reactions proceeded well leading to substituted indanes. The products were formed in moderate diastereo- and enantioselectivities (Scheme 59b).[238]

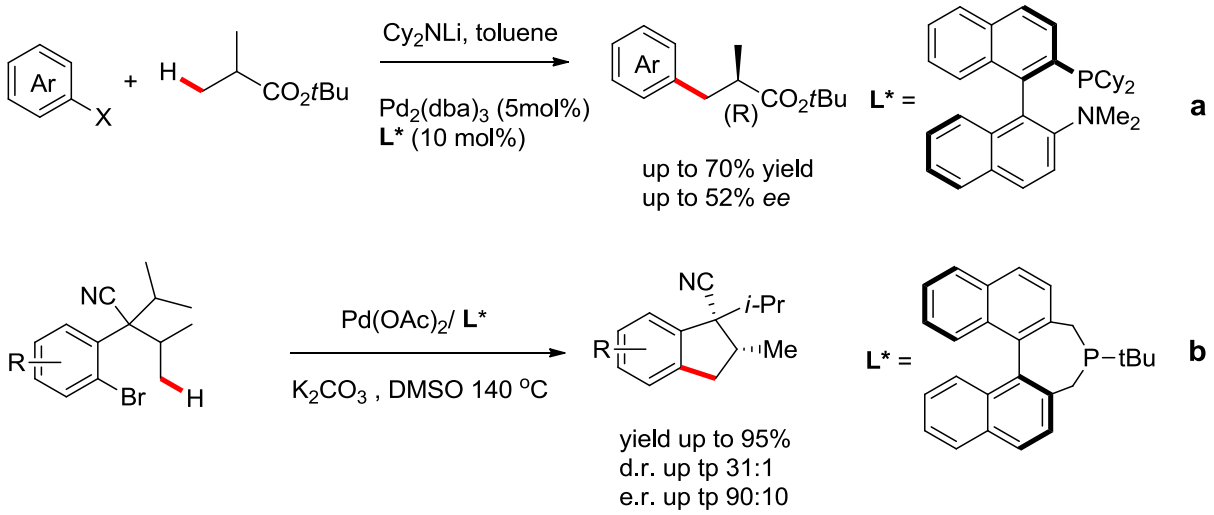

Scheme 59. **a**) Enantioselective *β* arylation *via* C(sp^3)-H activation. **b**) Stereoselective synthesis of indanes.

On the basis of the literature search we can conclude that C(sp^3)-H activation in catalysis remains one of the major challenges for chemists.

III.2. Synthesis of the Indoline Scaffold

III.2.I. Importance of Indolines in Medicinal Chemistry

Indoline is a common basic framework found in many naturally bioactive alkaloids, such as vinblastine (**153**) (an antimicrotubule drug used to treat certain kinds of cancer), (-)-physostigmine (**65**), strychnine (**154**) (notorious poison), and (+)-aspidospermidine (**155**) Figure 40),[239-242] and it is also found in several important pharmaceutically active compounds, such as pentropril[243,244] (**156**) (an angiotensin-converting enzyme (ACE) inhibitor and an antihypertensive drug). The indoline derivatives oleracein (**157 A**-**D**) were isolated from the edible plant *Portulaca oleracea* and are used in Chinese medicine.

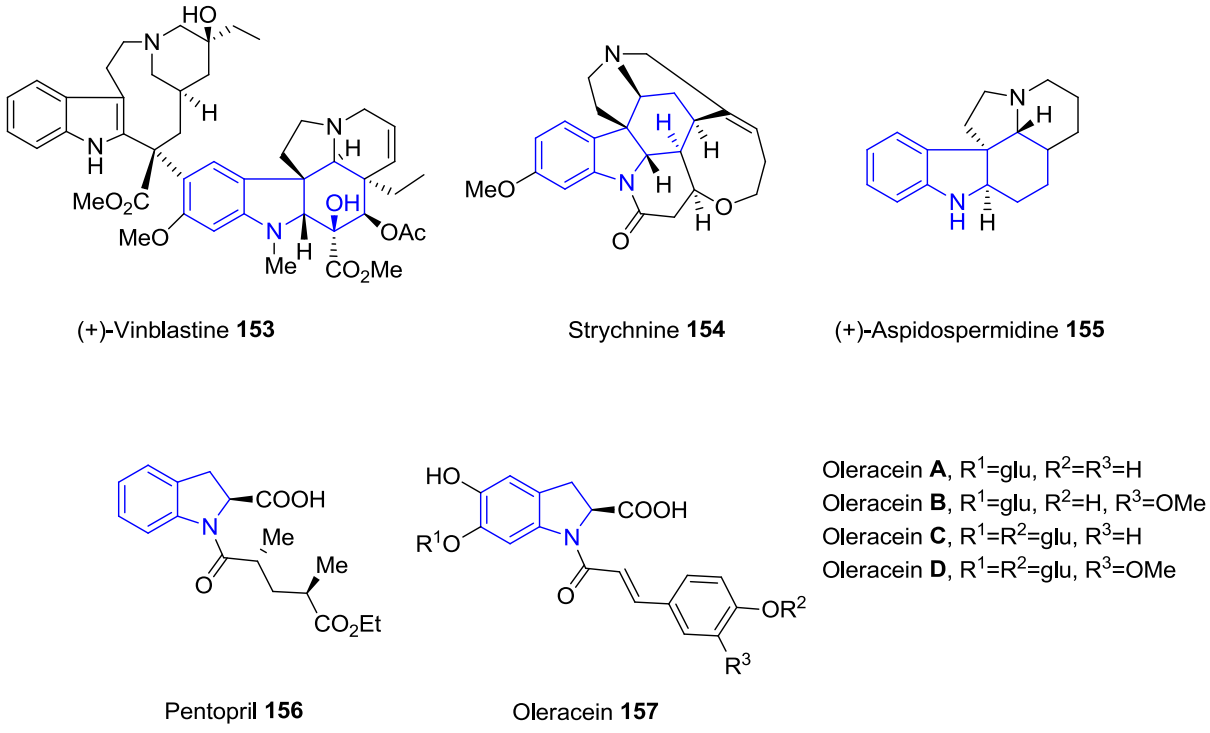

Figure 40. Representative bioactive indolines and its derivatives.

III.2.2. Synthesis of Indolines

To date, a large number of methodologies have been developed towards the indoline synthesis, including transition-metal-catalyzed reactions such as palladium-, copper- and nickel-catalyzed intramolecular aryl amination reactions and palladium-catalyzed C(sp^3)-H activation reaction, radical mediated reactions, intramolecular carbolithiation, intramolecular cycloaddition of ynamides and conjugated enynes, phenylildine(III)-mediated reactions and deoxygenation of oxindoles.[245] Also a few efficient enantioselective pathways towards

indoline synthesis have been developed such as the catalytic asymmetric hydrogenation of indoles,[246-248] the kinetic resolution of indolines[249], the asymmetric synthesis of indolines through intramolecular shifting of aromatic sulfinyl groups[250] and the synthesis of indolines *via* enantioselective copper-catalyzed desymmetric intramolecular *Ullmann* C-N coupling.[251] Most general methodologies are summarized in Figure 41.

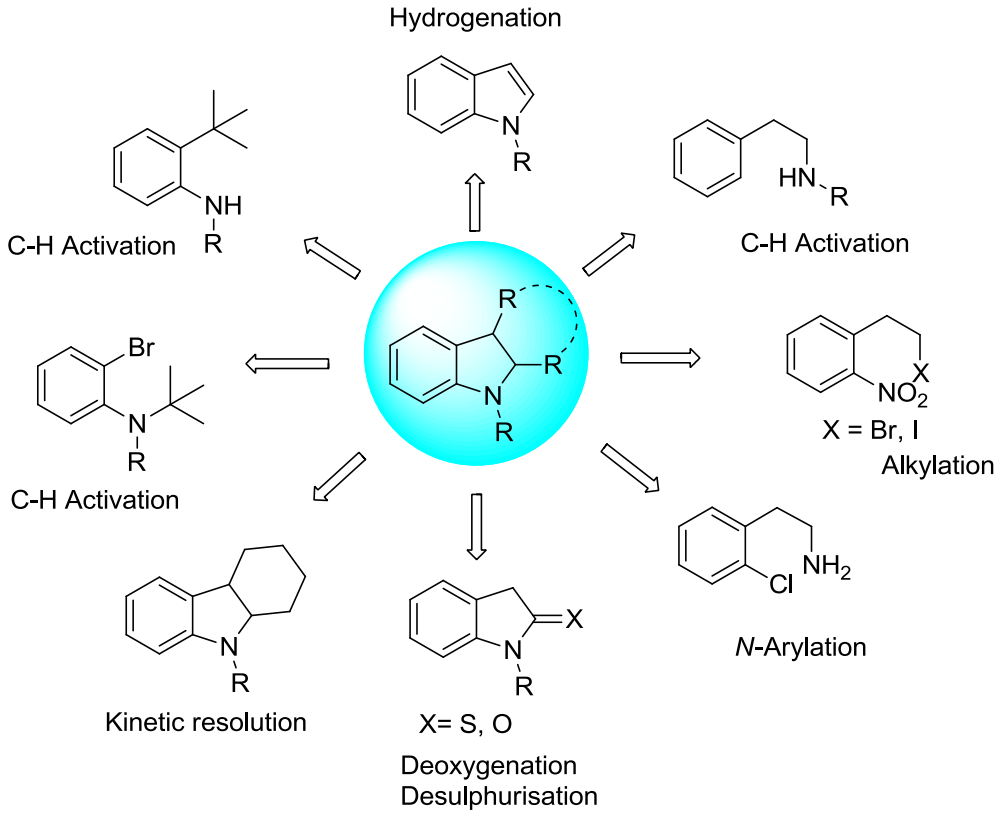

Figure 41. Approaches for the synthesis of indolines.

III.3. Concept

As it was already mentioned above, in 2008 *Fujii* and *Ohno* described a novel and convenient strategy for the synthesis of indolines *via* a Pd(0)-catalyzed C(sp^3)-H activation of unactivated alkyl groups of functionalized *N*-alkyl-2-bromoanilines and subsequent intramolecular cyclization, however, the corresponding indolines were formed as racemic mixtures. We proposed that this interesting transformation can proceed in asymmetric fashion with the help of our newly developed Pd-*NHC* catalysts. To the best of our knowledge efficient coupling reactions that can distinguish between two enantiotopic C-H bonds in an unactivated methylene group have not been reported (Scheme 60). Hence, the enantioselective version would represent a great progress in synthesis.

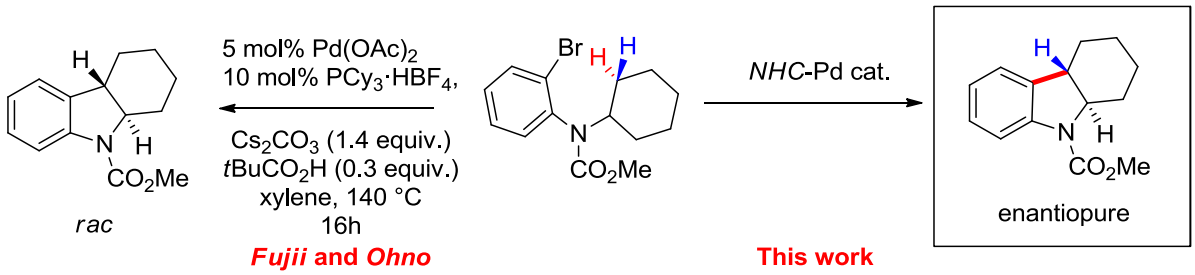

Scheme 60. Left: methodology developed by *Fujii* and *Ohno*. Right: our proposed strategy.

III.4. Results: Fused Indolines by Pd-Catalyzed Asymmetric C-C Coupling Involving an Unactivated Methylene Group[‡‡]

III.4.1. Synthesis of New Catalysts

To establish the most efficient catalyst in the enantioselective synthesis of indolines, we synthesized a number of Pd(*NHC*)(cinnamyl)I complexes. The complexes were prepared using a similar route as for the synthesis of complexes **100** and **102**. All Pd(*NHC*)(η^3-cinnamyl)I precatalysts were formed as a mixture of diastereoisomers in moderate to good yields (Figure 42).

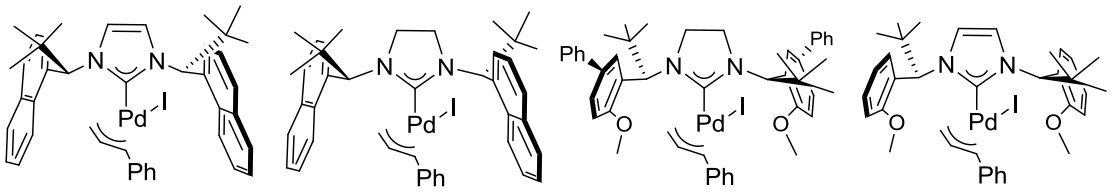

(*S*,*S*)-**158** (*S*,*S*)-**159** (*R*,*R*)-**160** (*R*,*R*)-**161**

Figure 42. (*S*,*S*)-**158**-38% yield, (*S*,*S*)-**159**-62% yield, (*R*,*R*)-**160**-83% yield, (*S*,*S*)-**161**-26% yield.

III.4.2. Optimization of Reaction Conditions

We started our study with *N*-cyclohexyl-substituted carbamate **162**. Under the reaction conditions we used previously for oxindole synthesis (Pd(dba)$_2$/*t*BuONa/DME/rt) fused indoline **163** was formed only in traces. A first positive result was obtained when the reaction was carried out under conditions developed by *Fujii* and *Ohno*. Under these conditions in the presence of precatalyst (*S*,*S*)-**100** the fused indoline **163** was formed in 36% yield and 86% *ee* (Table 15, entry 1). *Trans*-fusion in indoline **163** was indicated by the 12 Hz coupling

[‡‡] The study described in this chapter was carried out by the author of the thesis in collaboration with two postdoctoral associates (Dr. *M. Nakanishi* and Dr. *E. Larionov*)

constant in the ^{1}H-NMR spectrum.[234,249,252] Both the yield and enantiomeric ratio of indoline **163** increased strongly, when in place of the η^3-allyl complex (*S*,*S*)-**100**, the more reactive η^3-cinnamyl palladium complex (*S*,*S*)-**102** was used (Table 15, entry 2). It is noteworthy that in the absence of pivalic acid as an additive, only traces of the product were observed.[219] The reaction did not proceed at all at lower temperature (110 ˚C). Complex (*R*,*R*)-**161**, incorporating the enantiomeric *NHC* ligand with *o*-OMe aryl groups, afforded **163** in moderate 56% yield and 80% *ee* (entry 3).

Table 15. Screening of chiral *NHC*-palladium precursors in the asymmetric synthesis of fused indolines.

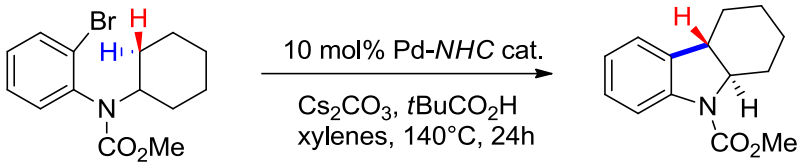

162 **163**

Entry[a]	Pd-*NHC*	Yield (%)[b]	E.r.[c]
1	(*S*,*S*)-**100**	36	93 : 7
2	(*S*,*S*)-**102**	73	97.5 : 2.5
3	(*S*,*S*)-**161**	56	10 : 90
4	(*S*,*S*)-**158**	89	97.5 : 2.5
5	(*S*,*S*)-**159**	9	78 : 22
6	(*R*,*R*)-**160**	9	n.d[d]
7[e]	$[Pd(cin)Cl]_2$/(*S*,*S*)-[**L14**H][I]	84	97.5 : 2.5
8[f]	$[Pd(cin)Cl]_2$/(*S*,*S*)-[**L14**H][I]	39	96 : 4
9[g]	$[Pd(cin)Cl]_2$/(*S*,*S*)-[**L14**H][I]	78	95 : 5

[a] Reaction conditions: **162** (0.2 mmol), Pd-*NHC* complex (0.02 mmol), pivalic acid (0.06 mmol), cesium carbonate (0.3 mmol), dry xylenes (2 mL). [b] Yield of product isolated after column chromatography. [c] The enantiomeric ratio was determined by HPLC on a chiral stationary phase (Chiral OD-H, *n*-hexane/*i*-PrOH 99:1, 0.5 mL/min^{-1}). The left column refers to the enantiomer shown. [d] n.d. = not determined. [e] $[Pd(\eta^3$-cinnamyl)$Cl]_2$ (0.01 mmol), (*S*,*S*)-[**L14**H][I] (0.02 mmol), cesium pivalate (0.2 mmol), cesium carbonate (0.3 mmol), dry xylenes (2 mL), 140 ˚C. [f] $[Pd(\eta^3$-cinnamyl)$Cl]_2$ (0.005 mmol), (*S*,*S*)-[**L14**H][I] (0.01 mmol), cesium pivalate (0.2 mmol), cesium carbonate (0.3 mmol), dry xylenes (2 mL), 140 ˚C. [g] $[Pd(\eta^3$-cinnamyl)$Cl]_2$ (0.005 mmol), (*S*,*S*)-[**L14**H][I] (0.01 mmol), cesium pivalate (0.2 mmol), cesium carbonate (0.3 mmol), dry xylenes (2 mL), dry mesitylene (160 ˚C).

A dramatic decrease of the yield and enantiomeric ratio of indoline **162** were found, when 4,5-dihydroimidazolium-derived *NHC*-palladium complexes **159** and **160** were used (entries 5 and 6).[§§] Complex (*S*,*S*)-**158** bearing imidazolium naphthyl-derived *NHC* ligand showed a significantly improved stability at elevated temperatures, and this had a beneficial effect on the yield and enantioselectivity of the coupling reaction (Table 15, entry 4).

Consequently, imidazolium salt (*S*,*S*)-[**L14**H][I], the precursor of the most efficient *NHC* ligand, was chosen for the *in situ* generation of Pd-*NHC* complex. Experimentally it was found that using an *in situ* generated catalyst in the presence of cesium pivalate and cesium carbonate in xylenes as solvent, the reaction gave indoline **162** in a good yield with high asymmetric induction (entry 7). The results perfectly matched those obtained from pre-assembled Pd-*NHC* catalyst (entry 2). When the catalyst loading was reduced to 5 mol% the yield of the cyclization reaction dropped (Table 15, entry 8), while heating of the reaction mixture in mesitylene at 160 ˚C helped to improve the yield up to 78% (entry 9).

III.4.3 Synthesis of Carbamates

A variety of carbamates was prepared from 2-bromoaniline derivatives according to the previously reported procedure.[234,253-255] 2-Bromoaniline derivative reacted with alkanone to produce imine, which was reduced *in situ* by $NaBH_4$. The corresponding *N*-alkyl-2-bromoaniline was transformed to the alkyl carbamate by treatment with the alkyl chloroformate under reflux conditions. Initially, the *N*-cyclohexyl derived carbamates bearing different substituents in the aniline part were prepared (Scheme 61).

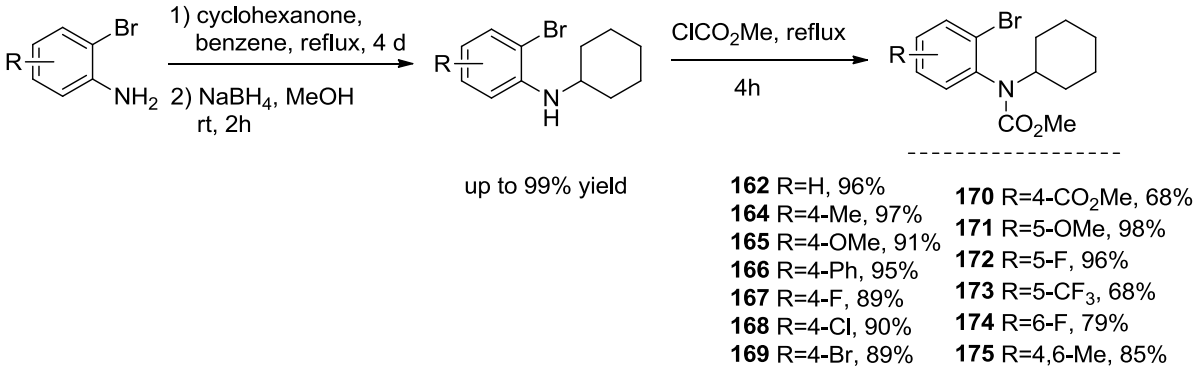

Scheme 61. Synthesis of carbamates **162**, **164**-**175**. Compound **164**-**175** were synthesized by Dr. *M. Nakanishi*.

[§§] Complex (*S*,*S*)-**159** decomposed by observation of precipitation of palladium black when heated in xylenes to 140 ˚C for 30 minutes. Complex (*S*,*S*)-**158** was recovered unchanged after the same treatment (confirmed by ^{1}H-NMR spectroscopy).

Also carbamates bearing different size of the cycloalkyl ring (*N*-cyclopentyl and *N*-cycloheptyl carbamates) were synthesized using the similar two-step procedure (Scheme 62).

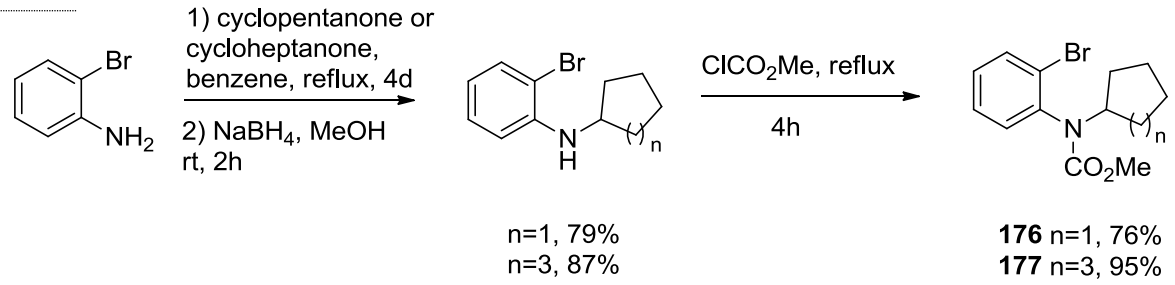

Scheme 62. Synthesis of carbamates **176** and **177** (prepared by Dr. *M. Nakanishi*).

A number of acyclic carbamates was prepared *via* reductive amination of ketones with *o*-bromoaniline (Table 16).

Table 16. Synthesis of acyclic carbamates **192**-**207**.

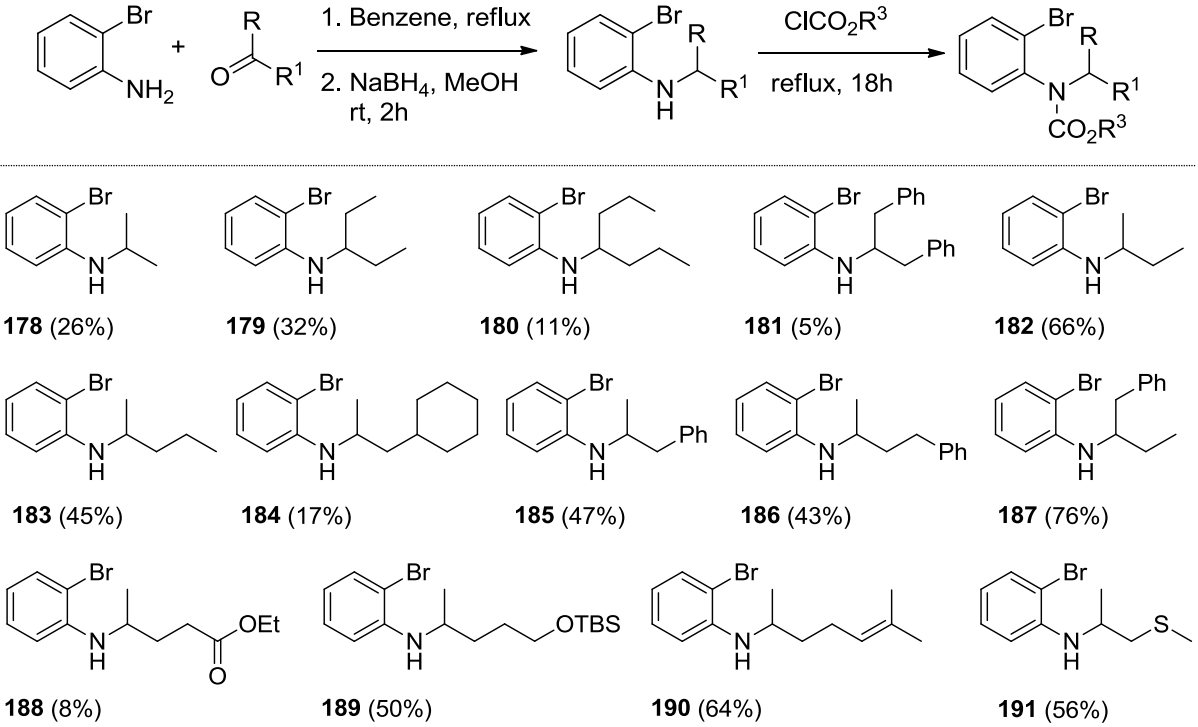

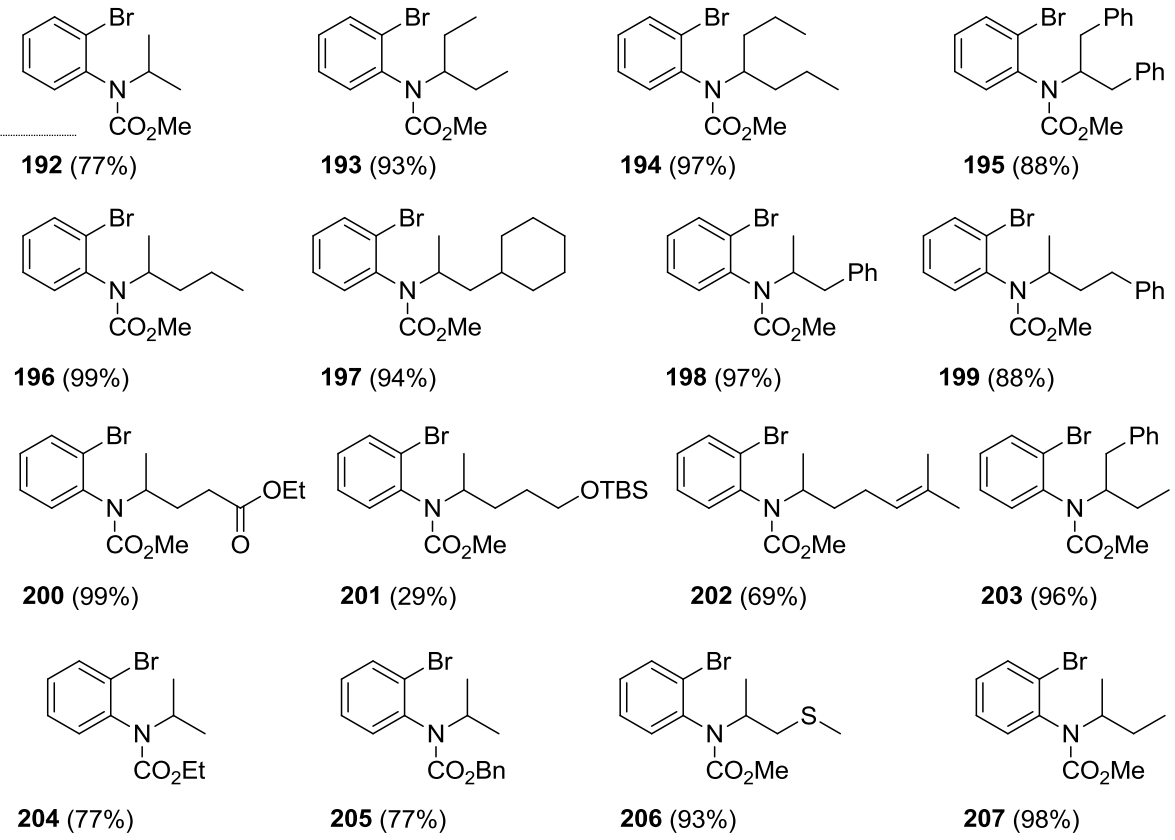

Compounds **179**-**181**, **183**-**184**, **187**, **193**-**197**, **203** were synthesized by Dr. *M. Nakanishi*.

A range of acyclic carbamates was synthesized *via* palladium-catalyzed amination[256] of 1,2-dibromoaniline (Table 17). The *Buchwald-Hartwig* coupling between 1,2-dibromobenzen and a primary amine led to the formation of *N*-alkyl-2-bromoaniline, which was further treated with a chloroformate giving the corresponding alkyl carbamate.

Table 17. Synthesis of carbamates **216**-**223** *via* Pd-catalyzed amination of 1,2-dibromoaniline.

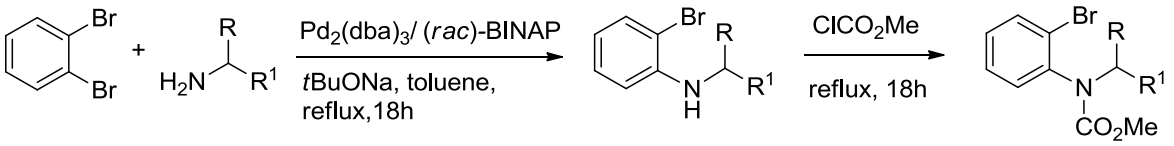

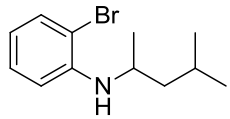

208 (59%)

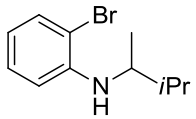

209 (62%)

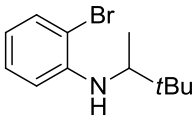

210 (55%)

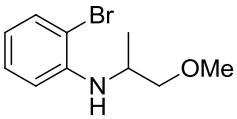

211 (58%)

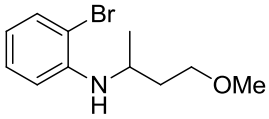

212 (76%)

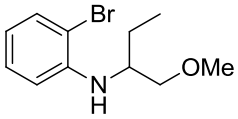

213 (55%)

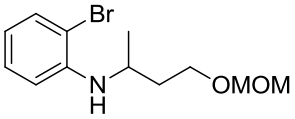

214 (63%)

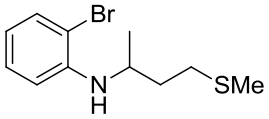

215 (61%)

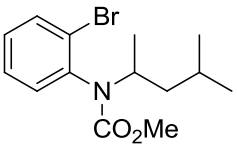

216 (91%)

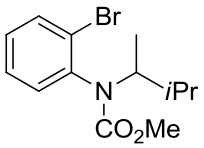

217 (88%)

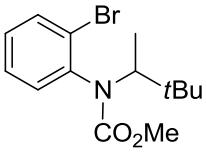

218 (48%)

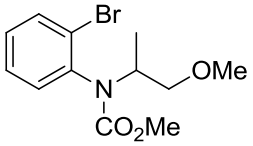

219 (87%)

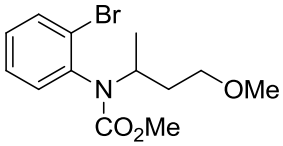

220 (69%)

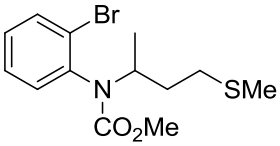

221 (96%)

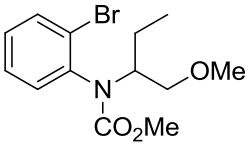

222 (95%)

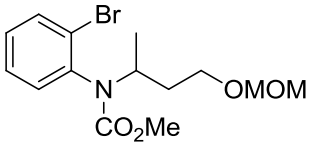

223 (86%)

Compounds **208**-**210**, **216**-**218** were prepared by Dr. *M. Nakanishi*.

Carbamates **224** and **225** bearing hydroxy and acetate groups, respectively, were easily prepared from the corresponding MOM-protected carbamate **223** (Scheme 63).

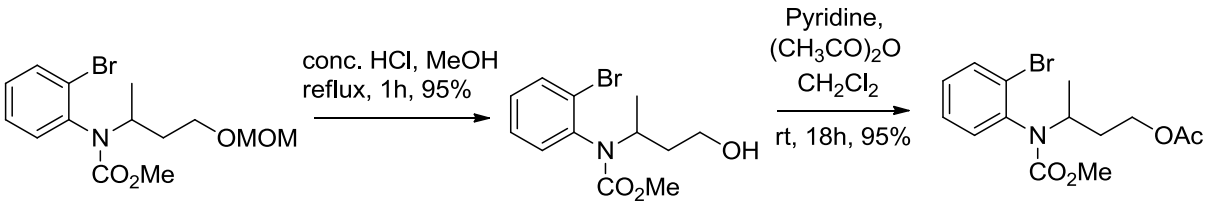

223 **224** **225**

Scheme 63. Synthesis of carbamates **224** and **225**.

The enantiopure carbamates **219**(*S*), **222**(*S*) and **228**-**230** were prepared in a six-step procedure as shown in Scheme 64. The commercially available amino acids were reduced by $LiAlH_4$ to the corresponding amino alcohols. After selective benzyl protection of the amino group, the hydroxyl group was easily protected using methyl iodide. The following selective cleavage of the benzyl protection under standard conditions Pd/C (1 atm H_2) led to the

formation of the methoxyamino derivatives. Final carbamates were obtained *via* palladium-catalyzed amination of 1,2-dibromoaniline (Scheme 64).

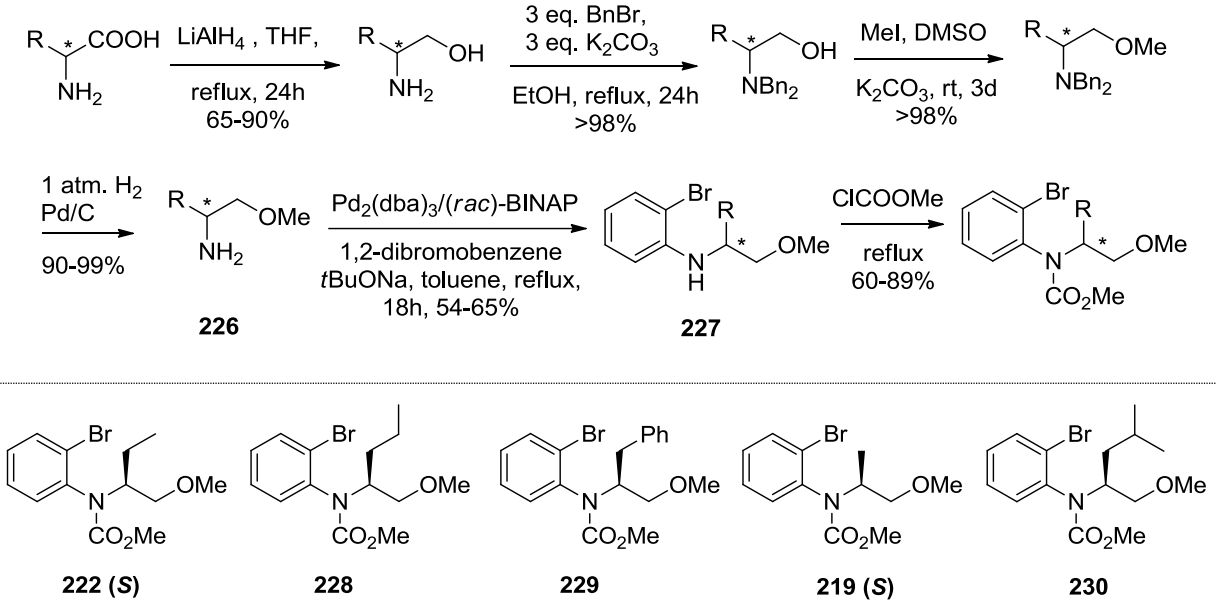

Scheme 64. Synthesis of enantiopure carbamates **219**(*S*), **222**(*S*) and **228**-**230**.

Both enantiomers of **198** were prepared according to the route shown in Scheme 65. The corresponding chiral amines ((*S*) - and (*R*) - 1-phenylpropan-2-amine) were obtained from commercially available (*L*)(-) or (*D*)(+)-norephedrine using the literature procedure.[257] The desired products (*S*)-**198** and (*R*)-**198** were synthesized *via* the standard palladium-catalyzed amination of 1,2-dibromoaniline (Scheme 65).

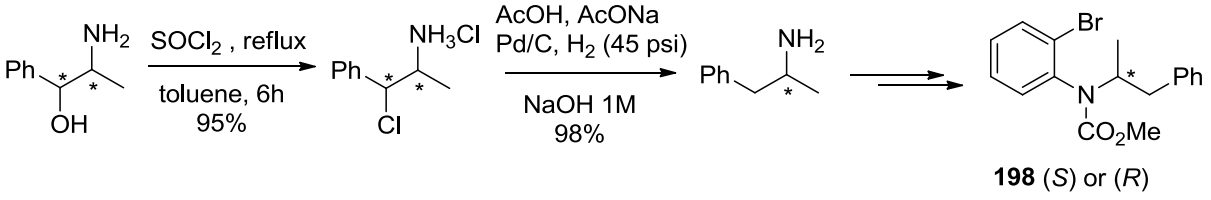

Scheme 65. Synthesis of (*S*)-**198** and (*R*)-**198**.

III.4.4. Substrate Scope for the Synthesis of Fused Indolines

Next, the substrate scope for the enantioselective Pd(*NHC*)-catalyzed synthesis of fused indolines *via* C(sp^3)-H activation of unactivated methylene group was investigated under established reaction conditions (Table 15, entry 9) and the results are listed in Table 18.

Table 18. Chiral Pd(*NHC*)-catalyzed asymmetric synthesis of fused indolines.

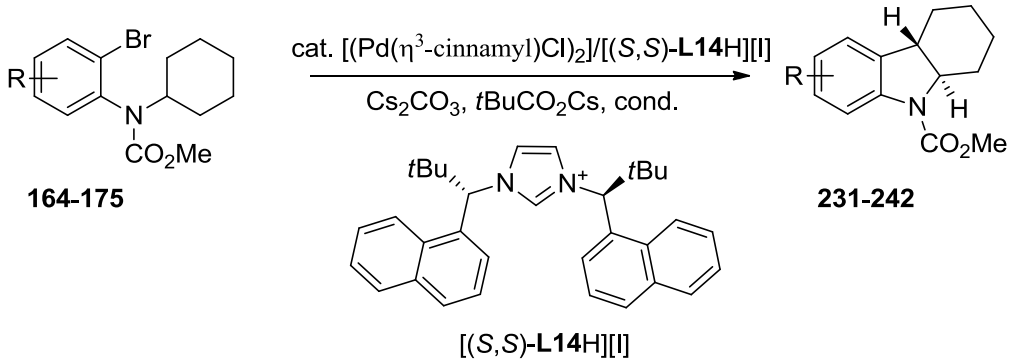

Entry	Substrate	R	Cond.[a] T [˚C]/*t*[h]	Prod.	Yield [%][b]	E.r.[c]
1	**164**	4-Me	160/3	**231**	82	95:5
2	**165**	4-MeO	160/3	**232**	84	94.5:5.5
3	**166**	4-Ph	160/3	**233**	88	96:4
4	**167**	4-F	140/24	**234**	81	96:4
5	**167**	4-F	160/3	**234**	59	90:10
6	**168**	4-Cl	140/24	**235**	30	63:37
7	**168**	4-Cl	160/3	**235**	13	55:45
8	**169**	4-Br	140/24	**236**	0[d]	n.d.
9	**170**	4-CO_2Me	160/3	**237**	82	89:11
10	**171**	5-MeO	140/24	**238**	55	96:4
11	**171**	5-MeO	160/3	**238**	24	90:10
12	**172**	5-F	160/3	**239**	70	93:7
13	**173**	5-CF_3	160/3	**240**	62	90:10
14	**174**	6-F	140/24	**241**	68	92:8
15	**175**	4,6-Me	160/3	**242**	88	96:4

[a] Conditions for reaction carried out at 140 ˚C: **carbamate** (0.2 mmol), [Pd(η^3-cinnamyl)Cl]$_2$ (0.01 mmol), (*S*,*S*)-[**L14**H][I] (0.02 mmol), cesium pivalate (0.2 mmol), cesium carbonate (0.3 mmol), dry xylenes (2 mL); conditions for reactions carried out at 160 ˚C: **carbamate** (0.2 mmol), [Pd(η^3-cinnamyl)Cl]$_2$ (0.005 mmol), (*S*,*S*)-[**L14**H][I] (0.01 mmol), cesium pivalate (0.2 mmol), cesium carbonate (0.3 mmol), dry mesitylene. [b] Yield of product isolated after flash column chromatography. [c] Enantiomeric ratio was determined by chiral HPLC. The left column refers to the enantiomer shown. [d] 0.1 mmol scale. N.d. = not determined. Carried out in collaboration with Dr. *M. Nakanishi*.

Extention to substituted aniline precursors showed that under these reaction conditions a fluoro group (Table 18, entry 5) is tolerated, but, not surprisingly, chloro and bromo groups are not (entries 6 and 8). Fortunately, the carbamates with electron-donor substituents at position C(4) gave improved product yields (Table 18, entries 1-3). In contrast, electron-withdrawing groups at C(4) decreased both products yields and enantioselectivities (Table 18, entries 4-9). The methoxy group at C(5) position of the aniline group reduced the product yield (entries 10 and 11). Fluoro and trifluoromethyl groups are reasonably well tolerated in this reaction (Table18, entries 12 and 13). Finally, entries 14 and 15 show that the reaction can be performed with C(6)-substituted carbamates (Table 18).

It was confirmed experimentally that the size of the cycloalkyl ring is of great important in this transformation. Thus, the C-H activation of the *N*-cyclopentyl carbamate derivative did not proceed at all (Table 19, entry 2). In contrast, *N*-cycloheptyl-substituted substrate gave better yield and even higher asymmetric induction than the corresponding *N*-cyclohexyl (Table 19, entries 3 and 4).

Table 19. Asymmetric synthesis of fused indolines.

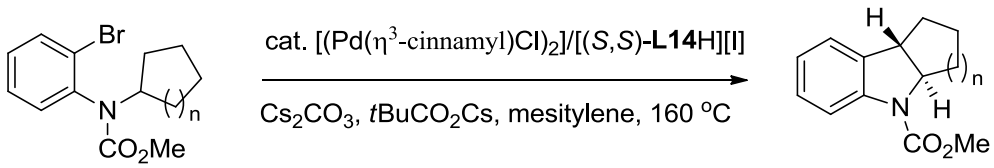

162,**176**,**177** **163**,**243**,**244**

Entry[a]	Substrate	n	*t* [h]	Product (yield %)[b]	E.r.[c]
1	**162**	2	3	**163**/(78)	95:5
2	**176**	1	24	**243**/(0)	-
3	**177**	3	3	**244**/(94)	97.5:2.5
4[d]	**177**	3	3	**244**/(88)	97.5:2.5

[a] Reaction conditions: **carbamate** (0.2 mmol), $[Pd(\eta^3\text{-cinnamyl})Cl]_2$ (0.005 mmol), (*S*,*S*)-[**L14**H][I] (0.01 mmol), cesium pivalate (0.2 mmol), cesium carbonate (0.3 mmol), dry mesitylene. [b] Yield of isolated product. [c] Enantiomeric ratios were determined by chiral HPLC. The left column refers to the enantiomer shown. [d] 1 mmol scale. Carried out in collaboration with Dr. *M. Nakanishi*.

III.4.5. Determination of Absolute Configuration

The absolute configuration of the fused indolines was determined by an X-ray structural analysis of compound **246**, which was obtained by hydrolysis of carbamate **245**. All other indolines were assigned configurations by analogy. As **245** was not directly accessible, it was prepared from **244** by reaction with tetra-*n*-butylammonium tribromide (Scheme 66). The X-ray structure shows that **246** have 5a*R*,10a*S* configuration (Figure 43).

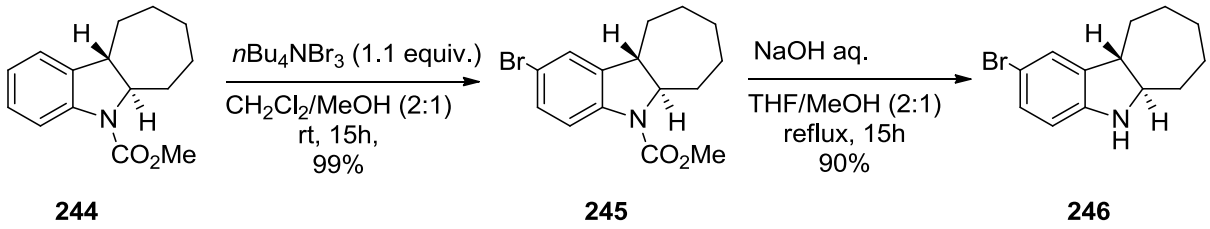

244 **245** **246**

Scheme 66. Bromination of fused indoline **244**.

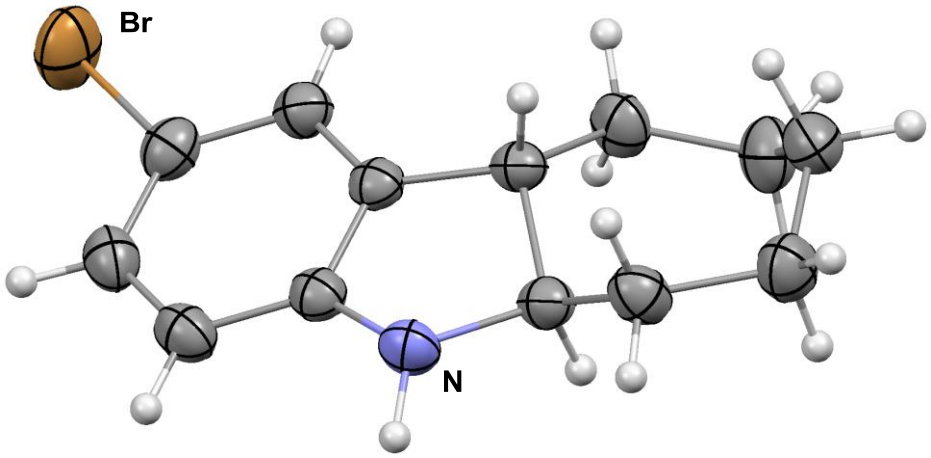

Figure 43. X-Ray structure of fused indoline (-)-(5a*R*,10a*S*)-**246**.[***]

III.4.6. Proposed Mechanism for Enantioselective Pd(NHC)-Catalyzed Synthesis of Fused Indolines via C(sp^3)-H Activation of the Unactivated Methylene Group.

The proposed reaction mechanism for this transformation is shown in Scheme 67. Initially, palladium dimer - $[Pd(\eta^3\text{-cinnamyl})Cl]_2$, is cleaved by the *NHC* ligand. The latter is generated *in situ* from *NHC*-HI and cesium pivalate. Nucleophilic addition of pivalate to the

[***] Carried out by Dr. *C. Besnard*.

cinnamyl ligand followed by alkene dissociation generates the Pd(0)-*NHC* active catalysts.[180,258] Following oxidative addition of carbamate **162** forms the palladacycle intermediate and a bromide ligand can be exchanged to pivalate. The C(sp^3)-H activation step occurs by an inner-sphere pivalate assisted concerted metalation-deprotonation (CMD).[259] On the methylene site, two enantiotopic C(sp^3)-H bonds can be perfectly distinguished as *trans*-fusion. The last reductive elimination produces desired indoline **163** and the regenerated Pd(0)-*NHC* active catalyst.

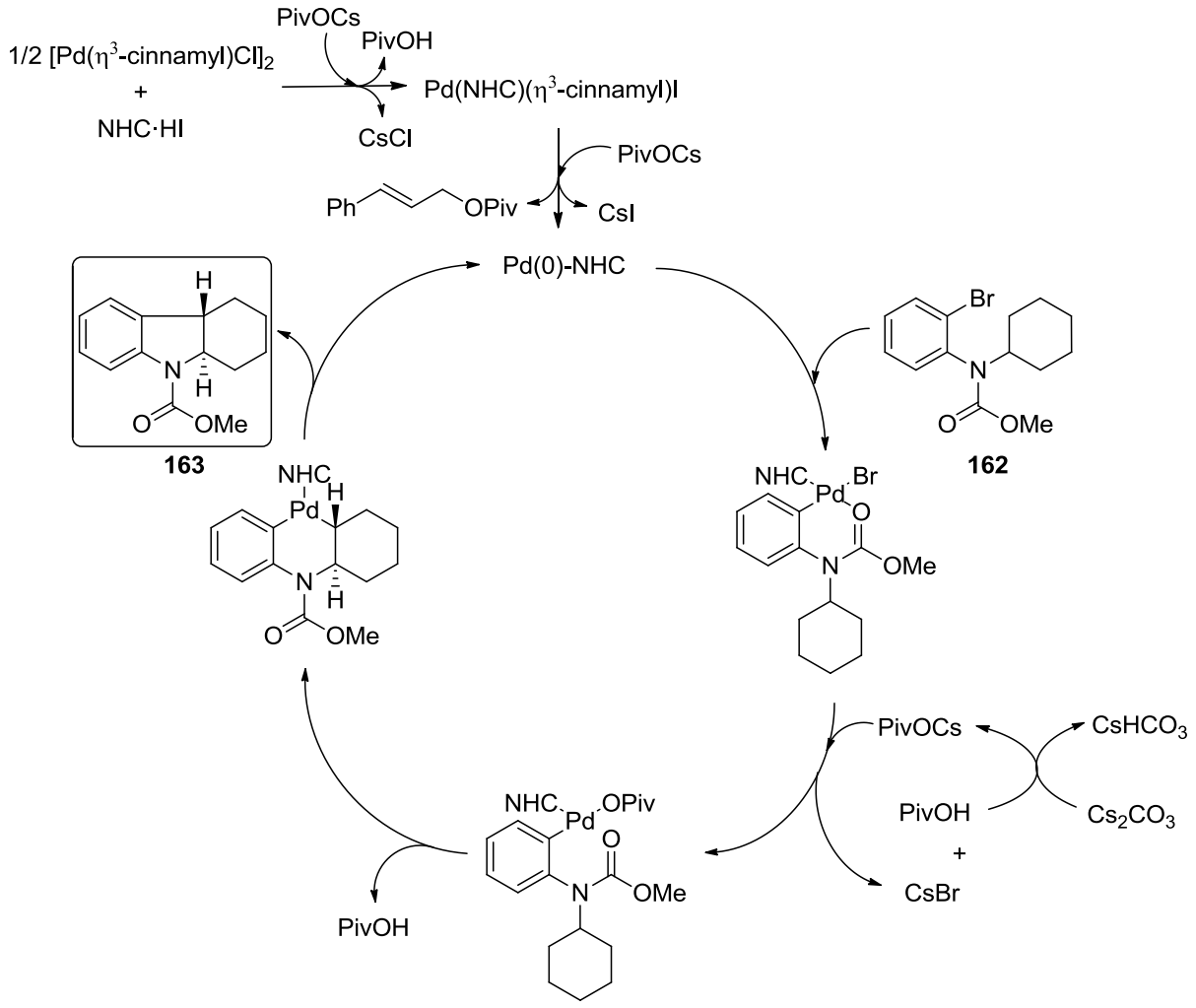

Scheme 67. Proposed catalytic cycle for the synthesis of fused indolines.

III.4.7. Highly Enantioenriched 2-Substituted and 2,3-Disubstituted Indolines via Regiodivergent Reaction of a Racemic Mixture (RRM).

Next, we focused our attention on the synthesis of enantioenriched 2-substituted and 2,3-disubstituted indolines. While this work was in progress, the enantioselective synthesis of 2-methylindolines *via* the same procedure but using chiral phosphine ligands was reported by

Kagan[260] and co-workers. In the presence of a Pd/(*R*,*R*)-Me-*DUPHOS* catalyst highly enantioenriched 2-methylindolines were prepared. However, attempts to extend the reaction under similar conditions to other members of this class of compounds were with little success. Recently, in 2012, the communication by *Cramer*[261] and co-workers appeared, which represent a more extensive study of a wide range of highly enantioenriched indolines. High asymmetric induction was provided by using new, sterically demanding monodentate phosphines in conjunction with bulky carboxylic acids.

Initially, prochiral substrates **192-195** were investigated under similar reaction conditions as for the fused indoline synthesis and the results are summarised in Table 20.

Table 20. Asymmetric synthesis of 2- and 2,3-disubstituted indolines.

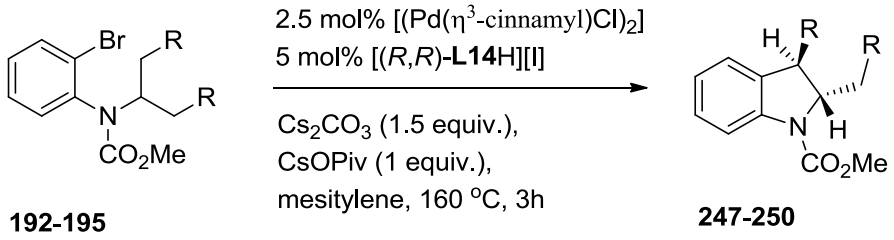

192-195 **247-250**

Entry[a]	Substrate	R	Product	Yield (%)[b]	Ee[c]
1	**192**	H	**247**	84	89
2[d]	**192**	H	**247**	86	90
3	**193**	Me	**248**	92	97
4	**194**	Et	**249**	91	95
5[e]	**195**	Ph	**250**	96	98

[a] Reaction conditions: [Pd(η^3-cinnamyl)Cl]$_2$ (2.5 mol%), (*R*,*R*)-[**L14**H][I] (5 mol%), **carbamate** (0.2 mmol), cesium pivalate (0.2 mmol), Cs_2CO_3 (0.3 mmol), dry mesitylene (2 mL). [b] Isolated yield of pure material. [c] Enantiomeric excess was determined by chiral HPLC. [d] Reaction conditions: [Pd(η^3-cinnamyl)Cl]$_2$ (5 mol%), (*R*,*R*)-[**L14**H][I] (10 mol%), **carbamate** (0.2 mmol), cesium pivalate (0.2 mmol), Cs_2CO_3 (0.3 mmol), dry xylenes (2 mL) at 140 °C for 24 h. [e] Reaction carried out with (*S*,*S*)-[**L14**H][I]. Carried out in collaboration with Dr. *M. Nakanishi*.

2-Methylindoline **247** was obtained in high yield (84%) and good enantioselectivity (89%) (Table 20, entry 1). Higher catalyst loading did not improve the yield and enantioselectivity of this system (entry 2). Gratefully, the product yield and asymmetric induction strongly increased with the *N*-3-isopentyl carbamate **193** and *N*-3-isooctyl

carbamate **194** where the cyclization involved not a methyl group but a C-H bond of a methylene unit (Table 20, entries 3 and 4). We found that Me activation in **193** would have led to the formation of a 6-membered ring product (a 2-ethyl-1,2,3,4-tetrahydroquinoline derivative), however this was completely absent in the crude product. As shown, and in accordance with the results obtained for fused indolines,[119] the *trans* products **247**-**250** were obtained exclusively.

The stereochemical assignment in **247** was determined by comparison with literature data[260] and that in **248** and **249** was tentatively made on the basis of the similarity of the CD spectra with the *trans*-fused indolines. Differences in the CD spectrum of **250** initially cast doubt on the stereochemical assignment in this compound. We resorted to a detailed *vibrational circular dichroism* (VCD)[†††] study.[262,263] Comparison of experimental results with the calculated VCD spectrum and IR spectrum proved that it was a *trans*-configuration. This was also done for **248**. Details are given in the experimental part.

Racemic substrate **207** was tested next. Interestingly, if the methyl group undergoes the cyclization reaction selectively, one can expect 2-substituted indolines as major products. However, if the CH_2 group participates in the reaction, then two additional pairs of diastereomers of enantiomeric indolines might form (Scheme **68**).

[†††] Carried out by Prof. Dr. *T. Bürgi*.

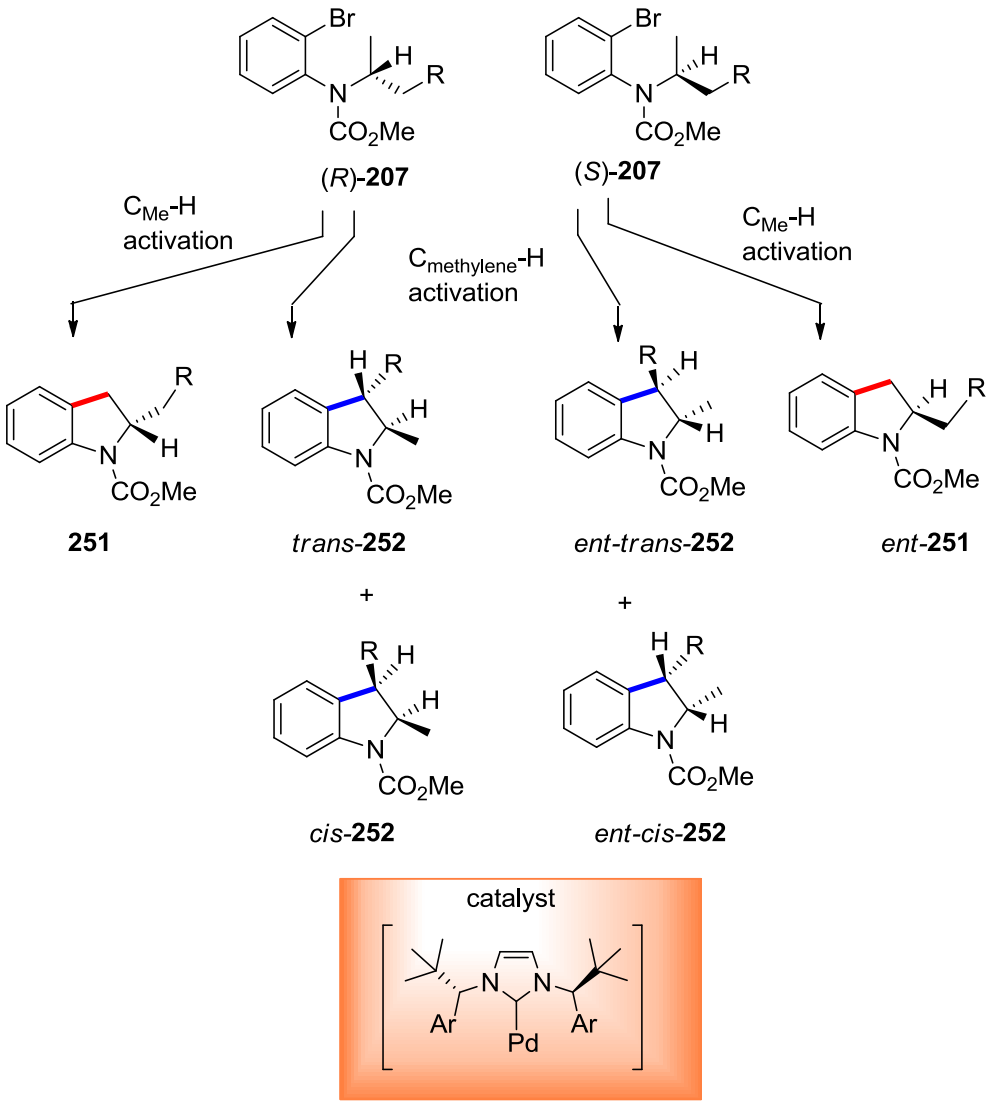

Scheme 68. Potential 2-substituted and 2,3-disubstituted indoline-products in the C_{Ar}-C_{sp3} coupling reaction of *rac* **207**.

Initially, the reaction of **207** was carried out with tricyclohexylphosphine (Table 21, entry 1) and with an achiral *NHC* ligand (entry 2). In both cases methyl C-H activation was the exclusive reaction pathway. This was also observed by *Anas, Cordi and Kagan*[260] with Me-DUPHOS ligand (entry 3). It was an expected result because the previous experience shows that C(sp^3)-H activation is easier in the methyl group than in the methylene group.

Interestingly, the chiral *NHC* ligands (*S*,*S*)-[**L14**H][I] and (*S*,*S*)-[**L5**H][I] generate two products, corresponding to both methyl- as well as methylene-C-H activation. In **207**, the former occurred with enantioselectivities around 70%, whereas the latter afforded *trans*-**252** as an enantiomerically pure diastereomer (entries 4 and 5). The products of the reactions of **207** with chiral *NHC*-Pd catalysts are the result of a regiodivergent reaction of a racemic

mixture[‡‡‡] (regiodivergent RRM).[264-266] No *cis*-products are formed in this reaction.

Table 21. Pd(*NHC*)-catalyzed synthesis of indolines from *rac*-**207**.

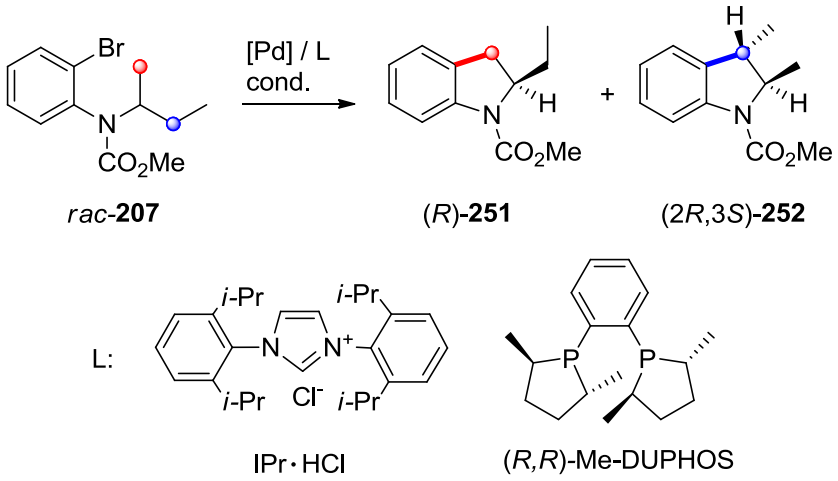

Entry	Ligand (L)	Ratio **251**:**252**[a] (% *ee*)	Yield (%)[b]
1[c]	$PCy_3 \cdot HBF_4$	100 : 0	90
2[d]	IPr·HCl	100 : 0	90
3[260]	(*R*,*R*)-Me-DUPHOS	100 (-23) : 0	65
4[e]	(*S*,*S*)-[**L14**H][I]	59 (68) : 35 (>99)	94
5[e]	(*S*,*S*)-[**L5**H][I]	57 (77) : 38 (>99)	95

[a] The ratio of products (*R*)-**251** and (*2R*,3*S*)-**252** was determined by ^{1}H-NMR. The enantiomeric excess was determined by chiral HPLC (AD-H column, *n*-hexane/*i*-PrOH = 99 : 1, 0.5 mL/min). [b] Isolated yield of the mixture of **251** and **252**. [c] Reaction conditions: $Pd(OAc)_2$ (10 mol%), PCy_3HBF_4 (20 mol%), carbamate **207** (0.2 mmol), pivalic acid (0.06 mmol), Cs_2CO_3 (0.3 mmol), dry xylenes (2 mL) [d] Reaction conditions: $[Pd(\eta^3\text{-cinnamyl})Cl]_2$ (5 mol%), IPr·HCl (10 mol%), carbamate **207** (0.2 mmol), cesium pivalate (0.2 mmol), Cs_2CO_3 (0.3 mmol), dry xylenes (2 mL). [e] Reaction conditions: $[Pd(\eta^3\text{-cinnamyl})Cl]_2$ (5 mol%), *NHC*·HI (10 mol%), **207** (0.2 mmol), cesium pivalate (0.2 mmol), Cs_2CO_3 (0.3 mmol), dry xylenes (2 mL).

Product (*R*)-**251** arises from the matched case of the reaction of substrate (*S*)-**207** and catalyst Pd(*S*,*S*)-**L14** (or Pd(*S*,*S*)-**L5**). It is formed in higher yield but lower enantioselectivity because the reaction of (*R*)-**207**/Pd(*S*,*S*)-**L14** (or (*R*)-**207**/Pd(*S*,*S*)-**L5**), the missmatched pair, produces not only (*2R*,3*S*)-**252** (catalyst control, excellent enantioselectivity), but also some

[‡‡‡] In the divergent reaction on a racemic mixture (RRM) both enantiomers of the substrate react with a chiral reagent at similar rates to form non-enantiomeric products. With excellent reagent control the products can be obtained in high yields (up to 50%) and asymmetric induction (>99% *ee*). There are three general categories of divergent RRM: a) Stereodivergent reactions on racemic mixtures (Generally a racemic starting material with resident stereo-centers is utilized, where in the divergent step, products form with a new stereogenic centers as diastereoisomers, which can be easily separated); b) Regiodivergent reactions on racemic mixtures (A racemic starting material reacts with a chiral non-racemic reagent producing enantioenriched regioisomers); c) Structurally divergent reactions on racemic mixtures (In the divergent step a racemic substrate reacts with a chiral reagent or catalyst producing two distinct enantioenriched compounds).

(*S*)-**251**. Figure 44 shows a plot of the progress of the reaction. The *ee* values for (*R*)-**251** and (*2R*,3*S*)-**252** are invariant over the course of the reaction.

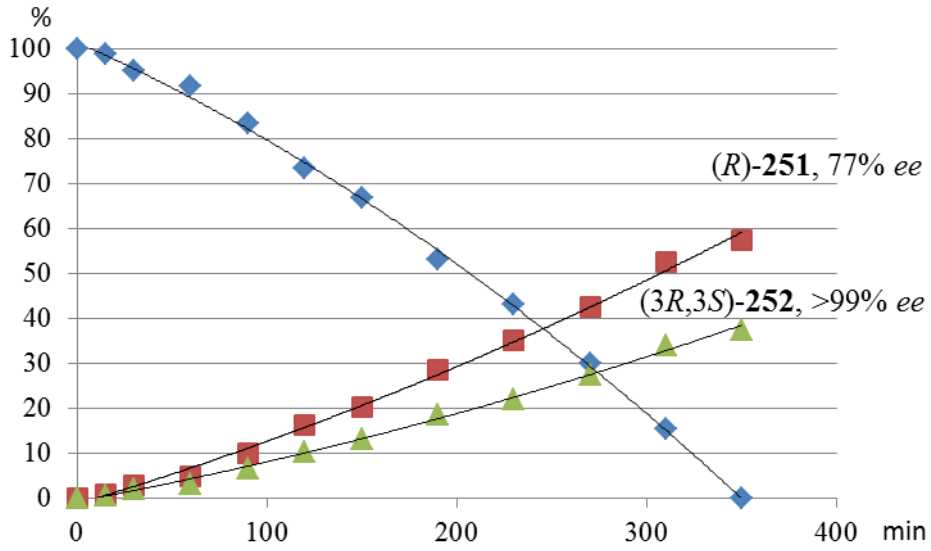

Figure 44. Evolution of the regiodivergent reaction of *rac*-**207**.

Next, to rationalize the regiodivergent RRM of this process, the activation barriers of CMD step for different pathways of C(sp^3)-H activation of carbamate **207** were calculated. The results show that with chiral *NHC* ligand the preference for the formation of *cis*-product *via* $C_{methylene}$-H activation is observed. The corresponding differences between activation barriers for *cis*- and *trans*-CH_2-activation are 15.9 kJ/mol for (*R*)-CH_2 and 8.8 kJ/mol for (*S*)-CH_2. In agreement with experiments, the CH_3-activation is more preferable for (*S*)-**207** than for (*R*)-**207**. The respective difference between activation barriers for *trans*-CH_2-activation is 16.9 kJ/mol in favour of (*R*)-CH_2 transition state (Figure 45). This is again in agreement with experimentally observed higher *ee*'s of product **252**.

The structures of corresponding TSs *trans*-(*R*)-CH_2 and *trans*-(*S*)-CH_2 are compared in Figure 46. It was noted, that there is a steric repulsion between substrate benzene ring and *o*-methyl group of *NHC* ligand in TS *trans*-(*S*)-CH_2 (distance between center of benzene ring and methyl-hydrogen is 2.321 Å) which increases energy of TS. An addition interaction of the second *o*-methyl group of *NHC* with the methyl group connected directly to the reacting carbon atom of the substrate increases further the energy of *trans*-(*S*)-CH_2, thus leading to high enantioselectivity of CH_2-activation.

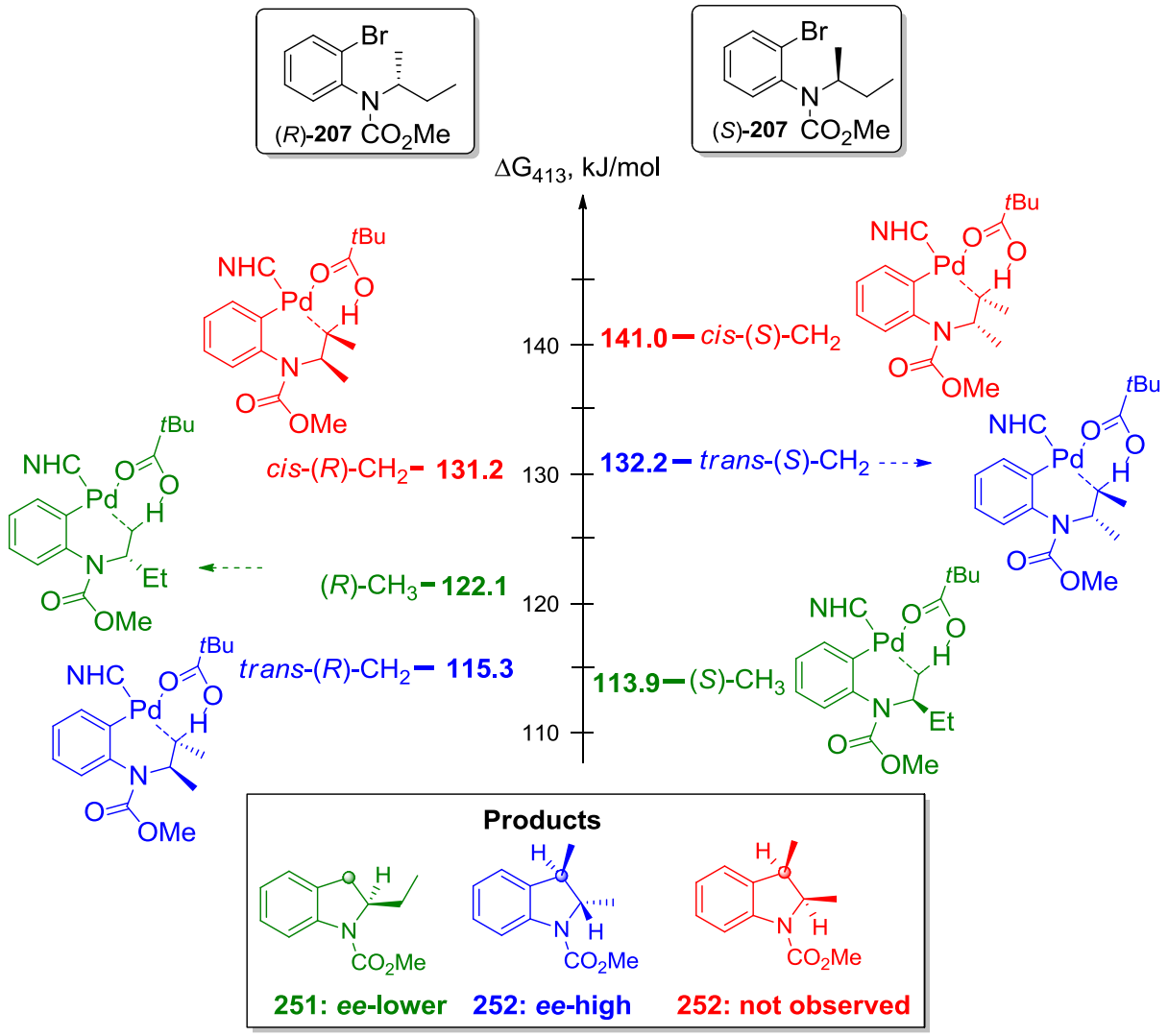

Figure 45. The activation barriers ($\Delta G^{\ddagger}_{413}$, gas phase) for CMD step with ligand (*S*,*S*)-[**L5**H][I] and substrate **207**. (*R*) and (*S*)-descriptors refer to the configuration of compound **207**.

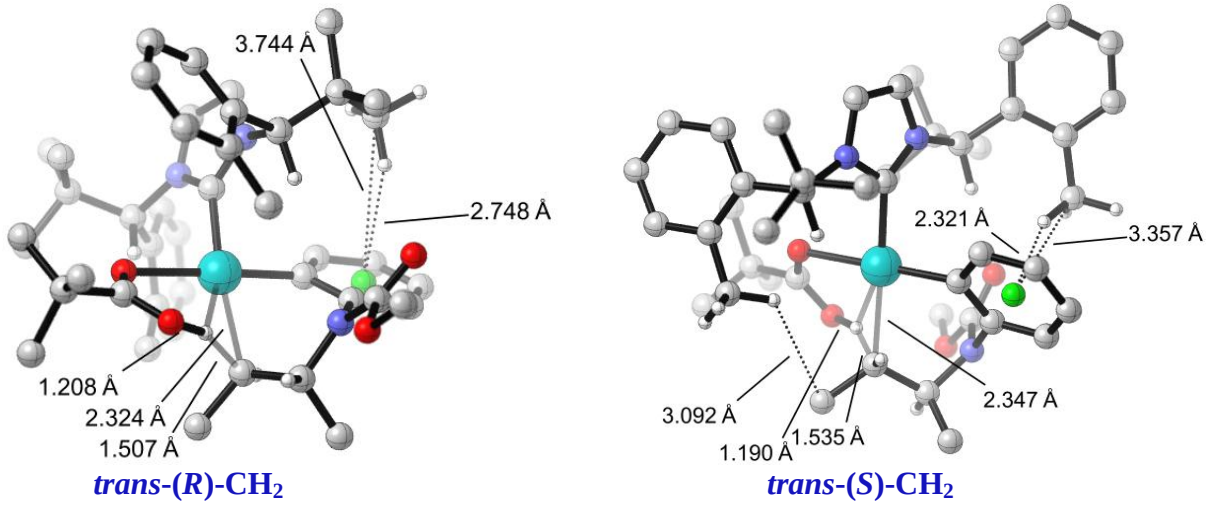

Figure 46. Structures of TSs for CH_2-activation of substrate **207**. Selected H atoms have been removed for clarity; center of substrate benzene ring is marked green. (*R*) and (*S*)-descriptors refer to the configuration of compound **207**.

We also have tried to correlate activation barriers, calculated relative to the most stable TS (*S*)-CH_3, with the respective experimental values (Table 22). Results show that the free energy barriers $\Delta\Delta G^{\ddagger}_{413}$ in the gas phase correlate very well with experimental ones (R^2 = 0.9819, RMSD = 1.8 kJ/mol). The largest deviation from experiment (3.3 kJ/mol) is observed for the TS *trans*-(*S*)-CH_2, which leads to the product (2*S*,3*R*)-**252**. Due to the low yield of this product (detected as a minor peak in HPLC) the error in the experiment relative to the free energy barrier is quite large.

Table 22. Comparison between experimental and calculated relative activation barriers for the regiodivergent RRM of carbamate **207**.

Activation mode	Experiment[a] $\Delta\Delta G^{\ddagger}_{413}$	Calculations $\Delta\Delta G^{\ddagger}_{413}$, kJ/mol $\Delta\Delta G^{\ddagger}$ gas phase	$\Delta\Delta G^{\ddagger}$ xylenes
(*S*)-CH_3	**0.0**	0	0
(*R*)-CH_3	**6.8**	8.2	10.3
***trans*-(*R*)-CH_2**	**1.0**	1.4	2.6
***trans*-(*S*)-CH_2**	**21.6**	18.3	23.8
Correlation coefficient R^2 [b]		**0.9819**	**0.9852**
RMSD, kJ/mol [b]		1.8	2.2

[a] See Scheme 68 for details. [b] Correlation coefficients R^2 and the root mean square deviations (RMSD) between calculated and experimental relative activation barriers.

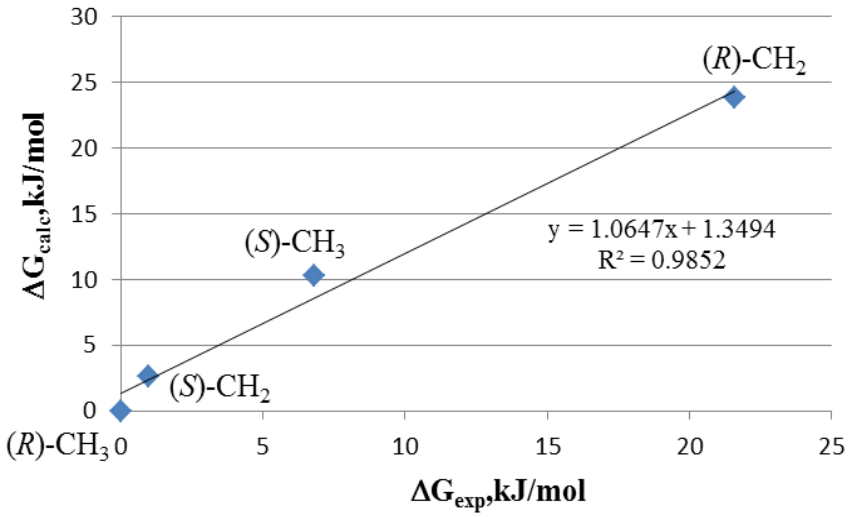

Figure 47. Correlation between experimental and calculated ($\Delta G^{\ddagger}_{413}$, xylenes) relative activation barriers for the regiodivergent RRM of carbamate **207** (blue squares).

A graphical representation of comparison between experimental and calculated activation barriers from Table 22 is shown in Figure 47. It is clearly seen, that the computations correlate well with the experimental data.

The ligand precursors (*S*,*S*)-[**L14**H][I] was then applied to the carbamates **203** and **222**. This data is summarized in Table 23. Both racemic carbamates **203** and **222** reacted in the coupling reaction producing a mixture of 2,3-disubstituted indolines in high yields and high enantioselectivities (Table 23, entries 1 and 2). The mixture was not separable by column chromatography. In case of carbamate **222**, a slightly higher temperature was required to complete the reaction (entry 2).

Table 23. Influence of substitution groups.

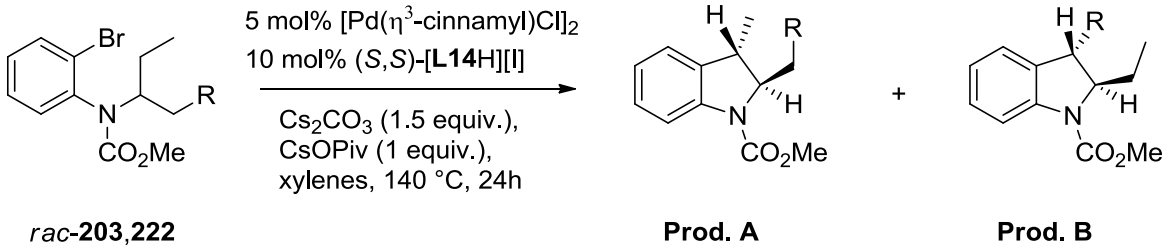

rac-**203**,**222** **Prod. A** **Prod. B**

Entry[a]	R	(**Prod. A**+**Prod. B**)/Yield [b]	**Prod.A** /Ee (%)[c]	**Prod.B** /Ee (%)[c]
1[d]	Ph	(**253**+**254**)/90 (1:0.9)	**253**/90	**254**/99
2[e]	MeO	(**255**+**256**)/81 (1:1)	**255**/96	**256**/88

[a] Condition: **carbamate** (0.2 mmol) (*S*,*S*)-[**L14**H][I] (10 mol%), [Pd(η^3-cinnamyl)Cl]$_2$ (5 mol%), cesium pivalate (1 equiv.) and of Cs_2CO_3 (1.5 equivs.) were used in dry xylenes at 140 °C for 24 h. [b] Determined by ^{1}H-NMR. [c] Enantiomeric excess (*ee*) was determined by chiral HPLC (see experimental section).[d] Carried out by Dr. *M. Nakanishi*. [e] **carbamate** (0.2 mmol), (*S*,*S*)-[**L14**H][I] (5 mol%), [Pd(η^3-cinnamyl)Cl]$_2$ (2.5 mol%), dry mesitylene, 160 °C, 3 h.

Both ligand precursors (*S*,*S*)-[**L14**H][I] and (*S*,*S*)-[**L5**H][I] were used in the reactions with differently substituted substrates and the results are listed in Tables 24 and 25. The coupling reactions proceeded in high yields (81%-99). Disubstituted indolines were generated with excellent enantiomeric purity. The exceptions were carbamates (**197**, **216**-**218**) containing branched alkyl groups, in this case only two substituted indolines formed *via* C(sp^3)$_{Me}$-H activation in high yields but low enantioselectivities (entries 13 and 20, Table 24; entries 1 and 2, Table 25). Interestingly, substrates **198**, **220** and **223** (entries 11, 12, 15 and 16) reacted with very high selectivity, and both products (2-subatituted and 2,3-disubstituted indolines) formed in high yields and asymmetric inductions. Up to 93% of the engaged

racemic starting material (**198**) was transformed into close to equal portions of separable highly enantioenriched indolines having different substitution patterns (**267** and **268**). In case of carbamate **225** only 2,3-disubstituted indoline **278** was obtained in high yield and excellent enantioselectivity (96%) (entry 17), while, carbamate **206** produced exclusively 2-substituted indoline **281** (entry 19).

Table 24. Chiral Pd(*NHC*)-catalyzed regiodivergent RRM of carbamates to give 2- and 2,3-disubstituted indolines.

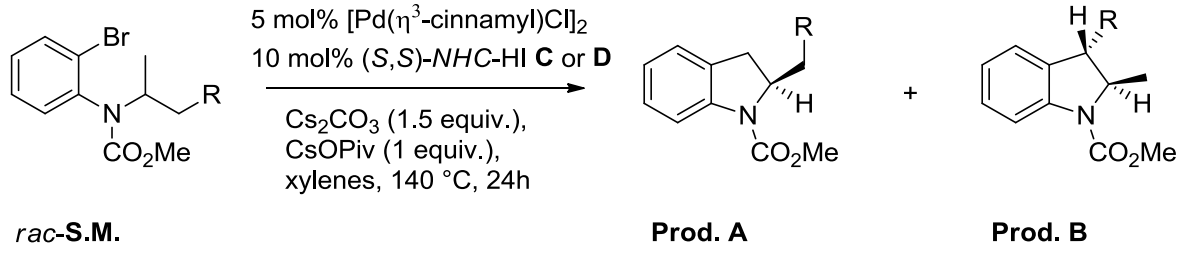

rac-**S.M.** **Prod. A** **Prod. B**

Entry[a]	S.M./R	*NHC HI*	**Prod. A**/ Yield (%)[b]/ Ee[c]	**Prod. B**/ Yield (%)[b]/ Ee[c]
1	**196**/Et	C	**257**/68[d]/44	**258**/22[d]/94
2	**196**/Et	D	**257**/61[d]/62	**258**/30[d]/96
3	**199**/CH_2Ph	C	**259**/65/27	**260**/26/99
4	**199**/CH_2Ph	D	**259**/62/47	**260**/32/99
5	**201**/$(CH_2)_2OTBS$	C	**261**/68/30	**262**/21/99
6	**201**/$(CH_2)_2OTBS$	D	**261**/55/55	**262**/30/99
7	**200**/$(CH_2)_2CO_2Et$	C	**263**/63/62	**264**/36/98
8	**200**/$(CH_2)_2CO_2Et$	D	**263**/54/69	**264**/31/98
9	**219**/OMe	C	**265**/62[d]/61	**266**/24[d]/99
10	**219**/OMe	D	**265**/57[d]/68	**266**/31[d]/99
11[e]	**198**/Ph	C	**267**/49/95	**268**/44/98
12	**198**/Ph	D	**267**/45/89	**268**/42/94
13	**197**/*c*Hex	D	**269**/81/25	**270**/0/-
14	**202**/prenyl	D	**271**/51/70	**272**/29/99
15	**220**/CH_2OMe	D	**273**/51/85	**274**/35/99
16	**223**/CH_2OMOM	D	**275**/45/78	**276**/44/99
17	**225**/CH_2OAc	D	**277**/0/-	**278**/42/96
18	**221**/CH_2SMe	D	**279**/56/74	**280**/29/95

19	**206**/SMe	D	**281**/45/95	**282**/0/-
20	**216**/*i*-Pr	D	**283**/86/9	**284**/0/-
21	**204**/Et	C	**285**/67[d]/61	**286**/26[d]/99
22	**204**/Et	D	**285**/56[d]/70	**286**/39[d]/99
23	**205**/Bn	C	**287**/56[d]/61	**288**/37[d]/99
24	**205**/Bn	D	**287**/47[d]/72	**288**/34[d]/99

(*S*,*S*)-*NHC*-HI: C = [**L14**H][I]; D = [**L5**H][I] [a] Reaction conditions: [Pd(η^3-cinnamyl)Cl]$_2$ (5 mol%), *NHC*-HI (10 mol%), **carbamate** (0.2 mmol), cesium pivalate (0.2 mmol), Cs_2CO_3 (0.3 mmol), dry xylenes (2 mL) at 140 ^oC for 24 h. [b] Isolated material unless otherwise indicated. [c] Enantiomeric excess (*ee*) was determined by chiral HPLC (see experimental section). [d] Not separated. Calculated by ^{1}H-NMR integration and based on the yield of mixtures of **Prod. A** and **Prod. B**. [e] 1 mmol scale of **198**.

Table 25. Chiral Pd(*NHC*)-catalyzed regiodivergent RRM of carbamates to give 2- and 2,3-disubstituted indolines.

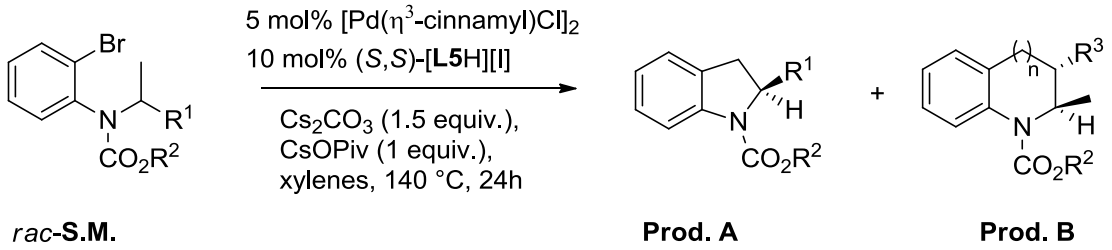

rac-**S.M.** **Prod. A** **Prod. B**

Entry[a]	Substrate/R^1/R^2	**Prod. A**/ Yield (%)[b]/ Ee[c]	**Prod. B**/ Yield (%)[b]/ Ee[c]
1	**217**/*i*-Pr/Me	**289**/84/4	**290**(n=0,R^3=2Me)/0
2	**218**/*t*Bu/Me	**291**/93/3	**292**(n=1,R^3=2Me)/0

[a] Reaction conditions: [Pd(η^3-cinnamyl)Cl]$_2$ (5 mol%), *NHC*-HI (10 mol%), **carbamate** (0.2 mmol), cesium pivalate (0.2 mmol), Cs_2CO_3 (0.3 mmol), dry xylenes (2 mL) at 140 ^oC for 24 h. [b] Isolated material unless otherwise indicated. [c] Enantiomeric excess (*ee*) was determined by chiral HPLC (see experimental section).

It follows from the above that starting with highly enantioenriched substrates, highly enantioenriched products can be obtained. This is demonstrated in Scheme 69. The reaction of (*S*)-**219** with the (*S*,*S*)-[**L14**]/Pd catalyst gives (*S*)-**265** exclusively (matched case), whereas the reaction of (*S*)-**219** with (*R*,*R*)- [**L14**]/Pd gives a mixture of products thereby confirming our interpretation of the data in Table 21 that this is the mismatched pair and it is responsible or the modest *ee* of **265** in the reactions of *rac*-**219** (Table 24, entries 9 and 10). An exception in this series is **198**. Here (*S*)-**198** reacts to give (*R*)-**267** selectively and (*R*)-**198** reacts to give (2*R*,3*S*)-**268** selectively. The *N*-protecting group in the enantioenriched carbamate **268** (98%

ee) was successfully cleaved producing (2*R*,3*S*)-2-methyl-3-phenylindoline **293** in 92% yield without the loss of enantiomeric purity (Scheme 69).

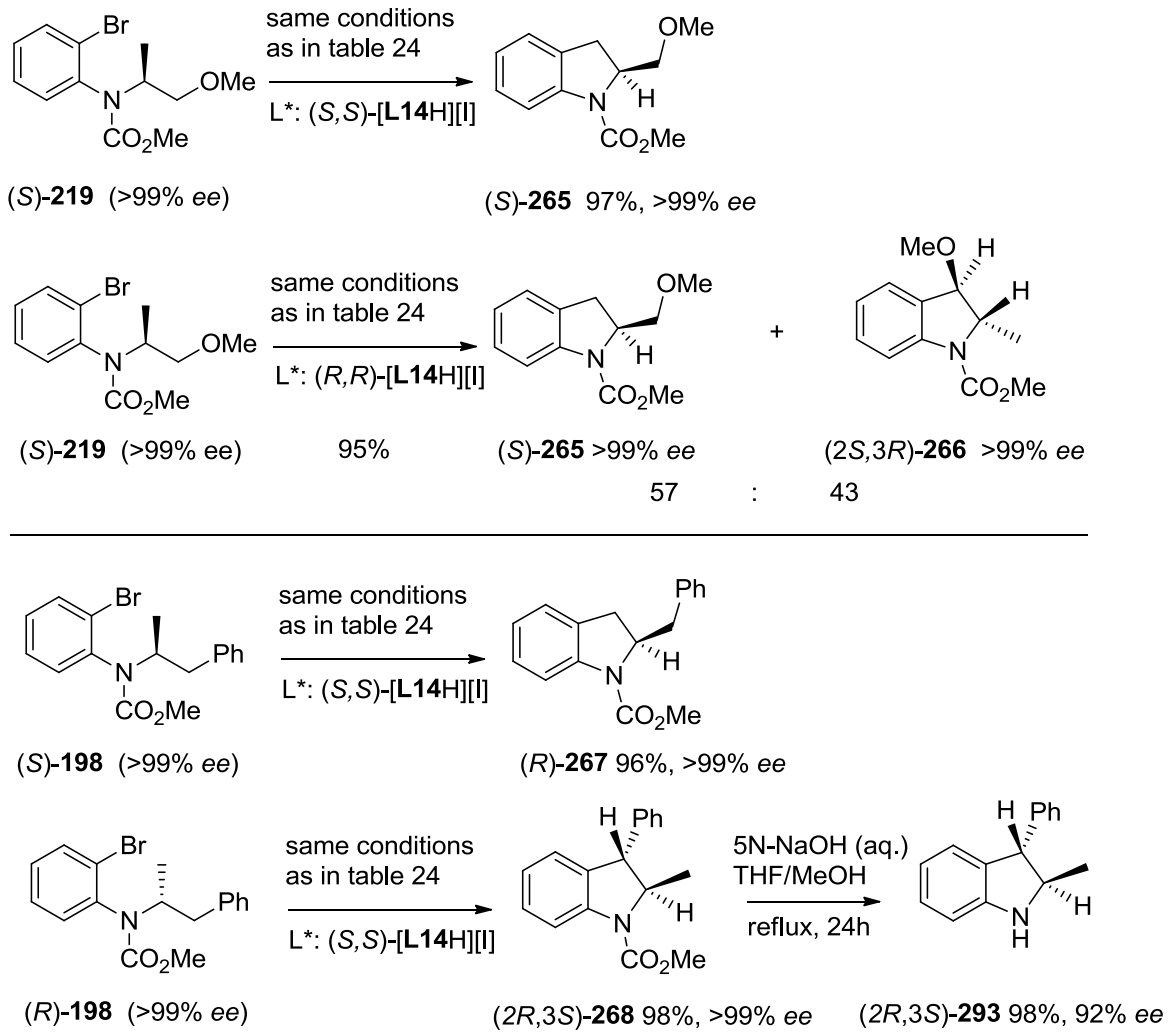

Scheme 69. Pd(*NHC*)-catalyzed synthesis of highly enantioenriched indolines *via* chiral *NHC*-palladium catalyzed regiodivergent reaction.

In order to extend this interesting methodology we investigated a series of enantiopure carbamates in Pd(*NHC*)-catalazed regiodivergent RRM and the results are shown in Table 26. All substrates in the presence of (*R*,*R*)-[**L14**H][I]/Pd catalytic system gave exclusively 2,3-disubstituted indolines *via* the methylene C-H activation next to methoxy group, while the reactions in the presence of (*S*,*S*)-[**L14**H][I]/Pd catalytic system produced exclusively 2,3-disubstituted indolines *via* a methylene C-H activation next to the alkyl group. All products formed in high yields. An exception was the reaction of carbamate **230** with (*S*,*S*)-[**L14**H][I]/Pd catalytic system, where the product did not form at all and only the starting material was recovered. The later result was expected, because as we found previously the C-H activation of the methylene group next to the secondary carbon is not feasible.

Table 26. Influence of substitution groups in enantioselective Pd(*NHC*)-catalyzed regiodivergent reaction.

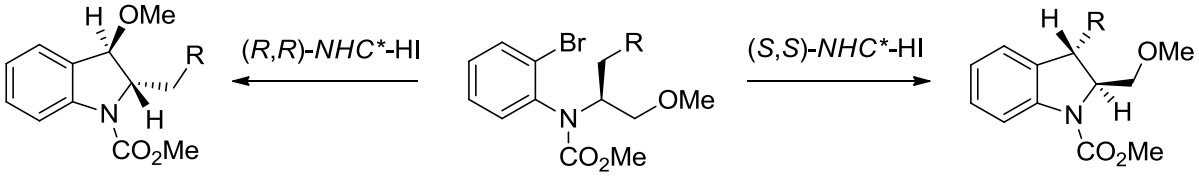

Prod. A (99% *ee*) **S.M.** (99% *ee*) **Prod. B** (99% *ee*)

Entry[a]	**S.M.**/R	Ligand	**Prod. A**/Yield(%)[b]	**Prod. B**/Yield(%)[b]
1	**222**/Me	(*R*,*R*)-[**L14**H][I]	**256**/86	**255**/0
2	**228**/Et	(*R*,*R*)-[**L14**H][I]	**294**/97	**295**/0
3	**229**/Ph	(*R*,*R*)-[**L14**H][I]	**296**/98	**297**/0
4	**230**/*i*-Pr	(*R*,*R*)-[**L14**H][I]	**298**/95	**299**/0
5	**222**/Me	(*S*,*S*)-[**L14**H][I]	**256**/0	**255**/85
6	**228**/Et	(*S*,*S*)-[**L14**H][I]	**294**/0	**295**/96
7	**229**/Ph	(*S*,*S*)-[**L14**H][I]	**296**/0	**297**/98
8[d]	**230**/*i*-Pr	(*S*,*S*)-[**L14**H][I]	**298**/0	**299**/0

[a] [**L14**H][I] (5 mol%), [Pd(η^3-cinnamyl)Cl]$_2$ (2.5 mol%), cesium pivalate (0.2 mmol), Cs_2CO_3 (0.3 mmol), dry mesitylene, 160 °C, 3 h. [b] Isolated yield. [d] S.M. was recovered.

Finally, the enantiopure indoline **297** was successfully crystallized and its X-ray structural analysis is shown in Figure 48. The picture clearly demonstrates *trans*-configuration of the formed 2,3-disubstituted indolines. This fact is in a perfect agreement with the results previously obtained from the vibrational circular dichroism (VCD) studies.

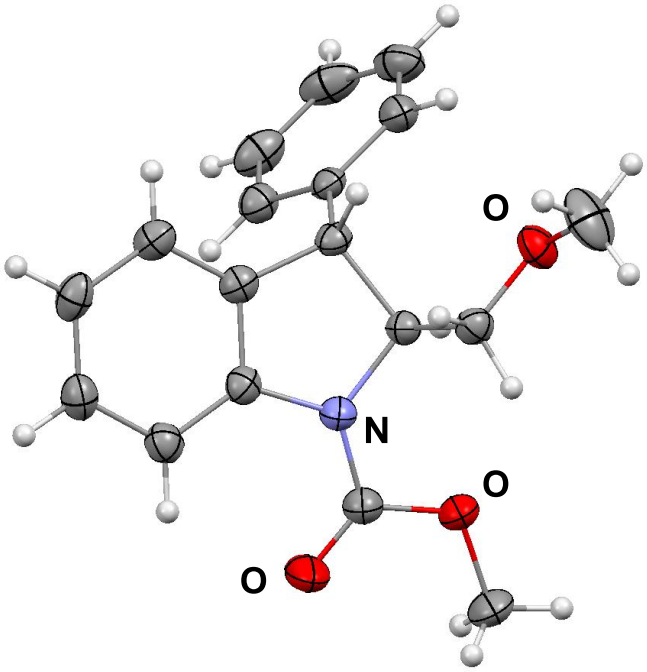

Figure 48. X-Ray structure of *trans*- indoline **297**.[§§§]

III.4.8. Conclusion

In conclusion, we have successfully applied new bulky chiral monodentate *N*-heterocyclic carbene ligands to the conversion of readily accessible carbamates into *trans*-fused[119,121], 2-substituted and 2,3-disubstituted[120] indolines *via* palladium-catalyzed Ar-X/unactivated C(sp^3)-H coupling. The reaction requires a temperature 140-160 ˚C. It is extraordinary that despite the high temperature, the synthesis of fused indolines occurs through high asymmetric recognition of the enantiotopic C-H bond in an unactivated methylene unit. In substrates with symmetrical $NCHR_2$ groups, very high asymmetric induction was obtained in those reactions where the catalyst had to distinguish between two enantiotopic methylene hydrogens. In substrates with unsymmetrical NCHRR' groups, Pd-phosphine and Pd-IPr catalysts showed a strong preference for the C_{Me}-H activation. It was therefore unexpected to find that the bulky chiral Pd-*NHC* catalysts directed this transformation to the regiodivergent reaction of a racemic mixture (RRM). In the ideal case where competition is between C-H activation of a methyl group and C-H activation of a benzyl fragment the catalyst transformed one enantiomer of a racemic mixture into a highly enantioenriched indoline *via* C_{Me}-H activation and the other enantiomer into equally highly enriched indolines *via* highly asymmetric $C_{methylene}$-H activation. The inductions found for

[§§§] Carried out by Dr. *C. Besnard*.

these homogeneous catalytic reactions are rather remarkable as they take place at high temperatures. To the best of our knowledge, these are the first examples of the direct synthesis of highly enatioenriched 2,3-*trans*-disubstituted indolines and regiodivergent reactions involving C-H activation.

IV Experimental Section

IV.1. General Remarks

Solvents were purified by filtration on drying columns (Al_2O_3) using a Solvtek© system. DME was distilled over Na/benzophenone. *t*BuONa was sublimed and weighted in the glove box. All reagents were purchased from commercial sources (Aldrich, Fluka and Acros) and used without further purification unless otherwise noted. LDA was produced by dropwise addition of *n*-butyllithium to 1 equiv. diisopropylamine in dry THF at 0 °C under a nitrogen atmosphere and stirring for 20-30 minutes prior to use. Reactions and manipulations involving organometallic or moisture sensitive compounds were carried out under purified nitrogen (or argon) in glassware dried by heating under vacuum. Molecular sieve (3 Å and 4 Å) were heated (160 °C) under vacuum (0.4 mbar) for 16 h. Cold bath: 0 ˚C: ise/water; -40 °C acetonitrile/dry ice; -60 °C toluene/dry ice; -78 °C acetone/dry ice. Reactions conducted below rt were cooled using a Thermo-Fisher Scientific Neslab Cryocool apparatus. Reactions performed above rt utilized an oil bath preheated to the stated temperature. Thin-layer chromatography was performed on EMD silica gel 60 F_{254} plates (0.25 mm). Melting points were determined on a Büchi 510 apparatus and are uncorrected. GC: *Hewlett Packard 6890* gas chromatograph with FID detection using a *Permabond OV-1701-0.25* column (25m x 0.32 mm ID). HPLC: Agilent 1100 series chromatograph. NMR: Bruker AMX-500, AMX-400 or AMX-300 FT. Chemical shifts are reported in ppm relative to tetramethylsilane. Data for ^{1}H are reported as chemical shift (δ ppm), multiplicity (s = singlet, d = doublet, t = triplet, q = quartet, quint = quintet, sex = sextet, sept = septet, m = multiplet), coupling constant, integration; data for ^{13}C are reported in terms of chemical shift. IR spectra: Perkin–Elmer Spectrum One. Neat liquids; Golden Gate accessory. HRMS: + TOF mode, ESI-MS mode, Applied Biosystems/Scix (Q-STA) spectrometer. Optical rotation was measured on Perkin Elmer 241 polarimeter using quartz cell 10 cm with sodium 589 nm filter. CD spectra: *Jasco J-715*, quartz cell (l = 1 cm). Analysis by HPLC was performed using an Agilent 1100 series chromatograph with a JASCO PU-980 pump and Agilent 1100 Series detection system.

IV.2. Synthesis of Chiral Amines

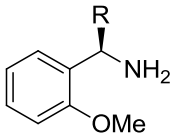

63, R = Me
64, R = *i*-Pr
65, R = *t*Bu

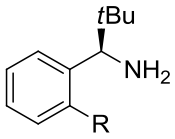

66, R = H
67, R = Me
68, R = O*n*-Pr
69, R = O*i*-Pr

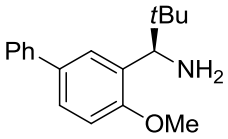

70

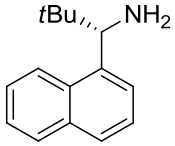

(*S*)-**104**

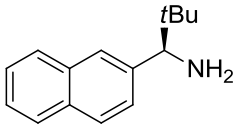

(*R*)-**105**

Highly enantioenriched chiral amines **63**-**66**[267,268], **67**[114], **70**[115] and **71a**[115,268,269] were prepared as previously described.

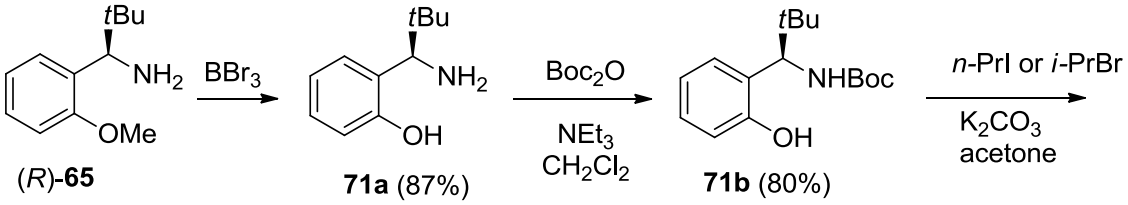

(*R*)-**65**

71a (87%)

71b (80%)

72a/R = *n*-Pr (99%)
72b/R = *i*-Pr (99%)

68 R = *n*-Pr (99%)
69 R = *i*-Pr (86%)

(*R*)-**71b**: To a solution of (*R*)-**71a** (2.22 g, 12.39 mmol) and triethylamine (2.2 mL, 15.5 mmol) in THF (70 mL) was added di-*tert*butyldicarbonate (3.45 g, 15.5 mmol) at rt. The reaction mixture was stirred for 18 h. The reaction was quenched with sat. aq. NH_4Cl, the aq. layer was extracted with CH_2Cl_2, and the combined organic layers were dried over $MgSO_4$ and concentrated in vacuum to give the *N*-Boc amine (2.75 g, 80%). The crude product was used without any further purification.

(*R*)-**72a**: To a solution of (*R*)-**71b** (1.0 g, 3.58 mmol) and *n*-PrI (2.5 g, 14.32 mmol) in acetone (60 mL) was added anhydrous K_2CO_3 (2.5 g, 17.9 mmol) and the mixture was refluxed for 20 h. After evaporation of acetone, the residue was filtered through a short silica gel pad and washed with ether. The product was obtained as pale-yellow oil (1.14 g, 99%) after evaporation of ether and used for the next step without further purification.

^{1}H-NMR (400 MHz, $CDCl_3$): δ 0.97 (*s*, 9H), 1.15 (t, *J* = 7.6 Hz, 3H), 1.46 (s, 9H), 1.88-1.97 (m, 2H), 3.95-4.05 (m, 2H), 6.90-6.95 (m, 2H), 7.14 (d, *J* = 7.0 Hz, 1H), 7.24 (t, *J* =

7.4 Hz, 1H). **^{13}C-NMR** (125 MHz, $CDCl_3$): δ 10.9, 14.1, 22.3, 22.7, 27.0, 28.2, 28.4, 69.5, 78.4, 111.7, 119.8, 127.9, 155.6, 156.7.

(*R*)-**72b**: To a solution of (*R*)-**71b** (642 mg, 2.30 mmol), *i*-PrBr (2.2 mL, 23 mmol), and Bu_4NI (170 mg, 20 mol%) in acetone (30 mL) was added anhydrous K_2CO_3 (3.8 g, 27.6 mmol) and the mixture was sealed and refluxed for 48 h. After evaporation of acetone, the residue was filtered through a short silica gel pad and washed with ether. The product was obtained as pale-yellow oil (0.74 g, 99%) after evaporation of ether and used for the next step without further purification.

^{1}H-NMR (500 MHz, $CDCl_3$): δ 0.97 (s, 9H), 1.42 (d, *J* = 4.8 Hz, 6H), 1.46 (s, 9H), 4.67 (m, 1H), 6.89-6.93 (m, 2H), 7.14 (d, *J* = 5.8 Hz, 1H), 7.30 (t, *J* = 5.8 Hz, 1H). **^{13}C-NMR** (125 MHz, $CDCl_3$): δ 22.00, 22.08, 27.1, 28.3, 28.5, 36.8, 69.5, 78.4, 112.7, 119.5, 127.7, 155.3, 155.6.

(*R*)-**68**: The mixture of (*R*)-**72a** (1.1 g, 3.46 mmol) and CF_3CO_2H (15 mL) with H_2O (0.9 mL) was stirred for 6 h at rt. The excess CF_3CO_2H was removed under vacuum and the residue was dissolved in ether and washed with sat. aq. $NaHCO_3$. After separation, the collected ether phase was washed with brine and dried with Na_2SO_4. After evaporation of ether, the crude free amine (*R*)-**2c** was obtained as yellow oil (0.78 g, 99%) by filtration though a short pad of silica gel and used directly for the next cyclization without further purification.

(*R*)-**69**: According to the same procedure as for preparation (*R*)-**68**, the crude free amine (*R*)-**69** was obtained as yellow oil with 96% yield and was used for the next step without further purification.

Rac-**104**: A 1 L round bottom three-neck flask equipped with a 4 cm Teflon-coated magnetic stir bar (oval shaped), reflux condenser fitted with a nitrogen (N_2) inlet, a glass stopper and a rubber septum was charged with 1-naphthonitrile (**103a**) (1.0 equiv., 25.0 g, 163.3 mmol) and 50 mL of dry diethyl ether (Et_2O). The reaction mixture was stirred at rt until all 1-naphthonitrile had dissolved (ca. 10 min). Under N_2, *tert*-butylmagnesium chloride (*t*BuMgCl) (1.05 equiv., 86.5 mL of 2.0 M solution in Et_2O, 171.3 mmol) was added at rt over 1 min *via* Teflon cannula followed by addition of copper (I) bromide (CuBr) (2.8 mol%, 0.70 g, 4.5 mmol). The vigorously stirred reaction mixture was then refluxed for 24 h (the reaction color turned to green-yellow after one hour). The reaction mixture was then cooled (-78

acetone / dry ice bath, external temperature), and 110 mL dry methanol (MeOH) was added cautiously by syringe under intensive stirring (the color of the reaction mixture turned to brown-grey) followed by addition of sodium borohydride ($NaBH_4$) (1.3 equiv., 8.06 g, 212.1 mmol). The reaction mixture was allowed to warm up to rt over a period of 6 h and stirred overnight (after 15 h the color of the reaction mixture was green). 110 mL of Water (H_2O) was added over a period of 10 min (the color of the solution turned to grey) and the reaction mixture was stirred for 30 min at rt. The precipitate was removed by filtration through a glass frit and washed with portions of Et_2O (total 500 mL). The filtrate was concentrated on a rotavap and then transferred to a 2-L separatory funnel, pre-charged with 100 mL H_2O. After extraction the organic phase was collected and the aqueous phase was extracted 2 times with 200 mL Et_2O. The combined organic phases were dried over Na_2SO_4. The solution was filtered (glass frit) and volatiles were removed by a rotavap (400 mmHg, 40 °C). The crude product (oil) was distilled under reduced pressure (0.5 mmHg) and the fraction coming over at 125-130 ˚C was collected. This fraction was taken up in 1 L of Et_2O and the solution was cooled to – 40 °C (acetone bath with dry ice, external temperature). Over a period of 3 h HCl gas (generated by addition of concentrated H_2SO_4 to solid NaCl) was passed through the vigorously stirred solution. The white precipitate of **104**·HCl formed was collected by filtration (glass frit) and washed with 500 mL of Et_2O. A 1-L one-necked round-bottomed flask was charged with **104**·HCl, 500 mL of Et_2O and 300 mL of 1 N aq. soln. of sodium hydroxide (NaOH). This was stirred until all solid was dissolved (ca. 30 min). The mixture was transferred to a 2-L separatory funnel and the organic layer was collected. The water phase was extracted with Et_2O (2×300 mL). The combined organic phases were dried over Na_2SO_4. Removal of volatiles under reduced pressure by rotavap (400 mmHg, 40 °C) afforded pure racemic amine **104** (22.6 g, 65%) as a white solid.

^{1}H-NMR (400 MHz, $CDCl_3$): δ 1.01 (s, 9H), 1.54 (bs, 2H), 4.82 (s, 1H), 7.47-7.57 (m, 3H), 7.74 (d, *J* = 7.4 Hz, 1H), 7.78 (d, *J* = 8.1 Hz, 1H), 7.88 (d, *J* = 8.4 Hz, 1H), 8.24 (d, *J* = 8.1 Hz, 1H). **^{13}C-NMR** (75 MHz, $CDCl_3$): δ 27.0, 36.4, 57.2, 123.9, 125.1, 125.2, 125.5, 127.2, 128.9, 132.5, 133.5, 140.7**. IR** (neat, cm^{-1}): 3366, 3296, 2962, 1948, 1594, 1509, 1473, 1389, 1358, 1328, 1069, 1026, 909, 872, 802, 780, 749, 633. **HRMS** (ESI): calcd. for $C_{15}H_{20}N_1$ ($[M+H]^+$): 214.159, found: 214.1593.

Rac-**105**: Applying the same procedure as for the synthesis of **104**, racemic amine **105** was obtained in 76% yield.

^{1}H-NMR (400 MHz, $CDCl_3$): δ 1.0 (s, 9H), 1.7 (bs, 2H), 3.98 (s, 1H), 7.48-7.55 (m, 3H), 7.81 (d, *J* = 2.5 Hz, 1H), 7.84 (s, 1H), 7.88 (d, *J* = 3.8 Hz, 2H). **^{13}C-NMR** (75 MHz, $CDCl_3$): δ 26.7, 35.4, 65.4, 125.4, 125.8, 126.84, 126.88, 127.0, 127.5, 127.9, 132.7, 133.0, 141.5. **IR** (neat, cm^{-1}): 3348, 3289, 2959, 1949, 1600, 1479, 1389, 1362, 1331, 1203, 940, 906, 865, 828, 756, 737, 591. **HRMS** (ESI): calcd. for $C_{15}H_{20}N_1$ ($[M+H]^+$): 214.159, found: 214.1584.

(*S*)-**104**: A 2-L round-bottom one-neck flask equipped with a 4 cm. Teflon-coated magnetic stir bar (oval shaped) and a reflux condenser was charged with *rac*-**104** (1.0 equiv., 34.0 g, 159.62 mmol), 1000 mL *i*-PrOH and 150 mL EtOAc. The reaction mixture was intensively mixed until all solid amine **104** was dissolved. (*L*)-malic acid (1 equiv., 21.4 g, 159.62 mmol) was added and the flask was immersed in a pre-heated oil bath (100 °C). The mixture was refluxed for one hour then cooled and kept overnight at +5 °C. The crystalline precipitate was collected on a glass frit and washed with 100 mL of cooled *i*-PrOH. After drying under vacuum, the salt of amine **104** (23.2 g, 67.04 mmol, 42% yield) was obtained with an amine enrichment of 88% *ee* (checked by HPLC after liberation: Chiracel OD-H column, *n*-hexane/*i*-PrOH = 99:1, 1.0 mL/min, 254 nm; t_R = 25.94 min. (major) and 21.56 min. (minor)). This salt (23.2 g, 67.04 mmol) was placed in a 2-L round-bottom one-neck flask equipped with a 4 cm. Teflon-coated magnetic stir bar (oval shaped) and reflux condenser. 800 mL *i*-PrOH and 130 mL EtOAc were added and the mixture was refluxed until the solid was dissolved (ca. 1h). The hot solution was left to cool and sit overnight (15 h) at rt. The white solid was filtered, washed with cold 100 mL *i*-PrOH and dried under vacuum. The solid was transferred to a 1-L round-bottom one-neck flask equipped with a 4 cm Teflon-coated magnetic stir bar (oval shaped). 300 mL of 1 N aq. NaOH soln. and 400 mL of Et_2O were added and the mixture was stirred vigorously. When all solid had dissolved, the mixture was transferred to a 2-L separatory funnel. After separation of the organic phase and extraction of the aq. phase with Et_2O (2×200 mL), the combined organic phases were dried over Na_2SO_4. Evaporation of volatiles under reduced pressure by rotavap (400 mmHg, 40 °C) afforded amine (*S*)-**104** in 38% yield as a white solid (12.9 g, 60.65 mmol, >99% *ee*). **M.p.** = 82-83 °C, $\mathbf{[\alpha]_D^{25}}$ = -59.1 (*c* = 1.0 in CH_2Cl_2).

(*R*)-**105**: A mixture of 2,2-dimethyl-1-(naphthalen-2-yl)propan-1-amine **105** (12.0 g, 56.25 mmol, 1 equiv.), *L*(+)-tartaric acid (8.44 g, 56.25 mmol, 1 equiv.), EtOH (400 mL) was refluxed until the solid was dissolved. The reaction mixture was allowed to cool to rt and stand at +5 °C overnight. The crystalline precipitate was filtered from the mother liquid and

washed with EtOH (100 mL). After drying under vacuum, the enantiomerically enriched salt (*R*)-**105** (9.18 g, 25.31 mmol, 45% yield) was obtained with 87% *ee* (checked by HPLC after liberation: Chiracel AS-H column, *n*-hexane/*i*-PrOH = 98:2, 1.0 mL/min, 254 nm; t_R = 6.44 min. (major) and 5.75 min. (minor)). The recrystallization was carried out. To the salt of amine **105** (9.18 g, 25.31 mmol, 87% *ee*) EtOH (300 mL) was added and reaction mixture was refluxed for 1 h. The hot solution was cooled to rt for 18 h, and crystals were filtered and dried under vacuum. The recrystallization gave the salt (7.72 g, 20.25 mmol). Following addition of NaOH (1N) and extraction with ether afforded (*R*)-**105** in total 36% yield as a white solid (4.31 g, 20.25 mmol, 99% *ee*). **M.p.** = 76-77 °C, $[\alpha]_D^{25}$ = -4.4 (*c* = 1.0 in CH_2Cl_2).

IV.3. Synthesis of Imidazolium and Dihydroimidazolium Salts (Chiral Carbene Precursors)

IV.3.1. Synthesis of Imidazolium Salts

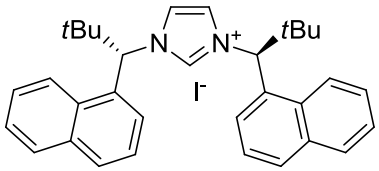

(*S*,*S*)-[**L14**H][I]: a) A 500 mL round-bottom 2-neck flask connected to the nitrogen line and equipped with a 1.5 cm Teflon-coated magnetic stir bar (oval shaped) and rubber septum was charged with aq. soln. of glyoxal (40%) (0.5 equiv., 5.92 mL, 52.101 mmol), CH_2Cl_2 (200 mL) and vigorously stirred with 40.0 g freshly dehydrated sodium sulfate (Na_2SO_4) for 10 minutes. After the addition of formic acid (98%) (7 mol%, 0.3 mL, 7.29 mmol) and (*S*)-**104** (1.0 equiv., 22.211 g, 104.20 mmol) the reaction mixture was allowed to stir for 5 minutes followed by addition of another 40.0 g of Na_2SO_4. During 18 h of stirring at rt the solution turned to yellow-green. The reaction mixture was filtered through the glass frit and Na_2SO_4 was washed with 50 mL CH_2Cl_2. The organic solvents were removed with rotary evaporator to yield the crude diimine, which was further purified by crystallization from MeOH. The crude diimine was introduced to MeOH 2L and reflux until all diimine was dissolved. After the solution was kept at rt for 18 h and during this time white crystalline needles was formed. Filtration of precipitate afforded pure diimine in 90% yield (23.3 g).

b) A dry 100 mL Schlenk tube connected to an N_2 manifold and equipped with a 1.5 cm Teflon-coated magnetic stir bar (oval shaped) and a rubber septum was charged with silver triflate AgOTf (1.5 equiv., 2.58 g, 10.044 mmol), 42 mL CH_2Cl_2 and chloromethyl

pivalate (1.5 equiv., 1.47 mL, 10.044 mmol). The mixture was stirred for 45 min. in the absence of light by which time the color of the reaction mixture had turned to yellow-pink. The resulting suspension was transferred under N_2, *via* a cannula equipped with a filter, into a 100 mL dry Schlenk tube preloaded with the solid diimine (1.0 equiv., 3.0 g, 6.696 mmol). This mixture was stirred in the absence of light at 40 °C for 24 h. After cooling to rt, the solvent was evaporated using a rotavap. Flash chromatography (fc) on SiO_2 (Et_2O/CH_2Cl_2 1:1) afforded 2.12 g of a brown product. This was taken up in dry acetone (100 mL). NaI (1.1 equiv., 1.10 g, 7.365 mmol) was added and the reaction mixture was stirred overnight (10 h). Volatiles were removed via a rotavap. The residue was taken up in a small amount of $CHCl_3$ and filtered through cotton. The above procedure (acetone, NaI, etc) was repeated. Column chromatography (CH_2Cl_2/Et_2O 1:1) afforded (*S*,*S*)-[**L14**H][I] (1.929 g, 49%) as light beige solid.

M.p. = 156-158 °C. $[\alpha]_D^{25}$ = +75 (*c* = 1.0 in CH_2Cl_2). **^{1}H-NMR** (400 MHz, $CDCl_3$): δ 1.18 (s, 18H) 6.75 (s, 2H), 7.42 (d, *J* = 7.3 Hz, 2H), 7.49 (d, *J* = 1.5 Hz, 2H), 7.52 (t, *J* = 7.8 Hz, 2H), 7.61 (dd, *J* = 6.9, 1.3 Hz, 1H), 7.63 (dd, *J* = 6.9, 1.3 Hz, 1H), 7.80 (dd, *J* = 8.2, 0.6 Hz, 2H), 7.83 (d, *J* = 8.2 Hz, 2H), 8.04 (d, *J* = 6.7 Hz, 2H), 8.79 (d, *J* = 8.7 Hz, 2H), 11.48 (s, 1H). **^{13}C-NMR** (100 MHz, $CDCl_3$): δ 28.1, 37.3, 67.0, 122.0, 123.9, 124.9, 126.5, 126.6, 128.1, 129.2, 130.2, 131.0, 132.1, 134.2, 138.3**. IR** (neat, cm^{-1}): 2962, 1599, 1536, 1476, 1369, 1140, 1030, 786, 756, 667. **HRMS** (ESI): calcd. for $C_{33}H_{37}N_2$ ($[M-I]^+$): 461.2956, found: 461.2970.

(*R*,*R*)-[**L16**H][I]: Applying the same procedure as for the synthesis of (*S*,*S*)-[**L14**H][I], imidazolium salt (*R*,*R*)-[**L16**H][I] was obtained in 39% yield from amine (*R*)-**105**.

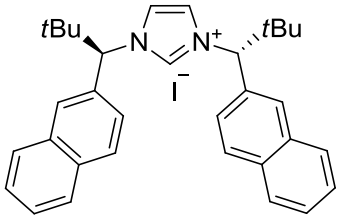

Yellow solid, **m.p.** = 195-197 °C. $[\alpha]_D^{25}$ = -90.3 (*c* = 1.0 in CH_2Cl_2). **^{1}H-NMR** (400 MHz, $CDCl_3$): δ 1.15 (s, 18H), 6.25 (s, 2H), 7.39-7.44 (m, 4H), 7.71-7.80 (m, 8H), 7.95-7.99 (m, 2H), 8.25 (s, 2H), 11.15 (s, 1H). **^{13}C-NMR** (100 MHz, $CDCl_3$): δ 27.4, 36.6, 73.6, 99.9, 122.4, 126.4, 126.5, 126.9, 127.4, 128.5, 128.6, 129.1, 132.2, 132.9, 133.0, 136.1. **IR** (neat,

cm^{-1}): 2962, 1536, 1475, 1369, 1138, 861, 782, 741, 668, 623, 538. **HRMS** (EI): calcd. for $C_{33}H_{37}N_2$ ($[M-I]^+$): 461.2951, found: 461.2958.

IV.3.2. Synthesis of Dihydroimidazolium Salts

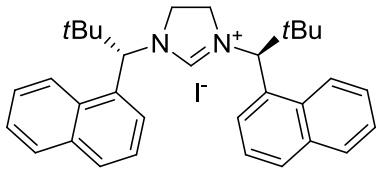

(*S*,*S*)-[**L15**H][I]: a) A 500 mL round-bottom 2-neck flask connected to an N_2 manifold and equipped with a 1.5 cm Teflon-coated magnetic stir bar (oval shaped) and a rubber septum was charged with an aq. soln. of glyoxal (0.5 equiv., 5.92 mL, 52.10 mmol, 40% in H_2O), CH_2Cl_2 (200 mL) and then was vigorously stirred with 40.0 g dehydrated sodium sulfate (Na_2SO_4) for 10 minutes. Formic acid (7 mol%, 0.3 mL, 7.29 mmol, 98%) and (*S*)-**104** (1.0 equiv., 22.211 g, 104.20 mmol) were added and the reaction mixture was stirred for 5 minutes followed by the addition of another 40.0 g of Na_2SO_4. During 18 h of stirring at rt the solution turned to yellow-green. The reaction mixture was filtered through a glass frit and Na_2SO_4 was washed with 50 mL CH_2Cl_2. The solution was evaporated on a rotavap to yield the crude diimine. This was taken up in 2L of MeOH and refluxed until all diimine was dissolved. The solution was left to cool to rt and kept at this temperature for 18 h. During this time white crystalline needles formed. Filtration afforded pure diimine (23.3 g, 90%).

b) The diimine (1.0 equiv., 8.0 g, 17.85 mmol) prepared as described above was introduced under N_2 to a 0 ºC solution of $LiAlH_4$ (3.0 equiv., 2.03 g, 53.55 mmol) in THF (200 mL). The reaction mixture was stirred overnight (10 h) at rt and then quenched by slow addition of an aq. sat. solution of NH_4Cl (50 mL) at 0 ˚C. The mixture was filtered through a short pad of Celite and the glass frit with Celite was carefully washed with 100 mL Et_2O. Removal of volatiles by a rotavap (100 mmbar, 40 ˚C) afforded crude diamine as pale-yellow oil (8.7 g, 99%). A 100 mL dry Schlenk tube connected to the N_2 manifold and equipped with a 1.5 cm Teflon-coated magnetic stir bar (oval shaped) and rubber septum was charged with diamine (8.7 g), $HC(OEt)_3$ (100 mL) and NH_4BF_4 (1.0 equiv., 1.85 g, 17.68 mmol). The stirred reaction mixture was heated to 125 ºC for 24 h. The excess of $HC(OEt)_3$ was removed under vacuum (0.5 mmbar, rt).

The crude product was dissolved in 300 mL acetone and NaI (1.2 equiv., 3.18 g, 21.21 mmol) was added. After stirring overnight (10 h), acetone was removed in *vacuo* (rotavap)

and the resultant solid was dissolved in 100 mL $CHCl_3$. The solution was filtered and the glass frit with precipitate was washed with 50 mL $CHCl_3$. After removal of solvent the cycle in the above paragraph was repeated. The crude product was dissolved in 100 mL of CH_2Cl_2, and 500 mL Et_2O was added. The pale-yellow precipitate was separated by filtration and washed with 100 mL Et_2O. Drying under *vacuum* (0.5 mmbar, rt) afforded (*S*,*S*)-[**L15**H][I] (9.47 g, 90%) as pale yellow solid.

M.p. = 270-272 °C. $[\alpha]_D^{25}$ = +81 (*c* = 1.0 in CH_2Cl_2). **^{1}H-NMR** (400 MHz, $CDCl_3$): δ 1.21 (s, 18H), 3.51-3.61 (m, 2H), 3.79-3.95 (m, 2H), 6.16 (s, 2H), 7.47 (t, *J* = 10.2 Hz, 2H), 7.54 (t, *J* = 10.2 Hz, 2H), 7.74 (d, *J* = 12.0 Hz, 4H), 7.88 (d, *J* = 12.0 Hz, 4H), 8.77 (d, *J* = 12.0 Hz, 2H), 11.21 (s, 1H). **^{13}C-NMR** (100 MHz, $CDCl_3$): δ 28.4, 29.7, 37.3, 48.4, 64.1, 123.7, 124.4, 126.4, 126.5, 128.1, 129.1, 129.8, 132.1, 134.2, 159.5. **IR** (neat, cm^{-1}): 2967, 2886, 1634, 1472, 1397, 1280, 1209, 1097, 1087, 800, 780, 630. **HRMS** (ESI): calcd. for $C_{33}H_{39}N_2$ ($[M-I]^+$): 463.3107, found: 463.3106.

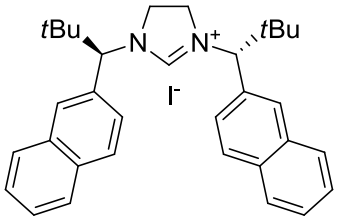

(*R*,*R*)-[**L17**H][I]: Applying the same procedure as for the synthesis of (*S*,*S*)-[**L15**H][I], carbene ligand precursor (*R*,*R*)-[**L17**H][I**]** was obtained in 91% yield as a yellow solid.

M.p. = 148-150 °C. $[\alpha]_D^{25}$ = -61.6 (*c* = 1.0 in CH_2Cl_2). **^{1}H-NMR** (400 MHz, $CDCl_3$): δ 1.20 (s, 18H), 3.95-4.04 (m, 2H), 4.07-4.15 (m, 2H), 5.49 (s, 2H), 7.47-7.51 (m, 4H), 7.64 (dd, *J* = 8.5, 1.8 Hz, 2H), 7.78-7.81 (m, 2H), 7.83 (s, 1H), 7.86 (s, 1H), 7.93-7.97 (m, 2H), 8.10 (d, *J* = 1.0 Hz, 2H), 10.5 (s, 1H). **^{13}C-NMR** (100 MHz, $CDCl_3$): δ 28.3, 36.9, 49.4, 71.9, 126.7, 126.8, 127.1, 127.6, 128.6, 128.8, 129.5, 131.8, 133.25, 133.28, 158.1. **IR** (neat, cm^{-1}): 2957, 1622, 1508, 1367, 1263, 1080, 861, 828, 745, 540. **HRMS** (EI): calcd. for $C_{33}H_{39}N_2$ ($[M-I]^+$): 463.3107, found: 463.3111.

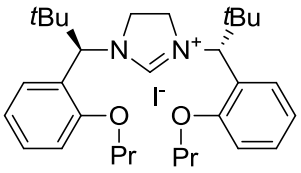

(*R*,*R*)-[**L10**H][I]: Applying the same procedure as for the synthesis of (*S*,*S*)-[**L15**H][I], carbene ligand precursor (*R*,*R*)-[**L10**H][I**]** was obtained in 66% yield.

M.p. = 93-95 °C. **[α]$_D^{20}$** = -60.8 (*c* = 0.5 in CH_2Cl_2). **^{1}H-NMR** (400 MHz, $CDCl_3$): δ 1.05 (t, *J* = 7.6 Hz, 6H), 1.20 (s, 18H), 1.81-1.90 (m, 4H), 3.95-4.05 (m, 4H), 4.16-4.29 (m, 4H), 5.24 (s, 2H), 6.97 (d, *J* = 8.3 Hz, 2H), 7.04 (t, *J* = 7.6 Hz, 2H), 7.37 (t, *J* = 7.8 Hz, 2H), 7.50 (dd, *J* = 1.5, 7.6 Hz, 2H), 8.52 (s, 1H). **^{13}C-NMR** (100 MHz, $CDCl_3$): δ 10.6, 22.3, 28.2, 36.4, 50.4, 69.9, 112.2, 120.4, 122.5, 129.4, 130.1, 156.4, 157.2. **IR** (neat, cm^{-1}): 2963, 2187, 1619, 1599, 1584, 1490, 1475, 1453. **HRMS** (EI): calcd. for $C_{31}H_{47}N_2O_2$ ($[M-I]^+$): 479.3632, found: 479.3635.

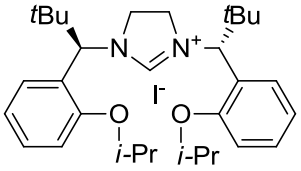

(*R*,*R*)-[**L11**H][I]: Applying the same procedure as for the synthesis of (*S*,*S*)-[**L15**H][I], carbene ligand precursor (*R*,*R*)-[**L11**H][I**]** was obtained in 71% yield.

M.p. = 102-104 °C. **[α]$_D^{20}$** = -65.5 (*c* = 0.5 in CH_2Cl_2). **^{1}H-NMR** (400 MHz, $CDCl_3$): δ 1.20 (s, 18H), 1.38 (t, *J* = 6.1 Hz, 12H), 4.17-4.27 (m, 4H), 4.63-4.71 (m, 2H), 5.21 (s, 2H), 6.96-7.03 (m, 4H), 7.33-7.38 (m, 2H), 7.49 (dd, *J* = 1.5, 7.6 Hz, 2H), 8.50 (s, 1H). **^{13}C-NMR** (100 MHz, $CDCl_3$): δ 21.9, 22.1, 28.2, 36.4, 50.2, 70.3, 113.2, 120.1, 123.1, 129.9, 155.2, 157.2. **IR** (neat, cm^{-1}): 2969, 2189, 1619, 1599, 1584, 1487, 1453. **HRMS** (EI): calcd. for $C_{31}H_{47}N_2O_2$ ($[M-I]^+$): 479.3632, found: 479.3629.

IV.4. General Procedure for the Synthesis of Amides

The requisite carboxylic acid (1.1 equiv.) and $SOCl_2$ (2.0 equiv.) were refluxed for 2 h. After removing of excess $SOCl_2$, pyridine or Et_3N (1.5 equiv.) in CH_2Cl_2 was added slowly at 0 °C followed by 2-bromoanyline (3-bromopyridin-2-amine or 2-bromopyridin-3-amine) (1.0 equiv.). The reaction mixture was stirred for 18 h at rt and then quenched with sat. aq. NH_4Cl

and extracted with EtOAc. F.c. (pentane/EtOAc 5:1) afforded the corresponding amide. This was added to the suspension of NaH in THF (1.5 equiv.) at 0 °C. The mixture was stirred for 1 h and cooled again to 0 °C and treated with MeI or (BnBr, MOMCl, BOMCl) (1.5 equiv.). The reaction was stirred overnight at rt. The mixture was then quenched with sat. aq. NH_4Cl and extracted with EtOAc. The organic solvent was evaporated by rotary evaporator and pure product was isolated by f.c. (silica gel; pentane/EtOAc 7:1). Spectroscopically, the amide exists as a mixture of two isomers.

N-(2-Bromophenyl)-*N*-methyl-2-phenylbutanamide (**74a**):

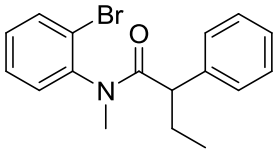

Oil, 83% yield. **^{1}H-NMR** (400 MHz, $CDCl_3$): δ 0.80-0.89 (m, 3H), 1.65-1.82 (m, 1.2H), 2.05-2.22 (m, 1.2H), 3.1 (t, *J* = 8 Hz, 0.8H), 3.21 (s, 3H), 3.22 (s, 0.24H), 6.65 (d, *J* = 12 Hz, 0.7H), 6.91-7.05 (m, 2H), 7.15-7.6 (m, 5.8H), 7.75 (d, *J* = 12 Hz, 0.7H). **^{13}C-NMR** (100 MHz, $CDCl_3$): δ 12.3, 12.6, 28.2, 28.4, 36.0, 51.0, 52.0, 123.4, 124.4, 126.71, 126.77, 127.9, 128.1, 128.3, 128.4, 128.6, 129.7, 130.5, 131.1, 131.8, 133.5, 134.0, 139.1, 140.2, 142.1, 142.5, 173.0; **IR** (neat, cm^{-1}): 2963, 1658, 1583, 1475, 1453. **HRMS** (ESI): calcd. for $C_{17}H_{18}BrNO$ ($[M+H]^+$): 332.0644, found: 332.0647.

N-(2-Bromophenyl)-*N*,3-dimethyl-2-phenylbutanamide (**74b**):

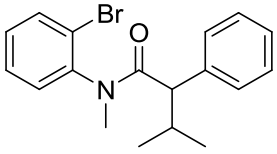

Yellow oil, 79% yield. **^{1}H-NMR** (400 MHz, $CDCl_3$): δ 0.52-0.56 (m, 4.4H), 1.10-1.15 (m, 4.4H), 2.38-2.51 (m, 1.5H), 2.71 (d, *J* = 13.6 Hz, 1H), 2.98 (d. *J* = 13.6 Hz, 0.5H), 3.19 (s, 3H), 3.23 (s, 1.4H), 6.59 (dd, *J* = 13.6 Hz, 1H), 6.91-7.05 (m, 3H), 7.11-7.49 (m, 8H), 7.61 (d, *J* = 4.0 Hz, 0.5H), 7.75 (d, *J* = 4.0 Hz, 1H). **^{13}C-NMR** (100 MHz, $CDCl_3$): δ 20.21, 20.25, 22.1, 22.7, 32.6, 32.8, 35.9, 36.0, 57.2, 58.2, 123.1, 124.5, 126.7, 128.0, 128.13, 128.16, 128.60, 128.64, 128.8, 129.71, 129.75, 130.9, 131.5, 133.6, 134.0, 138.5, 139.3, 142.0, 142.6, 172.9, 173.1. **IR** (neat, cm^{-1}): 2956, 1656, 1475, 1454, 1417. **HRMS** (ESI): calcd. for $C_{18}H_{20}BrNO$ ($[M+H]^+$): 346.0801, found: 346.0767.

N-(2-Bromophenyl)-*N*-methyl-2,3-diphenylpropanamide (**74c**):

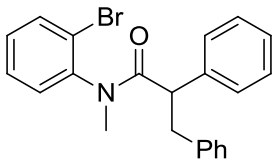

Oil, 69% yield. **^{1}H-NMR** (400 MHz, $CDCl_3$): δ 2.86 (dd, *J* = 11.6, 3.5 Hz, 0.6H), 2.99-3.04 (m, 1H), 3.13 (s, 2H), 3.39 (s, 3H), 3.50-3.61 (m, 3.2H), 6.23-6.25 (m, 0.6H), 6.65 (d, *J* = 8 Hz, 1H), 6.81-6.91 (m, 2H), 6.99 (d, *J* = 8 Hz, 2H), 7.1-7.35 (m, 16H), 7.60 (d, *J* = 8 Hz, 0.6H), 7.72 (d, *J* = 8 Hz, 1H). **^{13}C-NMR** (100 MHz, $CDCl_3$): δ 36.0, 36.2, 41.3, 41.6, 51.5, 52.7, 123.5, 123.8, 125.9, 126.4, 126.9, 127.0, 128.0, 128.21, 128.24, 128.28, 128.3, 128.5, 129.3, 129.4, 129.6, 129.7, 130.5, 131.0, 133.5, 133.6, 139.1, 139.2, 139.7, 139.9, 141.9, 142.2, 172.4, 172.5. **IR** (neat, cm^{-1}): 3060, 3027, 2925, 1659, 1600, 1583, 1494, 1475, 1453, 1418. **HRMS** (ESI): calcd. for $C_{22}H_{20}BrNO$ ($[M+H]^+$): 394.0801, found: 394.0767.

N-(2-Chlorophenyl)-*N*-methyl-2-p-tolylpropanamide (**75a**):

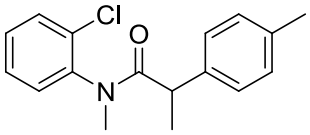

Yellow powder, **m.p.** = 82-83 °C, 76% yield. **^{1}H-NMR** (400 MHz, $CDCl_3$): δ 1.43 (d, *J* = 9.2 Hz, 1.4H), 1.45 (d, *J* = 9.2 Hz, 3H), 2.32 (s, 1.4H), 2.34 (s, 3H), 3.28 (s, 1.4H), 3.33 (s, 3H), 3.38 (q, *J* = 9.6 Hz, 1H), 3.56 (q, *J* = 9.6 Hz, 0.4H), 6.8 (dd, *J* = 10.4, 1.5 Hz, 1H), 6.92 (t, *J* = 8 Hz, 3H), 7.04 (t, *J* = 8 Hz, 3H), 7.17 (t, *J* = 1.6 Hz, 1H), 7.29-7.41 (m, 3H), 7.55 (d, (t, *J* = 10 Hz, 1H). **^{13}C-NMR** (100 MHz, $CDCl_3$): δ 20.0 20.5, 21.0, 36.0, 36.1, 42.8, 43.3, 127.3, 127.7, 127.82, 128.88, 129.1, 129.4, 129.5, 130.0, 130.3, 130.83, 130.87, 133.1, 133.8, 136.2, 137.6, 138.7, 140.8, 141.0, 174.1, 174.3. **IR** (neat, cm^{-1}): 2969, 1660, 1512, 1480, 1440. **HRMS** (EI): calcd. for $C_{17}H_{18}ClNO$ ($[M+H]^+$): 288.1149, found: 288.1145.

N-(2-Chlorophenyl)-*N*-methyl-2-(naphthalen-2-yl)propanamide (**75b**):

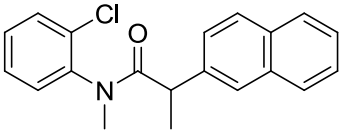

Oil, 86% yield. **^{1}H-NMR** (300 MHz, $CDCl_3$): δ 1.55 (d, *J* = 6.8 Hz, 4.2H), 3.25 (s, 4.3H), 3.57 (q, *J* = 6 Hz, 1H), 3.78 (q, *J* = 6 Hz, 0.4H), 6.68 (d, *J* = 5.7 Hz, 1H), 7.1 (t, *J* = 6.6 Hz, 1H), 7.21 (d, *J* = 6 Hz, 1H), 7.25 (d, *J* = 6 Hz, 0.4H), 7.3-7.41 (m, 3H), 7.42-7.51 (m, 3.4H), 7.63 (d, *J* = 6 Hz, 1H), 7.7-7.85 (m, 4H). **^{13}C-NMR** (75 MHz, $CDCl_3$): δ 19.9, 20.5, 36.1, 36.2, 43.5, 44.0, 125.4, 125.6, 125.7, 125.8, 125.9, 126.0, 126.6, 127.5, 127.6, 127.7, 127.8, 128.0, 128.1, 129.5, 129.6, 130.1, 130.4, 130.8, 130.9, 132.4, 132.5, 133.1, 133.3, 133.4, 143.0, 138.0, 139.2, 140.7, 173.8. **IR** (neat, cm^{-1}): 3056, 2971, 2931, 1659, 1586, 1480. **HRMS** (ESI): calcd. for $C_{20}H_{18}ClNO$ ($[M+H]^+$): 324.1118, found: 324.1149.

N-(2-Chlorophenyl)-*N*-methyl-2-phenylbutanamide (**75c**):

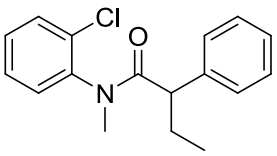

Oil, 91% yield. **^{1}H-NMR** (300 MHz, $CDCl_3$): δ 0.85 (m, 4.3H), 1.74 (m, 2H), 3.13 (m, 1.6H), 3.08 (t, *J* = 6 Hz, 1H), 3.22 (s, 3H), 3.24 (s, 1.3H), 3.31 (t, *J* = 6 Hz, 0.4H), 6.69 (d, *J* = 6 Hz, 1H), 6.92-7.01 (m, 2.8H), 7.11-7.29 (m, 5H), 7.31-7.45 (m, 3H), 7.59 (d, *J* = 6 Hz, 1H). **^{13}C-NMR** (75 MHz, $CDCl_3$): δ 12.4, 12.5, 28.0, 28.4, 35.9, 36.0, 51.0, 51.8, 126.7, 127.6, 127.92, 127.97, 128.1, 129.5, 130.4, 130.8, 131.0, 132.9, 140.2, 140.6, 173.2. **IR** (neat, cm^{-1}): 3027, 2964, 2930, 1659, 1586, 1480. **HRMS** (ESI): calcd. for $C_{17}H_{18}ClNO$ ($[M+H]^+$): 288.1151, found: 288.1149.

N-(2-Chlorophenyl)-*N*-methyl-2,3-diphenylpropanamide (**75d**):

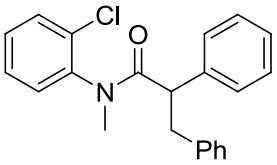

Oil, 74% yield. **^{1}H-NMR** (300 MHz, $CDCl_3$): δ 2.85-2.91 (m, 1H), 2.93-3.1 (m, 1.5H), 3.14 (s, 3H), 3.2 (s, 4H), 3.4-3.66 (m, 5H), 6.29 (d, *J* = 9 Hz, 1H), 6.66 (d, *J* = 9 Hz, 1H), 6.92-7.08 (m, 5H), 7.10-7.4 (m, 26H), 7.55 (d, *J* = 6 Hz, 1.3H). **^{13}C-NMR** (75 MHz, $CDCl_3$): δ 35.9, 36.1, 41.3, 41.4, 51.4, 52.4, 125.9, 126.3, 126.90, 126.99, 127.6, 127.8, 128.0, 128.1, 128.2, 128.30, 128.34, 129.2, 129.3, 129.4, 129.5, 130.3, 130.4, 130.9, 133.0, 139.3,

139.6, 139.9, 140.5, 172.6. **IR** (neat, cm^{-1}): 3027, 2928, 1659, 1585, 1480. **HRMS** (ESI): calcd. for $C_{22}H_{20}ClNONa$ ($[M+Na]^+$): 372.1153, found: 372.1125.

1-(8-Bromo-3,4-dihydroquinolin-1(2*H*)-yl)-2-phenylpropan-1-one (**77**):

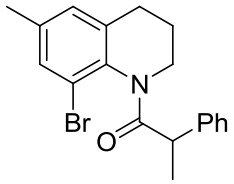

Solid, **m.p.** = 88-89 °C, 87% yield. **^{1}H-NMR** (400 MHz, $CDCl_3$): δ 1.29-1.57 (m, 6.1H), 1.85-1.98 (m, 1H), 2.22-2.38 (m, 2.4H), 2.39 (s, 3H), 2.76-2.83 (m, 1H), 3.96 (q, *J* = 7.2 Hz, 1H), 4.17 (q, *J* = 7.2 Hz, 0.34H), 4.6-4.67 (m, 1H), 6.78 (d, *J* = 6.8 Hz, 2H), 6.8 (s, 1H), 7.08-7.15 (m, 3H), 7.25-7.61 (m, 1.8H). **^{13}C-NMR** (100 MHz, $CDCl_3$): δ 18.7, 20.8, 23.8, 25.8, 41.7, 44.8, 120.4, 126.7, 127.6, 127.8, 128.8, 131.1, 136.4, 137.9, 139.9, 140.9, 174.4. **IR** (neat, cm^{-1}): 3026, 2931, 1661, 1477, 1452. **HRMS** (ESI): calcd. for $C_{19}H_{20}BrNO$ ($[M+H]^+$): 358.0808, found: 358.0785.

(*E*)-*N*-(2-Bromophenyl)-*N*,2-dimethyl-4-phenylbut-3-enamide (**81**):

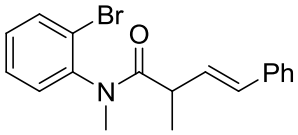

Oil, 88% yield. **^{1}H-NMR** (300 MHz, $CDCl_3$): δ 1.28 (d, *J* = 6 Hz, 2.6H), 1.34 (d, *J* = 6 Hz, 3.5H), 2.98-3.15 (m, 2H), 3.25 (s, 4.9H), 3.53 (q, *J* = 9 Hz, 0.37H), 5.97-6.35 (m, 3.3H), 7.2-7.46 (m, 14H), 7.71 (d, *J* = 10.5 Hz, 0.6H), 7.77 (d, *J* = 10.5 Hz, 1H). **^{13}C-NMR** (75 MHz, $CDCl_3$): δ 18.5, 18.6, 36.1, 41.5, 41.8, 123.6, 124.0, 126.2, 127.2, 127.4, 128.4, 128.54, 128.58, 128.8, 129.8, 130.1, 130.7, 130.8, 133.8, 134.0, 136.9, 137.2, 142.4, 142.7, 173.9, 174.3. **IR** (neat, cm^{-1}): 3058, 2974, 2930, 2869, 1661, 1583, 1475, 1446, 1427. **HRMS** (ESI): calcd. for $C_{18}H_{18}BrNO$ ($[M+H]^+$): 344.0644, found: 344.0622.

N-(2-Chlorophenyl)-*N*-methyl-2-phenylpropanamide (**84**):

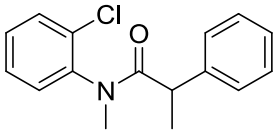

Oil, 87% yield. **^{1}H-NMR** (400 MHz, $CDCl_3$): δ 1.45 (d, *J* = 6.8 Hz, 1.4H), 1.46 (d, *J* = 6.8 Hz, 3H), 3.22 (s, 3H), 3.23 (s, 1.4H), 3.41 (q, *J* = 6.8 Hz, 1H), 3.61 (q, *J* = 6.8 Hz, 0.4H), 6.76 (d, *J* = 8 Hz, 1H), 6.91-7.05 (m, 3H), 7.17-7.41 (m, 8H), 7.24 (d, *J* = 8 Hz, 1H); **^{13}C-NMR** (100 MHz, $CDCl_3$): δ 20.0 20.5, 36.0, 36.2, 43.3, 43.8, 126.7, 127.4, 127.8, 128.0, 128.2, 128.4, 129.5, 129.6, 130.0, 130.4, 130.8, 133.1, 133.9, 140.6, 140.7, 140.9, 141.7, 173.9, 174.0; **IR** (neat, cm^{-1}): 3061, 2973, 2931, 1660, 1586, 1480, 1452, 1417. **HRMS** (ESI): calcd. for $C_{16}H_{16}ClNO$ ($[M+H]^+$): 274.0993, found: 274.0992.

N-(2-Bromo-4-methylphenyl)-*N*-methyl-2-phenylpropanamide (**85a**):

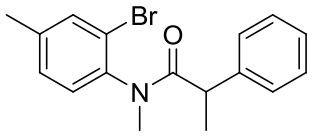

Yellow oil, 78% yield. **^{1}H-NMR** (400 MHz, $CDCl_3$): δ 1.46 (d, *J* = 12 Hz, 1.2H), 1.47 (d, *J* = 12 Hz, 3H), 2.43 (s, 3H), 2.45 (s, 1.2H), 3.19 (s, 3H), 3.21 (s, 1.2H), 3.42 (q, *J* = 8 Hz, 1H), 3.59 (q, *J* = 7 Hz, 0.38H), 6.66 (d, *J* = 8 Hz, 1H), 7.01-7.05 (m, 3.8H), 7.06-7.12 (m, 4.8H), 7.46 (s, 0.45H), 7.57 (s, 1H). **^{13}C-NMR** (100 MHz, $CDCl_3$): δ 20.1, 20.6, 20.8, 36.20, 36.23, 43.0, 43.8, 123.2, 123.6, 128.12, 128.17, 129.2, 129.54, 129.59, 130.3, 133.9, 134.3, 139.6, 139.8, 140.1, 140.7, 141.7, 173.9, 174.1. **IR** (neat, cm^{-1}): 3027, 2972, 2930, 1737, 1662, 1601, 1492, 1452, 1417. **HRMS** (ESI): calcd. for $C_{17}H_{18}BrNO$ ($[M+H]^+$): 332.0644, found: 332.0647.

N-(2-Bromo-4-isopropylphenyl)-*N*-methyl-2-phenylpropanamide (**85b**):

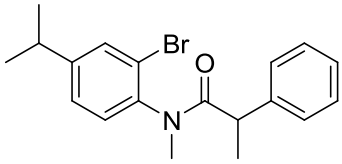

Oil, 85% yield. **^{1}H-NMR** (400 MHz, $CDCl_3$): δ 1.32 (d, *J* = 7.6 Hz, 6H), 1.34 (d, *J* = 7.6 Hz, 2.8H), 1.47 (d, *J* = 8 Hz, 1.1H), 1.48 (d, *J* = 8 Hz, 3H), 2.29-3.01 (m, 1.5H), 3.20 (s, 3H), 3.22 (s, 1.4H), 3.43 (q, *J* = 8 Hz, 1H), 3.60 (q, *J* = 6.8 Hz, 0.4H), 6.66 (d, *J* = 8Hz, 1H), 6.95-7.10 (m, 3.8H), 7.15-7.25 (m, 4H), 7.32 (s, 1H), 7.47 (s, 0.4H), 7.59 (s, 1H). **^{13}C-NMR** (100 MHz, $CDCl_3$): δ 20.03, 20.56, 23.8, 36.17, 36.19, 43.1, 43.9, 123.3, 123.8, 126.6, 126.7, 129.6, 131.8, 139.7, 139.9, 140.7, 141.8, 151.0, 173.9. **IR** (neat, cm^{-1}): 2962, 1664, 1491, 1453, 1416. **HRMS** (ESI): calcd. for $C_{19}H_{22}BrNO$ ($[M+H]^+$): 360.0957, found: 360.0940.

N-(2-Bromo-4,6-dimethylphenyl)-*N*-methyl-2-phenylpropanamide (**85c**):

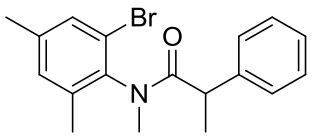

Solid, **m.p.** = 101-102 °C, 78% yield. **^{1}H-NMR** (400 MHz, $CDCl_3$): δ 1.46-1.51 (m, 6H), 2.39 (s, 3H), 3.12 (s, 3H), 3.43 (q, *J* = 8 Hz, 1H), 6.92 (s, 1H), 6.96-6.98 (m, 2H), 7.21-7.31 (m, 3H), 7.42 (s, 1H). **^{13}C-NMR** (100 MHz, $CDCl_3$): δ 17.5, 20.8, 20.9, 34.7, 44.0, 124.1, 126.7, 131.1, 131.4, 133.1, 138.2, 139.1, 139.6, 141.2, 174.1. **IR** (neat, cm^{-1}): 2983, 2927, 1657, 1476, 1452, 1415. **HRMS** (EI): calcd. for $C_{18}H_{20}BrNO$ ($[M+H]^+$): 346.0801, found: 346.0791.

N-(2-Bromo-5-(trifluoromethyl)phenyl)-*N*-methyl-2-phenylpropanamide (**85d**):

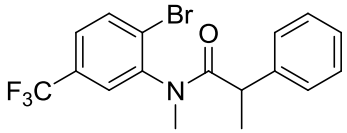

Solid, **m.p.** = 70-71 °C, 81% yield. **^{1}H-NMR** (400 MHz, $CDCl_3$): δ 1.48 (d, *J* = 6 Hz, 3.8H), 1.55 (d, *J* = 6 Hz, 0.2H), 3.18 (s, 3H), 3.20 (s, 0.8H), 3.25 (q, *J* = 8.2 Hz, 1H), 3.50 (q, *J* = 8.2 Hz, 0.2H), 6.8 (s, 1H), 6.91 (d, *J* = 12 Hz, 2H), 6.97-6.99 (m, 0.5H), 7.23-7.24 (m, 3.8H), 7.51 (d, *J* = 8 Hz, 1.5H), 7.73 (d, *J* = 8 Hz, 0.2H), 7.90 (d, *J* = 8 Hz, 1H). **^{13}C-NMR** (100 MHz, $CDCl_3$): δ 20.2, 20.5, 36.1, 43.8, 44.7, 121.5, 124.2, 126.2, 126.30, 126.34, 126.38, 126.9, 127.8, 128.0, 128.22, 128.26, 128.2, 128.33, 128.39, 128.7, 130.8, 131.1, 134.8, 140.1, 141.2, 142.8, 143.1, 173.2. **IR** (neat, cm^{-1}): 3029, 2932, 1668, 1602, 1575, 1415. **HRMS** (ESI): calcd. for $C_{17}H_{15}BrF_3NO$ ($[M+H]^+$): 386.0361, found: 386.0353.

N-(2-Bromo-5-fluorophenyl)-*N*-methyl-2-phenylpropanamide (**85e**):

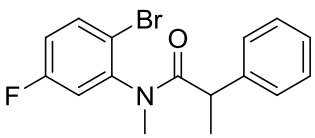

Solid, **m.p.** = 65-66 °C, 84% yield. **^{1}H-NMR** (400 MHz, $CDCl_3$): δ 1.47 (d, *J* = 6.8 Hz, 1H), 1.48 (d, *J* = 6.8 Hz, 3H), 3.23 (s, 3H), 3.23 (s, 1H), 3.39 (q, *J* = 6.8 Hz, 1H), 3.58 (q, *J* = 6.8 Hz, 0.34H), 6.42 (dd, *J* = 8.8, 3.1 Hz, 1H), 6.91-7.10 (m, 4H), 7,11-7.20 (m, 0.39H), 7.21-7.49 (m, 4.3H), 7.57 (q, *J* = 12 Hz, 0.37H), 7.71 (q, *J* = 12 Hz, 1H). **^{13}C-NMR** (100

MHz, $CDCl_3$): δ 20.2, 20.5, 36.0, 43.4, 44.4, 116.9, 117.0, 117.1, 117.2, 117.5, 118.20, 118.23, 118.3, 118.5, 118.81, 118.88, 126.84, 126.89, 127.2, 127.9, 128.2, 128.5, 134.1, 134.2, 134.7, 134.8, 140.3, 141.4, 143.40, 143.48, 143.5, 143.6, 160.7, 160.9, 162.7, 162.9, 173.4, 173.6. **IR** (neat, cm^{-1}): 3063, 3028, 2974, 2932, 1666, 1592, 1579, 1470, 1414. **HRMS** (ESI): calcd. for $C_{16}H_{15}BrFNO$ ($[M+H]^+$): 336.0393, found: 336.0397.

N-(2-Bromo-5-methoxyphenyl)-*N*-methyl-2-phenylpropanamide (**85f**):

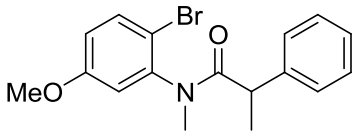

Yellow powder, **m.p.** = 87-88 °C, 89% yield. **^{1}H-NMR** (400 MHz, $CDCl_3$): δ 1.46 (d, *J* = 8.8 Hz, 3.7H), 3.21 (s, 3H), 3.22 (s, 0.8H), 3.4 (q, *J* = 9.2 Hz, 1H), 3.51 (s, 3H), 3.65 (q, *J* = 9.6 Hz, 0.31H), 3.9 (s, 0.71H), 6.17 (d, *J* = 3.6 Hz, 1H), 6.83 (dd, *J* = 11.8, 3.9 Hz, 1H), 6.85 (dd, *J* = 7.6, 2.7 Hz, 0.4H), 7.00-7.05 (m, 2H), 7.05-7.15 (m, 0.5H), 7.19-7.35 (m, 4H), 7.49 (d, *J* = 12 Hz, 0.5H), 7.55 (d, *J* = 12 Hz, 1H). **^{13}C-NMR** (100 MHz, $CDCl_3$): δ 20.2, 20.6, 36.0, 43.2, 44.3, 55.3, 55.8, 113.5, 115.3, 115.4, 115.7, 116.9, 126.6, 126.7, 127.5, 128.1, 128.1, 128.4, 133.6, 134.2, 140.6, 142.1, 142.7, 159.4, 173.5. **IR** (neat, cm^{-1}): 3062, 2932, 2837, 1661, 1589, 1572, 1475, 1453, 1411. **HRMS** (ESI): calcd. for $C_{17}H_{18}BrNO_2$ ($[M+H]^+$): 348.0593, found: 348.0587.

N-(2-Bromo-6-fluorophenyl)-N-methyl-2-phenylpropanamide (**85g**):

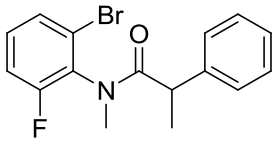

White solid, **m.p.** = 68-70 °C, 44% yield. **^{1}H-NMR** (400 MHz, $CDCl_3$): δ 1.41-1.45 (m, 4H), 3.14 (s, 3H), 3.16 (s, 1H), 3.34-3.43 (m, 1.3H), 6.8-6.9 (m, 3H), 6.9-6.98 (m, 0.6H), 7.15-7.25 (m, 5.4H), 7.34-7.39 (m, 0.6H), 7.5 (d, *J* = 8.0 Hz, 1H). **^{13}C-NMR** (100 MHz, $CDCl_3$): δ 20.1, 20.5, 35.2, 43.6, 44.4, 115.6, 115.8, 115.9, 116.1, 125.2, 126.8, 126.88, 127.2, 127.8, 128.3, 128.6, 128.7, 130.4, 130.5, 130.9, 140.8, 173.8. **IR** (neat, cm^{-1}): 3082, 2977, 2933, 1663, 1648, 1570, 1474, 1447, 1377, 1275, 1250, 1119, 1060, 1017, 869, 744, 696. **HRMS** (ESI) calcd. for $C_{16}H_{15}BrFNO$ ($[M+H]^+$) 336.0391, found 336.0395.

N-(2-Bromophenyl)-2-(2,3-dihydro-1H-inden-1-yl)-*N*-methylpropanamide (**89**):

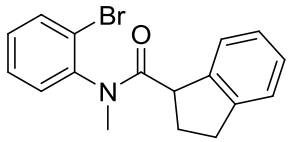

Yellow powder, **m.p.** = 123-124 °C, 83% yield. **^{1}H-NMR** (400 MHz, $CDCl_3$): δ 2.1-2.35 (m, 1.5H), 2.45-2.61 (m, 0.5H), 2.71-2.9 (m, 1H), 3.01-3.21 (m, 1H), 3.45 (d, *J* = 12 Hz, 3H), 3.78-3.92 (m, 1H), 7.18-7.55 (m, 7H), 7.75 (d, *J* = 12 Hz, 1H). **^{13}C-NMR** (100 MHz, $CDCl_3$): δ 31.0, 31.3, 32.0, 32.2, 36.0, 36.3, 48.4, 49.0, 123.5, 123.6, 123.9, 124.3, 124.7, 125.1, 126.3, 126.4, 127.0, 127.1, 129.0, 129.2, 129.8, 129.9, 130.1, 134.01, 134.05, 142.4, 142.8, 142.9, 143.0, 144.2, 144.7, 174.9, 175.1. **IR** (neat, cm^{-1}): 3023, 2940, 1664, 1583, 1475, 1434. **HRMS** (ESI): calcd. for $C_{17}H_{16}BrNO$ ($[M+H]^+$): 330.0488, found: 330.0489.

N-(2-Bromophenyl)-*N*-methyl-1,2-dihydrocyclobutabenzene-1-carboxamide (**106**):

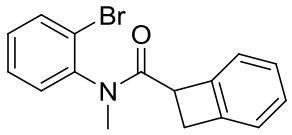

White solid, **m.p.** = 144-146 °C, 97% yield. **^{1}H-NMR** (300 MHz, $CDCl_3$): δ 2.9-3.04 (m 1.5H), 3.26 (s, 1.3H), 3.27 (s, 3H), 3.32 (dd, *J* = 13.6, 2.7 Hz, 0.7H), 3.53 (dd, *J* = 13.6, 2.7 Hz, 1H), 4.03-4.11 (m, 1.4H), 6.99-7.03 (m, 2H), 7.10-7.19 (m, 3.7H), 7.24-7.30 (m, 2H), 7.33-7.47 (m, 3H), 7.73 (dd, *J* = 8.0, 2.3 Hz, 1H). **^{13}C-NMR** (75 MHz, $CDCl_3$): δ 34.3, 35.5, 36.1, 45.2, 45.4, 122.3, 122.5, 122.8, 123.2, 123.6, 123.7, 127.0, 127.2, 127.7, 127.8, 128.9, 129.0, 129.9, 130.3, 130.4, 134.0, 134.07, 142.43, 142.47, 143.32, 143.63, 143.73, 144.5, 171,5, 171.8. **IR** (neat, cm^{-1}): 3066, 2931, 1651, 1580, 1472, 1455, 1420, 1375, 1311, 1259, 1117, 1031, 998, 765, 724, 668. **HRMS** (ESI): calcd. for $C_{16}H_{15}BrNO$ ($[M+H]^+$): 316.0331, found: 316.0320.

N-(2-Bromophenyl)-*N*-methyl-1,2,3,4-tetrahydronaphthalene-1-carboxamide (**107**):

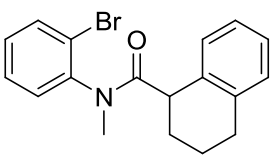

White solid, **m.p.** = 125-127 °C, 83% yield. **^{1}H-NMR** (400 MHz, $CDCl_3$): δ 1.46-1.58 (m, 2H), 1.88-2.11 (m, 6H), 2.64-2.74 (m, 2H), 2.81-2.89 (m, 2H), 3.28 (s, 3H), 3.32 (s, 3H), 3.56 (q, *J* = 16.9, 8.8 Hz, 2H), 7.06-7.13 (m, 7H), 7.23-7.29 (m, 2H), 7.32-7.44 (m, 4H), 7.48 (d, *J* = 7.8 Hz, 1H), 7.72 (d, *J* = 8 Hz, 2H). **^{13}C-NMR** (100 MHz, $CDCl_3$): δ 21.3, 21.4, 27.5, 29.1, 29.3, 36.2, 36.3, 43.2, 43.4, 123.40, 123.48, 125.83, 125.89, 126.41, 126.46, 127.7, 128.9, 129.1, 129.2, 129.53, 129.55, 129.8, 129.9, 130.0, 134.2, 134.9, 135.6, 137.4, 137.7, 142.77, 143.0, 175.5, 175.7. **IR** (neat, cm^{-1}): 3066, 2932, 1657, 1477, 1420, 1377, 1248, 1119, 1952, 1028, 958, 764, 751, 729. **HRMS** (ESI): calcd. for $C_{18}H_{19}BrNO$ ($[M+H]^+$): 344.0644, found: 344.0643.

N-(2-Bromophenyl)-*N*-methyl-6,7,8,9-tetrahydro-5*H*-benzo[7]annulene-5-carboxamide (**108**):

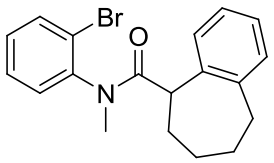

White solid, **m.p.** = 82-84 °C, 78% yield. **^{1}H-NMR** (400 MHz, $CDCl_3$): δ 1.17-1.26 (q, *J* = 13.1 Hz, 1H), 1.46-1.92 (m, 5.6H), 2.09-2.19 (m, *J* = 12.0 Hz, 1H), 2.34-2.39 (m, 0.14H), 2.49 (m, *J* = 5.8 Hz, 1H), 3.25 (t, *J* = 2.9 Hz, 3H), 3.48 (d, *J* = 9.8 Hz, 1H), 6.71 (dd, *J* = 6.8, 3.5 Hz, 1H), 6.93-7.19 (m, 6.9H), 7.66 (dd, *J* = 7.8, 4.3 Hz, 1H). **^{13}C-NMR** (100 MHz, $CDCl_3$): δ 27.4, 30.6, 30.9, 35.3, 35.7, 48.2, 123.4, 126.0, 126.4, 128.4, 129.1, 129.5, 129.8, 133.4, 140.5, 142.3, 174.4. **IR** (neat, cm^{-1}): 2923, 1656, 1472, 1384, 1286, 1126, 1049, 1030, 769, 747, 727, 697. **HRMS** (ESI): calcd. for $C_{19}H_{21}BrNO$ ($[M+H]^+$): 358.0801, found: 358.0799.

N-(2-Bromopyridin-3-yl)-*N*-methyl-2,3-dihydro-1*H*-indene-1-carboxamide (**109**):

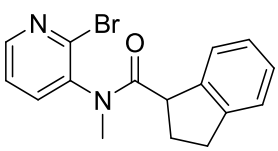

Yellow solid, **m.p.** = 78-80 °C, 75% yield. **^{1}H-NMR** (400 MHz, $CDCl_3$): δ 2.03-2.31 (m, 3H), 2.41-2.52 (m, 1H), 2.73-2.83 (m, 2H), 3.01-3.15 (m, 2H), 3.28 (s, 3H), 3.30 (s, 3H), 3.68-3.76 (m, 2H), 7.06 (d, *J* = 6.7 Hz, 1H), 7.11-7.22 (m, 6H), 7.31 (d, *J* = 4.3 Hz, 1H), 7.41-7.44 (m, 2H), 7.66 (dd, *J* = 1.7, 7.6 Hz, 1H), 7.81 (dd, *J* = 1.7, 7.6 Hz, 1H), 8.41-8.44 (m, 2H).

^{13}C-NMR (100 MHz, $CDCl_3$): δ 31.0, 31.2, 31.9, 32.1, 36.1, 36.3, 48.6, 49.1, 123.3, 123.8, 124.0, 124.3, 124.9, 125.1, 126.3, 126.5, 127.32, 127.38, 138.09, 138.15, 140.4, 140.5, 141.7, 142.3, 143.8, 144.0, 144.7, 149.5, 149.6, 174.5, 174.8. **IR** (neat, cm^{-1}): 3041, 2926, 2848, 1663, 1448, 1397, 1373, 1264, 1136, 1052, 811, 742, 632, 521. **HRMS** (ESI): calcd. for $C_{17}H_{17}BrNOS$ ($[M+H]^+$): 362.0209, found: 362.0110.

N-(2-Chloropyridin-3-yl)-*N*-methyl-1,2,3,4-tetrahydronaphthalene-1-carboxamide (**110**):

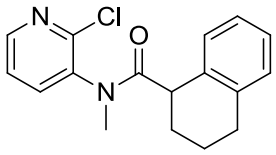

White solid, **m.p.** = 105-108 °C, 89% yield. **^{1}H-NMR** (400 MHz, $CDCl_3$): δ 1.44-1.56 (m, 2H), 1.82-1.87 (m, 1H), 1.92-2.03 (m, 4H), 2.65 (t, *J* = 5.7 Hz, 1H), 2.68 (t, *J* = 5.7 Hz, 1H), 2.78-2.89 (m, 2H), 3.28 (s, 3H), 3.33 (s, 3H), 3.51 (q, *J* = 7.6 Hz, 2H), 6.97-7.21 (m, 8H), 7.35-7.40 (m, 2H), 7.70 (dd, *J* = 7.7, 1.7 Hz, 1H), 7.82 (dd, *J* = 7.7, 1.7 Hz, 1H), 8.43-8.47 (m, 2H). **^{13}C-NMR** (100 MHz, $CDCl_3$): δ 21.0, 21.2, 27.3, 27.8, 29.0, 29.2, 36.1, 36.2, 43.3, 43.4, 123.6, 123.8, 125.93, 125.98, 126.64, 126.68, 127.4, 129.2, 129.6, 134.3, 135.0, 137.7, 138.3, 138.4, 138.5, 149.2, 149.3, 150.5, 150.6, 175.2, 175.4. **IR** (neat, cm^{-1}): 3052, 2933, 2849, 2343, 1660, 1556, 1451, 1405, 1370, 1348, 1249, 1140, 1072, 812, 751, 729, 641. **HRMS** (ESI): calcd. for $C_{17}H_{18}ClN_2O$ ($[M+H]^+$): 301.1048, found: 301.1227.

N-(2-Bromopyridin-3-yl)-*N*-methyl-1,2,3,4-tetrahydronaphthalene-1-carboxamide (**111**):

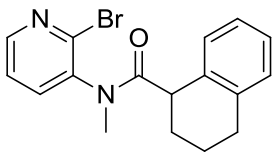

White solid, **m.p.** = 115-117 °C, 94% yield. **^{1}H-NMR** (400 MHz, $CDCl_3$): δ 1.47-1.58 (m, 2H), 1.83-2.11 (m, 6H), 2.65 (t, *J* = 5.1 Hz, 1H), 2.68 (t, *J* = 5.1 Hz, 1H), 2.78-2.87 (m, 1H), 3.28 (s, 3H), 3.33 (s, 3H), 3.44-3.53 (m, 2H), 6.98 (t, *J* = 4.6 Hz, 1H), 7.0-7.07 (m, 2H), 7.11 (t, *J* = 4.4 Hz, 4H), 7.31 (t, *J* = 4.3 Hz, 1H), 7.36-7.42 (m, 2H), 7.68 (dd, *J* = 7.8, 1.8 Hz, 1H), 7.78 (dd, *J* = 7.8, 1.8 Hz, 1H), 8.41 (dd, *J* = 9.8, 4.5 Hz, 2H). **^{13}C-NMR** (100 MHz, $CDCl_3$): δ 21.2, 21.4, 27.6, 28.0, 29.1, 29.3, 36.5, 43.6, 43.8, 123.9, 124.2, 126.0, 126.80,

126.84, 127.5, 129.3, 129.7, 129.8, 134.5, 135.3, 137.5, 137.9, 138.2, 140.4, 140.7, 143.8, 143.9, 149.7, 149.8, 175.2, 175.4. **IR** (neat, cm^{-1}): 2932, 1659, 1551, 1399, 1369, 1246, 1132, 1049, 812, 746. **HRMS** (ESI): calcd. for $C_{17}H_{18}BrNO_2$ ($[M+H]^+$): 345.0597, found: 345.0592.

N-(2-Bromopyridin-3-yl)-*N*-methyl-6,7,8,9-tetrahydro-5*H*-benzo[7]annulene-5-carboxamide (**112**):

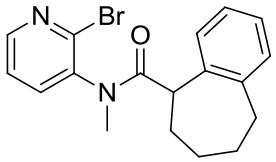

Colorless oil, 93% yield. **^{1}H-NMR** (400 MHz, $CDCl_3$): δ 1.16-1.23 (m, 1H), 1.49-1.70 (m, 2H), 1.73-1.78 (m, 1H), 1.90-1.95 (m, 1H), 2.12-2.20 (m, 2H), 2.48 (dd, *J* = 14.1, 5.2 Hz, 1H), 3.27 (s, 3H), 3.42 (d, *J* = 9.8 Hz, 1H), 6.94-6.96 (m, 3H), 7.05-7.13 (m, 3H), 8.25 (dd, *J* = 4.0, 2.4 Hz, 1H). **^{13}C-NMR** (100 MHz, $CDCl_3$): δ 27.3, 30.4, 30.5, 35.1, 35.7, 48.7, 123.1, 125.9, 126.7, 129.2, 137.8, 139.8, 140.0, 142.3, 143.7, 149.2, 174.0. **IR** (neat, cm^{-1}): 2925, 2850, 1737, 1665, 1446, 1397, 1376, 1267, 1241, 1134, 1116, 1051, 811, 743, 709, 633, 520. **HRMS** (ESI): calcd. for $C_{18}H_{20}N_2OBr$ ($[M+H]^+$): 359.0753, found: 359.0751.

N-(2-Bromo-4-methylphenyl)-*N*-methyl-1,2,3,4-tetrahydronaphthalene-1-carboxamide (**113**):

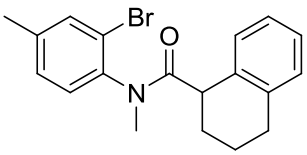

White solid, **m.p.** = 87-89 °C, 89% yield. **^{1}H-NMR** (400 MHz, $CDCl_3$): δ 1.47-1.56 (m, 1.9H), 1.85-2.0 (m, 5.8H), 2.36 (s, 2.7H), 2.38 (s, 3H), 2.64 (t, *J* = 5.2 Hz, 0.9H), 2.68 (t, *J* = 5.2 Hz, 1H), 2.78-2.89 (m, 2H), 3.26 (s, 3H), 3.3 (s, 2.7H), 3.59 (q, *J* = 8.9 Hz, 1.9H), 7.0-7.12 (m, 6.8H), 7.19 (t, *J* = 9.0 Hz, 2H), 7.24 (d, *J* = 8.2 Hz, 1H), 7.32 (d, *J* = 5.6 Hz, 0.9H), 7.35 (d, *J* = 8.0 Hz, 1H), 7.52 (s, 1.9H). **^{13}C-NMR** (100 MHz, $CDCl_3$): δ 20.84, 20.87, 21.3, 21.4, 27.9, 29.3, 36.31, 36.36, 43.1, 43.3, 122.9, 123.0, 125.7, 125.8, 126.3, 126.4, 127.7, 129.1, 129.4, 129.53, 129.59, 129.9, 134.5, 135.0, 135.7, 137.4, 137.6, 140.1, 140.3, 140.40, 140.42, 175.7, 175.9. **IR** (neat, cm^{-1}): 3047, 2934, 1658, 1493, 1369, 1246, 1124, 1049, 834, 745, 571. **HRMS** (ESI): calcd. for $C_{19}H_{21}BrNO$ ($[M+H]^+$): 358.0801, found: 358.0793.

N-(2-Bromo-4-methoxyphenyl)-*N*-methyl-1,2,3,4-tetrahydronaphthalene-1-carboxamide (**114**):

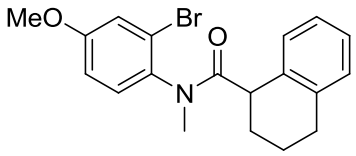

White solid, **m.p.** = 110-112 °C, 94% yield. **^{1}H-NMR** (400 MHz, $CDCl_3$): δ 1.47-1.58 (m, 1H), 1.83-2.07 (m, 6H), 2.62-2.69 (m, 1.9H), 2.80-2.89 (m, 2H), 3.24 (s, 3H), 3.28 (s, 2.7H), 3.59 (q, *J* = 8.3 Hz, 1.9H), 3.81 (s, 2.7H), 3.83 (s, 3H), 6.88-6.93 (m, 2H), 7.02-7.05 (m, 2.9H), 7.09-7.12 (m, 3.9H), 7.22 (d, *J* = 2.7 Hz, 1.9H), 7.26 (d, *J* = 8.6 Hz, 1H), 7.30-7.32 (m, 1H), 7.37 (d, *J* = 8.7 Hz, 0.9H). **^{13}C-NMR** (100 MHz, $CDCl_3$): δ 21.3, 21.4, 27.5, 27.9, 29.1, 29.3, 36.4, 36.5, 43.0, 43.2, 55.84, 55.87, 114.6, 114.7, 118.8, 119.0, 123.80, 123.86, 125.7, 125.8, 126.33, 126.38, 127.6, 129.1, 129.4, 129.5, 130.1, 130.2, 135.1, 135.5, 135.7, 135.8, 137.4, 137.7, 159.6, 175.9, 176.2. **IR** (neat, cm^{-1}): 3064, 2927, 1712, 1602, 1450, 1329, 1085, 796, 753, 734, 540. **HRMS** (ESI): calcd. for $C_{19}H_{21}BrNO_2$ ($[M+H]^+$): 374.0754, found: 374.0755.

N-(2-Bromo-4-fluorophenyl)-*N*-methyl-1,2,3,4-tetrahydronaphthalene-1-carboxamide (**115**):

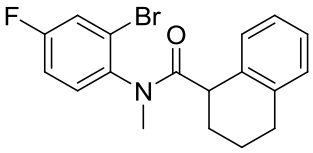

White solid, **m.p.** = 103-105 °C, 83% yield. **^{1}H-NMR** (400 MHz, $CDCl_3$): δ 1.45-1.50 (m, 2.6H), 1.81-2.06 (m, 6H), 2.64 (t, *J* = 5.3 Hz, 0.9H), 2.68 (t, *J* = 5.3 Hz, 1H), 3.25 (s, 3H), 3.29 (s, 2.7H), 3.53 (q, *J* = 7.0 Hz, 1.9H), 7.00-7.15 (m, 8.8H), 7.27-7.29 (m, 1H), 7.35 (dd, *J* = 5.4, 8.7 Hz, 1H), 7.44-7.47 (m, 2.7H). **^{13}C-NMR** (100 MHz, $CDCl_3$): δ 21.2, 21.3, 26.9, 27.5, 27.9, 29.1, 29.3, 36.40, 36.45, 43.2, 43.4, 115.9, 116.21, 116.28, 116.5, 121.2, 121.4, 121.5, 124.0 (dd, *J* = 3.6, 9.9 Hz), 125.8, 125.9, 126.51, 126.57, 127.59, 130.9 (dd, *J* = 4.8, 35.7 Hz), 134.8, 135.4, 137.5, 137.7, 139.13, 139.17, 139.44, 139.48, 160.3, 160.4, 162.8, 162.9, 175.6, 175.8. **IR** (neat, cm^{-1}): 3059, 2938, 2835, 1738, 1650, 1591, 1484, 1375, 1250, 1117, 880, 854, 739, 590. **HRMS** (ESI): calcd. for $C_{18}H_{18}BrFNO$ ($[M+H]^+$): 362.0550, found: 362.0550.

N-(2-Bromo-5-(trifluoromethyl)phenyl)-*N*-methyl-1,2,3,4-tetrahydronaphthalene-1-carboxamide (**116**):

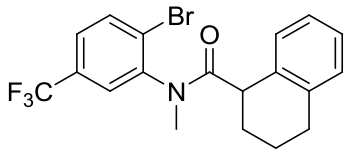

White solid, **m.p.** = 145-147 °C, 79% yield. **^{1}H-NMR** (400 MHz, $CDCl_3$): δ 1.48-1.58 (m, 1.7H), 1.82-2.08 (m, 5.8H), 2.64 (t, *J* = 5.5 Hz, 0.7H), 2.68 (t, *J* = 5.2 Hz, 1H), 3.29 (s, 3H), 3.32 (s, 2.1H), 3.46-3.52 (m, 1.7H), 6.95-7.01 (m, 0.7H), 7.04-7.08 (m, 1.7H), 7.09-7.14 (m, 3.7H), 7.23-7.28 (m, 1H), 7.52 (td, *J* = 2.0, 8.8 Hz, 1.7H), 7.62 (d, *J* = 1.8 Hz, 1H), 7.72 (d, *J* = 1.8 Hz, 0.7H), 7.87 (s, 1H), 7.89 (s, 0.7H). **^{13}C-NMR** (100 MHz, $CDCl_3$): δ 21.0, 21.1, 27.5, 27.8, 29.0, 29.2, 36.2, 36.4, 43.3, 43.5, 125.8, 126.0, 126.5, 126.6, 126.69, 127.0-127.16 (m), 127.5, 127.8, 127.9, 129.2, 129.3, 129.6, 131.3, 131.6, 131.7, 134.4, 135.0, 137.5, 137.7, 143.5, 143.8, 175.1, 175.3. **IR** (neat, cm^{-1}): 3068, 2937, 1738, 1654, 1421, 1333, 1168, 1120, 1076, 1027, 833, 738, 512. **HRMS** (ESI): calcd. for $C_{19}H_{18}BrNOF_3$ ($[M+H]^+$): 412.0518, found: 412.0508.

N-(2-Bromo-5-methoxyphenyl)-*N*-methyl-1,2,3,4-tetrahydronaphthalene-1-carboxamide (**117**):

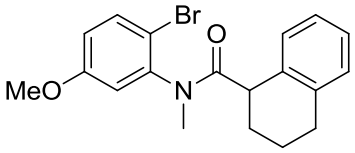

White solid, **m.p.** = 133-135 °C, 94% yield. **^{1}H-NMR** (400 MHz, $CDCl_3$): δ 1.47-1.58 (m, 2H), 1.87-2.11 (m, 6H), 2.64 (t, *J* = 5.2 Hz, 1H), 2.68 (t, *J* = 5.2 Hz, 1H), 2.80-2.89 (m, 2H), 3.26 (s, 3H), 3.3 (s, 3H), 3.56-3.62 (m, 2H), 3.78 (s, 3H), 3.82 (s, 3H), 6.79 (m, 2H), 6.89 (d, *J* = 2.9 Hz, 1H), 7.0 (d, *J* = 2.9 Hz, 1H), 7.04-7.12 (m, 7H), 7.31-7.35 (m, 1H), 7.56 (d, *J* = 3.3 Hz, 1H), 7.58 (d, *J* = 3.3 Hz, 1H). **^{13}C-NMR** (100 MHz, $CDCl_3$): δ 21.2, 21.3, 27.5, 28.0, 29.1, 29.3, 36.1, 36.2, 43.3, 43.4, 55.7, 55.8, 113.4, 133.5, 115.4, 115.7, 115.8, 125.80, 125.86, 126.3, 126.4, 127.6, 129.1, 129.52, 129.59, 134.3, 134.9, 135.6, 137.4, 137.7, 143.4, 143.6, 159.8, 159.9, 175.4, 175.6. **IR** (neat, cm^{-1}): 2936, 1658, 1589, 1475, 1418, 1371, 1282, 1221, 1116, 809, 740,504. **HRMS** (ESI): calcd. for $C_{19}H_{21}BrNO_2$ ($[M+H]^+$): 374.075, found: 374.0752.

N-(2-Bromo-3-(trifluoromethyl)phenyl)-*N*-methyl-1,2,3,4-tetrahydronaphthalene-1-carboxamide (**118**):

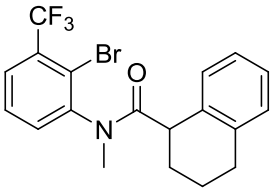

White solid, **m.p.** = 138-140 °C, 88% yield. **^{1}H-NMR** (400 MHz, $CDCl_3$): δ 1.45-1.56 (m, 2H), 1.81-2.0 (m, 6H), 2.64 (t, *J* = 4.0 Hz, 1H), 2.68 (t, *J* = 4.0 Hz, 1H), 2.81-2.89 (m, 2H), 3.27 (s, 3H), 3.32 (s, 3H), 3.45-3.49 (m, 2H), 7.01-7.07 (m, 3H), 7.09-7.12 (m, 4H), 7.27-7.29 (m, 1H), 7.50-7.59 (m, 3H), 7.68 (dd, *J* = 1.2, 7.8 Hz, 1H), 7.72-7.77 (m, 2H). **^{13}C-NMR** (100 MHz, $CDCl_3$): δ 21.1, 21.2, 27.5, 27.9, 29.0, 29.2, 36.31, 36.37, 43.4, 43.6, 125.85, 125.87, 126.5, 126.6, 127.4, 127.6-127.9 (m), 128.7, 129.0, 129.2, 129.51, 129.57, 133.3, 134.5, 135.2, 137.5, 137.8, 145.0, 145.3, 175.2, 175.4. **IR** (neat, cm^{-1}): 3459, 3016, 2970, 1740, 1663, 1426, 1369, 1215, 1228, 1134, 749, 517. **HRMS** (ESI): calcd. for $C_{19}H_{18}BrNOF_3$ ($[M+H]^+$): 412.0517, found: 412.0508.

N-(2-Bromophenyl)-6-methoxy-*N*-methyl-1,2,3,4-tetrahydronaphthalene-1-carboxamide (**119**):

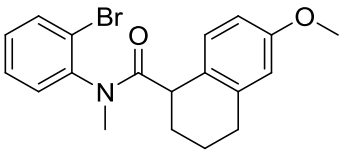

Colorless crystals, 63% yield, **m.p.** = 98-100 °C. **^{1}H-NMR** (300 MHz, $CDCl_3$): δ 1.41-1.55 (m, 1H), 1.83-2.06 (m, 3H), 2.58-2.67 (m, 1H), 2.77-2.89 (m, 1H), 3.28 (d, *J* = 9.0 Hz, 3H), 3.47 (q, *J* = 9.0 Hz, 1H), 3.75 (d, *J* = 0.81 Hz, 3H), 6.57 (t, *J* = 4.6 Hz, 1H), 6.70 (dd, *J* = 8.6, 2.1 Hz, 1H), 6.97 (d, *J* = 8.5 Hz, 0.5H), 7.21-7.29 (m, 1.5H), 7.35-7.48 (m, 2H), 7.71 (d, *J* = 7.9 Hz, 1H). **^{13}C-NMR** (75 MHz, $CDCl_3$): δ 21.3, 21.4, 27.8, 28.2, 29.6, 29.8, 36.42, 36.48, 42.6, 42.8, 55.40, 55.43, 112.4, 112.5, 113.8, 114.1, 123.5, 123.6, 127.4, 128.0, 128.8, 129.0, 129.3, 129.9, 130.0, 130.1, 130.2, 130.6, 134.34, 134.35, 138.9, 139.1, 143.0, 143.3, 158.12, 158.18, 175.8, 176.0. **IR** (neat, cm^{-1}): 2936, 1653, 1608, 1501, 1473, 1429, 1375, 1312, 1233, 1110, 1030, 869, 839, 816, 772, 730, 682, 642. **HRMS** (ESI): calcd. for $C_{19}H_{21}BrNO_2$ ($[M+H]^+$): 374.075, found: 374.0753.

N-(2-Bromophenyl)-6-chloro-*N*-methylchroman-4-carboxamide (**120**):

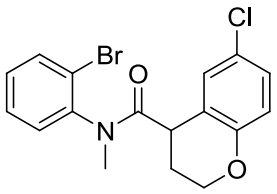

Colorless crystals, **m.p.** = 160-162 °C, 53% yield. **^{1}H-NMR** (300 MHz, $CDCl_3$): δ 1.85-1.95 (m, 3H), 2.25-2.36 (m, 1H), 3.26 (s, 3H), 3.3 (s, 3H), 3.49 (t, *J* = 5.9 Hz, 1H), 3.56 (t, *J* = 5.9 Hz, 1H), 3.95-4.05 (m, 2H), 3.96-4.05 (m, 2H), 4.37 (dd, *J* = 13.7, 2.8 Hz, 1H), 4.49 (dd, *J* = 13.7, 2.8 Hz, 1H), 6.73 (d, *J* = 8,7 Hz, 2H), 6.91 (d, *J* = 2.1 Hz, 1H), 7.04 (dd, *J* = 8.7, 2.2 Hz, 0.5H), 7.21 (d, *J* = 2.1 Hz, 1H), 7.29-7.34 (m, 3H), 7.43 (t, *J* = 8.4 Hz, 1H), 7.49 (d, *J* = 4.3 Hz. 2H), 7.74 (d, *J* = 8.0 Hz, 1H), 7.77 (d, *J* = 8.0 Hz, 1H). **^{13}C-NMR** (75 MHz, $CDCl_3$): δ 25.8, 26.2, 36.3, 36.5, 37.7, 38.4, 63.4, 63.9, 118.4, 118.7, 121.7, 122.1, 123.3, 123.4, 124.8, 124.9, 128.0, 128.3, 129.1, 129.5, 129.7, 130.1, 130.2, 130.3, 134.3, 134.5, 138.0, 142.3, 142.5, 152.7, 153.8, 173.3, 173.6. **IR** (neat, cm^{-1}): 2961, 2931, 2889, 1654, 1472, 1431, 1375, 1261, 1227, 1117, 1051, 1013, 904, 819, 768, 728, 685, 641, 621. **HRMS** (ESI): calcd. for $C_{17}H_{16}BrNO_2$ ($[M+H]^+$): 380.0047, found: 380.0037.

N-(2-Bromophenyl)-*N*-methylthiochroman-4-carboxamide (**121**):

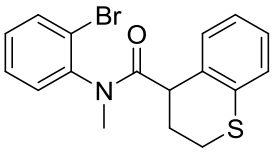

Yellow solid, **m.p.** = 123-125 °C, 90% yield. **^{1}H-NMR** (400 MHz, $CDCl_3$): δ 2.0-2.08 (m, 0.7H), 2.19-2.38 (m, 2.7H), 2.76-2.9 (m, 1.7H), 3.17-3.24 (m, 1.7H), 3.26 (s, 2.2H), 3.3 (s, 3H), 3.5 (dd, *J* = 8.0, 4.3 Hz, 1H), 3.57 (t, *J* = 5.4 Hz, 1H), 6.95-7.01 (m, 6.2H), 7.23-7.31 (m, 2.7H), 7.34-7.35 (m, 3.5H), 7.71 (d, *J* = 8.0 Hz, 1H), 7.74 (d, *J* = 8.0 Hz, 0.7H). **^{13}C-NMR** (100 MHz, $CDCl_3$): δ 24.2, 24.9, 26.6, 26.9, 29.7, 36.3, 36.36, 42.23, 42.63, 123.3, 123.9, 124.2, 126.7, 127.1, 127.19, 128.2, 129.0, 129.3, 129.8, 129.89, 130.1, 130.2, 130.6, 131.4, 132.7, 133.5, 133.8, 134.1, 134.4, 142.5, 142.6, 173.5, 173.7. **IR** (neat, cm^{-1}): 2925, 1649, 1472, 1418, 1373, 1300, 1243, 1117, 1028, 755, 738. **HRMS** (ESI): calcd. for $C_{17}H_{17}BrNOS$ ($[M+H]^+$): 362.0209, found: 362.0110.

N-Benzyl-*N*-(2-bromophenyl)thiochroman-4-carboxamide (**122**):

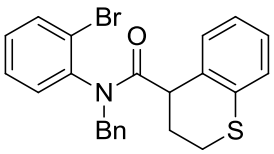

White solid, **m.p.** = 132-134 °C, 93% yield. **^{1}H-NMR** (400 MHz, $CDCl_3$): δ 2.13-2.20 (m, 1H), 2.36-2.50 (m, 2H), 2.54-2.63 (m, 1H), 2.94-2.98 (m, 1H), 3.06-3.09 (m, 1H), 3.39-3.47 (m, 2H). 3.62 (dd, *J* = 8.04, 4.2 Hz, 1H), 3.73 (t, *J* = 5.2 Hz, 1H), 4.19 (d, *J* = 14.2 Hz, 1H), 4.23 (d, *J* = 14.1 Hz, 1H), 5.93 (d, *J* = 14.2 Hz, 1H), 5.98 (d, *J* = 14.1 Hz, 1H), 6.99 (dt, *J* = 7.5, 1.9 Hz, 2H), 7.08-7.48 (m, 24H), 7.90 (dd, *J* = 7.8, 1.4 Hz, 1H), 7.94 (dd, *J* = 7.6, 1.8 Hz, 1H). **^{13}C-NMR** (100 MHz, $CDCl_3$): δ 24.0, 24.9, 26.7, 42.4, 42.7, 51.5, 51.7, 123.6, 123.8, 123.9, 124.2, 126.7, 127.1, 127.2, 127.6, 127.8, 128.0, 128.2, 128.53, 128.57, 129.4, 129.6, 130.1, 130.2, 130.8, 131.2, 131.4, 131.5, 132.9, 133.71, 133.76, 134.0, 134.3, 136.9, 137.2, 140.38, 140.39, 173.3, 173.4. **IR** (neat, cm^{-1}): 3056, 2920, 1648, 1470, 1432, 1390, 1297, 1239, 1197, 1084, 1030, 1010, 943, 756, 741, 704, 627, 562, 524. **HRMS** (ESI): calcd. for $C_{23}H_{21}BrNOS$ ($[M+H]^+$): 438.0521, found: 438.0520.

N-(2-Bromophenyl)-*N*-(methoxymethyl)thiochroman-4-carboxamide (**123**):

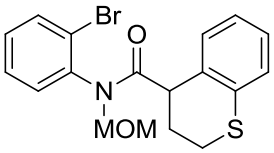

Yellow oil, 76% yield. **^{1}H-NMR** (400 MHz, $CDCl_3$): δ 1.99-2.07 (m, 1H), 2.18-2.28 (m, 2H), 2.34-2.42 (m, 1H), 2.81-2.90 (m, 2H), 3.21-3.27 (m, 2H), 3.46 (s, 3H), 3.49 (s, 3H), 3.53 (dd, *J* = 7.3, 4.2 Hz, 1H), 3.60 (t, *J* = 5.0 Hz, 1H), 4.47 (d, *J* = 10.1 Hz, 1H), 4.53 (d, *J* = 10.1 Hz, 1H), 5.64 (d, *J* = 10.1 Hz, 1H), 5.68 (d, *J* = 10.1 Hz, 1H), 6.95-7.11 (m, 7H), 7.24-7.44 (m, 7H), 7.72 (dd, *J* = 8.0, 0.8 Hz, 1H), 7.76 (dd, *J* = 8.0, 0.8 Hz, 1H). **^{13}C-NMR** (100 MHz, $CDCl_3$): δ 23.8, 24.6, 26.5, 26.6, 42.6, 42.7, 57.1, 57.4, 78.44, 78.48, 123.5, 123.6, 123.9, 124.2, 126.7, 127.31, 127.36, 128.2, 128.7, 129.0, 130.4, 130.5, 130.80, 130.87, 131.72, 131.79, 132.3, 133.7, 133.8, 134.0, 134.2, 139.8, 139.9, 174.5, 174.7. **IR** (neat, cm^{-1}): 3060, 2931, 1732, 1671, 1585, 1472, 1434, 1374, 1286, 1227, 1192, 1108, 1076, 1044, 1027, 913, 731, 650, 589, 517. **HRMS** (ESI): calcd. for $C_{18}H_{19}BrNO_2S$ ($[M+H]^+$): 392.0314, found: 392.0330.

N-((Benzyloxy)methyl)-*N*-(2-bromophenyl)thiochroman-4-carboxamide (**124**):

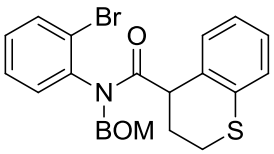

Yellow oil, 73% yield. **^{1}H-NMR** (400 MHz, $CDCl_3$): δ 1.99-2.06 (m, 1H), 2.21-2.29 (m, 2H), 2.38-2.44 (m, 1H), 2.78-2.92 (m, 2H), 3.20-3.28 (m, 2H), 3.55 (dd, *J* = 7.6, 4.3 Hz, 1H), 3.61 (t, *J* = 5.1 Hz, 1H), 4.62 (d, *J* = 10.4 Hz. 1H), 4.67 (d, *J* = 10.4 Hz. 1H), 4.71-4.81 (m, 4H), 5.77 (d, *J* = 10.4 Hz, 1H), 5.84 (d, *J* = 10.4 Hz, 1H), 6.96-7.13 (m, 7H), 7.27-7.43 (m, 18H), 7.73 (dd, *J* = 7.9, 1.3 Hz, 1H), 7.77 (dd, *J* = 8.0, 1.2 Hz, 1H). **^{13}C-NMR** (100 MHz, $CDCl_3$): δ 23.9, 24.7, 26.5, 26.9, 42.6, 42.8, 71.5, 71.7, 76.9, 84.0, 123.5, 123.7, 123.9, 124.2, 126.7, 127.31, 127.35, 127.38, 127.72, 127.75, 127.77, 128.2, 128.4, 128.7, 129.0, 130.3, 130.4, 130.7, 130.8, 131.7, 131.8, 132.3, 133.6, 133.8, 134.0, 134.2, 137.95, 137.96, 139.9, 140.0, 174.6, 174.8. **IR** (neat, cm^{-1}): 3059, 2928, 1736, 1671, 1584, 1472, 1370, 1225, 1047, 1026, 939, 731, 696, 582. **HRMS** (ESI): calcd. for $C_{24}H_{22}BrNO_2S$ ($[M+H]^+$): 468.0627, found: 468.0643.

N-(2-Bromophenyl)-*N*-methyl-1,2,3,4-tetrahydronaphthalene-2-carboxamide (**125**):

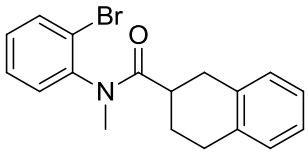

White solid, **m.p.** = 82-84 °C, 87% yield. **^{1}H-NMR** (400 MHz, $CDCl_3$): δ 1.86-2.05 (m, 3H), 2.11-2.16 (m, 1H), 2.39-2.91 (m, 8H), 3.08 (dd, *J* = 15.8, 11.7 Hz, 1H), 3.23 (dd, *J* = 15.8, 11.7 Hz, 1H), 3.242 (s, 3H), 3.25 (s, 3H), 6.97-7.07 (m, 8H), 7.20-7.24 (m, 2H), 7.32-7.40 (m, 4H), 7.65 (td, *J* = 7.8, 1.3 Hz, 2H). **^{13}C-NMR** (100 MHz, $CDCl_3$): δ 26.2, 26.9, 28.6, 28.7, 32.2, 32.7, 36.0, 36.1, 38.4, 38.6, 123.5, 123.7, 125.62, 125.65, 125.72, 125.78, 128.6, 128.8, 128.92, 128.95, 129.1, 129.2, 129.6, 129.7, 129.82, 129.85, 133.9, 134.0, 135.3, 135.4, 135.8, 135.9, 142.7, 175.6, 175.7. **IR** (neat, cm^{-1}): 3018, 2935, 1736, 1657, 1582, 1475, 1432, 1386, 1342, 1273, 1127, 1046, 1027, 742, 728, 642, 520. **HRMS** (ESI): calcd. for $C_{18}H_{19}NOBr$ ($[M+H]^+$): 344.0644, found: 344.0635.

IV.5. Catalytic Asymmetric Intramolecular *α*-Arylation Reactions

IV.5.1. General Procedure for Catalytic Asymmetric Intramolecular α-Arylation Reactions

Under N_2, a dried Schlenk tube was charged with 5 mol% $Pd(dba)_2$ (0.01 mmol), 5 mol% chiral carbine precursor (0.01 mmol) and *t*BuONa (0.3 mmol). Dimethoxyethane (DME) (1 mL) was added and the mixture was stirred for 10 min. The 2-bromo-*N*-alkylanilide (0.2 mmol) was then added as a solution in DME (3 mL). The reaction was stirred at rt and time indicated in the article and then quenched with aq. NH_4Cl and extracted with diethyl ether. The combined organic phases were washed with water and brine, and dried over Na_2SO_4. The product was isolated by f.c. over SiO_2 and the *ee* was determined by chiral HPLC.

IV.5.2. General Procedure for Kinetic Measurements of the Influence of Additives on the Catalytic Asymmetric Intramolecular α-Arylation of Amide (61)

Under Ar atmosphere, a dried Schlenk tube was charged with 5 mol% of catalyst (*S*,*S*)-[**L5**H][I] (0.01 mmol, 8.6 mg), additive 10 mol%, *t*BuONa (0.3 mmol, 28.8 mg) and decane (as an internal standard for GC measurment) (0.2 mmol, 38.9 μL). Dmiethoxyethane (DME) (1 mL) was added and the mixture was stirred for 5 minutes. Substrate **61** (0.2 mmol, 63.4 mg) was then added as a solution in DME (3 mL). The reaction was stirred at rt and aliquot (50 μL) was taken with defined period of time, filtered through the pipette with Celite and Silica gel and analysed by GC. Results are summarised in figure 31.

IV.5.3. General Procedure for Pd-Catalyzed α-Arylation of Amide (61) with Various Precatalysts

Under Ar atmosphere, a dried Schlenk tube was charged with 5 mol% of catalyst (0.01 mmol), 10 mol% of maleic anhydride (0.02 mmol, 1.96 mg), *t*BuONa (0.3 mmol, 28.8 mg) and decane (as an internal standard for GC measurment) (0.2 mmol, 38.9 μL). Dmiethoxyethane (DME) (1 mL) was added and the mixture was stirred for 5 minutes. Substrate **61** (0.2 mmol, 63.4 mg) was then added as a solution in DME (3 mL). The reaction was stirred at rt and aliquot (50 μL) was taken with defined period of time, filtered through the pipette with Celite and Silica gel and analysed by GC. Results are summarised in figure 37.

Oxindoles **62**, **93a**, **93c** and **94** are known compounds.[270]

(*S*)-1,3-Dimethyl-3-phenylindolin-2-one (**62**):[114]

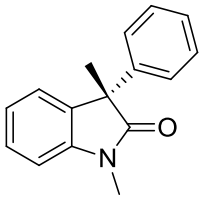

Oil, 99% yield (53.9 mg). $[\alpha]_D^{25}$ = -88.1 (*c* = 1.0 in CH_2Cl_2), 96% *ee* [Chiracel OD-H column, *n*-hexane/*i*-PrOH = 99:1, 1.0 mL/min, 254 nm; t_R = 16.76 min. (major) and 20.96 min. (minor)].

(*S*)-3-Ethyl-1-methyl-3-phenylindolin-2-one (**93a**):[270]

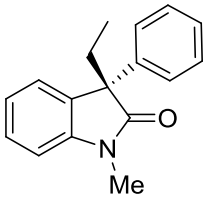

Oil, 85% yield (42.7 mg). $[\alpha]_D^{25}$ = -110.3 (*c* = 1.0 in CH_2Cl_2), 93% *ee* [Chiracel OD-H column, *n*-hexane/*i*-PrOH = 99:1, 1.0 mL/min, 254 nm; t_R = 16.46 min. (minor) and 20.36 min. (major)].

(*S*)-3-Isopropyl-1-methyl-3-phenylindolin-2-one (**93b**):

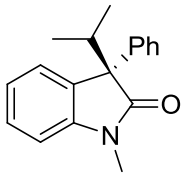

Oil, 80% yield (42.4 mg), $[\alpha]_D^{20}$ = -21.17 (*c* = 1.0 in CH_2Cl_2), 52% *ee* [Chiracel OD-H column, *n*-hexane/*i*-PrOH = 95:5, 1.0 mL/min, 254 nm; t_R = 10.66 min. (major) and 9.79 min. (minor)]. **^{1}H-NMR** (400 MHz, $CDCl_3$): δ 0.72 (d, *J* = 8.8 Hz, 3H), 1.00 (d, *J* = 8.8 Hz, 3H), 2.93-3.02 (m, 1H), 3.24 (s, 3H), 6.95 (d, *J* = 10.4 Hz, 1H), 7.19 (t, *J* = 10.4 Hz, 1H), 7.28-7.24 (m, 5H), 7.51 (d, *J* = 9.6 Hz, 2H). **^{13}C-NMR** (100 MHz, $CDCl_3$): δ 17.5, 26.2, 36.0, 60.8, 108.2, 122.0, 126.2, 127.1, 128.1, 129.5, 139.1, 144.4, 178.4. **IR** (neat, cm^{-1}): 3056, 2963,

2875, 1709, 1610, 1493, 1467. **HRMS** (ESI): calcd. for $C_{18}H_{19}NO$ ($[M+H]^+$): 266.1539, found: 266.1527.

(*S*)-3-Benzyl-1-methyl-3-phenylindolin-2-one (**93c**):[270]

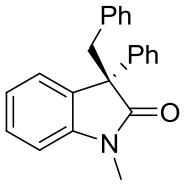

Oil, 86% yield (53.8 mg), $[\alpha]_D^{20}$ = -27.1 (*c* = 1.0 in CH_2Cl_2), 89% *ee* [Chiracel AS-H column, *n*-hexane/*i*-PrOH = 95:5, 1.0 mL/min, 254 nm; t_R = 7.52 min. (major) and 9.53 min. (minor)].

(*S*)-1'-Methyl-2,3-dihydrospiro[indene-1,3'-indolin]-2'-one (**94**):[270]

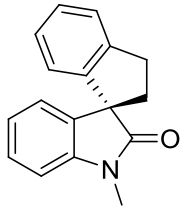

Yellow solid, **m.p.** = 113-115 °C, 99% yield (49.3 mg). $[\alpha]_D^{25}$ = -36.2 (*c* = 1.0 in CH_2Cl_2), 81% *ee* [Chiracel OD-H column, *n*-hexane/*i*-PrOH = 99:1, 1.0 mL/min, 254 nm; t_R = 25.94 min. (major) and 29.94 min. (minor)].

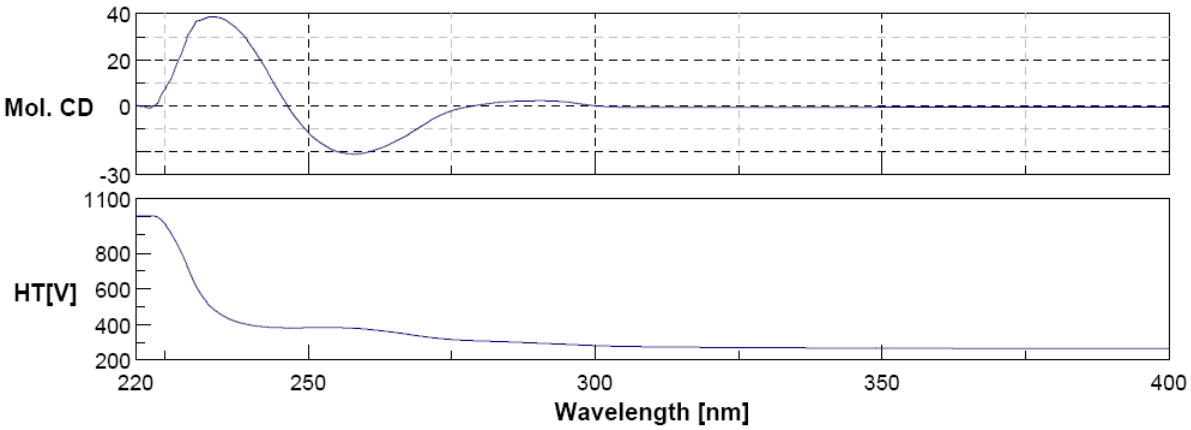

For CD spectrum: *c* = 0.0001 M in CH_2Cl_2.

(*S*)-1,3,5-Trimethyl-3-phenylindolin-2-one (**95a**):

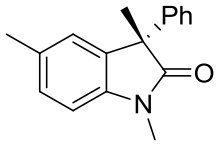

Oil, 98% yield (49.1 mg), $[\alpha]_D^{20}$ = -122.22 (*c* = 1.0 in CH_2Cl_2), 95% *ee* [Chiracel OD-H column, *n*-hexane/*i*-PrOH = 99:1, 1.0 mL/min, 254 nm; t_R = 17.25 min. (major) and 23.70 min. (minor)]. **^{1}H-NMR** (400 MHz, $CDCl_3$): δ 1.81 (s, 3H), 2.39 (s, 3H), 3.31 (s, 3H), 6.87 (d, *J* = 8 Hz, 1H), 7.06 (s, 1H), 7.20 (d, *J* = 6.4 Hz, 1H), 7.30-7.36 (m, 5H). **^{13}C-NMR** (100 MHz, $CDCl_3$): δ 21.2, 23.6, 26.5, 52.2, 108.0, 125.0, 127.2, 128.3, 132.3, 135.0, 140.8, 141.0, 179.5. **IR** (neat, cm^{-1}): 3022, 2968, 2868, 1710, 1619, 1599, 1498, 1452. **HRMS** (ESI): calcd. for $C_{17}H_{17}NO$ ($[M+H]^+$): 252.1382, found: 252.1375.

(*S*)-5-Isopropyl-1,3-dimethyl-3-phenylindolin-2-one (**95b**):

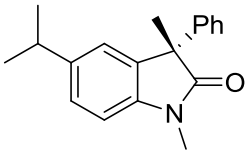

Oil, 98% yield (54.6 mg), $[\alpha]_D^{20}$ = -147.57 (*c* = 1.0 in CH_2Cl_2), 92% *ee* [Chiracel OD-H column, *n*-hexane/*i*-PrOH = 99:1, 1.0 mL/min, 254 nm; t_R = 14.00 min. (major) and 18.93 min. (minor)]. **^{1}H-NMR** (300 MHz, $CDCl_3$): δ 1.28 (d, *J* = 8 Hz, 6H), 1.85 (s, 3H), 2.92-2.99 (m, 1H), 3.29 (s, 3H), 6.90 (d, *J* = 8 Hz, 1H), 7.12 (s, 1H), 7.23-7.33 (m, 6H). **^{13}C-NMR** (75 MHz, $CDCl_3$): δ 23.8, 24.2, 24.4, 26.5, 33.9, 52.3, 108.0, 122.5, 125.7, 127.1, 134.8, 141.0, 141.2, 143.7, 179.5. **IR** (neat, cm^{-1}): 2958, 2930, 2869, 1710, 1618, 1599, 1495, 1458. **HRMS** (ESI): calcd. for $C_{19}H_{21}NO$ ($[M+H]^+$): 280.1695, found: 280.1680.

(*S*)-1,3,5,7-Tetramethyl-3-phenylindolin-2-one (**95c**):

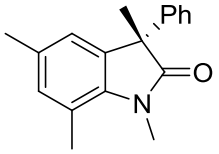

Oil, 82% yield (43.4 mg), $[\alpha]_D^{20}$ = -135.26 (*c* = 1.0 in CH_2Cl_2), 26% *ee* [Chiracel OD-H column, *n*-hexane/*i*-PrOH = 99:1, 1.0 mL/min, 254 nm; t_R = 20.04 min. (major) and 26.19 min. (minor)]. **^{1}H-NMR** (300 MHz, $CDCl_3$): δ 1.81 (s, 3H), 2.32 (s, 3H), 2.64 (s, 3H), 3.55 (s,

3H), 6.9 (d, *J* = 12 Hz, 2H), 7.30-7.35 (m, 5H). **^{13}C-NMR** (75 MHz, $CDCl_3$): δ 19.0, 20.8, 23.8, 29.8, 51.6, 119.5, 122.8, 126.7, 127.1, 128.5, 132.1, 132.2, 135.8, 138.5, 141.3, 180.2. **IR** (neat, cm^{-1}): 2968, 2927, 2868, 1706, 1600, 1477, 1458. **HRMS** (ESI): calcd. for $C_{18}H_{19}NO$ ($[M+H]^+$): 266.1539, found: 266.1532.

(*S*)-1,3-Dimethyl-3-phenyl-6-(trifluoromethyl)indolin-2-one (**95d**):

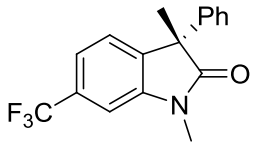

Oil, 98% yield (59.7 mg), **$[\alpha]_D^{20}$** = -66.54 (*c* = 1.0 in CH_2Cl_2), 95% *ee* [Chiracel OD-H column, *n*-hexane/*i*-PrOH = 99:1, 1.0 mL/min, 254 nm; t_R = 18.87 min. (major) and 27.57 min. (minor)]. **^{1}H-NMR** (400 MHz, $CDCl_3$): δ 1.86 (s, 3H), 3.34 (s, 3H), 7.18 (s, 1H), 7.29-7.45 (m, 7H). **^{13}C-NMR** (100 MHz, $CDCl_3$): δ 23.5, 26.6, 52.2, 105.0, 105.1, 119.8, 119.9, 124.4, 127.6, 130.5, 130.9, 138.7, 139.8, 143.9, 179.1. **IR** (neat, cm^{-1}): 3062, 2933, 1720, 1624, 1458. **HRMS** (ESI): calcd. for $C_{17}H_{14}F_3NO$ ($[M+H]^+$): 306.1100, found: 306.1086.

(*S*)-6-Fluoro-1,3-dimethyl-3-phenylindolin-2-one (**95e**):

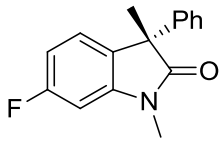

Colorless oil, 97% yield (49.5 mg), **$[\alpha]_D^{20}$** = -67.82 (*c* = 1.0 in CH_2Cl_2), 96% *ee* [Chiracel OD-H column, *n*-hexan/*i*-PrOH = 99:1, 1.0 mL/min, 254 nm, t_R = 18.87 min. (major) and 27.57 min. (minor)]. **^{1}H-NMR** (400 MHz, $CDCl_3$): δ 1.86 (s, 3H), 3.34 (s, 3H), 7.18 (s, 1H), 7.29-7.45 (m, 7H). **^{13}C-NMR** (100 MHz, $CDCl_3$): δ 23.5, 26.6, 52.2, 105.0, 105.1, 119.8, 119.9, 124.4, 127.6, 130.5, 130.9, 138.7, 139.8, 143.9, 179.1. **IR** (neat, cm^{-1}): 3062, 2933, 1720, 1624, 1458. **HRMS** (ESI): calcd. for $C_{17}H_{14}F_3NO$ ($[M+H]^+$): 306.1100, found: 306.1086.

(*S*)-6-Methoxy-1,3-dimethyl-3-phenylindolin-2-one (**95f**):

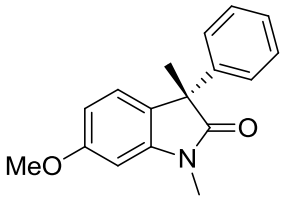

Oil, 99% yield (52.8 mg). $[\alpha]_D^{25}$ = -67.2 (*c* = 1.0 in CH_2Cl_2), 97% *ee* [Chiracel OD-H column, *n*-hexane/*i*-PrOH = 99:1, 1.0 mL/min, 254 nm; t_R = 31.79 min. (major) and 39.01 min. (minor)]. **^{1}H-NMR** (400 MHz, $CDCl_3$): δ 1.82 (s, 3H), 3.26 (s, 3H), 3.9 (s, 3H), 6.56 (s, 1H), 6.67 (dd, *J* = 10.9, 3.1 Hz, 1H), 7.14 (d, *J* = 10.8 Hz, 1H), 7.27-7.33 (m, 5H). **^{13}C-NMR** (100 MHz, $CDCl_3$): δ 24.0, 26.5, 51.6, 55.6, 96.3, 106.5, 124.8, 126.6, 126.7, 127.1, 128.5, 141.2, 144.5, 160.2, 180.0. **IR** (neat, cm^{-1}): 2932, 1715, 1624, 1600, 1505, 1460. **HRMS** (ESI): calcd. for $C_{17}H_{17}NO_2$ ($[M+H]^+$): 268.1332, found: 268.1320.

(*S*)-7-Fluoro-1,3-dimethyl-3-phenylindolin-2-one (**95g**):

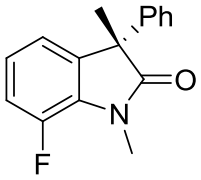

Oil, 96% yield (48.9 mg). $[\alpha]_D^{20}$ = -40.9 (*c* = 0.1 in CH_2Cl_2), 72% *ee* [Chiracel OD-H column, *n*-hexane/*i*-PrOH = 99:1, 1.0 mL/min, 254 nm; t_R = 8.92 min. (major) and 12.0 min. (minor)]. **^{1}H-NMR** (300 MHz, $CDCl_3$): δ 1.84 (s, 3H), 3.5 (d, *J* = 2.1 Hz, 3H), 6.95-7.15 (m, 3H), 7.28-7.41 (m, 5H). **^{13}C-NMR** (75 MHz, $CDCl_3$): δ 14.2, 23.8, 28.9, 29.0, 52.4, 60.4, 115.9, 116.1, 120.0, 120.1, 123.3, 123.35, 125.4, 126.5, 127.4, 128.6, 129.9, 137.7, 140.3, 146.6, 149.0, 179.1. **IR** (neat, cm^{-1}): 3057, 2973, 1717, 1631, 1631, 1480, 1366, 1334, 1279, 1235, 1098, 1054, 951, 776, 731, 696. **HRMS** (ESI): calcd. for $C_{16}H_{14}FNO$ ($[M+H]^+$): 256.1131, found: 256.1123.

(*S*)-1,8-Dimethyl-1-phenyl-5,6-dihydro-1*H*-pyrrolo[3,2,1-ij]quinolin-2(4H)-one (**96**):

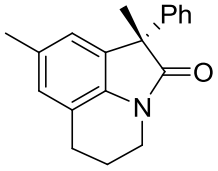

Oil, 87% yield (48.2 mg). $[\alpha]_D^{20}$ = -109.20 (*c* = 1.0 in CH_2Cl_2), 94% *ee* [Chiracel OD-H column, *n*-hexane/*i*-PrOH = 99:1, 1.0 mL/min, 254 nm; t_R = 24.33 min. (major) and 31.36 min. (minor)]. **^{1}H-NMR** (400 MHz, $CDCl_3$): δ 1.84 (s, 3H), 2.05-2.1 (m, 2H), 2.38 (s, 3H), 2.84 (t, *J* = 8 Hz, 2H), 3.78 (q, *J* = 4.8 Hz, 2H), 6.93 (d, *J* = 10 Hz, 2H), 7.27-7.35 (m, 5H). **^{13}C-NMR** (100 MHz, $CDCl_3$): δ 21.4, 23.7, 24.6, 39.1, 53.5, 120.1, 122.6, 126.7, 127.1, 127.3, 128.5, 131.7, 133.4, 136.6, 141.0, 178.3. **IR** (neat, cm^{-1}): 3021, 2928, 2868, 1703, 1626, 1491, 1432. **HRMS** (ESI): calcd. for $C_{19}H_{19}NO$ ($[M+H]^+$): 278.1539, found: 278.1538.

(*S*,*E*)-1,3-Dimethyl-3-styrylindolin-2-one (**15**):

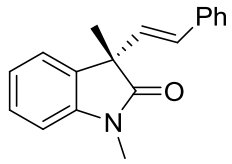

Oil, 96% yield (50.5 mg). $[\alpha]_D^{20}$ = -12.00 (*c* = 1.0 in CH_2Cl_2), 40% *ee* [Chiracel AS-H column, *n*-hexane/*i*-PrOH = 97:3, 1.0 mL/min, 254 nm; t_R = 9.69 min. (major) and 10.45 min. (minor)]. **^{1}H-NMR** (300 MHz, $CDCl_3$): δ 1.65 (s, 3H), 3.29 (s, 3H), 6.44 (q, *J* = 12 Hz, 2H), 6.95 (d, *J* = 4 Hz, 1H), 7.17 (t, *J* = 3 Hz, 1H), 7.20 (t, *J* = 3 Hz, 1H), 7.23-7.30 (m, 6H). **^{13}C-NMR** (75 MHz, $CDCl_3$): δ 23.1, 26.4, 50.7, 108.4, 122.6, 124.0, 126.5, 127.6, 128,2, 128.5, 129.9, 130.0, 132.9, 136.5, 143.0, 178.7. **IR** (neat, cm^{-1}): 3055, 2924, 2852, 1710, 1610, 1492, 1469, 1447. **HRMS** (ESI): calcd. for $C_{18}H_{17}NO$ ($[M+H]^+$): 264.1382, found: 264.1397.

(*S*)-1'-Methylspiro[bicyclo[4.2.0]octa[1(6),2,4]triene-7,3'-indolin]-2'-one (**126**):

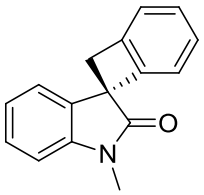

White solid, **m.p**. = 115.5-119.5 °C, 82% yield (38.5 mg). $[\alpha]_D^{25}$ = -16.6 (*c* = 0.5 in CH_2Cl_2), 52% *ee* [Chiracel AS-H column, *n*-hexane/*i*-PrOH = 95:5, 1.0 mL/min, 254 nm; t_R = 11.49 min. (major) and 17.21 min. (minor)]. **^{1}H-NMR** (300 MHz, $CDCl_3$): δ 3.29 (s, 3H), 3.46 (d, *J* = 13.4 Hz, 1H), 3.78 (d, *J* = 13.4 Hz, 1H), 6.88 (t, *J* = 7.3 Hz, 2H), 7.03 (td, *J* = 7.3, 0.9 Hz, 1H), 7.12 (dd, *J* = 9.0, 0.9 Hz, 1H), 7.21-7.35 (m, 5H). **^{13}C-NMR** (75 MHz, $CDCl_3$): δ 26.5, 42.8, 55.9, 108.0, 121.6, 122.7, 123.0, 123.2, 128.0, 128.5, 128.9, 130.6, 143.8, 143.9, 144.4, 177.0. **IR** (neat, cm^{-1}): 3059, 2926, 1716, 1661, 1613, 1583, 1552, 1512, 1467, 1372,

1262, 1129, 763, 746, 726. **HRMS** (ESI): calcd. for $C_{16}H_{14}NO$ ($[M+H]^+$): 236.2711, found: 236.2713.

(*S*)-1-Methyl-3',4'-dihydro-2'*H*-spiro[indoline-3,1'-naphthalen]-2-one (**127**):

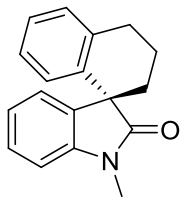

White solid, **m.p.** = 146-148 °C, 96% yield (50.5 mg). $\mathbf{[\alpha]_D^{25}}$ = +4.31 (*c* = 1.0 in CH_2Cl_2). 86% *ee* [Chiracel AS-H column, *n*-hexane/*i*-PrOH = 98:2, 1.0 mL/min, 254 nm; t_R = 11.26 min. (major) and 15.46 min. (minor)]. **^{1}H-NMR** (400 MHz, $CDCl_3$): δ 1.98-2.13 (m, 2H), 2.21-2.28 (m, 1H), 2.37-2.46 (m, 1H), 2.98-3.12 (m, 1H), 3.35 (s, 3H), 6.53 (d, *J* = 7.7 Hz, 1H), 6.98 (d, *J* = 7.8 Hz, 1H), 7.01 (t, *J* = 8.0 Hz, 1H), 7.07 (d, *J* = 8.0 Hz, 1H), 7.14 (d, *J* = 8.0 Hz, 1H), 7.18 (t, *J* = 8.0 Hz, 1H), 7.21 (d, *J* = 8.0 Hz, 1H), 7.37 (td, *J* = 8.0, 1.3 Hz, 1H). **^{13}C-NMR** (75 MHz, $CDCl_3$): δ 18.7, 26.5, 29.7, 34.0, 52.2, 108.0, 122.8, 124.0, 126.3, 127.1, 127.8, 128.0, 129.7, 135.1, 137.3, 137.8, 143.1, 180.5. **IR** (neat, cm^{-1}): 2933, 1707, 1610, 1491, 1342, 1255, 1125, 1091, 965, 749, 692. **HRMS** (ESI): calcd. for $C_{18}H_{17}NO$ ($[M+H]^+$): 264.1382, found: 264.1388.

(*S*)-1'-Methyl-6,7,8,9-tetrahydrospiro[benzo[7]annulene-5,3'-indolin]-2'-one (**128**):

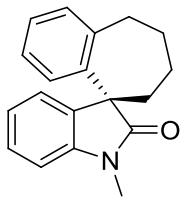

Yellow oil, 97% yield (53.8 mg). $\mathbf{[\alpha]_D^{25}}$ = -35.05 (*c* = 1.0 in CH_2Cl_2). 83% *ee* [Chiracel AS-H column, *n*-hexane/*i*-PrOH = 98:2, 1.0 mL/min, 254 nm; t_R = 7.76 min. (major) and 9.29 min. (minor)]. **^{1}H-NMR** (400 MHz, $CDCl_3$): δ 1.831.92 (m, 2H), 2.03-2.18 (m, 3H), 2.24-2.30 (m, 1H), 2.92-2.99 (qd, *J* = 7.4, 3.1 Hz, 1H), 3.24 (s, 3H), 3.6-3.67 (m, 1H), 6.58 (dd, *J* = 7.8, 1.2 Hz, 1H), 6.9 (d, *J* = 7.6 Hz, 1H), 6.94 (t, *J* = 9.6 Hz, 1H), 7.04-7.11 (m, 2H), 7.15 (d, *J* = 6.8 Hz, 1H), 7.21 (d, *J* = 6.8 Hz, 1H), 7.3 (td, *J* = 7.6, 1.1 Hz, 1H). **^{13}C-NMR** (100 MHz, $CDCl_3$): δ 23.0, 26.3, 27.2, 34.4, 35.4, 58.5, 108.2, 122.8, 124.2, 126.2, 127.3, 129.6, 131.6, 137.1, 138.9, 142.5, 143.0, 179.8. **IR** (neat, cm^{-1}): 2923, 1708, 1661,

1609, 1473, 1340, 1126, 1028, 973, 745, 726. **HRMS** (ESI): calcd. for $C_{19}H_{20}NO$ ($[M+H]^+$): 278.1539, found: 278.1539.

(*R*)-1,5-Dimethyl-3',4'-dihydro-2'*H*-spiro[indoline-3,1'-naphthalen]-2-one (**129**):

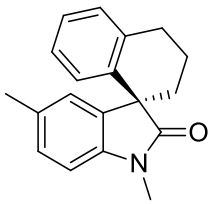

Glassy solid, 98% yield (54.2 mg). $[\alpha]_D^{25}$ = -2.11 (*c* = 1.0 in CH_2Cl_2). 87% *ee* [Chiracel AS-H column, *n*-hexane/*i*-PrOH = 99:1, 1.0 mL/min, 254 nm; t_R = 13.07 min. (minor) and 19.02 min. (major)]. **^{1}H-NMR** (400 MHz, $CDCl_3$): δ 1.91-2.05 (m, 2H), 2.16-2.22 (m, 1H), 2.27 (S, 3H), 2.33-2.39 (m, 1H), 2.92-3.06 (m, 2H), 3.27 (s, 3H), 6.48 (d, *J* = 8.4 Hz, 1H), 6.81 (d, *J* = 7.8 Hz, 1H), 6.88 (d, *J* = 0.5 Hz. 1H), 6.98 (t, *J* = 7.8 Hz, 1H), 7.08-7.14 (m, 2H), 7.17 (d, *J* = 8.0 Hz, 1H). **^{13}C-NMR** (100 MHz, $CDCl_3$): δ 18.8, 21.1, 26.5, 29.3, 34.0, 52.2, 107.7, 124.8, 126.3, 127.0, 128.0, 128.1, 129.6, 132.3, 135.3, 137.4, 137.8, 140.7, 180.4. **IR** (neat, cm^{-1}): 2932, 1703, 1619, 1601, 1496, 1449, 1344, 1258, 1097, 1053, 909, 804, 733, 697, 647. **HRMS** (ESI): calcd. for $C_{19}H_{20}NO$ ($[M+H]^+$): 278.1539, found: 278.1550.

(*R*)-5-Methoxy-1-methyl-3',4'-dihydro-2'*H*-spiro[indoline-3,1'-naphthalen]-2-one (**130**):

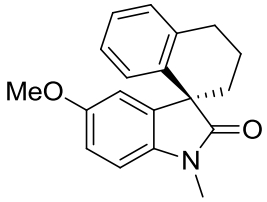

Yellow oil, 95% yield (55.6 mg). $[\alpha]_D^{25}$ = -6.31 (*c* = 0.5 in CH_2Cl_2). 89% *ee* [Chiracel AS-H column, *n*-hexane/*i*-PrOH = 99:1, 1.0 mL/min, 254 nm; t_R = 27.58 min. (minor) and 43.99 min. (major)]. **^{1}H-NMR** (400 MHz, $CDCl_3$): δ 1.91-2.03 (m, 2H), 2.18-2.22 (m, 1H), 2.38-2.40 (m, 1H), 2.91-3.06 (m, 2H), 3.26 (s, 3H), 3.72 (s, 3H), 6.48 (d, *J* = 7.7 Hz, 1H), 6.67 (s, 1H), 6.81 (d, *J* = 1 Hz, 2H), 6.96 (t, *J* = 7.5 Hz, 1H), 7.11 (t, *J* = 7.9 Hz, 1H), 7.16 (d, *J* = 7.4 Hz, 1H). **^{13}C-NMR** (100 MHz, $CDCl_3$): δ 18.9, 26.7, 27.1, 29.4, 34.2, 52.7, 55.9, 108.4, 111.7, 112.2, 126.5, 127.2, 128.2, 129.8, 135.2, 136.8, 137.9, 138.8, 156.3, 180.3. **IR**

(neat, cm^{-1}): 2930, 1739, 1706, 1635, 1492, 1434, 1363, 1285, 1216, 1117, 1029, 737, 515. **HRMS** (ESI): calcd. for $C_{19}H_{20}NO_2$ ($[M+H]^+$): 294.1488, found: 294.1493.

(*R*)-5-Fluoro-1-methyl-3',4'-dihydro-2'*H*-spiro[indoline-3,1'-naphthalen]-2-one (**131**):

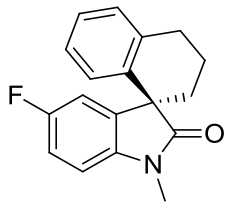

Yellow solid, **m.p.** = 124-126 °C, 89% yield (50.0 mg). $[\alpha]_D^{25}$ = -3.24 (*c* = 1.0 in CH_2Cl_2). 74% *ee* [Chiracel OD-H column, *n*-hexane/*i*-PrOH = 99:1, 1.0 mL/min, 254 nm; t_R = 23.92 min. (minor) and 32.66 min. (major)]. **^{1}H-NMR** (400 MHz, $CDCl_3$): δ 1.91-2.02 (m, 2H), 2.20-2.24 (m, 1H), 2.32-2.41 (m, 1H), 3.28 (s, 3H), 6.46 (d, *J* = 7.7 Hz, 1H), 6.80-6.85 (m, 2H), 6.96-7.01 (m, 2H), 7.11-7.18 (m, 2H). **^{13}C-NMR** (100 MHz, $CDCl_3$): δ 18.7, 26.6, 26.9, 29.1, 33.9, 52.5, 52.6, 108.40, 108.48, 112.0, 112.3, 113.9, 114.1, 126.4, 127.3, 127.8, 129.8, 134.5, 137.7, 138.7, 138.8, 139.05, 139.07, 158.2, 160.5, 164.1, 180.14, 180.16. **IR** (neat, cm^{-1}): 3058, 2933, 1719, 1611, 1487, 1466, 1339, 1183, 1183, 1079, 1022, 913, 751, 696, 515. **HRMS** (ESI): calcd. for $C_{18}H_{17}FNO$ ($[M+H]^+$): 282.1288, found: 282.1278.

(*R*)-1-Methyl-6-(trifluoromethyl)-3',4'-dihydro-2'*H*-spiro[indoline-3,1'-naphthalen]-2-one (**132**):

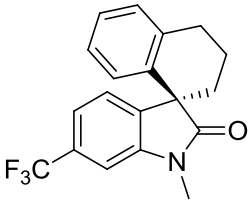

Yellow solid, **m.p.** = 159-161 °C, 77% yield (50.9 mg). $[\alpha]_D^{25}$ = -2.85 (*c* = 1.0 in CH_2Cl_2). 51% *ee* [Chiracel OD-H column, *n*-hexane/*i*-PrOH = 99:1, 1.0 mL/min, 254 nm; t_R = 22.00 min. (minor) and 43.99 min. (major)]. **^{1}H-NMR** (400 MHz, $CDCl_3$): δ 1.92-2.04 (m, 2H), 2.18-2.22 (m, 1H), 2.34-2.42 (m, 2H), 2.95-3.08 (m, 2H), 3.33 (s, 3H), 6.44 (dd, *J* = 7.8, 0.5 Hz, 1H), 6.98 (td, *J* = 7.7, 1.4 Hz, 1H), 7.13-7.20 (m, 4H), 7.29 (d, *J* = 7.8 Hz, 1H). **^{13}C-NMR** (100 MHz, $CDCl_3$): δ 18.6, 26.6, 26.9, 29.1, 33.9, 52.2, 104.7 (q, *J* = 3.7 Hz), 119.9 (q, *J* = 3.7 Hz), 122.7, 124.2, 125.4, 126.5, 127.4, 127.8, 128.1, 129.9, 130.2, 130.5, 130.8, 134.1, 137.8, 141.0, 143.7, 180.0. **IR** (neat, cm^{-1}): 2943, 1701, 1621, 1452, 1314, 1256, 1159, 1109,

972, 890, 825, 747, 665, 553. **HRMS** (ESI): calcd. for $C_{19}H_{17}NOF_3$ ($[M+H]^+$): 332.1256, found: 332.1269.

(*R*)-6-Methoxy-1-methyl-3',4'-dihydro-2'*H*-spiro[indoline-3,1'-naphthalen]-2-one (**133**):

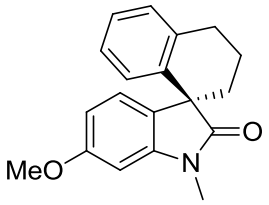

Solid, **m.p.** = 161-163 °C, 91% yield (53.3 mg). $[\alpha]_D^{25}$ = -6.11 (*c* = 1.0 in CH_2Cl_2). 77% *ee* [Chiracel OD-H column, *n*-hexane/*i*-PrOH = 99:1, 1.0 mL/min, 254 nm; t_R = 33.38 min. (minor) and 38.87 min. (major)]. **^{1}H-NMR** (400 MHz, $CDCl_3$): δ 1.93-2.05 (m, 2H), 2.15-2.18 (m, 1H), 2.32-2.41 (m, 1H), 2.89-3.05 (m, 2H), 3.27 (s, 3H), 3.83 (s, 3H), 6.49-6.51 (m, 3H), 6.94-6.98 (m, 2H), 7.11 (td, *J* = 7.3, 1.1 Hz, 1H), 7.16 (d, *J* = 7.4 Hz, 1H). **^{13}C-NMR** (100 MHz, $CDCl_3$): δ 18.8, 26.5, 29.2, 34.2, 51.7, 55.5, 96.0, 106.4, 124.5, 126.3, 126.9, 127.9, 129.6, 135.6, 137.7, 144.3, 160.0, 181.0. **IR** (neat, cm^{-1}): 2933, 1707, 1620, 1503, 1452, 1369, 1257, 1228, 1090, 1064, 1028, 969, 828, 775, 738, 582. **HRMS** (ESI): calcd. for $C_{19}H_{20}NO_2$ ($[M+H]^+$): 294.1488, found: 294.1499.

(*R*)-1-Methyl-4-(trifluoromethyl)-3',4'-dihydro-2'*H*-spiro[indoline-3,1'-naphthalen]-2-one (**134**):

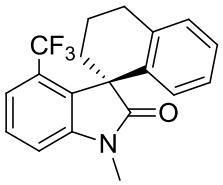

Yellow glassy solid, 95% yield (62.8 mg). 4% *ee* [Chiracel OD-H column, *n*-hexane/*i*-PrOH = 99:1, 1.0 mL/min, 254 nm; t_R = 23.07 min. (minor) and 27.59 min. (major)]. **^{1}H-NMR** (400 MHz, $CDCl_3$): δ 1.85-191 (m, 1H), 1.98 (dt, *J* = 13.7, 3.4 Hz, 1H), 2.36 (td, *J* = 13.6, 3.4 Hz, 1H), 2.59-2.71 (m, 1H), 2.87-2.99 (m, 2H), 3.26 (s, 3H), 6.35 (d, *J* = 7.72 Hz, 1H), 6.93 (t, *J* = 7.2 Hz, 1H), 7.09 (d, *J* = 7.5 Hz, 1H), 7.12 (dd, *J* = 10.5, 1.08 Hz, 1H), 7.17 (d, *J* = 7.5 Hz, 1H), 7.30 (d, *J* = 8.0 Hz, 1H), 7.46 (t, *J* = 7.9 Hz, 1H). **^{13}C-NMR** (100 MHz, $CDCl_3$): δ 18.5, 26.6, 29.1, 32.3, 52.2, 111.1, 120.9 (q, *J* = 4.8 Hz), 125.0, 126.0, 126.4,

126.7, 126.8, 127.0, 128.8, 129.6, 133.47, 133.49, 134.3, 138.1, 145.3, 179.2. **IR** (neat, cm^{-1}): 2926, 1711, 1609, 1491, 1472, 1454, 1334, 1303, 1168, 1121, 1096, 964, 801, 742, 702, 548. **HRMS** (ESI): calcd. for $C_{19}H_{17}NOF_3$ ($[M+H]^+$): 332.1256, found: 332.1259.

(*S*)-6'-Methoxy-1-methyl-3',4'-dihydro-2'*H*-spiro[indoline-3,1'-naphthalen]-2-one (**135**):

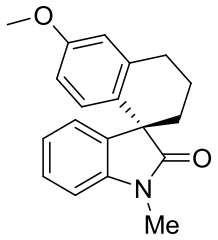

Yellow oil, 92% yield (53.9 mg). $[\alpha]_D^{25}$ = -11.13 (*c* = 1.0 in CH_2Cl_2). 88% *ee* [Chiracel AS-H column, *n*-hexane/*i*-PrOH = 98:2, 1.0 mL/min, 254 nm; t_R = 19.19 min. (major) and 27.01 min. (minor)]. **^{1}H-NMR** (300 MHz, $CDCl_3$): δ 1.89-2.0 (m, 2H), 2.1-2.2 (m, 1H), 2.31-2.43 (m, 1H), 2.88-3.0 (m, 2H), 3.27 (s, 3H), 3.74 (s, 3H), 6.38 (d, *J* = 9.0 Hz, 1H), 6.54 (dd, *J* = 9.0, 3.0 Hz, 1H), 6.68 (d, *J* = 2.1 Hz, 1H), 6.91 (d, *J* = 9.0 Hz, 1H), 6.98-7.07 (m, 2H), 7.28 (t, *J* = 6.0 Hz, 1H). **^{13}C-NMR** (100 MHz, $CDCl_3$): δ 18.9, 26.6, 29.8, 34.4, 51.8, 55.3, 108.1, 113.2, 114.0, 122.9, 124.1, 127.9, 129.2, 137.6, 139.4, 143.3, 158.5, 180.8. **IR** (neat, cm^{-1}): 2932, 1703, 1607, 1491, 1467, 1341, 1255, 1240, 1161, 1090, 1036, 965, 838, 745, 690. **HRMS** (ESI): calcd. for $C_{19}H_{20}NO_2$ ($[M+H]^+$): 294.1488, found: 294.1492.

(*R*)-6-Chloro-1'-methylspiro[chroman-4,3'-indolin]-2'-one (**136**):

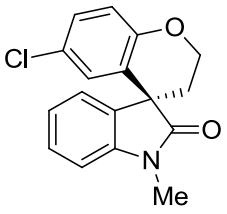

White solid, **m.p.** = 68-70 °C, 98% yield (58.7 mg). $[\alpha]_D^{25}$ = -45.37 (*c* = 1.0 in CH_2Cl_2). 88% *ee* [Chiracel AS-H column, *n*-hexane/*i*-PrOH = 98:2, 1.0 mL/min, 254 nm; t_R = 14.37 min. (major) and 26.40 min. (minor)]. **^{1}H-NMR** (300 MHz, $CDCl_3$): δ 2.13-2.27 (m, 2H), 3.29 (s, 3H), 4.32-4.38 (m, 1H), 4.80-4.88 (m, 1H), 6.41 (d, *J* = 2.2 Hz, 1H), 6.87 (d, *J* = 8.8 Hz, 1H), 6.95 (d, *J* = 8.8 Hz, 1H), 7.08 (d, *J* = 4.5 Hz, 3H), 7.32-7.38 (m, 1H). **^{13}C-NMR** (75 MHz, $CDCl_3$): δ 26.6, 31.9, 47.8, 62.0, 77.2, 108.4, 119.1, 122.3, 123.4, 123.8, 125.3,

127.8, 128.8, 129.0, 134.0, 143.4, 154.1, 178.5. **IR** (neat, cm^{-1}): 2962, 1706, 1610, 1470, 1370, 1346, 1253, 1037, 815, 746, 701. **HRMS** (ESI): calcd. for $C_{17}H_{15}ClNO_2$ ($[M+H]^+$): 300.0785, found: 300.0791.

(*R*)-1-Methylspiro[indoline-3,4'-thiochroman]-2-one (**138**):

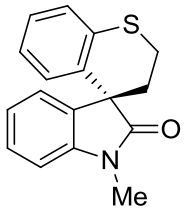

Yellow solid, **m.p.** = 134-136 °C, 98% yield (55.1 mg). $[\alpha]_D^{25}$ = -25.69 (*c* = 1.0 in CH_2Cl_2). 90% *ee* [Chiracel OD-H column, *n*-hexane/*i*-PrOH = 99:1, 1.0 mL/min, 254 nm; t_R = 47.34 min. (major) and 67.95 min. (minor)]. **^{1}H-NMR** (400 MHz, $CDCl_3$): δ 2.22-2.28 (m, 1H), 2.38-2.44 (m, 1H), 3.10-3.16 (m, 1H), 3.29 (s, 3H), 3.58-3.64 (m, 1H), 6.52 (d, *J* = 8.0 Hz, 1H), 6.85 (t, *J* = 8.0 Hz, 1H), 6.93 (d, *J* = 8.0 Hz, 1H), 7.04 (t, *J* = 8.0 Hz, 2H), 7.06 (t, *J* = 8.0 Hz, 1H), 7.32 (t, *J* = 8.0 Hz, 1H). **^{13}C-NMR** (75 MHz, $CDCl_3$): δ 22.1, 26.5, 32.4, 51.0, 108, 3, 123.1, 124.3, 124.4, 127.2, 127.6, 128.4, 128.9, 131.4, 135.6, 142.9, 179.2. **IR** (neat, cm^{-1}): 2924, 2848, 1705, 1608, 1469, 1344, 1242, 1124, 1087, 948, 741, 540. **HRMS** (ESI): calcd. for $C_{17}H_{15}NOS$ ($[M+H]^+$): 282.0947, found: 282.0947.

(*R*)-1-Benzylspiro[indoline-3,4'-thiochroman]-2-one (**138**):

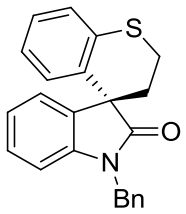

Yellow solid, **m.p.** = 135-138 °C, 94% yield (67.1 mg). $[\alpha]_D^{25}$ = -19.24 (*c* = 1.0 in CH_2Cl_2). 84% *ee* [Chiracel AS-H column, *n*-hexane/*i*-PrOH = 95:5, 1.0 mL/min, 254 nm; t_R = 17.71 min. (major) and 33.81 min. (minor)]. **^{1}H-NMR** (400 MHz, $CDCl_3$): δ 2.29-2.36 (m, 1H), 2.45-2.51 (m, 1H), 3.12-3.18 (m, 1H), 3.66-3.72 (m, 1H), 4.98 (dd, *J* = 18.5, 15.6 Hz, 2H), 6.52 (dd, *J* = 7.9, 1.1 Hz, 1H), 6.79 (d, *J* = 7.8 Hz, 1H), 6.82 (td, *J* = 7.9, 1.2 Hz, 1H), 6.97 (td, *J* = 7.5, 0.8 Hz, 1H), 7.05 (td, *J* = 8.4, 1.3 Hz, 1H), 7.11 (d, *J* = 7.2 Hz, 1H), 7.16 (t, *J* = 7.8 Hz, 2H), 7.22-7.28 (m, 1H), 7.29-7.31 (m, 4H). **^{13}C-NMR** (100 MHz, $CDCl_3$): δ 22.1, 32.7, 43.8, 50.9, 109.3, 123.1, 124.3, 124.5, 127.36, 127.39, 127.69, 127.79, 128.3, 128.91,

128.97, 131.4, 133.7, 135.5, 135.9, 142.0, 179.2. **IR** (neat, cm^{-1}): 3058, 2926, 1707, 1658, 1609, 1470, 1432, 1384, 1349, 1299, 1186, 1079, 1029, 942, 740, 726, 697. **HRMS** (ESI): calcd. for $C_{23}H_{20}NOS$ ($[M+H]^+$): 358.1260, found: 358.1257.

(*R*)-1-(Methoxymethyl)spiro[indoline-3,4'-thiochroman]-2-one (**139**):

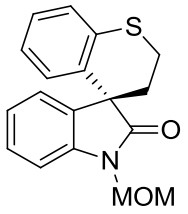

Glassy solid, 97% yield (60.3 mg). $[\alpha]_D^{25}$ = -24.69 (*c* = 1.0 in CH_2Cl_2). 86% *ee* [Chiracel AS-H column, *n*-hexane/*i*-PrOH = 99:1, 1.0 mL/min, 254 nm; t_R = 18.80 min. (major) and 22.08 min. (minor)]. **^{1}H-NMR** (400 MHz, $CDCl_3$): δ 2.28-2.34 (m, 1H), 2.39-2.45 (m, 1H), 3.07-3.14 (m, 1H), 3.36 (s, 3H), 3.63-3.69 (m, 1H), 5.18 (d, *J* = 10.8 Hz, 1H), 5.22 (d, *J* = 10.8 Hz, 1H), 6.55 (dd, *J* = 7.8, 1.2 Hz, 1H), 6.85 (td, *J* = 7.9, 1.3 Hz, 1H), 7.06-7.19 (m, 4H), 7.20 (dd, *J* = 7.9, 1.1 Hz, 1H), 7.32 (td, *J* = 7.7, 1.2 Hz, 1H). **^{13}C-NMR** (100 MHz, $CDCl_3$): δ 22.0, 32.9, 51.2, 56.4, 71.5, 109.7, 123.7, 124.4, 124.5, 127.3, 127.7, 128.5, 128.9, 131.2, 133.7, 135.0, 141.1, 179.7. **IR** (neat, cm^{-1}): 3054, 2933, 1715, 1609, 1485, 1466, 1343, 1288, 1229, 1118, 1086, 1069, 911, 742, 613, 509. **HRMS** (ESI): calcd. for $C_{18}H_{18}NO_2S$ ($[M+H]^+$): 312.1052, found: 312.1067.

(*R*)-1-((Benzyloxy)methyl)spiro[indoline-3,4'-thiochroman]-2-one (**140**):

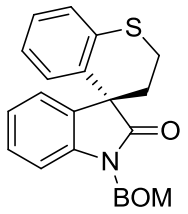

Glassy solid, 94% yield (72.7 mg). $[\alpha]_D^{25}$ = -23.12 (*c* = 1.0 in CH_2Cl_2). 86% *ee* [Chiracel AS-H column, *n*-hexane/*i*-PrOH = 99:1, 1.0 mL/min, 254 nm; t_R = 24.18 min. (major) and 30.76 min. (minor)]. **^{1}H-NMR** (400 MHz, $CDCl_3$): δ 2.24-2.36 (m, 2H), 3.06-3.10 (m, 1H), 3.63-3.69 (m, 1H), 4.57 (d, *J* = 11.8 Hz, 1H), 4.61 (d, *J* = 11.8 Hz, 1H), 5.30 (d, *J* = 11.0 Hz, 1H), 5.34 (d, *J* = 11.0 Hz, 1H), 6.52 (d, *J* = 8.6 Hz, 1H), 6.84 (t, *J* = 8.0 Hz, 1H), 7.06-7.11 (m, 1H), 7.15-7.21 (m, 5H), 7.28-7.35 (m, 5H). **^{13}C-NMR** (100 MHz, $CDCl_3$): δ 25.4, 32.7, 51.2, 69.9, 70.9, 109.8, 123.7, 124.3, 124.5, 127.3, 127.7, 127.8, 127.9, 128.4,

128.5, 128.9, 131.2, 135.0, 137.3, 141.2, 179.6. **IR** (neat, cm^{-1}): 3058, 2925, 1716, 1610, 1485, 1467, 1432, 1343, 1218, 1050, 944, 799, 740, 696, 670, 507. **HRMS** (ESI): calcd. for $C_{24}H_{22}NO_2S$ ($[M+H]^+$): 388.1365, found: 388.1377.

(*S*)-1-Methyl-3',4'-dihydro-1'*H*-spiro[indoline-3,2'-naphthalen]-2-one (**141**):

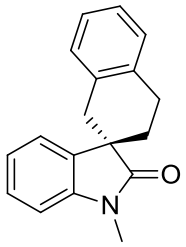

Colorless crystals, **m.p.** = 125-127 °C, 75% yield (39.4 mg). $[\alpha]_D^{25}$ = -58.2 (*c* = 0.5 in CH_2Cl_2). 56% *ee* [Chiracel AS-H column, *n*-hexane/*i*-PrOH = 99:1, 1.0 mL/min, 254 nm; t_R = 21.92 min. (minor) and 45.10 min. (major)]. **^{1}H-NMR** (400 MHz, $CDCl_3$): δ 1.72-1.78 (m, 1H), 2.25-2.33 (m, 1H), 2.67 (dd, *J* = 16.3, 1.8 Hz, 1H), 3.08-3.11 (m, 2H), 3.24 (d, *J* = 1.6 Hz, 0.5H), 3.27 (s, 3H), 3.36 (d, *J* = 1.6 Hz, 0.5H), 6.75 (dd, *J* = 7.9, 1.2 Hz, 1H), 6.86-6.89 (m, 2H), 6.98-7.07 (m, 2H), 7.14-7.24 (m, 3H). **^{13}C-NMR** (100 MHz, $CDCl_3$): δ 25.6, 26.4, 30.1, 36.2, 46.8, 108.0, 122.3, 123.9, 126.1, 126.2, 127.8, 128.7, 129.5, 133.6, 134.0, 135.4, 142.8, 180.3. **IR** (neat, cm^{-1}): 2924, 1711, 1664, 1611, 1492, 1470, 1376, 1350, 1253, 1092, 1024, 965, 749, 524. **HRMS** (ESI): calcd. for $C_{18}H_{18}NO$ ($[M+H]^+$): 264.1382, found: 264.1370.

(*R*)-1'-Methyl-2,3-dihydrospiro[indene-1,3'-pyrrolo[3,2-b]pyridin]-2'(1'*H*)-one (**142**):

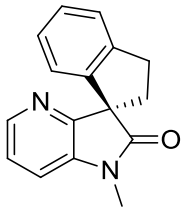

Yellow solid, **m.p.** = 129-131 °C, 99% yield (49.5 mg). $[\alpha]_D^{25}$ = -29.75 (*c* = 1.0 in CH_2Cl_2). 86% *ee* [Chiracel AS-H column, *n*-hexane/*i*-PrOH = 90:10, 1.0 mL/min, 254 nm; t_R = 9.93 min. (major) and 11.33 min. (minor)]. **^{1}H-NMR** (400 MHz, $CDCl_3$): δ 2.63 (t, *J* = 7.9 Hz, 2H), 3.28 (s, 3H), 3.32-3.45 (m, 2H), 6.62 (d, *J* = 7.6 Hz, 1H), 7.06 (t, *J* = 7.5 Hz, 1H), 7.12 (dd, *J* = 7.8, 1.4 Hz, 1H), 7.16 (d, *J* = 5.0 Hz, 1H), 7.21 (td, *J* = 7.4, 0.8 Hz, 1H), 7.35 (d, *J* = 7.5 Hz, 1H), 8.18 (dd, *J* = 5.0, 1.3 Hz, 1H). **^{13}C-NMR** (100 MHz, $CDCl_3$): δ 26.2, 32.0,

35.7, 60.7, 114.0, 122.7, 122.9, 125.3, 126.9, 128.2, 138.5, 142.3, 143.5, 145.5, 155.3, 178.2. **IR** (neat, cm^{-1}): 2929, 1707, 1598, 1445, 1323, 1304, 1131, 1080, 1032, 947, 790, 774, 754, 654, 579. **HRMS** (ESI): calcd. for $C_{16}H_{15}N_2O$ ($[M+H]^+$): 251.1178, found: 251.1186.

(*R*)-1'-Methyl-3,4-dihydro-2H-spiro[naphthalene-1,3'-pyrrolo[3,2-b]pyridin]-2'(1'H)-one (**143**):

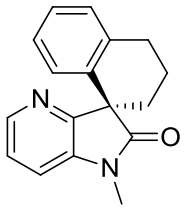

Yellow solid, **m.p.** = 126-128 °C, 99% yield (52.3 mg). $[\alpha]_D^{25}$ = -74.52 (*c* = 1.0 in CH_2Cl_2). 91% *ee* [Chiracel AS-H column, *n*-hexane/*i*-PrOH = 99:1, 1.0 mL/min, 254 nm; t_R = 36.36 min. (minor) and 41.23 min. (major)]. **^{1}H-NMR** (400 MHz, $CDCl_3$): δ 2.10-2.20 (m, 2H), 2.27-2.33 (m, 2H), 3.0 (t, *J* = 6.1 Hz, 2H), 3.3 (s, 3H), 6.4 (d, *J* = 7.7 Hz, 1H), 6.95 (t, *J* = 7.3 Hz, 1H), 7.09-7.18 (m, 4H), 8.18 (dd, *J* = 4.7, 1.5 Hz, 1H). **^{13}C-NMR** (100 MHz, $CDCl_3$): δ 18.4, 26.2, 29.2, 32.3, 52.4, 114.1, 122.5, 126.3, 127.3, 127.4, 130.1, 133.3, 138.0, 138.3, 143.3, 157.4, 178.9. **IR** (neat, cm^{-1}): 2933, 1714, 1600, 1491, 1461, 1429, 1365, 1330, 1108, 1029, 755, 625. **HRMS** (ESI): calcd. for $C_{17}H_{17}NO_2$ ($[M+H]^+$): 265.1335, found: 265.1333.

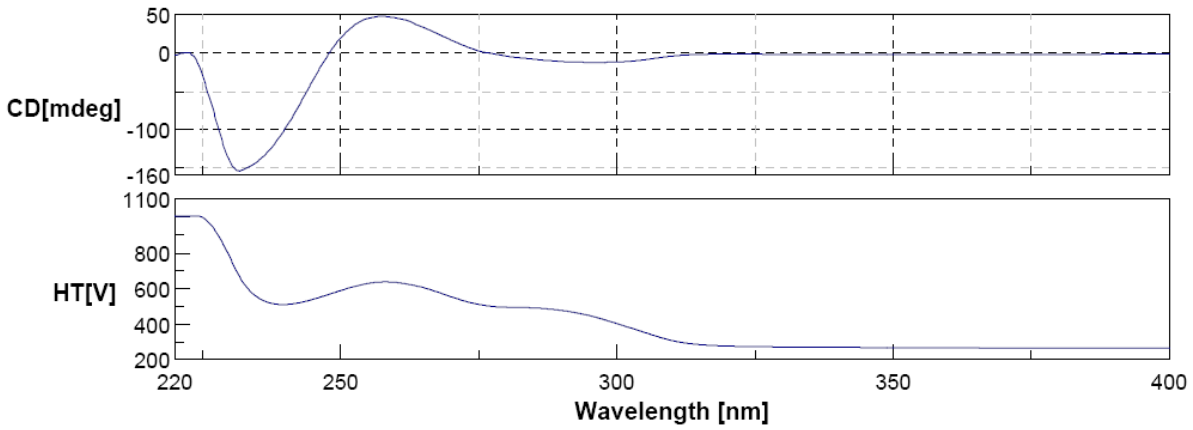

For CD spectrum: *c* = 0.0001 M in CH_2Cl_2.

(*R*)-1'-Methyl-6,7,8,9-tetrahydrospiro[benzo[7]annulene-5,3'-pyrrolo[3,2-b]pyridin]-2'(1'H)-one (**144**):

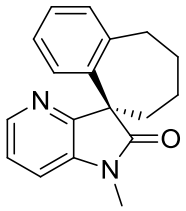

Yellow solid, **m.p.** = 112-114 °C, 99% yield (55.1 mg). $\mathbf{[\alpha]_D^{25}}$ = -88.69 (*c* = 1.0 in CH_2Cl_2). 90% *ee* [Chiracel OD-H column, *n*-hexane/*i*-PrOH = 99:1, 1.0 mL/min, 254 nm; t_R = 29.60 min. (major) and 33.62 min. (minor)]. **^{1}H-NMR** (400 MHz, $CDCl_3$): δ 1.87-2.25 (m, 6H), 3.25-3.32 (m, 1H), 3.28 (s, 3H), 3.50-3.57 (m, 1H), 6.59 (dd, *J* = 7.8, 0.7 Hz, 1H), 6.96 (td, *J* = 7.7, 1.4 Hz, 1H), 7.07-7.11 (m, 2H), 7.14-7.18 (m, 2H). **^{13}C-NMR** (100 MHz, $CDCl_3$): δ 23.7, 26.0, 27.4, 34.4, 34.8, 58.6, 114.2, 122.3, 126.0, 127.4, 128.8, 131.7, 137.3, 137.7, 143.0, 143.9, 156.7, 178.6. **IR** (neat, cm^{-1}): 2930, 1703, 1600, 1447, 1365, 1323, 1301, 1216, 1164, 1093, 978, 796, 758, 690, 637, 538. **HRMS** (ESI): calcd. for $C_{18}H_{19}N_2O$ ($[M+H]^+$): 279.1491, found: 279.1479.

IV.6. General Procedure for the Synthesis of [Pd(η^3-cinnamyl or allyl)(*NHC*)I] Complexes

In an N_2 filled drybox [Pd(π-cinnamyl or allyl)Cl]$_2$ (0.1 mmol, 1.0 equiv.), imidazolium salt (0.2 mmol, 2.0 equiv.) and *t*BuONa (0.2 mmol, 2.0 equiv.) were placed into a dried Schlenk tube. Dimethoxyethane (DME) (4 mL, freshly distilled over Na and benzophenone) was added and the mixture was stirred at rt for 24 h and then quenched with aq. NH_4Cl and extracted with CH_2Cl_2. The combined organic phases were washed with water and brine, and dried over $MgSO_4$. The resulting crude product was purified by flash column chromatography (silica gel; ethyl acetate : *n*-hexane = 7 : 1) to give [Pd(η^3-cinnamyl or allyl)(*NHC*)I] complex shown by ^{1}H-NMR to consist of a mixture of diastereoisomers (in case of [Pd(η^3-cinnamyl)(*NHC*)I] complexes) or isomers (in case of [Pd(η^3-allyl)(*NHC*)I] complexes).

(*S*,*S*)-(**100**):

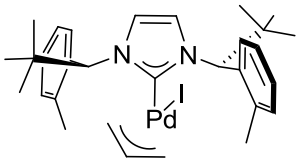

Recrystallization from pentane/acetone gave a yellow solid shown by NMR to consist of a 1: 0.9 mixture of *endo*- and *exo*-isomers. A crystal suitable for X-ray analysis was obtained by diffusion of pentane into an acetone solution of the complex. 83% yield, **m.p.** = 193-195 ^{o}C (decomp.). **100a**: **^{1}H-NMR** (500 MHz, $CDCl_3$): δ 0.95 (s, 9H), 1.11 (s, 9H), 2.27 (d, *J* = 12.0 Hz, 1H), 2.53 (s, 3H), 2.65 (bs, 4H), 2.96 (d, *J* = 14 Hz, 1H). 4.33 (d, *J* = 2.2, 7.6 Hz, 1H), 4.63-4.71 (m, 1H), 5.94 (s, 1H), 6.04 (s, 1H), 6.93 (d, *J* = 7.6 Hz, 1H), 7.04-7.15 (m, 6H), 7.39-7.41 (m, 1H), 7.64 (d, *J* = 1.9 Hz, 1H), 7.71 (d, *J* = 2.2 Hz, 1H). **100b**: **^{1}H-NMR** (500 MHz, $CDCl_3$): δ 0.96 (s, 8.1H), 1.13 (s, 8.1H), 1.57 (d, *J* = 13.0 Hz, 0.9H), 2.5 (s, 2.7H), 2.57 (s, 2.7H), 2.87 (d, *J* = 13.6 Hz, 0.9H), 3.4 (d, *J* = 7.0 Hz, 0.9H), 4.23 (dd, *J* = 1.9, 7.3 Hz, 0.9H), 5.01-5.12 (m, 0.9H), 5.73 (s, 0.9H), 6.45 (s, 0.9H), 7.04-7.15 (m, 6.3H), 7.30-7.35 (m, 0.9H), 7.64 (d, *J* = 1.9 Hz, 0.9H), 7.73 (d, *J* = 1.9 Hz, 0.9H).

^{13}C-NMR (100 MHz, $CDCl_3$): δ 21.8, 21.9, 22.5, 22.6, 27.9, 28.2, 28.66, 28.69, 36.8, 36.9, 37.1, 54.9, 58.6, 66.6, 68.1, 68.3, 68.4, 68.5, 112.5, 114.4, 118.5, 119.0, 121.0, 121.3, 125.2, 125.3, 125.4, 126.8, 126.6, 127.3, 127.4, 127.6, 127.9, 128.42, 128.46, 130.6, 130.9, 131.26, 131.29, 135.4, 135.5, 136.1, 136.4, 137.0, 137.1, 138.3, 138.7, 184.5, 184.7. **IR** (neat, cm^{-1}): 2964, 1479, 1400, 1365, 1223, 1161, 1103, 906, 846, 742, 689, 631. **HRMS** (EI): calcd for $C_{30}H_{41}N_2Pd$ ($[M-I]^+$): 535.2304, found: 535.2294. **Element analysis calcd** (%) for $C_{30}H_{41}IN_2Pd$ (662): C 54.35%, H 6.23, N 4.23, found for $C_{30}H_{41}IN_2Pd \times 0.02CH_2Cl_2$ C 54.25, H 6.22, N 4.21.

(*S*,*S*)-(**102**):

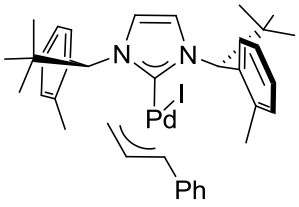

Yellow solid, **m.p.** = 105-110 °C, 89% yield. $[\alpha]_D^{25}$ = -142.5 (*c* = 1.0 in CH_2Cl_2). **^{1}H-NMR** (400 MHz, $CDCl_3$): δ 0.48 (s, 6H), 1.0 (s, 6H), 1.01 (s, 9H), 1.09 (s, 6H), 1.14 (s, 9H),

1.15 (s, 6H), 1.6 (d, *J* = 12.6 Hz, 1H), 2.29 (d, *J* = 11.5 Hz, 1H), 2.36 (s, 2H), 2.45 (d, *J* = 6.2 Hz, 1H), 2.51 (d, *J* = 3.6 Hz, 5H), 2.67-2.73 (m, 6H), 2.76 (s, 2.6H), 3.02 (d, *J* = 13.0 Hz, 0.6H), 3.29 (dd, *J* = 7.0, 1.9 Hz, 1H), 3.94 (d, *J* = 7.2 Hz, 0.17H), 4.12 (d, *J* = 7.5 Hz, 1.2H), 4.42 (d, *J* = 11.7 Hz, 0.17H), 4.54 (d, *J* = 12.7 Hz, 1H), 4.74 (d, *J* = 13.2 Hz, 0.8H), 5.02 (s, 0.65H), 5.06-5.14 (m, 0.17H), 5.23-5.31 (m, 0.8H), 5.67-5.78 (m, 2H), 5.84 (s, 1H), 5.99 (d, *J* = 10.5 Hz, 1.7H), 6.31 (d, *J* = 7.6 Hz, 1H), 6.35 (d, *J* = 8.3 Hz, 0.7H), 6.46 (s, 1H), 6.48 (s, 0.2H), 6.57 (s, 0.7H), 6.63 (t, *J* = 7.9 Hz, 0.36H), 6.91-7.47 (m, 42.4H), 7.54-7.59 (m, 0.6H), 7.64 (td, *J* = 6.6, 2.0 Hz, 2.6H), 7.73 (dd, *J* = 4.9, 2.0 Hz, 2H). **^{13}C-NMR** (100 MHz, $CDCl_3$): δ 14.1, 21.5, 21.7, 21.8, 22.0, 22.3, 22.7, 22.8, 26.9, 27.6, 28.0, 28.3, 28.4, 28.5, 28.73, 28.79, 28.8, 31.6, 36.0, 36.2, 36.92, 36.99, 37.0, 37.21, 37.24, 37.26, 37.4, 37.5, 49.0, 53.9, 62.3, 68.3, 68.6, 77.2, 79.01, 79.04, 85.8, 89.5, 107.4, 107.6, 109.0, 118.7, 119.1, 119.4, 119.6, 119.7, 121.2, 121.4, 125.1, 125.2, 125.3, 125.4, 125.5, 126.0, 126.3, 126.8, 126.9, 127.01, 127.06, 127.1, 127.35, 127.37, 127.4, 127.5, 127.6, 127.9, 128.0, 128.1, 128.20, 128.27, 128.3, 128.4, 128.56, 128.57, 128.64, 128.68, 128.9, 129.0, 130.7, 131.0, 131.2, 131.30, 131.34, 131.35, 135.3, 135.4, 135.9, 136.6, 136.4, 136.5, 137.13, 137.19, 137.92, 137.95, 138.3, 138.4, 138.7, 138.8, 139.3, 139.6, 183.6, 183.71, 183.79. **IR** (neat, cm^{-1}): 688, 745, 846, 907, 1030, 1104, 1162, 1225, 1366, 1400, 1417, 1478, 1598, 1673, 2959. **HRMS** (EI): calcd. for $C_{36}H_{45}N_2Pd$ ($[M-I]^+$): 611.2635, found: 611.2612. **Element analysis calcd** (%) for $C_{36}H_{46}IN_2Pd$ (739): C 58.50%, H 6.14%, N 3.79% found for $C_{36}H_{45}IN_2Pd$: C 58.27%, H 6.04%, N 3.29%.

(*S*,*S*)-(**158**):

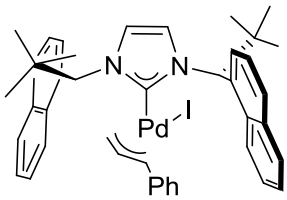

Yellow solid, 38% yield, **m.p.** = 205-207 °C (decomp.). **$[\alpha]_D^{25}$** = -47.4 (*c* = 1.0 in CH_2Cl_2). **^{1}H-NMR** (500 MHz, $CDCl_3$): δ 0.5 (d, *J* = 12.4 Hz, 1H), 0.59 (s, 4.5H), 1.0 (s, 2.2H), 1.05 (s, 13.7H), 1.07 (s, 17H), 1.12 (s, 15H), 1.18 (s, 13H), 1.22 (s, 6H), 1.27 (s, 2.2H), 1.84 (d, *J* = 6.4 Hz, 1H), 2.12 (d, *J* = 11.3 Hz, 1H), 2.29 (d, *J* = 12.6 Hz, 0.1H), 2.62 (d, *J* = 13 Hz, 0.19H), 2.83 (d, *J* = 13 Hz, 0.19H), 2.93 (dd, *J* = 6.9, 1.2 Hz, 1H), 3.61 (d, *J* = 7.5 Hz, 0.3H), 3.79-3.86 (m, 1H), 3.98 (d, *J* = 12.7 Hz, 1H), 4.13 (q, *J* = 14.2 Hz, 1H), 4.67 (d, *J* = 13.3 Hz, 1H), 5.48-5.61 (m, 1H), 5.85 (d, *J* = 7.2 Hz, 0.1H), 6.17 (d, *J* = 7.4 Hz, 0.6H), 6.48

(s, 1H), 6.64 (s, 1H), 6.75 (s, 1H), 6.95 (t, *J* = 7.7 Hz, 0.6H), 6.95 (t, *J* = 7.7 Hz, 0.6H), 6.99 (d, *J* = 7.2 Hz, 0.2H), 7.06 (d, *J* = 7.1 Hz, 0.2H), 7.17-7.64 (m, 50.6H), 7.73 (t, *J* = 7.8 Hz, 4H), 7.78-7.96 (m, 18H), 8.15 (d, *J* = 8.6 Hz, 1H), 8.19 (d, *J* = 8.9 Hz, 1H), 8.34 (d, *J* = 8.5 Hz, 1H), 8.68 (d, *J* = 8.6 Hz, 0.2H), 8.78 (d, *J* = 8.7 Hz, 1H). **^{13}C-NMR** (125 MHz, $CDCl_3$): δ 14.1, 14.2, 21.0, 22.7, 26.9, 28.1, 28.5, 28.7, 28.93, 28.95, 29.0, 29.7, 31.9, 35.7, 36.0, 36.4, 36.8, 36.90, 36.95, 47.6, 52.8, 53.4, 60.1, 60.4, 62.6, 65.6, 66.6, 67.1, 67.2, 67.6, 77.7, 82.8, 86.8, 90.1, 107.6, 108.1, 108.5, 110.4, 119.0, 119.1, 119.4, 119.7, 119.8, 119.9, 120.8, 121.1, 123.9, 124.2, 124.4, 124.67, 124.69, 124.72, 124.76, 124.86, 124.89, 124.9, 125.1, 125.2, 125.32, 125.38, 125.4, 125.5, 125.60, 125.67, 125.71, 125.74, 125.81, 125.84, 125.90, 125.94, 126.02, 126.04, 126.08, 126.1, 126.2, 126.4, 126.7, 126.8, 126.9, 127.4, 127.6, 127.7, 127.90, 127.95, 128.0, 128.1, 128.2, 128.51, 128.58, 128.6, 128.72, 128.77, 128.83, 128.85, 129.1, 129.2, 129.4, 132.20, 132.28, 132.3, 132.5, 132.7, 132.9, 133.5, 133.6, 133.7, 133.8, 133.9, 134.03, 134.07, 134.9, 135.6, 135.7, 135.5, 136.9, 137.2, 137.8, 138.7, 139.0, 139.9. **IR** (neat, cm^{-1}): 527, 547, 689, 754, 782, 910, 1027, 1162, 1190, 1220, 1366, 1399, 1424, 1475, 1596, 2959. **HRMS** (EI): calcd. for $C_{42}H_{45}N_2Pd$ ($[M\text{-}I]^+$): 685.2768, found: 685.2777. **Element analysis calcd** (%) for $C_{42}H_{45}IN_2Pd$ (811): C 62.19%, H 5.59%, N 3.45% found for $C_{42}H_{45}IN_2Pd$: C 62.11%, H 5.54%, N 3.44%.

(*S*,*S*)-(**159**):

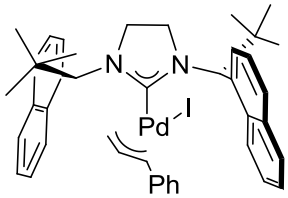

Yellow solid, **m.p.** = 227-229 °C (decomp.). 62% yield. **$[\alpha]_D^{25}$** = -53.1 (*c* = 1.0 in CH_2Cl_2). **^{1}H-NMR** (500 MHz, $CDCl_3$): δ 0.5 (d, *J* = 12.4 Hz, 1H), 1.01 (s, 9H), 1.06 (s, 9H), 1.07 (s, 9H), 1.13 (s, 9H), 1.84 (d, *J* = 6.0 Hz, 0.7H), 2.09 (d, *J* = 11.2 Hz, 0.7H), 3.11 (dd, *J* = 6.9, 1.2 Hz, 0.5H), 3.54-3.61 (m, 0.5H), 4.03-4.09 (m, 2H), 4.15-4.43 (m, 7H), 4.79 (d, *J* = 13.4 Hz, 0.7H), 5.6 (td, *J* = 12.5, 7.0 Hz, 0.5H), 6.22 (s, 0.8H), 6.29 (d, *J* = 9.0 Hz, 2H), 6.88 (s, 1H), 7.09 (t, *J* = 7.1 Hz, 0.8H), 7.21 (dd, *J* = 7.5, 2.4 Hz, 3H), 7.31 (q, *J* = 7.8 Hz, 3H), 7.38-7.65 (m, 23H), 7.71 (d, *J* = 7.9 Hz, 1H), 7.74 (d, *J* = 7.9 Hz, 1H), 7.80-7.89 (m, 6H), 7.91 (d, *J* = 8.2 Hz, 1H), 8.19 (dd, *J* = 8.9, 5.6 Hz, 2H), 8.25 (d, *J* = 8.6 Hz, 1H), 8.79 (d, *J* = 8.7 Hz, 1H). **^{13}C-NMR** (125 MHz, $CDCl_3$): δ 28.0, 28.82, 28.88, 28.9, 29.0, 29.7, 35.2, 35.9, 36.2, 36.35, 36.37, 36.9, 47.1, 48.4, 48.8, 49.5, 50.2, 51.2, 54.0, 65.01, 65.03, 65.09, 65.5,

86.5, 91.0, 107.8, 109.2, 123.5, 124.2, 124.51, 124.55, 124.59, 124.7, 124.9, 125.1, 125.3, 125.50, 125.52, 125.57, 125.6, 125.7, 125.8, 125.92, 125.96, 126.1, 126.21, 126.26, 126.4, 126.7, 126.8, 127.2, 127.5, 127.72, 127.77, 127.8, 127.9, 128.0, 128.1, 128.3, 128.40, 128.43, 128.49, 128.6, 128.7, 128.81, 128.85, 129.0, 132.3, 132.5, 132.6, 133.0, 133.2, 133.4, 133.7, 134.0, 134.20, 134.23, 137.6, 138.7, 138.9, 140.1, 216.3, 216.9, 217.8. **IR** (neat, cm^{-1}): 600, 691, 750, 780, 1123, 1261, 1429, 1476, 1596, 1671, 2924. **HRMS** (EI): calcd. for $C_{42}H_{47}N_2Pd$ ($[M-I]^+$): 685.2768, found: 685.2777. **Element analysis calcd** (%) for $C_{42}H_{47}IN_2Pd$ (813): C 62.04%, H 5.83%, N 3.45% found for $C_{42}H_{47}IN_2Pd$: C 61.59%, H 5.72%, N 3.32%.

(*R*,*R*)-(**160**):

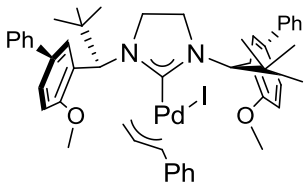

Yellow solid, **m.p.** = 86-88 °C (decomp.). 83% yield. $[\alpha]_D^{25}$ = +57.1 (*c* = 1.0 in CH_2Cl_2). **^{1}H-NMR** (400 MHz, $CDCl_3$): δ 1.01 (s, 6.6H), 1.04 (s, 9H), 1.05 (s, 9H), 1.1 (s, 6.6H), 1.84 (d, *J* = 10.7 Hz, 0.5H), 2.26 (d, *J* = 11.4 Hz, 1H), 2.58 (d, *J* = 6.6 Hz, 1H), 3.32 (d, *J* = 6.0 Hz, 0.6H), 3.41 (s, 2H), 3.48 (q, *J* = 7.0 Hz, 1H), 3.8 (d, *J* = 5.0 Hz, 0.6H), 3.8 (s, 2.7H), 3.88 (s, 3H), 3.92 (s, 3H), 3.97-4.16 (m, 5H), 4.2-4.25 (m, 1.5H), 4.35 (q, *J* = 9.9 Hz, 1H), 4.52-4.57 (m, 1.6H), 4.99 (br.s, 0.7H), 5.65-5.73 (m, 1.5H), 5.69 (s, 0.6H), 6.13 (s, 1H), 6.33 (s, 0.6H), 6.78 (d, *J* = 8.6 Hz, 0.6H), 6.94 (d, *J* = 8.6 Hz, 2H), 7.02 (d, *J* = 8.6 Hz, 1.5H), 7.09-7.20 (m, 5H), 7.28-7.57 (m, 31H). **^{13}C-NMR** (100 MHz, $CDCl_3$): δ 14.1, 22.7, 26.9, 27.5, 28.4, 28.6, 28.65, 28.7, 28.8, 29.3, 29.6, 29.7, 31.9, 34.7, 35.5, 35.9, 35.93, 36.0, 36.3, 48.2, 48.8, 49.0, 49.2, 49.7, 49.8, 50.2, 50.3, 52.4, 53.4, 54.7, 55.0, 55.06, 55.2, 55.8, 62.4, 62.5, 62.9, 63.3, 86.2, 88.0, 107.6, 107.9, 109.9, 111.1, 111.4, 111.45, 111.5, 111.6, 125.9, 125.97, 126.2, 126.27, 126.36, 126.38, 126.43, 126.46, 126.59, 126.6, 126.7, 126.8, 126.9, 126.92, 126.95, 127.0, 127.02, 127.1, 127.15, 127.17, 127.4, 128.11, 128.15, 128.2, 128.5, 128.6, 128.8, 128.9, 128.98, 129.0, 130.5, 131.6, 131.9, 132.4, 132.7, 138.7, 138.8, 140.4, 140.7, 140.8, 141.4, 141.8, 156.0, 156.5, 156.7, 156.82, 156.84, 214.9, 216.2. **IR** (neat, cm^{-1}): 589, 727, 761, 906, 1022, 1246, 1435, 1483, 1605, 2960. **HRMS** (EI): calcd. for $C_{48}H_{55}N_2O_2Pd$ ($[M-I]^+$): 797.3292, found: 797.3290. **Element analysis calcd** (%) for $C_{48}H_{55}IN_2O_2Pd$ (925): C 62.31%, H 5.99%, N 3.03% found for $C_{48}H_{55}IN_2O_2Pd$: C 62.03%, H 6.01%, N 2.68%.

(*R*,*R*)-(**161**):

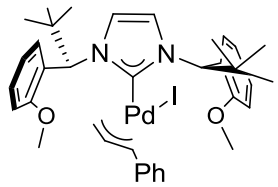

Yellow solid, **m.p.** = 110-112 °C. 26%, $[\alpha]_D^{25}$ = +38.1 (*c* = 1.0 in CH_2Cl_2). **^{1}H-NMR** (400 MHz, $CDCl_3$): δ 0.45 (s, 6H), 0.83 (s, 1.8H), 0.94 (s, 6H), 0.96 (s, 6H), 1.00 (s, 1.8H), 1.06 (s, 6H), 1.10 (s, 6H), 1.19 (t, *J* = 7.2 Hz, 3H), 1.24 (t, *J* = 7.2 Hz, 3H), 1.95 (d, *J* = 12.4 Hz, 0.8H), 2.03 (s, 2H), 2.30 (d, *J* = 11.6 Hz, 0.8H), 2.57 (d, *J* = 6.8 Hz, 0.8H), 2.61 (d, *J* = 12.8 Hz, 0.2H), 2.99 (d, *J* = 13.2Hz, 0.8H), 3.03 (d, *J* = 14.8 Hz, 0.2H), 3.16 (d, *J* = 7.2 Hz, 0.8H), 3.42-3.50 (m, 1H), 3.47 (s, 3H), 3.75 (s, 2H), 3.78 (s, 3H), 3.81 (s, 3H), 3.82 (s, 2H), 3.91 (s, 2H), 4.02-4.26 (m, 3.3H), 4.59 (dd, *J* = 13.2, 12.8 Hz, 1H), 5.15-5.40 (m, 1.8H), 5.64-5.88 (m, 1.8H), 6.17 (s, 0.8H), 6.20 (s, 1H), 6.29-6.37 (m, 1.3H), 6.38 (s, 1H), 6.41 (s, 0.2H), 6.61 (s, 0.8H), 6.69 (d, *J* = 8.4 Hz, 1H), 6.77-6.98 (m, 12H), 7.07-7.48 (m, 18H), 7.48-7.54 (m, 2.5H), 7.58 (s, 1H), 7.63 (d, *J* = 8.4 Hz, 1.8H). **^{13}C-NMR** (100 MHz, $CDCl_3$): δ 14.4, 15.5, 21.3, 27.6, 28.0, 28.2, 28.7, 28.8, 28.9, 35.5, 36.4, 36.6, 36.7, 36.9, 49.7, 52.6, 55.0, 55.1, 55.4, 55.7, 56.0, 60.6, 65.4, 65.5, 66.1, 85.9, 87.6, 107.7, 108.2, 109.8, 110.9, 111.1, 111.4, 111.5, 111.9, 119.7, 119.8, 120.0, 120.0, 120.2, 120.3, 120.9, 126.0, 126.1, 126.3, 126.7, 127.6, 128.3, 128.3, 128.4, 128.5, 128.6, 128.7, 128.9, 129.0, 129.4, 129.8, 139.1, 139.5, 156.5, 156.9, 157.2, 183.5, 184.4, 185.6. **IR** (neat, cm^{-1}): 690, 729, 750, 804, 853, 909, 1027, 1107, 1163, 1184, 1200, 1242, 1289, 1323, 1367, 1402, 1418, 1461, 1492, 1600, 1723, 2961. **HRMS** (ESI) calcd. for $C_{36}H_{45}N_2O_2Pd$ 643.2510, found 643.2527. **Element analysis calcd** (%) for $C_{36}H_{47}IN_2O_2Pd$ (711): C 55.93%, H 6.13%, N 3.62% found for $C_{36}H_{47}IN_2O_2Pd$: C 56.06%, H 5.93%, N 3.14%.

(*S*,*S*)-(**101**):

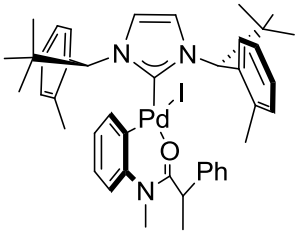

$Pd(dba)_2$ (115 mg, 0.2 mmol, 1.0 equiv.), chiral carbene precursor (*S*,*S*)-[**L5**H][I] (103.3 mg, 0.2 mmol, 1.0 equiv.) and *t*BuONa (19.2 mg, 0.2 mmol, 1.0 equiv.) were placed

into a dried Schlenk tube under N_2. Dimethoxyethane (DME) (2 mL) (freshly distilled over Na and benzophenone) was added and the reaction mixture stirred for one hour at rt. Substrate **61** (63.6 mg, 0.2 mmol, 1.0 equiv.) was then added as a solution in DME (2 mL). The reaction was stirred at ambient temperature for 24 h and then quenched with aq. NH_4Cl and extracted with CH_2Cl_2. The combined organic phases were washed with water and brine, and dried over $MgSO_4$. After evaporation of volatiles, the residue was purified by f.c. over SiO_2 (Hexane/EtOAc 7/1) to give 3 (111 mg, 65%) as yellow solid shown by NMR to consist of a 1:1 mixture of diastereoisomers. By preparative f.c. over SiO_2 (Hexane/EtOAc/CH_2Cl_2 10/1/0.5) both diastereoisomers were separately isolated. The crystals suitable for X-ray analysis were obtained by diffusion of pentane into an acetone solution of complex.

Diastereoisomer (*S*,*S*)-**101a**: Yellow solid, **m.p.** = 185-187 °C (decomp.). $\mathbf{[\alpha]_D^{25}}$ = -68.4 (*c* = 1.0 in CH_2Cl_2), **^{1}H-NMR** (500 MHz, $CDCl_3$): δ 0.53 (s, 8H), 1.25 (s, 8H), 1.58 (d, *J* = 6.8 Hz, 3H), 2.03 (s, 3H), 3.12 (s, 3H), 3.56 (s, 3H), 3.96 (q, *J* = 6.7 Hz, 1H), 4.85 (dd, *J* = 7.6, 1.4 Hz, 1H), 5.89 (s, 1H), 6.05 (td, *J* = 7.7, 1.4 Hz, 1H), 6.79 (td, *J* = 6.9, 1.4 Hz, 1H), 6.86 (dd, *J* = 8.2, 1.4 Hz, 1H), 6.87 (d, *J* = 7.4 Hz, 1H), 6.99-7.02 (m, 2H), 7.04 (td, *J* = 7.9, 1.1 Hz, 1H), 7.09 (td, *J* = 7.5, 1.4 Hz, 2H), 7.2 (t, *J* = 6.9 Hz, 1H), 7.22 (s, 1H), 7.35 (dd, *J* = 7.8, 0.9 Hz, 1H), 7.4 (tt, *J* = 10.8, 6.4, 1.2 Hz, 1H), 7.46 (t, *J* = 7.1 Hz, 1H), 7.54 (d, *J* = 2.1 Hz. 1H), 7.69 (d, *J* = 2.1 Hz, 1H), 7.88 (d, *J* = 7.1 Hz, 2H). **^{13}C-NMR** (125 MHz, $CDCl_3$): δ 21.0, 21.9, 22.5, 26.8, 28.1, 28.9, 36.5, 37.1, 37.5, 45.7, 67.5, 67.7, 115.3, 119.2, 119.7, 124.0, 124.7, 125.0, 126.9, 127.0, 127.3, 128.0, 129.1, 129.2, 130.7, 131.4, 135.8, 136.9, 137.0, 138.4, 138.6, 138.9, 139.1, 139.3, 172.8, 174.5. **IR** (neat, cm^{-1}): 2959, 1591, 1478, 1450, 1421, 1400, 1225, 1162, 1065, 1028, 906, 845, 745, 697. **HRMS** (EI): calcd. for $C_{43}H_{52}N_3OPd$ ($[M-I]^+$): 732.3139, found: 732.3127. **Element analysis calcd** (%) for $C_{43}H_{52}IN_3OPd$ (860): C 60.04%, H 6.09%, N 4.88% found for $C_{43}H_{52}IN_3OPd$: C 60.24%, H 6.38%, N 4.66%.

Diastereoisomer (*S*,*S*)-**101b**: **^{1}H-NMR** (500 MHz, $CDCl_3$): δ 0.58 (s, 9H), 1.22 (s, 9H), 1.76 (d, *J* = 6.9 Hz, 3H), 2.98 (s, 3H), 3.12 (s, 3H), 3.4 (s, 3H), 4.08 (q, *J* = 6.8 Hz, 1H), 4.86 (dd, *J* = 7.6, 1.4 Hz, 1H), 6.04 (td, *J* = 7.4, 1.2 Hz, 1H), 6.33 (s, 1H), 6.56 (dd, *J* = 8.0, 1.2 Hz, 1H), 6.72 (td, *J* = 8.5, 1.4 Hz, 1H), 7.08 (t, *J* = 8.1 Hz, 2H), 7.11 (dd, *J* = 6.5, 1.2 Hz, 1H), 7.13 (s, 2H), 7.16 (dd, *J* = 7.1, 1.5 Hz, 2H), 7.19 (bs, 1H), 7.21 (d, *J* = 1.5 Hz, 2H), 7.22 (d, *J* = 7.6 Hz, 2H), 7.24 (bs, 1H), 7.31 (t, *J* = 7.0 Hz, 2H), 7.4 (dd, *J* = 7.8, 0.8 Hz, 1H), 7.56 (d, *J* = 2.1 Hz, 1H), 7.69 (d, *J* = 2.1 Hz, 1H). **^{13}C-NMR** (125 MHz, $CDCl_3$): δ 21.72, 21.78, 22.74, 28.1, 28.9, 36.6, 37.2, 38.6, 45.8, 67.6, 68.1, 116.3, 119.1, 120.1, 124.9, 125.2, 127.1,

127.21, 127.29, 127.5, 129.0, 129.1, 131.5, 135.8, 136.6, 136.8, 137.7, 139.0, 139.9, 140.5, 140.6, 172.5, 176.1.

(*S*,*S*)-(**145**):

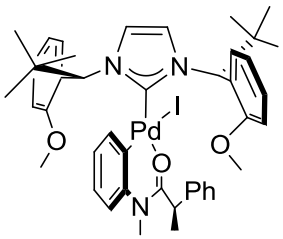

According to the same procedure as for the preparation of (*S*,*S*)-**101**, complex (*S*,*S*)-**145** was obtained in 58% yield as a yellow solid. (mixture of diastereoisomers), **m.p.** = 138-140 °C (decomp.). $[\alpha]_D^{25}$ = -57.1 (*c* = 1.0 in CH_2Cl_2), **^{1}H-NMR** (400 MHz, $CDCl_3$): δ 0.58 (s, 9H), 0.64 (s, 9H), 1.17 (s, 9H), 1.21 (s, 9H), 1.52 (d, *J* = 6.5 Hz, 3H), 1.69 (d, *J* = 6.5 Hz, 3H), 3.16 (s, 3H), 3.45 (s, 3H), 3.60 (s, 3H), 3.66 (s, 3H), 3.97 (s, 4H), 4.17 (q, *J* = 6.3 Hz, 1H), 4.99-5.08 (m, 2H), 5.98-6.08 (m, 3H), 6.52 (d, *J* = 7.6 Hz, 1H), 6.63-6.96 (m, 14H), 7.15-7.40 (m, 18H), 7.50 (s, 2H), 7.63 (d, *J* = 4.7 Hz, 2H), 7.81 (d, *J* = 6.6 Hz, 2H). **^{13}C-NMR** (100 MHz, $CDCl_3$): δ 16.5, 21.3, 22.4, 28.1, 28.3, 28.5, 35.9, 36.0, 36.4, 37.8, 38.3, 45.5, 45.7, 48.6, 55.4, 56.1, 84.0, 112.3, 112.63, 112.64, 115.0, 115.9, 119.9, 120.1, 123.4, 124.4, 124.5, 127.1, 127.2, 127.4, 128.3, 128.4, 128.5, 128.68, 128.69, 129.09, 129.1, 129.4, 130.1, 139.2, 139.7, 139.8, 140.4, 140.6, 157.3, 158.4, 175.0, 175.2, 180.6, 180.9. **IR** (neat, cm^{-1}): 2967, 1655, 1596, 1492, 1450, 1402, 1245, 1162, 1107, 1054, 1028, 909, 852, 803, 751, 728, 698, 630, 562. **HRMS** (EI): calcd. for $C_{43}H_{52}N_3O_3Pd$ ($[M\text{-}I]^+$): 764.3037, found: 764.3025. **Element analysis calcd** (%) for $C_{43}H_{52}IN_3O_3Pd$ (892): C 57.89%, H 5.87%, N 4.71% found for $C_{43}H_{52}IN_3O_3Pd$: C 58.63%, H 5.84%, N 5.18%.

(*S*,*S*)-(**146**):

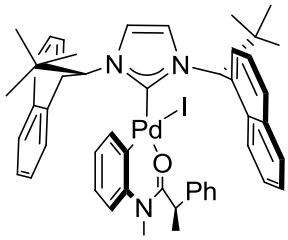

According to the same procedure as for the preparation of (*S*,*S*)-**101**, complex (*S*,*S*)-**146** was obtained in 64% yield as a yellow solid. (mixture of diastereoisomers), **m.p.** = 155-

158 °C $[\alpha]_D^{25}$ = -35.3 (*c* = 1.0 in CH_2Cl_2). **^{1}H-NMR** (400 MHz, $CDCl_3$): δ 0.73 (s, 9H), 0.86 (s, 5.8H), 1.31 (s, 5.8H), 1.35 (s, 9H), 1.51-1.54 (m, 5.6H), 3.49 (s, 1.9H), 3.57 (s, 3H), 3.92 (q, *J* = 6.7 Hz, 1H), 4.18 (q, *J* = 6.7 Hz, 0.59H), 4.97 (d, *J* = 7.5 Hz, 1.59H), 5.96 (t, *J* = 7.4 Hz, 0.6H), 6.04-6.08 (m, 1H), 6.39 (t, *J* = 7.7 Hz, 1H), 6.45 (d, *J* = 8.0 Hz, 0.6H), 6.61 (t, *J* = 7.9 Hz, 0.6H), 6.70 (d, *J* = 2.2 Hz, 3H), 6.98-8.07 (m, 43H), 8.50 (d, *J* = 8.5 Hz, 0.6H), 9.23 (d, *J* = 8.8 Hz, 0.6H), 9.42 (d, *J* = 8.7 Hz, 1H). **^{13}C-NMR** (100 MHz, $CDCl_3$): δ 21.5, 22.5, 26.9, 28.8, 28.9, 29.2, 36.54, 36.56, 36.9, 37.0, 37.5, 38.3, 44.1, 45.8, 66.46, 66.49, 67.1, 67.4, 114.4, 115.4, 119.5, 119.70, 119.74, 123.6, 123.8, 124.0, 124.12, 124.17, 124.2, 124.5, 124.7, 124.8, 124.9, 125.2, 125.3, 125.4, 125.7, 126.0, 126.2, 126.5, 126.62, 126.68, 126.9, 127.0, 127.1, 127.2, 127.5, 127.7, 127.8, 128.0, 128.1, 128.2, 128.3, 128.4, 128.52, 128.57, 129.0, 129.2, 129.4, 129.7, 130.9, 132.8, 133.2, 133.3, 133.4, 133.5, 133.70, 133.73, 133.77, 134.2, 134.5, 134.7, 135.3, 135.5, 137.1, 137.7, 138.2, 138.35, 138.38, 138.8, 139.7, 140.4, 173.4, 173.7, 175.2, 175.3. **IR** (neat, cm^{-1}): 3050, 2961, 1660, 1597, 1556, 1476, 1449, 1399, 1367, 1219, 1161, 1066, 1026, 783, 755, 697, 531. **HRMS** (EI): calcd. for $C_{49}H_{52}N_3OPd$ ([M-I]$^+$):804.3137, found: 804.3139. **Element analysis calcd** (%) for $C_{49}H_{52}IN_3OPd$ (932): C 63.13%, H 5.62%, N 4.51% found for $C_{49}H_{52}IN_3OPd$: C 63.49%, H 6.01%, N 4.50%.

IV.7. Catalytic Enantioselective Synthesis of a 3-Aryl-3-benzyl-oxindole (51) Exhibiting anti-Tumor Activity

3-(3-Chlorophenyl)-2-(3-methoxyphenyl)propanoic acid (**147a**):

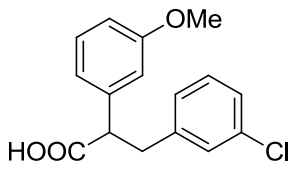

LDA was prepared by adding a 1.7M *n*BuLi (2 equiv., 14 mL soln. in pentane, 24.0 mmol) into freshly distilled diisopropylamine (2 equiv., 3.4 mL, 24.0 mmol) in THF (10 mL) and stirred for half an hour. 2-(3-methoxyphenyl)acetic acid (1 equiv., 2.0 g, 12.0 mmol) was added to the magnetically stirred solution at -78 °C. This was followed by the introduction of 3-chloro benzyl bromide (1 equiv., 2.46 g, 12 mmol. The reaction mixture was warmed to rt.and stirred for 16 h before quenching with 2M aq.soln. of HCl (50 mL) followed by extraction with AcOEt (3×20 mL). The organic layer was dried ($MgSO_4$), filtered, and the solvents were evaporated to give crude **147a** (3.17 g, 91%), which was used in the next step without further purification. **^{1}H-NMR** (400 MHz, $CDCl_3$): δ 3.03 (dd, *J* = 6.9, 13.8 Hz, 1H),

3.39 (dd, *J* = 6.9,13.8 Hz, 1H), 3.82 (s, 3H), 3.87 (m, 1H), 6.86 (d, *J* = 7.5 Hz, 1H), 6.88 (s, 1H), 6.92 (d, *J* = 7.5, 1H), 7.03 (m, 1H), 7.18 (m, 3H), 7.28 (d, *J* = 7.5 Hz, 1H). **^{13}C-NMR** (100 MHz, $CDCl_3$): δ 38.7, 53.1, 55.2, 113.1, 113.8, 120.4, 126.7, 127.1, 129.0, 129.6, 129.8, 134.11, 138.9, 140.6, 159.8.

N-(2-Bromo-5-chlorophenyl)-3-(3-chlorophenyl)-2-(3-methoxyphenyl)propanamide (**148**):

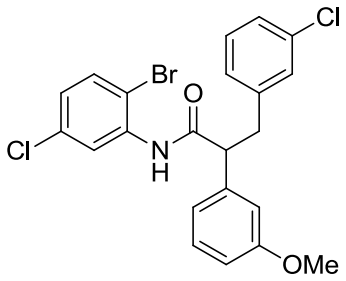

3-(3-Chlorophenyl)-2-(3-methoxyphenyl)propanoic acid (1 equiv., 2.0 g, 6.88 mmol) was reflux with $SOCl_2$ (3 equiv., 2.45 g, 20.6 mmol) for 2 h. The excess of $SOCl_2$ was removed under vacuum. To the crude acid chloride Et_3N (1.5 equiv., 1.04 g, 10.3 mmol) in CH_2Cl_2 (20 mL) was added at 0 °C followed by the addition of 2-bromo-5-chloroaniline (1 equiv., 1.4 g, 6.88 mmol). The resulting reaction mixture was stirred for 16 h at rt before quenching by the addition of an aq. soln. of NH_4Cl (10 mL). Extraction with CH_2Cl_2 (3×40 mL), drying over $MgSO_4$, and evaporation of volatiles afforded **148** (2.93 g, 89%). This was used in the next step without purification. Colorless oil. **^{1}H-NMR** (400 MHz, $CDCl_3$): δ 3.07 (dd, *J* = 7.9, 13.8 Hz, 1H), 3.61 (dd, *J* = 7.9, 13.8 Hz, 1H), 3.79 (m, 1H), 3.81 (s, 3H), 6.84 (m, 2H), 6.92 (m, 1H), 7.01 (m, 1H), 7.14 (d, *J* = 3.4 Hz, 3H), 7.29 (m, 1H), 7.34 (d, *J* = 8.5 Hz, 1H), 7.59 (bs, 1H), 8.42 (d, *J* = 1.7 Hz, 1H). **^{13}C-NMR** (100 MHz, $CDCl_3$): δ 38.3, 55.3, 56.2, 110.8, 113.5, 113.9, 118.6, 118.7, 120.6, 121.3, 125.1, 126.6, 127.2, 129.0, 129.6, 130.4, 132.7, 134.1, 134.2, 136.3, 139.3, 141.1, 160.2, 170.6. **IR** (neat, cm^{-1}): 3287, 3075, 2933, 2836, 1723, 1655, 1600, 1574, 1519, 1494, 1402, 1355, 1304, 1260, 1233, 1202, 1187, 1156, 1089, 1032, 996, 872, 858, 807, 787, 777, 695, 653.

N-((Benzyloxy)methyl)-N-(2-bromo-5-chlorophenyl)-3-(3-chlorophenyl)-2-(3-methoxyphenyl)propanamide (**149**):

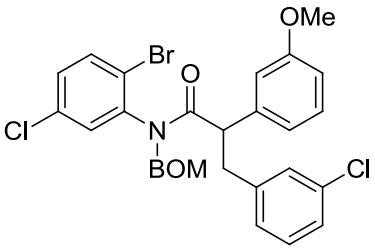

A suspension of NaH (1.5 equiv., 0.075 g, 3.13 mmol) in THF (10 mL) at 0 °C was treated with **148** (1 equiv., 1.0 g, 2.087 mmol) and the reaction mixture was stirred for 1 h at rt. Cooling to 0 °C was followed by slow addition of BOMCl (benzyl chloromethyl ether) (1.5 equiv., 0.49 g, 3.13 mmol). The reaction mixture was allowed to warm to rt, stirred for 20 h, quenched by the addition of aq. soln. of NH_4Cl (30 mL), extracted with AcOEt (3×40 mL), and dried over ($MgSO_4$). Solvent removal under reduced pressure and purification by flash chromatography (f.c) (pentane/EtOAc 7:1) gave **149** (0.937 g, 75%). Colorless oil. **^{1}H-NMR** (400 MHz, $CDCl_3$): δ 2.83 (dd, *J* = 3.9, 13.5 Hz, 1H), 2.87 (dd, *J* = 6.7, 13.6 Hz, 2H), 3.34 (t, *J* = 7.2 Hz, 2H), 3.50 (m, 3H), 3.58 (dd, *J* = 3.8, 11.0 Hz, 1H), 3.72 (s, 5H), 3.78 (s, 3H), 4.39 (d, *J* = 6.4 Hz, 1H), 4.50 (d, *J* = 10.6 Hz, 2H), 4.59 (d, *J* = 4.7 Hz, 3H), 5.64 (d, *J* = 10.6 Hz, 2H), 5.72 (d, *J* = 10.7 Hz, 1H), 6.42 (m, 6H), 6.70 (m, 2H), 6.80 (td, *J* = 2.1, 7.3, 7.9 Hz, 3H), 6.90 (m, 2H), 7.15 (m, 12H), 7.35 (m, 22H), 7.50 (d, *J* = 8.6 Hz, 1H), 7.60 (d, *J* = 8.6 Hz, 2H). **^{13}C-NMR** (100 MHz, $CDCl_3$) δ 40.4, 41.4, 52.0, 53.5, 55.2, 69.9, 70.9, 71.2, 75.8, 76.4, 88.6, 91.6, 113.2, 113.4, 113.7, 120.2, 120.8, 121.8, 122.1, 126.4, 127.0, 127.6, 127.8, 127.9, 128.4, 128.5, 129.4, 129.4, 129.5, 129.8, 129.9, 130.2, 130.4, 132.6, 133.3, 133.5, 133.8, 133.9, 134.3, 134.5, 137.6, 137.6, 139.4, 139.9, 140.0, 140.2, 141.4, 159.6, 159.9, 172.5, 172.7. **IR** (neat, cm^{-1}): 2938, 1674, 1596, 1578, 1464, 1402, 1257, 1147, 1116, 1090, 1049, 875, 812, 777, 731, 693.

N-(2-Bromo-5-chlorophenyl)-3-(3-chlorophenyl)-N-(methoxymethyl)-2-(3-methoxy phenyl)propanamide (**150**):

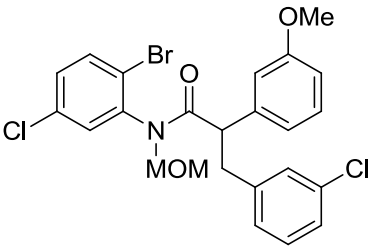

Synthesized using the same procedure as detailed for **149.** Scale 4.17 mmol of **148**. MOMCl (chloromethyl methyl ether) (1.5 equiv., 0.5 g, 6.26 mmol). **150** (1.87 g, 86%). Colorless oil. **^{1}H-NMR** (400 MHz, $CDCl_3$) mixture of rotamers: δ 2.82 (m, 1.4H), 3.22 (s, 1.4H), 3.29 (t, *J* = 6.7 Hz, 1 H), 3.35 (s, 3H), 3.45 (m, 2H), 3.71 (s, 3H), 3.77 (s, 1.4H), 4.28 (d, *J* = 10.5 Hz, 0.4H), 4.34 (d, *J* = 10.4 Hz, 1H), 5.52 (d, *J* = 10.4 Hz, 1H), 5.56 (d, *J* = 10.5 Hz, 0.4 H), 6.30 (d, *J* = 2.3 Hz, 0.4H), 6.36 (s, 1H), 6.41 (m, 2H), 6.67 (d, *J* = 7.6 Hz, 0.4H), 6.73 (s, 0.4H), 6.78 (d, *J* = 8.1 Hz, 1.4H), 6.91 (t, *J* = 3.8 Hz, 1H), 7.04 (s, 1.4H), 7.19 (m, 6H), 7.50 (d, *J* = 8.6 Hz, 0.4H), 7.58 (d, *J* = 8.5 Hz, 1H). **^{13}C-NMR** (100 MHz, $CDCl_3$): δ 40.4, 41.4, 52.1, 53.4, 55.2, 56.8, 56.9, 77.6, 78.0, 113.5, 113.1, 113.3, 113.7, 120.1, 126.4, 127.7, 129.3, 129.4, 130.1, 133.2, 133.9, 139.5, 139.9, 139.9, 140.2, 141.4, 141.4, 159.6, 159.9, 172.5, 172.7. **IR** (neat, cm^{-1}): 2937, 2833, 1674, 1596, 1577, 1465, 1436, 1400, 1362, 1257, 1113, 1079, 1029, 1003, 913, 875, 814, 776, 727, 693, 523. **HRMS** (EI): calcd. for $C_{24}H_{23}NO_3Cl_2Br$ ($[M+H]^+$): 522.0232, found: 522.0223.

(*R*)-6-Chloro-3-(3-chlorobenzyl)-1-(methoxymethyl)-3-(3-methoxyphenyl)indolin-2-one (**151**):

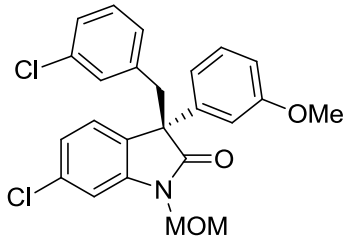

Under N_2, a dried Schlenk tube was charged with $Pd(dba)_2$ (5 mol%, 5.7 mg, 0.01 mmol), (R,R)-[**L12**H][I] (5 mol%, 7.02 mg, 0.01 mmol) and *t*BuONa (1.5 equiv., 28.8 mg, 0.3 mmol). Toluene (1 mL) was added and the mixture was stirred for 30 min at rt. After **150** (1 equiv., 104.6 mg, 0.2 mmol) was added as a soln. in toluene (3 mL), the reaction was stirred at 50 ˚C for 48 h. After the reaction mixture was quenched with sat. aq. soln. NH_4Cl (10 mL) and extracted with AcOEt (3×10 mL), the combined organic phases were washed with water (10 mL), brine (10 mL), and dried over ($MgSO_4$). Purification by f.c (pentane/AcOEt 10:1) afforded (*R*)-**151** (76.0 mg, 86% yield). Yellow oil. $\mathbf{[\alpha]_D^{20}}$ = +1.71 (*c* = 1.0, CH_2Cl_2). 90% *ee* [Chiracel AD-H column, *n*-hexane/*i*-PrOH = 99:1, 1.0 mL/min, 254 nm; t_R = 39.22 min (major) and 65.18 min (minor)]. **^{1}H-NMR** (400 MHz, $CDCl_3$): δ 2.95 (s, 3H), 3.42 (d, *J* = 13.0 Hz, 1H), 3.71 (d, *J* = 13.0 Hz, 1H), 3.79 (s, 3H), 4.88 (d, *J* = 11.0, 1H), 4.92 (d, *J* = 11.0 Hz, 1H), 6.72 (d, *J* = 7.6 Hz, 1H), 6.84 (dd, *J* = 2.4, 8.2 Hz, 1H), 6.98 (m, 5H),

7.06 (dd, *J* = 1.7, 7.9 Hz, 1H), 7.13 (dd, *J* = 1.8, 7.9 Hz, 1H), 7.20 (d, *J* = 8.0 Hz, 1H), 7.27 (t, *J* = 7.8 Hz, 1H). **^{13}C-NMR** (100 MHz, $CDCl_3$): δ 43.0, 55.3, 55.9, 58.1, 71.7, 110.6, 112.6, 113.5, 119.2, 122.9, 126.4, 127.1, 128.4, 128.6, 129.0, 129.8, 130.2, 133.7, 134.4, 137.4, 140.6, 143.2, 159.8, 177.70. **IR** (neat, cm^{-1}): 2933, 2834, 1720, 1604, 1487, 1432, 1394, 1340, 1290, 1240, 1179, 1129, 1081, 1049, 971, 915, 875, 781, 746, 686, 658. **HRMS** (EI): calcd. for $C_{24}H_{21}NO_3Cl_2Na$ ($[M]^+$): 464.0790, found: 464.0791.

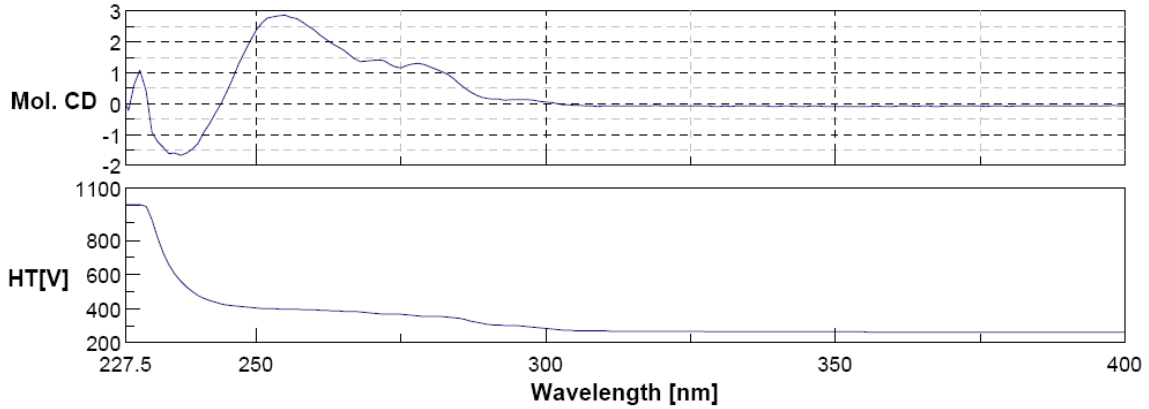

For CD spectrum: *c* = 0.0001 M in CH_2Cl_2.

(*S*)-1-((Benzyloxy)methyl)-6-chloro-3-(3-chlorobenzyl)-3-(3-methoxyphenyl)indolin-2-one (**152**):

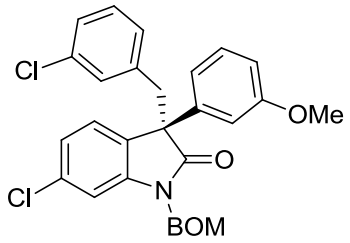

Under N_2, a dried Schlenk tube was charged with $Pd(dba)_2$ (5 mol%, 5.7 mg, 0.01 mmol), (S,S)-[**L14**H][I] (5 mol%, 5.8 mg, 0.01 mmol) and *t*BuONa (1.5 equiv., 28.8 mg, 0.3 mmol). Dimethoxyethane (DME) (1 mL) was added and the mixture was stirred for 10 min at rt. After amide **149** (1 equiv., 0.119 g, 0.2 mmol) was added as a soln. in toluene (3 mL), the reaction was stirred at rt for 48 h, quenched with sat. aq. soln. NH_4Cl (10 mL), and extracted with AcOEt (3×10 mL). The combined organic phases were washed with water (20 mL), brine (20 mL), and dried over ($MgSO_4$). The crude product was purified by f.c. (Pentane/AcOEt 10:1) giving (S)-**152** (0.032 mg, 31%). Yellow oil. $[\alpha]_D^{20}$ = -1.89 (*c* = 1.0, CH_2Cl_2). 86% *ee* HPLC (Chiralcel AD-H column, *n*-hexane/*i*-PrOH = 95:5, 1.0 mL/min, 254 nm; t_R = 17.80

min (minor) and 39.38 min (major)]. **^{1}H-NMR** (400 MHz, $CDCl_3$): δ 3.49 (d, *J* = 13.1 Hz, 1H), 3.76 (d, *J* = 13.0 Hz, 1H), 3.85 (s, 3H), 3.98 (d, *J* = 11.6 Hz, 1H), 4.18 (d, *J* = 11.6 Hz, 1H), 5.02 (d, *J* = 11.2 Hz, 1H), 5.12 (d, *J* = 11.2 Hz, 1H), 6.81 (d, *J* = 6.8 Hz, 1H), 6.90 (m, 2H), 7.01 (m, 8H), 7.28 (m, 11H). **^{13}C-NMR** (100 MHz, $CDCl_3$): δ 43.0, 55.33, 58.1, 69.8, 70.1, 110.8, 112.61, 113.62, 119.3, 123.0, 126.4, 127.2, 127.9, 128.1, 128.3, 128.7, 129.1, 129.8, 130.3, 133.7, 134.5, 136.9, 137.3, 140.6, 143.2, 159.8, 177.6. **IR** (neat, cm^{-1}): 2921, 2852, 1725, 1606, 1488, 1458, 1290, 1259, 1083, 1021, 800, 744, 696. **HRMS** (EI): calcd. for $C_{30}H_{25}NO_3Cl_2Na$ ($[M+Na]^+$): 540.1127, found: 540.1103.

(*R*)-6-Chloro-3-(3-chlorobenzyl)-3-(3-methoxyphenyl)indolin-2-one (**51**):

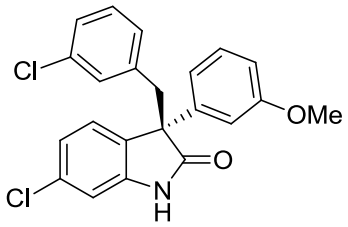

To a solution of oxindole **151** (1 equiv., 76 mg, 0.17 mmol) in CH_3CN (6 mL) at 0 °C were added trimethylsilyl chloride (4.5 equiv., 83 mg, 0.76 mmol), NaI (4.5 equiv., 114 mg, 0.76 mmol) and the resulting mixture was stirred at 0° for 1 h. The reaction was quenched with sat. aq. soln. $NaHCO_3$ (6 mL) and extracted with AcOEt (2×15 mL). The organic layers were combined, washed with brine (20 ml), dried over (Na_2SO_4), filtered, and concentrated in vacuum. MeOH (40 mL) at rt was added followed by Et_3N (3 equiv., 52.0 mg, 0.51 mmol). This mixture was stirred at 60 °C for 30 min. After cooling to rt, the reaction was quenched with sat. aq. soln. NH_4Cl (20 mL) and hexane/AcOEt (1/1, 100 mL) was added. The organic layer was separated and the aqueous layer was extracted with hexane (2×30 mL). The organic layers were combined, washed with brine (100 mL), dried over (Na_2SO_4), filtered, and concentrated in vacuum. The residue was purified by f.c. (hexane/AcOEt 5/1) to afford (*R*)-**51** (61.6 mg, 91%). Recrystallization from dichloromethane-hexane gave (*R*)-**51** (53.0 mg, 79%). White solid, **m.p.** = 164.5-166.5 °C. **$[\alpha]_D^{20}$** = +8.7 (*c* = 1.0, CH_2Cl_2). 96% *ee* [Chiracel OD-H column, *n*-hexane/*i*-PrOH = 70:30, 1.0 mL/min, 254 nm; t_R = 6.98 min (minor) and 23.91 min (major)]. **^{1}H-NMR** (400 MHz, $CDCl_3$): δ 3.53 (d, *J* = 12.8 Hz, 1H), 3.64 (d, *J* = 12.8 Hz, 1H), 3.78 (s, 3H), 6.74 (d, *J* = 1.8 Hz, 1H), 6.87 (m, 2H), 7.05 (m, 6H), 7.28 (m, 2H). **^{13}C-NMR** (100 MHz, $CDCl_3$): δ 41.7, 54.2, 58.4, 109.8, 112.2, 112.7, 118.7, 121.6, 126.4, 126.4, 128.2, 128.7, 129.3, 129.7, 130.7, 133.0, 133.6, 137.9, 141.0, 142.9, 159.9, 180.3. **IR** (neat, cm^{-1}):

3222, 2930, 2835, 1711, 1612, 1596, 1485, 1454, 1431, 1322, 1255, 1221, 1174, 1069, 1037, 859, 786, 691, 635, 590. **HRMS** (EI): calcd. for $C_{22}H_{17}Cl_2NO_2$ ($[M]^+$): 398.0706, found: 398.0709.

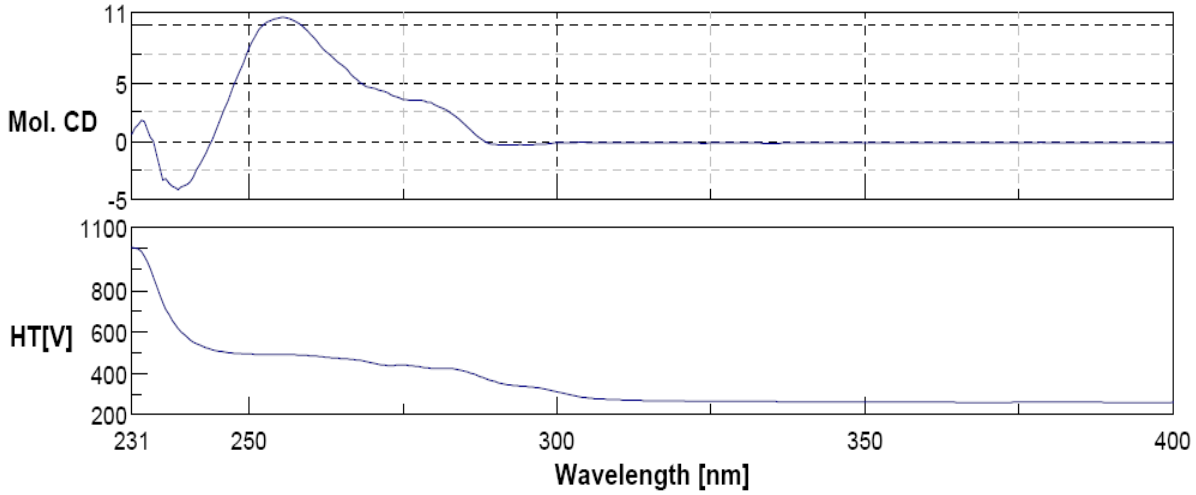

For CD spectrum: c = 0.0001 M in CH_2Cl_2.

IV.8. Synthesis of *N*-Cycloalkyl-2-Bromoaniline

IV.8.1. Representative Procedure 1 for *N*-Alkyl-2-Bromoaniline by Reductive Amination[256]

2-Bromoaniline (1.7 g, 10 mmol), molecular sieves 4Å (2.5 g) and alkanone (2-5 equiv.) was dissolved in benzene (50 mL). The reaction mixture was stirred refluxed with Dean-Stark apparatus for 4 days. The reaction mixture was filtered through celite and washed with diethyl ether. The filtrate was evaporated by rotary evaporator and dried under vacuum. The crude imine was dissolved in absolute methanol (50 mL) and $NaBH_4$ (3 equiv.) was added slowly under nitrogen. The reaction mixture as stirred for 2 h. 1*N*-KOH aq. (50 mL) was added and the extracted with dichloromethane. The organic phase was dried over Na_2SO_4. After filtration and evaporation, the residue was purified by flush column chromatography (silica gel; diethyl ether/pentane as eluent) affording *N*-alkyl-*o*-bromoaniline.

IV.8.2. Representative Procedure 2 for Palladium-Catalyzed N-Arylation[271]

$Pd_2(dba)_3$ (2 mol%), *rac*-BINAP (6 mol%), and sodium *t*BuONa (1.4 equiv.) were successfully filled into a schlenk flask. After the flask was evacuated and backfilled with nitrogen, dry toluene, amine (1.1 equiv.) and 1,2-dibromobenzene (1 equiv.) was added under

nitrogen. The resulting reaction mixture was stirred at 110 °C in the shield Schlenk tube for 24 h. The reaction mixture was cooled down to rt and diluted with ethylacetate (10 mL) followed by filtration through the pad of celite. The filtrate was evaporated by rotary evaporator and the volatiles were removed under high vacuum. The residue was purified by flash column chromatography (silica gel; diethyl ether/pentane as eluent) to afford 2-bromo-*N*-alkylaniline.

2-Bromo-*N*-isopropylaniline (**178**):[234]

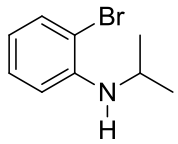

Colorless oil, 26% yield. **^{1}H-NMR** (400 MHz, $CDCl_3$): δ 1.24 (d, *J* = 6.4, 6H), 3.64 (oct, *J* = 6.4, 1H), 4.13 (d, *J* = 6.8 Hz, 1H), 6.51 (td, *J* = 7.6, 1.6 Hz, 1H), 6.63 (dd, *J* = 7.6, 1.6Hz, 1H), 7.15 (dd, *J* = 7.6, 1.6 Hz, 1H), 7.39 (dd, *J* = 8, 1.6 Hz, 1H). **^{13}C-NMR** (100 MHz, $CDCl_3$): δ 23.1, 44.5, 110.0, 112.0, 117.4, 128.6, 132.7, 144.4. **IR** (neat, cm^{-1}): 3405, 2966, 2929, 1595, 1506, 1462, 1425, 1384, 1366, 1318, 736, 1285, 1175, 1153, 1112, 1017. **HRMS** (ESI): calcd. for $C_9H_{12}NBr$ ($[M]^+$): 213.0153, found 213.0150.

2-Bromo-*N*-(sec-butyl)aniline (**182**):[234]

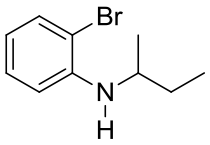

Colorless oil, 66% yield. **^{1}H-NMR** (400 MHz, $CDCl_3$): δ 0.95 (t, *J* = 7.6 Hz, 1H), 1.20 (t, *J* = 6.4 Hz, 1H), 1.45-1.67 (m, 2H), 3.32-3.47 (m, 1H), 4.13 (d, *J* = 6.8 Hz, 1H), 6.50 (td, *J* = 8, 1.6 Hz, 1H), 6.61 (dd, *J* = 8, 0.8 Hz, 1H), 7.14 (td, *J* = 7.6, 0.8 Hz, 1H), 7.39 (dd, *J* = 8, 1.6 Hz, 1H).

2-Bromo-*N*-(pentan-2-yl)aniline (**183**):

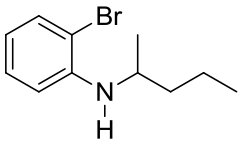

Colorless oil, 45% yield. **^{1}H-NMR** (400 MHz, $CDCl_3$): δ 0.91 (t, *J* =7.2 Hz, 1H), 1.19 (d, *J* = 6.4 Hz, 1H), 1.31-1.65 (m, 4H), 3.40-3.56 (m, 1H), 3.95-4.35 (brd, 1H), 6.50 (td, *J* = 7.6, 1.6 Hz, 1H), 6.61 (dd, *J* = 8.4, 1.2 Hz, 1H), 7.13 (dd, *J* = 7.2, 1.2 Hz, 1H), 7.39 (dd, *J* = 8, 1.6 Hz, 1H). **^{13}C-NMR** (100 MHz, $CDCl_3$): δ 14.3, 19.5, 20.9, 39.4, 48.6, 110.0, 111.8, 117.3, 128.6, 132.7, 144.6. **IR** (neat, cm^{-1}): 3408, 2960, 2930, 2871, 1595, 1508, 1459, 1426, 1378, 1321, 1286, 1166, 1112, 1048, 1018, 739. **HRMS** (ESI): calcd. for $C_{11}H_{17}BrN$ ($[M+H]^+$): 242.0538, found 242.0534.

2-Bromo-*N*-(1-phenylpropan-2-yl)aniline (**185**):

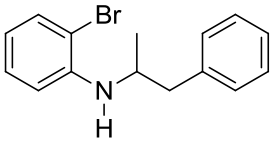

Colorless oil, 47% yield. **^{1}H-NMR** (400 MHz, $CDCl_3$): δ 1.20 (d, *J* = 6.4 Hz, 3H), 2.71 (qd, *J* = 13.2, 4.8 Hz, 2H), 3.72-3.86 (m, 1H), 4.10-4.42 (brd, 1H), 6.54 (td, *J* = 7.6, 1.2 Hz, 1H), 6.70 (dd, *J* = 8.4, 1.6 Hz, 1H), 7.13-7.26 (m, 4H), 7.26-7.34 (m, 2H), 7.42 (dd, *J* = 7.6, 1.6 Hz, 1H). **^{13}C-NMR** (100 MHz, $CDCl_3$): δ 20.3, 42.5, 49.8, 110.2, 112.0, 117.7, 126.6, 128.6, 128.7, 129.7, 132.8, 138.4, 144.1. **IR** (neat, cm^{-1}): 3401, 3063, 3026, 2967, 2926, 1594, 1453, 1427, 1377, 1319, 1283, 1245, 1201, 1151, 1112, 1046, 1016, 737. **HRMS** (ESI): calcd. for $C_{15}H_{16}BrN$ ($[M]^+$): 289.0466, found 289.0462.

2-Bromo-*N*-(4-phenylbutan-2-yl)aniline (**186**):[272]

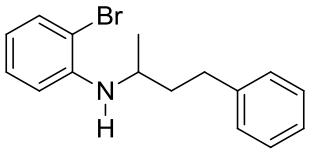

Colorless oil, 43% yield. **^{1}H-NMR** (400 MHz, $CDCl_3$): δ 1.26 (d, *J* = 6.4 Hz, 3H), 1.76-2.00 (m, 2H), 2.73 (t, *J* = 8 Hz, 2H), 3.44-3.58 (m, 1H), 4.02-4.30 (brd, 1H), 6.48-6.56 (m, 2H), 7.12 (td, *J* = 7.6, 1.6 Hz, 1H), 7.15-7.22 (m, 3H), 7.25-7.32 (m, 2H), 7.41 (dd, *J* = 8.4, 1.6 Hz, 1H). **^{13}C-NMR** (100 MHz, $CDCl_3$): δ 21.0, 32.6, 38.9, 48.2, 110.1, 112.0, 117.5, 126.1, 128.6, 132.7, 141.9, 144.3. **IR** (neat, cm^{-1}): 3403, 3062, 3026, 2965, 1595, 1506, 1457, 1426, 1378, 1320, 1286, 1190, 1161, 1094, 1061, 1017. **HRMS** (EI): calcd. for $C_{16}H_{18}BrN$ ($[M]^+$): 303.0623, found 303.0620.

Ethyl 4-((2-bromophenyl)amino)pentanoate (**188**):

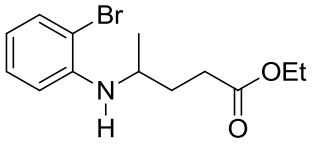

Colorless oil, 8% yield. **^{1}H-NMR** (400 MHz, $CDCl_3$): δ 1.22 (t, *J* = 7.2 Hz, 3H), 1.22 d, *J* = 6.4 Hz, 3H), 1.78-2.00 (m, 2H), 2.41 (t, *J* = 7.6 Hz, 2H), 4.11 (q, *J* = 7.2 Hz, 1H), 4.11 (brd, 1H), 6.52 (td, *J* = 8, 1.2 Hz, 1H), 6.64 (dd, *J* = 8.4, 1.2 Hz, 1H), 7.14 (d, *J* = 7.8, 1.2 Hz, 1H), 7.39 (dd, *J* = 8, 1.6 Hz, 1H). **^{13}C-NMR** (100 MHz, $CDCl_3$): δ 14.4, 20.9, 31.2, 31.9, 48.4, 60.7, 110.2, 112.0, 117.7, 128.7, 132.8, 144.3, 173.7. **IR** (neat, cm^{-1}): 3383, 2972, 1729, 1595, 1506, 1460, 1428, 1375, 1320, 1258, 1215, 1178, 1119, 1095, 1017,739. **HRMS** (ESI): calcd. for $C_{13}H_{19}BrNO_2$ ($[M+H]^+$): 300.0593, found 300.0597.

2-Bromo-*N*-(5-((tert-butyldimethylsilyl)oxy)pentan-2-yl)aniline (**188**):

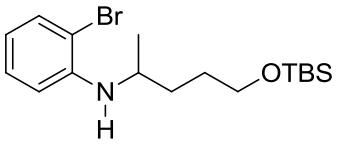

Colorless oil, 50% yield. **^{1}H-NMR** (400 MHz, $CDCl_3$): δ 0.03 (s, 3H), 0.03 (s, 3H), 0.87 (s, 9H), 1.21 (d, *J* = 6.4 Hz, 3H), 3.44-3.56 (m, 1H), 3.62 (t, *J* = 6 Hz, 2H), 3.98-4.32 (brd, 1H), 6.50 (td, *J* = 8, 1.6 Hz, 1H), 6.61 (dd, *J* = 8, 1.2 Hz, 1H), 7.13 (td, *J* = 7.6, 1.6 Hz, 1H), 7.38 (dd, *J* = 7.6, 1.6 Hz, 1H). **^{13}C-NMR** (100 MHz, $CDCl_3$): δ -5.1, 18.6, 21.0, 26.2, 29.5, 33.4, 48.7, 63.2, 110.0, 111.9, 117.3, 128.6, 132.7, 144.5. **IR** (neat, cm^{-1}): 3409, 2929, 2857, 1596, 1460, 1427, 1381, 1285, 1252, 1206, 1092, 1017, 939, 833, 737. **HRMS** (ESI): calcd. for $C_{17}H_{31}BrNOSi$ ($[M+H]^+$): 372.1335, found 372.1336.

2-Bromo-*N*-(6-methylhept-5-en-2-yl)aniline (**190**):

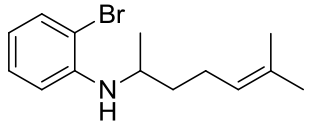

Colorless oil, 64% yield. **^{1}H-NMR** (400 MHz, , $CDCl_3$): δ 1.25 (d, *J* = 6.3 Hz, 3H), 1.50-1.59 (m, 1H), 1.61 (s, 3H), 1.67 (dd, *J* = 14.1, 6.7 Hz, 1H), 1.71-1.75 (m, 4H), 2.13 (q, *J* = 7.4 Hz, 2H), 3.39-3.69 (m, 1H), 4.18 (s, 1H), 5.16 (tt, *J* = 7.2, 1.4 Hz, 1H), 6.54 (td, *J* = 7.8,

1.5 Hz, 1H), 6.64 (dd, *J* = 8.2, 1.2 Hz, 1H), 7.12-7.24 (m, 1H), 7.43 (dd, *J* = 7.9, 1.5 Hz, 1H). **^{13}C-NMR** (100 MHz, $CDCl_3$): δ 17.9, 20.9, 24.8, 26.0, 37.2, 48.3, 110.0, 111.8, 117.2, 123.9, 128.6, 132.7, 144.6. **IR** (neat, cm^{-1}): 3410, 2965, 2923, 2857, 1595, 1507, 1458, 1377, 1321, 1017, 830, 737, 657. **HRMS** (ESI): calcd. for $C_{14}H_{21}BrN$ ($[M+H]^+$): 282.0851, found 282.0847.

2-Bromo-*N*-(1-(methylthio)propan-2-yl)aniline (**191**):

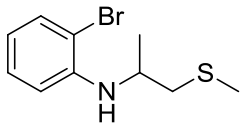

Colorless oil, 56% yield. **^{1}H-NMR** (400 MHz, $CDCl_3$): δ 1.36 (d, *J* = 6.4 Hz, 3H), 2.16 (s, 3H), 2.63 (dd, *J* = 13.3, 6.8 Hz, 1H), 2.80 (dd, *J* = 13.3, 4.7 Hz, 1H), 3.74 (dp, *J* = 12.9, 6.5 Hz, 1H), 4.46 (d, *J* = 7.3 Hz, 1H), 6.57 (td, *J* = 7.6, 1.4 Hz, 1H), 6.65 (dd, *J* = 8.2, 1.0 Hz, 1H), 7.21-7.12 (m, 1H), 7.43 (dd, *J* = 7.9, 1.5 Hz, 1H). **^{13}C-NMR** (100 MHz, $CDCl_3$): δ 16.9, 20.4, 40.9, 48.5, 110.3, 111.9, 118.0, 128.6, 132.9, 144.0. **IR** (neat, cm^{-1}): 3383, 2968, 2915, 1744, 1593, 1500, 1457, 1426, 1316, 1284, 1150, 1016, 957, 738. **HRMS** (ESI): calcd. for $C_{10}H_{14}NBrS$ ($[M]^+$): 259.0025, found: 259.0026.

2-Bromo-*N*-(1-methoxypropan-2-yl)aniline (**211**):

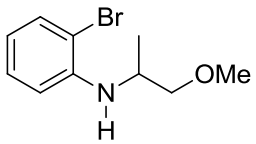

Colorless oil, 58% yield. **^{1}H-NMR** (400 MHz, $CDCl_3$): δ 1.25 (d, *J* = 6.4 Hz, 3H), 3.38 (s, 3H), 3.42 (qd, *J* = 9.6, 4.8 Hz, 2H), 3.61-3.73 (m, 1H), 4.15-4.85 (brd, 1H), 6.53 (td, *J* = 8, 1.6 Hz, 1H), 6.67 (dd, *J* = 8, 1.2 Hz, 1H), 7.14 (td, *J* = 7.6, 1.6 Hz, 1H), 7.40 (dd, *J* = 8, 1.6 Hz, 1H). **^{13}C-NMR** (100 MHz, $CDCl_3$): δ 18.2, 48.7, 59.4, 110.4, 112.1, 117.9, 128.6, 132.8, 144.4. **IR** (neat, cm^{-1}): 3403, 2977, 2926, 2879, 2829, 1595, 1504, 1457, 1428, 1388, 1369, 1284, 1239, 1198, 1166, 1100, 1018, 986, 922, 738. **HRMS** (ESI): calcd. for $C_{10}H_{15}BrNO$ 244.0331, found 244.0327.

2-Bromo-*N*-(1-methoxybutan-2-yl)aniline (**213**):

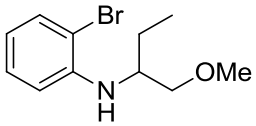

Colorless oil, 55% yield. **^{1}H-NMR** (400 MHz, $CDCl_3$): δ 0.99 (t, *J* = 7.5 Hz, 2H), 1.59 (dt, *J* = 14.0, 7.1 Hz, 1H), 1.67-1.84 (m, 1H), 3.38 (s, 2H), 3.39-3.55 (m, 2H), 4.39-4.42 (brm, 1H), 6.54 (td, *J* = 7.8, 1.5 Hz, 1H), 6.67 (dd, *J* = 8.2, 1.3 Hz, 1H), 7.11-7.21 (m, 1H), 7.42 (dd, *J* = 7.9, 1.5 Hz, 1H). **^{13}C-NMR** (100 MHz, $CDCl_3$): δ 10.7, 25.1, 54.7, 59.4, 74.2, 110.2, 111.9, 117.6, 128.6, 132.7, 133.9, 144.7. **IR** (neat, cm^{-1}): 3402, 3070, 2965, 2927, 2876, 1738, 1595, 1506, 1459, 1430, 1284, 1237, 1196, 1104, 1017, 960, 925, 936, 738. **HRMS** (ESI): calcd. for $C_{11}H_{17}BrN_1O$ ($[M+H]^+$): 258.0488, found 258.0491.

2-Bromo-*N*-(4-(methoxymethoxy)butan-2-yl)aniline (**214**):

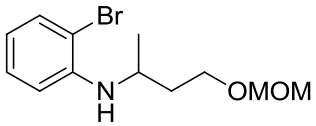

Colorless oil, 63% yield. **^{1}H-NMR** (400 MHz, $CDCl_3$): δ 1.01 (t, *J* = 7.5 Hz, 3H), 1.57-1.66 (m, 1H), 1.87 – 1.70 (m, 1H), 3.37 (s, 3H), 3.46-3.53 (m, 1H), 3.59 (dd, *J* = 9.8, 4.9 Hz, 2H), 3.65 (dd, *J* = 9.8, 4.4 Hz, 2H), 4.45 (d, *J* = 7.5 Hz, 2H), 4.64 (dd, *J* = 8.7, 6.5 Hz, 2H), 6.54 (td, *J* = 7.8, 1.5 Hz, 2H), 6.67 (dd, *J* = 8.3, 1.1 Hz, 3H), 7.15 (ddd, *J* = 8.6, 7.4, 1.5 Hz, 2H), 7.41 (dd, *J* = 7.9, 1.5 Hz, 2H). **^{13}C-NMR** (100 MHz, $CDCl_3$): δ 10.6, 25.1, 54.6, 55.5, 69.1, 96.9, 110.2, 111.9, 117.6, 128.6, 132.7, 144.7. **IR** (neat, cm^{-1}): 3403, 2932, 1595, 1506, 1460, 1320, 1151, 1107, 1044, 1018, 918, 740. **HRMS** (EI): calcd. for $C_{12}H_{18}N_1O_2Br$ ($[M]^+$): 287.0515, found: 287.0517.

Methyl (2-bromophenyl)(isopropyl)carbamate (**192**):[234]

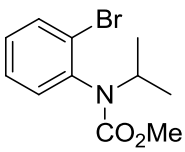

White solid, **m.p.** = 47 °C, 77% yield. **^{1}H-NMR** (400 MHz, $CDCl_3$): δ 1.01 (d, *J* = 7.2 Hz, 3H), 1.30 (d, *J* = 6.4 Hz, 3H), 3.61 (s, 3H), 4.36-4.42 (m, 1H), 7.15 (dd, *J* = 7.6, 1.6 Hz, 1H), 7.17 (d, *J* = 7.6 Hz, 1H), 7.30 (td, *J* = 7.6, 1.6 Hz, 1H), 7.62 (d, *J* = 7.6, 1.2 Hz, 1H). **^{13}C-**

NMR (100 MHz, $CDCl_3$): δ 19.8, 22.8, 50.5, 53.0, 126.1, 128.0, 129.1, 130.8, 133.6, 138.6, 155.4. **IR** (neat, cm^{-1}): 2977, 1706, 1586, 1477, 1441, 1390, 1368, 1319, 1276, 1265, 1249, 1194, 1134, 1095, 1051, 980, 955, 861, 785, 755, 726. **HRMS** (ESI): calcd. for $C_{11}H_{14}NNaO_2Br$ ($[M]^+$): 294.0100, found 253.0099.

Methyl (2-bromophenyl)(pentan-2-yl)carbamate (**196**):

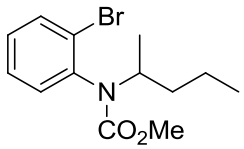

Colorless oil, 99% yield. **^{1}H-NMR** (400 MHz, $CDCl_3$): δ 0.85 (t, *J* = 7.2 Hz, 1.2H), 0.91-1.00 (m, 4H), 1.07-1.53 (m, 3.8H), 1.61-1.77 (m, 1H), 3.61 (s, 3H), 4.10-4.24 (m, 0.4H), 4.30-4.55 (m, 0.6H), 7.10-7.22 (m, 2H), 7.26-7.34 (m, 1H), 7.38 (d, *J* = 8, 1H). **^{13}C-NMR** (100 MHz, $CDCl_3$): δ 14.2, 14.2, 17.3, 20.0, 20.4, 52.9, 53.0, 54.3, 55.7, 125.8, 126.3, 128.0, 128.8, 128.9, 130.5, 138.4, 139.6, 155.3, 155.7. **IR** (neat, cm^{-1}): 2957, 2872, 1605, 1585, 1475, 1440, 1390, 1319, 1264, 1191, 1056, 1028, 951, 911, 869, 785, 761, 746, 728. **HRMS** (ESI): calcd. for $C_{13}H_{19}BrNO_2$ ($[M+H]^+$): 300.0593, found 300.0604.

Methyl (2-bromophenyl)(1-phenylpropan-2-yl)carbamate (**198**):

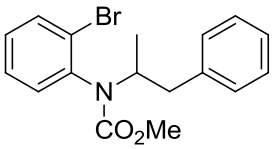

White solid, **m.p.** = 102 °C, 97% yield. **^{1}H-NMR** (400 MHz, $CDCl_3$): δ 0.90 (d, *J* = 6.8 Hz, 1.7H), 0.83 (d, *J* = 6.8 Hz, 1.3H), 2.44 (dd, *J* = 12.8, 9.2 Hz, 0.4H), 2.78 (dd, *J* = 12.8, 10 Hz, 0.6H), 3.27 (dd, *J* = 12.8, 8.4 Hz, 0.6H), 3.33-3.43 (m, 0.4H), 3.65 (s, 3H), 4.10-4.26 (m, 0.4H), 4.34-4.64 (m, 0.6H), 6.70 (d, *J* = 7.2 Hz, 0.4H), 7.05-7.37 (m, 7.6H), 7.56-7.66 (m, 1H). **^{13}C-NMR** (100 MHz, $CDCl_3$): δ 16.3, 19.3, 40.8, 43.3, 53.0, 53.1, 56.3, 59.2, 125.3, 126.2, 126.6, 128.2, 128.2, 128.6, 128.9, 129.2, 129.6, 130.6, 130.7, 133.6, 138.9, 139.5, 140.3, 155.2, 155.6. **IR** (neat, cm^{-1}): 3062, 3027, 2978, 2951, 1704, 1585, 1475, 1440, 1388, 1325, 1293, 1191, 1167, 1069, 1029, 983, 951, 915, 860, 830, 761, 744, 729, 700. **HRMS** (ESI): calcd. for $C_{17}H_{19}BrNO_2$ ($[M+H]^+$): 348.0593, found 348.0589.

Methyl (2-bromophenyl)(4-phenylbutan-2-yl)carbamate (**199**):

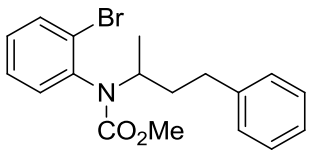

White solid, **m.p.** = 61 °C, 88% yield. **^{1}H-NMR** (400 MHz, $CDCl_3$): δ 1.12 (d, *J* = 6.8 Hz, 1.9H),): 1.48 (d, *J* = 6.8 Hz, 1.1H), 1.55-1.67 (m, 0.4H), 1.82-1.99 (m, 0.6H), 2.08-2.26 (m, 1H), 2.70 (d, *J* = 8.4 Hz, 0.7H), 2.81 (t, *J* = 8.4 Hz, 1.3H), 3.71 (s, 3H), 4.23-4.39 (m, 0.4H), 4.49-4.67 (m, 0.6H), 7.15-7.45 (m, 8H), 7.70 (td, *J* = 8.4, 1.2 Hz, 1H). **^{13}C-NMR** (100 MHz, $CDCl_3$): δ 17.3, 20.2, 33.3, 33.6, 35.9, 39.0, 53.0, 53.1, 54.5, 55.7, 125.7, 126.1, 126.1, 126.3, 128.2, 128.5, 128.6, 128.9, 129.1, 133.7, 138.5, 141.8, 142.0, 155.4, 155.8. **IR** (neat, cm^{-1}): 3026, 2950, 1705, 1585, 1475, 1440, 1389, 1317, 1190, 1060, 1043, 952, 750, 724. **HRMS** (ESI): calcd. for $C_{15}H_{20}NO_4$ ($[M+H]^+$): 278.1386, found 278.1390.

Ethyl 4-((2-bromophenyl)(methoxycarbonyl)amino)pentanoate (**200**):

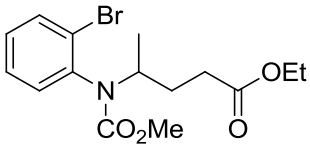

Colorless oil, >99% yield. **^{1}H-NMR** (400 MHz, $CDCl_3$): δ 0.99 (d, *J* = 6.8 Hz, 2H), 1.45-1.28 (m, 3.2H), 1.34 (d, *J* = 6.8 Hz, 1H), 1.54-1.68 (m, 0.8H), 1.68-1.81 (m, 2H), 1.77-1.91 (m, 0.7H), 1.97-2.14 (m, 1H), 2.36 (t, *J* = 7.6 Hz, 0.7H), 2.45 (t, *J* = 7.6 Hz, 1.3H), 3.61 (s, 3H), 4.02-4.20 (m, 2.3H), 4.30-4.56 (m, 0.7H), 7.11-7.23 (m, 2H), 7.26-7.35 (m, 1H), 7.62 (d, *J* = 7.6 Hz, 1H). **^{13}C-NMR** (100 MHz, $CDCl_3$): δ 14.4, 17.4, 19.9, 29.3, 31.8, 32.1, 53.0, 53.2, 53.8, 55.7, 60.6, 60.7, 125.5, 126.3, 128.2, 128.2, 129.0, 129.1, 130.5, 130.6, 133.7, 133.8, 138.2, 139.5, 155.8. **IR** (neat, cm^{-1}): 2980, 1706, 1586, 1475, 1441, 1390, 1319, 1129, 1119, 1076, 1029, 946, 856, 785, 758. **HRMS** (ESI): calcd. for $C_{15}H_{21}BrNO_4$ ($[M+H]^+$): 358.0648, found 358.0640.

Methyl (2-bromophenyl)(5-((*tert*-butyldimethylsilyl)oxy)pentan-2-yl)carbamate (**201**):

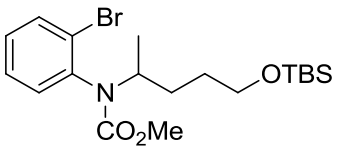

Colorless oil, 29% yield. **^{1}H-NMR** (400 MHz, $CDCl_3$): δ -0.04 (s, 1H), -0.03 (s, 1H), 0.04 (s, 3.8H), 0.08 (s, 0.8H), 0.82 (s, 3.2H),), 0.88 (d *J* = 6.8 Hz, 1.1H), 0.89 (s, 5H), 0.98 (d *J* = 6.8 Hz, 1.9H),), 1.34 (d *J* = 6.8 Hz, 1.1H), 1.44-1.85 (m, 4H), 3.47-3.74 (m, 2H), 3.61 (s, 3H), 4.08-4.28 (m, 0.4H), 4.40-4.58 (m, 0.6H) 7.10-7.23 (m, 2H), 7.29 (td, *J* = 8, 1.2 Hz, 1H), 7.14 (d, *J* = 8, 1.2 Hz, 1H), 7.38 (dd, *J* = 8, 1.2 Hz, 1H). **^{13}C-NMR** (100 MHz, $CDCl_3$): δ -5.2, -5.1, 15.5, 17.6, 18.5, 18.6, 20.1, 26.2, 26.2, 30.0, 30.5, 33.4, 53.0, 53.1, 54.2, 55.8, 63.1, 125.8, 126.4, 128.1, 128.9, 129.0, 130.6, 130.7, 138.2, 155.9 . **IR** (neat, cm^{-1}): 2952, 2857, 1711, 1586, 1475, 1441, 1390, 1321, 1252, 1192, 1090, 1030, 1006, 939, 833, 774, 729. **HRMS** (ESI): calcd. for $C_{19}H_{33}BrNO_3Si$ 430.1407, found 430.1406.

Methyl (2-bromophenyl)(6-methylhept-5-en-2-yl)carbamate (**202**):

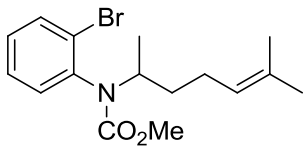

Colorless oil, 69% yield. **^{1}H-NMR** (400 MHz, $CDCl_3$): δ 0.99 (d, *J* = 6.9 Hz, 5H), 1.13-1.28 (m, 1H), 1.35 (d, *J* = 6.7 Hz, 3H), 1.44-1.59 (m, 6H), 1.62 (s, 6H), 1.65 (s, 3H), 1.70 (s, 6H), 1.72-1.87 (m, 3H), 1.98 (q, *J* = 7.6, 6.8 Hz, 3H), 2.08 (q, *J* = 7.5 Hz, 4H), 3.62 (s, 6H), 4.11-4.31 (brm, 2H), 4.43 (brm, 2H), 5.04 (tt, *J* = 7.0, 1.3 Hz, 2H), 5.16 (t, *J* = 7.1 Hz, 2H), 7.10-7.24 (m, 7H), 7.27-7.36 (m, 2H), 7.52-7.72 (m, 3H). **^{13}C-NMR** (100 MHz, $CDCl_3$): δ 17.2, 17.9, 19.9, 25.4, 25.7, 25.9, 34.0, 37.1, 53.0, 53.09, 54.4, 55.6, 110.3, 123.9, 125.8, 126.3, 128.0, 128.8, 129.0, 130.5, 130.6, 132.2, 133.6, 138.5, 139.6, 155.3, 155.7. **IR** (neat, cm^{-1}): 2974, 2926, 2853, 1708, 1586, 1475, 1440, 1389, 1314, 1265, 1191, 1110, 1072, 1029, 761. **HRMS** (ESI): calcd. for $C_{16}H_{23}NO_2Br$ ($[M+H]^+$): 340.0906, found: 340.0905.

Methyl (2-bromophenyl)(1-(methylthio)propan-2-yl)carbamate (**206**):

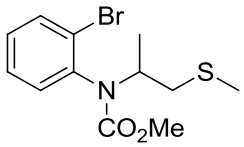

Colorless oil, 93% yield. **^{1}H-NMR** (400 MHz, $CDCl_3$): δ 1.09 (d, *J* = 6.9 Hz, 3H), 1.44 (d, *J* = 6.8 Hz, 1.5H), 2.11 (s, 1.5H), 2.20 (s, 3H), 2.40 (dd, *J* = 13.2, 9.2 Hz, 0.5H), 2.65 (dd, *J* = 13.3, 8.3 Hz, 1H), 2.86 (dd, *J* = 13.3, 8.3 Hz, 1H), 3.16 (d, *J* = 8.6 Hz,0.5H), 3.62 (s, 4.5H), 4.09-4.18 (m, 0.5H), 4.52-4.54 (m, 1H), 7.13-7.16 (m, 0.5H), 7.18 (dd, *J* = 7.4, 1.7 Hz,

1H), 7.23 (dd, *J* = 7.8, 1.5 Hz, 1H), 7.29-7.33 (m, 2H), 7.61-7.64 (m, 1.5H). **^{13}C-NMR** (100 MHz, $CDCl_3$): δ 15.8, 15.9, 16.3, 18.6, 38.5, 40.3, 52.8, 53.0, 53.2, 56.4, 125.1, 125.9, 128.0, 128.1, 128.9, 129.1, 130.7, 130.9, 133.5, 138.0, 139.7, 154.9, 155.5. **IR** (neat, cm^{-1}): 2958, 2918, 1744, 1706, 1576, 1501, 1457, 1426, 1318, 1284, 1143, 1018, 953, 720. **HRMS** (EI): calcd. for $C_{12}H_{16}BrNO_2S$ 317.0080, found 317.0080.

Methyl (2-bromophenyl)(*sec*-butyl)carbamate (**207**):[234]

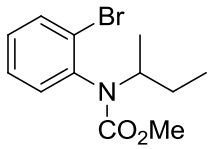

Colorless oil, 98% yield. **^{1}H-NMR** (400 MHz, $CDCl_3$): δ 0.87 (t, *J* = 7.6 Hz, 1H), 0.96 (d, *J* = 6.8 Hz, 2H), 0.98 (t, *J* = 7.6 Hz, 2H), 1.32 (d, *J* = 6.4 Hz, 1H), 1.45-1.60 (m, 0.8H), 1.66-1.84 (m, 1.2H), 3.61 (s, 3H), 4.01-4.13 (m, 0.5H), 4.22-4.44 (m, 0.5H), 7.09-7.22 (m, 2H), 7.25-7.33 (m, 1H), 7.54-7.66 (m, 1H). **^{13}C-NMR** (100 MHz, $CDCl_3$): δ 11.3, 11.8, 16.8, 19.3, 26.9, 29.9, 52.9, 53.0, 55.9, 57.5, 125.7, 126.3, 128.0, 128.8, 128.9, 130.5, 133.5, 138.4, 139.6, 155.2, 155.8. **IR** (neat, cm^{-1}): 2968, 2877, 1706, 1585, 1475, 1439, 1389, 1325, 1310, 1295, 1266, 1244, 1191, 1120, 1093, 1052, 1028, 998, 953, 935, 840, 753. **HRMS** (ESI): calcd. for $C_{12}H_{17}BrN$ 286.0437, found 286.0432.

Methyl (2-bromophenyl)(1-methoxypropan-2-yl)carbamate (**219**):

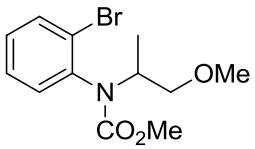

White solid, 87% yield, **m.p.** = 39 ºC. **^{1}H-NMR** (400 MHz, $CDCl_3$): δ 0.98 (d, *J* = 6.8 Hz, 2H), 1.39 (d, *J* = 6.8 Hz, 1H), 3.27 (s, 1.3H), 3.39 (s, 1.7H), 3.42 (d, *J* = 6.4 Hz, 2H), 3.61 (s, 2.4H), 3.74-3.85 (m, 0.6H), 4.00-4.12 (m, 0.3H), 4.40-4.80 (m, 0.7H), 7.25-7.34 (m, 2H), 7.60 (t, *J* = 7.6 Hz, 1H). **^{13}C-NMR** (100 MHz, $CDCl_3$): δ 14.4, 16.7, 52.7, 52.9, 53.1, 73.9, 74.8, 124.9, 126.2, 128.0, 128.1, 128.7, 129.1, 130.9, 131.4, 133.3, 133.3, 155.0, 155.8. **IR** (neat, cm^{-1}): 2951, 2582, 1706, 1586, 1475, 1441, 1375, 1318, 1268, 1194, 1154, 1103, 1073, 1029, 1045, 982, 958, 928, 786, 759, 728. **HRMS** (ESI): calcd. for $C_{12}H_{17}BrNO_3$ 302.0386, found 302.0390.

Methyl (2-bromophenyl)(4-(methoxymethoxy)butan-2-yl)carbamate (**223**):

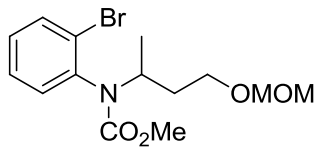

Colorless oil, 86% yield. **^{1}H-NMR** (400 MHz, $CDCl_3$): 0.95 (t, *J* = 7.5 Hz, 3H), 1.03 (t, *J* = 7.5 Hz, 3H), 1.25-1.36 (m, 1H), 1.57-1.64 (m, 1.7H), 1.86-1.93 (m, 1.7H), 3.27 (s, 2.4H), 3.38 (s, 3H), 3.50 (dd, *J* = 10.1, 5.1 Hz, 1H), 3.64 (s, 5.5H), 4.11-3.76 (m, 3.5H), 4.28-4.32 (m, 1.7H), 4.50 (dd, *J* = 20.2, 6.4 Hz, 2H), 4.68 (dd, *J* = 20.2, 6.4 Hz, 2H), 7.14 (qd, *J* = 8.1, 1.7 Hz, 4H), 7.31 (tt, *J* = 8.0, 2.2 Hz, 5H), 7.36 (dd, *J* = 7.9, 1.8 Hz, 2H), 7.42 (d, *J* = 9.5 Hz, 1H), 7.61 (ddd, *J* = 7.9, 3.7, 1.2 Hz, 5H). **^{13}C-NMR** (100 MHz, $CDCl_3$): δ 11.6, 11.7, 22.3, 24.6, 24.6, 53.0, 53.1, 55.4, 55.6, 60.2, 62.9, 67.3, 67.9, 96.7, 125.1, 126.0, 128.0, 128.2, 128.6, 128.8, 130.4, 131.1, 133.4, 133.4, 138.9, 140.8, 155.9. **IR** (neat, cm^{-1}): 2950, 1707, 1585, 1440, 1296, 1147, 1108, 1043, 917, 756, 728. **HRMS** (ESI): calcd. for $C_{14}H_{20}BrN_1O_4Na$ ($[M+Na]^+$): 368.0467, found: 368.0477.

Methyl (2-bromophenyl)(1-methoxybutan-2-yl)carbamate (**222**):

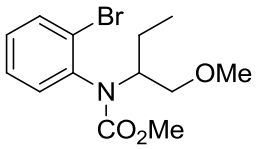

Colorless oil, 95% yield. **^{1}H-NMR** (400 MHz, $CDCl_3$): δ 0.94 (t, *J* = 7.5 Hz, 3H), 1.02 (t, *J* = 7.5 Hz, 2H), 1.25 (h, *J* = 7.5 Hz, 1.5H), 1.55 - 1.72 (m, 2H), 1.83-1.90 (m, 2H), 3.23 (s, 2H), 3.29-3.36 (m, 1H), 3.39 (s, 3H), 3.48 (dd, *J* = 10.2, 6.9 Hz, 1H), 3.54-3.69 (m, 6H), 3.69-3.87 (m, 2H), 4.00 (qd, *J* = 7.2, 5.0 Hz, 0.8H), 4.33 (p, *J* = 6.6 Hz, 1.6H), 7.11-7.17 (m, 3H), 7.27-7.43 (m, 4.8H), 7.61 (d, *J* = 7.5 Hz, 1.9H). **^{13}C-NMR** (100 MHz, $CDCl_3$): δ 11.7, 11.8, 22.3, 24.5, 53.0, 53.2, 58.8, 58.9, 60.0, 60.6, 62.8, 72.2, 72.7, 125.1, 126.1, 128.1, 128.2, 128.6, 128.8, 130.5, 131.2, 133.3, 138.7, 140.7, 155.5, 155.9. **IR** (neat, cm^{-1}): 2953, 2878, 1707, 1586, 1475, 1440, 1378, 1297, 1267, 1194, 1095, 1027, 949, 756, 728, 687. **HRMS** (EI): calcd. for $C_{13}H_{18}NO_3BrNa$ ($[M+Na]^+$): 338.0362, found: 338.0371.

Methyl (2-bromophenyl)(4-hydroxybutan-2-yl)carbamate (**224**):

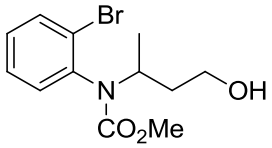

Colorless oil, 95% yield. **^{1}H-NMR** (400 MHz, $CDCl_3$): δ 0.98 (t, *J* = 7.5 Hz, 3H), 1.02 (t, *J* = 7.4 Hz, 1.6H), 1.53-1.99 (m, 3.6H), 2.54-2.75 (m, 0.4H), 3.31 (s, 0.8H), 3.65 (s, 4.6H), 3.71-3.98 (m, 3.9H), 4.10 (brs, 1.3H), 7.10-7.21 (m, 1.5H), 7.26-7.37 (m, 3H), 7.58-7.66 (m, 1.5H). **^{13}C-NMR** (100 MHz, $CDCl_3$): δ 11.5, 11.7, 21.8, 23.6, 53.3, 53.4, 60.5, 63.1, 64.0, 65.1, 124.8, 128.4, 128.5, 129.0, 130.2, 130.3, 133.6, 133.7, 140.4, 156.4, 156.9. **IR** (neat, cm^{-1}): 3442, 2954, 1684, 1585, 1474, 1442, 1309, 1266, 1192, 1048, 1027, 754, 728, 686. **HRMS** (EI): calcd. for $C_{12}H_{16}Br_1N_1O_3Na$ ($[M+Na]^+$): 324.0205, found: 324.0216.

3-((2-Bromophenyl)(methoxycarbonyl)amino)butyl acetate (**225**):

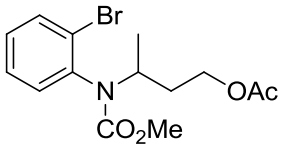

Colorless oil, 95% yield. **^{1}H-NMR** (400 MHz, $CDCl_3$): δ 0.94 (t, *J* = 7.5 Hz, 3H), 1.02 (t, *J* = 7.5 Hz, 2.8H), 1.20-1.35 (m, 1H), 1.66-1.77 (m, 1H), 1.82 (dd, *J* = 13.3, 6.6 Hz, 2H), 1.90 (s, 3H), 2.04 (s, 3H), 3.61 (s, 6H), 4.15-4.31 (m, 4.6H), 4.39 (dd, *J* = 11.2, 4.0 Hz, 1H), 7.09-7.18 (m, 2H), 7.20-7.33 (m, 4H), 7.56-7.63 (m, 2H). **^{13}C-NMR** (100 MHz, $CDCl_3$): δ 11.4, 11.6, 20.9, 21.1, 22.3, 24.7, 53.2, 59.8, 60.7, 64.0, 64.5, 125.3, 125.9, 128.1, 128.2, 128.9, 129.0, 130.3, 130.5, 133.6, 133.7, 139.1, 155.6, 155.7, 170.7, 170.8. **IR** (neat, cm^{-1}): 2965, 1740, 1707, 1585, 1440, 1297, 1224, 1028, 757, 729. **HRMS** (EI): calcd. for $C_{14}H_{18}Br_1N_1O_4Na$ ($[M+Na]^+$): 366.0311, found: 366.0319.

IV.8.3. Synthesis of Enantioenriched Carbamates

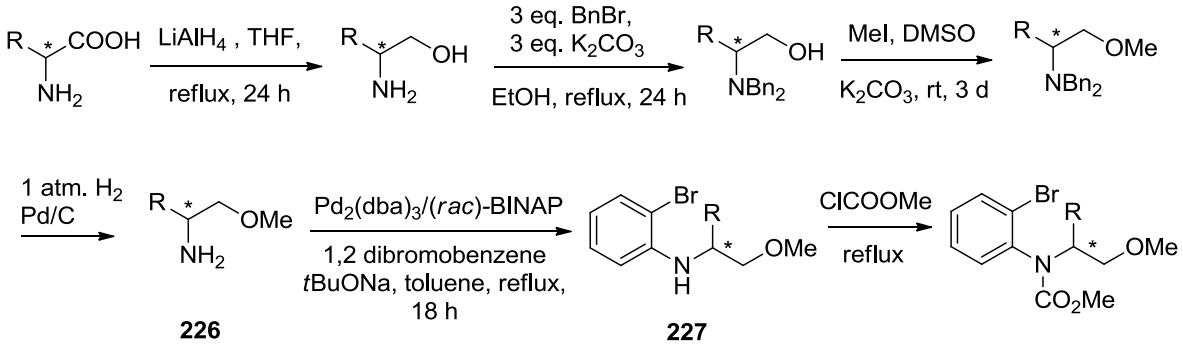

Enantiopure methoxyamino derivatives were prepared from the corresponding chiral amino acids in 4 steps as previously described.[273-276] Carbamates **219**(*S*), **222**(*S*), and **228**-**230** were synthesized according to the general procedure 2.

(*S*)-2-Bromo-*N*-(1-methoxypentan-2-yl)aniline (**227a** (R = *n*-Pr)):

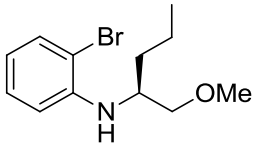

Colorless oil, 59% yield. **^{1}H-NMR** (400 MHz, $CDCl_3$): δ 0.84-0.90 (m, 4H), 0.95 (d, *J* = 7.3 Hz, 3H), 1.39-1.45 (m, 1H), 1.64-1.78 (m, 1H), 3.38 (s, 3H), 3.44-3.61 (m, 3H), 4.35-4.39 (m, 1H), 6.54 (td, *J* = 7.6, 1.5 Hz, 1H), 6.68 (d, *J* = 8.2 Hz, 1H), 7.13-7.17 (m, 4H), 7.41 (dd, *J* = 7.9, 1.5 Hz, 2H). **^{13}C-NMR** (100 MHz, $CDCl_3$): δ 14.1, 19.3, 34.5, 52.9, 59.2, 74.5, 111.7, 117.4, 128.4, 32.6, 144.5. **IR** (neat, cm^{-1}): 3407, 2923, 2869, 1738, 1595, 1508, 1458, 1377, 1320, 1194, 1109, 1018, 988, 744, 699. **HRMS** (ESI): calcd. for $C_{12}H_{19}BrNO$ ($[M+H]^+$): 272.0644, found 272.0642.

(*S*)-B-bromo-*N*-(1-methoxy-3-phenylpropan-2-yl)aniline (**227b** (R = Bn)):

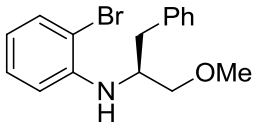

Colorless oil, 67% yield. **^{1}H-NMR** (400 MHz, $CDCl_3$): δ 3.02 (d, *J* = 6.5 Hz, 1H), 3.40 - 3.50 (m, 3H), 3.81-3.87 (m, 1H), 4.67 (d, *J* = 8.1 Hz, 1H), 6.62 (td, *J* = 7.7, 1.4 Hz, 1H), 6.78 (dd, *J* = 8.2, 1.1 Hz, 1H), 7.24 (ddd, *J* = 8.4, 7.3, 1.4 Hz, 1H), 7.27-7.35 (m, 3H), 7.35-7.44 (m, 2H), 7.49 (dd, *J* = 7.9, 1.5 Hz, 1H). **^{13}C-NMR** (100 MHz, $CDCl_3$): δ 37.2, 54.0,

59.1, 72.5, 110.3, 111.7, 117.7, 126.5, 128.5, 129.5, 132.7, 138.1, 144.0. **IR** (neat, cm^{-1}): 3402, 3026, 2923, 1739, 1593, 1505, 1454, 1431, 1366, 1319, 1231, 1202, 1119, 1069, 1016, 968, 738, 698, 638. **HRMS** (ESI): calcd. for $C_{16}H_{19}BrNO$ ($[M+H]^+$): 320.0644, found 320.0641.

(*S*)-2-Bromo-*N*-(1-methoxy-4-methylpentan-2-yl)aniline (**227c** (R = *i*Bu)):

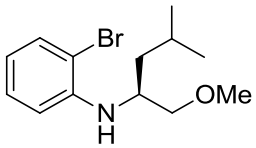

Colorless oil, 64% yield. **^{1}H-NMR** (300 MHz, $CDCl_3$): δ 0.96 (dd, *J* = 6.5, 1.8 Hz, 3.5H), 1.04 (dd, *J* = 6.6, 1.8 Hz, 4H), 1.43-1.70 (m, 2H), 1.71-1.95 (m, 1H), 3.35-3.45 (m, 4H), 3.52 (ddd, *J* = 9.3, 3.9, 1.7 Hz, 1H), 3.65 (brs, 1H), 4.39 (brs, 0.9H), 6.58 (td, *J* = 7.6, 1.5 Hz, 0.7H), 6.75 (dd, *J* = 8.2, 1.3 Hz, 1H), 7.15-7.27 (m, 1H), 7.46 (dt, *J* = 7.9, 1.6 Hz, 0.6H), 7.61-7.70 (m, 0.2 H). **^{13}C-NMR** (75 MHz, $CDCl_3$): δ 22.5, 23.1, 24.9, 41.6, 51.3, 59.2, 74.8, 110.0, 111.6, 117.4, 124.8, 128.51, 128.54, 132.6, 133.7, 144.5. **IR** (neat, cm^{-1}): 3406, 2954, 1594, 1507, 1458, 1429, 1320, 1194, 1111, 1016, 972, 738, 700. **HRMS** (ESI): calcd. for $C_{13}H_{21}N_1O_1Br$ ($[M+H]^+$): 286.0801, found 286.0803.

(*S*)-Methyl (2-bromophenyl)(1-methoxypentan-2-yl)carbamate (**228**):

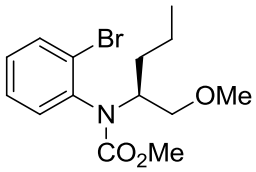

Colorless oil, 89% yield. **$[\alpha]_D^{25}$** = +7.09 (*c* = 1.0 in CH_2Cl_2), >99% *ee*. **^{1}H-NMR** (400 MHz, $CDCl_3$): δ 0.86 (t, *J* = 7.2 Hz, 3H), 0.93 (t, *J* = 7.3 Hz, 2H), 1.12 - 1.27 (m, 1H), 1.27 - 1.58 (m, 3H), 1.67-1.92 (m, 3H), 3.22 (s, 2H), 3.32 (dd, *J* = 9.9, 4.8 Hz, 1H), 3.44 (dd, *J* = 10.2, 7.4 Hz, 1H), 3.55 (dd, *J* = 10.4, 4.4 Hz, 1H), 3.61 (s, 4H), 3.67-3.89 (m, 2H), 4.00-4.07 (m, 1H), 4.37-4.51 (m, 1H), 7.08-7.17 (m, 3H), 7.26-7.41 (m, 5H), 7.59 (dd, *J* = 7.8, 2.7 Hz, 2H). **^{13}C-NMR** (100 MHz, $CDCl_3$): δ 14.1, 20.3, 31.1, 33.5, 52.8, 52.9, 57.9, 58.6, 61.0, 72.3, 72.9, 124.8, 125.9, 127.9, 128.0, 128.4, 128.7, 130.3, 131.1, 133.1, 133.2, 138.4, 140.6, 155.2, 155.8. **IR** (neat, cm^{-1}): 2958, 2872, 1707, 1585, 1474, 1439, 1318, 1295, 1193, 1104, 1058, 1028, 950, 918, 762, 728. **HRMS** (ESI): calcd. for $C_{14}H_{20}BrNO_3$ ($[M]^+$): 330.0699, found 330.0704.

(*S*)-Methyl (2-bromophenyl)(1-methoxy-3-phenylpropan-2-yl)carbamate (**229**):

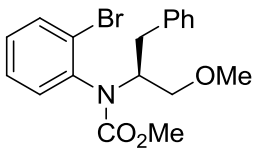

Colorless oil, 96% yield. $[\alpha]_D^{25}$ = -4.77 (*c* = 1.0 in CH_2Cl_2). **^{1}H-NMR** (400 MHz, $CDCl_3$): δ 2.62 (dd, *J* = 13.3, 9.5 Hz, 1H), 3.19 (s, 1.8H), 3.25 (dd, *J* = 13.2, 6.5 Hz, 1H), 3.37 (s, 4H), 3.45-3.68 (m, 1H), 3.65 (dd, *J* = 10.0, 4.6 Hz, 1H), 3.71 (s, 1H), 3.72 (s, 3H), 3.77-3.94 (m, 1H), 4.22-4.29 (m, 0.5H), 4.45-4.52 (m, 1H), 6.97 (d, *J* = 7.7 Hz, 1H), 7.13-7.43 (m, 11H), 7.64 (dd, *J* = 8.0 Hz, 1H), 7.66 (d, *J* = 11.3, 0.5H). **^{13}C-NMR** (100 MHz, $CDCl_3$): δ 14.2, 21.1, 35.5, 37.3, 52.9, 53.0, 58.5, 58.6, 60.4, 61.4, 62.5, 70.6, 72.0, 124.8, 125.5, 126.4, 126.5, 128.0, 128.0, 128.5, 128.5, 128.6, 128.7, 129.2, 129.3, 130.9, 133.1, 138.7, 139.2, 155.1, 155.6. **IR** (neat, cm^{-1}): 3027, 2950, 1706, 1584, 1474, 1440, 1297, 1190, 1116, 1067, 1028, 951, 761, 747, 700. **HRMS** (EI): calcd. for $C_{18}H_{20}BrNO_3$ ($[M]^+$): 337.0621, found 337.0615.

(*S*)-Methyl (2-bromophenyl)(1-methoxy-4-methylpentan-2-yl)carbamate (**230**):

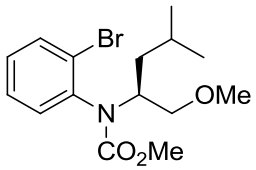

Colorless oil, 97% yield. $[\alpha]_D^{25}$ = +10.2 (*c* = 1.0 in CH_2Cl_2), >99% *ee*. **^{1}H-NMR** (300 MHz, $CDCl_3$): δ 0.94 (dd, *J* = 11.2, 5.7 Hz, 14H), 1.04 (dt, *J* = 14.1, 7.1 Hz, 1H), 1.37 (dt, *J* = 13.7, 6.8 Hz, 1H), 1.51-1.90 (m, 4H), 3.27 (s, 2.4H), 3.34 (dd, *J* = 9.8, 4.7 Hz, 1H), 3.38-3.56 (m, 6H), 3.65 (s, 5H), 3.83 (dd, *J* = 19.4, 11.1 Hz, 2H), 3.99-4.23 (m, 0.8H), 4.40-4.73 (m, 1H), 7.11-7.19 (m, 1.6H), 7.27-7.42 (m, 3.4H), 7.55-7.70 (m, 1.4H). **^{13}C-NMR** (75 MHz, $CDCl_3$): δ 22.2, 22.5, 22.8, 23.0, 25.2, 25.4, 37.9, 40.3, 52.8, 52.9, 55.9, 58.6, 59.6, 72.5, 73.2, 124.8, 126.0, 127.8, 128.0, 128.3, 128.8, 130.3, 131.1, 133.1, 133.2, 138.1, 140.7, 155.1, 155.9. **IR** (neat, cm^{-1}): 2954, 1707, 1585, 1474, 1440, 1316, 1293, 1193, 1110, 1060, 1029, 759. **HRMS** (ESI): calcd. for $C_{15}H_{23}N_1O_3Br$ ($[M+H]^+$): 344.0855, found 344.0849.

IV.8.4. Preparation of Enantio-pure (R)- and (S)-Methyl-(2-bromophenyl)(1-phenylpropan-2-yl)carbamate (198)

Preparation of (S)- and (R)-1-Phenylpropan-2-amine:[257]

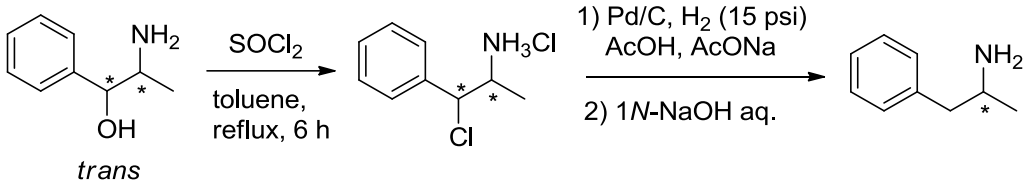

To the solution of (*L*)-(-)-norephedrine (4.0 g, 26.5 mmol, 1 equiv.) in toluene (40 mL), thionyl chloride (4.0 g, 33.6 mmol, 1.26 equiv.) was slowly added and the reaction mixture stirred at 60 °C for 6 h. After cooling down the reaction mixture to 10 °C, the product started to be precipitated. The solid was collected by filtration, washed with toluene (20 mL) and dried in vacuo to afford the crude (*L*)-(-)-chloroamphetamine hydrochloride in 95% yield (5.1 g).

The glass vessel with magnetic stirring was charged with (*L*)-(-)-chloroamphetamine hydrochloride (5.0 g, 24.2 mmol), water (12 mL) and activated carbon (5 g). Then 0.31 g of Pd/C (50 wt% water wet) was charged into the vessel along with sodium acetate (4.5 g, 54 mmol), and acetic acid (11.0 g, 183 mmol). The glassware was filled with hydrogen gas (balloon pressurized hydrogen atmosphere) and stirred at 20 °C for 24 h. The Pd/C and activated carbon was filtered through pad celite and washed with water. The pH of the filtrate was adjusted to greater than pH 12 with sodium hydroxide. The crude product was extracted from aqueous with ethyl acetate, washed with brine and dried over $MgSO_4$. After filtration, organic solvent was removed by rotary evaporator and in vacuo affording (*S*)-1-phenylpropan-2-amine in 98% yield (3.2 g).

(*S*)-1-Phenylpropan-2-amine: Colorless oil, $[\alpha]_D^{25}$ = +23.1 (*c* = 1.0 in CH_2Cl_2), >99% *ee*, [chiral column: AD-H, *n*-hexane/*i*-PrOH = 99 : 1, 0.5 mL/min, 254 nm; t_R = 29.56 min. (major)].

(*R*)-1-Phenylpropan-2-amine: Colorless oil, $[\alpha]_D^{25}$ = -24.15 (*c* = 1.0 in CH_2Cl_2), >99% *ee* [chiral column: AD-H, *n*-hexane/*i*-PrOH = 99 : 1, 0.5 mL/min, 254 nm; t_R = 32.24 min. (major)].

Synthesis of (S)- and (R)-(198):

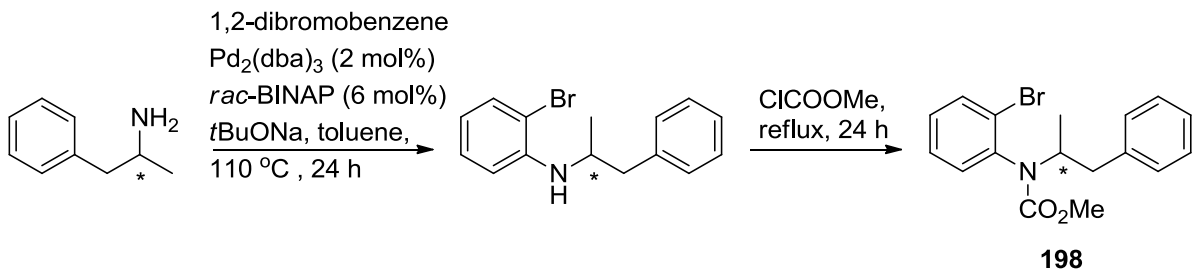

198

(*R*)-Methyl (2-bromophenyl)(1-phenylpropan-2-yl)carbamate **198**: $[\alpha]_D^{25}$ = -29.15 (*c* = 1.0 in CH_2Cl_2), 99% *ee*, [chiral column: AD-H, *n*-hexane/*i*-PrOH = 99 : 1, 0.5 mL/min, 254 nm; t_R = 34.56 min. (minor) and 52.62 min. (major)].

(*S*)-Methyl (2-bromophenyl)(1-phenylpropan-2-yl)carbamate **198**: $[\alpha]_D^{25}$ = +30.8 (*c* = 1.0 in CH_2Cl_2), >99% *ee*, [chiral column: AD-H, *n*-hexane/*i*-PrOH = 99 : 1, 0.5 mL/min, 254 nm; t_R = 34.39 min. (major)].

IV.9. Palladium-Catalyzed Synthesis of Indolines

IV.9.1. Representative Racemic Synthesis of Indolines Using $PCy_3 \cdot HBF_4$ as a Ligand

Carbamate (0.2 mmol, 1 equiv.), $Pd(OAc)_2$ (4.5 mg, 0.02 mmol), pivalic acid (6.1 mg, 0.06 mmol), cesium carbonate (97.5 mg, 0.3 mmol) and $PCy_3 \cdot HBF_4$ (14.7 mg, 0.04 mmol) were successfully filled into a Schlenk flask. After the flask was evacuated and backfilled with nitrogen, dry xylenes was added under nitrogen and the resulting reaction mixture was stirred at 140 °C overnight (17-24 h). The reaction mixture was cooled down to rt and diluted with dichloromethane (2 mL) followed by filtration through celite. The filtrate was evaporated under high vacuum. The residue was purified by f.c. (silica gel; diethyl acetate : pentane = 1 : 30 as eluent) to afford the racemic indoline.

IV.9.2. Racemic Synthesis of Indoline (251) Using $PCy_3 \cdot HBF_4$ as a Ligand

Substrate **207** (57.2 mg, 0.2 mmol), $Pd(OAc)_2$ (4.5 mg, 0.02 mmol), pivalic acid (6.1 mg, 0.06 mmol), cecium carbonate (97.5 mg, 0.3 mmol), and $PCy_3 \cdot HBF_4$ (14.7 mg, 0.04 mmol) were placed into a Schlenk flask. After the flask was evacuated and backfilled with nitrogen, dry xylenes 2 mL were added under nitrogen and the resulting reaction mixture was stirred at 140 °C in the Schlenk tube behind a protective shield for 17 h. The reaction mixture

was cooled to rt and diluted with dichloromethane (2 mL) followed by filtration through a pad of celite. The filtrate was evaporated by rotary evaporator and the volatiles were removed under vacuum. The residue was purified by f.c. (silica gel; diethyl acetate : pentane = 1 : 30 as eluent) to afford the racemic indoline **251** in 91% yield (37.3 mg).

IV.9.3. Racemic Synthesis of Indoline (251) Using IPr·HCl as a Ligand

Carbamate **207** (57.2 mg, 0.2 mmol), cesium carbonate (97.5 mg, 0.3 mmol), [Pd(π-cinnamyl)Cl]$_2$ (5.2 mg, 0.01 mmol), cesium pivalate (46.8 mg, 0.2 mmol) and IPr·HCl (8.5 mg, 0.02 mmol) were placed in a Schlenk flask. After the flask was evacuated and backfilled with nitrogen, dry xylene 2 mL was added under nitrogen. The resulting reaction mixture was stirred at 140 °C in the Schlenk tube behind a protective shield for 17 h. The reaction mixture was cooled to rt and diluted with dichloromethane (2 mL) followed by filtration through the pad of celite. The filtrate was evaporated by rotary evaporator and the volatiles were removed under vacuum. The residue was purified by f.c. (silica gel; diethyl acetate : pentane = 1 : 30 as eluent) to afford the indoline **251** in 91% yield (37.5 mg).

IV.9.4. Representative Procedure for the Asymmetric Pd(NHC)-Catalyzed C-H Activation

Carbamate **207** (62.4 mg, 0.2 mmol), cesium carbonate (97.5 mg, 0.3 mmol), [Pd(π-cinnamyl)Cl]$_2$ (2.6 mg, 0.005 mmol), cesium pivalate (46.8 mg, 0.2 mmol) and *NHC*·HI (0.01 mmol) were placed in a Schlenk flask. After the flask was evacuated and backfilled with nitrogen, dry mesitylene (2 mL) was added under nitrogen. The resulting reaction mixture was stirred at 160 °C in the Schlenk tube behind a protective shield for 3 h. The reaction mixture was cooled to rt and diluted with dichloromethane (2 mL) followed by filtration through a pad of celite. The filtrate was evaporated by rotary evaporator and the volatiles were removed under vacuum. The residue was purified by f.c. (silica gel; diethyl acetate : pentane = 1 : 30 as eluent) to afford the indoline methyl carbamate **251**.

(*S*)-Methyl 2-methylindoline-1-carboxylate (**247**):[260]

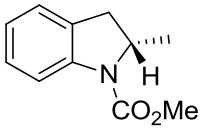

Colorless oil, 84% yield (32.1 mg). $[\alpha]_D^{20}$ = +52.0 (*c* = 0.5 in CH_2Cl_2). 90% *ee*. [Chiral column: AS-H, *n*-hexane/*i*-PrOH = 99 : 1, 0.5 mL/min, 254 nm); t_R = 11.7 min

(minor) and 13.6 min (major)]. **^{1}H-NMR** (400 MHz, $CDCl_3$): 1.27 (d, *J* = 7.2 Hz, 1H), 2.62 (dd, *J* = 16, 2 Hz, 1H), 3.35 (dd, *J* = 16, 9.6 Hz, 1H), 3.83 (s, 3H), 4.40-4.65 (m, 1H), 6.57 (t, *J* = 7.2 Hz, 1H), 7.14 (d, *J* = 7.6 Hz, 1H), 7.17 (t, *J* = 7.6 Hz, 1H), 7.44-8.10 (brd, 1H).

(*R*)-Methyl 2-ethylindoline-1-carboxylate (**251**):

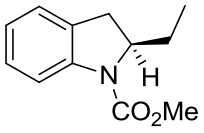

(*S*,*S*)-[**L14**H][I] was used. Colorless oil, 57% yield calcd. by NMR (23.2 mg), 77% *ee*. [Chiral column: AD-H, *n*-hexane/*i*-PrOH = 99 : 1, 0.5 mL/min, 254 nm; t_R = 21.44 min. (major) and 26.68 (minor)]. **^{1}H-NMR** (400 MHz, $CDCl_3$): 0.86 (t, *J* = 7.6 Hz, 3H), 1.49-1.63 (m, 1H), 1.67-1.87 (m, 1H), 2.74 (dd, *J* = 16, 2.4 Hz, 1H), 3.27 (dd, *J* = 16, 9.6 Hz, 1H), 3.82 (s, 3H), 4.28-4.46 (m, 1H), 6.94 (td, *J* = 7.2, 0.8 Hz, 1H), 7.12 (d, *J* = 7.6 Hz, 1H), 7.15 (t, *J* = 7.6 Hz, 1H), 7.34-8.10 (m, 1H).

(*R*)-Methyl 2-ethylindoline-1-carboxylate (**251**) and (2*R*,3*S*)-methyl 2,3-dimethylindoline-1-carboxylate (**252**):

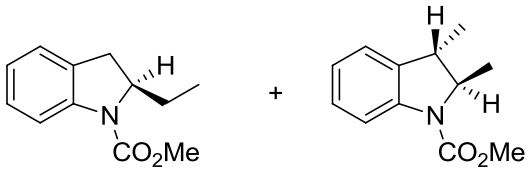

(*S*,*S*)-[**L14**H][I] was used. Colorless oil-**252**, 38% yield (15.5 mg) calcd. by NMR, >99% *ee* [Chiral column: AD-H, *n*-hexane/*i*-PrOH = 99 : 1, 0.5 mL/min, 254 nm; t_R = 15.19 min. (major)]. **251** + **252**: **^{1}H-NMR** (400 MHz, $CDCl_3$): δ 0.88 (t, *J* = 7.4 Hz, 4H), 1.23 (d, *J* = 7.0 Hz, 2.6H), 1.29 (d, *J* = 6.3 Hz, 2.2H), 1.52-1.63 (m, 1.4H), 1.77 (brd, 1H), 2.76 (d, *J* = 16.0 Hz, 1H), 2.85 (q, *J* = 6.8 Hz, 0.65H), 3.28 (dd, *J* = 16.0, 9.6 Hz, 1H), 3.83 (s, 5H), 4.05 (brd, 0.65H), 4.38 (brd, 1H), 6.93-7.00 (m, 1.65H), 7.13-7.21 (m, 3.5H), 7.77 (brd, 1.65H). **251** + **252**: **^{13}C-NMR** (100 MHz, $CDCl_3$): δ 9.1, 20.5, 21.8, 27.3, 32.90, 32.97, 43.0, 52.4, 60.6, 63.4, 115.2, 115.3, 122.7, 122.8, 124.3, 124.8, 127.3, 127.7, 153.8.

(2*R*,3*S*)-Methyl 2-ethyl-3-methoxyindoline-1-carboxylate (**255**):

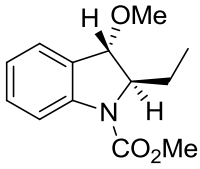

Colorless oil, 40.5% yield (19 mg) calcd. by NMR. $[\alpha]_D^{25}$ = -27.60 (*c* = 1.0 in CH_2Cl_2), 96% *ee*. [Chiral column: (*R*,*R*)-Whelk-O1, *n*-hexane/*i*-PrOH = 99 : 1, 0.5 mL/min, 254 nm; 40.03 min. (major) and t_R = 52.56 min. (minor)]. **^{1}H-NMR** (400 MHz, $CDCl_3$): δ 0.95 (t, *J* = 7.5 Hz, 3H), 1.41- 1.59 (m, 1H), 1.80 (brm, 1H), 3.35 (s, 1H), 3.85 (s, 1H), 4.26 (brm, 1H), 4.40 (s, 1H), 7.04 (td, *J* = 7.4, 0.7 Hz, 1H), 7.29-7.40 (m, 2H), 7.93 (brd, 1H). **^{13}C-NMR** (100 MHz): δ 9.5, 25.1, 52.7, 55.2, 66.5, 82.5, 116.0, 122.8, 126.5, 130.4, 143.2, 153.5. **IR** (neat, cm^{-1}): 2965, 1703, 1604, 1481, 1440, 1389, 1344, 1282, 1190, 1138, 1087, 1056, 933, 753, 642. **HRMS** (EI): calcd. for $C_{13}H_{17}NO_3Na$ ($[M+Na]^+$): 258.1101, found: 258.1104.

(2*S*,3*S*)-Methyl 2-(methoxymethyl)-3-methylindoline-1-carboxylate (**256**):

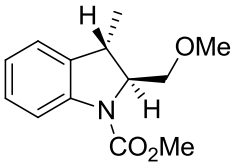

Colorless oil, 40.5% yield (19 mg) calcd. by NMR. $[\alpha]_D^{25}$ = -9.53 (*c* = 1.0 in CH_2Cl_2), 88% *ee*. [Chiral column: (*R*,*R*)-Whelk-O1, *n*-hexane/*i*-PrOH = 99 : 1, 0.5 mL/min, 254 nm; 22.76 min. (major) and t_R = 25.61 min. (minor)]. ^{1}H NMR (400 MHz, $CDCl_3$): 1.28 (d, *J* = 7.1 Hz, 3H), 3.27 (qd, *J* = 7.1, 2.0 Hz, 1H), 3.36 (s, 3H), 3.62 (dd, *J* = 9.2, 4.0 Hz, 1H), 3.87 (s, 3H), 4.17 (brm, 1H), 6.93 – 7.07 (m, 1H), 7.18 (dd, *J* = 15.9, 7.6 Hz, 2H), 7.70 (brd, 1H). **^{13}C-NMR** (100 MHz): δ 22.3, 38.6, 52.8, 59.3, 66.3, 72.9, 115.4, 123.2, 124.5, 127.7, 136.1, 154.0. **IR** (neat, cm^{-1}): 2958, 1702, 1482, 1440, 1385, 1333, 1310, 1280, 1193, 1137, 1059, 748. **HRMS** (EI): calcd. for $C_{13}H_{17}N_1O_3Na$ ($[M+Na]^+$): 258.1100, found: 258.1102.

(*R*)-Methyl 2-propylindoline-1-carboxylate (**257**):

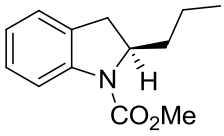

(*S*,*S*)-[**L14**H][I] was used. Colorless oil, 68% yield (29.7 mg) calcd. by NMR. 61% *ee* [Chiral column: AS-H, *n*-hexane = 100 : 0, 0.5 mL/min, 254 nm; t_R = 22.79 min. (major) and 29.39 (minor)]. **^{1}H-NMR** (400 MHz, $CDCl_3$): δ 0.90 (t, *J* = 7.6 Hz, 3H), 1.22-1.39 (m, 2H), 1.22-1.39 (m, 2H), 1.45-1.56 (m, 1H), 2.73 (dd, *J* = 16, 2 Hz, 1H), 3.27 (dd, *J* = 16, 9.6 Hz, 1H), 3.82 (s, 3H), 4.34-4.56 (brd, 1H), 6.94 (td, *J* = 7.6, 1.2 Hz, 1H), 7.12(d, *J* = 8 Hz, 1H), 7.16 (t, *J* = 7.6 Hz, 1H), 7.26-8.40 (brd, 1H). **^{13}C-NMR** (100 MHz, $CDCl_3$): δ 14.2, 18.3, 33.6, 37.0, 52.6, 59.5, 115.5, 122.9, 125.0, 127.5, 130.6, 154.0. **IR** (neat, cm^{-1}): 2957, 2871, 1702, 1603, 1485, 1441, 1390, 1330, 1290, 1270, 1239, 1221, 1193, 1135, 1059, 1022, 751. **HRMS** (ESI): calcd. for $C_{13}H_{18}NO_2$ ($[M+H]^+$): 220.1332, found 220.1320.

(*R*)-Methyl 2-propylindoline-1-carboxylate (**257**) and (2*R*,3*S*)-methyl 3-ethyl-2-methylindoline-1-carboxylate (**258**):

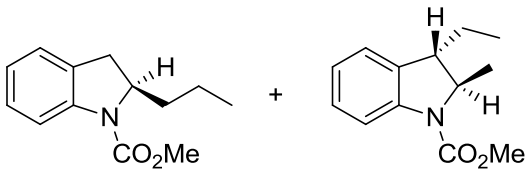

(*S*,*S*)-[**L14**H][I] was used. Colorless oil-**258**: 22% yield (9.6 mg) calcd. by NMR, 96% *ee* [Chiral column: AS-H, *n*-hexane/*i*-PrOH = 100 : 0, 0.5 mL/min, 254 nm; t_R = 17.81 min. (major) and 19.87 (minor)]. **257** + **258**: **^{1}H-NMR** (400 MHz, $CDCl_3$): δ 0.90-0.95 (m, 4.7H), 1.27-1.36 (m, 4H), 1.48-1.59 (m, 2H), 1.72 (brd, 1.4H), 2.67 (t, *J* = 6.4 Hz, 0.5H), 2.74 (dd, *J* = 16.0, 1.8 Hz, 1H), 3.28 (dd, *J* = 16.0, 9.6 Hz, 1H), 3.84 (s, 4.5H), 4.18 (brd, 0.5H), 4.44 (brd, 1H), 6.93-7.00 (m, 1.5H), 7.13-7.22 (m, 3H), 7.65 (brd, 1.5H). **257** + **258**: **^{13}C-NMR** (100 MHz, $CDCl_3$): δ 11.1, 14.0, 18.1, 29.0, 33.4, 36.7, 49.9, 52.4, 59.3, 61.0, 115.3, 122.6, 122.7, 124.8, 127.3, 127.7, 153.5, 153.7.

(*R*)-Methyl 2-phenethylindoline-1-carboxylate (**259**):

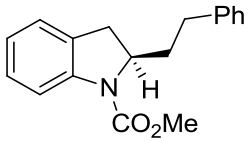

(*S*,*S*)-[**L5**H][I] was used. Colorless oil, 62% yield (34.8 mg), $[\alpha]_D^{20}$ = -19.4 (*c* = 1.0 in CH_2Cl_2), 47% *ee*, [Chiral column: (*R*,*R*)-Whelk-O1, *n*-hexane/*i*-PrOH = 99 : 1, 0.5 mL/min, 254 nm; t_R = 28.26 min. (major) and 47.58 min. (minor)]. **^{1}H-NMR** (400 MHz, $CDCl_3$): δ 1.80-1.96 (m, 1H), 2.00-2.18 (m, 1H), 2.52-2.72 (m, 2H), 2.82 (dd, *J* = 16, 2 Hz, 1H), 3.32

(dd, *J* = 16, 9.6 Hz, 1H), 3.81 (s, 3H), 4.34-4.60 (brd, 1H), 6.96 (t, *J* = 7.2, 0.8 Hz, 1H), 7.10-7.22 (m, 5H), 7.26-7.30 (m, 2H), 7.40-8.10 (brd, 1H). **^{13}C-NMR** (125 MHz, $CDCl_3$): δ 15.5, 31.3, 33.6, 36.2, 52.7, 59.3, 66.0, 115.6, 123.0, 125.1, 126.1, 127.6, 128.5, 130.3, 141.5, 142.1, 153.9. **IR** (neat, cm^{-1}): 3027, 2952, 2858, 1701, 1602, 1484, 1440, 1389, 1330, 1289, 1225, 1191, 1130, 1056, 942, 840, 749. **HRMS** (ESI): calcd. for $C_{18}H_{20}NO_2$ ($[M+H]^+$): 282.1488, found 282.1480.

(2*R*,3*S*)-Methyl 3-benzyl-2-methylindoline-1-carboxylate (**260**):

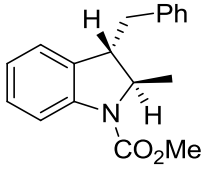

(*S*,*S*)-[**L5**H][I] was used. Colorless oil, 32% yield (17.9 mg). **$[\alpha]_D^{25}$** = +15.4 (*c* = 0.5 in CH_2Cl_2), >99% *ee*, [Chiral column: (*R*,*R*)-Whelk-O1, *n*-hexane/*i*-PrOH = 99 : 1, 0.5 mL/min, 254 nm; t_R = 19.86 min. (major)]. **^{1}H-NMR** (400 MHz, $CDCl_3$): δ 1.12 (d, *J* = 6.4 Hz, 3H), 2.69-2.82 (m, 2H), 3.02 (t, *J* = 14.9 Hz, 1H), 3.78 (s, 3H), 4.18 (brd, 1H), 6.85-6.93 (m, 2H), 7.08 (d, *J* = 6.9 Hz, 2H), 7.13-7.27 (m, 4H), 7.59 (brd, 1H). **^{13}C-NMR** (100 MHz, $CDCl_3$): δ 20.9, 42.4, 49.9, 52.6, 60.8, 115.6, 122.7, 125.3, 126.6, 128.2, 128.6, 129.4, 139.0. **IR** (neat, cm^{-1}): 2947, 1701, 1601, 1482, 1439, 1387, 1280, 1190, 1059, 748, 698. **HRMS** (EI): calcd. for $C_{18}H_{20}NO_2$ ($[M+H]^+$): 282.1488, found: 282.1479.

(*R*)-Methyl 2-(3-((tert-butyldimethylsilyl)oxy)propyl)indoline-1-carboxylate (**261**):

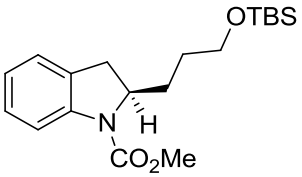

(*S*,*S*)-[**L14**H][I] was used. Colorless oil, 68% yield (47.4 mg). **$[\alpha]_D^{25}$** = -18.8 (*c* = 1.0 in CH_2Cl_2), 55% *ee*, [Chiral column: (*R*,*R*)-Whelk-O1, *n*-hexane/*i*-PrOH = 99 : 1, 0.5 mL/min, 254 nm; t_R = 18.65 min. (major) and 24.72 min. (minor)]. **^{1}H-NMR** (400 MHz, $CDCl_3$): 0.00 (s, 3H), 0.01 (s, 3H), 0.86 (s, 9H), 1.41-1.67 (m, 3H), 1.70-1.84 (m, 1H), 2.75 (dd, *J* = 16, 2 Hz, 1H), 3.28 (dd, *J* = 16, 9.6 Hz, 1H), 3.58 (t, *J* = 6.4 Hz, 2H), 3.81 (s, 3H), 4.30-4.60 (brd, 1H), 6.94 (td, *J* = 7.2, 0.8 Hz, 1H), 7.12 (d, *J* = 7.2 Hz, 1H), 7.16 (t, *J* = 7.6 Hz, 1H), 7.40-8.20 (brd, 1H). **^{13}C-NMR** (125 MHz, $CDCl_3$): δ 18.5, 26.1, 28.3, 31.2, 33.6,

52.6, 59.5, 63.1, 115.5, 122.9, 125.0, 127.6, 130.5, 154.0. **IR** (neat, cm^{-1}): 2952, 2930, 2857, 1705, 1603, 1486, 1463, 1441, 1390, 1330, 1307, 1284, 1251, 1227, 1191, 1132, 1093, 1059, 1022, 983, 833, 751. **HRMS** (EI) calcd. for $C_{19}H_{32}NO_3Si$ ($[M+H]^+$): 350.2145, found 350.2150.

(2*R*,3*S*)-Methyl 3-(2-((*tert*-butyldimethylsilyl)oxy)ethyl)-2-methylindoline-1 carboxylate (**262**):

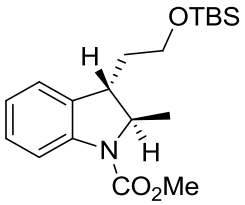

(*S*,*S*)-[**L14**H][I] was used. Colorless oil, 21% yield (14.6 mg). $[\alpha]_D^{25}$ = +6.6 (*c* = 0.5 in CH_2Cl_2), >99% *ee*, [Chiral column: (*R*,*R*)-Whelk-O1, *n*-hexane/*i*-PrOH = 99 : 1, 0.5 mL/min, 254 nm; t_R = 14.03 min. (major)]. **^{1}H-NMR** (400 MHz, $CDCl_3$): δ 0.06 (d, *J* = 3.4 Hz, 6H), 0.91 (s, 9H), 1.26 (d, *J* = 6.4 Hz, 3H), 1.69-1.74 (m, 2H), 2.96 (t, *J* = 6.7 Hz, 1H), 3.71 (d, *J* = 6.0 Hz, 2H), 3.83 (s, 3H), 4.26-4.30 (m, 1H), 6.97 (td, *J* = 7.4, 0.9 Hz, 1H), 7.15-7.21 (m, 2H), 7.61 (brd, 1H). **^{13}C-NMR** (100 MHz, $CDCl_3$): δ 5.0, 1.2, 18.4, 20.6, 26.1, 39.0, 45.1, 52.6, 60.6, 61.3, 115.6, 122.8, 125.0, 127.9, 134.4. **IR** (neat, cm^{-1}): 2926, 2854, 1705, 1602, 1485, 1440, 1389, 1250, 1094, 1054, 938, 832, 749. **HRMS** (EI): calcd. for $C_{19}H_{32}NO_3Si$ $[M+H]^+$: 350.2145, found: 350.2137.

(*R*)-Methyl 2-(3-ethoxy-3-oxopropyl)indoline-1-carboxylate (**263**):

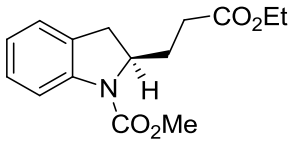

(*S*,*S*)-[**L14**H][I] was used. Colorless oil, 63% yield (55.4 mg). $[\alpha]_D^{20}$ = -31.78 (*c* = 1.0 in CH_2Cl_2), 69% *ee*, [Chiral column: OD-H, *n*-hexane/*i*-PrOH = 99 : 1, 0.5 mL/min, 254 nm; t_R = 20.54 min. (major) and 25.08 (minor)]. **^{1}H-NMR** (400 MHz, $CDCl_3$): δ 1.21 (t, *J* = 7.2 Hz, 3H), 1.88-2.79 (m, 1H), 2.21-2.38 (m, 2H), 2.71 (dd, *J* = 16.4, 2.4 Hz, 1H), 3.32 (dd, *J* = 16, 9.6 Hz, 1H), 3.82 (s, 3H), 4.09 (q, *J* = 7.2 Hz, 2H), 4.44-4.63 (brd, 1H), 6.95 (td, *J* = 7.6, 0.8 Hz, 1H), 7.12 (d, *J* = 7.2 Hz, 1H), 7.16 (t, *J* = 7.6 Hz, 1H), 7.48-7.80 (brd, 1H). **^{13}C-NMR** (100 MHz, $CDCl_3$): δ 14.4, 30.1, 30.2, 52.8, 58.6, 60.7, 115.8, 123.2, 125.0, 127.7, 130.1,

153.9, 173.2. **IR** (neat, cm^{-1}): 2956, 1503, 1435, 1441, 1389, 1285, 1225, 1186, 1130, 1089, 1057, 1023, 941, 859, 753. **HRMS** (EI): calcd. for $C_{15}H_{19}NO_4Na$ ($[M+Na]^+$): 300.1206, found 300.1206.

(2*R*,3*S*)-Methyl 3-(2-ethoxy-2-oxoethyl)-2-methylindoline-1-carboxylate (**264**):

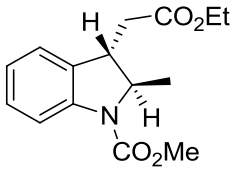

(*S*,*S*)-[**L14**H][I] was used. Colorless oil, 36% yield (19.9 mg). $[\alpha]_D^{20}$ = -8.43 (*c* = 0.5 in CH_2Cl_2). 98% *ee*, [Chiral column: AS-H, *n*-hexane/*i*-PrOH = 99 : 1, 0.5 mL/min, 254 nm; t_R = 17.04 min. (major) and 19.01 (minor)]. **^{1}H-NMR** (400 MHz, $CDCl_3$): δ 1.31 (t, *J* = 7.1 Hz, 3H), 1.37 (d, *J* = 6.4 Hz, 3H), 2.56-2.58 (m, 2H), 3.30 (t, *J* = 7.4 Hz, 1H), 3.89 (s, 3H), 4.22 (qd, *J* = 7.2, 1.7 Hz, 2H), 4.27 (brd, 1H), 7.03 (t, *J* = 7.4 Hz, 1H), 7.22 (d, *J* = 7.4 Hz, 1H), 7.27 (t, *J* = 7.6 Hz, 1H), 7.47-7.88 (m, 1H). **^{13}C-NMR** (100 MHz, $CDCl_3$): δ 14.2, 20.4, 28.4, 29.7, 40.6, 44.2, 52.5, 60.7, 61.5, 115.5, 122.9, 124.8, 128.3, 171.7. **IR** (neat, cm^{-1}): 2958, 1704, 1602, 1484, 1440, 1336, 1281, 1170, 1059, 1023, 752. **HRMS** (EI): calcd. for $C_{15}H_{20}NO_4$ ($[M+H]^+$): 278.1386, found: 278.1380.

(*S*)-Methyl 2-(methoxymethyl)indoline-1-carboxylate (**265**):

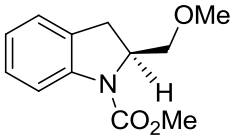

(*S*,*S*)-[**L14**H][I] was used. Colorless oil, 62% yield (27.4 mg) calcd. by NMR. 67% *ee* [Chiral column: AD-H, *n*-hexane/*i*-PrOH = 99 : 1, 0.5 mL/min, 254 nm; t_R = 29.45 min. (major) and 34.67 (minor)]. **^{1}H-NMR** (400 MHz, $CDCl_3$): δ 3.01 (dd, *J* = 16.4, 2.4 Hz, 1H), 3.25 (dd, *J* = 16, 9.6 Hz, 1H), 3.58 (dd, *J* = 9.2, 4 Hz, 1H), 3.83 (s, 3H), 4.50-4.70 (m, 1H), 7.14 (d, *J* = 7.6 Hz, 1H), 7.15 (t, *J* = 8.4 Hz, 1H), 7.32-8.00 (brd, 1H). **^{13}C-NMR** (125 MHz, $CDCl_3$): δ 31.3, 52.5, 58.1, 59.0, 72.9, 115.2, 122.9, 124.9, 127.2, 130.1, 141.8, 153.6. **IR** (neat, cm^{-1}): 2926, 1702, 1602, 1484, 1462, 1440, 1379, 1332, 1308, 1282, 1225, 1192, 1137, 1116, 1055, 1021, 972, 939, 860, 833, 752, 712. **HRMS** (ESI): calcd. for $C_{12}H_{15}NO_3Na$ ($[M+Na]^+$): 244.0944, found 244.0944.

(*S*)-Methyl 2-(methoxymethyl)indoline-1-carboxylate (**265**) and (2*R*,3*S*)-methyl 3-methoxy-2-methylindoline-1-carboxylate (**266**):

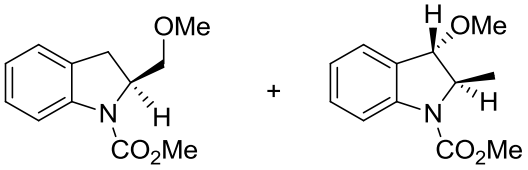

(*S*,*S*)-[**L14**H][I] was used. Colorless oil-**266**, 24% yield (10.6 mg) calcd. by NMR. >99% *ee* [Chiral column: AD-H, *n*-hexane/*i*-PrOH = 99 : 1, 0.5 mL/min, 254 nm; t_R = 27.67 min. (major)]. **265** + **266**: **^{1}H-NMR** (400 MHz, $CDCl_3$): δ 1.26 (d, *J* = 7.0 Hz, 1.5H), 3.03 (dd, *J* = 16.2, 2.1 Hz, 1H), 3.27 (dd, *J* = 16.4, 9.7 Hz, 1H), 3.33 (s, 1.5H), 3.34 (s, 3H), 3.60 (dd, *J* = 9.0, 3.9 Hz, 1H), 3.84 (s, 4.5H), 4.29 (brd, 0.5H), 4.39 (brd, 0.5H), 4.61 (brd, 1H), 6.96 (t, *J* = 7.4 Hz, 1H), 7.04 (t, *J* = 7.4 Hz, 0.5H), 7.14-7.18 (m, 2H), 7.33-7.39 (m, 1H), 7.70 (brd, 1.5H). **265** + **266**: **^{13}C-NMR** (100 MHz, $CDCl_3$): δ 14.3, 18.5, 28.4, 31.4, 52.6, 53.0, 55.1, 58.2, 58.7, 59.1, 61.0, 72.9, 74.7, 84.7, 115.3, 115.9, 122.6, 123.0, 125.0, 127.3, 127.9, 128.0, 128.9, 130.4, 131.2, 133.2, 155.7.

(*R*)-Methyl 2-benzylindoline-1-carboxylate (**267**):

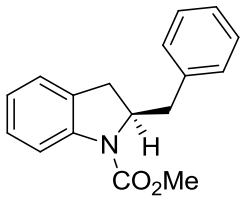

(*S*,*S*)-[**L5**H][I] was used. Colorless oil, 45% yield (24.1 mg), 94% *ee*. **$[\alpha]_D^{25}$** = -21.25 (*c* = 1.0 in CH_2Cl_2), >99% *ee*, [Chiral column: AD-H, *n*-hexane/*i*-PrOH = 99 : 1, 0.5 mL/min, 254 nm; t_R = 36.51 min. (major)]. **^{1}H-NMR** (400 MHz, $CDCl_3$): δ 2.61 (dd, *J* = 12.8, 10 Hz, 1H), 2.80 (dd, *J* = 16, 1.6 Hz, 1H), 3.13 (dd, *J* = 16.4, 9.6 Hz, 1H), 3.00-3.42 (m, 1H), 3.84 (s, 3H), 4.60-4.80 (m, 1H), 6.98 (t, *J* = 7.2 Hz, 1H), 7.15 (d, *J* = 7.6 Hz, 1H), 7.17-7.28 (m, 4H), 7.28-7.36 (m, 2H), 7.38-8.30 (brd, 1H). **^{13}C-NMR** (125 MHz, $CDCl_3$): δ 32.7, 40.3, 52.5, 60.6, 115.3, 122.8, 125.1, 126.5, 127.0, 127.5, 128.4, 128.7, 129.5, 137.7, 141.6, 153.6. **IR** (neat, cm^{-1}): 3064, 3029, 2948,2913, 1855, 1703, 1602, 1484, 1441, 1391, 1359, 1309, 1275, 1232, 1191, 1145, 1128, 1087, 1058, 1020, 939, 918, 894, 870, 759, 698. **HRMS** (ESI): calcd. for $C_{17}H_{18}NO_2$ ($[M+H]^+$): 268.1332, found 268.1338.

(2*R*,3*S*)-Methyl 2-methyl-3-phenylindoline-1-carboxylate (**268**):

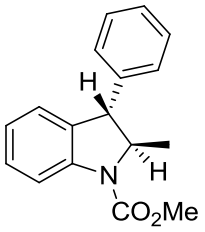

(*S*,*S*)-[**L5**H][I] was used. Colorless oil, 42% yield (22.4 mg). $[\alpha]_D^{20}$ = +110.15 (*c* = 1.0 in CH_2Cl_2), >99% *ee* [Chiral column: AD-H, *n*-hexane/*i*-PrOH = 99 : 1, 0.5 mL/min, 254 nm; t_R = 31.89 min. (major)]. **^{1}H-NMR** (400 MHz, $CDCl_3$): δ 1.46 (d, *J* = 6.1 Hz, 3H), 3.85 (s, 3H), 3.98 (d, *J* = 1.8 Hz, 1H), 4.39 (brd, 1H), 6.99 (t, *J* = 7.3 Hz, 1H), 7.03-7.06 (m, 3H), 7.20-7.29 (m, 4H), 7.81 (brd, 1H). **^{13}C-NMR** (100 MHz, $CDCl_3$): δ 21.5, 52.7, 54.5, 64.8, 115.6, 123.3, 126.0, 127.1, 127.3, 128.4, 128.9, 144.2, 153.8. **IR** (neat, cm^{-1}): 3022, 2959, 2855, 1731, 1605, 1486, 1467, 1381, 1244, 1224, 1019, 745, 689. **HRMS** (EI): calcd. for $C_{17}H_{18}NO_2$ ($[M+H]^+$): 268.1332, found: 268.1332.

(*R*)-Methyl 2-(cyclohexylmethyl)indoline-1-carboxylate (**269**):

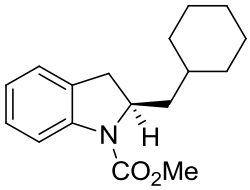

(*S*,*S*)-[**L5**H][I] was used. Colorless oil, 81% yield (44.2 mg), 25% *ee*. [Chiral column: (*R*,*R*)-Whelk-O1, *n*-hexane/*i*-propanol = 99 : 1, 1.0 mL/min, 254 nm); t_R = 10.3 min (major) and 14.1 min (minor)]. **^{1}H-NMR** (400 MHz, $CDCl_3$): δ 0.86-1.06 (m, 2H), 1.07-1.41 (m, 5H), 1.50-1-2.00 (m, 7H), 2.71 (dd, *J* = 15.6, 1.6 Hz, 1H), 3.25 (d, *J* = 15.6, 9.2 Hz, 1H), 3.81 (s, 3H), 4.35-4.65 (brd, 1H), 6.94 (td, *J* = 7.6, 0.8 Hz, 1H), 7.13 (d, *J* = 7.2 Hz, 1H), 7.16 (t, *J* = 7.6 Hz, 1H), 7.40-8.24 (brd, 1H). **^{13}C-NMR** (100 MHz, $CDCl_3$): δ 26.3, 26.5, 26.7, 32.6, 34.0, 34.4, 42.4, 52.6, 57.8, 115.7, 122.9, 125.2, 127.6, 130.6, 153.8. **IR** (neat, cm^{-1}): 2921, 2850, 1703, 1602, 1485, 1441, 1391, 1329, 1309, 1291, 1275, 1230, 1192, 1130, 1085, 1057, 1021, 968, 934, 896, 855, 751. **HRMS** (ESI): calcd. for $C_{17}H_{24}NO_2$ ($[M+H]^+$): 274.1801, found 240.1800.

(*R*)-Methyl 2-(4-methylpent-3-en-1-yl)indoline-1-carboxylate (**271**):

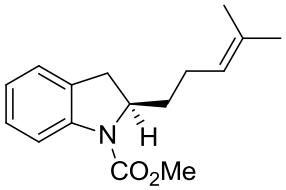

Colorless oil. 51% yield (25.5 mg) calcd. by NMR. 70% *ee*. [Chiral column: AD-H, *n*-hexane/*i*-PrOH = 99 : 1, 0.5 mL/min, 254 nm; t_R = 22.08 min. (major) and 32.49 min. (minor)]. **^{1}H-NMR** (400 MHz, $CDCl_3$): δ 1.58 (s, 3H), 1.68 (s, 3H), 1.69-1.82 (brm, 1 H), 2.01 (q, *J* = 7.4 Hz, 2H), 2.80 (dd, *J* = 16.0, 2.0 Hz, 2H), 3.30 (dd, *J* = 16.0, 9.7 Hz, 2H), 3.85 (s, 3H), 4.45 (brs, 1H), 5.11 (t, *J* = 7.0 Hz, 1H), 6.97 (td, *J* = 7.4, 0.9 Hz, 1H), 7.18 (dd, *J* = 15.1, 7.5 Hz, 2H), 7.78 (brd, 1H). **^{13}C-NMR** (100 MHz, $CDCl_3$): δ 17.8, 23.7, 25.9, 33.5, 34.6, 52.6, 59.4, 115.5, 122.9, 123.6, 125.0, 127.5, 130.6, 132.3, 153.9. **IR** (neat, cm^{-1}): 2953, 2924, 2857, 1708, 1603, 1486, 1442, 1392, 1332, 1287, 1193, 1132, 1060, 752. **HRMS** (EI): calcd. for $C_{16}H_{20}N_1O_2$ ($[M+H]^+$): 258.1488, found: 258.1480.

(*R*)-Methyl 2-(4-methylpent-3-en-1-yl)indoline-1-carboxylate (**271**) and (2*R*,3*S*)-methyl 2-methyl-3-(3-methylbut-2-en-1-yl)indoline-1-carboxylate (**272**):

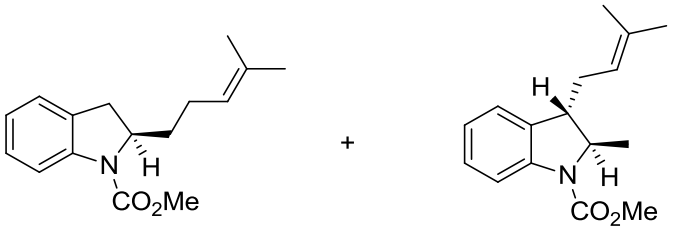

Colorless oil-**272**. 29% yield (15 mg) calcd. by NMR. >99% *ee*. [Chiral column: AD-H, *n*-hexane/*i*-PrOH = 99 : 1, 0.5 mL/min, 254 nm; t_R = 25.03 min. (major)]. **271** + **272**: **^{1}H-NMR** (400 MHz, $CDCl_3$): δ 1.25 (d, *J* = 6.3 Hz, 2H), 1.52 (s, 1.8H), 1.58 (s, 3H), 1.67 (d, *J* = 0.8 Hz, 3H), 1.71 (d, *J* = 0.6 Hz, 2H), 2.01 (q, *J* = 7.4 Hz, 2.2H), 2.17-2.24 (m, 1H), 2.68 – 2.93 (m, 1.6H), 3.29 (dd, *J* = 16.0, 9.6 Hz, 1H), 3.84 (s, 5H), 4.15 (brm, 0.59H), 4.44 (brm, 1H), 5.10-5.15 (m, 1.5H), 6.89-7.06 (m, 1.6H), 7.09-7.23 (m, 3H), 7.66 (brd, 1.6H). **271** + **272**: **^{13}C-NMR** (100 MHz, $CDCl_3$): δ 153.9, 141.9, 134.4, 132.3, 130.5, 127.9, 127.5, 125.0, 123.6, 122.9, 122.8, 121.1, 115.5, 61.0, 59.4, 52.6, 48.8, 34.9, 34.6, 33.5, 26.0, 25.9, 23.7, 20.9, 18.1, 17.8. **271** + **272**: **IR** (neat, cm^{-1}): 2954, 2925, 2856, 1703, 1602, 1484, 1440, 1388, 1331, 1309, 1283, 1191, 1132, 1058, 934, 840, 750.

(*S*)-Methyl 2-(2-methoxyethyl)indoline-1-carboxylate (**273**):

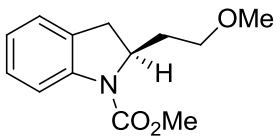

Colorless oil. 51% yield (24.0 mg). 85% *ee*. $[\alpha]_D^{20}$ = -1.10 (*c* = 1.0 in CH_2Cl_2). [Chiral column: AD-H, *n*-hexane/*i*-PrOH = 99 : 1, 0.5 mL/min, 254 nm; t_R = 38.80 min. (minor) and 54.87 min. (major)]. **^{1}H-NMR** (400 MHz, $CDCl_3$): δ 1.73-1.81 (m, 1H), 2.06-2.09 (m, 1H), 2.84 (d, *J* = 16.0 Hz, 1H), 3.28 (s, 3H), 3.30-3.34 (m, 1H), 3.44 (t, *J* = 5.8 Hz, 1H), 3.84 (s, 3H), 4.57 (brm, 1H), 6.96 (t, *J* = 7.4 Hz, 1H), 7.13-7.19 (m, 2H), 7.76 (brd, 1H). ^{13}C NMR (100 MHz, $CDCl_3$): δ 33.6, 34.4, 52.5, 57.4, 58.6, 69.2, 115.4, 122.8, 124.9, 127.4, 146.4, 153.7. **IR** (neat, cm^{-1}): 2952, 1701, 1602, 1484, 1440, 1387, 1330, 1308, 1288, 1220, 1191, 1115, 1056, 1021, 854, 751, 710, 640. **HRMS** (EI): calcd. for $C_{13}H_{17}NO_3Na$ ($[M+Na]^+$): 258.1100, found: 258.1105.

(2*R*,3*S*)-Methyl 3-(methoxymethyl)-2,3-dimethylindoline-1-carboxylate (**274**):

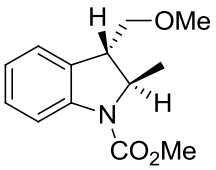

Colorless oil, 35% yield (16.4 mg). >99% *ee*. $[\alpha]_D^{20}$ = +51.61 (*c* = 1.0 in CH_2Cl_2). [Chiral column: AD-H, *n*-hexane/*i*-PrOH = 99 : 1, 0.5 mL/min, 254 nm; t_R = 27.24 min. (major)]. **^{1}H-NMR** (400 MHz, $CDCl_3$): δ 1.35 (d, *J* = 4.8 Hz, 3H), 3.05-3.10 (m, 1H), 3.31-3.36 (m, 1H), 3.40 (d, *J* = 2,5 Hz, 3H), 3.44-3.48 (m, 1H), 3.89 (s, 3H), 4.43 (bs, 1H), 7.01-7.04 (m, 1H), 7.23-7.31 (m, 2H), 7.84 (brd, 1H). ^{13}C NMR (100 MHz, $CDCl_3$): δ 20.8, 48.7, 52.5, 58.9, 75.4, 115.4, 122.7, 125.2, 128.4, 130.1, 141.7, 153.6. **IR** (neat, cm^{-1}): 2927, 1703, 1602, 1484, 1439, 1386, 1313, 1279, 1191, 1136, 1104, 1060, 969, 863, 751, 707, 596. **HRMS** (EI): calcd. for $C_{13}H_{17}N_1O_3Na$ ($[M+Na]^+$): 258.1100, found: 258.1101.

(*S*)-Methyl 2-(2-(methoxymethoxy)ethyl)indoline-1-carboxylate (**275**):

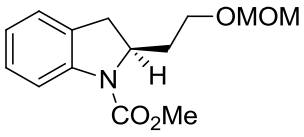

Colorless oil, 45% yield (23.8 mg). 78% *ee*. $[\alpha]_D^{20}$ = -1.15 (*c* = 1.0 in CH_2Cl_2). [Chiral column: AS-H, *n*-hexane/*i*-PrOH = 99 : 1, 0.5 mL/min, 254 nm; 14.94 min. (minor) and t_R = 15.74 min. (major)]. **^{1}H-NMR** (400 MHz, $CDCl_3$): δ 0.94 (t, *J* = 7.5 Hz, 3H), 1.24-1.36 (m, 1H), 1.39-1.55 (m, 1H), 1.80 (brd, 1H), 3.43 (s, 3H), 3.85 (s, 3H), 4.27 (brm, 1H), 4.64-4.83 (m, 2H), 7.04 (t, *J* = 7.5 Hz, 1H), 7.28-7.42 (m, 2H), 7.91 (s, 1H). **^{13}C-NMR** (100 MHz, $CDCl_3$): δ 9.5, 24.9, 29.9, 52.7, 55.7, 67.7, 94.3, 116.0, 122.9, 126.6, 130.4, 143.2, 153.3. **IR** (neat, cm^{-1}): 2955, 1703, 1602, 1483, 1440, 1388, 1333, 1280, 1140, 1061, 1033, 917, 748. **HRMS** (EI): calcd. for $C_{14}H_{19}N_1O_4Na$ ($[M+Na]^+$): 288.1206, found: 288.1202.

(2*R*,3*S*)-Methyl 3-((methoxymethoxy)methyl)-2-methylindoline-1-carboxylate (**276**):

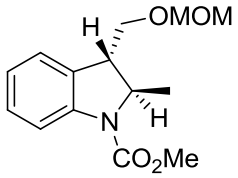

Colorless oil, 44% yield (23.3. mg). 99% *ee*. $[\alpha]_D^{20}$ = +15.35 (*c* = 1.0 in CH_2Cl_2). [Chiral column: AD-H, *n*-hexane/*i*-PrOH = 99 : 1, 0.5 mL/min, 254 nm; 35.76 min. (minor) and t_R = 39.61 min. (major)]. **^{1}H-NMR** (400 MHz, $CDCl_3$): δ 1.29 (d, *J* = 7.1 Hz,3), 3.26 (td, *J* = 7.1, 2.2 Hz, 1H), 3.32 (s, 3H), 3.47-3.61 (m, 1H), 3.75 (dd, *J* = 9.0, 4.4 Hz, 1H), 3.86 (s, 3H), 4.07-4.23 (m, 1H), 4.58 (dd, *J* = 9.8, 6.5 Hz, 2H), 6.99 (t, *J* = 7.9 Hz, 1H), 7.14-7.20 (m, 2H), 7.69 (brd, 1H). **^{13}C-NMR** (100 MHz, $CDCl_3$): δ 22.3, 29.9, 38.7, 52.8, 55.5, 66.5, 68.1, 96.9, 115.4, 123.2, 124.4, 127.7, 136.0, 154.0. **IR** (neat, cm^{-1}): 2955, 1705, 1605, 1482, 1440, 1390, 1282, 1141, 1023, 929, 915, 754. **HRMS** (EI): calcd. for $C_{14}H_{19}N_1O_4Na$ ($[M+Na]^+$): 288.1206, found: 288.1199.

(2*R*,3*S*)-Methyl 3-(acetoxymethyl)-2-methylindoline-1-carboxylate (**278**):

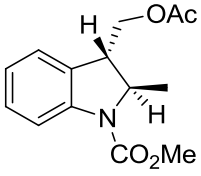

Colorless oil, 42% yield (22.1 mg). 96% *ee*. $[\alpha]_D^{20}$ = -8.64 (*c* = 0.5 in CH_2Cl_2). [Chiral column: AS-H, *n*-hexane/*i*-PrOH = 99 : 1, 0.5 mL/min, 254 nm; 27.63 min. (minor) and t_R = 32.05 min. (mojor)]. **^{1}H-NMR** (400 MHz, $CDCl_3$): δ 1.23-1.27 (m, 1H), 1.27 (d, *J* = 7.7 Hz, 3H), 1.94 (s, 1H), 3.13 (q, *J* = 7.2 Hz, 1H), 3.86 (s, 3H), 4.12-4.30 (m, 3H), 6.99 (td, *J* = 7.4, 0.8 Hz, 1H), 7.14 (d, *J* = 7.2 Hz, 1H), 7.20 (t, *J* = 7.8 Hz, 1H), 7.70 (s, 1H). **^{13}C-NMR** (100

MHz, $CDCl_3$): δ 20.6, 21.9, 38.5, 52.7, 64.3, 65.3, 106.6, 115.2, 123.1, 124.0, 127.7, 135.3, 153.7, 170.8. **IR** (neat, cm^{-1}): 2970, 1739, 1594, 1570, 1455, 1440, 1370, 1331, 1234, 1207, 1117, 1087, 816, 746. **HRMS** (EI): calcd. for $C_{14}H_{17}N_1O_4Na$ ($[M+Na]^+$): 286.1049, found: 286.1045.

(*S*)-Methyl 2-(2-(methylthio)ethyl)indoline-1-carboxylate (**279**):

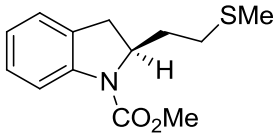

Yellow oil, 56% yield (28.1 mg). 74% *ee*. $[\alpha]_D^{20}$ = +44.26 (*c* = 1.0 in CH_2Cl_2). [Chiral column: (*R*,*R*)-Whelk-O1, *n*-hexane/*i*-PrOH = 99 : 1, 0.5 mL/min, 254 nm; 34.13 min. (minor) and t_R = 45.84 min. (major)]. **^{1}H-NMR** (400 MHz, $CDCl_3$): δ 1.81-1.88 (m, 1H), 2,03-2.06 (m, 1H), 2.09 (s, 3H), 2.42-2.57 (m, 2H), 2.75 (dd, *J* = 16.1, 1.7 Hz, 1H), 3.33 (dd, *J* = 16.0, 9.6 Hz, 1H), 3.84 (s, 3H), 4.56-4.62 (brm. 1H), 6.96 (td, *J* = 7.4, 0.7 Hz, 1H), 7.13-7.02 (m, 2H), 7.78 (brd, 1H). **^{13}C-NMR** (100 MHz): δ 15.5, 29.8, 33.6, 34.1, 52.7, 58.7, 115.6, 123.1, 125.0, 127.7, 130.2, 141.9, 153.8. **IR** (neat, cm^{-1}): 2915, 1699, 1601, 1483, 1439, 1387, 1284, 1224, 1190, 1128, 1055, 749, 711. **HRMS** (EI): calcd. for $C_{13}H_{17}N_1O_2Na$ ($[M+Na]^+$): 274.0872, found: 274.0875.

(2*R*,3*S*)-Methyl 2,3-dimethyl-3-((methylthio)methyl)indoline-1-carboxylate (**280**):

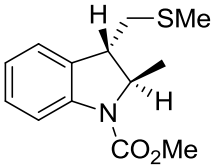

Yellow solid, **m.p.** = 43-45 ˚C, 29% yield (14.5 mg). 74% *ee*. $[\alpha]_D^{20}$ = -15.46 (*c* = 1.0 in CH_2Cl_2). [Chiral column: (*R*,*R*)-Whelk-O1, *n*-hexane/*i*-PrOH = 99 : 1, 0.5 mL/min, 254 nm; 19.96 min. (minor) and t_R = 24.71 min. (major)]. **^{1}H-NMR** (400 MHz, $CDCl_3$): δ 1.20-1.31 (m, 1H), 1.46 (d, *J* = 6.3 Hz, 3H), 3.86 (s, 3H), 4.84 (brs, 1H), 4.97 (s, 1H), 5.47 (d, *J* = 2.4 Hz, 1H), 7.02 (td, *J* = 7.5, 0.7 Hz, 1H), 7.28 (t, *J* = 7.6 Hz, 1H), 7.44 (d, *J* = 7.6 Hz, 1H), 7.95 (brd, 1H). **^{13}C-NMR** (100 MHz, $CDCl_3$): δ 22.5, 52.7, 60.4, 101.6, 116.0, 120.8, 123.0, 130.2, 147.4. **IR** (neat, cm^{-1}): 2954, 1705, 1643, 1601, 1477, 1465, 1438, 1381, 1318, 1276, 1207, 1146, 1060, 869, 747, 707, 613.

(*S*)-Methyl 2-((methylthio)methyl)indoline-1-carboxylate (**281**):

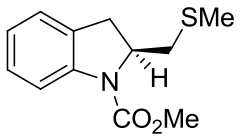

Yellow oil, 45% yield (21.3 mg). 97% *ee*. $[\alpha]_D^{20}$ = +45.69 (*c* = 1.0 in CH_2Cl_2). [Chiral column: AD-H, *n*-hexane/*i*-PrOH = 99 : 1, 0.5 mL/min, 254 nm; 34.46 min. (minor) and t_R = 37.04 min. (major)]. **^{1}H-NMR** (400 MHz, $CDCl_3$): δ 2.16 (s, 3H), 2.54 (dd, *J* = 13.1, 9.7 Hz, 1H), 2.81-2.97 (m, 1H), 3.04 (dd, *J* = 16.4, 1.7 Hz, 1H), 3.34 (dd, *J* = 16.4, 9.5 Hz, 1H), 3.86 (s, 3H), 4.60 (brs, 1H), 6.98 (t, *J* = 7.7 Hz, 1H), 7.16-7.19 (m, 2H), 7.76 (brd, 1H). **^{13}C-NMR** (100 MHz, $CDCl_3$): δ 15.8, 33.2, 38.2, 52.8, 58.6, 115.4, 123.2, 125.2, 127.7, 128.3, 133.6, 153.8. **IR** (neat, cm^{-1}): 2952, 1701, 1601, 1483, 1439, 1386, 1319, 1284, 1127, 1056, 1024, 750, 602. **HRMS** (EI): calcd. for $C_{12}H_{15}N_1O_2Na$ ($[M+Na]^+$): 260.0715. found: 260.0707.

(*R*)-Ethyl 2-ethylindoline-1-carboxylate (**285**):

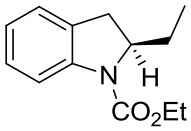

(*S*,*S*)-[**L14**H][I] was used. Colorless oil, 67% yield (29.5 mg) calcd. by NMR, 61% *ee* [Chiracel AS-H column, *n*-hexane/*i*-PrOH = 100:0, 0.5 mL/min, 254 nm; t_R = 20.67 min. (major) and 28.23 (minor)].

(*R*)-Ethyl 2-ethylindoline-1-carboxylate (**285**) and (2*R*,3*S*)-ethyl 2,3-dimethylindoline-1-carboxylate (**286**):

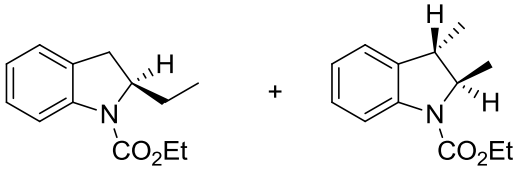

(*S*,*S*)-[**L14**H][I] was used. **286** 23% yield (10.1 mg) calcd. by NMR, 99% *ee* [Chiracel AS-H column, *n*-hexane/*i*-PrOH = 100:0, 0.5 mL/min, 254 nm; t_R = 16.31 min. (major) and 19.46 (minor)]. **285** + **286**: **^{1}H-NMR** (400 MHz, $CDCl_3$): δ 0.88 (t, *J* = 7.4 Hz, 3H), 1.23 (d, *J* = 7.0 Hz, 2.3H), 1.29 (d, *J* = 6.3 Hz, 2.3H), 1.34-1.39 (m, 5.4H), 1.53-1.64 (m, 1H), 1.78 (bs, 1H), 2.75 (dd, *J* = 16.1, 2.0 Hz, 1H), 2.84 (qd, 7.0, 2.1 Hz, 0.7H), 3.28 (dd, *J* = 16.0, 9.6 Hz, 1H), 4.06 (bs, 0.7H), 4.26-4.34 (m, 3.5H), 4.4 (bs, 1H), 6.95 (td, *J* = 7.4, 0.8 Hz, 1H), 6.98

(td, *J* = 7.4, 0.8 Hz, 0.7H), 7.13-7.21 (m, 3.7H), 7.73 (bs, 1.7H). **285** + **286**: **^{13}C-NMR** (100 MHz, $CDCl_3$): δ 9.1, 14.6, 20.5, 21.8, 27.3, 32.9, 43.0, 60.5, 61.3, 63.3, 115.3, 122.6, 122.7, 124.3, 124.8, 127.3, 127.6, 153.4.

(*R*)-Benzyl 2-ethylindoline-1-carboxylate (**287**):

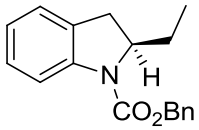

(*S*,*S*)-[**L14**H][I] was used. 56% yield (34.3 mg) calcd. by NMR. 61% *ee* [Chiracel AS-H column, *n*-hexane/*i*-PrOH = 99:1, 0.5 mL/min, 254 nm; t_R = 12.63 min. (major) and 14.55 (minor)].

(*R*)-Benzyl 2-ethylindoline-1-carboxylate (**287**) and (2*R*,3*S*)-benzyl 2,3-dimethylindoline-1-carboxylate (**288**):

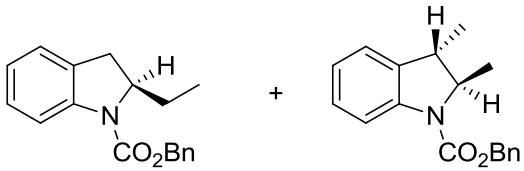

(*S*,*S*)-[**L14**H][I] was used. **288** 37% yield (20.8 mg) calcd. by NMR. 99% *ee* [Chiracel AS-H column, *n*-hexane/*i*-PrOH = 99:1, 0.5 mL/min, 254 nm; t_R = 10.97 min. (major)]. **287** + **288**: **^{1}H-NMR** (400 MHz, $CDCl_3$): δ 0.88 (t, *J* = 7.3 Hz, 3H), 1.25 (d, *J* = 7.0 Hz, 2.4H), 1.31 (d, *J* = 6.3 Hz, 2.4H), 1.56-1.67 (m, 1.4H), 1.8 (bs, 1H), 2.77 (dd, *J* = 16.0, 2.0 Hz, 1H), 2.87 (qd, *J* = 7.0, 2.1 Hz, 0.74H), 3.30 (dd, *J* = 16.0, 9.6 Hz, 1H), 4.11-4.14 (m, 0.74H), 4.45 (bs, 1H), 5.19-5.34 (m, 3.5H), 6.95-7.02 (m, 1.8H), 7.15-7.20 (m, 3.6H), 7.32-7.46 (m, 8.9H), 7.85 (bs, 1.74H). **287** + **288**: **^{13}C-NMR** (100 MHz, $CDCl_3$): δ 9.1, 20.6, 21.8, 27.6, 29.7, 33.0, 43.0, 60.6, 63.5, 67.1, 99.9, 115.4, 122.8, 122.9, 124.3, 124.8, 127.4, 127.7, 128.0, 128.13, 128.17, 128.2, 128.62, 128.63, 136.3, 153.2.

(*S*)-Methyl 2-isopropylindoline-1-carboxylate (**289**):

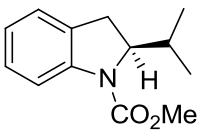

Colorless oil, 84% yield (36.8 mg), 4% *ee*. [Chiral column: AS-H, *n*-hexane/*i*-propanol = 99 : 1, 0.5 mL/min, 254 nm); ret. time = 9.8 min (major) and 11.5 min (minor)]. **^{1}H-NMR** (400 MHz, $CDCl_3$): δ 0.67 (d, *J* = 6.8 Hz, 3H), 0.90 (d, *J* = 6.8 Hz, 3H), 2.12-2.36 (m, 1H), 2.82 (dd, *J* = 16.4, 2.8 Hz, 1H), 3.14 (td, *J* = 16.4, 10 Hz, 1H), 3.82 (s, 3H), 4.26-4.50 (brd, 1H), 6.92 (td, *J* = 7.6, 1.2 Hz, 1H), 7.10 (d, *J* = 7.6 Hz, 1H), 7.14 (t, *J* = 7.6 Hz, 1H), 7.32-8.30 (brd, 1H). **^{13}C-NMR** (100 MHz, $CDCl_3$): δ 15.5, 16.4, 18.5, 18.6, 29.1, 29.9, 31.1, 52.6, 64.2, 115.4, 115.8, 122.9, 123.0, 124.4, 127.4, 131.1, 131.3, 142.8, 154.3. IR (neat, cm^{-1}): 2959, 2874, 1702, 1602, 1485, 1464, 1441, 1390, 1338, 1314, 1282, 1224, 1193, 1127, 1086, 1039, 1023, 996, 845, 766, 746. **HRMS** (EI): calcd. for $C_{13}H_{18}NO_2$ ($[M+H]^+$): 220.1332, found 220.1324.

(*S*)-Methyl 2-(*tert*-butyl)indoline-1-carboxylate (**291**):

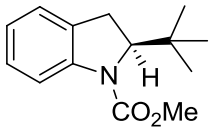

Colorless oil, 93% yield (43.3 mg), 3% *ee*. [Chiral column: (*R*,*R*)-Whelk-O1, *n*-hexane/*i*-propanol = 99 : 1, 1 mL/min, 254 nm); ret. time = 9.0 min (major) and 11.8 min (minor)]. **^{1}H-NMR** (400 MHz, $CDCl_3$): δ 0.81 (s, 9H), 2.84 (d, *J* = 16 Hz, 1H), 3.20 (dd, *J* = 16, 9.6, Hz, 1H), 3.79 (s, 3H), 4.35 (d, *J* = 9.6 Hz, 1H), 6.94 (td, *J* = 7.2, 0.8 Hz, 1H), 7.10 (d, *J* = 7.6 Hz, 1H), 7.14 (t, *J* = 7.6 Hz, 1H), 7.26-7.80 (m, 1H). **^{13}C-NMR** (100 MHz, $CDCl_3$): δ 26.1, 30.9, 36.7, 52.7, 67.7, 116.8, 123.4, 124.0, 127.2, 132.7, 143.5, 155.6. **IR** (neat, cm^{-1}): 2959, 1703, 1601, 1487, 1439, 1369, 1341, 1323, 1276, 1227, 1192, 1156, 1127, 1087, 1058, 1043, 1016, 995, 974, 931, 845, 774. **HRMS** (EI): calcd. for $C_{14}H_{20}NO_2$ ($[M+H]^+$): 234.1498, found 234.1488.

IV.9.5. Pd(NHC)-Catalyzed Synthesis of Indolines via Regiodivergent Reaction from Enantiopure Carbamates

(*S*)-Methyl 2-(methoxymethyl)indoline-1-carboxylate (**265**):

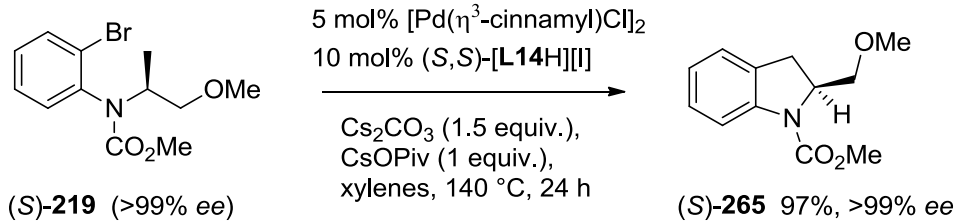

(*S*)-**219** (>99% *ee*) → (*S*)-**265** 97%, >99% *ee*

Carbamate (*S*)-**219** (60.4 mg, 0.2 mmol), cesium carbonate (97.5 mg, 0.3 mmol), [Pd(π-cinnamyl)Cl]$_2$ (5.2 mg, 0.01 mmol), cesium pivalate (46.8 mg, 0.2 mmol) and (*S*,*S*)-[**L14**H][I] (11.8 mg, 0.02 mmol) were placed in a Schlenk flask. After the flask was evacuated and backfilled with nitrogen, dry xylenes (2 mL) was added under nitrogen. The resulting reaction mixture was stirred at 140 °C in the Schlenk tube behind a protective shield for 24 h. The reaction mixture was cooled to rt and diluted with dichloromethane (2 mL) followed by filtration through a pad of celite. The filtrate was evaporated by rotary evaporator and the volatiles were removed under vacuum. The residue was purified by f.c. (silica gel; diethyl acetate : pentane = 1 : 30 as eluent) to afford the indoline methyl carbamate (*R*)-**265** in 97% yield (42.8 mg) and >99% *ee* [Chiral column: AD-H, *n*-hexane/*i*-PrOH = 99 : 1, 0.5 mL/min, 254 nm; t_R = 28.44 min. (major)].

(2*S*,3*R*)-Methyl 3-methoxy-2-methylindoline-1-carboxylate (**266**)**:**

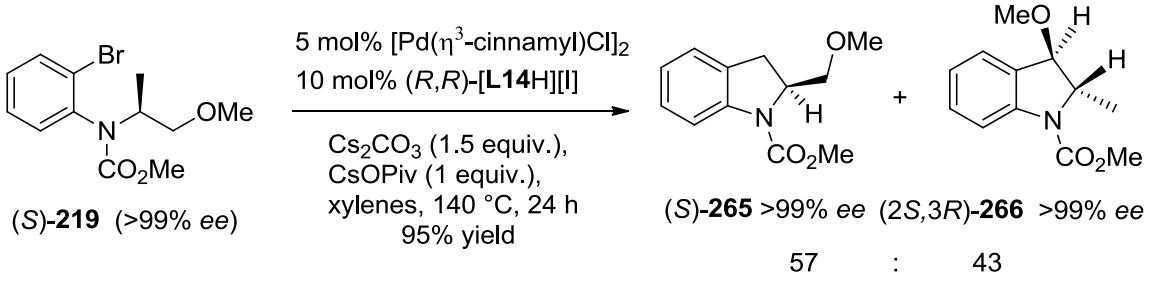

Carbamate (*S*)-**219** (60.4 mg, 0.2 mmol), cesium carbonate (97.5 mg, 0.3 mmol), [Pd(π-cinnamyl)Cl]$_2$ (5.2 mg, 0.01 mmol), cesium pivalate (46.8 mg, 0.2 mmol) and (*R*,*R*)-[**L14**H][I] (11.8 mg, 0.02 mmol) were placed in a Schlenk flask. After the flask was evacuated and backfilled with nitrogen, dry xylenes (2 mL) was added under nitrogen. The resulting reaction mixture was stirred at 140 °C in the Schlenk tube behind a protective shield for 24 h. The reaction mixture was cooled to rt and diluted with dichloromethane (2 mL) followed by filtration through a pad of celite. The filtrate was evaporated by rotary evaporator and the volatiles were removed under vacuum. The residue was purified by f.c. (silica gel; diethyl acetate : pentane = 1 : 30 as eluent) to afford the mixture of indolines (*R*)-**265** (>99% *ee*) in 54.1 % yield (25.2 mg; yield calcd. by NMR), [Chiral column: AD-H, *n*-hexane/*i*-PrOH = 99 : 1, 0.5 mL/min, 254 nm; t_R = 28.70 min. (major)] and (2*S*,3*R*)-**266** (>99% *ee*) in 40.8 % yield (18.1 mg; yield calcd. by NMR) [Chiral column: AD-H, *n*-hexane/*i*-PrOH = 99 : 1, 0.5 mL/min, 254 nm; t_R = 26.17 min. (major)].

(*R*)-Methyl 2-benzylindoline-1-carboxylate (**267**):

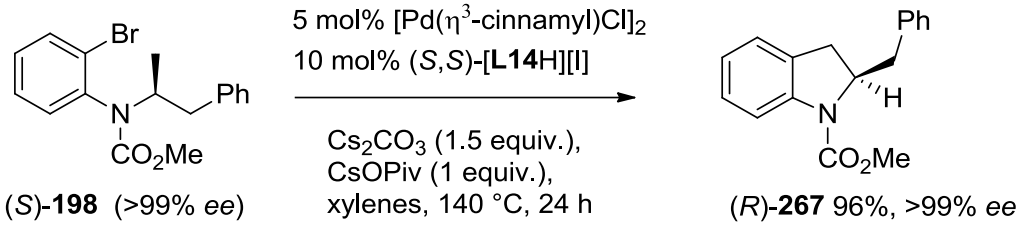

(*S*)-**198** (>99% *ee*) (*R*)-**267** 96%, >99% *ee*

The same procedure as for (*S*)-**265** applied to the synthesis of (*R*)-**267**. Carbamate (*S*)-**198** was used. (*R*)-**267** formed in 96% yield (51.2 mg), >99% *ee* [Chiral column: AD-H, *n*-hexane/*i*-PrOH = 99 : 1, 0.5 mL/min, 254 nm; t_R = 36.51 min. (major)].

(2*R*,3*S*)-Methyl 2-methyl-3-phenylindoline-1-carboxylate (**268**):

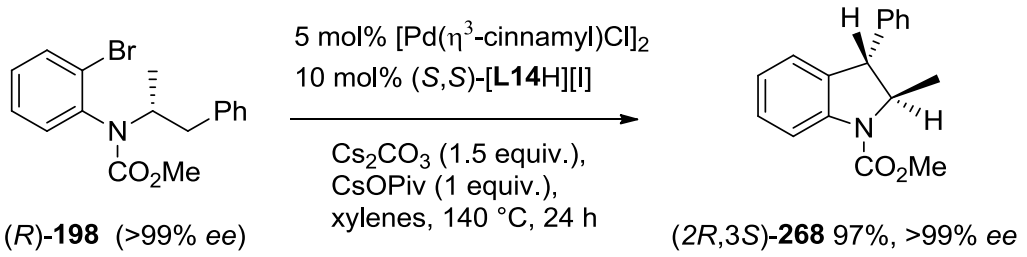

(*R*)-**198** (>99% *ee*) (2*R*,3*S*)-**268** 97%, >99% *ee*

The same procedure as for (2*S*,3*R*)-**266** applied to the synthesis of (2*R*,3*S*)-**268**. Carbamate (*R*)-**198** was used. (2*R*,3*S*)-**268** formed in 97% yield (51.8 mg), >99% *ee* [Chiral column: AD-H, *n*-hexane/*i*-PrOH = 99 : 1, 0.5 mL/min, 254 nm; t_R = 31.71 min. (major)].

(2*S*,3*R*)-Methyl 3-methoxy-2-propylindoline-1-carboxylate (**294**):

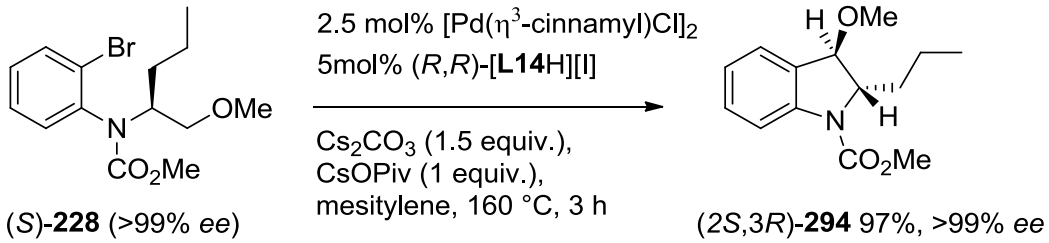

(*S*)-**228** (>99% *ee*) (2*S*,3*R*)-**294** 97%, >99% *ee*

Colorless oil, 97% yield (48.3 mg). $[\alpha]_D^{20}$ = -23.24 (*c* = 1.0 in CH_2Cl_2). >99% *ee*. **^{1}H-NMR** (400 MHz, $CDCl_3$): δ 0.94 (t, *J* = 7.2 Hz, 3H), 1.26-1.50 (m, 3H), 1.69 (brm, 1H), 3.34 (s, 3H), 3.83 (s, 3H), 4.34 (brm, 1H), 4.38 (s, 1H), 7.04 (t, *J* = 7.4 Hz, 1H), 7.34-7.50 (m, 2H), 7.51-7.91 (brd, 1H). **^{13}C-NMR** (100 MHz, $CDCl_3$): δ 14.0, 18.3, 55.1, 65.0, 68.9, 70.8, 107.2, 115.9, 122.6, 130.3, 160.1. **IR** (neat, cm^{-1}): 2957, 2821, 1704, 1604, 1481, 1440, 1389, 1336,

1304, 1285, 1268, 1190, 1138, 1087, 1057, 1022, 937, 750. **HRMS** (EI): calcd. for $C_{14}H_{19}BrNO_3$ ($[M]^+$) 249.1360, found 249.1362.

(2*S*,3*S*)-Methyl 3-ethyl-2-(methoxymethyl)indoline-1-carboxylate (**295**):

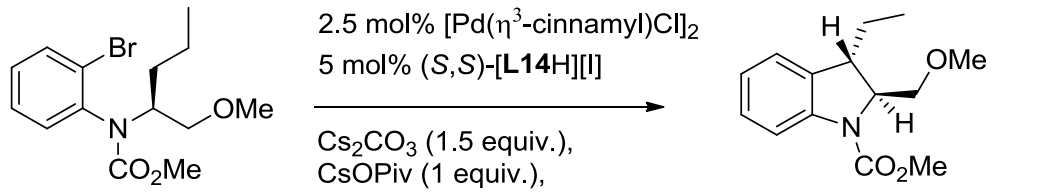

(*S*)-**228** (>99% *ee*) (*2S*,3*S*)-**295** 96%, >99% *ee*

Colorless oil, 96% yield (47.8 mg). $[\alpha]_D^{20}$ = -3.57 (*c* = 1.0 in CH_2Cl_2). >99% *ee*. **^{1}H-NMR** (400 MHz, $CDCl_3$): δ 0.94 (t, *J* = 7.4 Hz, 3H), 1.60 (dh, *J* = 13.9, 6.8 Hz, 2H), 3.07 (t, *J* = 6.6 Hz, 1H), 3.34 (s, 3H), 3.56 (dd, *J* = 9.0, 3.8 Hz, 1H), 3.85 (s, 3H), 4.27 (s, 1H), 6.99 (t, *J* = 7.4 Hz, 1H), 7.18 (dd, *J* = 14.4, 7.4 Hz, 2H), 7.29-8.05 (brm, 1H). **^{13}C-NMR** (100 MHz, $CDCl_3$): δ 10.9, 22.3, 29.1, 45.2, 52.6, 59.1, 63.7, 72.9, 115.3, 122.9, 124.9, 127.6, 134.4. **IR** (neat, cm^{-1}): 2959, 2925, 1703, 1601, 1482, 1461, 1440, 1378, 1333, 1280, 1193, 1138, 1113, 1059, 1022, 743. **HRMS** (ESI): calcd. for $C_{14}H_{20}NO_3$ ($[M+H]^+$): 250.1437, found 250.1431.

(2*S*,3*R*)-Methyl 2-benzyl-3-methoxyindoline-1-carboxylate (**296**):

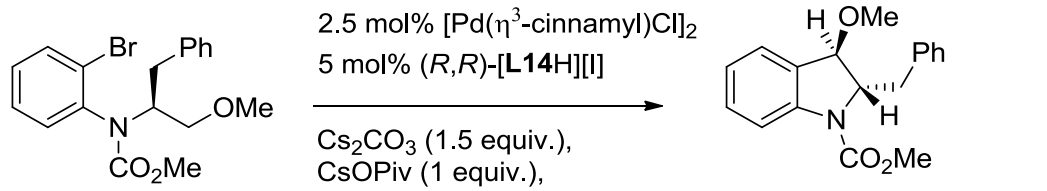

(*S*)-**229** (>99% *ee*) (*2S*,3*R*)-**296** 98%, >99% *ee*

Colorless oil, 98% yield (58.2 mg). $[\alpha]_D^{20}$ = -24.18 (*c* = 1.0 in CH_2Cl_2). >99% *ee*. **^{1}H-NMR** (400 MHz, $CDCl_3$): δ 2.47-2.58 (m, 1H), 3.08 (brs, 3H), 3.15-3.47 (m, 1H), 3.87 (brs, 3H), 4.43 (s, 1H), 4.50-4.61 (m, 1H), 7.12 (t, *J* = 7.2 Hz, 1H), 7.20-7.51 (m, 2H), 7.51- 8.14 (m, 1H). **^{13}C-NMR** (100 MHz, $CDCl_3$): δ 38.0, 52.7, 55.2, 59.2, 66.2, 81.8, 115.9, 122.9, 126.6, 126.8, 127.4, 128.1, 128.6, 129.5, 130.5, 137.0. **IR** (neat, cm^{-1}): 2952, 1704, 1603, 1481, 1440, 1389, 1346, 1316, 1272, 1190, 1136, 1087, 1055, 1034, 968, 755. **HRMS** (EI): calcd. for $C_{18}H_{19}NO_3$ ($[M]^+$): 297.1360, found 297.1359.

(2*S*,3*S*)-Methyl 2-(methoxymethyl)-3-phenylindoline-1-carboxylate (**297**):

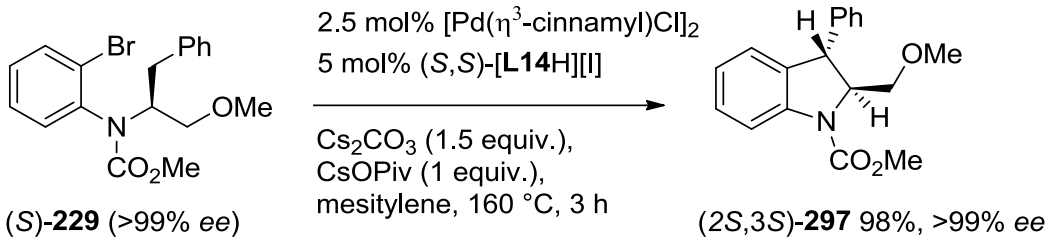

(*S*)-**229** (>99% *ee*) (*2S*,3*S*)-**297** 98%, >99% *ee*

White solid, **m.p.** = 117-119 °C, 98% yield (58.2 mg). $[\alpha]_D^{20}$ = +69.59 (*c* = 1.0 in CH_2Cl_2). >99% *ee*. **^{1}H-NMR** (400 MHz, $CDCl_3$): δ 3.46 (s, 3H), 3.53 (t, *J* = 9.0 Hz, 1H), 3.76 (dd, *J* = 9.4, 3.8 Hz, 1H), 3.89 (s, 3H), 4.47-4.55 (m, 2H), 7.01-7.18 (m, 4H), 7.21-7.37 (m, 4H), 7.46-8.13 (brd, 1H). **^{13}C-NMR** (100 MHz, $CDCl_3$): δ 49.3, 52.7, 59.2, 67.2, 72.7, 115.4, 123.4, 126.0, 126.8, 127.4, 128.1, 128.7, 144.1. **IR** (neat, cm^{-1}): 2929, 2818, 1703, 1599, 1481, 1440, 1377, 1302, 1261, 1189, 1136, 1122, 1047, 964, 760. **HRMS** (ESI): calcd. for $C_{18}H_{20}NO_3$ ($[M+H]^+$): 298.1437, found 298.1438.

(2*S*,3*R*)-Methyl 2-isobutyl-3-methoxyindoline-1-carboxylate (**298**):

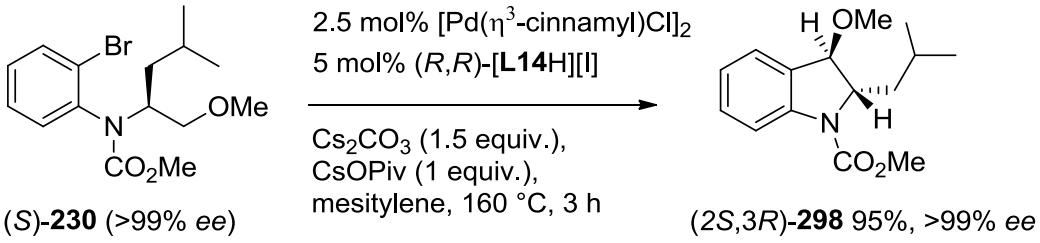

(*S*)-**230** (>99% *ee*) (*2S*,3*R*)-**298** 95%, >99% *ee*

Colorless oil, 95% yield (49.9 mg). $[\alpha]_D^{20}$ = -30.98 (*c* = 1.0 in CH_2Cl_2). >99% *ee*. **^{1}H-NMR** (400 MHz, $CDCl_3$): δ 0.96 (d, *J* = 6.5 Hz, 3H), 1.04 (d, *J* = 5.0 Hz, 3H), 1.25-1.29 (m, 1H), 1.46-1.56 (m, 1H), 1.74 (brs, 1H), 3.33 (s, 3H), 3.83 (s, 3H), 4.35 (s, 2H), 7.04 (t, *J* = 7.4 Hz, 1H), 7.30-7.39 (m, 2H), 7.85 (brd, 1H). **^{13}C-NMR** (75 MHz, $CDCl_3$): δ 21.7, 23.5, 24.7, 40.8, 52.5, 55.1, 63.9, 116.0, 122.6, 126.5, 130.3, 133.3, 153.1. **IR** (neat, cm^{-1}): 2955, 1708, 1604, 1481, 1440, 1388, 1289, 1273, 1192, 1128, 1089, 1056, 934, 883, 753, 621. **HRMS** (EI): calcd. for $C_{15}H_{21}NO_3$ ($[M]^+$): 263.1516, found 263.1518.

IV.10. Synthesis of (2*R*,3*S*)-2-Methyl-3-Phenylindoline (293)

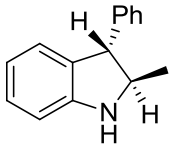

To a solution of (2*R*,3*S*)-**268** (53.4 mg, 0.2 mmol, 1 equiv.) in THF/MeOH (2.5 mL/ 5 mL) was added 5*N*-NaOH aq. (2 mL, 10 mmol, 50 equiv.). This mixture was refluxed for 24 h. After cooling to rt it was extracted with CH_2Cl_2. The combined organic phases were dried over Na_2SO_4. After filtration and evaporation the crude residue was purified by f. c. (silica gel; eluent: ethyl acetate:pentane = 1:20) affording indoline (2*R*,3*S*)-**293** as a colorless oil in 92% yield (38.4 mg,)

$[\alpha]_D^{20}$ = +35.0 (*c* = 0.5 in CH_2Cl_2). >99% *ee*. [Chiral column, AD-H, *n*-hexane/*i*-PrOH = 99:1, 0.5 mL/min, 254 nm, t_R = 20.36 min. (major)]. **^{1}H-NMR** (400 MHz, $CDCl_3$): δ 1.31 (d, *J* = 6.0 Hz, 3H), 3.84 (q, *J* = 5.9 Hz, 1H), 3.92 (d, *J* = 9.6 Hz, 1H), 6.65-6.69 (m, 2H), 6.79-6.82 (m, 2H), 7.70 (tt, *J* = 7.6, 1.0 Hz, 1H), 7.22-7.26 (m, 2H), 7.29-7.33 (m, 2H). **^{13}C-NMR** (100 MHz, $CDCl_3$): δ 20.5, 57.2, 65.6, 109.5, 119.2, 125.1, 127.0, 127.9, 128.7, 128.9, 132.6, 142.8, 151.0. **IR** (neat, cm^{-1}): 3364, 3028, 2963, 2854, 1732, 1605, 1482, 1464, 1375, 1245, 1214, 1017, 746, 698. **HRMS** (ESI): calcd. for $C_{18}H_{19}N_2O$ ($[M+H]^+$): 210.1277, found: 210.1280

IV.11. IR and Vibrational Circular Dichroism (VCD) Spectra[****]

IR and vibrational circular dichroism (VCD) spectra were recorded on a Bruker PMA 50 accessory coupled to a Tensor 27 Fourier transform infrared spectrometer. A photoelastic modulator (Hinds PEM 90) set at l/4 retardation was used to modulate the handedness of the circular polarized light. Demodulation was performed by a lock-in amplifier (SR830 DSP). An optical low-pass filter (< 1800 cm^{-1}) in front of the photoelastic modulator was used to enhance the signal/noise ratio. Solutions of ca. 10 mg in 500 µl CD_2Cl_2were prepared and measured in a cell equipped with CaF_2 windows and a 130 µm spacer. The neat solvent served as the reference. For both the sample and reference 8400 scans at 4 cm^{-1} resolution were averaged.

[****] Carried out by *Prof. T. Bürgi*.

IV.11.1. Computational Methods

Density functional theory (DFT) as implemented in Gaussian03 was used to study the structure of **246** and **268** and to calculate the corresponding IR and VCD spectra.(ref Gausian) The calculations were performed using the b3lyp functional[277] and a 6-31G(d) basis set.[278] Prior to the calculation of the spectra all degrees of freedom were completely relaxed. IR and VCD spectra were constructed from calculated dipole and rotational strengths using the GaussView program.[††††]

IV.11.2 Discussion of Results

VCD spectroscopy was used to determine the stereochemistry of the indolines **248** and **268**. For both compounds four isomers are possible, corresponding to the *cis* and *trans* arrangement of the two substituents and the corresponding enantiomers. In addition one has to consider conformational freedom. For the phenyl-methyl compound two conformers are possible corresponding to the arrangement of the ester group. For the methyl-ethyl compound additionally three positions are feasible for the ethyl group leading to a total of six conformers for each stereoisomer. All the conformers were calculated. The discussion presented here is however based only on the most stable conformer of the corresponding compound. A more detailed discussion will be given elsewhere.

Indoline (**248**):

The IR and VCD spectra of the *cis* and *trans* compound are quite similar, particularly for the carbonyl vibration, the weak band measure around 1600 cm^{-1} and the group of bands slightly below 1500 cm^{-1} (calculated slightly above 1500 cm^{-1}). A clear distinction is possible based on the strong band measure at around 1400 cm^{-1} (calculated at 1460 cm^{-1}). For the *cis* compound this band is calculated positive in the VCD and has opposite phase as the carbonyl

[††††] Gaussian 03, Revision C.01, M. J. Frisch, G. W. Trucks, H. B. Schlegel, G. E. Scuseria, M. A. Robb, J. R. Cheeseman, J. A. Montgomery, Jr., T. Vreven, K. N. Kudin, J. C. Burant, J. M. Millam, S. S. Iyengar, J. Tomasi, V. Barone, B. Mennucci, M. Cossi, G. Scalmani, N. Rega, G. A. Petersson, H. Nakatsuji, M. Hada, M. Ehara, K. Toyota, R. Fukuda, J. Hasegawa, M. Ishida, T. Nakajima, Y. Honda, O. Kitao, H. Nakai, M. Klene, X. Li, J. E. Knox, H. P. Hratchian, J. B. Cross, V. Bakken, C. Adamo, J. Jaramillo, R. Gomperts, R. E. Stratmann, O. Yazyev, A. J. Austin, R. Cammi, C. Pomelli, J. W. Ochterski, P. Y. Ayala, K. Morokuma, G. A. Voth, P. Salvador, J. J. Dannenberg, V. G. Zakrzewski, S. Dapprich, A. D. Daniels, M. C. Strain, O. Farkas, D. K. Malick, A. D. Rabuck, K. Raghavachari, J. B. Foresman, J. V. Ortiz, Q. Cui, A. G. Baboul, S. Clifford, J. Cioslowski, B. B. Stefanov, G. Liu, A. Liashenko, P. Piskorz, I. Komaromi, R. L. Martin, D. J. Fox, T. Keith, M. A. Al-Laham, C. Y. Peng, A. Nanayakkara, M. Challacombe, P. M. W. Gill, B. Johnson, W. Chen, M. W. Wong, C. Gonzalez, and J. A. Pople, Gaussian, Inc., Wallingford CT, 2004.

band. For the *trans* this band is calculated strongly negative and has the same phase as the carbonyl band, as is observed in the experiment. In the experiment there is a positive band at 1460, which is due to another conformer.

Conclusion: Analysis of the VCD spectra strongly indicates that the measured compound corresponds to the *trans* compound and the enantiomer corresponds to the one considered in the calculation.

Indoline (**268**):

The IR and VCD spectra of the *cis* and *trans* compound are again quite similar. Also in this case the region around the strong band measure slightly below 1400 cm^{-1} (calculated slightly above 1400 cm^{-1}) is most conclusive. For the *cis* there are positive and negative bands, whereas for the *trans* only strong negative bands are calculated. The experiment reveals two strong positive bands, where the stronger one corresponds to a relatively weak band in the IR. This is a strong indication for the *trans* configuration. Furthermore, for the *cis* a relatively strong carbonyl band in the VCD is predicted, in contrast to the experiment. The bands calculated for the *trans* have opposite sign compared to the measured spectrum, which shows that the enantiomer considered in the calculation has opposite absolute configuration with respect to the measured compound.

Conclusion: Analysis of the VCD spectra strongly indicates that the measured compound corresponds to the *trans* compound and the enantiomer measured has opposite absolute configuration with respect to the one calculated.

Indoline (**248**) (Experimental spectra):

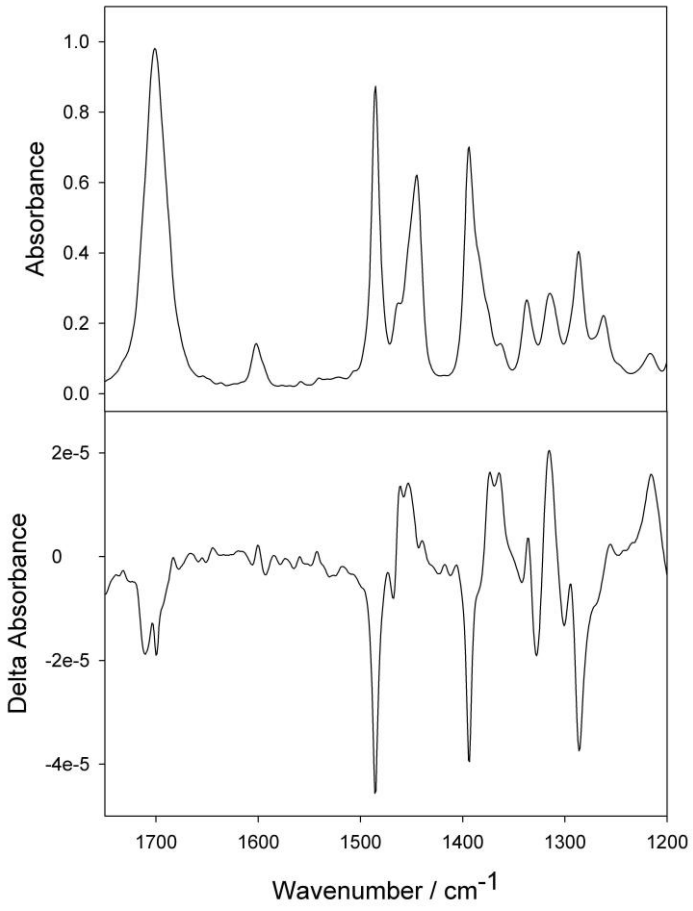

(2*S*,3*R*)-Methyl 2-ethyl-3-methylindoline-1-carboxylate (**248**):

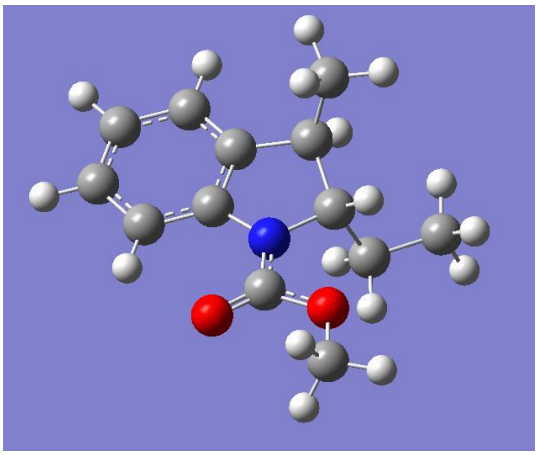

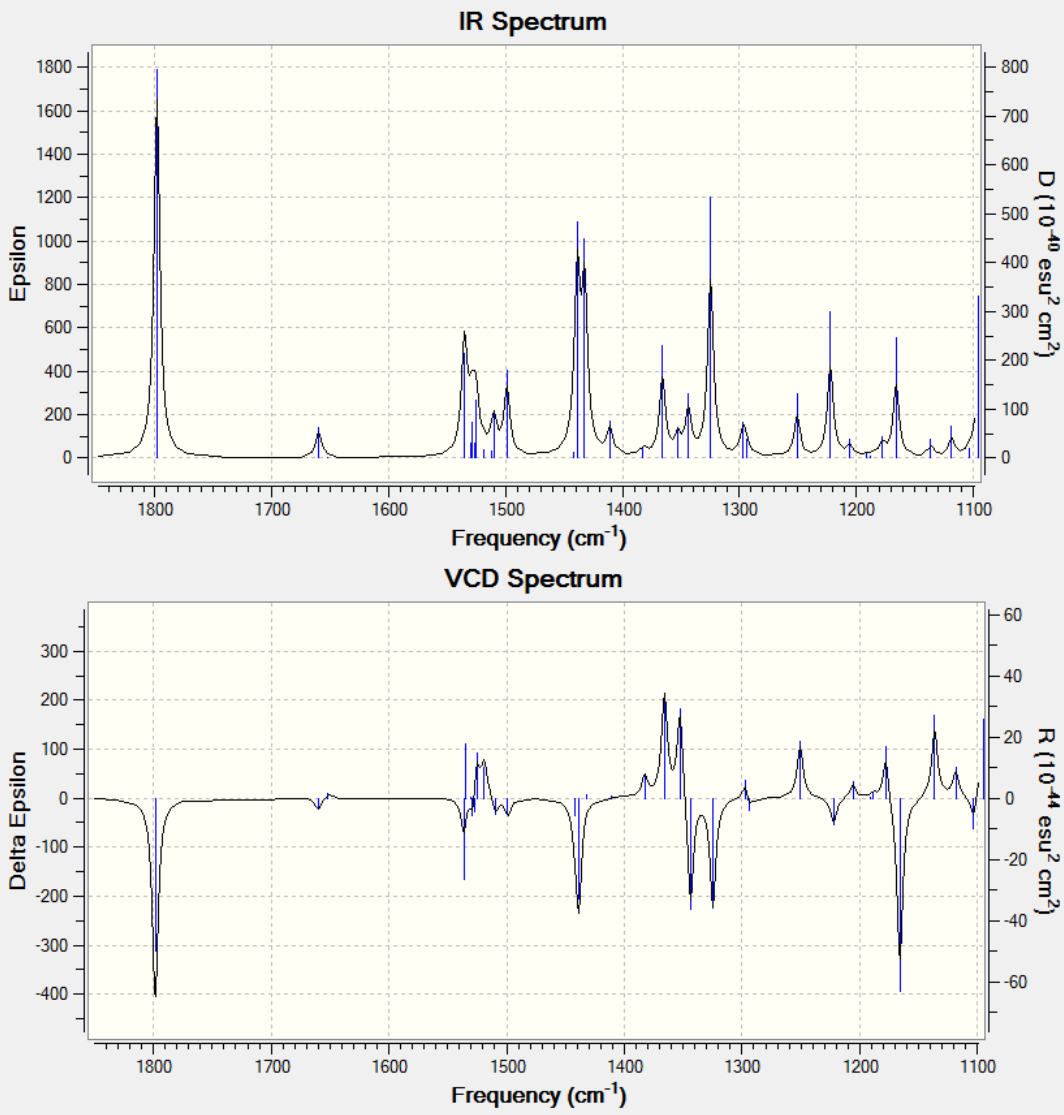

(2*S*,3*S*)-Methyl 2-ethyl-3-methylindoline-1-carboxylate (**248**):

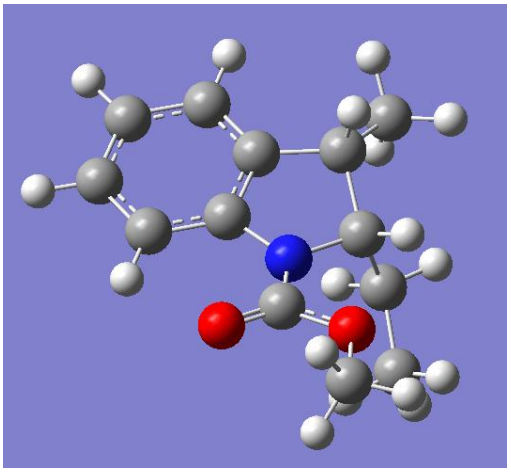

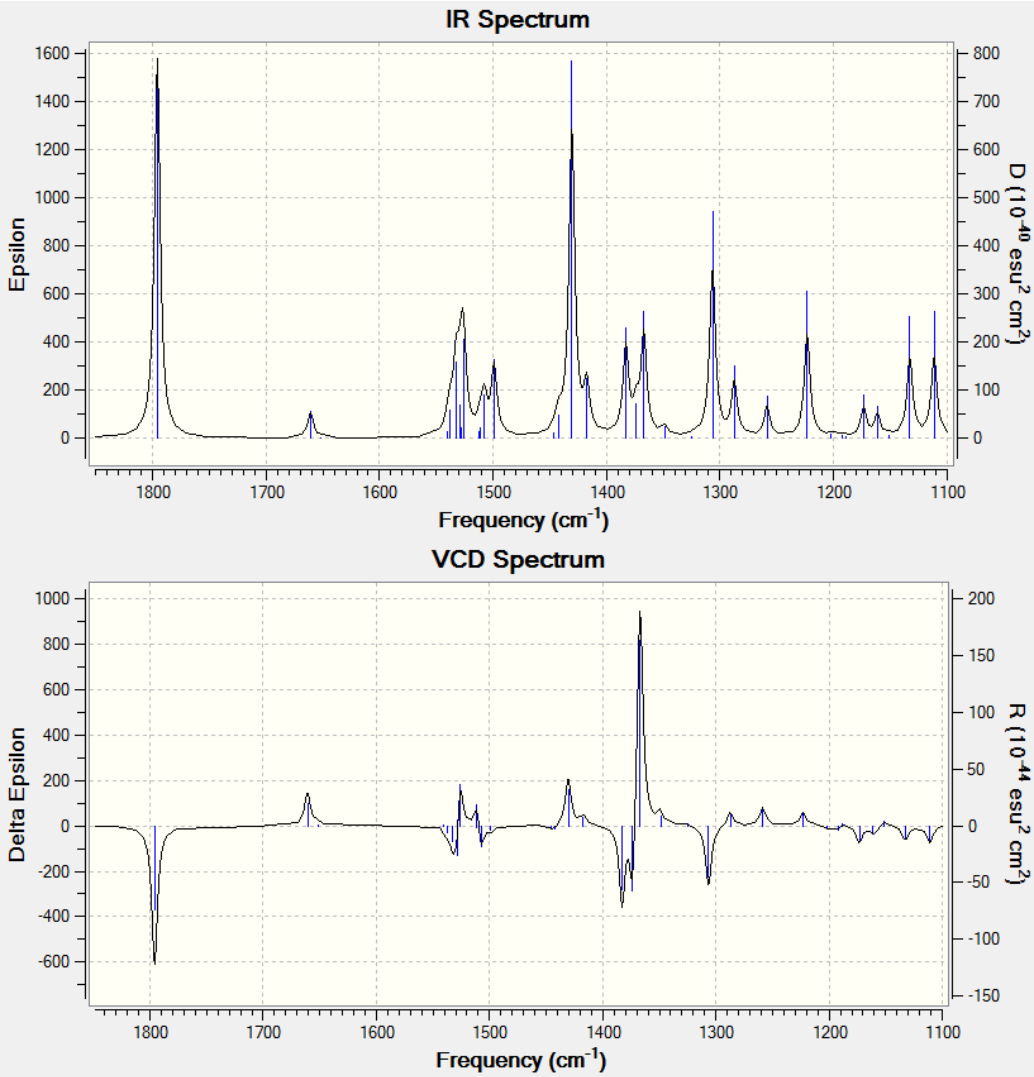
IR Spectrum
Epsilon
D (10^{-40} esu^2 cm^2)
Frequency (cm^{-1})
VCD Spectrum
Delta Epsilon
R (10^{-44} esu^2 cm^2)
Frequency (cm^{-1})

Indoline (**268**) (Experimental spectra):

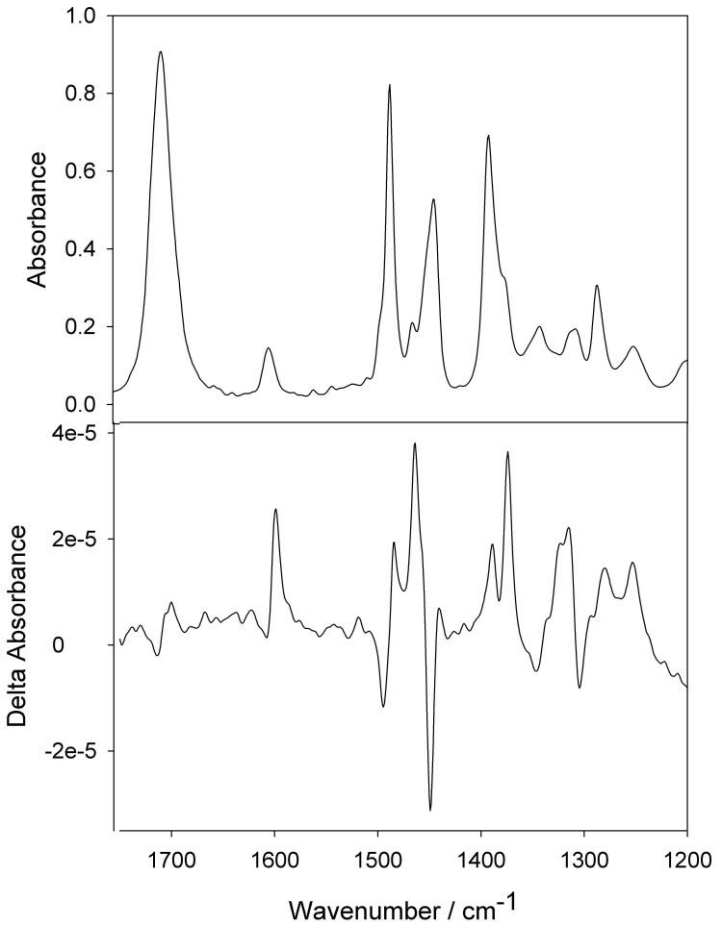

(2*S*,3*R*)-methyl 2-methyl-3-phenylindoline-1-carboxylate (**268**):

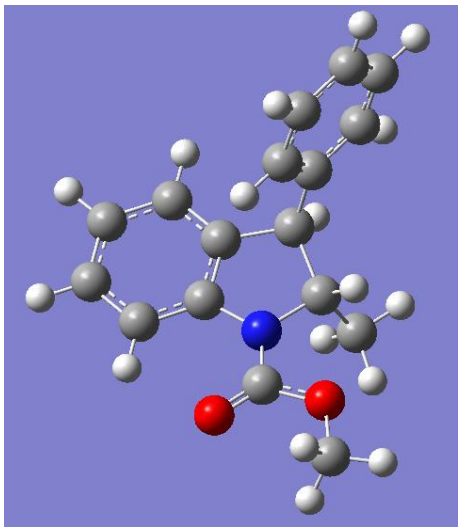

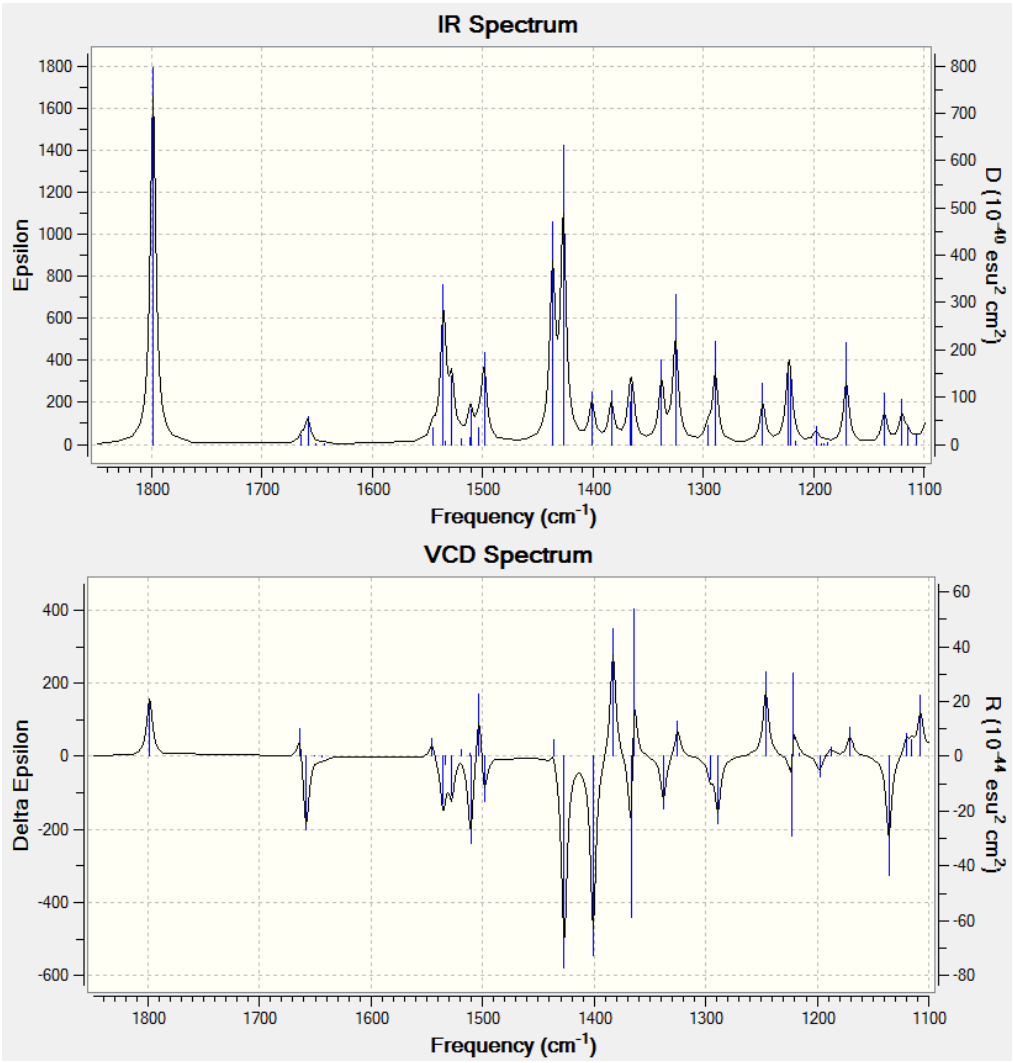

(2*R*,3*R*)-methyl 2-methyl-3-phenylindoline-1-carboxylate (**268**):

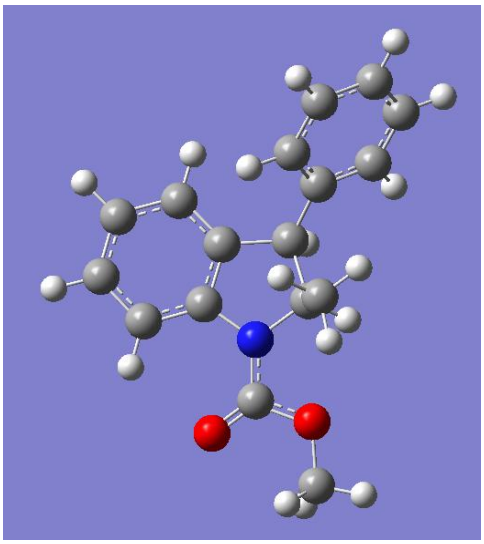

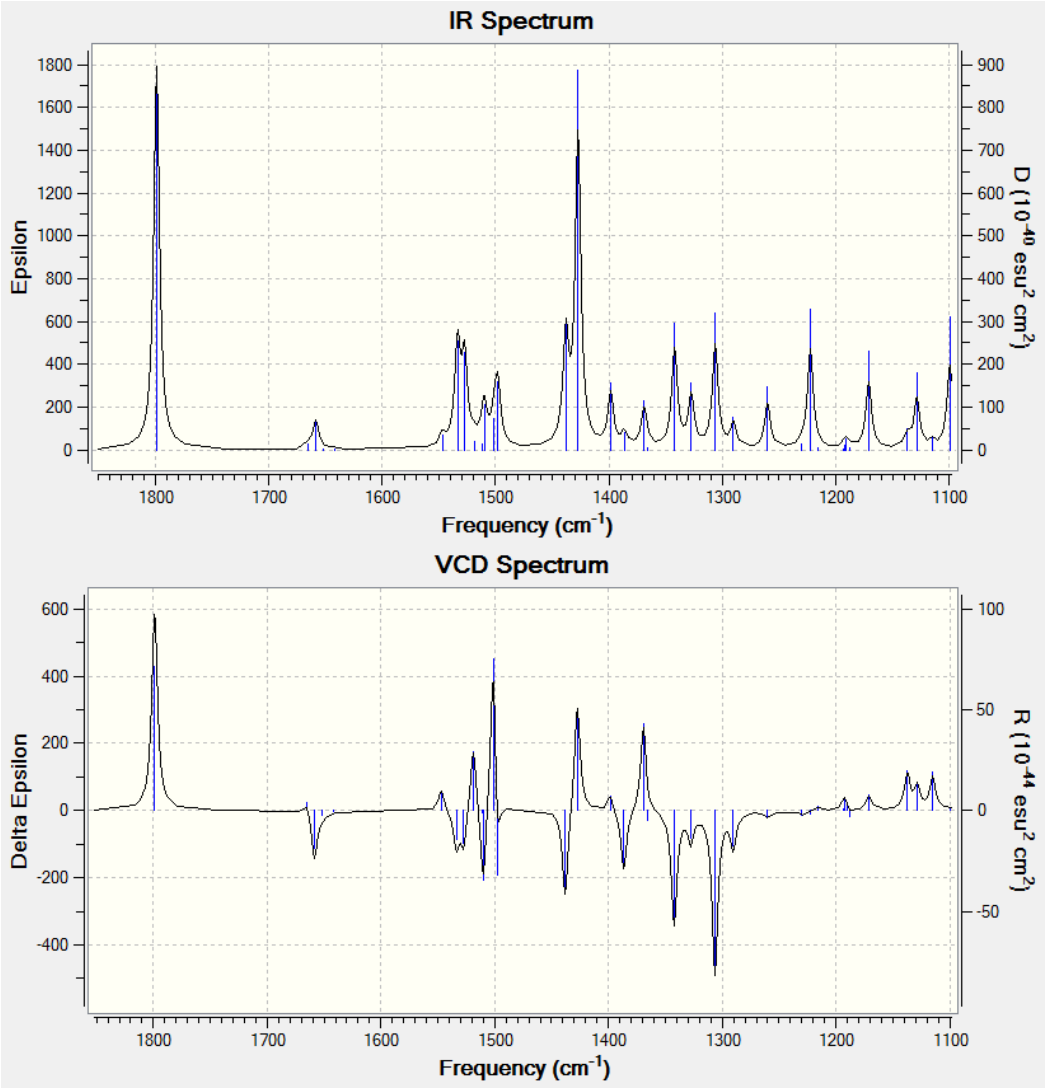
IR Spectrum
Epsilon
D (10^{-40} esu^2 cm^2)
Frequency (cm^{-1})
VCD Spectrum
Delta Epsilon
R (10^{-44} esu^2 cm^2)
Frequency (cm^{-1})

Compounds Index

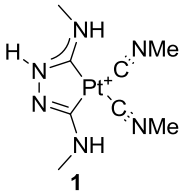

1

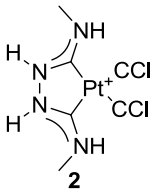

2

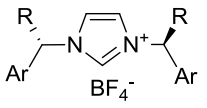

3 (R=Me, Ar=1-Naphthyl)
4 (R=Et, Ar=Mes)

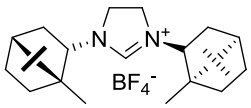

5

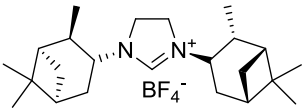

6

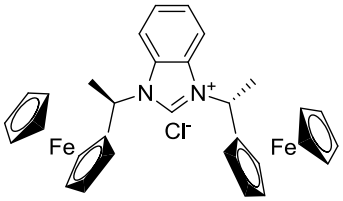

7

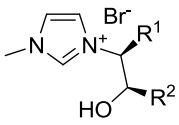

8 (R^1 = H)
9 (R^2 = H)

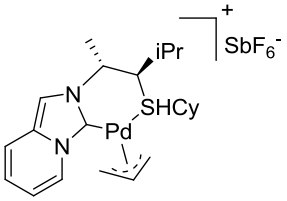

10

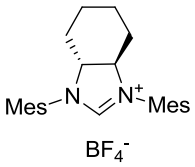

11

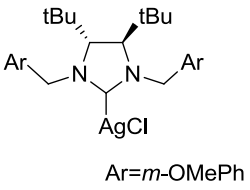

Ar=*m*-OMePh

12

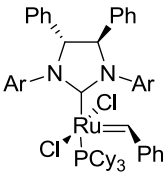

13

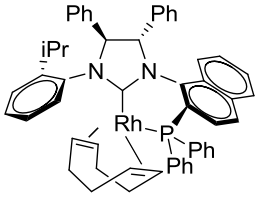

14

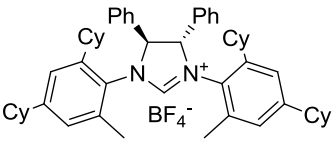

15

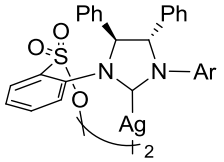

16 (Ar=2,4,6-(*i*-Pr)Ph)
17 (2,6-(*i*-Pr)Ph)

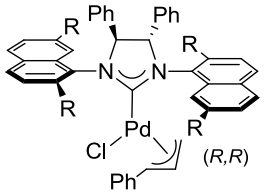

18 (R=*i*Pr)
19 (R=Cyoct)

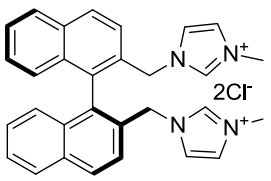

20

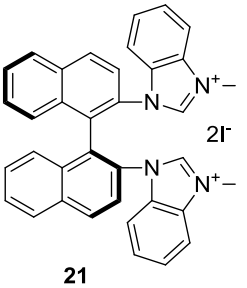

21

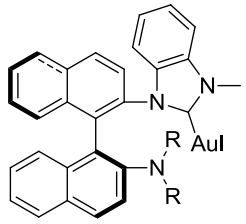

22

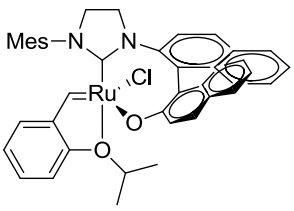

23

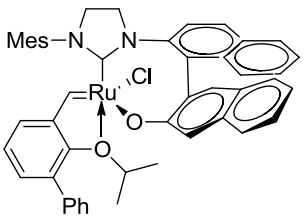

24

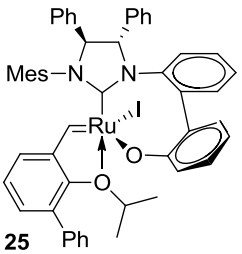

25

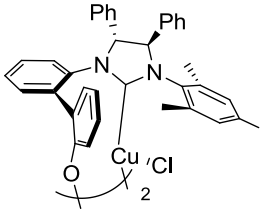

26

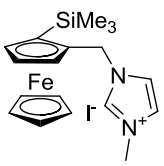

27

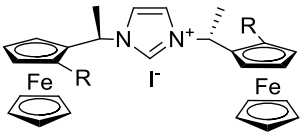

28 (R=$SiMe_3$)
29 (R=PPh_2)

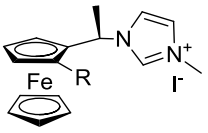

30 (R=SPh)
31 (R=PPh_2)

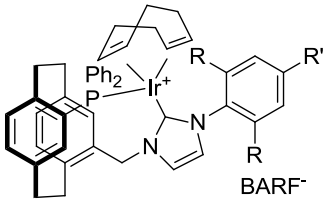

32a R = R' = H
32b R = R' = Me
32c R = ^{i}Pr, R' = H

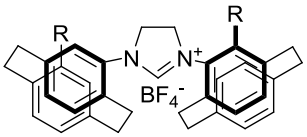

33a R = H
33b R = Ph
33c R = Cy
33d R = *o*-anisyl

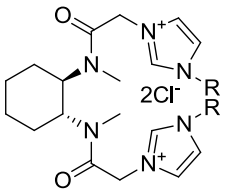

34

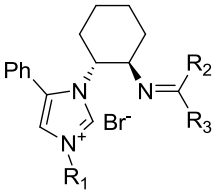

35

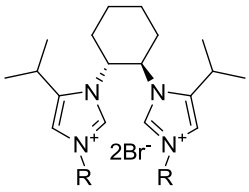

36

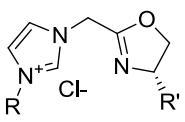

37

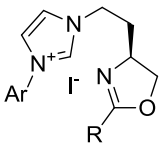

38

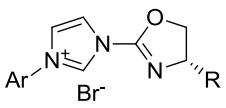

39

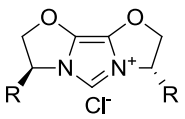

40a (R=*i*Pr)
40b (R=*t*Bu)
40c (R=Bn)

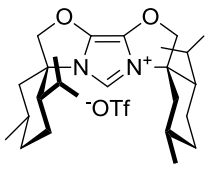

41

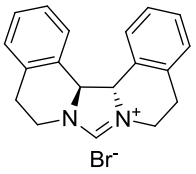

42

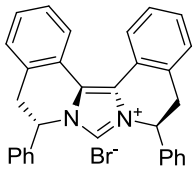

43

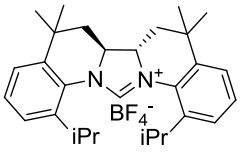

44

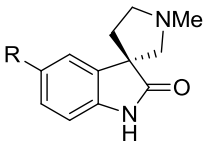

45 R = OMe
46 R = H

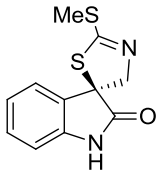

47

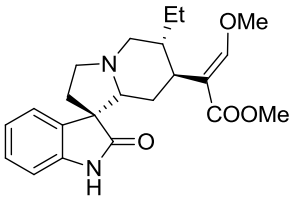

48

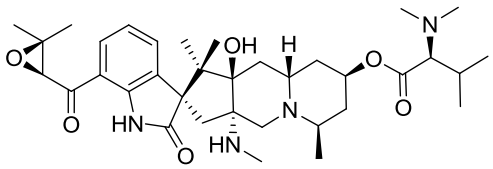

49

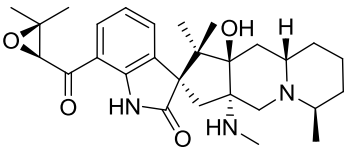

50

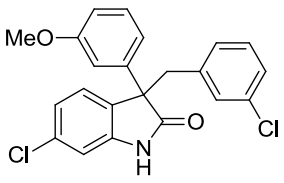

(*rac*)-**51**

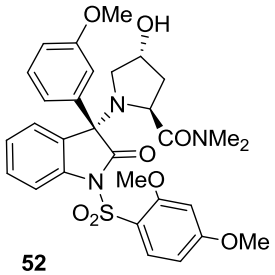

52

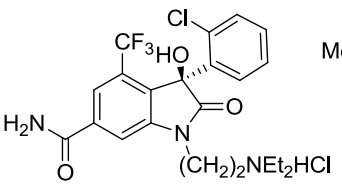

53

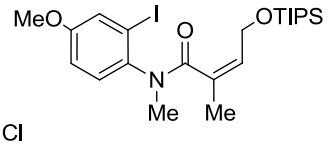

54

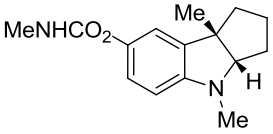

55

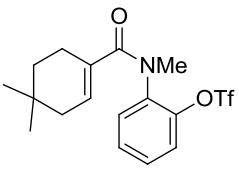

56

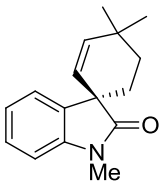

57

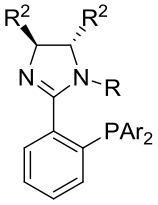

R = 2-naphthyl

58 Ar = R^2 = 3,5-$F_2C_6H_3$

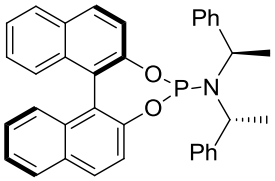

59

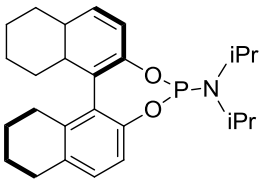

60

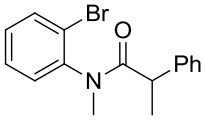

61

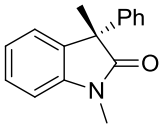

(*S*)-**62**

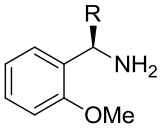

63, R = Me
64, R = *i*Pr
65, R = *t*Bu

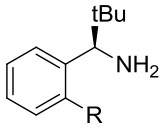

66, R = H
67, R = Me
68, R = O*n*Pr
69, R = O*i*Pr

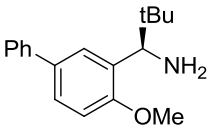

70

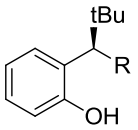

71a (R = NH_2)
71b (R = NHBoc)

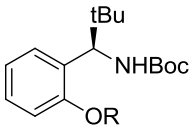

72a/R = *n*Pr
72b/R = *i*Pr

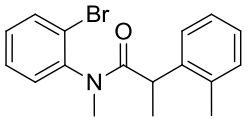

73a

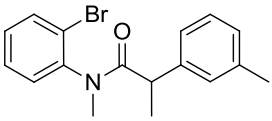

73b

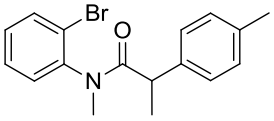

73c

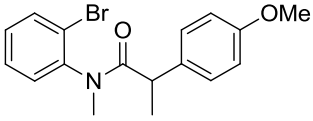

73d

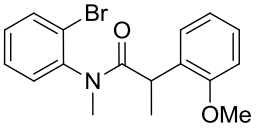

73e

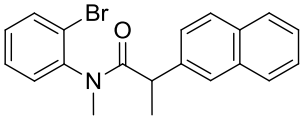

73f

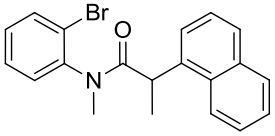

73g

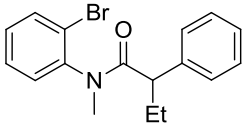

74a

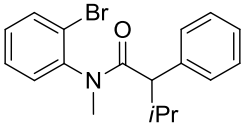

74b

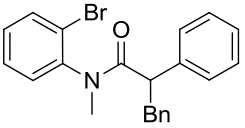

74c

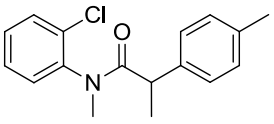

75a

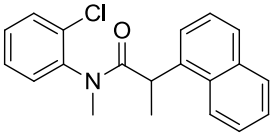

75b

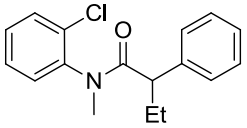

75c

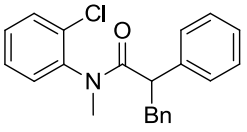

75d

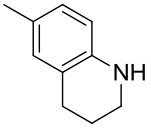

76

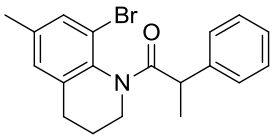

77

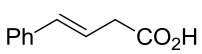

78

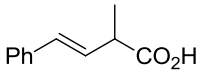

79

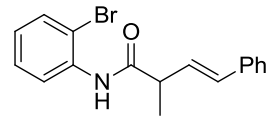

80

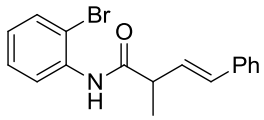

81

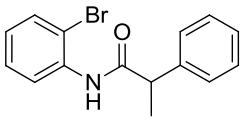

82

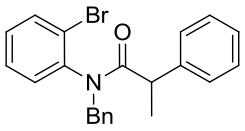

83

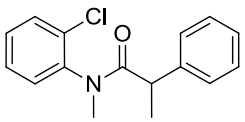

84

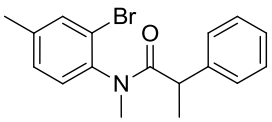

85a

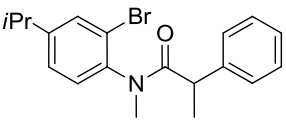

85b

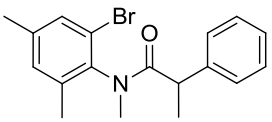

85c

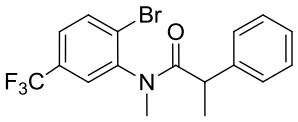

85d

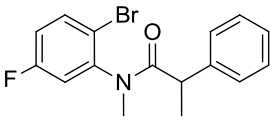

85e

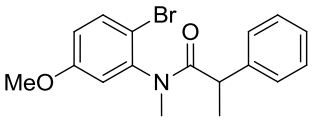

85f

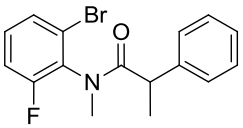

85g

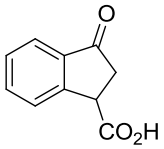

86

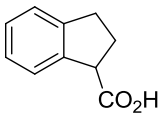

87

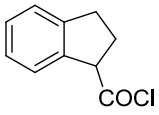

88

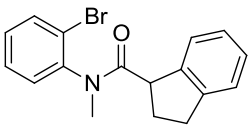

89

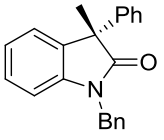

(*S*)-**90**

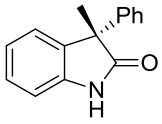

(*S*)-**91**

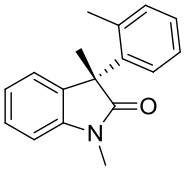

(*S*)-**92a**

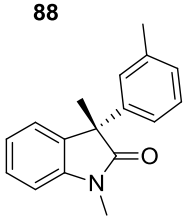

(*S*)-**92b**

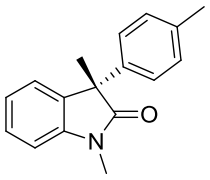

(*S*)-**92c**

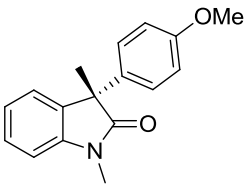

(*S*)-**92d**

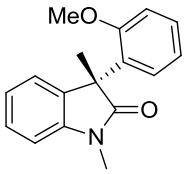

(*S*)-**92e**

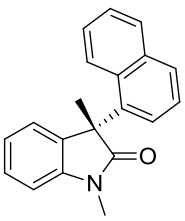

(*S*)-**92f**

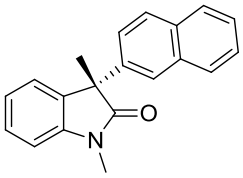

(*S*)-**92g**

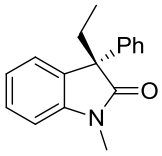

(*S*)-**93a**

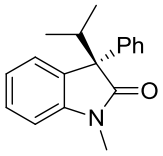

(*S*)-**93b**

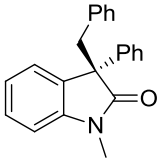

(*S*)-**93c**

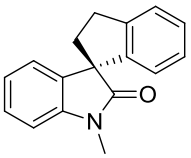

(*S*)-**94**

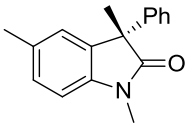

(*S*)-**95a**

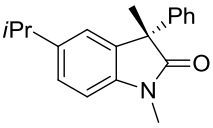

(*S*)-**95b**

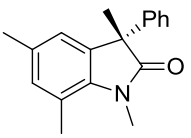

(*S*)-**95c**

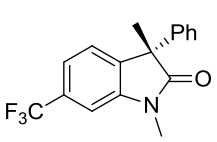

(*S*)-**95d**

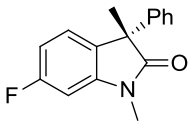

(*S*)-**95e**

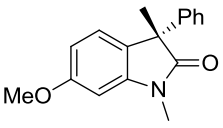

(*S*)-**95f**

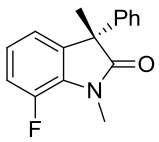

(*S*)-**95g**

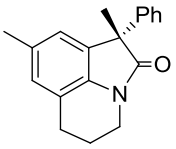

(*S*)-**96**

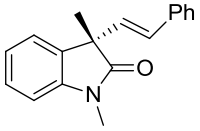

(*S*)-**97**

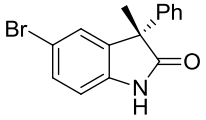

(*S*)-**98**

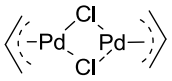

99

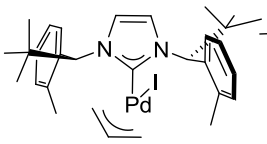

(*S*,*S*)-**100**

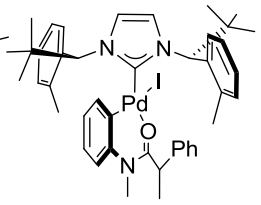

(*S*,*S*) - **101**

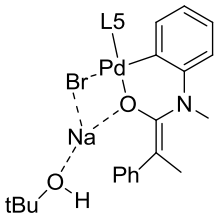

101'

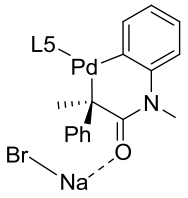

101"

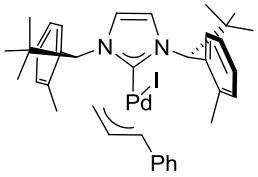

(*S*,*S*) - **102**

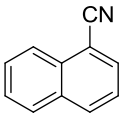

103a

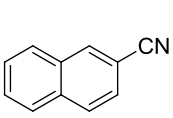

103b

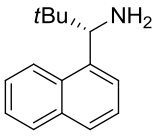

(*S*)-**104**

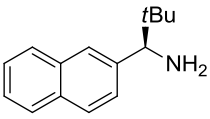

(*R*)-**105**

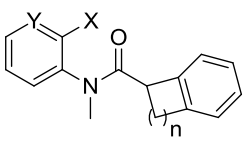

106; Y = CH, n = 1, X = Br
107; Y = CH, n = 3, X = Br
108; Y = CH, n = 4, X = Br
109; Y = N, n = 2, X = Br
110; Y = N, n = 2, X = Cl
111; Y = N, n = 3, X = Br
112; Y = N, n = 4, X = Br

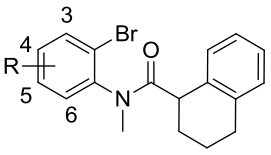

113; C(4)-Me
114; C(4)-OMe
115; C(4)-F
116; C(5)-CF_3
117; C(5)-OMe
118; C(3)-CF_3

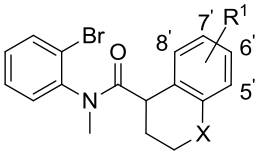

119; X = CH_2, C(6')-OMe
120; X = O, C(7')-Cl
121; X = S, R^1 = H

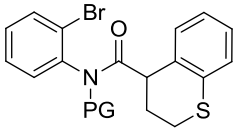

122; PG = Bn
123; PG = MOM
124; PG = BOM

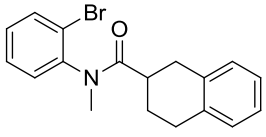

125

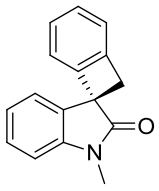

(S)-**126**

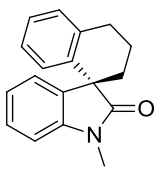

(*S*)-**127**

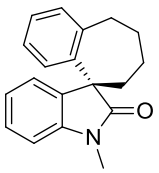

(*S*)-**128**

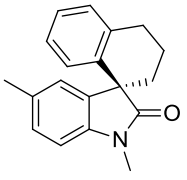

(*R*)-**129**

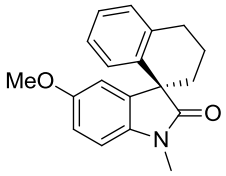

(*R*)-**130**

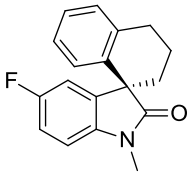

(*R*)-**131**

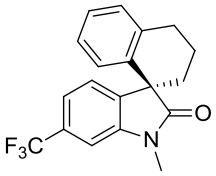

(*R*)-**132**

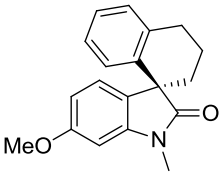

(*R*)-**133**

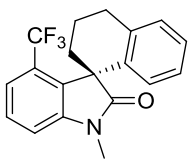

(*R*)-**134**

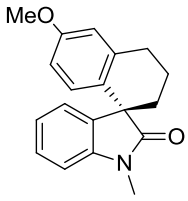

(*S*)-**135**

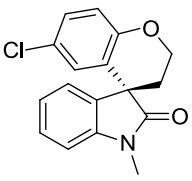

(*R*)-**136**

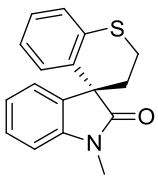

(*R*)-**137**

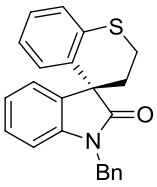

(*R*)-**138**

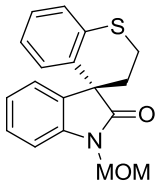

(*R*)-**139**

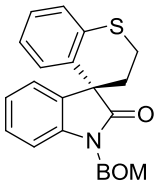

(*R*)-**140**

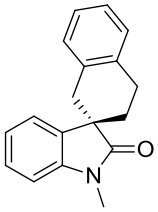

(*S*)-**141**

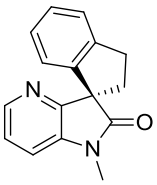

(*R*)-**142**

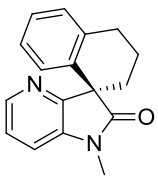

(*R*)-**143**

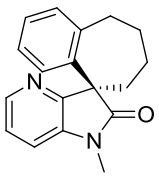

(*R*)-**144**

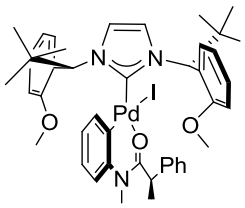

(*S*,*S*) - **145**

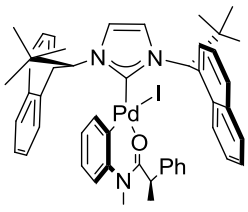

(*S*,*S*) - **146**

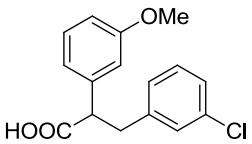

147a

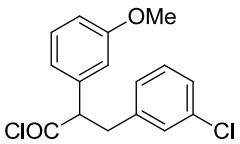

147b

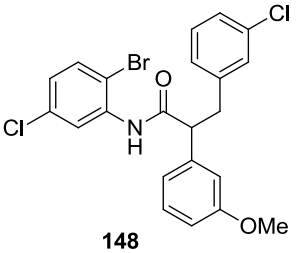

148

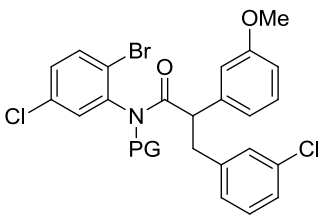

PG = BOM, **149**
PG = MOM, **150**

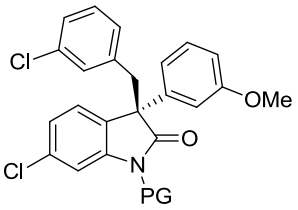

PG = MOM, (*R*)-**151**
PG = BOM, (*S*)-**152**

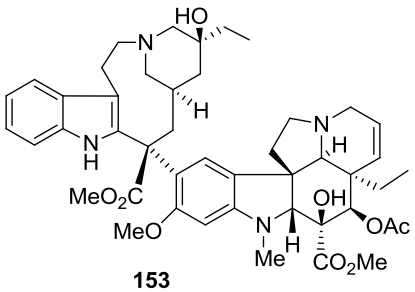

153

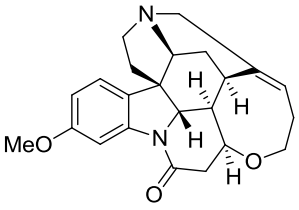

154

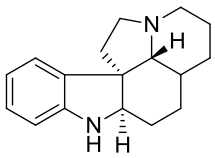

155

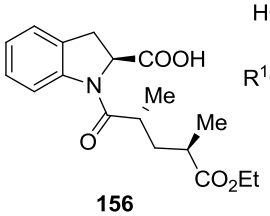

156

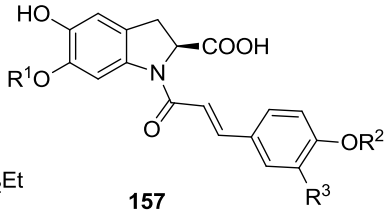

157

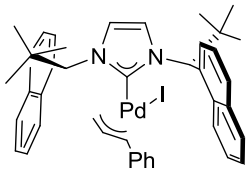

(*S*,*S*)-**158**

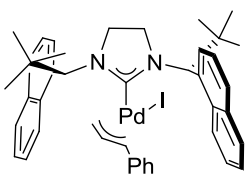

(*S*,*S*)-**159**

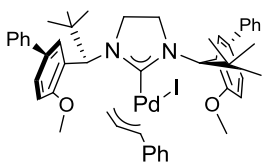

(*R*,*R*)-**160**

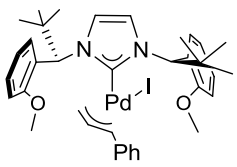

(*R*,*R*)-**161**

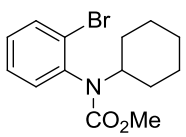

162

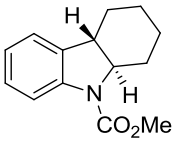

(4a*S*,9a*R*)-**163**

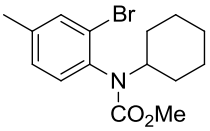

164

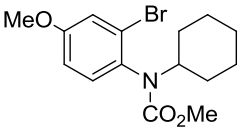

165

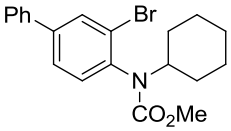

166

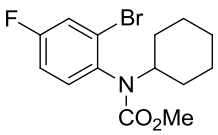

167

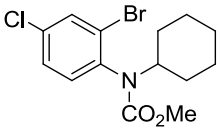

168

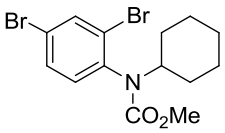

169

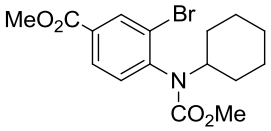

170

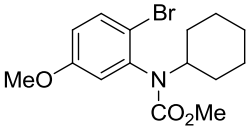

171

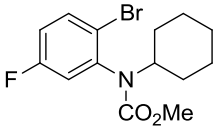

172

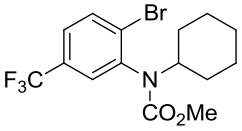

173

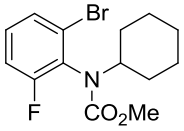

174

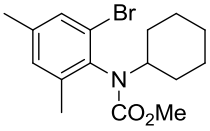

175

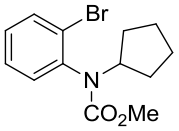

176

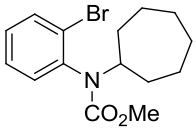

177

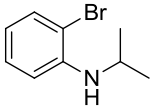

178

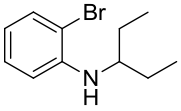

179

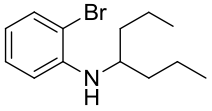

180

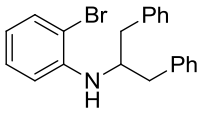

181

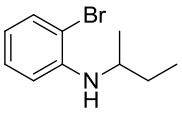

182

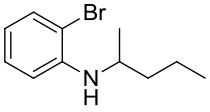

183

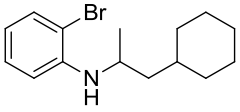

184

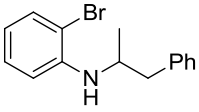

185

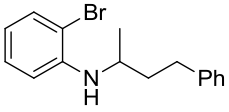

186

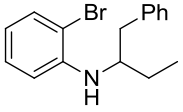

187

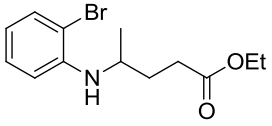

188

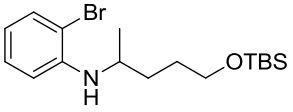

189

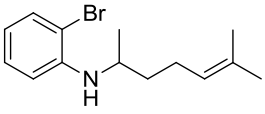

190

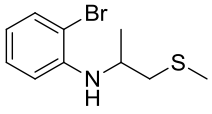

191

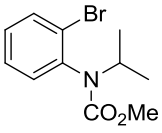

192

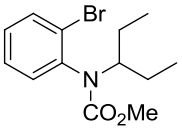

193

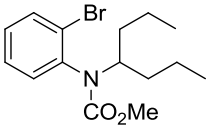

194

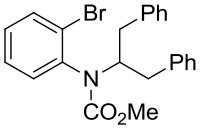

195

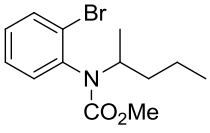

196

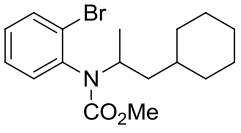

197

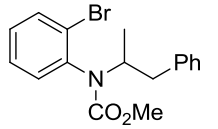

198

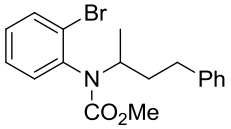

199

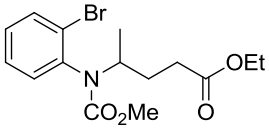

200

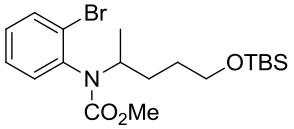

201

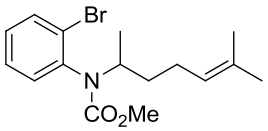

202

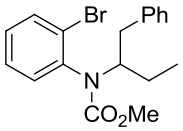

203

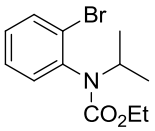

204

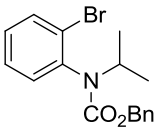

205

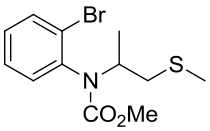

206

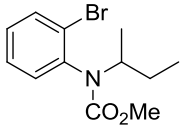

207

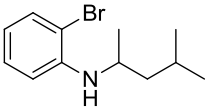

208

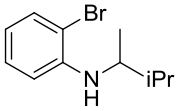

209

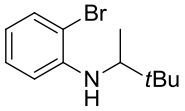

210

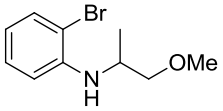

211

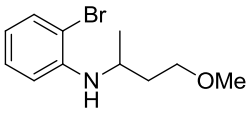

212

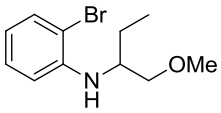

213

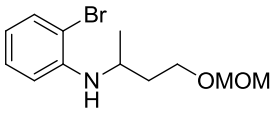

214

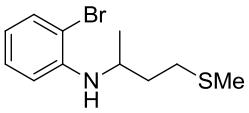

215

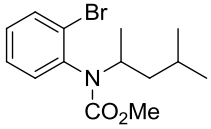

216

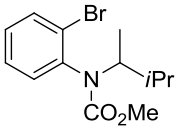

217

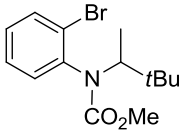

218

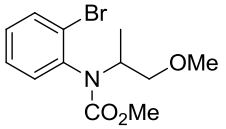

219

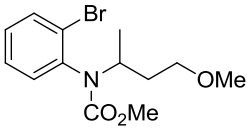

220

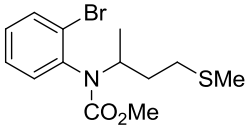

221

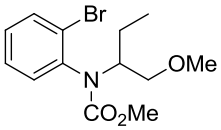

222

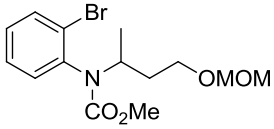

223

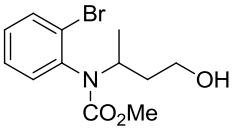

224

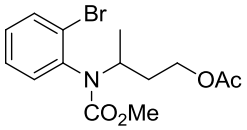

225

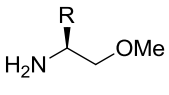

(*S*)-**226**

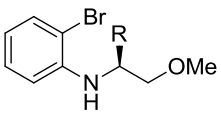

(*S*)-**227a** (R=*n*Pr)
(*S*)-**227b** (R=Bn)
(*S*)-**227c** (R=*i*Bu)

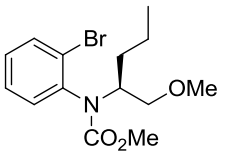

(*S*)-**228**

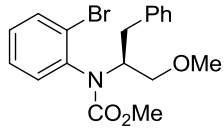

(*S*)-**229**

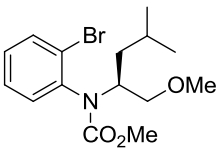

(*S*)-**230**

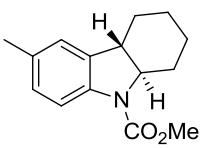

(4a*S*,9a*R*)-**231**

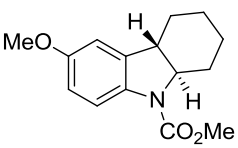

(4a*S*,9a*R*)-**232**

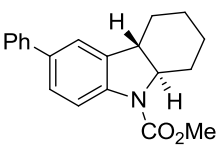

(4a*S*,9a*R*)-**233**

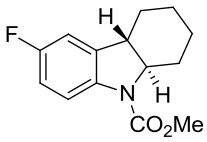

(4a*S*,9a*R*)-**234**

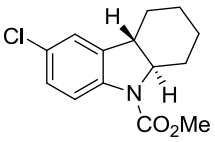

(4a*S*,9a*R*)-**235**

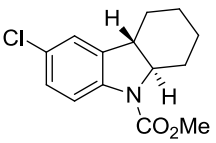

(4a*S*,9a*R*)-**236**

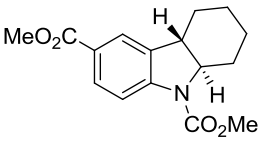

(4a*S*,9a*R*)-**237**

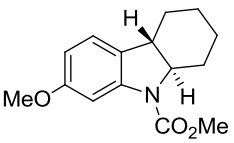

(4a*S*,9a*R*)-**238**

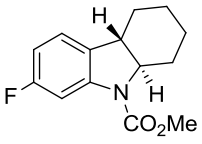

(4a*S*,9a*R*)-**239**

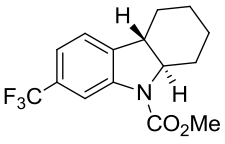

(4a*S*,9a*R*)-**240**

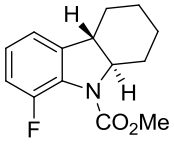

(4a*S*,9a*R*)-**241**

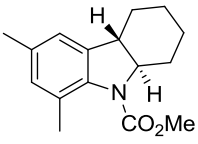

(4a*S*,9a*R*)-**242**

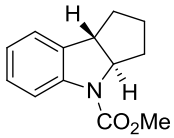

(3a*R*,8b*S*)-**243**

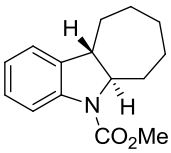

(5a*R*,10a*S*)-**244**

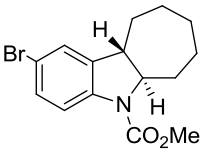

(5a*R*,10a*S*)-**245**

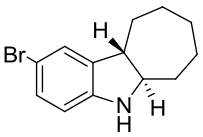

(5a*R*,10a*S*)-**246**

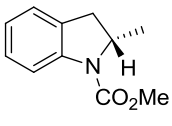

(*S*)-**247**

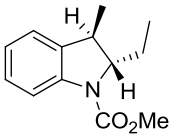

(2*S*,3*R*)-**248**

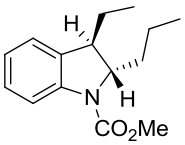

(2*S*,3*R*)-**249**

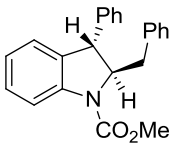

(2*R*,3*S*)-**250**

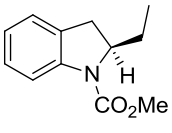

(*R*)-**251**

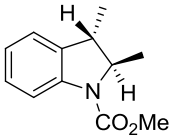

(2*R*,3*S*)-**252**

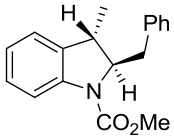

(2*R*,3*S*)-**253**

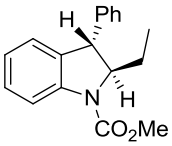

(2*R*,3*S*)-**254**

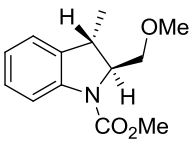

(2*S*,3*S*)-**255**

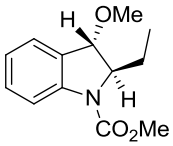

(2*R*,3*S*)-**256**

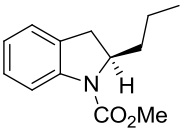

(*R*)-**257**

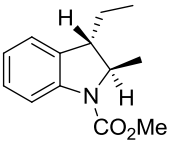

(2*R*,3*S*)-**258**

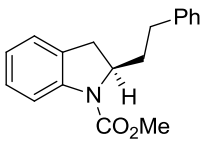

(*R*)-**259**

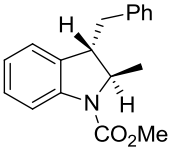

(2*R*,3*S*)-**260**

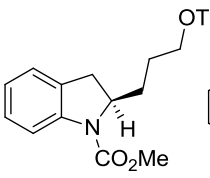

(*R*)-**261**

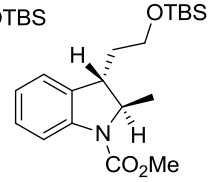

(2*R*,3*S*)-**262**

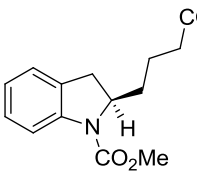

(*R*)-**263**

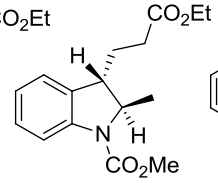

(2*R*,3*S*)-**264**

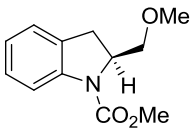

(*S*)-**265**

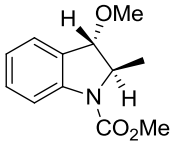

(2*R*,3*S*)-**266**

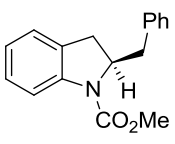

(*R*)-**267**

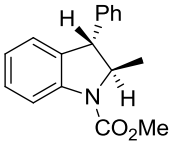

(2*R*,3*S*)-**268**

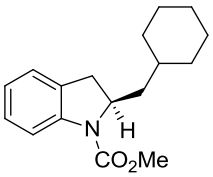

(*R*)-**269**

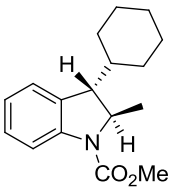

(2*R*,3*S*)-**270**

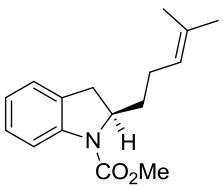

(*R*)-**271**

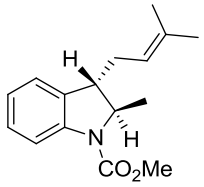

(2*R*,3*S*)-**272**

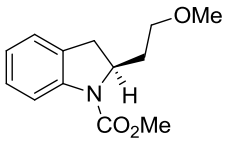

(*R*)-**273**

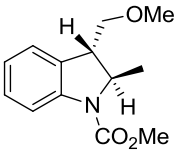

(2*R*,3*S*)-**274**

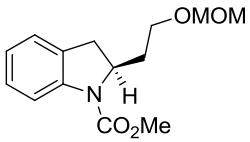

(*R*)-**275**

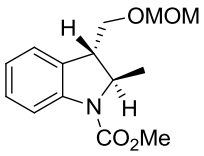

(2*R*,3*S*)-**276**

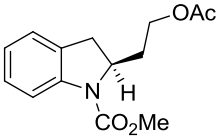

(*R*)-**277**

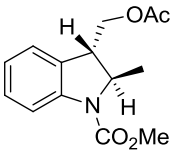

(2*R*,3*S*)-**278**

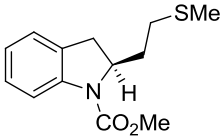

(*R*)-**279**

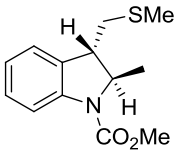

(2*R*,3*S*)-**280**

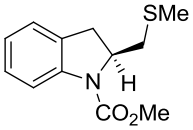

(*R*)-**281**

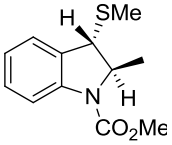

(2*R*,3*S*)-**282**

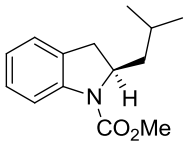

(*S*)-**283**

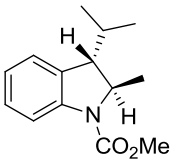

(*R*)-**284**

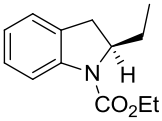

(*R*)-**285**

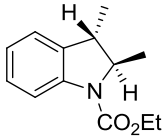

(2*R*,3*S*)-**286**

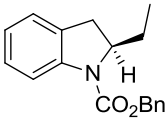

(*R*)-**287**

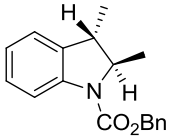

(2*R*,3*S*)-**288**

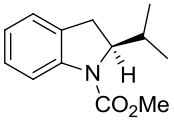

(*R*)-**289**

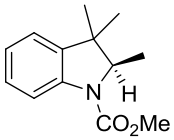

(2*R*,3*S*)-**290**

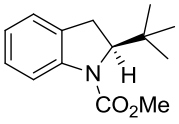

(*S*)-**291**

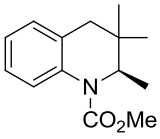

(*R*)-**292**

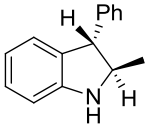

(2*R*,3*S*)-**293**

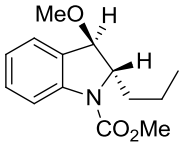

(2*S*,3*R*)-**294**

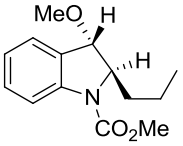

(2*R*,3*S*)-**294**

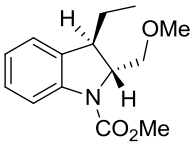

(2*R*,3*R*)-**295**

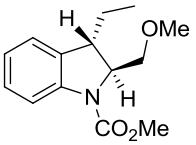

(2*S*,3*S*)-**295**

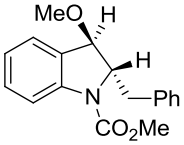

(2*S*,3*R*)-**296**

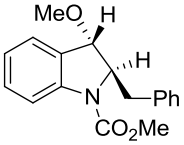

(2*R*,3*S*)-**296**

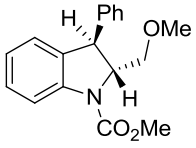

(2*R*,3*R*)-**297**

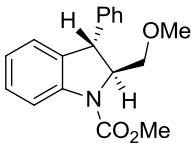

(2*S*,3*S*)-**297**

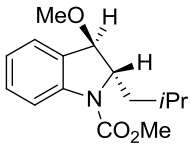

(2*S*,3*S*)-**298**

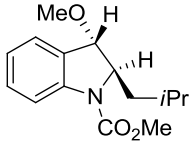

(2*R*,3*S*)-**298**

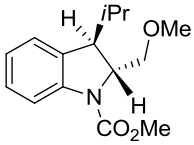

(2*R*,3*R*)-**299**

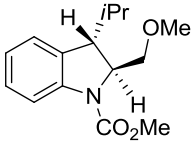

(2*S*,3*S*)-**299**

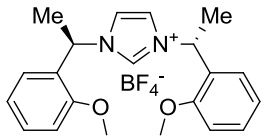

(*R*,*R*)-[**L1**H][BF_4^-]

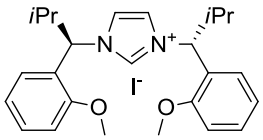

(*R*,*R*)-[**L2**H][I^-]

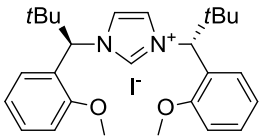

(*R*,*R*)-[**L3**H][I^-]

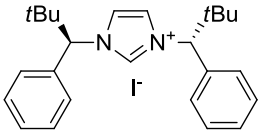

(*R*,*R*)-[**L4**H][I^-]

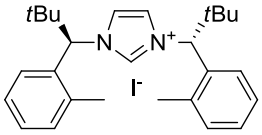

(*R*,*R*)-[**L5**H][I^-]

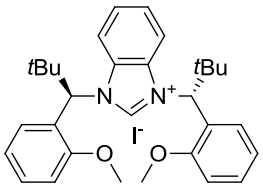

(*R*,*R*)-[**L6**H][**I**]

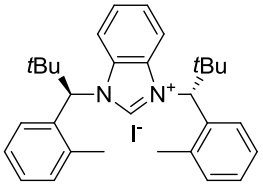

(*R*,*R*)-[**L7**H][**I**]

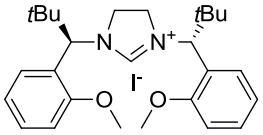

(*R*,*R*)-[**L8**H][**I**]

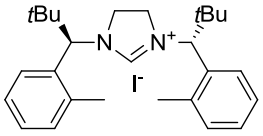

(*R*,*R*)-[**L9**H][**I**]

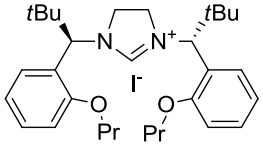

(*R*,*R*)-[**L10**H][I^-]

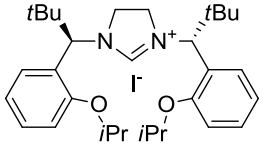

(*R*,*R*)-[**L11**H][I^-]

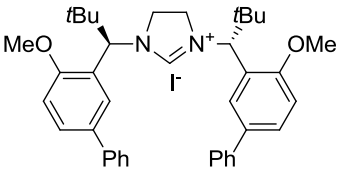

(*R*,*R*)-[**L12**H][I^-]

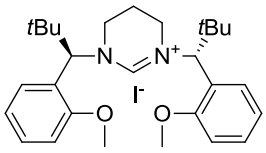

(*R*,*R*)-[**L13**H][**I**]

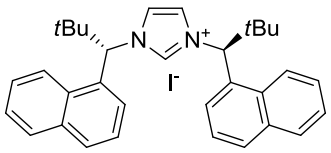

(*S*,*S*)-[**L14**H][**I**]

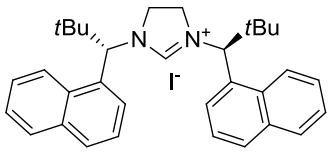

(*S*,*S*)-[**L15**H][**I**]

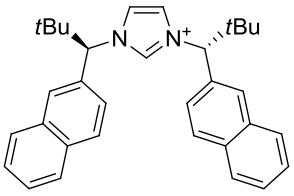

(*R*,*R*)-[**L16**H][**I**]

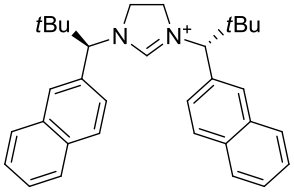

(*R*,*R*)-[**L17**H][**I**]

Crystallographic Data

*Crystallographic Data for (S,S)-**100**:*

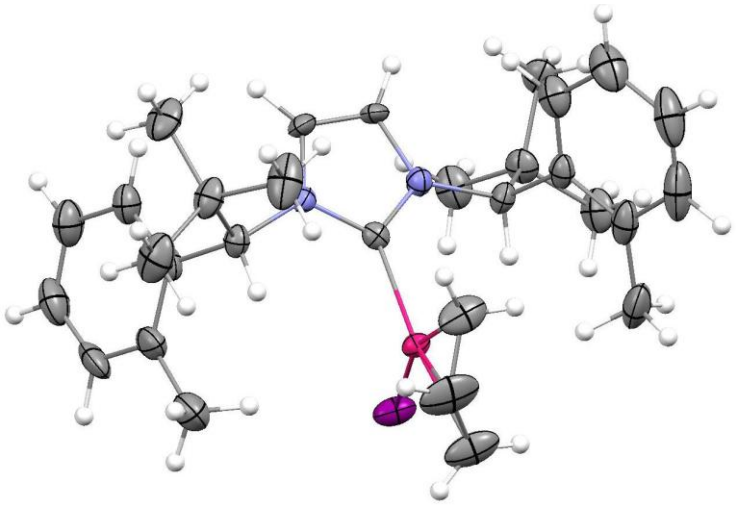

Crystal data and structure refinement for

Identification code	
Empirical formula	$C_{30}H_{41}IN_2Pd$
Formula weight	663.0
Temperature/K	N/A
Crystal system	monoclinic
Space group	C2
a/Å	23.098(2)
b/Å	8.4741(4)
c/Å	16.0210(13)
α/°	90.00000
β/°	107.205(10)
γ/°	90.00000
Volume/Å^3	2995.5(4)
Z	4
ρ_{calc}mg/mm^3	1.47
m/mm^{-1}	1.67
F(000)	1336.0
Crystal size/mm^3	.363 × .182 × .046
2Θ range for data collection	N/A to 53.4°
Index ranges	$-29 \le h \le 29$, $-10 \le k \le 10$, $-20 \le l \le 20$
Reflections collected	18692
Independent reflections	6294[R(int) = .027]
Data/restraints/parameters	6294/N/A/322
Goodness-of-fit on F^2	1.50(2)
Final R indexes [I>=2σ (I)]	R_1 = 0.0230, wR_2 = N/A
Final R indexes [all data]	R_1 = N/A, wR_2 = 0.0240
Largest diff. peak/hole / e Å^{-3}	1.11/-0.86
Flack parameter	-.01(2)

Bond Distance (Angstroms)

Pd	I	2.6500(6)	C8	C9	1.370(14)
Pd	C1	2.043(6)	C9	C10	1.405(9)
Pd	C101	2.144(6)	C12	C13	1.532(8)
Pd	C102	2.156(8)	C12	C14	1.540(10)
Pd	C103	2.207(8)	C12	C15	1.540(11)
N1	C1	1.369(8)	C16	C17	1.540(7)
N1	C3	1.378(8)	C16	C24	1.574(10)
N1	C4	1.489(8)	C17	C18	1.399(10)
N2	C1	1.365(8)	C17	C22	1.394(10)
N2	C2	1.376(8)	C18	C19	1.405(9)
N2	C16	1.484(8)	C18	C23	1.511(11)
C2	C3	1.349(9)	C19	C20	1.354(12)
C4	C5	1.542(7)	C20	C21	1.369(14)
C4	C12	1.565(9)	C21	C22	1.403(7)
C5	C6	1.417(9)	C24	C25	1.523(12)
C5	C10	1.369(10)	C24	C26	1.519(12)
C6	C7	1.416(9)	C24	C27	1.548(7)
C6	C11	1.502(12)			

Bond Angles (Degrees)

I	Pd	C1	93.26(14)	C4	C12	C14	115.3(6)
C1	N1	C3	110.6(5)	C4	C12	C15	106.6(5)
C1	N1	C4	122.0(5)	C13	C12	C14	109.5(6)
C3	N1	C4	127.5(6)	C13	C12	C15	107.9(6)
C1	N2	C2	110.4(5)	C14	C12	C15	107.4(6)
C1	N2	C16	121.9(5)	N2	C16	C17	111.0(5)
C2	N2	C16	127.6(5)	N2	C16	C24	113.5(5)
Pd	C1	N1	125.6(4)	C17	C16	C24	116.0(5)
Pd	C1	N2	129.8(5)	C16	C17	C18	121.2(6)
N1	C1	N2	104.7(5)	C16	C17	C22	120.6(6)
N2	C2	C3	107.6(5)	C18	C17	C22	118.2(6)
N1	C3	C2	106.8(6)	C17	C18	C19	118.9(7)
N1	C4	C5	109.6(5)	C17	C18	C23	122.1(6)
N1	C4	C12	113.9(5)	C19	C18	C23	119.0(7)
C5	C4	C12	114.9(5)	C18	C19	C20	121.9(8)
C4	C5	C6	120.8(6)	C19	C20	C21	120.4(6)
C4	C5	C10	119.7(6)	C20	C21	C22	119.1(8)
C6	C5	C10	119.5(6)	C17	C22	C21	121.5(8)
C5	C6	C7	116.5(7)	C16	C24	C25	105.9(7)
C5	C6	C11	123.8(6)	C16	C24	C26	116.4(6)
C7	C6	C11	119.7(7)	C16	C24	C27	107.6(6)
C6	C7	C8	122.9(8)	C25	C24	C26	109.6(6)
C7	C8	C9	120.5(6)	C25	C24	C27	109.3(6)
C8	C9	C10	118.4(9)	C26	C24	C27	107.9(7)
C5	C10	C9	122.2(7)	C101	C102	C103	129.4(10)
C4	C12	C13	109.9(6)				

*Crystallographic Data for (S,S)-**101a**:*

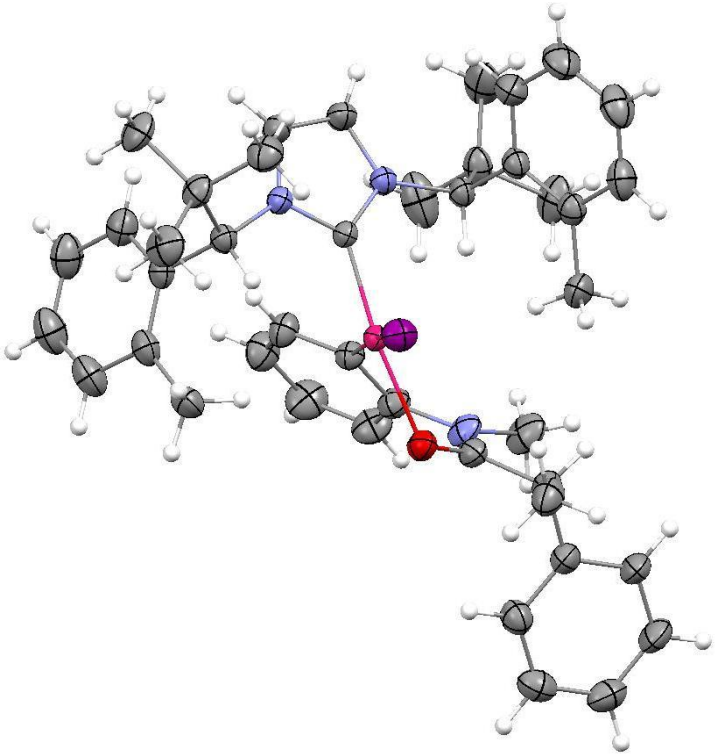

Crystal data and structure refinement for

Identification code	
Empirical formula	$C_{43}H_{52}IN_3OPd$
Formula weight	860.21
Temperature/K	220.0
Crystal system	orthorhombic
Space group	$P2_12_12_1$
a/Å	12.0004(3)
b/Å	17.2806(3)
c/Å	19.1879(4)
α/°	90
β/°	90
γ/°	90
Volume/Å^3	3979.07(14)
Z	4
ρ_{calc}mg/mm^3	1.436
m/mm^{-1}	1.278
F(000)	1752.0
Crystal size/mm^3	0.60 × 0.20 × 0.10
2Θ range for data collection	4.64 to 67.04°
Index ranges	$-18 \le h \le 18$, $-26 \le k \le 26$, $-29 \le l \le 29$
Reflections collected	156906
Independent reflections	15509[R(int) = 0.0745]
Data/restraints/parameters	15509/0/442
Goodness-of-fit on F^2	0.967
Final R indexes [I>=2σ (I)]	R_1 = 0.0390, wR_2 = 0.0659
Final R indexes [all data]	R_1 = 0.0423, wR_2 = 0.0665
Largest diff. peak/hole / e Å^{-3}	0.86/-1.42
Flack parameter	0.001(14)

Bond Distance (Angstroms)

Pd1	C1	2.854(3)	
Pd1	C31	1.951(3)	
Pd1	C32	1.982(3)	
Pd1	I2	2.7101(3)	
C3	C12	1.534(5)	
C4	C18	1.523(5)	
C4	C1	1.532(4)	
C4	C35	1.520(4)	
C5	C12	1.525(5)	
O6	C1	1.261(4)	
C7	C24	1.562(4)	
C7	C28	1.533(5)	
C7	C37	1.514(5)	
C7	C43	1.540(5)	
C8	C16	1.500(5)	
C9	C15	1.375(6)	
C9	C26	1.387(5)	
N10	C13	1.481(4)	
N10	C1	1.322(4)	
N10	C34	1.445(4)	
C11	C15	1.366(6)	
C11	C16	1.398(5)	
C12	C30	1.574(4)	
C12	C38	1.537(5)	
N14	C30	1.481(4)	
N14	C31	1.370(3)	
N14	C36	1.371(4)	
C16	C17	1.396(4)	
C17	C26	1.388(5)	
C17	C30	1.531(4)	
C19	C35	1.390(5)	
C19	C40	1.378(5)	
N21	C24	1.493(4)	
N21	C25	1.383(4)	
N21	C31	1.364(3)	
C22	C33	1.397(5)	
C22	C46	1.381(6)	
C23	C45	1.388(4)	
C23	C47	1.380(5)	
C24	C39	1.527(4)	
C25	C36	1.348(4)	
C27	C33	1.509(5)	
C29	C41	1.389(5)	
C29	C46	1.375(6)	
C32	C34	1.403(4)	
C32	C45	1.406(4)	
C33	C39	1.398(4)	
C34	C49	1.399(5)	
C35	C44	1.374(5)	
C39	C41	1.396(4)	
C40	C42	1.384(5)	
C42	C48	1.377(6)	
C44	C48	1.390(5)	
C47	C49	1.377(5)	

Bond Angles (Degrees)

O6	Pd1	C31	169.05(10)		
O6	Pd1	C32	85.40(10)		
O6	Pd1	I2	89.13(6)		
C1	Pd1	C31	145.21(10)		
C1	Pd1	C32	73.64(11)		
C1	Pd1	I2	103.74(7)		
C31	Pd1	C32	88.52(11)		
C31	Pd1	I2	98.00(8)		
C32	Pd1	I2	170.86(8)		
C18	C4	C1	111.3(3)		
C18	C4	C35	110.3(3)		
C1	C4	C35	112.7(3)		
Pd1	O6	C1	113.7(2)		
C24	C7	C28	109.4(3)		
C24	C7	C37	116.3(3)		
C24	C7	C43	106.2(3)		
C28	C7	C37	109.4(3)		
C28	C7	C43	108.1(3)		
C37	C7	C43	107.1(3)		
C15	C9	C26	119.1(4)		
C13	N10	C1	122.3(3)		
C13	N10	C34	115.9(3)		
N10	C1	Pd1	91.11(18)		
N10	C1	O6	122.4(3)		
C24	N21	C25	127.3(2)		
C24	N21	C31	121.6(2)		
C25	N21	C31	110.9(2)		
C33	C22	C46	121.4(3)		
C45	C23	C47	119.7(3)		
C7	C24	N21	114.1(2)		
C7	C24	C39	115.2(2)		
N21	C24	C39	110.6(2)		
N21	C25	C36	106.8(3)		
C17	C26	C9	121.5(4)		
C41	C29	C46	119.7(4)		
C12	C30	N14	113.1(2)		
C17	C30	C12	115.7(2)		
C17	C30	N14	111.0(2)		
N14	C31	Pd1	129.5(2)		
N14	C31	N21	104.1(2)		
N21	C31	Pd1	126.06(19)		
Pd1	C32	C34	119.4(2)		
Pd1	C32	C45	123.7(2)		
C34	C32	C45	116.3(3)		

C1 N10 C34	121.8(3)	C22 C33 C39	119.4(3)
C15 C11 C16	121.9(4)	C27 C33 C22	117.5(3)
C3 C12 C5	108.6(3)	C27 C33 C39	123.1(3)
C3 C12 C30	115.1(3)	N10 C34 C32	120.9(3)
C3 C12 C38	110.1(3)	N10 C34 C49	117.8(3)
C5 C12 C30	105.7(3)	C32 C34 C49	121.3(3)
C5 C12 C38	107.5(3)	C4 C35 C19	120.1(3)
C30 C12 C38	109.4(3)	C4 C35 C44	121.7(3)
C30 N14 C31	121.3(2)	C19 C35 C44	118.1(3)
C30 N14 C36	127.7(2)	N14 C36 C25	107.3(3)
C31 N14 C36	111.0(2)	C24 C39 C33	121.0(3)
C9 C15 C11	120.0(4)	C24 C39 C41	120.7(3)
C8 C16 C11	118.0(3)	C33 C39 C41	118.3(3)
C8 C16 C17	123.8(3)	C19 C40 C42	120.3(4)
C11 C16 C17	118.3(3)	C39 C41 C29	121.6(3)
C16 C17 C26	119.1(3)	C40 C42 C48	118.8(3)
C16 C17 C30	120.2(3)	C35 C44 C48	120.9(3)
C26 C17 C30	120.6(3)	C32 C45 C23	122.4(3)
C35 C19 C40	121.2(3)	C22 C46 C29	119.6(4)
C4 C1 Pd1	135.7(2)	C23 C47 C49	119.9(3)
C4 C1 O6	117.5(3)	C44 C48 C42	120.6(4)
C4 C1 N10	120.1(3)	C34 C49 C47	120.4(3)

*Crystallographic Data for (S,S)-**101b***:

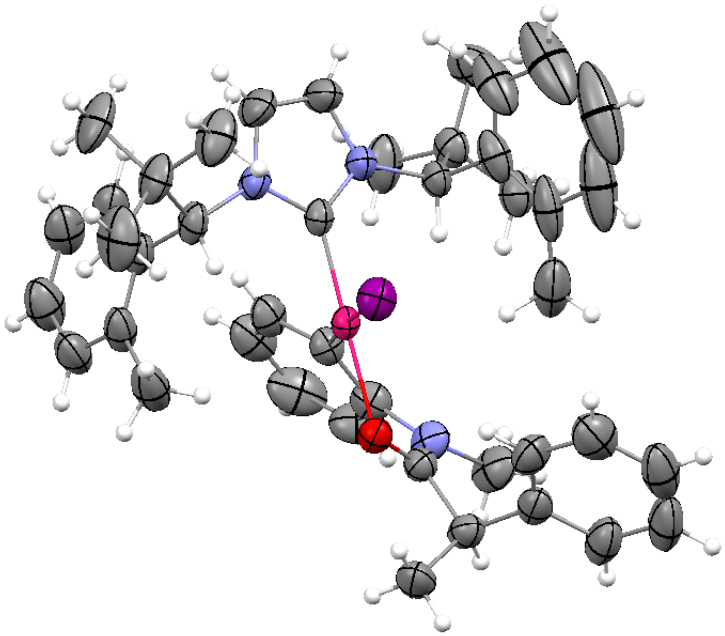

Crystal data

$C_{43}H_{52}IN_3OPd \cdot 0.4(C_3H_6O)$	$V = 4473\ (5)$ Å^3
$M_r = 883.44$	$Z = 4$
Monoclinic, $P2_1$	Mo $K\alpha$ radiation, $\lambda = 0.71073$ Å
$a = 12.749\ (10)$ Å	$\mu = 1.14$ mm^{-1}
$b = 17.994\ (8)$ Å	$T = 220$ K
$c = 19.866\ (10)$ Å	0.50 × 0.30 × 0.15 mm
$\beta = 101.056\ (10)°$	

Data collection

Stoe IPDS diffractometer	19243 independent reflections
Absorption correction: Multi-scan XDS (Kabsch, 1993)	17321 reflections with $I > 2.0\sigma(I)$
$T_{min} = 0.71$, $T_{max} = 0.84$	$R_{int} = 0.032$
49265 measured reflections	

Refinement

$R[F^2 > 2\sigma(F^2)] = 0.027$	H-atom parameters constrained
$wR(F^2) = 0.069$	$\Delta\rho_{max} = 0.74$ e Å^{-3}
$S = 0.92$	$\Delta\rho_{min} = -0.83$ e Å^{-3}
19243 reflections	Absolute structure: Flack (1983), 9079 Friedel-pairs
956 parameters	Flack parameter: 0.065 (11)
22 restraints	

Bond Distance (Angstroms)

Pd1—I2	2.7102 (11)	Pd51—C71	1.967 (4)
Pd1—O3	2.100 (2)	O53—C54	1.248 (4)
Pd1—C7	1.990 (3)	C54—N55	1.348 (5)
Pd1—C21	1.966 (3)	C54—C63	1.533 (5)
O3—C4	1.250 (4)	N55—C56	1.445 (5)
C4—N5	1.356 (4)	N55—C62	1.477 (5)
C4—C13	1.512 (4)	C56—C57	1.402 (6)
N5—C6	1.438 (5)	C56—C61	1.395 (6)
N5—C12	1.470 (4)	C57—C58	1.399 (5)
C6—C7	1.402 (5)	C58—C59	1.375 (6)
C6—C11	1.399 (5)	C59—C60	1.369 (8)
C7—C8	1.400 (5)	C60—C61	1.390 (8)
C8—C9	1.384 (5)	C63—C64	1.534 (6)
C9—C10	1.376 (7)	C63—C65	1.514 (6)
C10—C11	1.385 (7)	C65—C70	1.365 (7)
C13—C14	1.534 (5)	C65—C66	1.398 (6)
C13—C15	1.522 (5)	C70—C69	1.393 (7)
C15—C16	1.390 (5)	C69—C68	1.356 (9)
C15—C20	1.384 (5)	C68—C67	1.343 (10)
C16—C17	1.377 (7)	C67—C66	1.383 (8)
C17—C18	1.349 (8)	C71—N72	1.363 (4)
C18—C19	1.387 (7)	C71—N75	1.354 (4)
C19—C20	1.379 (6)	N72—C73	1.377 (5)
C21—N22	1.359 (4)	N72—C88	1.481 (4)
C21—N25	1.361 (4)	C73—C74	1.337 (6)
N22—C23	1.384 (4)	C74—N75	1.383 (5)
N22—C38	1.483 (4)	N75—C76	1.476 (4)
C23—C24	1.342 (5)	C76—C81	1.516 (6)
C24—N25	1.382 (4)	C76—C77	1.584 (5)
N25—C26	1.477 (4)	C81—C87	1.387 (8)
C26—C27	1.556 (5)	C81—C82	1.404 (8)
C26—C31	1.516 (5)	C87—C86	1.416 (11)
C27—C28	1.516 (6)	C86—C85	1.347 (18)
C27—C29	1.541 (6)	C85—C84	1.375 (17)
C27—C30	1.524 (5)	C84—C82	1.402 (9)
C31—C32	1.401 (6)	C82—C83	1.482 (10)
C31—C37	1.406 (5)	C77—C78	1.529 (6)
C32—C33	1.510 (6)	C77—C79	1.528 (6)
C32—C34	1.398 (6)	C77—C80	1.521 (6)
C34—C35	1.391 (8)	C88—C93	1.525 (6)
C35—C36	1.360 (8)	C88—C89	1.563 (6)
C36—C37	1.382 (6)	C93—C99	1.396 (5)
C38—C39	1.558 (5)	C93—C94	1.402 (6)
C38—C43	1.522 (5)	C99—C98	1.370 (7)
C39—C40	1.547 (7)	C98—C97	1.380 (8)
C39—C41	1.521 (5)	C97—C96	1.369 (7)
C39—C42	1.538 (6)	C96—C94	1.386 (7)
C43—C44	1.416 (6)	C94—C95	1.510 (6)
C43—C49	1.390 (6)	C89—C91	1.532 (7)
C44—C45	1.494 (7)	C89—C92	1.537 (8)
C44—C46	1.411 (6)	C89—C90	1.548 (7)
C46—C47	1.354 (8)	O99—C118	1.223 (13)
C47—C48	1.377 (9)	C118—C101	1.383 (17)
C48—C49	1.393 (7)	C118—C102	1.43 (2)
Pd51—I52	2.7069 (11)	O103—C104	1.18 (3)
Pd51—O53	2.083 (3)	C104—C105	1.50 (3)
Pd51—C57	1.993 (4)	C104—C106	1.43 (3)

Bond Angles (Degrees)

I2—Pd1—O3	91.26 (7)	I52—Pd51—C71	91.42 (12)
I2—Pd1—C7	176.20 (10)	O53—Pd51—C71	177.78 (12)
O3—Pd1—C7	85.27 (12)	C57—Pd51—C71	91.82 (15)
I2—Pd1—C21	94.61 (10)	Pd51—O53—C54	120.5 (2)
O3—Pd1—C21	173.41 (11)	O53—C54—N55	123.5 (3)
C7—Pd1—C21	88.79 (13)	O53—C54—C63	117.5 (3)
Pd1—O3—C4	119.6 (2)	N55—C54—C63	118.9 (3)
O3—C4—N5	122.0 (3)	C54—N55—C56	119.9 (3)
O3—C4—C13	118.6 (3)	C54—N55—C62	119.8 (4)
N5—C4—C13	119.4 (3)	C56—N55—C62	119.0 (3)
C4—N5—C6	121.1 (3)	N55—C56—C57	123.2 (3)
C4—N5—C12	119.8 (3)	N55—C56—C61	116.0 (4)
C6—N5—C12	118.5 (3)	C57—C56—C61	120.7 (4)
N5—C6—C7	122.9 (3)	C56—C57—Pd51	118.6 (3)
N5—C6—C11	116.3 (3)	C56—C57—C58	116.8 (4)
C7—C6—C11	120.7 (4)	Pd51—C57—C58	124.3 (3)
C6—C7—Pd1	118.0 (2)	C57—C58—C59	122.8 (5)
C6—C7—C8	117.4 (3)	C58—C59—C60	119.3 (5)
Pd1—C7—C8	124.6 (3)	C59—C60—C61	120.4 (4)
C7—C8—C9	122.1 (4)	C56—C61—C60	119.9 (5)
C8—C9—C10	119.3 (4)	C54—C63—C64	108.5 (3)
C9—C10—C11	120.8 (4)	C54—C63—C65	111.4 (3)
C6—C11—C10	119.6 (4)	C64—C63—C65	110.5 (4)
C4—C13—C14	108.3 (3)	C63—C65—C70	122.1 (4)
C4—C13—C15	112.2 (3)	C63—C65—C66	118.9 (5)
C14—C13—C15	110.1 (3)	C70—C65—C66	118.8 (5)
C13—C15—C16	120.3 (4)	C65—C70—C69	120.4 (5)
C13—C15—C20	121.7 (3)	C70—C69—C68	119.6 (6)
C16—C15—C20	117.9 (4)	C69—C68—C67	121.3 (6)
C15—C16—C17	120.7 (5)	C68—C67—C66	120.1 (5)
C16—C17—C18	120.8 (5)	C65—C66—C67	119.8 (6)
C17—C18—C19	119.8 (4)	Pd51—C71—N72	127.1 (2)
C18—C19—C20	119.9 (5)	Pd51—C71—N75	127.3 (2)
C15—C20—C19	120.9 (4)	N72—C71—N75	105.6 (3)
Pd1—C21—N22	127.5 (2)	C71—N72—C73	109.7 (3)
Pd1—C21—N25	126.9 (2)	C71—N72—C88	122.6 (3)
N22—C21—N25	105.4 (3)	C73—N72—C88	127.6 (3)
C21—N22—C23	110.0 (3)	N72—C73—C74	107.5 (4)
C21—N22—C38	122.4 (3)	C73—C74—N75	107.4 (4)
C23—N22—C38	127.6 (3)	C74—N75—C71	109.8 (3)
N22—C23—C24	107.2 (3)	C74—N75—C76	128.5 (3)
C23—C24—N25	107.4 (3)	C71—N75—C76	121.7 (3)
C24—N25—C21	109.9 (3)	N75—C76—C81	110.0 (3)
C24—N25—C26	127.8 (3)	N75—C76—C77	114.2 (3)
C21—N25—C26	122.1 (2)	C81—C76—C77	114.3 (3)
N25—C26—C27	114.6 (3)	C76—C81—C87	120.8 (5)
N25—C26—C31	110.6 (3)	C76—C81—C82	120.1 (5)
C27—C26—C31	114.4 (3)	C87—C81—C82	119.0 (5)
C26—C27—C28	110.3 (3)	C81—C87—C86	121.1 (9)
C26—C27—C29	106.7 (3)	C87—C86—C85	119.6 (10)
C28—C27—C29	107.9 (4)	C86—C85—C84	119.8 (9)
C26—C27—C30	116.3 (3)	C85—C84—C82	122.7 (10)
C28—C27—C30	109.0 (4)	C81—C82—C84	117.7 (8)
C29—C27—C30	106.3 (3)	C81—C82—C83	124.7 (5)

C26—C31—C32	121.5 (3)	C84—C82—C83	117.5 (8)
C26—C31—C37	119.6 (3)	C76—C77—C78	109.2 (3)
C32—C31—C37	119.0 (4)	C76—C77—C79	105.7 (3)
C31—C32—C33	122.6 (4)	C78—C77—C79	107.5 (4)
C31—C32—C34	118.6 (4)	C76—C77—C80	115.4 (4)
C33—C32—C34	118.8 (4)	C78—C77—C80	110.9 (4)
C32—C34—C35	121.4 (5)	C79—C77—C80	107.7 (4)
C34—C35—C36	119.7 (4)	N72—C88—C93	109.4 (3)
C35—C36—C37	120.6 (5)	N72—C88—C89	114.8 (4)
C31—C37—C36	120.7 (4)	C93—C88—C89	115.2 (3)
N22—C38—C39	114.4 (3)	C88—C93—C99	119.4 (4)
N22—C38—C43	110.6 (3)	C88—C93—C94	122.3 (4)
C39—C38—C43	115.3 (3)	C99—C93—C94	118.2 (4)
C38—C39—C40	107.5 (3)	C93—C99—C98	122.4 (4)
C38—C39—C41	116.3 (3)	C99—C98—C97	119.2 (4)
C40—C39—C41	109.9 (4)	C98—C97—C96	119.1 (5)
C38—C39—C42	106.4 (3)	C97—C96—C94	122.9 (5)
C40—C39—C42	109.2 (4)	C93—C94—C96	118.2 (4)
C41—C39—C42	107.4 (3)	C93—C94—C95	122.6 (4)
C38—C43—C44	121.1 (3)	C96—C94—C95	119.2 (5)
C38—C43—C49	120.0 (4)	C88—C89—C91	114.9 (4)
C44—C43—C49	118.9 (4)	C88—C89—C92	105.9 (4)
C43—C44—C45	123.6 (4)	C91—C89—C92	108.0 (4)
C43—C44—C46	117.0 (5)	C88—C89—C90	109.8 (3)
C45—C44—C46	119.4 (4)	C91—C89—C90	109.1 (5)
C44—C46—C47	122.9 (5)	C92—C89—C90	108.9 (5)
C46—C47—C48	120.5 (5)	O99—C118—C101	124.1 (14)
C47—C48—C49	118.4 (5)	O99—C118—C102	122.6 (13)
C48—C49—C43	122.3 (5)	C101—C118—C102	113.2 (12)
I52—Pd51—O53	90.52 (7)	O103—C104—C105	126 (3)
I52—Pd51—C57	176.46 (11)	O103—C104—C106	124 (3)
O53—Pd51—C57	86.22 (14)	C105—C104—C106	110 (3)

Hydrogen-bond Geometry (Angstroms)

Hydrogen-bond geometry (Å, º)

D—H···*A*	*D*—H	H···*A*	*D*···*A*	*D*—H···*A*
C20—H201···O3	0.94	2.59	3.186 (9)	121
C90—H902···C73	0.98	2.53	3.155 (9)	122
C85—H851···O99^{i}	0.94	2.14	3.010 (9)	152
C102—H1022···O103^{ii}	1.07	2.54	3.549 (9)	156

*Crystallographic Data for (S,S)-**146***:

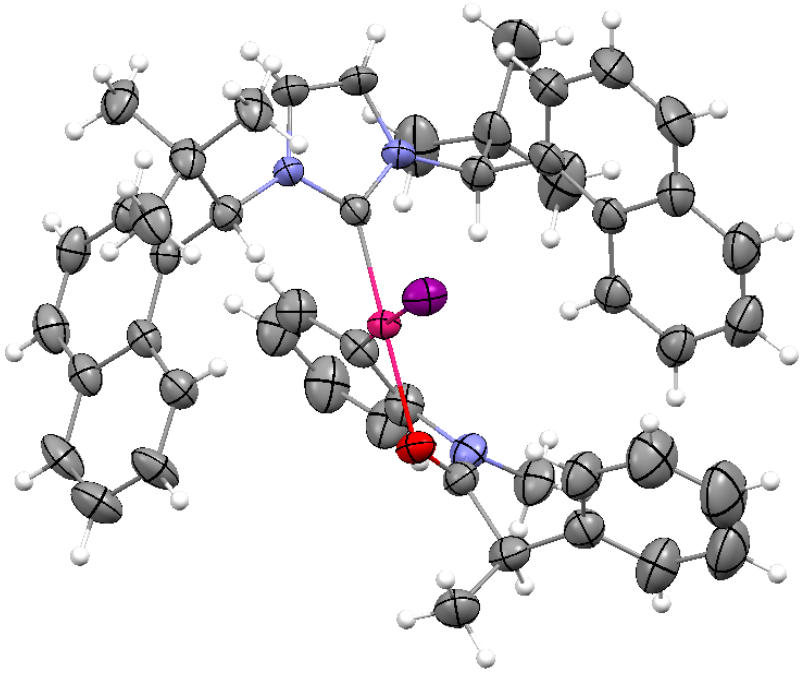

Crystal data

$C_{49}H_{52}I_1N_3O_1Pd_1 \cdot 0.5(C_5H12)$	$V = 4788.4\ (3)\ Å^3$
$M_r = 968.35$	$Z = 4$
Orthorhombic, $P2_12_12_1$	Mo $K\alpha$
$a = 10.3995\ (3)$ Å	$\mu = 1.07\ mm^{-1}$
$b = 15.6586\ (6)$ Å	$T = 180$ K
$c = 29.4050\ (10)$ Å	$0.30 \times 0.20 \times 0.05$ mm

Data collection

Serial diffractometer	10646 independent reflections
Absorption correction: integration Gaussian Integration (Busing and Levy, 1957)	9438 reflections with $I > 2.0\sigma(I)$
$T_{min} = 0.69$, $T_{max} = 0.95$	$R_{int} = 0.040$
10646 measured reflections	

Refinement

$R[F^2 > 2\sigma(F^2)] = 0.034$	?
$wR(F^2) = 0.066$	$\Delta\rho_{max} = 1.27\ e\ Å^{-3}$
$S = 0.90$	$\Delta\rho_{min} = -1.12\ e\ Å^{-3}$
10605 reflections	Absolute structure: Flack (1983), 0 Friedel-pairs

Bond Distance (Angstroms)

I1—Pd2	2.6955 (4)	C41—C42	1.403 (6)
Pd2—O3	2.093 (3)	C42—C43	1.357 (6)
Pd2—C7	2.004 (4)	C43—C44	1.415 (6)
Pd2—C37	1.965 (4)	C44—C45	1.430 (5)
O3—C4	1.227 (5)	C44—C49	1.423 (6)
C4—N5	1.347 (5)	C45—C46	1.420 (5)
C4—C20	1.537 (6)	C46—C47	1.372 (6)
N5—C6	1.461 (6)	C47—C48	1.388 (6)
N5—C16	1.476 (5)	C48—C49	1.354 (7)
C6—C7	1.371 (6)	C57—C58	1.536 (6)
C6—C11	1.411 (6)	C57—C62	1.524 (6)
C7—C8	1.393 (6)	C57—C66	1.541 (6)
C8—C9	1.400 (6)	C71—C72	1.333 (6)
C9—C10	1.381 (8)	C72—N73	1.385 (5)
C10—C11	1.368 (7)	N73—C74	1.476 (5)
C20—C21	1.496 (6)	C74—C75	1.529 (6)
C20—C32	1.526 (6)	C74—C92	1.572 (6)
C21—C22	1.379 (7)	C75—C76	1.378 (6)
C21—C26	1.405 (7)	C75—C80	1.417 (6)
C22—C23	1.384 (7)	C76—C77	1.395 (7)
C23—C24	1.365 (10)	C77—C78	1.369 (7)
C24—C25	1.395 (10)	C78—C79	1.397 (7)
C25—C26	1.383 (8)	C79—C80	1.422 (6)
C37—N38	1.349 (5)	C79—C84	1.413 (7)
C37—N73	1.361 (4)	C80—C81	1.428 (6)
N38—C39	1.479 (5)	C81—C82	1.361 (6)
N38—C71	1.394 (5)	C82—C83	1.412 (7)
C39—C40	1.515 (5)	C83—C84	1.360 (8)
C39—C57	1.574 (5)	C92—C93	1.526 (7)
C40—C41	1.383 (5)	C92—C97	1.529 (7)
C40—C45	1.430 (5)	C92—C101	1.541 (7)

Bond Angles (Degrees)

I1—Pd2—O3	92.76 (8)	C42—C43—C44	120.6 (4)
I1—Pd2—C7	177.05 (13)	C43—C44—C45	119.6 (4)
O3—Pd2—C7	85.41 (14)	C43—C44—C49	120.4 (4)
I1—Pd2—C37	90.84 (10)	C45—C44—C49	119.9 (4)
O3—Pd2—C37	176.06 (14)	C44—C45—C40	118.9 (3)
C7—Pd2—C37	90.93 (16)	C44—C45—C46	116.6 (4)
Pd2—O3—C4	121.0 (3)	C40—C45—C46	124.5 (4)
O3—C4—N5	124.2 (4)	C45—C46—C47	121.3 (4)
O3—C4—C20	117.9 (4)	C46—C47—C48	121.6 (4)
N5—C4—C20	117.9 (4)	C47—C48—C49	119.6 (4)
C4—N5—C6	120.3 (3)	C44—C49—C48	121.0 (4)
C4—N5—C16	121.3 (4)	C39—C57—C58	106.1 (4)
C6—N5—C16	117.5 (4)	C39—C57—C62	116.0 (3)

N5—C6—C7	122.9 (4)	C58—C57—C62	107.0 (4)
N5—C6—C11	115.5 (4)	C39—C57—C66	110.1 (3)
C7—C6—C11	121.5 (4)	C58—C57—C66	108.2 (4)
C6—C7—Pd2	119.9 (3)	C62—C57—C66	109.2 (4)
C6—C7—C8	117.1 (4)	N38—C71—C72	107.5 (4)
Pd2—C7—C8	123.0 (3)	C71—C72—N73	107.6 (3)
C7—C8—C9	122.3 (5)	C72—N73—C37	109.3 (3)
C8—C9—C10	119.0 (5)	C72—N73—C74	128.4 (3)
C9—C10—C11	119.9 (5)	C37—N73—C74	122.3 (3)
C6—C11—C10	120.1 (5)	N73—C74—C75	111.1 (4)
C4—C20—C21	110.2 (4)	N73—C74—C92	114.8 (3)
C4—C20—C32	109.4 (4)	C75—C74—C92	113.9 (3)
C21—C20—C32	110.6 (4)	C74—C75—C76	119.7 (4)
C20—C21—C22	122.1 (4)	C74—C75—C80	121.3 (4)
C20—C21—C26	118.9 (5)	C76—C75—C80	119.0 (4)
C22—C21—C26	118.8 (5)	C75—C76—C77	122.3 (5)
C21—C22—C23	119.9 (5)	C76—C77—C78	119.2 (5)
C22—C23—C24	121.2 (7)	C77—C78—C79	120.8 (5)
C23—C24—C25	120.2 (7)	C78—C79—C80	120.1 (5)
C24—C25—C26	118.8 (7)	C78—C79—C84	119.9 (5)
C21—C26—C25	121.0 (6)	C80—C79—C84	120.0 (5)
Pd2—C37—N38	127.7 (3)	C79—C80—C75	118.4 (4)
Pd2—C37—N73	125.9 (3)	C79—C80—C81	116.1 (4)
N38—C37—N73	106.4 (3)	C75—C80—C81	125.5 (4)
C37—N38—C39	122.0 (3)	C80—C81—C82	122.7 (4)
C37—N38—C71	109.3 (3)	C81—C82—C83	120.1 (5)
C39—N38—C71	128.7 (3)	C82—C83—C84	119.1 (5)
N38—C39—C40	110.3 (3)	C79—C84—C83	121.8 (5)
N38—C39—C57	114.5 (3)	C74—C92—C93	109.4 (4)
C40—C39—C57	114.6 (3)	C74—C92—C97	107.3 (4)
C39—C40—C41	120.5 (3)	C93—C92—C97	109.0 (5)
C39—C40—C45	121.1 (3)	C74—C92—C101	114.1 (5)
C41—C40—C45	118.4 (4)	C93—C92—C101	109.9 (4)
C40—C41—C42	122.3 (4)	C97—C92—C101	107.0 (4)
C41—C42—C43	120.1 (4)		

Without modeling the solvent, the refinement converges to low R factors (R 0.0485 Rw 0.00770 using all reflections). However, some remaining density appears in the Fourier difference map. This remaining electron density, located in voids present in the structure (2 voids per unit-cell), forms an elongated pattern which is consistent with a pentane molecule. The solvent molecules are however too disorder to be properly modeled. Squeeze was therefore used to model the contribution of the solvent. The number of electrons found by squeeze per void is somewhat higher than the number of electrons in a pentane molecule (56 vs. 42 electrons per pentane molecule) but the size and shape of the void seem consistent with a pentane molecule.

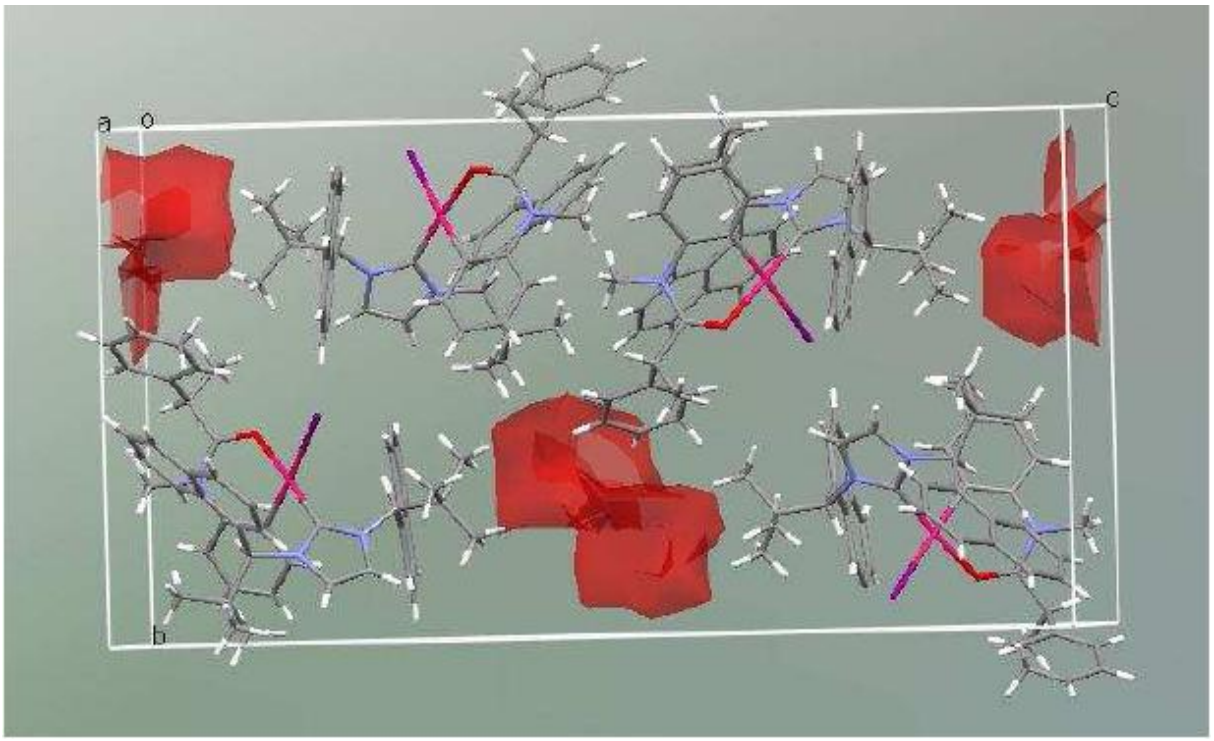

Main voids found per squeeze (in P1)

	x	y	z	Volume(Å^3)	Number of electrons
	-0.047	0.250	0.000	361	57
	0.031	0.750	0.500	361	56

There are 2 voids per unit-cell which correspond of half a solvent molecule per formula-unit.

This half-pentane molecule was added to the formula.

*Crystallographic Data for (S,S)-**297***:

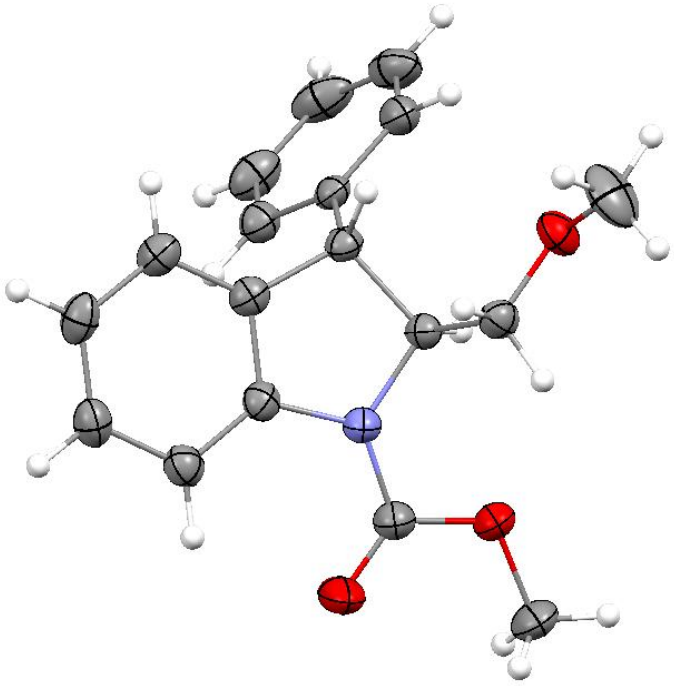

Crystal data

$C_{18}H_{19}NO_3$	$D_x = 1.292$ Mg m^{-3}
$M_r = 297.34$	Cu $K\alpha$ radiation, $\lambda = 1.5418$ Å
Orthorhombic, $P2_12_12_1$	Cell parameters from 3813 reflections
$a = 7.60231$ (8) Å	$\theta = 2.6$–$73.1°$
$b = 11.84409$ (13) Å	$\mu = 0.71$ mm^{-1}
$c = 16.97416$ (19) Å	$T = 180$ K
$V = 1528.39$ (3) Å^3	Block
$Z = 4$	0.3 × 0.3 × 0.2 mm
$F(000) = 632$	

Data collection

SuperNova, Dual, Cu at zero, Atlas diffractometer	1747 independent reflections
Radiation source: SuperNova (Cu) X-ray Source	1714 reflections with $I > 2\sigma(I)$
Mirror monochromator	$R_{int} = 0.017$
Detector resolution: 10.4679 pixels mm^{-1}	$\theta_{max} = 73.3°$, $\theta_{min} = 4.6°$
ω scans	$h = -9 \rightarrow 5$
Absorption correction: Multi-scan *CrysAlis PRO*, Agilent Technologies, Version 1.171.35.21 (release 20-01-2012 CrysAlis171 .NET) (compiled Jan 23 2012,18:06:46) Empirical absorption correction using spherical harmonics, implemented in SCALE3 ABSPACK scaling algorithm.	$k = -13 \rightarrow 14$
$T_{min} = 0.645$, $T_{max} = 1.000$	$l = -16 \rightarrow 20$
4982 measured reflections	

Refinement

Refinement on F^2

Least-squares matrix: Full

$R[F^2 > 2\sigma(F^2)] = 0.029$

$wR(F^2) = 0.076$

$S = 1.09$

1747 reflections

201 parameters

0 restraints

Primary atom site location: Structure-invariant direct methods

Secondary atom site location: Difference Fourier map

Hydrogen site location: Inferred from neighbouring sites

H-atom parameters constrained

$w = 1/[\sigma^2(F_o^2) + (0.0388P)^2 + 0.2668P]$ where $P = (F_o^2 + 2F_c^2)/3$

$(\Delta/\sigma)_{max} < 0.001$

$\Delta\rho_{max} = 0.18$ e Å^{-3}

$\Delta\rho_{min} = -0.17$ e Å^{-3}

Absolute structure: Flack H D (1983), Acta Cryst. A39, 876-881 In the absence of sigificant anomalous scatterine, Friedel pairs were merged.

Bond Distance (Angstroms)

N1—C10	1.359 (2)	C3—C17	1.518 (2)
N1—C2	1.4853 (19)	C3—C4	1.512 (2)
N1—C9	1.418 (2)	C5—C4	1.382 (2)
O15—C14	1.413 (2)	C5—C6	1.391 (2)
O15—C16	1.405 (2)	C17—C18	1.391 (2)
O12—C10	1.349 (2)	C17—C22	1.389 (2)
O12—C13	1.447 (2)	C4—C9	1.393 (2)
O11—C10	1.208 (2)	C9—C8	1.381 (2)
C2—C3	1.560 (2)	C18—C19	1.385 (3)
C2—C14	1.521 (2)	C22—C21	1.390 (3)
C7—C6	1.386 (3)	C20—C19	1.383 (3)
C7—C8	1.393 (3)	C20—C21	1.380 (3)

Bond Angles (Degrees)

C10—N1—C2	125.54 (14)	C18—C17—C3	118.93 (14)
C10—N1—C9	123.97 (14)	C22—C17—C3	122.45 (15)
C9—N1—C2	110.44 (12)	C22—C17—C18	118.57 (16)
C16—O15—C14	112.30 (15)	C5—C4—C3	129.39 (14)
C10—O12—C13	114.48 (14)	C5—C4—C9	119.79 (15)
O12—C10—N1	111.07 (14)	C9—C4—C3	110.82 (14)
O11—C10—N1	125.03 (17)	C4—C9—N1	109.31 (14)
O11—C10—O12	123.91 (16)	C8—C9—N1	128.97 (15)
N1—C2—C3	104.12 (12)	C8—C9—C4	121.71 (16)
N1—C2—C14	112.51 (12)	C19—C18—C17	121.25 (17)
C14—C2—C3	110.41 (12)	C7—C6—C5	119.97 (16)
C6—C7—C8	121.33 (16)	C17—C22—C21	120.19 (17)
C17—C3—C2	112.46 (12)	C21—C20—C19	119.76 (18)
C4—C3—C2	102.93 (12)	C9—C8—C7	117.75 (16)
C4—C3—C17	114.93 (13)	C20—C19—C18	119.64 (19)
O15—C14—C2	106.07 (12)	C20—C21—C22	120.59 (19)
C4—C5—C6	119.42 (16)		

Abbreviations

Ad:	adamantly	**DMAP**:	4-dimethylaminopyridine
A_H:	height parameter	**DME**:	ethylene glycol dimethyl ether
A_L:	length parameter	**DMF**:	*N*,*N*-dimethylformamide
Ar:	aryl	**DMSO**:	dimethyl sulfoxide
aq:	aqueous	**dr**:	diastereomeric ratio
AROM/CM:	asymmetric ring-openning/cross metathesis	**ee**:	enantiomeric excess
		EDG:	electron donating group
atm:	atmosphere	**equiv.**:	equivalent
BArF$^-$:	tris(perfluorophenyl)borane	**ES/ESI**:	electron spray ionisation
BDE:	bond dissociation energy	**EWG**:	electron withdrawing group
BINAP:	2,2'-bis(diphenylphosphion)-1,1'-binaphthyl	**GC**:	gas chromatography
		f.c.:	flash chromatography
BINOL:	1,1'-Bi-2-naphtol	**h**:	hour
Boc:	*tert*-butoxycarbonyl	**h*v***:	light, electromagnetic radiation
BOM:	benzyloxymethyl		
Bn:	benzyl	**HOMO**:	highest occupied molecular orbital
brs:	broad singlet		
brm:	broad multiplet	**HPLC**:	high performance liquid chromatography
C:	concentration		
calcd:	calculated	***i*-Pr**:	*iso*-propyl, 2-propyl
cat:	catalyst	**IR**:	infrared spectroscopy
***c*Hex**:	cyclohexane	**LDA**:	lithium diisopropylamide
COD:	1,5-cyclooctadiene	**m**:	multiplet
conv:	conversion	**Me**:	methyl
dba:	*trans*,*trans*-dibenzylide-neacetone	**min**:	minute
		MO:	molecular orbital
DCM:	dichloromethane	**MS**:	molecular sieves, mass spectrometry (low resolution)
DCC:	*N*,*N'*-dicyclohexyl-carbodiimide		
		m/z:	mass/charge ratio
de:	diastereomeric excess	N_2:	dinitrogen, molecular nitrogen
dd:	doublet of doublets	**n.d.**:	not determined
DFT:	density functional theory	***NHC***:	*N*-heterocyclic carbene

NMR:	nuclear magnetic resonance
***n*-Pr**:	1-propyl
Ph:	phenyl
q:	quartet
rac:	racemic
rt:	room temperature
s:	singlet
t:	time
T:	temperature
***t*Bu**:	*tert*-butyl
TEP:	*Tolman* electronic parameter
THF:	tetrahydrofurane
TM:	transition-metal
TOF:	turnover frequency
TON:	turnover number
%V_{bur}:	percent buried volume
ROCM:	ring-opening cross metathesis
S.M.:	starting material

Symbols

δ:	chemical shift
Δ:	substraction
J:	coupling constant
k:	rate constant
l:	length

Units

°:	degree
Å:	Ångström
d:	day
°C:	degree Celsius
Hz:	hertz (Hz, MHz)
K:	degree Kelvin
M:	molarity
mmol:	millimole
ppm:	parts per million

Literature

(1) Tschugajeff, L.; Skanawy-Grigorjewa, M. P., A. *Anorg. Chem.* **1925**, *148*, 37.

(2) Chugaev, L.; Skanawy-Grigorjewa, M. *J. Russ. Chem. Soc.* **1915**, *47*, 776.

(3) Rouschias, G.; Shaw, B. L. *Chem. Commun.* **1970**, 183.

(4) Butler, W. M.; Enemark, J. H.; Parks, J.; Balch, A. L. *Inorg. Chem.* **1973**, *12*, 451.

(5) Stork, J. R.; Olmstead, M. M.; Balch, A. L. *Inorg. Chem.* **2004**, *43*, 7508.

(6) Burke, A. B.; Balch, A. L.; Enemark, J. H. *J. Am. Chem. Soc.* **1970**, *92*, 2555.

(7) Öfele, K. *J. Organomet. Chem.* **1968**, *12*, 42.

(8) Wanzlick, H.-W.; Schönherr, H.-J. *Angew. Chem. Int. Ed.* **1968**, *7*, 141.

(9) Lappert, M. F. *J. Organomet. Chem.* **1988**, *358*, 185.

(10) Lappert, M. F. *J. Organomet. Chem.* **1975**, *100*, 139.

(11) Arduengo, A. J.; Harlow, R. L.; Kline, M. *J. Am. Chem. Soc.* **1991**, *113*, 361.

(12) Arduengo, A. J.; Bertrand, G. *Chem. Rev.* **2009**, *109*, 3209.

(13) Schuster, O.; Yang, L. R.; Raubenheimer, H. G.; Albrecht, M. *Chem. Rev.* **2009**, *109*, 3445.

(14) Lin, J. C. Y.; Huang, R. T. W.; Lee, C. S.; Bhattacharyya, A.; Hwang, W. S.; Lin, I. J. B. *Chem. Rev.* **2009**, *109*, 3561.

(15) Arnold, P. L.; Casely, I. J. *Chem. Rev.* **2009**, *109*, 3599.

(16) Poyatos, M.; Mata, J. A.; Peris, E. *Chem. Rev.* **2009**, *109*, 3677.

(17) Corberan, R.; Mas-Marza, E.; Peris, E. *Eur. J. Inorg. Chem.* **2009**, 1700.

(18) Hahn, F. E.; Jahnke, M. C. *Angew. Chem. Int. Ed.* **2008**, *47*, 3122.

(19) Herrmann, W. A. *Angew. Chem. Int. Ed.* **2002**, *41*, 1290.

(20) Scholl, M.; Ding, S.; Lee, C. W.; Grubbs, R. H. *Org. Lett.* **1999**, *1*, 953.

(21) Scott, N. M.; Dorta, R.; Stevens, E. D.; Correa, A.; Cavallo, L.; Nolan, S. P. *J. Am. Chem. Soc.* **2005**, *127*, 3516.

(22) Fortman, G. C.; Nolan, S. P. *Chem. Soc. Rev.* **2011**, *40*, 5151.

(23) Magill, A. M.; Cavell, K. J.; Yates, B. F. *J. Am. Chem. Soc.* **2004**, *126*, 8717.

(24) Huang, J. K.; Schanz, H. J.; Stevens, E. D.; Nolan, S. P. *Organometallics* **1999**, *18*, 2370.

(25) Fürstner, A.; Alcarazo, M.; Krause, H.; Lehmann, C. W. *J. Am. Chem. Soc.* **2007**, *129*, 12676.

(26) Dorta, R.; Stevens, E. D.; Nolan, S. P. *J. Am. Chem. Soc.* **2004**, *126*, 5054.

(27) Hillier, A. C.; Sommer, W. J.; Yong, B. S.; Petersen, J. L.; Cavallo, L.; Nolan, S. P. *Organometallics* **2003**, *22*, 4322.

(28) Dorta, R.; Stevens, E. D.; Scott, N. M.; Costabile, C.; Cavallo, L.; Hoff, C. D.; Nolan, S. P. *J. Am. Chem. Soc.* **2005**, *127*, 2485.

(29) Leuthausser, S.; Schwarz, D.; Plenio, H. *Chem. Eur. J.* **2007**, *13*, 7195.

(30) Cazin, C. S. J. *N-Heterocyclic Carbenes in Transition Metal Catalysis and Organocatalysis* **2011**.

(31) Tolman, C. A. *Chem. Rev.* **1977**, *77*, 313.

(32) Cavallo, L.; Correa, A.; Costabile, C.; Jacobsen, H. *J. Organomet. Chem.* **2005**, *690*, 5407.

(33) Kelly, R. A.; Clavier, H.; Giudice, S.; Scott, N. M.; Stevens, E. D.; Bordner, J.; Samardjiev, I.; Hoff, C. D.; Cavallo, L.; Nolan, S. P. *Organometallics* **2008**, *27*, 202.

(34) Clavier, H. C., A.; Cavallo, L.; Escudero-Adán, E. C.; Benet-Buchholz, J.; Slawin, A. M. Z.; Nolan, S. P. *Eur. J. Inorg. Chem.* **2009**, 1767.

(35) Bazinet, P.; Ong, T. G.; O'Brien, J. S.; Lavoie, N.; Bell, E.; Yap, G. P. A.; Korobkov, I.; Richeson, D. S. *Organometallics* **2007**, *26*, 2885.

(36) Gaillard, S.; Bantreil, X.; Slawin, A. M. Z.; Nolan, S. P. *Dalton Trans.* **2009**, 6967.

(37) Wurtz, S.; Lohre, C.; Frohlich, R.; Bergander, K.; Glorius, F. *J. Am. Chem. Soc.* **2009**, *131*, 8344.

(38) Kiyomori, A.; Marcoux, J. F.; Buchwald, S. L. *Tetrahedron Letters* **1999**, *40*, 2657.

(39) Chan, B. K. M.; Chang, N. H.; Grimmett, M. R. *Aust. J. Chem.* **1977**, *30*, 2005.

(40) Ozdemir, I.; Demir, S.; Cetinkaya, B.; Toupet, L.; Castarlenas, R.; Fischmeister, C.; Dixneuf, P. H. *Eur. J. Inorg. Chem.* **2007**, 2862.

(41) Herrmann, W. A.; Kocher, C.; Goossen, L. J.; Artus, G. R. J. *Chem. Eur. J.* **1996**, *2*, 1627.

(42) Bildstein, B.; Malaun, M.; Kopacka, H.; Wurst, K.; Mitterbock, M.; Ongania, K. H.; Opromolla, G.; Zanello, P. *Organometallics* **1999**, *18*, 4325.

(43) Huang, J. K.; Nolan, S. P. *J. Am. Chem. Soc.* **1999**, *121*, 9889.

(44) Glorius, F.; Altenhoff, G.; Goddard, R.; Lehmann, C. *Chem. Commun.* **2002**, 2704

(45) Gridnev, A. A.; Mihaltseva, I. M. *Synth. Commun.* **1994**, *24*, 1547.

(46) Furstner, A.; Alcarazo, M.; Cesar, V.; Lehmann, C. W. *Chem. Commun.* **2006**, 2176.

(47) Grasa, G. A.; Viciu, M. S.; Huang, J. K.; Nolan, S. P. *J. Org. Chem.* **2001**, *66*, 7729.

(48) Bon, R. S.; Hong, C. G.; Bouma, M. J.; Schmitz, R. F.; de Kanter, F. J. J.; Lutz, M.; Spek, A. L.; Orru, R. V. A. *Org. Lett.* **2003**, *5*, 3759.

(49) Bon, R. S.; van Vliet, B.; Sprenkels, N. E.; Schmitz, R. F.; de Kanter, F. J. J.; Stevens, C. V.; Swart, M.; Bickelhaupt, F. M.; Groen, M. B.; Orru, R. V. A. *J. Org. Chem.* **2005**, *70*, 3542.

(50) Bon, R. S.; de Kanter, F. J. J.; Lutz, M.; Spek, A. L.; Jahnke, M. C.; Hahn, F. E.; Groen, M. B.; Orru, R. V. A. *Organometallics* **2007**, *26*, 3639.

(51) Enders, D.; Gielen, H.; Raabe, G.; Runsink, J.; Teles, J. H. *Chem. Ber.* **1996**, *129*, 1483.

(52) Wang, F. J.; Liu, L. J.; Wang, W. F.; Li, S. K.; Shi, M. *Coordin Chem Rev* **2012**, *256*, 804.

(53) Guillen, F.; Winn, C. L.; Alexakis, A. *Tetrahedron: Asymmetry* **2001**, *12*, 2083.

(54) Alexakis, A.; Winn, C. L.; Guillen, F.; Pytkowicz, J.; Roland, S.; Mangeney, P. *Adv. Synth. Catal.* **2003**, *345*, 345.

(55) Winn, C. L.; Guillen, F.; Pytkowicz, J.; Roland, S.; Mangeney, P.; Alexakis, A. *J. Organomet. Chem.* **2005**, *690*, 5672.

(56) Urban, S.; Ortega, N.; Glorius, F. *Angew. Chem. Int. Ed.* **2011**, *50*, 3803.

(57) Ortega, N.; Urban, S.; Beiring, B.; Glorius, F. *Angew. Chem. Int. Ed.* **2012**, *51*, 1710.

(58) Urban, S.; Beiring, B.; Ortega, N.; Paul, D.; Glorius, F. *J. Am. Chem. Soc.* **2012**, *134*, 15241.

(59) Sato, Y.; Hinata, Y.; Seki, R.; Oonishi, Y.; Saito, N. *Org. Lett.* **2007**, *9*, 5597.

(60) Lee, S.; Hartwig, J. F. *J. Org. Chem.* **2001**, *66*, 3402.

(61) Seo, H.; Kim, B. Y.; Lee, J. H.; Park, H. J.; Son, S. U.; Chung, Y. K. *Organometallics* **2003**, *22*, 4783.

(62) Arnold, P. L.; Rodden, M.; Davis, K. M.; Scarisbrick, A. C.; Blake, A. J.; Wilson, C. *Chem. Commun.* **2004**, 1612.

(63) Clavier, H.; Coutable, L.; Guillemin, J. C.; Mauduit, M. *Tetrahedron: Asymmetry* **2005**, *16*, 921.

(64) Pytkowicz, J.; Roland, S.; Mangeney, P. *Tetrahedron: Asymmetry* **2001**, *12*, 2087.

(65) Seiders, T. J.; Ward, D. W.; Grubbs, R. H. *Org. Lett.* **2001**, *3*, 3225.

(66) Bappert, E.; Helmchen, G. *Synlett* **2004**, 1789.

(67) Mahandru, G. M.; Liu, G.; Montgomery, J. *J. Am. Chem. Soc.* **2004**, *126*, 15316.

(68) Chaulagain, M. R.; Sormunen, G. J.; Montgomery, J. *J. Am. Chem. Soc.* **2007**, *129*, 9568.

(69) Liu, P.; Montgomery, J.; Houk, K. N. *J. Am. Chem. Soc.* **2011**, *133*, 6956.

(70) Gao, F.; McGrath, K. P.; Lee, Y.; Hoveyda, A. H. *J. Am. Chem. Soc.* **2010**, *132*, 14315.

(71) Akiyama, K.; Gao, F.; Hoveyda, A. H. *Angew. Chem. Int. Ed.* **2010**, *49*, 419.

(72) Gao, F.; Hoveyda, A. H. *J. Am. Chem. Soc.* **2010**, *132*, 10961.

(73) Luan, X. J.; Mariz, R.; Robert, C.; Gatti, M.; Blumentritt, S.; Linden, A.; Dorta, R. *Org. Lett.* **2008**, *10*, 5569.

(74) Luan, X. J.; Wu, L. L.; Drinkel, E.; Mariz, R.; Gatti, M.; Dorta, R. *Org. Lett.* **2010**, *12*, 1912.

(75) Wu, L.; Falivene, L. D., E.Grant, S.Linden, A.Cavallo, L.; Dorta, R. *Angew. Chem. Int. Ed.* **2012**, *51*, 1.

(76) Clyne, D. S.; Jin, J.; Genest, E.; Gallucci, J. C.; RajanBabu, T. V. *Org. Lett.* **2000**, *2*, 1125.

(77) Duan, W. L.; Shi, M.; Rong, G. B. *Chem. Commun.* **2003**, 2916.

(78) Zhang, T.; Shi, M. *Chem. Eur. J.* **2008**, *14*, 3759.

(79) Xu, Q.; Zhang, R.; Zhang, T.; Shi, M. *J. Org. Chem.* **2010**, *75*, 3935.

(80) Ma, G. N.; Zhang, T.; Shi, M. *Org. Lett.* **2009**, *11*, 875.

(81) Liu, Z.; Shi, M. *Tetrahedron* **2010**, *66*, 2619.

(82) Liu, Z.; Shi, M. *Organometallics* **2010**, *29*, 2831.

(83) Wang, W. F.; Yang, J. M.; Wang, F. J.; Shi, M. *Organometallics* **2011**, *30*, 3859.

(84) Van Veldhuizen, J. J.; Garber, S. B.; Kingsbury, J. S.; Hoveyda, A. H. *J. Am. Chem. Soc.* **2002**, *124*, 4954.

(85) Van Veldhuizen, J. J.; Gillingham, D. G.; Garber, S. B.; Kataoka, O.; Hoveyda, A. H. *J. Am. Chem. Soc.* **2003**, *125*, 12502.

(86) Van Veldhuizen, J. J.; Campbell, J. E.; Giudici, R. E.; Hoveyda, A. H. *J. Am. Chem. Soc.* **2005**, *127*, 6877.

(87) Khan, R. K. M. B., R. V.; Torker, S.; Li, B.; Hoveyda, A. H. *J. Am. Chem. Soc.* **2012**, *134*, 12774.

(88) Bolm, C.; Kesselgruber, M.; Raabe, G. *Organometallics* **2002**, *21*, 707.

(89) Broggini, D.; Togni, A. *Helv. Chim. Acta* **2002**, *85*, 2518.

(90) Gischig, S.; Togni, A. *Organometallics* **2004**, *23*, 2479.

(91) Seo, H.; Park, H.; Kim, B. Y.; Lee, J. H.; Son, S. U.; Chung, Y. K. *Organometallics* **2003**, *22*, 618.

(92) Gischig, S.; Togni, A. *Eur. J. Inorg. Chem.* **2005**, 4745.

(93) Bolm, C.; Focken, T.; Raabe, G. *Tetrahedron: Asymmetry* **2003**, *14*, 1733.

(94) Focken, T.; Raabe, G.; Bolm, C. *Tetrahedron: Asymmetry* **2004**, *15*, 1693.

(95) Ma, Y. D.; Song, C.; Ma, C. Q.; Sun, Z. J.; Chai, Q.; Andrus, M. B. *Angew. Chem. Int. Ed.* **2003**, *42*, 5871.

(96) Focken, T.; Rudolph, J.; Bolm, C. *Synthesis* **2005**, 429.

(97) Jacobsen, E. N. *Accounts Chem. Res.* **2000**, *33*, 421.

(98) Noyori, R.; Ohkuma, T. *Angew. Chem. Int. Ed.* **2001**, *40*, 40.

(99) Perry, M. C.; Cui, X. H.; Burgess, K. *Tetrahedron: Asymmetry* **2002**, *13*, 1969.

(100) Ludovic, G.; Douthwaite, R. E. *Organometallics* **2003**, *22*, 4187.

(101) Bonnet, L. G.; Douthwaite, R. E.; Hodgson, R. *Organometallics* **2003**, *22*, 4384.

(102) Herrmann, W. A.; Goossen, L. J.; Spiegler, M. *Organometallics* **1998**, *17*, 2162.

(103) Nanchen, S.; Pfaltz, A. *Chem. Eur. J.* **2006**, *12*, 4550.

(104) Powell, M. T.; Hou, D. R.; Perry, M. C.; Cui, X. H.; Burgess, K. *J. Am. Chem. Soc.* **2001**, *123*, 8878.

(105) Perry, M. C.; Cui, X. H.; Powell, M. T.; Hou, D. R.; Reibenspies, J. H.; Burgess, K. *J. Am. Chem. Soc.* **2003**, *125*, 113.

(106) Gade, L. H.; Cesar, V.; Bellemin-Laponnaz, S. *Angew. Chem. Int. Ed.* **2004**, *43*, 1014.

(107) Cesar, V.; Bellemin-Laponnaz, S.; Wadepohl, H.; Gade, L. H. *Chem. Eur. J.* **2005**, *11*, 2862.

(108) Herrmann, W. A.; Baskakov, D.; Herdtweck, E.; Hoffmann, S. D.; Bunlaksananusorn, T.; Rampf, F.; Rodefeld, L. *Organometallics* **2006**, *25*, 2449.

(109) Baskakov, D.; Herrmann, W. A.; Herdtweck, E.; Hoffmann, S. D. *Organometallics* **2007**, *26*, 626.

(110) Liu, L. T.; Ishida, N.; Ashida, S.; Murakami, M. *Org. Lett.* **2011**, *13*, 1666.

(111) Berlin, J. M.; Goldberg, S. D.; Grubbs, R. H. *Angew. Chem. Int. Ed.* **2006**, *45*, 7591.

(112) Funk, T. W.; Berlin, J. M.; Grubbs, R. H. *J. Am. Chem. Soc.* **2006**, *128*, 1840.

(113) Song, C.; Ma, C. Q.; Ma, Y. D.; Feng, W. H.; Ma, S. T.; Chai, Q.; Andrus, M. B. *Tetrahedron Letters* **2005**, *46*, 3241.

(114) Kundig, E. P.; Seidel, T. M.; Jia, Y. X.; Bernardinelli, G. *Angew. Chem. Int. Ed.* **2007**, *46*, 8484.

(115) Jia, Y. X.; Hillgren, J. M.; Watson, E. L.; Marsden, S. P.; Kundig, E. P. *Chem. Commun.* **2008**, 4040.

(116) Arao, T.; Kondo, K.; Aoyama, T. *Tetrahedron Lett.* **2006**, *47*, 1417.

(117) Park, J. K.; Lackey, H. H.; Rexford, M. D.; Kovnir, K.; Shatruk, M.; McQuade, D. T. *Org. Lett.* **2010**, *12*, 5008.

(118) Sakaguchi, S.; Powrie, F.; Ransohoff, R. M. *Nature Med.* **2012**, *18*, 630.

(119) Nakanishi, M.; Katayev, D.; Besnard, C.; Kundig, E. P. *Angew. Chem. Int. Ed.* **2011**, *50*, 7438.

(120) Katayev, D.; Nakanishi, M.; Burgi, T.; Kundig, E. P. *Chem. Sci.* **2012**, *3*, 1422.

(121) Nakanishi, M.; Katayev, D.; Besnard, C.; Kundig, E. P. *Chimia* **2012**, *66*, 241.

(122) Bernardinelli, G. H.; Kundig, E. P.; Meier, P.; Pfaltz, A.; Radkowski, K.; Zimmermann, N.; Neuburger-Zehnder, M. *Helv. Chim. Acta* **2001**, *84*, 3233.

(123) Bernardinelli, G.; Gillet, S.; Kundig, P.; Liu, R. G.; Ripa, A.; Saudan, L. *Synthesis* **2001**, 2040.

(124) Saudan, L. A.; Bernardinelli, G.; Kundig, E. P. *Synlett* **2000**, 483.

(125) Kundig, E. P.; Meier, P. *Helv. Chim. Acta* **1999**, *82*, 1360.

(126) Goehring, R. R.; Sachdeva, Y. P.; Pisipati, J. S.; Sleevi, M. C.; Wolfe, J. F. *J. Am. Chem. Soc.* **1985**, *107*, 435.

(127) Marti, C.; Carreira, E. M. *Eur. J. Org. Chem.* **2003**, 2209.

(128) da Silva, J. F. M.; Garden, S. J.; Pinto, A. C. *J. Brazil. Chem. Soc.* **2001**, *12*, 273.

(129) Lin, H.; Danishefsky, S. J. *Angew. Chem. Int. Ed.* **2003**, *42*, 36.

(130) Galliford, C. V.; Scheidt, K. A. *Angew. Chem. Int. Ed.* **2007**, *46*, 8748.

(131) Fensome, A.; Adams, W. R.; Adams, A. L.; Berrodin, T. J.; Cohen, J.; Huselton, C.; Illenberger, A.; Kern, J. C.; Hudak, V. A.; Marella, M. A.; Melenski, E. G.; McComas, C. C.; Mugford, C. A.; Slayden, O. D.; Yudt, M.; Zhang, Z. M.; Zhang, P. W.; Zhu, Y.; Winneker, R. C.; Wrobel, J. E. *J. Med. Chem.* **2008**, *51*, 1861.

(132) Jossang, A.; Jossang, P.; Hadi, H. A.; Sevenet, T.; Bodo, B. *J. Org. Chem.* **1991**, *56*, 6527.

(133) Anderton, N.; Cockrum, P. A.; Colegate, S. M.; Edgar, J. A.; Flower, K.; Vit, I.; Willing, R. I. *Phytochemistry* **1998**, *48*, 437.

(134) Suchy, M.; Kutschy, P.; Monde, K.; Goto, H.; Harada, N.; Takasugi, M.; Dzurilla, M.; Balentova, E. *J. Org. Chem.* **2001**, *66*, 3940.

(135) Mugishima, T.; Tsuda, M.; Kasai, Y.; Ishiyama, H.; Fukushi, E.; Kawabata, J.; Watanabe, M.; Akao, K.; Kobayashi, J. *J. Org. Chem.* **2005**, *70*, 9430.

(136) Luk, K. C. S., S. S.; Zhang, J.; Zhamg, Z. *PCT Int. Appl. 2006136606* **2006**, *121*, 34.

(137) Bernard, K.; Bogliolo, S.; Ehrenfeld, J. *Br. J. Pharmacol.* **2005**, *144*, 1037.

(138) Claudine, S. L. G.; Sylvain, D.; Gabrielle, B.; Maurice, M.; Jacques, S.; Rolf, G.; Guy, G.; Gilles, G. *Stress* **2003**, *6*, 199.

(139) Tokunaga, T.; Hume, W. E.; Umezome, T.; Okazaki, K.; Ueki, Y.; Kumagai, K.; Hourai, S.; Nagamine, J.; Seki, H.; Taiji, M.; Noguchi, H.; Nagata, R. *J. Med. Chem.* **2001**, *44*, 4641.

(140) Tokunaga, T.; Hume, W. E.; Nagamine, J.; Kawamura, T.; Taiji, M.; Nagata, R. *Bioorg. Med. Chem. Lett.* **2005**, *15*, 1789.

(141) Tomita, D.; Yamatsugu, K.; Kanai, M.; Shibasaki, M. *J. Am. Chem. Soc.* **2009**, *131*, 6946.

(142) Magnus, P.; Turnbull, R. *Org. Lett.* **2006**, *8*, 3497.

(143) Ghosh, A. K.; Schiltz, G.; Perali, R. S.; Leshchenko, S.; Kay, S.; Walters, D. E.; Koh, Y.; Maeda, K.; Mitsuya, H. *Bioorg. Med. Chem. Lett.* **2006**, *16*, 1869.

(144) O'Connor, S. J. L., Z. *Synlett* **2003**, 2135.

(145) Trost, B. M.; Brennan, M. K. *Synthesis* **2009**, 3003.

(146) Zhou, F.; Liu, Y. L.; Zhou, J. A. *Adv. Synth. Catal.* **2010**, *352*, 1381.

(147) Klein, J. E. M. N.; Taylor, R. J. K. *Eur. J. Org. Chem.* **2011**, 6821.

(148) Ashimori, A.; Bachand, B.; Calter, M. A.; Govek, S. P.; Overman, L. E.; Poon, D. J. *J. Am. Chem. Soc.* **1998**, *120*, 6488.

(149) Ashimori, A.; Bachand, B.; Overman, L. E.; Poon, D. J. *J. Am. Chem. Soc.* **1998**, *120*, 6477.

(150) Ashimori, A. B., B.; Calter, M. A.; Govek, S. P.; Overman, L. A.; Poon, D. J. *J. Am. Chem. Soc.* **1998**, *120*, 6488.

(151) Ashimori, A. B., B.; Overman, L. E.; Poon, D. J. *J. Am. Chem. Soc.* **1998**, *120*, 6477.

(152) Matsuura, T. O., L. E.; Poon, D. J. *J. Am. Chem. Soc.* **1998**, *120*, 6500.

(153) Dounay, A. B.; Hatanaka, K.; Kodanko, J. J.; Oestreich, M.; Overman, L. E.; Pfeifer, L. A.; Weiss, M. M. *J. Am. Chem. Soc.* **2003**, *125*, 6261.

(154) Busacca, C. A.; Grossbach, D.; So, R. C.; O'Brien, E. M.; Spinelli, E. M. *Org. Lett.* **2003**, *5*, 1595.

(155) Pinto, A. J., Y.; Neuville, L.; Zhu, J. *Chem. Eur. J.* **2007**, *13*, 961.

(156) Yasui, Y.; Kamisaki, H.; Takemoto, Y. *Org. Lett.* **2008**, *10*, 3303.

(157) Yasui, Y.; Kinugawa, T.; Takemoto, Y. *Chem. Commun.* **2009**, 4275.

(158) Reddy, V. J.; Douglas, C. J. *Org. Lett.* **2010**, *12*, 952.

(159) Yin, L.; Kanai, M.; Shibasaki, M. *Angew. Chem. Int. Ed.* **2011**, *50*, 7620.

(160) Wu, L.; Falivene, L.; Drinkel, E.; Grant, S.; Linden, A.; Cavallo, L.; Dorta, R. *Angew. Chem. Int. Ed.* **2012**, *51*, 1.

(161) Spallek, M. J.; Riedel, D.; Rominger, F.; Hashmi, A. S. K.; Trapp, O. *Organometallics* **2012**, *31*, 1127.

(162) Jia, Y. X.; Katayev, D.; Bernardinelli, G.; Seidel, T. M.; Kundig, E. P. *Chem. Eur. J.* **2010**, *16*, 6300.

(163) Herrmann, W. A.; Bohm, V. P. W.; Gstottmayr, C. W. K.; Grosche, M.; Reisinger, C. P.; Weskamp, T. *J. Organomet. Chem.* **2001**, *617*, 616.

(164) Juaristi, E.; Hernandez-Rodriguez, M.; Lopez-Ruiz, H.; Avina, J.; Munoz-Muniz, O.; Hayakawa, M.; Seebach, D. *Helv. Chim. Acta* **2002**, *85*, 1999.

(165) Ebbers, E. J.; Ariaans, G. J. A.; Bruggink, A.; Zwanenburg, B. *Tetrahedron: Asymmetry* **1999**, *10*, 3701.

(166) Fananas, F. J.; Granados, A.; Sanz, R.; Ignacio, J. M.; Barluenga, J. *Chem. Eur. J.* **2001**, *7*, 2896.

(167) Mermerian, A. H.; Fu, G. C. *J. Am. Chem. Soc.* **2005**, *127*, 5604.

(168) Scarborough, C. C.; Bergant, A.; Sazama, G. T.; Guzei, I. A.; Spencer, L. C.; Stahl, S. S. *Tetrahedron* **2009**, *65*, 5084.

(169) Viciu, M. S.; Navarro, O.; Germaneau, R. F.; Kelly, R. A.; Sommer, W.; Marion, N.; Stevens, E. D.; Cavallo, L.; Nolan, S. P. *Organometallics* **2004**, *23*, 1629.

(170) Malhotra, S. K.; Johnson, F. *J. Am. Chem. Soc.* **1965**, *87*, 5493.

(171) Hoffmann, R. W. *Chem. Rev.* **1989**, *89*, 1841.

(172) Hoffmann, R. W. *Angew. Chem. Int. Ed.* **2000**, *39*, 2054.

(173) Pregosin, P. S.; Salzmann, R. *Coordin Chem Rev* **1996**, *155*, 35.

(174) Hansson, S.; Norrby, P. O.; Sjogren, M. P. T.; Akermark, B.; Cucciolito, M. E.; Giordano, F.; Vitagliano, A. *Organometallics* **1993**, *12*, 4940.

(175) Gogoll, A.; Ornebro, J.; Grennberg, H.; Backvall, J. E. *J. Am. Chem. Soc.* **1994**, *116*, 3631.

(176) Burckhardt, U.; Baumann, M.; Trabesinger, G.; Gramlich, V.; Togni, A. *Organometallics* **1997**, *16*, 5252.

(177) Brown, J. M.; Hulmes, D. I.; Guiry, P. J. *Tetrahedron* **1994**, *50*, 4493.

(178) Albinati, A.; Kunz, R. W.; Ammann, C. J.; Pregosin, P. S. *Organometallics* **1991**, *10*, 1800.

(179) Clavier, H.; Nolan, S. P. *Chem. Commun.* **2010**, *46*, 9260.

(180) Marion, N.; Navarro, O.; Mei, J. G.; Stevens, E. D.; Scott, N. M.; Nolan, S. P. *J. Am. Chem. Soc.* **2006**, *128*, 4101.

(181) Espinet, P.; Echavarren, A. M. *Angew. Chem. Int. Ed.* **2004**, *43*, 4704.

(182) Perez-Rodriguez, M.; Braga, A. A. C.; Garcia-Melchor, M.; Perez-Temprano, M. H.; Casares, J. A.; Ujaque, G.; de Lera, A. R.; Alvarez, R.; Maseras, F.; Espinet, P. *J. Am. Chem. Soc.* **2009**, *131*, 3650.

(183) Belletire, J. L.; Howard, H.; Donahue, K. *Synth. Commun.* **1982**, *12*, 763.

(184) Ting, P. C.; Kaminski, J. J.; Sherlock, M. H.; Tom, W. C.; Lee, J. F.; Bryant, R. W.; Watnick, A. S.; Mcphail, A. T. *J. Med. Chem.* **1990**, *33*, 2697.

(185) Cheung, M.; Hunter, R. N.; Peel, M. R.; Lackey, K. E. *Heterocycles* **2001**, *55*, 1583.

(186) Adams, C.; Aldous, D. J.; Amendola, S.; Bamborough, P.; Bright, C.; Crowe, S.; Eastwood, P.; Fenton, G.; Foster, M.; Harrison, T. K. P.; King, S.; Lai, J.; Lawrence, C.; Letallec, J. P.; McCarthy, C.; Moorcroft, N.; Page, K.; Rao, S.; Redford, J.; Sadiq, S.; Smith, K.; Souness, J. E.; Thurairatnam, S.; Vine, M.; Wyman, B. *Bioorg. Med. Chem. Lett.* **2003**, *13*, 3105.

(187) Wood, E. R.; Kuyper, L.; Petrov, K. G.; Hunter, R. N.; Harris, P. A.; Lackey, K. *Bioorg. Med. Chem. Lett.* **2004**, *14*, 953.

(188) Marfat, A.; Carta, M. P. *Tetrahedron Letters* **1987**, *28*, 4027.

(189) Robinson, R. P.; Donahue, K. M. *J. Org. Chem.* **1991**, *56*, 4805.

(190) Bacque, E.; El Qacemi, M.; Zard, S. Z. *Org. Lett.* **2004**, *6*, 3671.

(191) Saito, T.; Furukawa, N.; Otani, T. *Org. Biomol. Chem.* **2010**, *8*, 1126.

(192) Ackermann, L.; Vicente, R.; Hofmann, N. *Org. Lett.* **2009**, *11*, 4274.

(193) Wolfe, J. F.; Sleevi, M. C.; Goehring, R. R. *J. Am. Chem. Soc.* **1980**, *102*, 3646.

(194) Okuda, S.; Robison, M. M. *J. Am. Chem. Soc.* **1959**, *81*, 740.

(195) Robinson, R. P.; Donahue, K. M.; Son, P. S.; Wagy, S. D. *J. Heterocyclic Chem.* **1996**, *33*, 287.

(196) Ficken, G. E.; Kendall, J. D. *J. Chem. Soc.* **1961**, 747.

(197) Barker, M. W.; Mchenry, W. E. *J. Org. Chem.* **1979**, *44*, 1175.

(198) Smith, K.; El-Hiti, G. A.; Pritchard, G. J.; Hamilton, A. *J. Chem. Soc., Perkin Trans. 1* **1999**, 2299.

(199) Dey, C.; Kundig, E. P. *Chem. Commun.* **2012**, *48*, 3064.

(200) Dey, C.; Katayev, D.; Ylijoki, K. E. O.; Kundig, E. P. *Chem. Commun.* **2012**, *48*, 10957.

(201) Lemhadri, M.; Fall, Y.; Doucet, H.; Santelli, M. *Synthesis* **2009**, 1021.

(202) Terrier, O. B., J. C.; Rosa-Calatrava, M. *WO 2012/059696 A1* **2012**, 11.

(203) Fukuyama, T.; Liu, G. *J. Am. Chem. Soc.* **1996**, *118*, 7426.

(204) Arndtsen, B. A.; Bergman, R. G.; Mobley, T. A.; Peterson, T. H. *Accounts Chem. Res.* **1995**, *28*, 154.

(205) Davies, H. M. L.; Manning, J. R. *Nature* **2008**, *451*, 417.

(206) Labinger, J. A.; Bercaw, J. E. *Nature* **2002**, *417*, 507.

(207) Kakiuchi, F.; Chatani, N. *Adv. Synth. Catal.* **2003**, *345*, 1077.

(208) Dick, A. R.; Sanford, M. S. *Tetrahedron* **2006**, *62*, 2439.

(209) Godula, K.; Sames, D. *Science* **2006**, *312*, 67.

(210) Dyker, G. *Angew. Chem. Int. Ed.* **1999**, *38*, 1699.

(211) Hassan, J.; Sevignon, M.; Gozzi, C.; Schulz, E.; Lemaire, M. *Chem. Rev.* **2002**, *102*, 1359.

(212) Goj, L. A.; Gunnoe, T. B. *Curr. Org. Chem.* **2005**, *9*, 671.

(213) Campeau, L. C.; Fagnou, K. *Chem. Commun.* **2006**, 1253.

(214) Alberico, D.; Scott, M. E.; Lautens, M. *Chem. Rev.* **2007**, *107*, 174.

(215) Chen, X.; Engle, K. M.; Wang, D. H.; Yu, J. Q. *Angew. Chem. Int. Ed.* **2009**, *48*, 5094.

(216) McGlacken, G. P.; Bateman, L. M. *Chem. Soc. Rev.* **2009**, *38*, 2447.

(217) Bellina, F.; Rossi, R. *Tetrahedron* **2009**, *65*, 10269.

(218) Ackermann, L.; Vicente, R. *Org. Lett.* **2009**, *11*, 4922.

(219) Lafrance, M.; Fagnou, K. *J. Am. Chem. Soc.* **2006**, *128*, 16496.

(220) Garcia-Cuadrado, D.; Braga, A. A. C.; Maseras, F.; Echavarren, A. M. *J. Am. Chem. Soc.* **2006**, *128*, 1066.

(221) Ackermann, L.; Vicente, R.; Althammer, A. *Org. Lett.* **2008**, *10*, 2299.

(222) Caron, L.; Campeau, L. C.; Fagnou, K. *Org. Lett.* **2008**, *10*, 4533.

(223) Lafrance, M.; Lapointe, D.; Fagnou, K. *Tetrahedron* **2008**, *64*, 6015.

(224) Pascual, S.; de Mendoza, P.; Braga, A. A. C.; Maseras, F.; Echavarren, A. M. *Tetrahedron* **2008**, *64*, 6021.

(225) Liegault, B.; Lapointe, D.; Caron, L.; Vlassova, A.; Fagnou, K. *J. Org. Chem.* **2009**, *74*, 1826.

(226) Liegault, B.; Petrov, I.; Gorelsky, S. I.; Fagnou, K. *J. Org. Chem.* **2010**, *75*, 1047.

(227) Jazzar, R.; Hitce, J.; Renaudat, A.; Sofack-Kreutzer, J.; Baudoin, O. *Chem. Eur. J.* **2010**, *16*, 2654.

(228) Baudoin, O. *Chem. Soc. Rev.* **2011**, *40*, 4902.

(229) Dyker, G. *Angew. Chem. Int. Ed.* **1992**, *31*, 1023.

(230) Dyker, G. *Angew. Chem. Int. Ed.* **1994**, *33*, 103.

(231) Dyker, G. *Chem. Ber.* **1994**, *127*, 739.

(232) Lafrance, M.; Gorelsky, S. I.; Fagnou, K. *J. Am. Chem. Soc.* **2007**, *129*, 14570.

(233) Rousseaux, S.; Davi, M.; Sofack-Kreutzer, J.; Pierre, C.; Kefalidis, C. E.; Clot, E.; Fagnou, K.; Baudoin, O. *J. Am. Chem. Soc.* **2010**, *132*, 10706.

(234) Watanabe, T.; Oishi, S.; Fujii, N.; Ohno, H. *Org. Lett.* **2008**, *10*, 1759.

(235) Shi, B. F.; Maugel, N.; Zhang, Y. H.; Yu, J. Q. *Angew. Chem. Int. Ed.* **2008**, *47*, 4882.

(236) Wasa, M.; Engle, K. M.; Lin, D. W.; Yoo, E. J.; Yu, J. Q. *J. Am. Chem. Soc.* **2011**, *133*, 19598.

(237) Renaudat, A.; Jean-Gerard, L.; Jazzar, R.; Kefalidis, C. E.; Clot, E.; Baudoin, O. *Angew. Chem. Int. Ed.* **2010**, *49*, 7261.

(238) Martin, N.; Pierre, C.; Davi, M.; Jazzar, R.; Baudoin, O. *Chem. Eur. J.* **2012**, *18*, 4480.

(239) Zhang, H. J.; Boonsombat, J.; Padwa, A. *Org. Lett.* **2007**, *9*, 279.

(240) Bui, T.; Syed, S.; Barbas, C. F. *J. Am. Chem. Soc.* **2009**, *131*, 8758.

(241) Wang, T.; Xu, Q. G.; Yu, P.; Liu, X. X.; Cook, J. M. *Org. Lett.* **2001**, *3*, 345.

(242) Iyengar, R.; Schildknegt, K.; Morton, M.; Aube, J. *J. Org. Chem.* **2005**, *70*, 10645.

(243) Rakhit, A.; Hurley, M. E.; Tipnis, V.; Coleman, J.; Rommel, A.; Brunner, H. R. *J. Clin. Pharmacol.* **1986**, *26*, 156.

(244) Xiang, L.; Xing, D. M.; Wang, W.; Wang, R. F.; Ding, Y.; Du, L. J. *Phytochemistry* **2005**, *66*, 2595.

(245) Liu, D. Y.; Zhao, G. W.; Xiang, L. *Eur. J. Org. Chem.* **2010**, 3975.

(246) Kuwano, R.; Sato, K.; Kurokawa, T.; Karube, D.; Ito, Y. *J. Am. Chem. Soc.* **2000**, *122*, 7614.

(247) Kuwano, R.; Kashiwabara, M.; Sato, K.; Ito, T.; Kaneda, K.; Ito, Y. *Tetrahedron: Asymmetry* **2006**, *17*, 521.

(248) Kuwano, R.; Kashiwabara, M. *Org. Lett.* **2006**, *8*, 2653.

(249) Arp, F. O.; Fu, G. C. *J. Am. Chem. Soc.* **2006**, *128*, 14264.

(250) Garcia Ruano, J. L.; Parra, A.; Marcos, V.; del Pozo, C.; Catalan, S.; Monteagudo, S.; Fustero, S.; Poveda, A. *J. Am. Chem. Soc.* **2009**, *131*, 9432.

(251) Zhou, F. G., J.; Liu, J.; Ding, K.; Yu, S.; Cai, Q. *J. Am. Chem. Soc.* **2012**, *134*, 14326.

(252) Wang, D. S.; Chen, Q. A.; Li, W.; Yu, C. B.; Zhou, Y. G.; Zhang, X. M. *J. Am. Chem. Soc.* **2010**, *132*, 8909.

(253) Rousseaux, S.; Davi, M.; Sofack-Kreutzer, J.; Pierre, C.; Kefalidis, C. E.; Clot, E.; Fagnou, K.; Baudoin, O. *J. Am. Chem. Soc.*, *132*, 10706.

(254) Omar-Amrani, R.; Schneider, R.; Fort, Y. *Synthesis* **2004**, 2527.

(255) Mei, T. S.; Wang, X. S.; Yu, J. Q. *J. Am. Chem. Soc.* **2009**, *131*, 10806.

(256) Cho, D. J.; Wu, C. J.; Sujith, S.; Han, W. S.; Kang, S. O.; Lee, B. Y. *Organometallics* **2006**, *25*, 2133.

(257) Buenger, G. D., J.; Jass, P.; Michalson, E.; Schiesher, M. *US 2009/0292143A1* **2009**.

(258) Viciu, M. S.; Germaneau, R. F.; Navarro-Fernandez, O.; Stevens, E. D.; Nolan, S. P. *Organometallics* **2002**, *21*, 5470.

(259) Rousseaux, S.; Gorelsky, S. I.; Chung, B. K. W.; Fagnou, K. *J. Am. Chem. Soc.* **2010**, *132*, 10692.

(260) Anas, S.; Cordi, A.; Kagan, H. B. *Chem. Commun.* **2011**, *47*, 11483.

(261) Saget, T.; Lemouzy, S. J.; Cramer, N. *Angew. Chem. Int. Ed.* **2012**, *51*, 2238.

(262) Nafie, L. A.; Keiderling, T. A.; Stephens, P. J. *J. Am. Chem. Soc.* **1976**, *98*, 2715.

(263) Nafie, L. A. *Annu. Rev. Phys. Chem.* **1997**, *48*, 357.

(264) Kagan, H. B. *Tetrahedron* **2001**, *57*, 2449.

(265) Vedejs, E.; Jure, M. *Angew. Chem. Int. Ed.* **2005**, *44*, 3974.

(266) Miller, L. C.; Sarpong, R. *Chem. Soc. Rev.* **2011**, *40*, 4550.

(267) Pache, S.; Botuha, C.; Franz, R.; Kundig, E. P.; Einhorn, J. *Helv. Chim. Acta* **2000**, *83*, 2436.

(268) Bernardinelli, G.; Fernandez, D.; Gosmini, R.; Meier, P.; Ripa, A.; Schupfer, P.; Treptow, B.; Kundig, E. P. *Chirality* **2000**, *12*, 529.

(269) Kundig, E. P.; Botuha, C.; Lemercier, G.; Romanens, P.; Saudan, L.; Thibault, S. *Helv. Chim. Acta* **2004**, *87*, 561.

(270) Jia, Y. X.; Kundig, E. P. *Angew. Chem. Int. Ed.* **2009**, *48*, 1636.

(271) Rivas, F. M.; Riaz, U.; Giessert, A.; Smulik, J. A.; Diver, S. T. *Org. Lett.* **2001**, *3*, 2673.

(272) Bailey, H. V.; Heaton, W.; Vicker, N.; Potter, B. V. L. *Synlett* **2006**, 2444.

(273) Guo, Z. Q.; Wu, D. P.; Zhu, Y. F.; Tucci, F. C.; Regan, C. F.; Rowbottom, M. W.; Struthers, R. S.; Xie, Q.; Reijmers, S.; Sullivan, S. K.; Sai, Y.; Chen, C. *Bioorg. Med. Chem. Lett.* **2005**, *15*, 3685.

(274) Wyszogrodzka, M.; Mows, K.; Kamlage, S.; Wodzifiska, J.; Plietker, B.; Haag, R. *Eur. J. Org. Chem.* **2008**, 53.

(275) Wyszogrodzka, M.; Haag, R. *Langmuir* **2009**, *25*, 5703.

(276) Kordes, M.; Winsel, H.; de Meijere, A. *Eur. J. Org. Chem.* **2000**, 3235.

(277) Becke, A. D. *J. Chem. Phys.* **1993**, *98*, 5648.

(278) Ditchfie.R; Hehre, W. J.; Pople, J. A. *J. Chem. Phys.* **1971**, *54*, 724.